UNCLASSIFIED

| AD NUMBER |
| --- |
| ADB022011 |
| LIMITATION CHANGES |

TO:

Approved for public release; distribution is unlimited.

FROM:

Distribution authorized to U.S. Gov't. agencies only; Test and Evaluation; APR 1976. Other requests shall be referred to Air Force Flight Dynamics Laboratory, FXB, Wright-Patterson, AFB, OH 45433.

| AUTHORITY |
| --- |

afal ltr dtd 22 may 1978

THIS PAGE IS UNCLASSIFIED

THIS REPORT HAS BEEN DELIMITED
AND CLEARED FOR PUBLIC RELEASE
UNDER DOD DIRECTIVE 5200.20 AND
NO RESTRICTIONS ARE IMPOSED UPON
ITS USE AND DISCLOSURE,

DISTRIBUTION STATEMENT A

APPROVED FOR PUBLIC RELEASE;
DISTRIBUTION UNLIMITED,

AFFDL-TR-76-76

# LIGHT EXPERIMENTAL SUPERCRUISER
# CONCEPTUAL DESIGN

*THE BOEING AEROSPACE COMPANY*
*SEATTLE, WASHINGTON 98124*

JULY 1976

OCT 18 1977

Final Report for Period June 1975 – March 1976

AIR FORCE FLIGHT DYNAMICS LABORATORY
AIR FORCE WRIGHT AERONAUTICAL LABORATORIES
AIR FORCE SYSTEMS COMMAND
WRIGHT-PATTERSON AIR FORCE BASE, OHIO 45433

This technical report has been reviewed and is approved for publication.
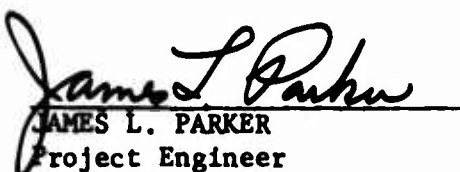
JAMES L. PARKER
Project Engineer

R. L. HAAS
Chief
Vehicle Synthesis Branch

FOR THE COMMANDER

ROBERT D. MCKELVEY, Col USAF
Chief, Aeromechanics Division

| REPORT DOCUMENTATION PAGE | READ INSTRUCTIONS BEFORE COMPLETING FORM |
|---|---|

| 1. REPORT NUMBER | 2. GOVT ACCESSION NO. | 3. RECIPIENT'S CATALOG NUMBER |
|---|---|---|
| AFFDL-TR-76-76 | | |

| 4. TITLE (and Subtitle) | 5. TYPE OF REPORT & PERIOD COVERED |
|---|---|
| LIGHT EXPERIMENTAL SUPERCRUISE CONCEPTUAL DESIGN | Final Report, June 1975-March 1976 |
| | 6. PERFORMING ORG. REPORT NUMBER |
| | D180-19115-5 |

| 7. AUTHOR(s) | 8. CONTRACT OR GRANT NUMBER(s) |
|---|---|
| B. D. Nelson, W. D. Middleton, N. Baullinger, P. Osterbeck L. Alberts | F33615-75-C-3150 |

| 9. PERFORMING ORGANIZATION NAME AND ADDRESS | 10. PROGRAM ELEMENT, PROJECT, TASK AREA & WORK UNIT NUMBERS |
|---|---|
| Boeing Military Airplane Development Boeing Aerospace Company Seattle, Washington 98124 | 12070118 |

| 11. CONTROLLING OFFICE NAME AND ADDRESS | 12. REPORT DATE |
|---|---|
| Air Force Flight Dynamics Laboratory AFFDL/FXB Wright-Patterson Air Force Base Dayton, Ohio 45433 | July 1976 |
| | 13. NUMBER OF PAGES |
| | 319 |

| 14. MONITORING AGENCY NAME & ADDRESS(if different from Controlling Office) | 15. SECURITY CLASS. (of this report) |
|---|---|
| Same | Unclassified |
| | 15a. DECLASSIFICATION/DOWNGRADING SCHEDULE |

16. DISTRIBUTION STATEMENT (of this Report)

Distribution limited to U.S. Government Agencies only; Test and Evaluation (April 1976). Other requests for this document must be referred to Air Force Flight Dynamics Laboratory (AFFDL/FXB), Wright-Patterson Air Force Base, Ohio 45433.

17. DISTRIBUTION STATEMENT (of the abstract entered in Block 20, if different from Report)

18. SUPPLEMENTARY NOTES

19. KEY WORDS (Continue on reverse side if necessary and identify by block number)

LES Concept Technology Assessment, Arrow Configuration, Canard Configuration, Supercruise Aerodynamics, Combat Persistence, Mission Performance, Low Profile Cockpit, Composite Structures, Flight Controls, Subsystems, J101/J7 Study A9 Engine Installation, Vehicle Parametric Trades, Armament, Wind Tunnel Test Requirements, Analysis/Evaluation Procedures, Prototype Costs.

20. ABSTRACT (Continue on reverse side if necessary and identify by block number)

A conceptual design study has been completed to investigate the application of advanced technologies in a low cost experimental fighter that could double the cruise speed of current and emerging fighters. Conceptual design studies were conducted with USAF/AFFDL sponsorship under Contract F33615-75-C-3150. Wind tunnel tests were conducted under a Boeing independent research program to verify performance results.

The Light Experimental Supercruiser concept employs six major technologies.

DD FORM 1473 EDITION OF 1 NOV 65 IS OBSOLETE
1 JAN 73

a modified existing engine. Technologies are: 1) Advanced supersonic aerodynamics, 2) Low Profile cockpit, 3) Damage tolerant composite structure, 4) Digital fiber-optic flight controls, and 5) Two-Dimensional Airframe Integrated Exhaust System. The air vehicle design is based on NASA SCAT 15 arrow wing research and is powered by a modified General Electric J101 engine.

2) Variable Camber Wing Geometry

# TABLE OF CONTENTS

## LIST OF ILLUSTRATIONS

### SECTION 2.0

## LIST OF ILLUSTRATIONS
### SECTION 3.0 (Continued)

# LIST OF ILLUSTRATIONS

## SECTION 3.0 (Continued)

## SECTION 4.0

# LIST OF ILLUSTRATIONS
## SECTION 4.0 (Continued)

## SECTION 5.0

# LIST OF ILLUSTRATIONS

## SECTION 5.0 (Continued)

## LIST OF ILLUSTRATIONS

### APPENDIX A

### APPENDIX B

# LIST OF ILLUSTRATIONS (Continued)

# LIST OF TABLES

## LIST OF SYMBOLS AND ABBREVIATIONS

| | | |
|---|---|---|
| a.c. | - | Aerodynamic center |
| AIN | - | Airframe Integrated Nozzle |
| b | - | Projected wing span |
| $\bar{C}$ or MAC | - | Mean aerodynamic chord or reference wing chord |
| $C_D$ | - | Drag Coefficient |
| c.g. | - | Center of gravity |
| $C_L$ | - | Lift coefficient |
| $C_{L_{\alpha=0}}$ | - | Lift coefficient at zero angle of attack |
| $C_{L_{\delta e}}$ | - | Elevator lift effectiveness coefficient (1/rad) |
| $C_\ell$ | - | Rolling moment coefficient about x-axis |
| $C_m$ | - | Pitching moment coefficient about center of gravity |
| $C_n$ | - | Yawing moment coefficient |
| $C_{n_\beta}$ | - | Change in yawing moment coefficient with variation in side slip angle, total airplane, (1/rad) |
| $C_{n_{\beta VT}}$ | - | $C_{n_\beta}$ due to vertical tail only (1/rad) |
| $C_{n_{\delta R}}$ | - | Rudder yawing moment effectiveness coefficient (1/rad) |
| $C_p$ | - | Pressure coefficient ($\Delta P/q$) |
| $C_Y$ | - | Side force coefficient |
| D | - | Drag (lbs) |
| $F_n$ | - | Installed thrust (lbs) |
| g | - | Acceleration of gravity (ft/sec$^2$) or maneuver load factor |
| $h_p$ | - | Pressure altitude (feet) |
| $I_X$ | - | Moment of inertia about x-axis (slug, ft$^2$) |
| KEAS | - | Knots, equivalent airspeed |
| L | - | Lift or length |
| LES | - | Light Experimental Supercruiser |
| LWF | - | Light Weight Fighter |
| M | - | Mach number |
| $M_{cr}$ | - | Cruise Mach number |
| N, n | - | Structural design load factor |
| p | - | Static pressure |
| $P_S$ | - | Specific excess power |
| q | - | Dynamic pressure (lb/ft$^2$) |
| R | - | Airplane range or combat radius (N.MI.) |

LIST OF SYMBOLS AND ABBREVIATIONS (Continued)

RAD, rad - Radians

S          - Reference wing area ($ft^2$)

$S_e$      - Elevator surface area ($ft^2$)

t/c        - Wing thickness to chord ratio

TOGW       - Takeoff gross weight (lbs)

V          - Velocity (feet per second or knots)

W          - Airplane weight (lbs)

$\frac{W}{S}$  - Wing loading (lbs per $ft^2$)

WBL        - Wing Buttock Line (inches from centerline)

$X_{c.g.}$ - Longitudinal location of c.g. in percent of reference chord

$X_{a.c.}$ - Longitudinal location of aerodynamic center in percent of reference wing chord

$\alpha$   - Angle of attack (degrees)

$\beta$    - Side slip angle

$\delta_e$ - Elevator deflection, trailing edge down=pos (degrees)

$\dot{\theta}$ - Turn rate (degrees/second)

$\ddot{\theta}$ - Angular acceleration in pitch about c.g. ($rad/sec^2$)

$\Gamma_R$ - First order roll mode time constant (sec.)

$\emptyset$ - Bank angle (degrees)

$\omega_{nd}$ - Undamped natural frequency of the Dutch Roll oscillation (rad/sec)

# 1.0 INTRODUCTION

Past studies have shown the desirability of penetration of hostile territory at supersonic speeds to enhance aircraft survivability against enemy defenses (Reference 1). Studies have also been done to evaluate the technologies which contribute to this capability. A study conducted by the Air Force Flight Dynamics Laboratory (Reference 2) identified composite structure, supersonic wave drag and propulsion-airframe integration to be the important technologies for supersonic penetrator aircraft. In subsequent studies (References 3 and 4) engines, avionics, and weapons were also identified as technology areas requiring advancement.

The purpose of the present study was to define a fighter aircraft demonstration which incorporates the airframe technologies that allow the combination of air superiority fighter performance with an efficient supersonic cruise capability. A useful load and a derivative of an existing engine were assumed in achieving an aircraft design of minimum size. A demanding air superiority mission was defined as a design goal. The concept selected as a result of this study is intended to be the smallest and lowest cost aircraft which could demonstrate the combination of technologies that have been assessed to be relevant to a supersonic cruise fighter aircraft.

The possibility of attaining the three major objectives has motivated this design effort:

1. Design of an air vehicle that could double the cruise speed over existing fighters and carry a useful payload.

2. Maneuverability equal to emerging air combat fighters so that the combat arena could be enlarged to include supersonic as well as transonic speeds.

1

## 1.0 INTRODUCTION (Continued)

3. Employment of advanced technologies to reduce fighter size (reflecting reductions in signature, cost, fuel efficiency, storage, etc.) and use of an existing engine requiring a minimum development effort.

New technologies employed in LES include 1) advanced supersonic aerodynamics, 2) variable camber wing geometry, 3) low profile cockpit, 4) damage tolerant composite structures, 5) digital fiber-optic flight controls and 6' two-dimensional airframe integrated exhaust system.

This study has identified many uncertainties associated with the application of these advanced technologies. Although development programs are needed to alleviate these uncertainties, an experimental airplane program could focus these efforts towards a common objective.

This study represents the results of four months of conceptual level design work. It is intended to be used solely for purposes of definition of an aircraft program required to achieve the goals as defined. It is not intended to be a final design but rather a tool to help evaluate the option of fabrication and flight test of a demonstrator aircraft for supersonic cruise fighter technologies.

The engineering effort was conducted at Seattle, Washington, under the direction of R. Hardy, Chief of Aerodynamics and Propulsion Technology, Research and Engineering Division, Boeing Aerospace Company. Design Study Manager was B. D. Nelson and principal engineers were W.D. Middleton and N. Baullinger (Aerodynamic Design); P. Osterbeck (Parametric Studies and Performance).

Major contributions were made by the following engineering specialists:

2

## 1.0 INTRODUCTION (Continued)

| | | |
|---|---|---|
| L. Alberts | - | Propulsion Performance |
| W. 3rennan | - | Flight Systems |
| S. Butchart | - | Air Vehicle Configuration |
| A. Grisham | - | Stress Analysis - ISAS |
| M. McKinney | - | Structures Design |
| D. Neilson | - | Loads & Stress |
| R. Rankin | - | Mass Properties |
| D. Redmond | - | Air Vehicle Configuration |
| W. Sander | - | Cockpit Design |
| B. Sutherland | - | Energy Maneuver |
| B. Tricoli | - | Propulsion Installation |
| F. Watts | - | Life Cycle Costs |
| 0. Foard | - | Prototype Costs |
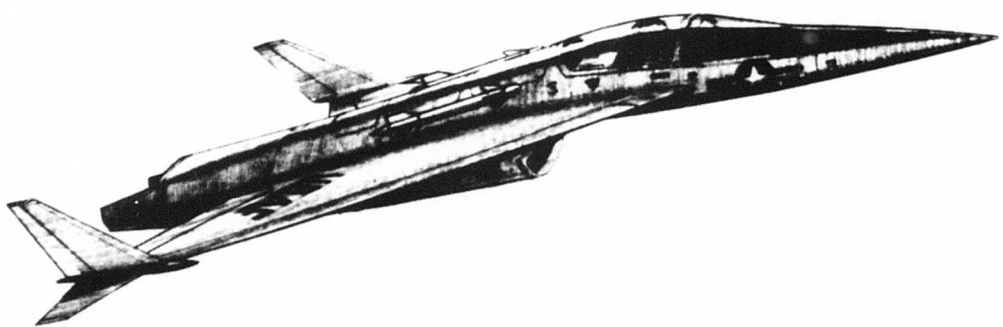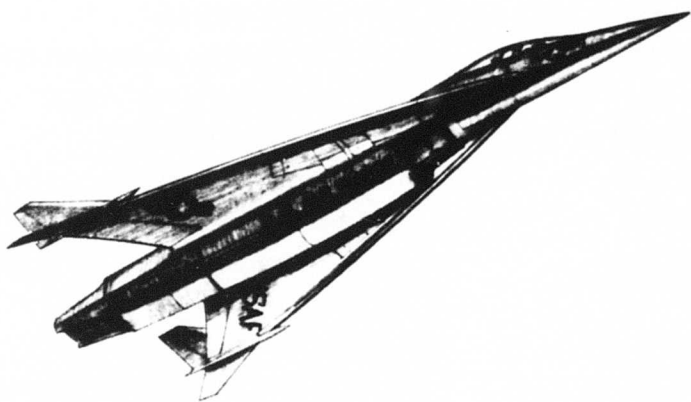
Figure 1.    Light Experimental Supercruiser — Model 985-213

4

## 2.0   SUMMARY

A Light Experimental Supercruiser (LES) air vehicle concept has been de-
fined to show the performance potential of a low cost demonstration of
advanced technologies with direct application to Advanced Tactical
Fighters.  The design concept selected from the parametric analysis for
refinement is the Boeing Model 985-213 shown in Figure 1.

This vehicle is designed to cruise at supersonic speeds using non-after-
burning (dry) thrust and demonstrate Light Weight Fighter combat capa-
bility.  The aircraft was configured so that the internal and external
aerodynamics provide low drag at the design Mach number of 1.8.  Com-
bat capability comparable to emerging air superiority fighters was
achieved through a wing loading of 50 psf and a thrust loading of 1.32.
The design gross weight of the aircraft was 12,500 lbs with a useful
load of 4330 lbs.

The cost of a two-aircraft, experimental prototype program was estimated
to be 83 million dollars.  The airframe and flight test costs were $46
million.  The total program cost includes the development of all of the
subsystem advanced technologies discussed below.  Details are given in
section 3.11.

Six areas of technology have been incorporated to achieve the LES con-
cept.  These technologies along with their benefits are:
  o  Supersonic Aerodynamics - Efficient supersonic cruise (supercruise)
     with combat persistence and high sustained load factors
  o  Variable Camber Wing Geometry - Transonic maneuver
  o  Low-Profile Cockpit - Supercruise, high maneuver, stealth
  o  Damage-Tolerant Composite Structure - Fuel weight fraction,
     survivability airplane size, stealth, cost
  o  Digital Fiber-optic Flight Control System - Supercruise high
     maneuverability
  o  Two-Dimensional Airframe Integrated Exhaust System - Combat
     agility, control augmentation, landing field length reduction.

19.7 FEET

15°

30°

9.3 FEET

44 FEET
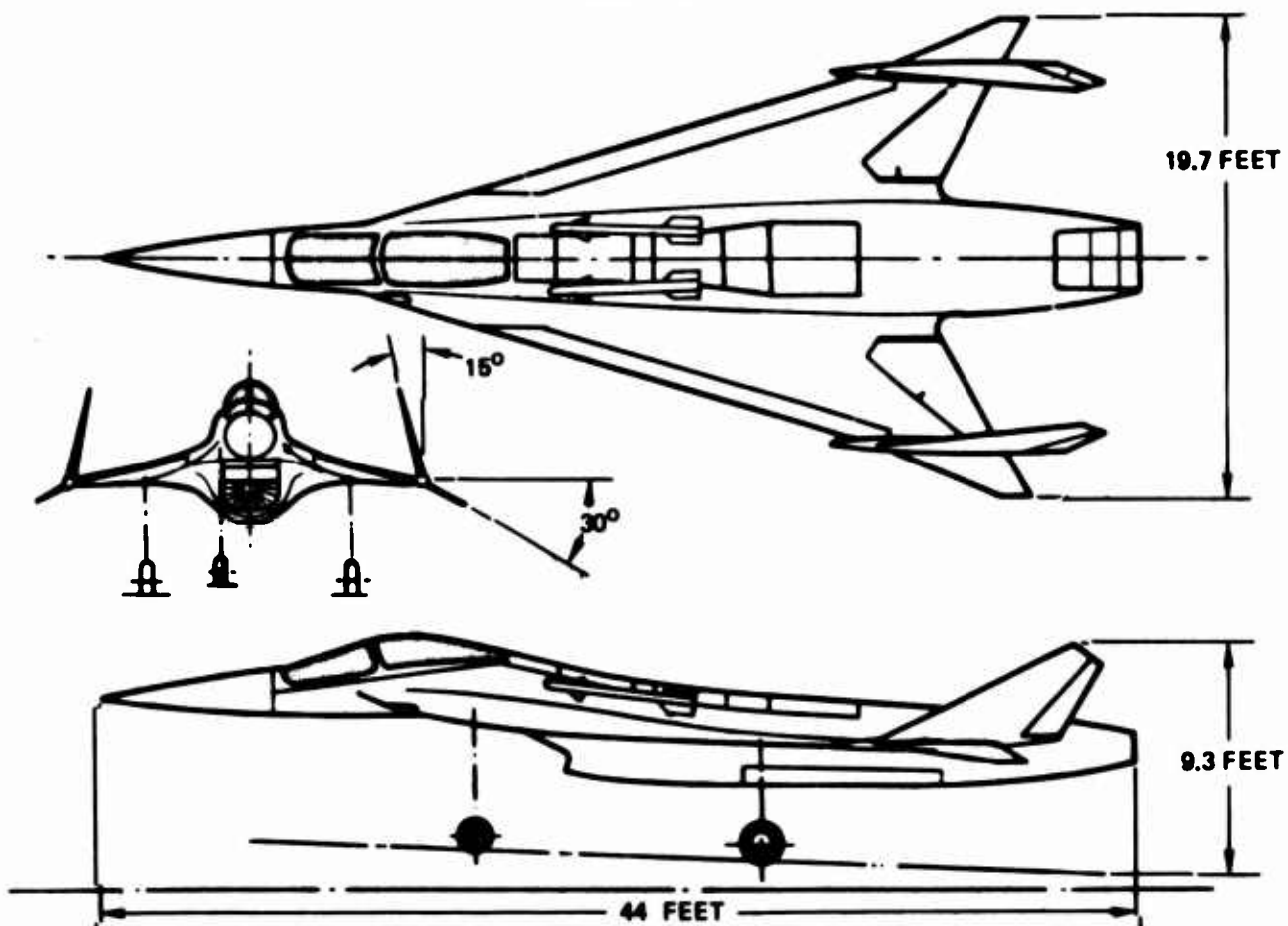
POINT DESIGN WEIGHTS
- DESIGN MISSION          12,500 POUNDS
- OVERLOAD MISSION        16,780 POUNDS
- OPERATING WEIGHT        8,530
- FULL INTERNAL FUEL      3,830
- WEIGHT EMPTY            7,910
- PAYLOAD – DESIGN MISSION   340
- PAYLOAD – A/G MISSION      4,000
- AVIONICS – DAY A/A         380

PERFORMANCE OBJECTIVES
CRUISE – M = 1.8 @ 50K
PERSISTENCE @ M = 0.9/30K    4 TURNS
                M = 2.0/40K    3 TURNS
MAX S.L. M = 1.2
MAX 50K M = 2.2
LANDING SPEED = 130 KTS

PROPULSION
- ENGINE – (1) GE J101/J7A9
- INLET – 3 SHOCK VAR-RAMP
- NOZZLE – BOEING 2D-AIN

MANEUVER DEVICES
- LEADING EDGE – VARI-CAMBER
- TRIM – NEUTRAL STABILITY
- CONTROL – ELEVONS & THRUST VECTORING
- DRAG MODULATION – AIN REVERSER
- LIFT – LOW W/S + VAR-CAMBER

FEATURES
- LO-PROFILE/HIGH ACCELERATION COCKPIT
- DAMAGE TOLERANT COMPOSITE STRUCTURE
- AIRFRAME INTEGRATED NOZZLE – 2D
- SUPERSONIC CRUISE/DRY THRUST
- DIGITAL FBW FLIGHT CONTROLS
- LOW WAVE DRAG AERODYNAMICS
- INTEGRATED DRAG MODULATION

GEOMETRY

| | WING | VERT |
|---|---|---|
| - WING AREA | 266 | 38 |
| - L.E. SWEEP | 74 | 52 |
| - ASPECT RATIO | 1.46 | 0.88 |
| - TAPER RATIO | 0.19 | 0.32 |
| - THICKNESS RATIO | 0.04 – 0.03 | 0.048 – 0.03 |
| - MAC, INCHES | 227 | |

WETTED AREA & FINENESS RATIO
- BODY FINENESS RATIO (NET)    14.2
- OVERALL FINENESS RATIO l/√A_MAX    11.2
- WETTED AREA    785 FEET²
- b²/SWET    0.48

ARMAMENT
CANNON – XM197 - 3 BBL - 20MM + 250 RDS AMMO
MISSILES (A/A) (-2) "CLAW"

Figure 2.   LES Three View – Model 985-213

6

## 2.0   SUMMARY (Continued)

This engineering study has emphasized the performance of the airplane and engine. Airframe and system design layout was carried to the point where internal arrangement verified adequate volume for equipment and fuel. Airframe and system analysis was concluded when equipment comple- ment and structural weights could project a viable air vehicle.

## 2.1   DESIGN GOALS

Supercruise, supersonic persistence, supersonic maneuver and transonic maneuver are combined in the design goals for LES. Combat capability like that of the Light Weight Fighter (LWF) are required and the fighter concept must be based on an existing engine design, the General Electric J101/J7 Study A9, a derivative of the J101-GE-100 engine. The specific goals were:

Supercruise - For this design study supercruise has been defined as effi- cient cruise (aerodynamic design defined at the supersonic cruise condi- tion) at speeds above $M = 1.6$ with intermediate (military) thrust.

Supersonic Persistence - The number of turns at Mach 2.0 and 40,000 feet with max augmented thrust and thrust equal drag ($P_S = 0$). At least three Mach 2.0 turns are desired at a combat radius of 200 N.Mi. Per- sistence is measured through the flight envelope.

Missions - The LES design mission is shown in Figure 3. A 200 N.Mi. radius with LWF combat was specified. This mission is intended to demon- strate capability of the LES concept. In addition two other mission capabilities were measured; a maximum supersonic radius mission and an overload mission also shown in Figure 3.

7

**DESIGN MISSION**

LWF COMBAT

M = 2.0

M = 1.2

CRUISE M = 1.8 @ 50K

M = 0.9

200 N.MI.

LWF COMBAT
4 TURNS (M0.9@30K)
3 TURNS (M1.2@30K)
ACCEL M0.9-1.6
EXPEND WEAPONS
340 LBS

CLIMB @ MIN TIME & FUEL

20 MIN
LOITER

**MAX SUPERSONIC RADIUS**

ALT

M = 1.8@50K

1 TURN
EXPEND
WEAPONS

CLIMB
MIN TIME & FUEL

XXX N.MI.

20 MIN
LOITER

MISSION RADIUS

**OVERLOAD SUPERSONIC RADIUS**

2 x 2,000 A/G WPNS

M = 1.8@50K

1 TURN
RELEASE
4,000 POUNDS

CLIMB
MIN TIME & FUEL

XXX N.MI.

MISSION RADIUS

*Figure 3.   LES — Mission Profiles*

8

## 2.1    DESIGN GOALS (Continued)

Flight Envelope - The desired and resulting flight envelopes for LES are
shown in Figure 4.  A cruise design point of Mach 1.8 was set as a goal
from studies that investigated M = 1.6 to 2.2.  Several limits can be
imposed on LES performance that may degrade overall capability.  These
are illustrated on Figure 5.  Available engine data limits performance
estimates to 60,000 feet altitude and Mach 2.0.  An additional altitude
limit may be imposed by continuous operation at high altitudes without
a pressure suit.  This limit, set at 50,000 feet, would require the LES
to cruise at non-optimum conditions.

The supersonic cruise speed also places a requirement for a high per-
formance ejection capability (600 KEAS).  Escape performance can be met
with a STENCIL SIIIS seat previously qualified but modified for 50° re-
clination in the LES low-profile cockpit.  In order to achieve the de-
sired flight limits, windmill start with full vehicle secondary power
extraction required emergency power system for lower speeds to pre-
serve flight control power and aid in engine air start.  Emergency power
is provided by a Ram Air Turbine and Jet Fuel Starter.

## 2.2    PERFORMANCE

Performance was calculated both with and without altitude restriction.
A summary of the results are shown on Table 1.  The penalties resulting
from limiting this particular aircraft to 50,000 feet altitude are ex-
treme.  A 50% loss in the combat persistance occurs if the aircraft is
not allowed to cruise at its optimum condition.  Careful consideration
should be given to allowing unrestricted cruise altitudes in certain
combat conditions.  The purpose of the high speed flight is to enhance
the survivability.  Aircraft designs of the LES type will possess good
maneuverability at high altitude and therefore should be more survivable.
Some increase in vulnerability would be experienced, however, which would
have to be traded off against the improved survivability.

9
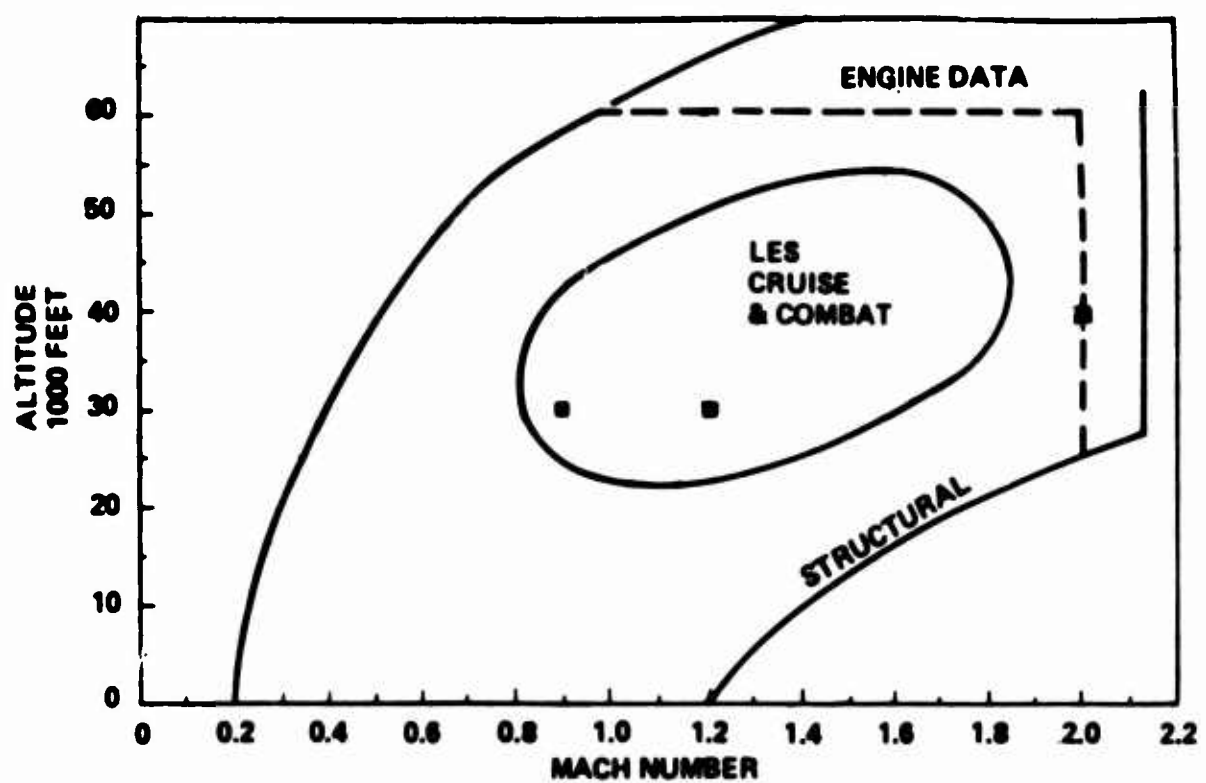
Figure 4.   LES — Flight Envelopes
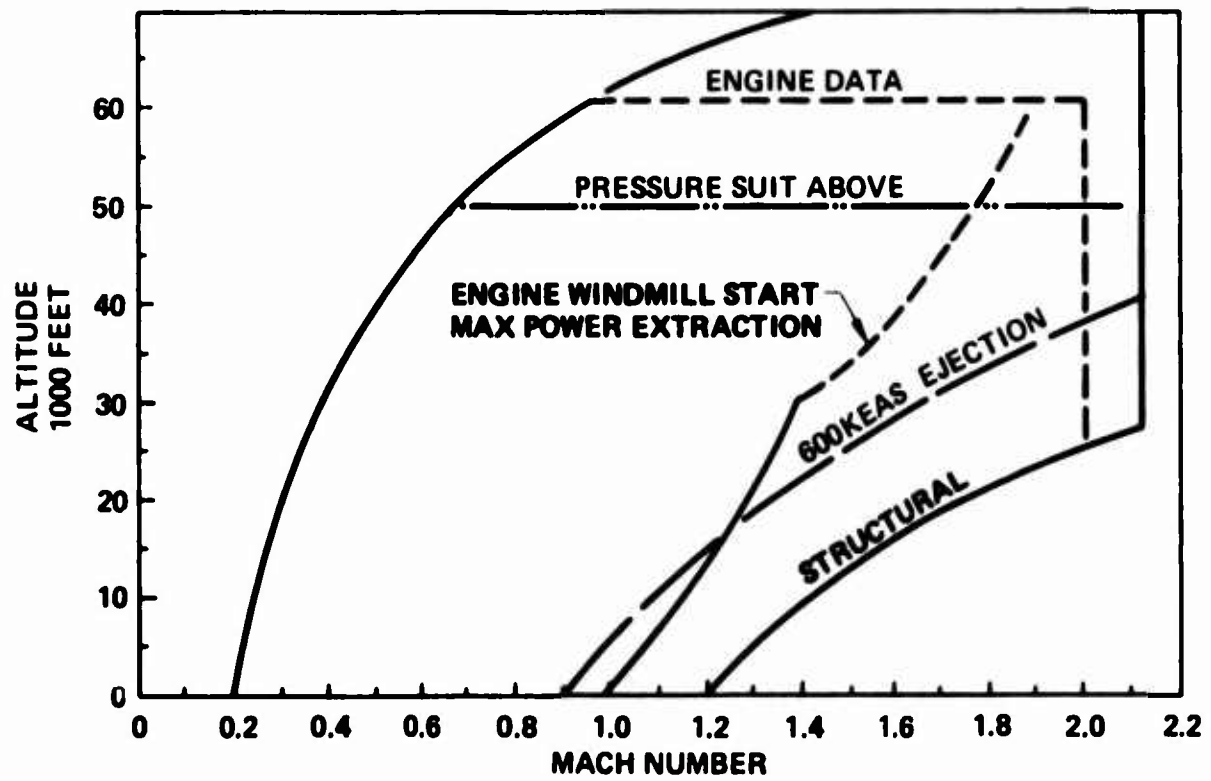


Figure 5.   LES — Flight Limits

## 2.2 PERFORMANCE (Continued)

*Table 1.   Performance Summary (985-213)*

| MISSION PERFORMANCE | M 1.8/50K Cruise | Optimum Cruise |
|---|---|---|
| Percent of Design Mission Combat at 200 n. mi. ▷ | 26 % | 61 % |
| Maximum Supersonic Radius | 255 n. mi. | 420 n. mi. |
| Overload Supersonic Radius | 210 n. mi. | 275 n. mi. |

| COMBAT PERFORMANCE | 0.9M/30K | 1.2M/30K | 2.0M/40K |
|---|---|---|---|
| Number of Turns at 200 n.mi. | | | |
| M 1.8/50K Cruise | 2.7 | 1.7 | 1.0 |
| Optimum Cruise | 6.3 | 4.1 | 2.3 |
| Maximum Sustained Load Factor | 4.9 | 5.5 | 5.8 |
| Maximum Turn Rate Degrees/Sec. | 9.8 | 8.3 | 5.4 |

▷4 turns at 0.9M/30K + 3 turns at 1.2M/30K + accel fuel (0.9M→1.6M).

As assessed, the model 985-213 was unable to achieve the DESIGN MISSION objective as shown in Figure 6 regardless of restrictions in cruise conditions.   Restricting the cruise altitude to 50,000 feet as a pressure suit limit, 26 percent of the LWF combat maneuver is shown in Figure 6 at the 200 n. mi. radius with cruise at Mach 1.8.   Because the cruise L/D is significantly improved with altitude, 50 percent of the design combat capability is estimated at 60,000 feet.   The best cruise speed on dry thrust is estimated to be Mach 1.60.   With this and an optimum cruise climb flight profile, the LES -213 could attain 61 percent of LWF combat turn performance.   Further wing tailoring will be required to improve the performance at lower altitudes.   The cruise drag polar providing the above performance is depicted in Figure 7.

## 2.2 PERFORMANCE (Continued)

A deficiency in performance level is attributed to an insufficient margin in non-afterburning thrust minus drag of the assessed airplane. Figure 8 indicates that at 55,000 feet and average cruise conditions, a Mach number capability of 1.65 exists using dry thrust. To compensate for the increment in thrust required at 1.8 Mach, an interpolation between intermediate thrust and minimum augmentation was employed. This approach was used only as an interim solution as drag reduction potential and possible dry thrust improvements must be more carefully investigated. Reasonable progress in these areas is anticipated.

The relative importance of technology application and evaluation accuracy on mission radius is depicted by the sensitivity information in Figure 9. Significant losses or improvements in performance can result from relatively small perturbations in weight, drag and engine performance.
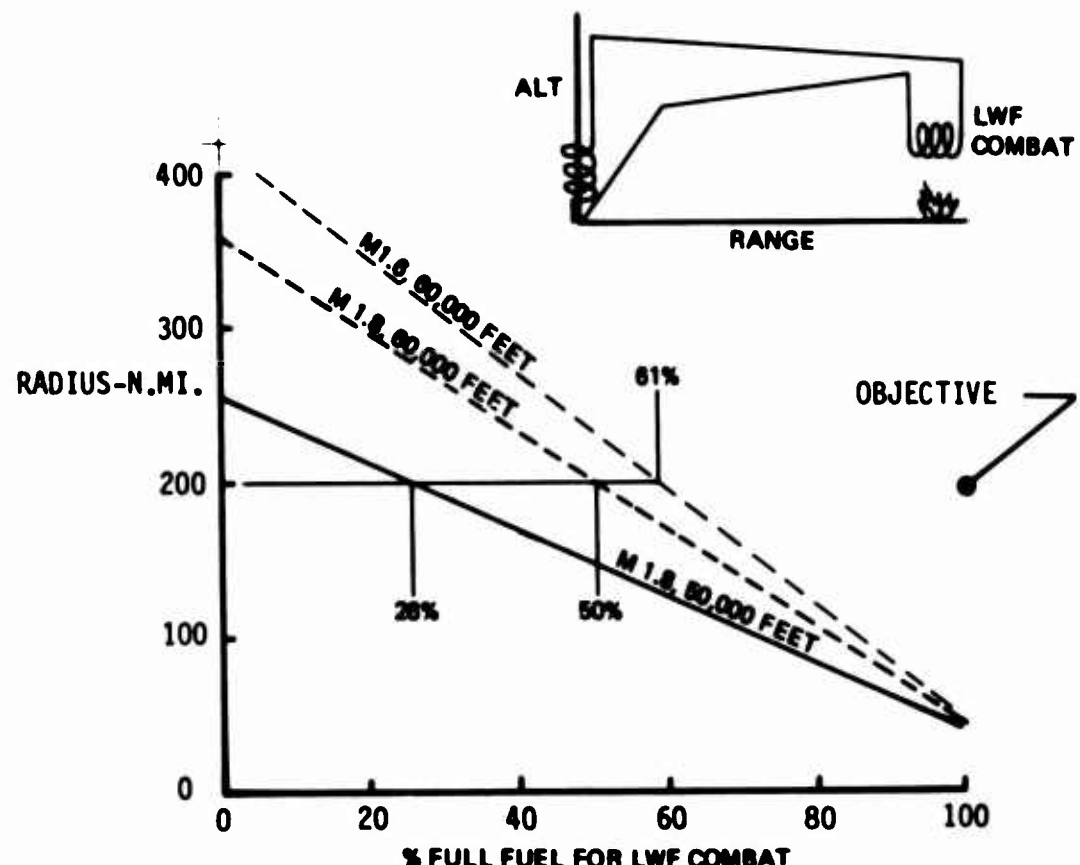
Figure 6. Design Mission Performance
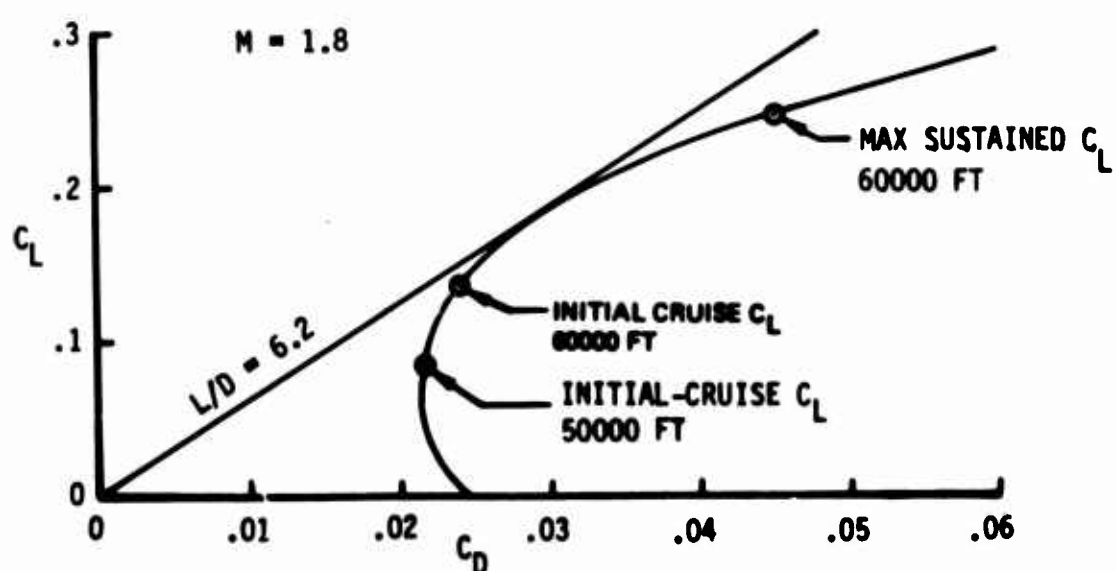


Figure 7. Aerodynamic Efficiency for Design Mission

13
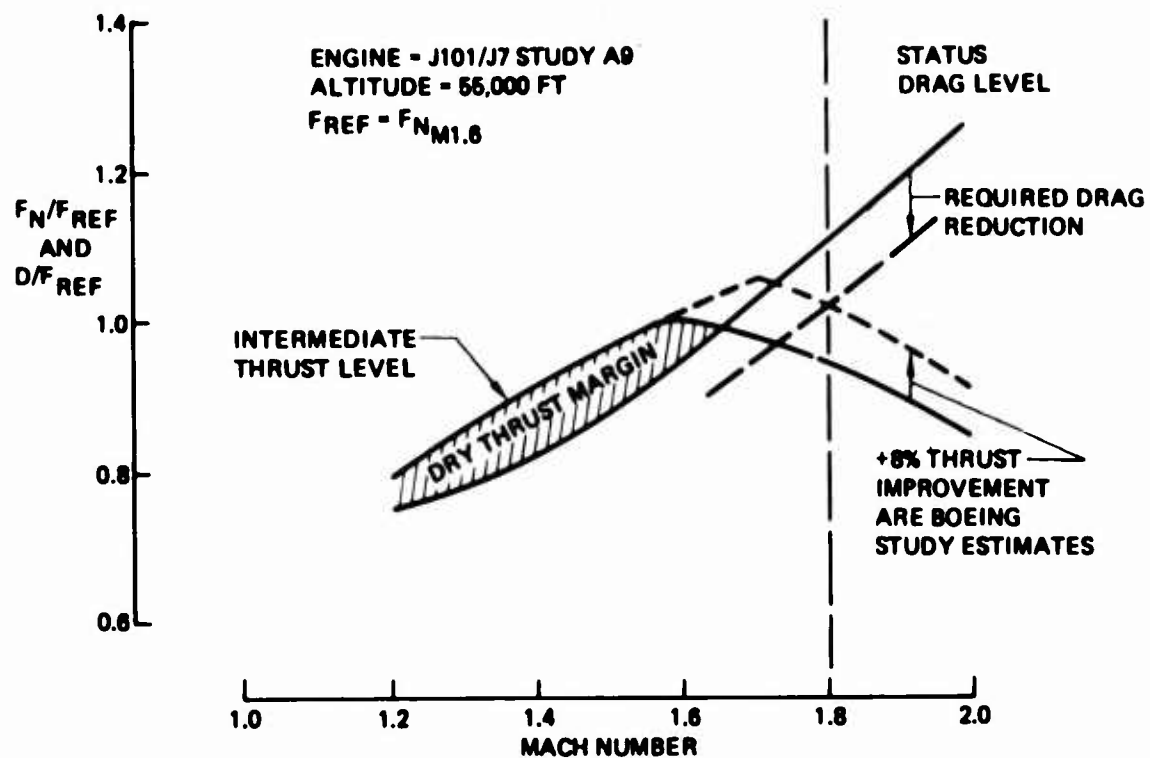
Figure 8. Thrust/Drag Matching
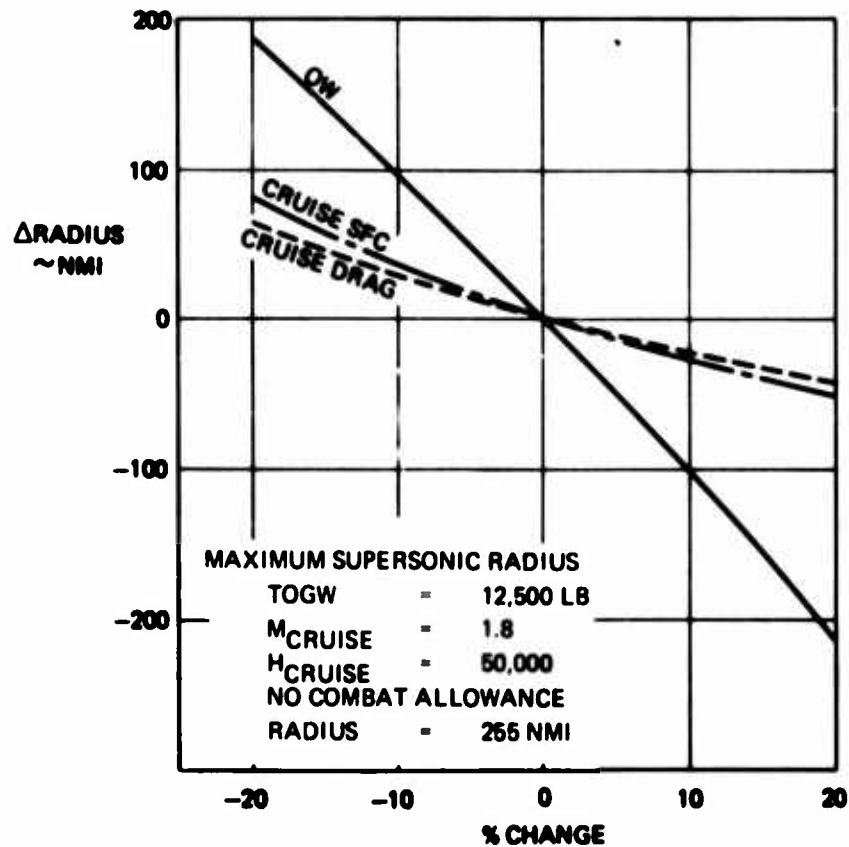


Figure 9. LES Sensitivity to Technology Variations

14

## 2.3  TECHNOLOGY ASSESSMENT

Several previous studies (Reference 1 - 4) have assessed the technologies which are relevant to aircraft that require a combination of supersonic cruise efficiency and fighter combat performance.  The benefits of such technologies have been assessed for their contribution to improvements in the mission capabilities of deep strike fighter aircraft. The present study explores the feasibility of combining the airframe related technologies in a minimum cost demonstration aircraft.  An existing engine derivative is employed in this aircraft design study to, avoid the time and expenses associated with the development of a new engine.

The design features of LES-213 have evolved with this goal and the constraint of a fixed engine cycle.  If the engine characteristics are improved to provide increased dry thrust then future improvements can be traded between higher cruise speed and better fighter characteristics. Figure 8 focuses on the primary technical risk.  Here the current estimates of engine and airplane performance results in only a 5 percent dry thrust margin for cruise across the Mach range.  However, dry thrust improvements up to 8 percent, may be possible for a short-life experimental engine.  Also an examination of the drag elements suggests drag reduction may be achieved through further refinement of the airplane general arrangement.  These improvements may make Mach 1.8 supercruise capability an achievable goal.

The design approach and compromises necessary to achieve this cruise performance are discussed in this section along with specific areas of program risk and technology applications.

### 2.3.1 AERODYNAMICS

This section briefly describes the results of the cruise drag analysis, the possible improvements, and the recommended studies considered necessary to assure a viable supercruise configuration from an Aerodynamic standpoint.

## 2.3.1 AERODYNAMICS (Continued)

In order to achieve the low supersonic drag level necessary for efficient cruise, the technology from the NASA advanced supersonic transport (AST) program has been applied to the design of fighter aircraft. Although the maximum cruise speed of this airplane is slower than that contemplated for the AST, the SCAT 15 wing with increased camber was applied for this initial iteration to take advantage of the large data base which exists for that planform. High angle of attack operation consistent with fighter requirements, surfaces unique theoretical versus experimental deficiences in the analysis of highly swept wings. Free vorted calculation method development along with wind tunnel data correlation is necessary to enhance the aerodynamic design guidance in this area. A wind tunnel test program to provide missing design data is described in Section 5.6.

Supersonic cruise efficiency of this airplane is comprised by the relatively low wing loading dictated by transonic maneuver require-ments and approach speeds. Alternate means of improving lift and drag characteristics at high angles of attack could therefore provide signi-ficant advantages in overall design efficiency. Improved variable camber devices, planform modifications, vectored thrust and wing con-tour refinement resulting from the above mentioned improved aerodynamics analysis methods offer this potential.

Supersonic design and assessment of the -213 for this study was accomplished in the manner described in Section 3.4. The wing/body contours were optimized for a 1.8M cruise condition at $C_L = 0.1$. Figure 10 summarizes the cruise lift to drag ratio with Mach number. A value of 6.2 at 1.8 Mach represents a 50 percent improvement over comparable configurations designed for subsonic cruise but with supersonic capability. As a consequence, a transonic penalty is accepted. To minimize this penalty during subsonic maneuver operations at high lift coefficients, a variable camber leading edge concept was assumed.
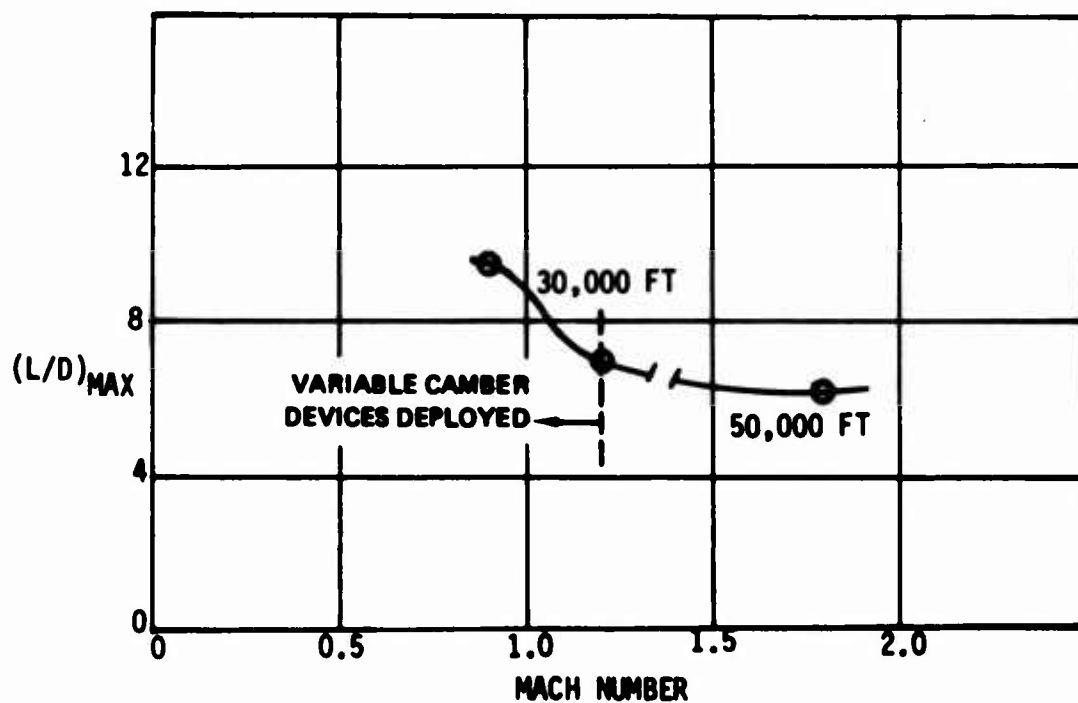


Figure 10. LES-213 Aerodynamic Cruise Efficiency

2.3.1 AERODYNAMICS (Continued)

While it is anticipated that further potential can be achieved through wing and wing-body contour changes, these characteristics served as the basis for the performance discussed in Sections 2.2 and 3.10.

Component identification of the total zero-lift drag is presented in Figure 11. Skin friction is the predominate term at Mach = 0.9. Supersonic drag on the other hand is comprised of four major components; skin friction, wave drag, camber and trim drag and the drag of miscellaneous components. Detail design and analysis may lead to potential zero lift drag reductions. For example, Figure 12 indicates miscellaneous components, camber, trim and wing refinements may offer this potential.

The wind tunnel model shown in Figure 13 was built and tested to aid in aerodynamic estimating methodology applied to this study contract. Application of the results of these subsonic, transonic and supersonic tests to this study was not possible as analysis work continues subsequent to the writing of this report.

Overall, this initial work conducted on the LES concept appears quite promising. Supersonic configuration one-g design techniques developed for larger, slimmer supersonic transports were applied with reasonable success. Further iterations of the design and analysis process can lead to additional performance capabilities and a significant edge over opponent fighter aircraft of the future. Specific recommended follow-on aerodynamic studies are listed below and on Page 22:

- o    Refine wing design and wing-body contours
- o    Enrich Aerodynamics methodology with LES wind tunnel results
- o    Investigate potential reduction of miscellaneous drag items
- o    Improve assessment of aft-body wave drag for 2-D Airframe Integrated Nozzle
- o    Continue refinement of cockpit design
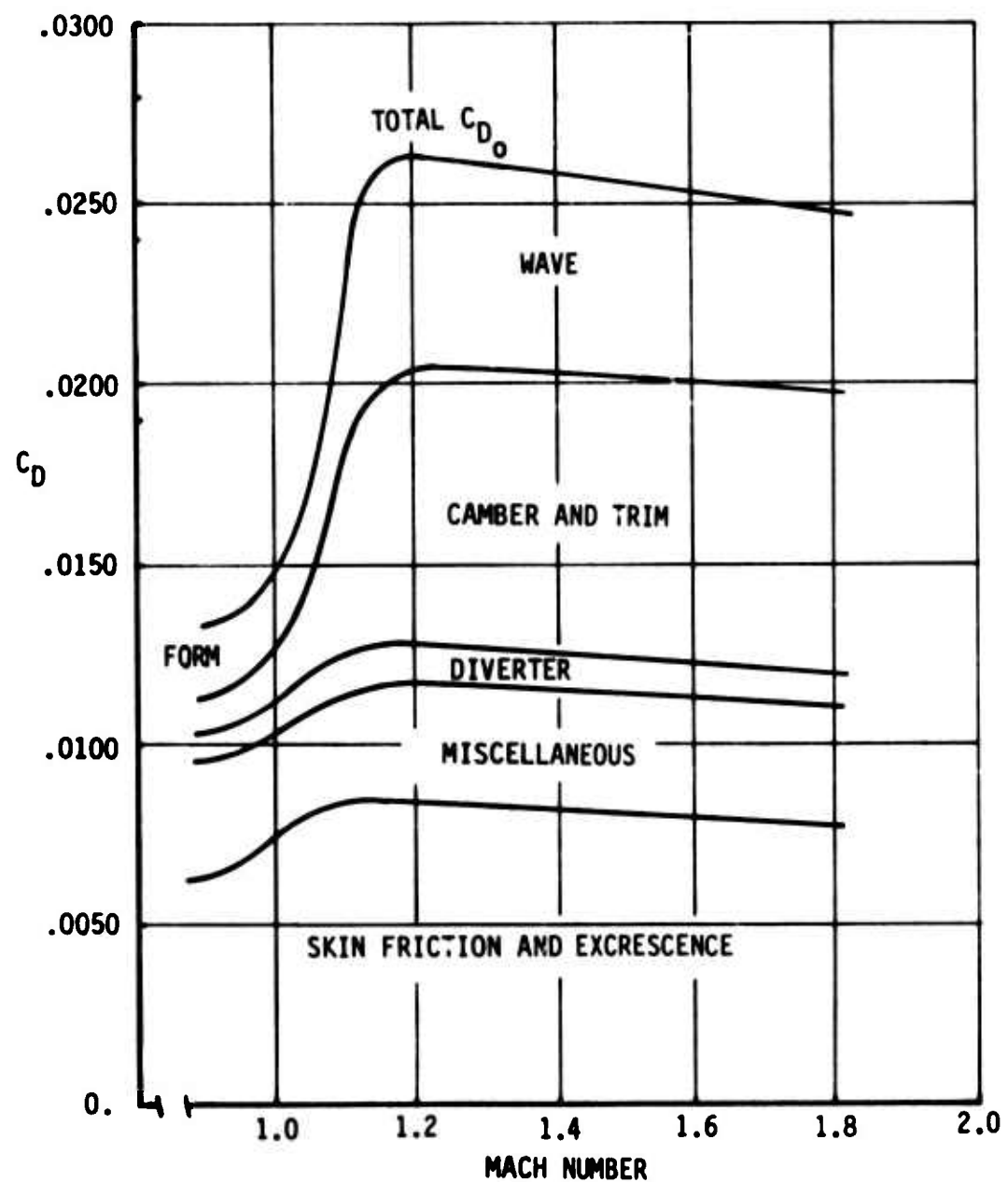
*Figure 11.* *Zero—Lift Drag Components*
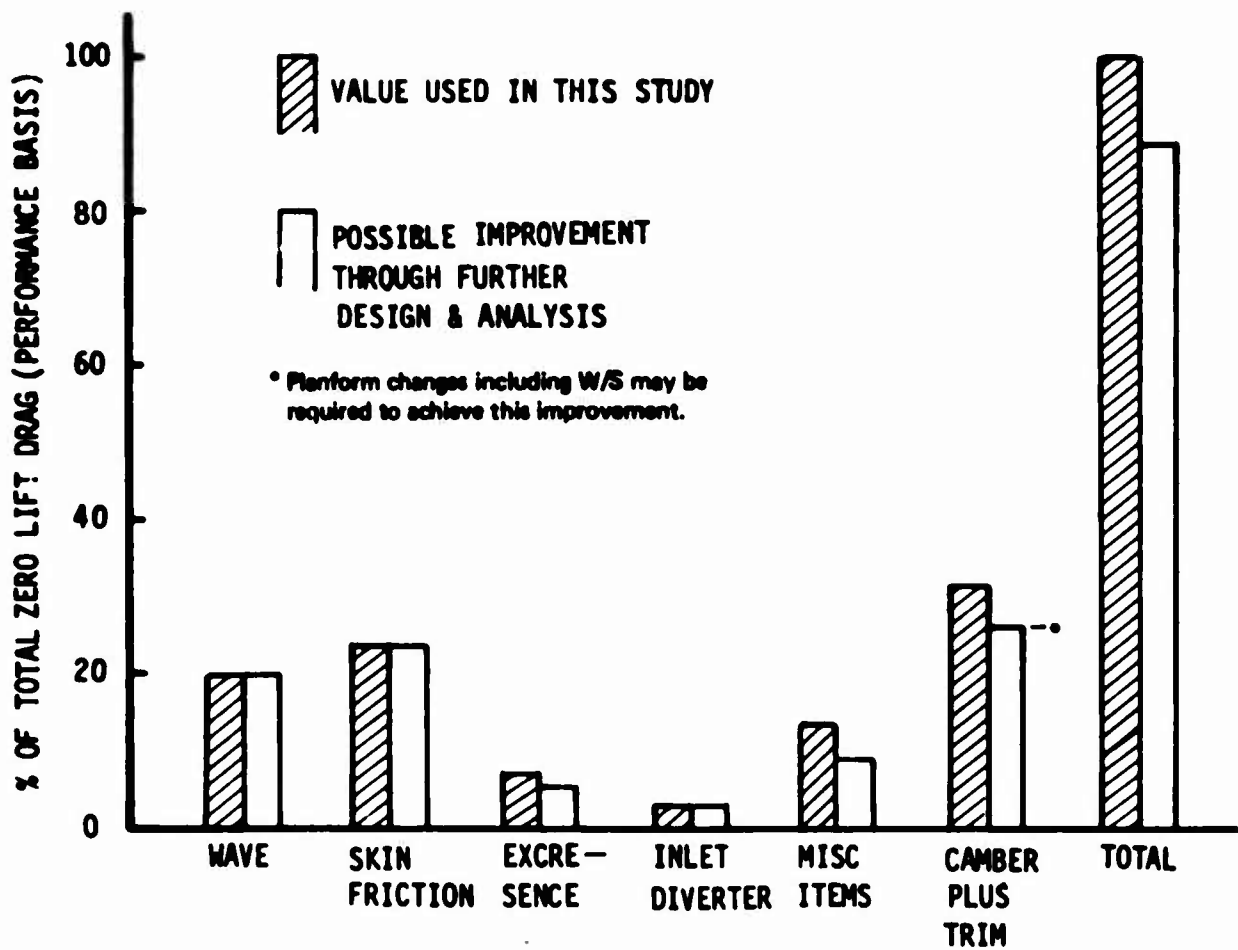
*Figure 12. Zero-Lift Drag Summary (Mach 1.8, 50,000 Feet)*

Figure 13.  LES Wind Tunnel Model Picture

21
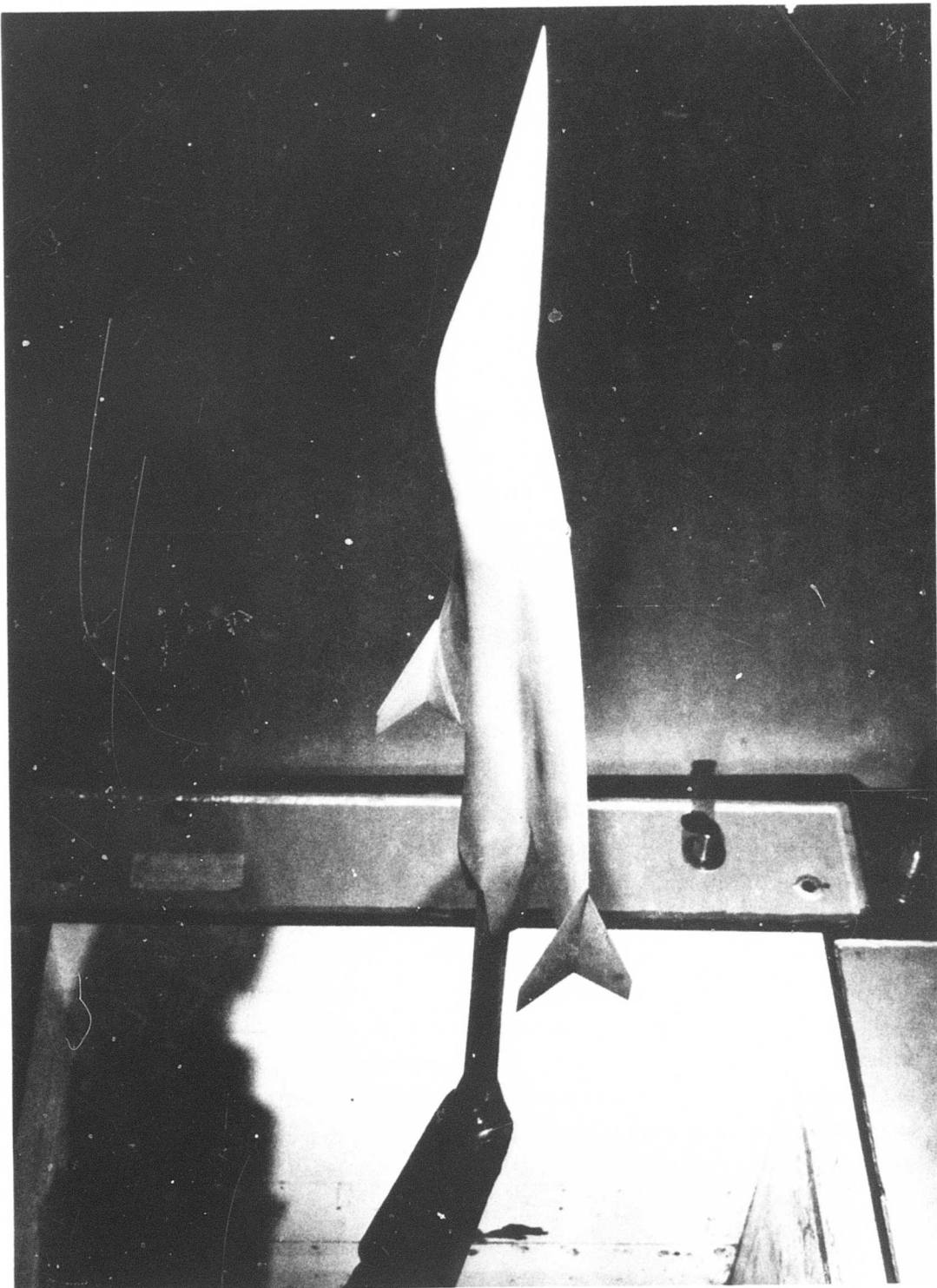
## 2.3.1 AERODYNAMICS (Continued)

      c     Investigate variable camber benefits in transonic regime

      o     Improve pitch and lateral control power.

## 2.3.2 COCKPIT DESIGN

The importance of forebody drag is shown in Figures 14 and 15. The effects are shown on body area distribution in the cockpit if enlarged to accommodate a standard pressure suit and provide more total "visibility out" to the pilot. The additional cross section would assure pilot protection at higher cruise altitudes (60,000 feet) with current USAF regulations. The effect on supersonic drag is shown two ways. At Mach 1.8 the 17 counts additional drag represent a 7% increase in total drag (Figure 15). Also shown is the influence of forebody change to body wave drag. Forebody drag increases from 60% to 71% of the total body. Employment of a cockpit for MIL-STD 850 vision and pressure suit would appear to eliminate any chance for supercruise if other drag levels are not reduced.

An intermediate design is possible which would provide MIL-STD-850 vision and without space for pressure suit. Cockpit development would then include pilot life support systems for operation at high altitude with damage tolerance. Development of the low profile cockpit should emphasize pilot human factors to provide good working environment and life support. Development should be centered on pilot workload with simulators and centrifuge testing. The seat selected for LES is a Stencel SIIIS modified for reclination of seat rails to 54%. This provides a seat back angle of 50°. Configuration rigging of the seat pan angle and head rest are changes required for this seat. High performance ejection (600 KTS) is predicted for this seat configuration by Stencel.

22
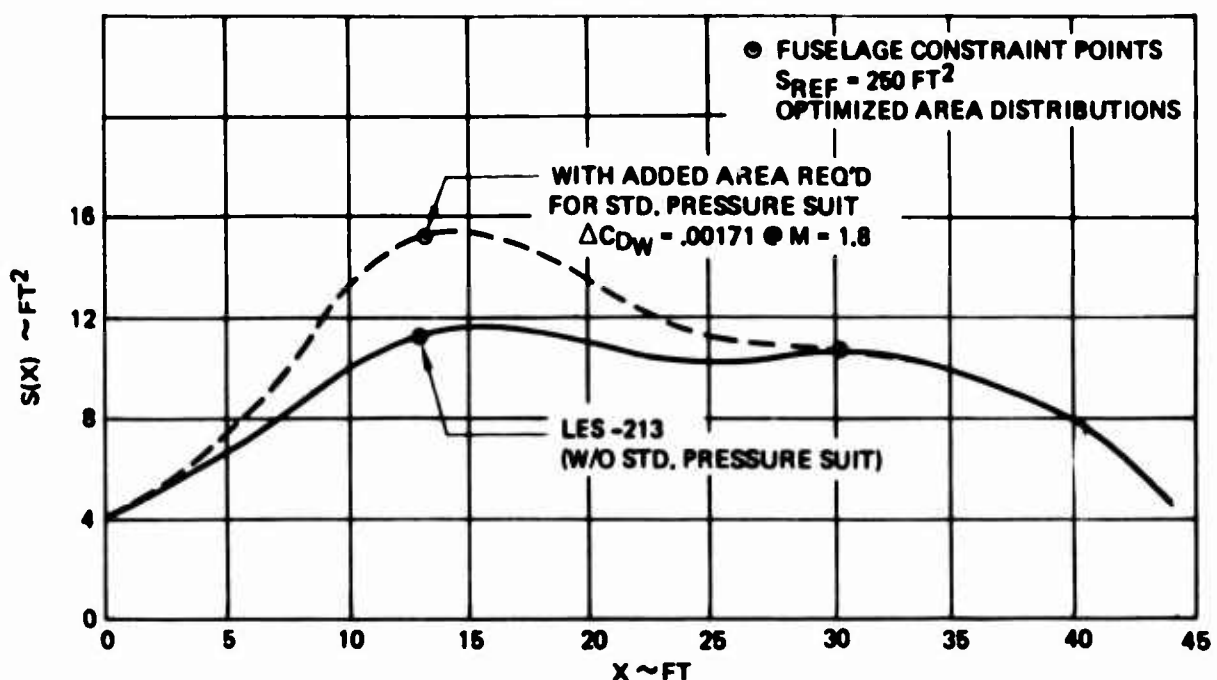
Figure 14.    Fuselage Area Change Due to Cockpit Modifications
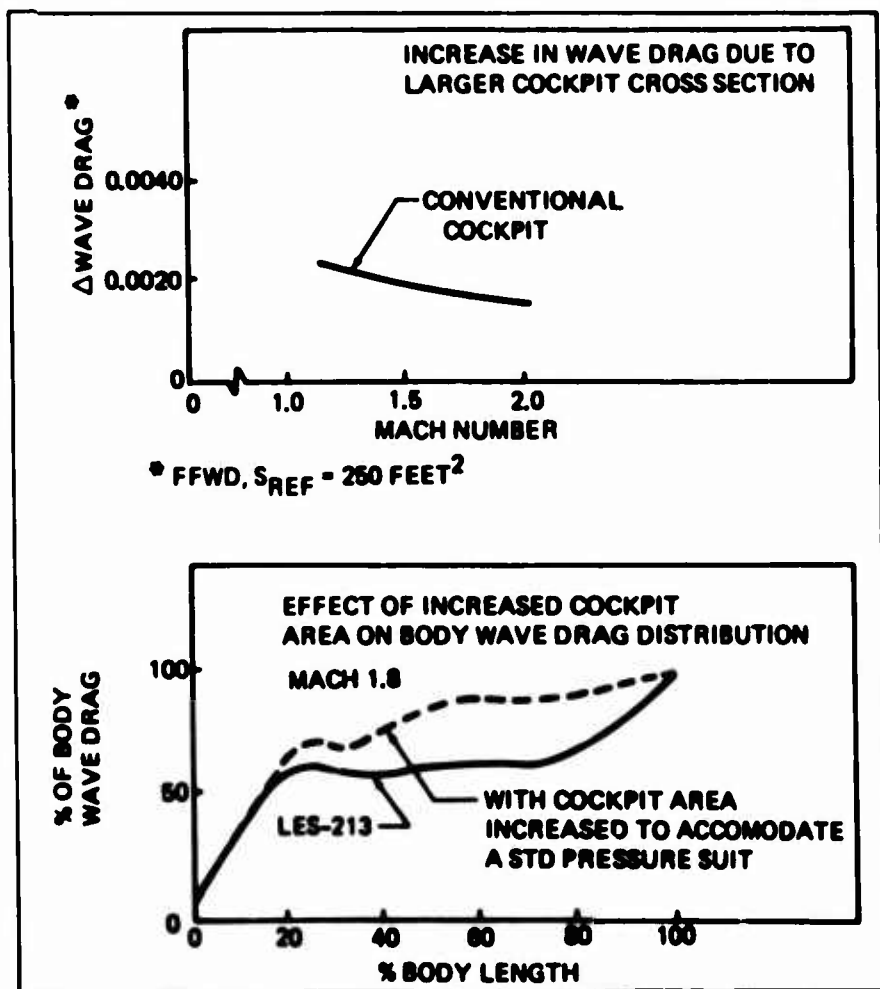


Figure 15.    Drag Produced by Standard Cockpit

## 2.3.2 COCKPIT DESIGN (Continued)

One critical feature of this cockpit design is the itegration of in-
strument panel with the canopy hatch and the side opening operation
for ingress and egress. Primary concern for this design is the ability
to predict canopy path during ejection. For this reason alternate cano-
py hatch designs should be evaluated during development of the LES low-
profile cockpit. One alternate design worthy of serious study is the
concept proposed by AFFDL whereby the canopy and panel hinge separately.
The canopy incorporates aft hinging while the panel and windshield
hinges at the forward end to provide a "q" shield during ejection. Both
canopy designs are shown in Figure 16.

## COCKPIT DEVELOPMENT

Advanced Displays--Cne of the major problems associated with the cockpit
layout using state-of-the-art instruments and electrical-electronic con-
trol panels is the interference between such equipment and the body of
the pilot. The present cockpit layout places backup radio controls at
the extreme aft vision limit - or beyond. To actuate the knobs and
switches the pilot's arm must be slipped back beside the seat-confined
by the cockpit sill beam. The pilot's shoulder may move forward re-
stricting his downward view. Development is needed to consolidate the
visual instruments and necessary tactile controls forward of the pilot
as shown in the "DIAS" panel configuration Figure 17. By use of the
MPD/MKB display units and the HUD the pilot's visual "load" is reduced
and his required head movement within the cockpit virtually eliminated.
The pilot's required lateral arm movements are reduced. Because of the
simplified arrangement and ease of access, instrument and control main-
tenance time should be reduced.
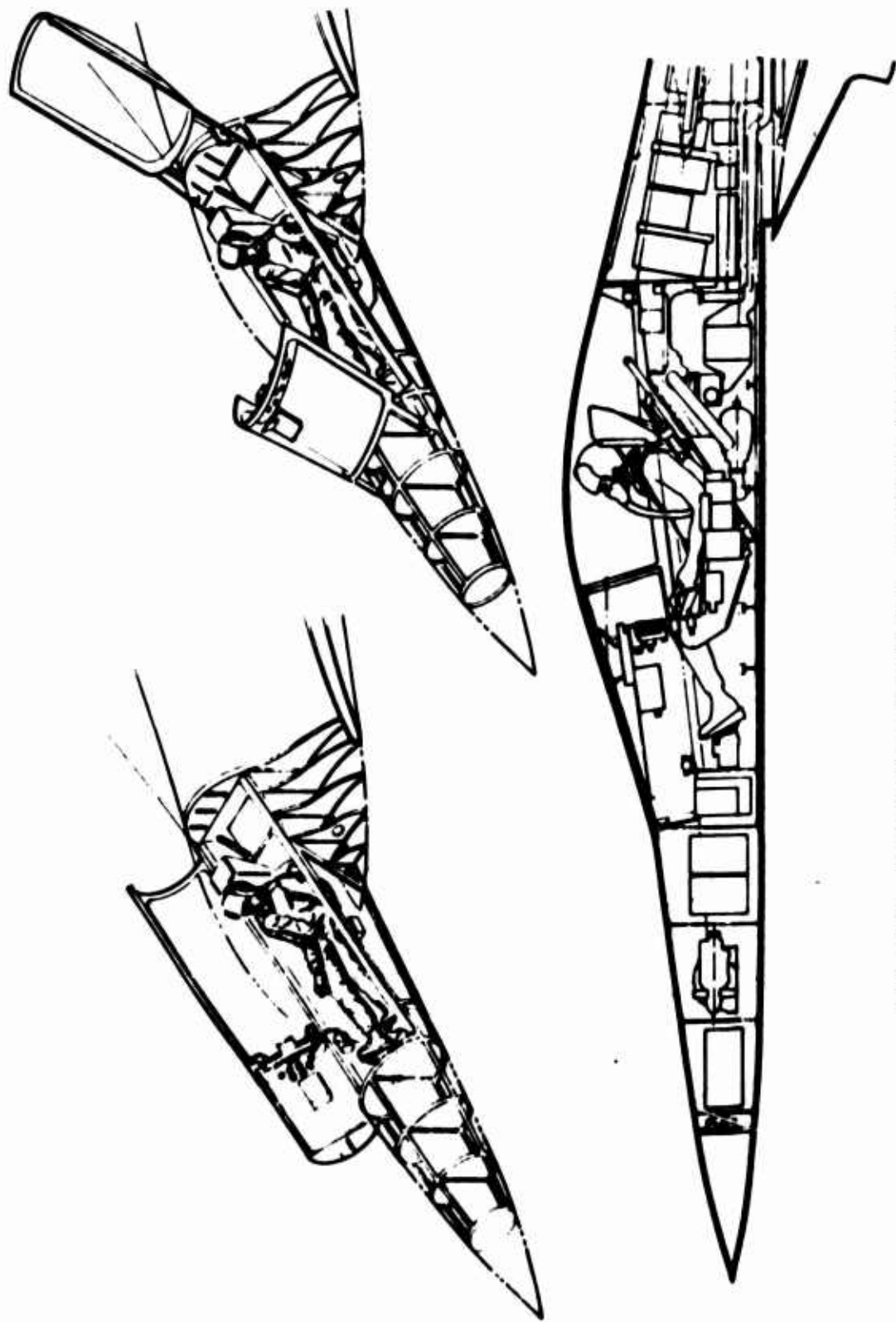
Figure 16. Low Profile Cockpit Design — Canopy Jettison Options

25

**OFFSHELF DISPLAYS**

**ADVANCED DISPLAYS**
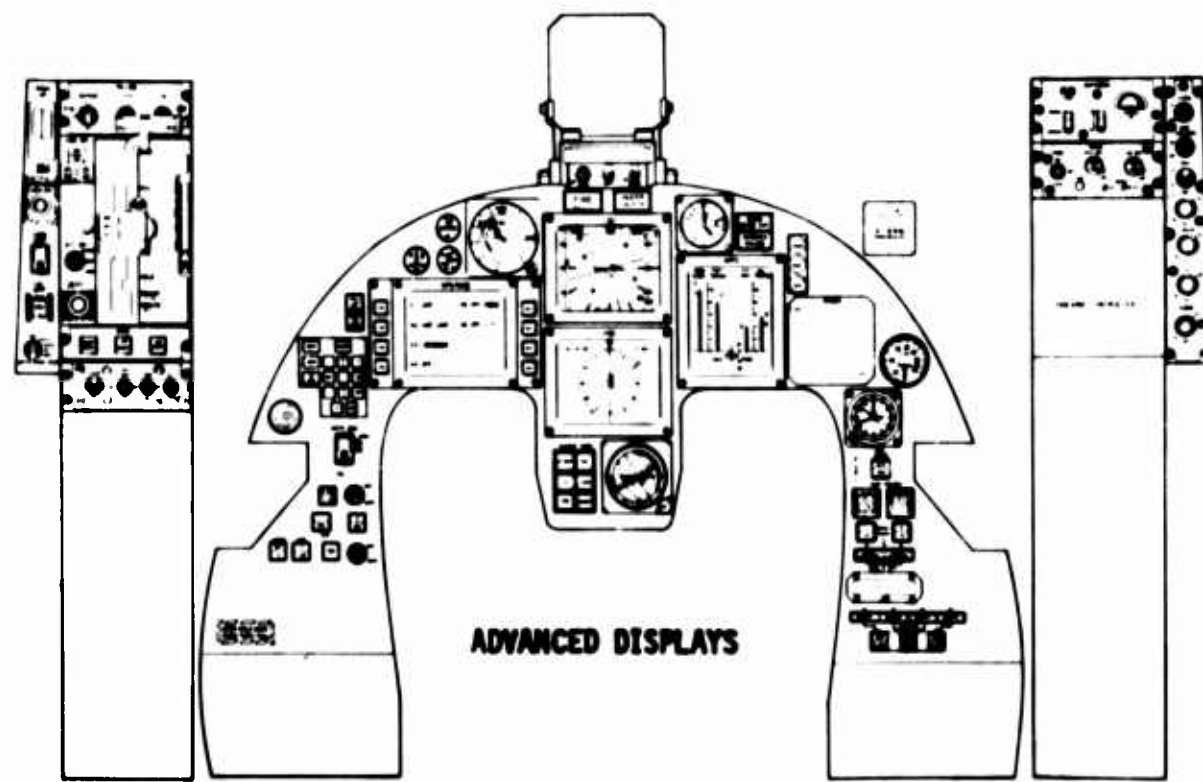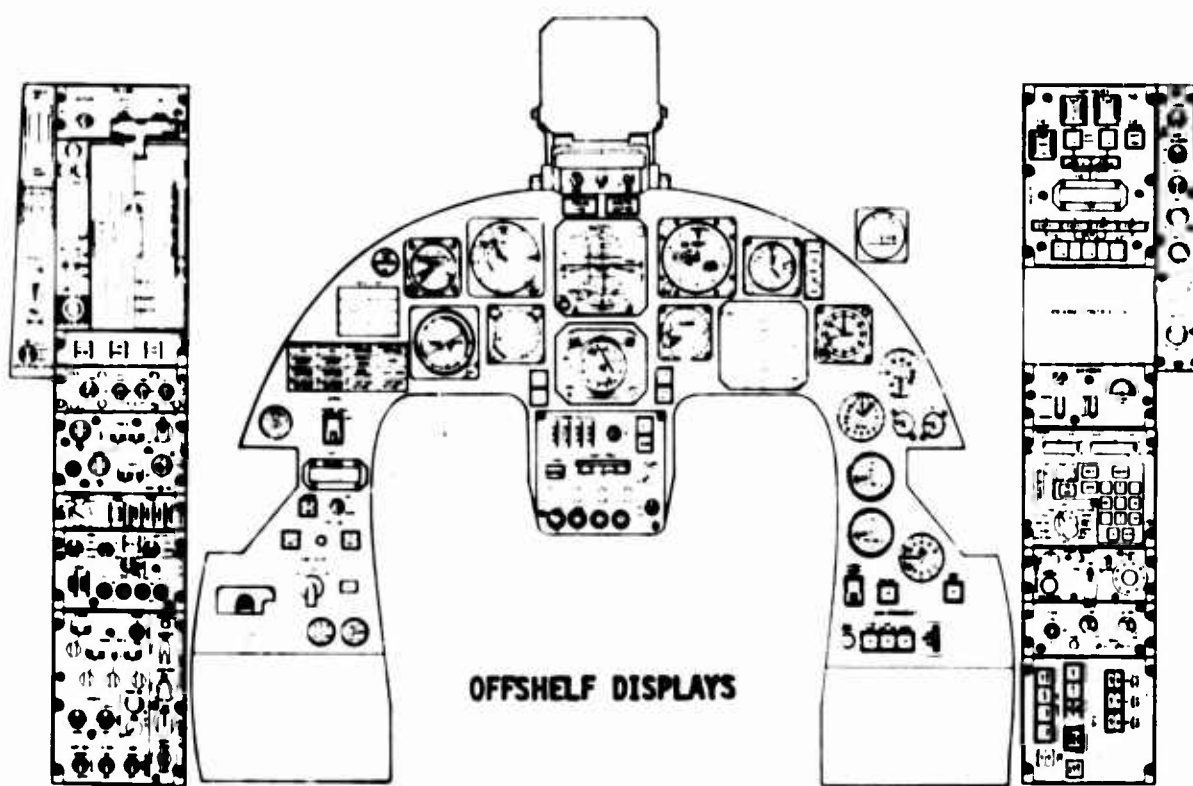
Figure 17. Cockpit Panel Layouts

26

## 2.3    TECHNOLOGY ASSESSMENT (Continued)

### 2.3.3    COMPOSITE AIRFRAME & DAMAGE TOLERANCE

A unitized fiber composite structure was employed using a hybrid skin with a multi-spar support arrangement.  Advanced composites were selected for structural efficiency.  A structural weight saving of approximately 20 percent and a potential cost saving of 9 percent are estimated compared to an aluminum airframe (Reference Weight and Cost Evaluation, Sections 3.9 and 3.11).  The aerodynamically tailored configuration with a highly blended wing-body and extensive use of double curvatures makes fiber composites a logical choice for ease of manufacturing.  Figure 18 shows the LES structural arrangement.

Damage tolerance design practice was employed in the material and concept selection by concentrating bending loads in the multiple spar caps for load path redundancy and using damage tolerant hybrid skin with graphite/epoxy and fiberglass.  Spar spacing and attachment concept were selected to provide resistance to 23 mm HE projectiles with the associated overpressure and hydraulic ram effects.  Small fighter type aircraft require a structure that is damage tolerant, lightweight, and with low manufacturing cost.  These requirements are complicated by the difficulty of providing simple continuous load paths while providing access for engine accessories, equipment and housing for landing gear.

Only a small portion of the total effort was spent in the structural design and analysis of the airframe; further work is therefore recommended in the following areas:

  o Structural design criteria.  Conduct trade studies on load factors, design speeds, sink rates, maneuver capabilities, threat requirements, and damage tolerance requirements.

27

Figure 18. Isometric — LES Structural Arrangement
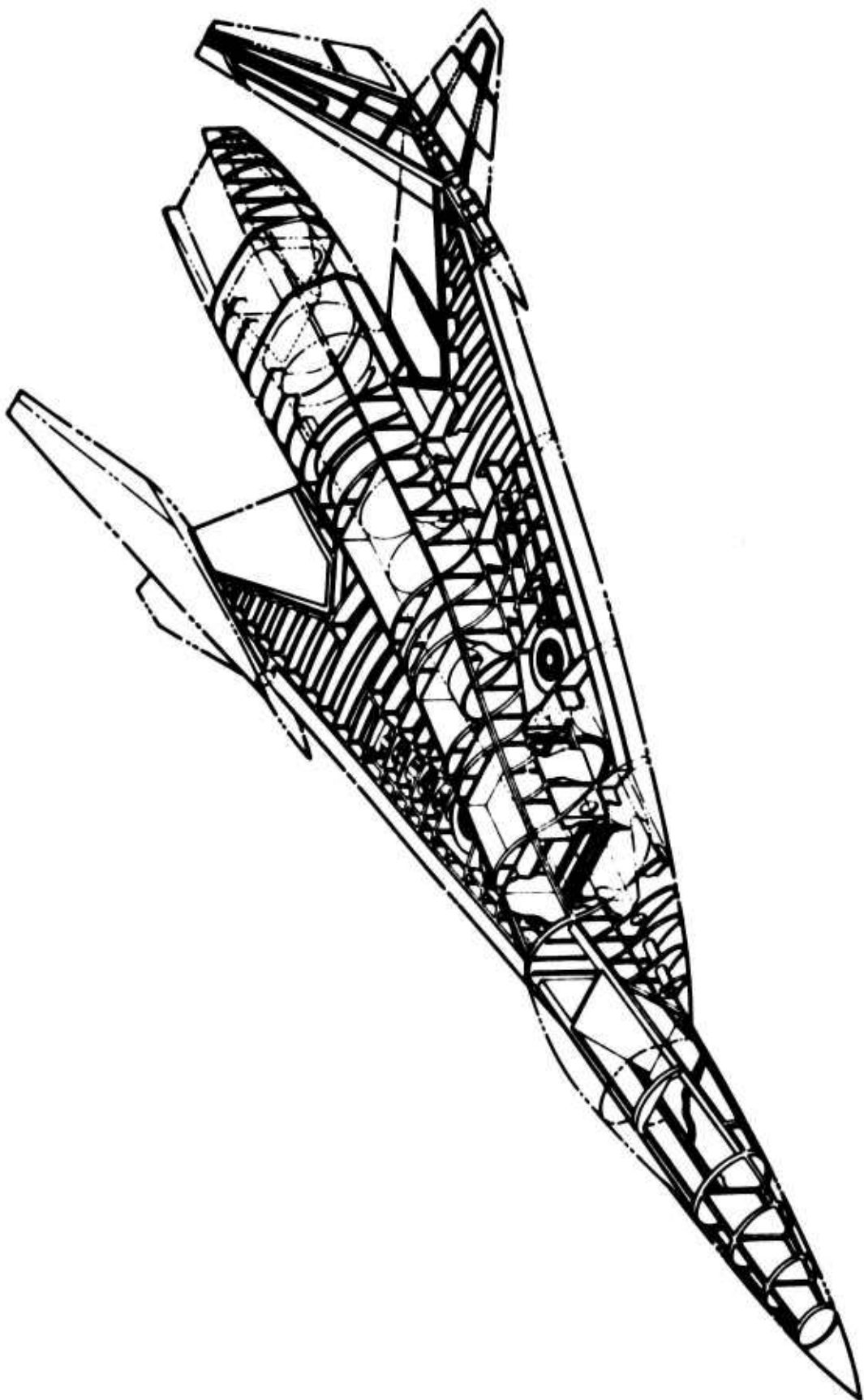
2.3.3 COMPOSITE AIRFRAME AND DAMAGE TOLERANCE (Continued)

o   Expand external load analysis to include additional flight
    and ground conditions such that all major structural components
    are sized by critical or near critical conditons.

o   Evaluate alternate structural concepts to provide improved
    load paths in the wing/body structure, increased t/c at
    fin attachment, rearrangement of elevon for improved aft
    body load paths and damage tolerance.

o   Establish preliminary flutter speed.  Aeroelastically tailor
    structure to satisfy strength, flutter, and control surface
    effectiveness criteria at minimum structural weight.

o   Establish structural and fatigue allowables that address
    material degradation effects due to humidity, temperature,
    aging and cyclic loading.

The data obtained to date on the Navy Battle Damage Tolerant Wing
Structural Development Program (Reference 5) indicate that the separation
of bending and torsional material, redundant unidirectional spar elements
and a hybrid skin is desired for resisting the 23 mm HE threat.  This
program should be supplemented with a program of design, fabrication and
test of components aimed at the structural problems of small fighter type
aircraft.  Several items requiring development effort are:

1.  Practical joints for the unidirectional graphite chords of spars,
    ribs and bulkheads.

2.  Structural design of major joints; manufacturing breaks, fin-to-
    wing joint, landing gear attachment concept, etc.

3.  Manufacturing feasibility and cost evaluation.

## 2.3 TECHNOLOGY ASSESSMENT (Continued)

### 2.3.4 FLIGHT CONTROLS

A preliminary evaluation of Model 985-213 stability and control charac-
teristics was performed and the following conclusions drawn:

1.  A flight-critical, three-axis automatic flight control system will
    be required.

2.  The elevon surfaces are marginally adequate, but may have to be
    increased in size or augmented by a thrust vectoring control.

In supersonic flight, the airplane will be balanced with a relatively
small static margin so that trim drag may be minimized, and maneuver-
ability enhanced. Since there is little possibility of fuel transfer
for rapid c.g. control, the airplane will probably be statically unstable
in subsonic flight. Such a balance philosophy will require a sophistica-
ted automatic system so that angle of attack or load factor limits are not
exceeded.

Arrow wings display a tendency toward pitchup. If wind tunnel tests re-
veal such characteristics on LES, there are several ways to improve the
situation. Either reducing the sweep of the trailing edge or reducing
the sweep of the leading edge outboard of the fins, or both, will reduce
pitchup. Another possibility would be to depend upon an automatic system
to limit angle of attack.

Although Model 985-213 has a comparatively light wing loading, the highly
swept planform has a low lift curve slope, consequently high angles of
attack will be reached in air-to-air combat. High angles of attack
usually cause degradation in lateral-directional stability characteristics.
The configuration will have to be carefully tailored in the development
phase so that a spin-resistant airplane is achieved. An automatic sys-
tem may be useful to augment desirable characteristics.

2.3.4 FLIGHT CONTROLS (Continued)

The inherent roll damping of the supercruiser planform is low. To bring the roll time constant within limits suitable for air-to-air combat, artificial roll damping will be necessary.

Model 985-213 will exhibit high values of $C_{l\beta}$ and low $C_{n\beta}$. Together with low roll inertia and high yaw inertia, the aerodynamic characteristics will give rise to poor Dutch roll damping and high $\phi/\beta$ ratio. Stability augmentation will be required to overcome these undesirable effects.

Analysis (Section 3.5) shows a full symmetric elevon deflection is necessary for takeoff rotation, and nearly full antisymmetric deflection is required for adequate roll response in combat.

Fortunately, these two requirements do not occur simultaneously, and a control priority system may be devised. However, further study is required to isolate the critical condition for combined pitch and roll control. Should the presently installed surfaces prove deficient, a number of solutions are available. The alternatives include: increase in control surface chord, addition of a pitch control surface and use of vectored thrust for pitch control.

In addition to the augmentation functions described above, standard pilot relief modes as Mach hold and altitude hold will be furnished by the Flight Control System. Fly-by-wire control, without mechanical backup, will be used throughout. Digital computation will be employed, with functions that are critical to flight safety integrated into a set of triply redundant computers, while non-flight-critical processing is performed in a single central, or mission, computer. This flight management concept will provide a safe, reliable system at light weight. Experience from the HLH fly-by-wire system and the YC-14 digital computers and STOL control system will provide a solid foundation upon which to build a Flight Control System of the future.

2.3    TECHNOLOGY ASSESSMENT (Continued)

2.3.5  ENGINE-NOZZLE-AIRFRAME INTEGRATION

Engine Performance--Supercruise performance is heavily dependent on the
engine cycle, engine technology and low supersonic drag.  Any existing
engine could have been selected as the subject of this supercruise study.
Based on engine/airplane matching trade studies, a version of the General
Electric J101 was selected because its characteristics are closest to
those desired for the Light Experimental Supercruiser.  Its advanced
technology provides better thrust per frontal area and thrust per volume
than other small engines.  The availability of advanced technology in
thrust sizes near 15,000 lbs allow airplane designs in the 10,000 to
15,000 lb range.  Airplanes in this size class produce a useful capability
for experimental development.  The engine used here is a J101/J7 Study
A9 and its cycle characteristics at supercruise conditions produce a
thrust lapse with Mach number above 1.6 that limits dry thrust supercruise
speed.

Installation--The engine and exhaust system installation for the -213
configuration is not a conventional design.  The exhaust system is a two-
dimensional wedge nozzle concept where airframe and exhaust nozzle
structural integration is utilized to minimize weight.  This concept is
considerably different from the conventional engine mounted axisymmetric
nozzle design not only because of the basic geometry, but also in the
structural integration of traditional airframe and exhaust nozzle.

Recently completed studies of the 2-D Airframe Integrated Nozzle (AIN)
show that the concept is feasible from a structural and actuation stand-
point at reasonable weights (Reference 6).  Nozzle cooling requirements,
an important concern for non-axisymmetric nozzles, were found to be
comparable to cooling requirements of high performance axisymmetric C-D
nozzles, by proper management of nozzle air supply.  In addition, this
study showed promise of Radar Cross Section and Infra Red suppression
due to nozzle geometry without large performance penalty. The design
studies also identified areas that require further development work

32

## 2.3.5  ENGINE-NOZZLE-AIRFRAME INTEGRATION (Continued)

including Finwall cooling panel fatigue life, heat transfer rig tests,
development of an airframe-to-engine seal, a nozzle cooling system
control and independent nozzle throat expansion area control.  A full
scale development program is estimated to require approximately 48
months, the first 18 months of which are component development testing.

Wind Tunnel Test Data--Thrust/drag performance evaluation of the 2-D AIN
has been based primarily on static and wind tunnel test data of single
and twin nozzle/aftbody models (References 7 and 8).  The wind tunnel
tests were conducted in a cooperative exploratory program with NASA
Langley Research Center under Navy (NAPTC) and Boeing IR&D funding.
Tests have been conducted in the transonic (Mach 0.60 to 1.2) and super-
sonic (Mach 2.0) flight regimes with high pressure exhaust flow simulation.
Results of these investigations indicate thrust/drag performance of a
single 2-D AIN as designed for the -213 configuration is competitive with
current engine mounted variable geometry axisymmetric C-D nozzles
at transonic and supersonic speeds.  High thrust vectoring efficiency and
jet induced lift can be obtained using the two-dimensional centerbody
wedge deflected to vector jet exhaust thrust downward.  In addition,
thrust-reversing capabilities of panels symmetrically deployed from the
centerbody wedge are very effective for inflight operation and may also
be employed for improved deceleration during the landing.

Wind tunnel evaluation of the 2-D AIN thrust/drag performance for the
specific LES airplane geometry where the canopy fuselage, wing, and
nozzle/aftbody geometries can be simulated has not been accomplished.
Such a wind tunnel investigation should also include an axisymmetric
C-D nozzle installation to assess "round versus square" nozzle/aftbody
performance in the installed environment.

33

## 2.3.5 ENGINE-NOZZLE-AIRFRAME INTEGRATION

It is concluded that for the 2-D AIN concept the design is feasible from a mechanical/structural standpoint, has thrust/drag performance that is competitive with C-D axisymmetric exhaust nozzles, and offers potential thrust vectoring/induced lift and inflight thrust reversing benefits. There are several development tasks that must be accomplished that include thrust/drag performance evaluation for the specific LES airplane geometry and full scale component development.

## 2.3.6 STEALTH TECHNOLOGY

LES was not designed specifically for stealth but the LES configuration geometry offers many potential solutions to aircraft detectable observables. Table 2 identifies the major vehicle observables (elements of vehicle detection), emission characteristics, elusiveness and technology trades. A sharp nose, low profile cockpit, blended body, high wing sweep, canted vertical fins, a shielded inlet, a 2-D centerbody wedge nozzle, coupled with small size and supersonic speed at high altitude, all contribute to stealth research in supercruise missions.

*Table 2. Vehicle Observables*

| Observables | Aircraft Emission Characteristics | Vehicle Elusiveness | Threat Versus Technology Trades |
|---|---|---|---|
| RCS<br>IR<br>Visual<br>Acoustic | Geometry<br>Propulsion<br>External Stores<br>Antenna & Sensors<br>Materials | Speed<br>Altitude<br>Size<br>Shape<br>Maneuvers<br>EW<br>IRCM<br>Coatings | Detection Threshold<br>Weight<br>Performance<br>Mission<br>Avionics<br>Cost<br>Development Risk |
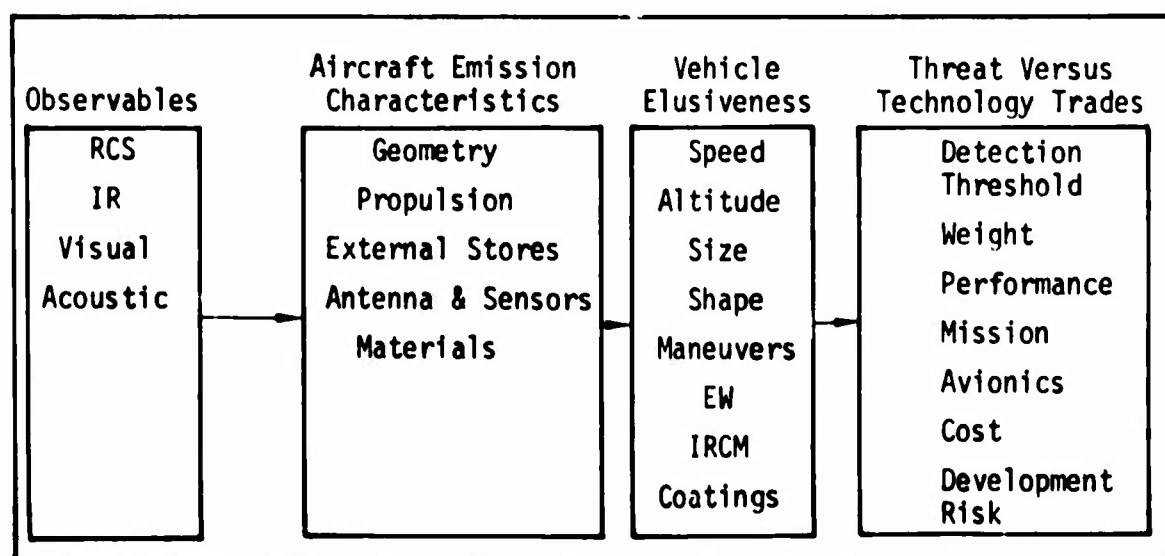
# 3.0 LES SELECTED CONFIGURATION

This section describes the LES air vehicle (Model 985-213) its sub-
systems, airframe, performance mass properties and estimated cost
for a two vehicle experimental program.

## 3.1 DESIGN CHARACTERISTICS (985-213)

The primary design characteristics are summarized in this section. The
general arrangement drawing is shown in Figure 19. The air vehicle
is designed to a Mach 1.8 area distribution with a blended wing body.
A NASA SCAT 15 arrow wing planform with a $74^o$ leading edge sweep is
incorporated to minimize wave drag with low wing loading. At 12,500
lbs. the vehicle encloses a volume of approximately 375 cu. ft. The
volume is distributed through critical cross sections created by the
pilot's station in the lo-profile cockpit and the wing rear spar.
Body camber is employed to fit wing root airfoil contours for best
cruise drag and pitching moment. Over the nose vision is limited to
$7^o$ down at cruise to minimize canopy drag while providing an effective
gun sight capability. A 2-D Airframe Integrated Nozzle is used to
close out the body. The two dimensional centerbody wedge design of
the 2-D AIN allows lengthening the aft body, improving the aft body
fineness ratio and reducing boat tail angles without imposing signifi-
cant thrust or weight penalties.

Wing--The Light Experimental Supercruiser described is an arrow wing
design based on NASA/SCAT-15 research with low wing loading (50 PSF)
and flexible skin variable camber leading edge. The basic wing is
cambered and twisted for a design cruise lift coefficient of 0.1. The
wing is twisted about the 75% chord line to provide a simple hinge for
trailing edge elevons. Wing tip panels (of -213) are fixed with $30^o$
negative dihedral to reduce overall dihedral effect and contribute to
directional stability. Wing structure is skin and spar construction
with bending loads carried in the spars and torsion in the skin. Fuel

CROSS SECTIONAL AREA ~ FT²
BODY PERIMETER    ~   FT

20

15

10

5

$A_{CAP}$=4.0 FT²

WBL 32.0

STA 100

WL 100    STA 113.5

WL 100    STA 184

STA 213

STA 238

STA 26

WL 100

GROUND PLANE

BODY DESIGN REF AREA

ACTUAL BODY AREA

GROSS AREA

M-18 WING AREA + FIN AREA
( SOB - WBL 18 )

BODY WETTED AREA (SOB=WBL 25)

GROSS FUEL
VOLUME

WING FUEL VOLUME

SIDE

CENTER

$A_{DIM}$ = 41 SQ FT

WING FUEL
1200 LB

WBL 320

WBL 400

MAC

BL 353.0

STA 100

WL 100

STA 113.9

WL 100    STA 184

STA 218

STA 297

STA 292.5

STA 435.5

STA 230

STA 340

STA 391

STA 292

GROUND PLANE

15°

STA 505

WL 100 WRP    WL 98.0

STA 473

WL 100

53 FT

44 FT

SIZE
A PROJECTED FRONTAL A
A PROJECTED PROFILE AR
A PROJECTED PLANFORM A
$\sqrt{A_1^2 + A_2^2 + A_3^2}$

BODY DESIGN REF AREA

GROSS AREA

M+18 WING AREA + FIN AREA
( SOB + WBL B)

BODY WETTED AREA (SOB=WBL 25)

GROSS FUEL VOLUME

WING FUEL VOLUME

$A_{DH} = 41$ SQ FT

SIDE CENTER

WBL 400

BL 35 10

BL 917

STA 435.5

STA 391

STA 473

**SIZE FACTOR**

| | |
|---|---|
| A PROJECTED FRONTAL AREA | 30.5 FT² |
| A PROJECTED PROFILE AREA | 136.7 FT² |
| A PROJECTED PLANFORM AREA | 326.6 FT² |
| $\sqrt{A_1^2 + A_2^2 + A_3^2}$ = | 356.4 FT² |

WL 100 WRP
WL 96 0 ENG ₵

8.3 FT

WL 100

DESIGN CHARACTERISTICS

REFERENCE GEOMETRY

| | | | WING | | H TAIL | V TAIL |
|---|---|---|---|---|---|---|
| L E SWEEP | | deg | 74E | 74/65E | | 65 |
| AREA | S | ft² | 250 | 2665 | | 38 |
| DIHEDRAL | Γ | deg | — | | | 15 |
| ASPECT RATIO | R | | 934 | 145 | | 68 |
| TAPER RATIO | λ | | 19 | 044 | | 32 |
| B A C | C | ft | 189 | | | |
| INCIDENCE | i | deg | | | | |
| THICKNESS RATIO | t/c | | 04 | 03 | | 04 78 03 |
| TAIL VOLUME COEF | V | | | | | |
| AIRFOIL SECTION | | | | | | |
| L E FLAP AREA | S | ft² | 27 | | | |
| T E FLAP AREA | S | ft² | — | | | |
| L E FLAP DEFL | i | deg | 35 | | | |
| T E FLAP DEFL | i | deg | — | | | |
| CONTROL AREA | S | ft² | 18 | | | 95 |
| CONTROL DEFL | i | deg | 30 | | | ±30 |
| T CHGT | | | | | | |
| EXPOSED AREA | | ft² | | 159 | | 65 |

WEIGHT SUMMARY LBS

| | BASIC DESIGN MISSION | |
|---|---|---|
| STRUCTURE | 3650 | |
| PROPULSION | 2770 | |
| FIXED EQUIP | 1490 | |
| WEIGHT EMPTY | 7910 | |
| NON-EXP USEFUL LOAD | 620 | |
| OPERATING WEIGHT | 8530 | |
| FUEL | 3630 | |
| PAYLOAD | 340 | |
| EXT PLD PROVISIONS | | |
| GROSS WT | 12,500 | |

WETTED AREA FT²

| | | |
|---|---|---|
| WING SWEPT | 74 | |
| BODY STREET | 420 | |
| WING INTERF | 29 | |
| GAP INTERF | — | |
| AERO BODY | 391 | |
| EXPOSED WING | 318 | |
| AIR INDUC | — | |
| EXP VERTICAL | 76 | |
| TOTAL AERO | 785 | |

AERO REV

DESIGN NOTES

POWER PLANT : J101/J7 STUDY A9  15,000 LB CLASS

INLET : DOUBLE RAMP VARIABLE GEOMETRY M 2.0 SHOCK-ON-LIP
ACAP = 40 FT²

LANDING GEAR : NOSE — (2) 20 x 5.5 ; 14 PLY , 230 PSI , 200 GPM
MAIN — (1) 16 x 4.4 ; 8 PLY , 120 PSI , 160 GPM

ARMAMENT : (2) CLAW MISSILES SEMISUBMERGED
(1) M197 20MM GUN  250 RDS AMMO

▷ WING DEFINED FROM WBL 00 TO WBL 917

▷ TOTAL WING INCLUDING TIP

REVISION 'A'

INCHES

Figure 19.  General Arrangement LES Model 985-21

37 & 38

3

## 3.1 DESIGN CHARACTERISTICS (Continued)

is carried in integral wing tanks to the fin stations. Vertical fins house fuel surge tanks and overboard vents. Wing geometry is further described in section 5.0 of this document.

The following section describes airplane geometry and accessibility.

Internal Arrangement--All major components and subsystems are shown on the inboard profile, Figure 20, to represent the integrated design. In the system descriptions frequent reference will be made to this drawing. Part of those descriptions are summarized here to provide understanding of the philosophy.

First the vehicle aerodynamic envelope is considered inviolate to assure low supersonic wave drag. In the course of packaging design some compromise is to be expected.

Weights and Balance--The LES balances at 55% to 60% of Mean Aerodynamic Chord (MAC). To accomplish this, equipment placement has been located as far aft as possible. The resulting arrangement places lower density equipment in the forebody section. Fuel system capacity is 3800 lbs. Fuel transfer is available to move airplane c.g. approximately 4% MAC. This is possible by virtue of the aft body fuel tanks.

Ground Attitude--The airplane sets rather high in comparison to others of the same size class. Body camber and chin inlet arrangement force a choice of high nose and long nose gear or a lower nose with negative angle of attack on the wing during ground roll. The high nose attitude was selected to minimize nose wheel lift off speed. The main gear length was sized by engine removal clearance and nozzle clearance at touchdown angles. This arrangement produces approximately 34 inches clearance under the body and allows ample room for addition of low drag stores pallet and clearance for loading up to 2,000 lb. bombs.

OXYGEN SUPPLY

SIDE ARM CONTROLLER

NOSE GEAR ACTUATOR

RO RADAR

RAM AIR TURBINE

FWD AVIONICS

HUD UNIT

THROTTLE

BLAST TUBE

ECS UNIT

MUZZLE GAS DIFFUSER

AFT AVIONICS

M-197 GUN

AMMO BOX

SINGLE POINT REFUEL RECEPTACLE

GUN START BOTTLE

FUEL TRANS SYS

FUEL

HYD MOTOR GENERATOR

FUEL/AIR STARTER

GPI

LE DRIVE UNIT

MAIN GEAR ACTUATOR

ECS UNIT

AMMO BOX

TRAPEZE ACTUATOR

CLAW
MISSILE

M-197 GUN

NOSE GEAR

FWD AVIONICS

HUD

BLAST TUBE

RAMP

THROAT ACTUATOR

AMMO BOX

EJECTION SEAT

FUEL

RAIL

CLAW

M-197 GUN

RAMP

FWD AVIONICS

HUD UNIT

AMMUNITION BOX

AFT AVIONICS

RO RADAR

OXYGEN SUPPLY

FUEL

RAM AIR TURBINE

EJECTION SEAT
50° SEAT BACK
ANGLE

MOISTURE
SEPERATOR

ECS UNIT

ELECT POWER
SHIELD

INVERTER

ELECT SYS
CONTROLS

THROAT ACTUATOR

OIL / AIR HX

HYD MOTOR GENERATOR

Figure 20. Inboard Profile — LES Model 985-213

41 & 42

## 3.1 DESIGN CHARACTERISTICS (Continued)

Lo-Profile Cockpit--The cockpit arrangement for low wave drag places the pilot in a fixed semi-supine seat with back angle $50^0$ aft of the vertical. This fixed high "g" seat requires special canopy designs to provide for emergency escape. Because of the small cross-sectional area,windshield and instrument panel must be integrated and designed to move together for pilot leg clearance during normal ingress and egress as well as emergency escape.

Maintainability--Simple rules were followed for maintainability and servicing. The primary guidelines are as follows:

1. Locate equipment to require a minimum number of openings in addition to the natural openings of wheel wells, canopy hatch, and engine bay access doors.

2. Package avionics and equipment in 40 lb. units for easy removal by one man.

3. Locate equipment access on upper body and usc upper wing for work platforms.

4. Leave lower body free of access doors except for services to connect body mounted external stores.

Accessibility--Major access to equipment and subsystem components is through upper body openings (Figure 21). All access covers are hinged and non-structural. This arrangement is a result of the structural configuration which forms an inverted horseshoe frame from the very forward radar bulkhead to the engine face.

Access to the engine mount system and the engine/airframe accessory pack is provided at the top of the body. Installation/removal of the gas generator section of the engine (including the afterburner flame holders and ignition system) is raised/lowered vertically through an opening in the bottom of body structure. Aft of the gas generator section, the
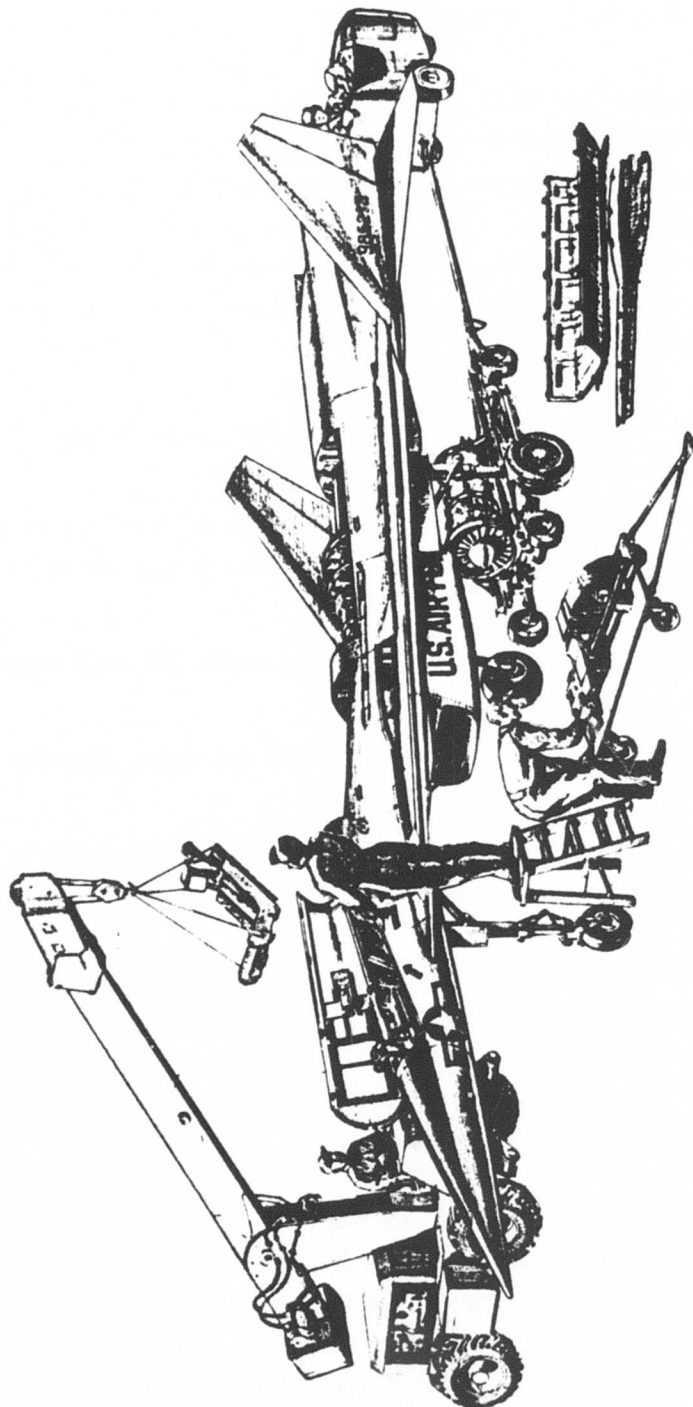
Figure 21.    LES Accessibility – Maintenance and Servicing

## 3.1 DESIGN CHARACTERISTICS (Continued)

non-circular afterburner duct and center body wedge nozzle are integrated into airframe monocoque structure. A circular interface (between the gas generator section and the aft body integrated exhaust system) is located forward of the flameholders and is sealed by a rolling bellows design. Access to nozzle actuators is through the drag modulation/reverser panels on upper and lower surface of the variable geometry centerbody. A work stand is necessary to provide good working height for the nose and cockpit sections. The upper wing surface serves as a work stand for upper body equipment bays and the gun bay. A standard "Air-Log" trailer is usable for engine removal.

Removal of heavy equipment such as ejection seat, cannon and aircraft accessory drive system require hoist equipment. Other equipment and electronic boxes are intended to weigh 40 lbs. or less for one man removal.

The lower body is clear of access doors. As such the inlet duct section of the body is monocoque with only the engine bay door breaking the lower body. The absence of access on the lower fuselage is intentional to leave unobstructed space for low drag weapon carriage.

Armament Loading--The "CLAW" air-to-air missiles are mounted semi-submerged on the upper body. This location provides low drag and good sensor up look angles. Hoist loading is possible but ample space is available on top of the wing for two men to position the 80 lb. missiles on their rail launchers. Ammunition loading is all manual from the upper wing work area.

## 3.2 AIRFRAME

This section describes the structural arrangement, materials selection, loads and stress analysis and landing gear arrangement for LES concept 985-213.

LES Composite Structure--The determining factors in the design concept of the structure are, blending of wing and body structure which causes extreme changes in direction of the exterior panels in the spanwise direction and placement of the engine with its access requirements. The structural arrangement is shown in Figure 22.

The structural concept under investigation in the Battle Damage Tolerant Wing Structure Development Program (Reference 5) is used in this airplane. This concept uses multi-spar construction with the wing bending loads carried by the spars and wing torsion carried in the skin panels. The skin panels are designed with $\pm45^0$ graphite for wing torsion and $0^0$ S-Glass for improved damage tolerance (30% thickness of required graphite). The S-Glass increases the damage tolerance of the panel by increasing the strain at failure by approximately 100% and also the additional panel thickness increases panel stability and shear capability. This panel design does not require edge inserts or filler material where fuel pressure loads require mechanical fasteners to be installed and is more economical to build than the sandwich design.

The upper and lower panels are mechanically attached to the spars. Tests run in the Battle Damage Tolerant Wing Structural Development Program (Reference 5) show the mechanical attachment to be far superior to bonding these panels to the spars due to high internal pressures associated with 23 mm HE and the hydraulic ram effects in the fuel tank areas.

The spar concept consists of a sandwich web with $(\pm45^0/90^0)$ graphite face sheets on fiberglass honeycomb and $0^0$ graphite chords. Fiberglass honeycomb core is used to avoid potential corrosion problems associated with

46

AL WIRE MESH
.003 DIA ·120·120
TYPICAL FOR EXTERIOR SKINS

CHORD
0° GRAPHITE

SKIN
±45° GRAPHITE/EPOXY
WOVEN CLOTH (70%)
0° S GLASS (30%)

WEB
±45° GRAPHITE/EPOXY
WOVEN CLOTH (60%)
0°-90° S·GLASS/EPOXY
WOVEN CLOTH (40%)

## 2C4
NO SCALE

↑ UP
← FWD

FIBERGLASS HONEYCOMB

ACCESS PANEL
±45° GRAPHITE/EPOXY WOVEN CLOTH (60%)
0°-90° S·GLASS/EPOXY WOVEN CLOTH (40%)

UPPER LONGERON
0° GRAPHITE

SKIN
SEE 2C4 c13

FACE SHEETS
±45° GRAPHITE/EPOXY CLOTH 60%
0°-90° S·GLASS/EPOXY CLOTH 40%

FIBERGLASS HONEYCOMB

## 1C4
NO SCALE
(ROTATED 90°)

↑ UP
← INBD

---

¢ AIRPLANE

UPPER LONGERON

ACCESS DO
ENGINE AC

SIDE WA
ACCESS

LOWER

ENGINE

RIB
SIDE OF BODY

MAIN LANDING GEAR

## 1A5
B. STA 336.

FORWARD ENGINE SUPPORT

ACCESS
ENGINE

UPPER

SIDE
ENG

FRONT SPAR

RIB
SIDE OF BODY

LOWER L

ACCESS DOO
ENGINE REM

## 2A4
B. STA 390.5

UPPER LONGERON

VERTICAL STABILIZER

S
E

WL 100

TIP FIN

LOWER LONGERON

ACCESS DO
ENGINE RE

## 1A4
B. STA 434

1

**1A5**
B STA 336.

- ₵ AIRPLANE
- ACCESS DOOR ENGINE ACCESSORIES
- SIDE WALL ACCESSORY COMPARTMENT
- FRONT SPAR
- WL 100
- LOWER LONGERON
- ENGINE INLET

**2A4**
B STA 390.5

- ACCESS DOOR ENGINE ACCESSORIES
- UPPER LONGERON
- SIDE WALL ENGINE COMPARTMENT
- WL 100
- LOWER LONGERON
- ACCESS DOOR ENGINE REMOVAL

**1A4**
B STA 434

- SIDE WALL ENGINE COMPARTMENT
- RIB - SIDE OF BODY
- WL 100
- FRONT SPAR
- FLAPERON
- ACCESS DOOR ENGINE REMOVAL

**3A6**
B STA 214

- CANOPY
- ₵ AIRPLANE
- UPPER LONGERON
- SIDE WALL ELECTRONIC BAY
- SUPPORT FITTING NOSE LANDING GEAR
- RIB SIDE OF BODY
- WL 100
- BLAST TUBE CANNON
- PRESSURE DECK COCKPIT

**2A6**
B STA 238

- ACCESS DOOR ELECTRONIC BAY
- UPPER LONGERON
- SIDE WALL ELECTRONIC BAY
- RIB SIDE OF BODY
- FRONT SPAR
- ACCESS DOOR CANNON
- WL 100
- NOSE LANDING GEAR
- RAMP · ENGINE INLET

**1A6**
B STA 262

- ACCESS DOOR CANNON AMMUNITION
- SIDE WALL AMMUNITION BAY
- RIB SIDE OF BODY
- FRONT SPAR
- UPPER LONGERON
- ACCESS DOOR CANNON
- WL 100
- NOSE LANDING GEAR
- RAMP · ENGINE INLET

**2A5**
B STA 298

- ACCESS DOOR EQUIPMENT
- SIDE WALL EQUIPMENT BAY
- RIB SIDE OF BODY
- FRONT SPAR
- WL 100
- ENGINE INLET

- ACCESS DOORS EQUIPMENT
- ₵

- B STA 0
- B STA 26
- ACCESS DOOR EQUIPMENT
- WL 100

ACCESS DOOR
ENGINE ACCESSORIES

ACCESS DOOR
CANNON AMMUNITION

PRESSURE SHELL

CROSSBEAM
SILL BEAM

ACCESS DOOR
ELECTRONIC BAY

SUPPORT FITTING
NOSE LANDING GEAR

ACCESS DOORS
EQUIPMENT

SILL BEAM

ACCESS DOOR
CANNON

FRONT SPAR

ACCESS DOOR
EQUIPMENT

RIB
SIDE OF BODY

UPPER LONGERON

CROSSBEAM
SILL BEAM

CANOPY

SILL BEAM

PRESSURE BEAM

PRESSURE SHELL

B STA
200

WL 100

WIN

B STA
0

B STA
26

B STA
108

B STA
160

CANOPY

B STA
214

B STA
238

B STA
262

B STA
298

B STA
336

ACCESS DOOR
EQUIPMENT

SILL BEAM
COCKPIT

CROSSBEAM

ACCESS DOOR
ELECTRONIC BAY

ACCESS DOOR
CANNON AMMUNITION

UPPER LONGERON

WL 100

PRESSURE SHELL
COCKPIT

3A6 C9

2A6 B9

1A6 B9

2A5 A9

1A5 C11

ENGINE INLET

LOWER LONGERON

3

ACCESS DOORS
AFT ENGINE SUPPORT

1C4

2C4

2-D NOZZLE PLUG

FLAPERON

ACCESS DOORS
ACCESSORIES

NITION

VERTICAL STABILIZER SUPPORT

ESS DOOR
NNON

FRONT SPAR

RIB
SIDE OF BODY

UPPER LONGERON

WING SPAR-STUB
(TYP)

WING SPAR-CARRYTHRU

TIP FIN

B STA
262

B STA
298

B STA
336

B STA
390 S

B STA
434

B STA
555

ACCESS DOOR
ELECTRONIC BAY

ACCESS DOOR
CANNON AMMUNITION

UPPER LONGERON

ACCESS DOOR
ENGINE ACCESSORIES

AFT ENGINE SUPPORT

2-D NOZZLE PLUG

PB9

2A5 A9

1A5 C11

2A4 B11

1A4 A11

ACCESS DOOR
ENGINE REMOVAL

FORWARD ENGINE SUPPORT

ENGINE INLET

LOWER LONGERON

LEFT HAND SIDE VIEW

UP

FWD

47 & 48

*Figure 22. Structural Arrangement — LES Model 985–213*

4

## 3.2 AIRFRAME (Continued)

aluminum honeycomb core. The spar webs are flat, constant thickness honeycomb to reduce fabrication costs. The basic multi-spar design will carry 'imit load with any one spar failed. The wing-body blend area at the side of the engine forms a natural torque box for spar load redistribution.

Body bending loads are carried by lower longerons of $0^o$ graphite located on the lower surface along the sides of the engine removal doors, and by $0^o$ graphite beams located at the sides of the upper engine accessories access doors. All point load applications are distributed into the composite (graphite-epoxy) airframe by machined titanium fittings.

For lightning protection, the exterior surface of all composite skins is covered by aluminum wire mesh, .003 x 120 x 120, laid up in the panel and bonded to the ground system of the airplane. Other techniques for Electro-Magnetic Pulse (EMP) protection are being studied under government sponsorship and these results will be considered in future designs of LES structure.

Landing Gear--The landing gear arrangement is a conventional tricycle arrangement with $55^o$ lateral turnover. The nose gear is offset from the centerline to accommodate the inlet duct. The need for low-wave drag has dictated the location for engine accessories above the wing behind the wing carry over spars. While this arrangement minimized body cross-sectional area, it eliminates useful gear stowage space below the inlet duct. The compromise nose gear arrangement does not unduly complicate the wing root structure for stowage because the opposite wing carries the cannon and its loads in similar structure. With nose gear down, the nose wheel is located ahead of the inlet and is offset from the center producing wheel/inlet relationship similar to many twin inlet airplane arrangements. The main gear requires a shrink link to retract into the wing wheel well. This is brought about by gear down length requirements

3.2 AIRFRAME (Continued)

and the use of an unswept front spar. A more detailed design study should compare the benefits and penalties of an alternate design which would add modest sweep to the rear spar, increase nose down ground attitude 1/2 degree and increase body clearance height five inches.

Canopy Design--The canopy design represents a compromise of over the nose visibility in favor of reduced supersonic wave drag. Canopy contours are cylindrical in cross section. A constant radius of 13 inches wrapped in a toriod provides smooth canopy fairing between windshield and rear fairing. Canopy frame structure is of graphite-epoxy hinged along the right hand sill-beam. Integration of the instrument panel and canopy frame facilitates all pilot ingress and egress modes and serves to reduce the total weight of this counterbalanced unit. Canopy and windshield materials are primarily polycarbonate.

Loads and Stress Analysis--An integrated aeroelastic loads and stress analysis cycle of a typical wing/fuselage structural arrangement for the LES 985-213 airplane has been conducted with the Boeing Integrated Structural Analysis System (ISAS), which is described in appendix A.

The external load envelope is based on three symmetric 6.5 g balanced maneuvers at speed altitude combinations representing some of the expected critical conditions; namely, Mach = .85 at 30,000 ft, Mach = 1.2 at 40,000 ft. and Mach = 1.8 at 50,000 ft. The airload distributions are based on two-dimensional potential flow theory with the limitations of linear, nonviscous, attached flow. An idealized structural arrangement is somewhat different from the final arrangement shown in Figure 22.

The limitations of the analysis are well recognized; however, the aerodynamic and structural approximations are adequate to indicate that the use of graphite-epoxy composite materials used in this type of structural arrangement can provide a strong and light-weight structure. Structural

3.2 AIRFRAME (Continued)

weight for idealized strength material of the 60 ft$^2$ main load carrying portion of the integrated wing/fuselage structure is 196 lb. per airplane (3.27 lb/sq. ft.).

The external aerodynamic/weight load grid together with the section of the airplane structure analyzed is shown in Figure 23. The general design procedure is to obtain initial structure sizes and flexibilities by applying the external loads that would occur on a rigid airplane. A new set of loads incorporating flexibility effects can then be calculated and applied. A second structural sizing follows to complete an aeroelastic loop. In this case, no significant load changes were evident and no further aeroelastic iterations were necessary. Mechanical properties used for the graphite/epoxy structure are shown in Figure 24. These values were extracted from the Air Force Advanced Composite Design Guide.

In the structural concept for the wing, spanwise uniaxial fiberglass was used (30% of the skin gage thickness) to improve damage tolerance and buckling strength of the $\pm45^\circ$ oriented graphite/epoxy skin. In the initial analysis, the fiberglass was not considered as part of the load carrying structure, but was used in calculating skin weight. Subsequent analyses show that the uniaxial fiberglass reacts approximately the same magnitude of load as the $\pm45^\circ$ Graphite/Epoxy skins in the spanwise direction. While this provides a margin of safety of 30-50% in a majority of the structure analyzed, the combined thermal and moisture degradation effects of Graphite/Epoxy will offset part of these margins of safety.

Partial program output is machine generated plots of the unloaded structure as viewed from various perspectives. The structural deflections that result from application of design loads are presented in Figure 25 where the washout at the wing tip in a high load maneuver can be seen. Deflections are proportional to vector lengths.
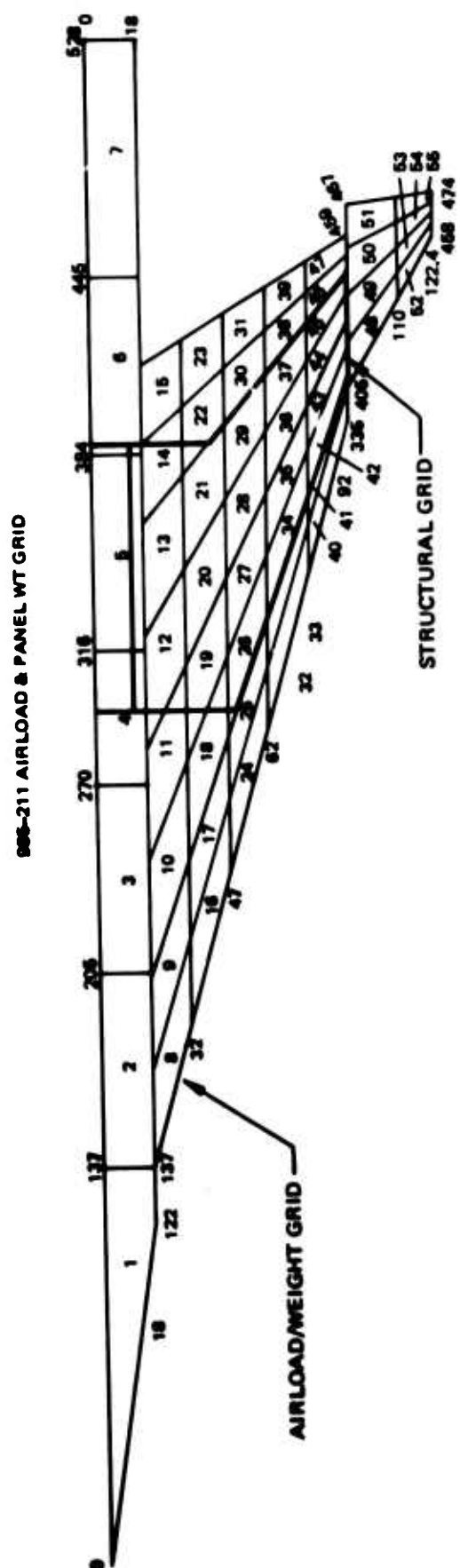
Figure 23. External Load and Structural Model Grids

**GRAPHITE/EPOXY PROPERTIES**

| DENSITY LB/IN³ | t – in LAYER | MODULI X 10⁻³ KSI | | | POISSON'S RATIO | TENSION KSI | | COMPRESSION KSI | | SHEAR KSI |
|---|---|---|---|---|---|---|---|---|---|---|
| | | $E_X$ | $E_Y$ | $G_o$ | | $F_X$ | $F_Y$ | $F_X$ | $F_Y$ | $F_{XY}$ |
| 0.058 | 0.005 | 21 | 1.7 | 0.66 | 0.21 | 180 ▲ | 12 | 180 ▲ | | 12 |

▶ EFFECTIVE ALLOWABLE IS APPROX. 115 KSI WHEN CREDIT IS TAKEN FOR 30% FIBERGLASS IN THE SKIN.

**MINIMUM GAGES**

| $t_{min}$ – in | | | $A_{min}$ -in² |
|---|---|---|---|
| FUEL TANK COVER | OUTBOARD COVER | SHEAR WEBS | SPAR |
| 0.1 | 0.07 | 0.08 | 0.03 |

**COMPOSITE LAY-UP**

SKIN: ±45° GR/EP – FOR TORSIONAL STRENGTH AND STIFFNESS
30% (0°) FIBERGLASS – TO PREVENT BUCKLING AND INCREASE FRACTURE TOUGHNESS

SPAR CHORDS: 0° GR/EP – FOR BENDING STRENGTH AND STIFFNESS
±45° GR/EP – FOR SHEAR TRANSFER FROM SKIN TO SPAR WEBS

SPAR WEBS: 60% ±45° GR/EP – FOR SHEAR STRENGTH AND STIFFNESS
40% ±45° FIBERGLASS – FOR BUCKLING RESISTANCE AND FRACTURE TOUGHNESS

Figure 24. Structural Model - Plan View
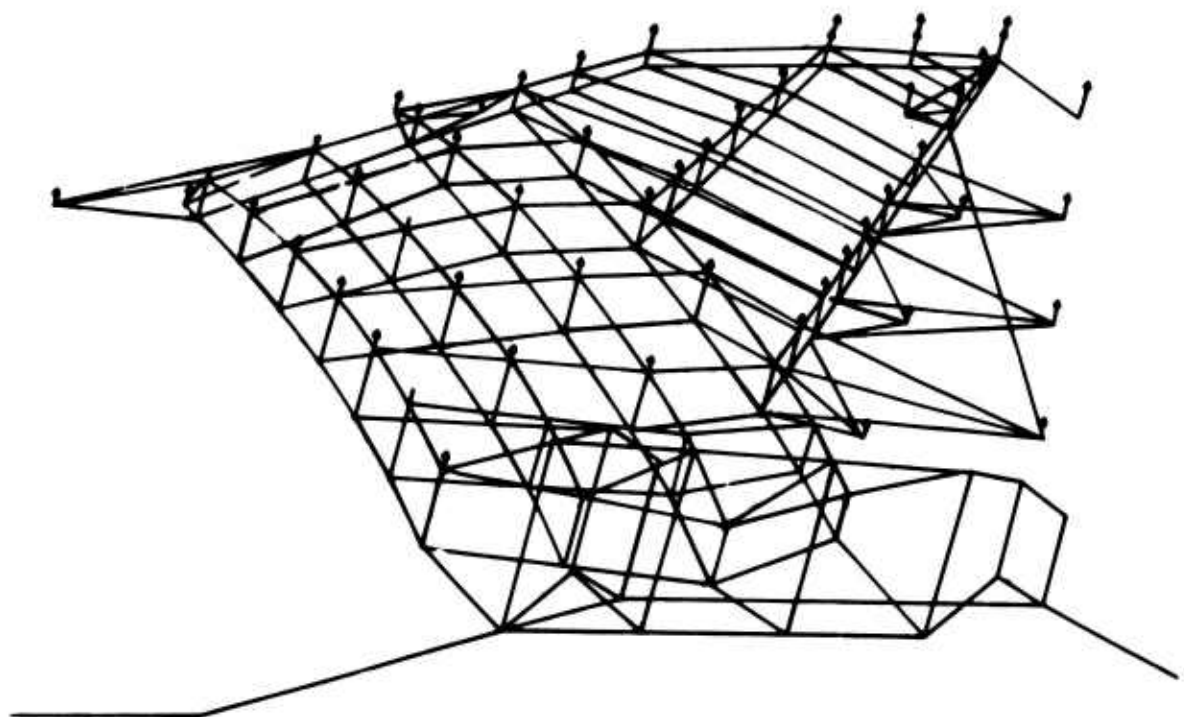
*Figure 25. Structural Deflections Under Design Load*

## 3.3 PROPULSION SYSTEM INSTALLATION

### ENGINE DESCRIPTION AND INSTALLATION

The baseline powerplant for the LES study is a derivative of the General Electric J101-GE-100 engine. This engine (designated the J101/J7 Study A9) is a dual rotor, low bypass ratio, medium cycle pressure ratio engine with a mix flow augmentor and scheduled C-D axisymmetric exhaust nozzle. The J101/J7 Study A9 engine incorporates a flared fan to increase the engine airflow and bypass ratio with a slight increase in maximum turbine temperature over the J101-GE-100. Additional J101/J7 Study A9 modifications consist of the following:

o New three finger single actuation exhaust nozzle, (slaved A9/A8),
o Revised exhaust nozzle area schedule,
o Rescheduled augmentor for improved low reheat performance,
o Revised fan speed and turbine inlet temperature schedule.

LES Installation--For this configuration study, the J101/J7/A9 engine was modified to relocate engine accessories and to accept a 2-D Airframe Integrated Nozzle. No internal modifications are required in the gas generator. Engine accessories and a new gear box have been moved to a top mounted location to utilize an existing heavy strut (at 12 o'clock position) to house the main power takeoff shaft as shown in Figure 26. Engine installation utilizes the existing mounts. This arrangement allows engine and aircraft accessories to be "hidden" between body spar frames for reduced airplane cross sectional area.

Inlet Duct System--Air induction is through a single 2-dimensional horizontal ramp inlet. The diffuser transitions from 2-dimensional at the throat to circular at the engine face. Approximately 10 inches ahead of the compressor face is a flexible joint in the circular duct section which accommodates duct/engine misalignment as well as thermal growth of the duct section. Alignment of the engine with the inlet duct is aided by adjusting the length of the side and rear engine mount links.

AIRFRAME MOUNTED
ACCESSORY GEARBOX

E.S.
200.0

A

THRUST MOUNT
SIDE RESTRAINT ONE SIDE

SEC A·A

FLEX JOINT

E.S.
178.60

THRUST MOUNT

A
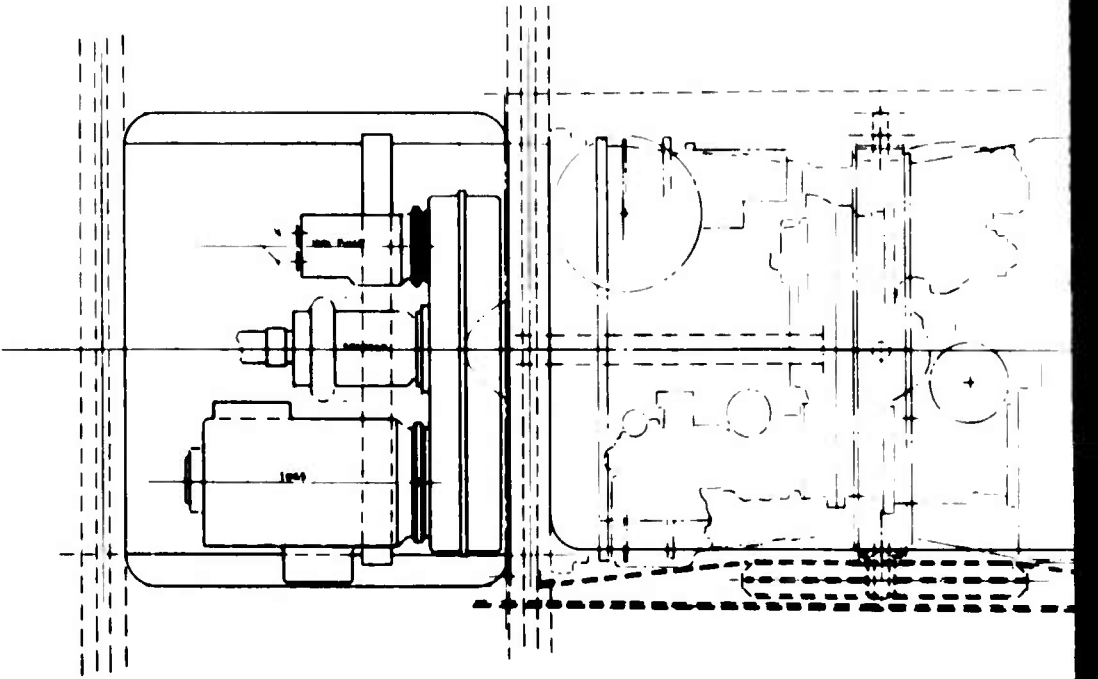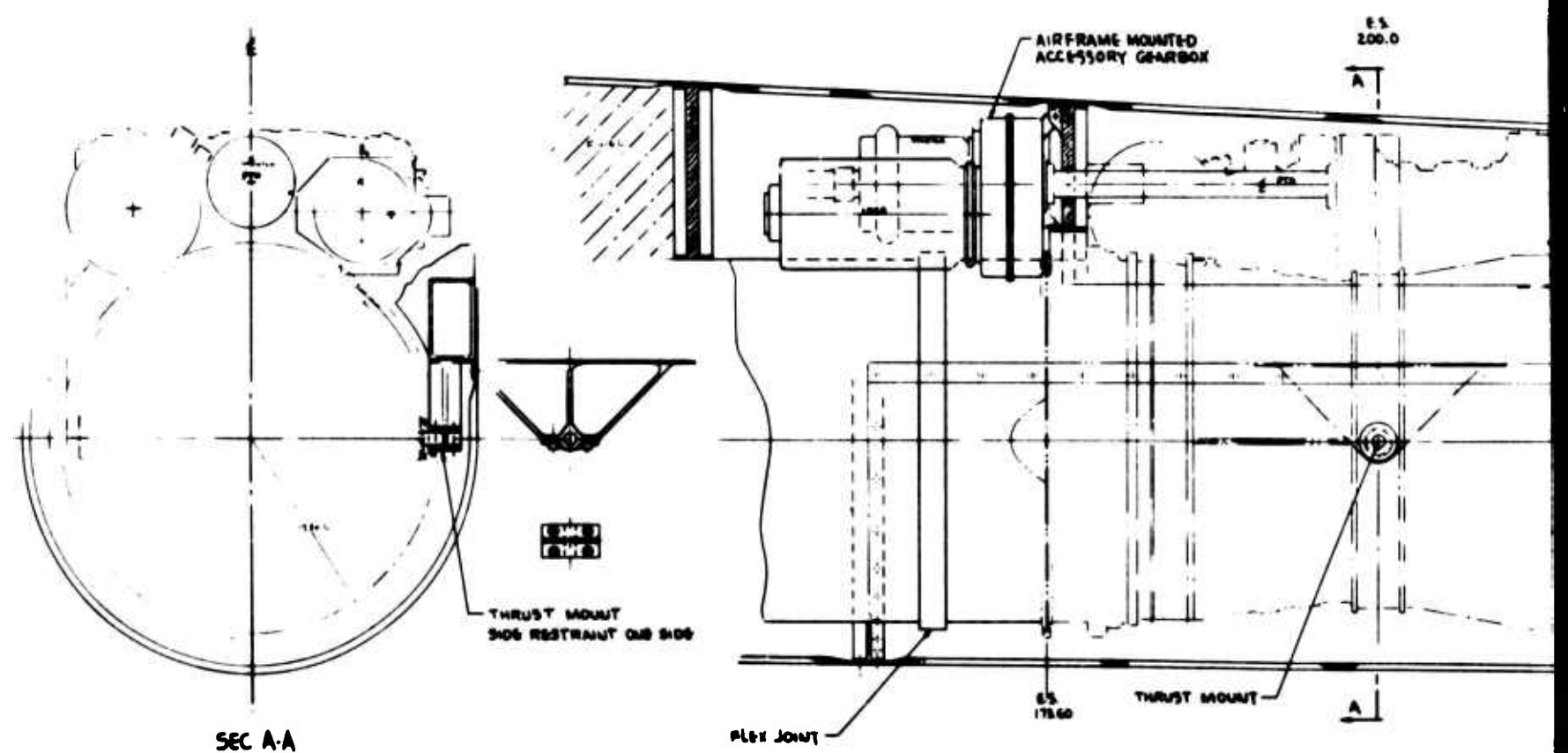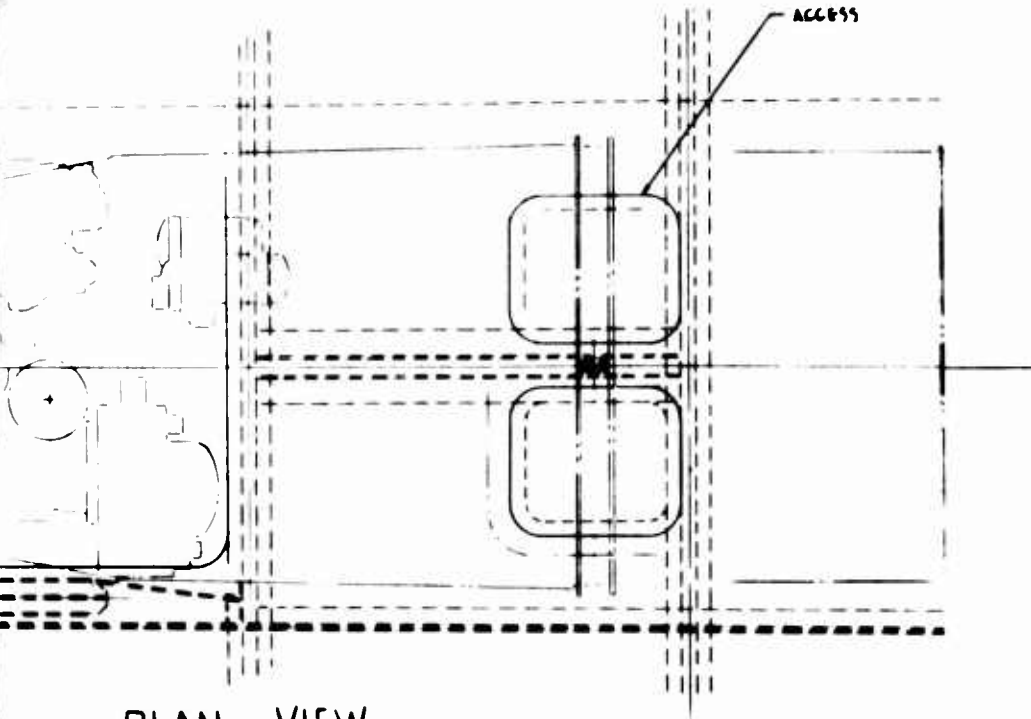
PLAN VIEW
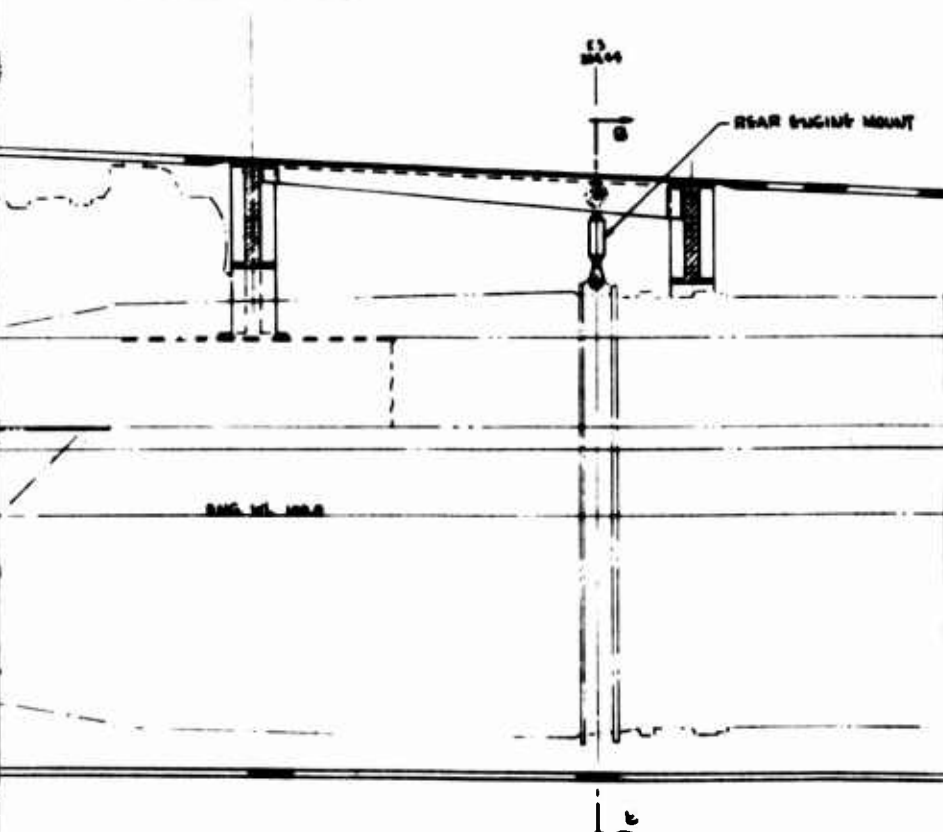
SIDE VIEW
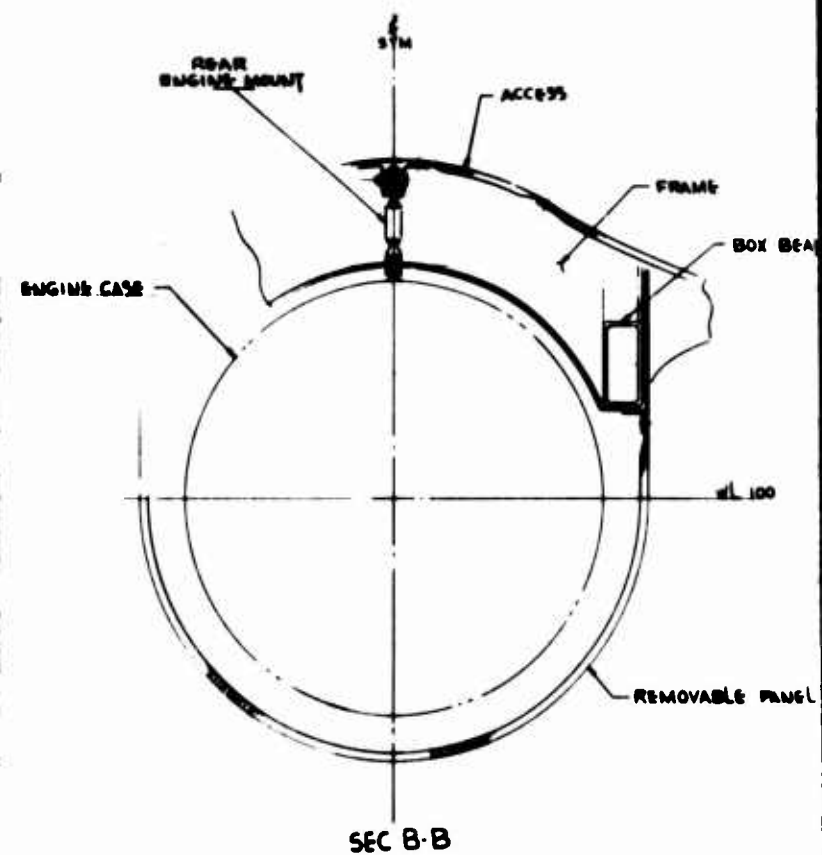
**Figure 28. Engine/Airframe Accessory Installation**

57 & 58

## 3.3 PROPULSION SYSTEM INSTALLATION (Continued)

Engine Mounting--Engine thrust is transmitted into the integrated wing/
fuselage structure through the lower body longerons. The forward thrust
mounts consist of pins inserted into spherical bearings on the horizontal
centerline of the engine case at engine station 200.0. There is no side
restraint on the thrust mounts and the engine can be translated laterally
in the engine compartment by adjustment of the side mount tangential
link located at the top centerline of the engine. At engine station
244.44, is the rear engine mount, which consists of an adjustable verti-
cal link, hung from the wing/fuselage structure. The rear mount will
only react vertical load and will permit engine movement laterally as
well as fore and aft.

2-D Nozzle Description and Mounting--The augmentor duct and axisymmetric
C-D nozzle combination of the basic engine are removed and replaced with
the 2D Airframe Integrated Nozzle installation. A circular interface
between the engine and the 2-D AIN exhaust system is located aft of the
rear mount, but forward of the flameholder location and sealed by a gas
tight rolling-bellows. The flexible joint permits 3-axis movement,
accommodates thermal expansion, and isolates all nozzle loads from the
engine case.

The 2-D exhaust system features a two-dimensional variable geometry
centerbody wedge, capable of independent $A_8$ (primary nozzle throat area)
and $A_9$ (nozzle exit area) control installed in a fixed geometry duct.
The exhaust duct transitions from circular at the flexible seal joint
to "square" (super ellipse cross section) at the nozzle throat station.
The duct cross section remains constant from the nozzle throat station
to the nozzle exit station. Sidewall extensions form low drag booms and
provide centerbody wedge support aft of the nozzle exit plane. Inte-
grated airframe structure provides the pressure vessel and outer struc-
tural support for the afterburner liners, sidewalls, and centerbody
wedge. The variable area centerbody wedge is supported in four locations,

### 3.3  PROPULSION SYSTEM INSTALLATION (Continued)

all four share vertical loads and one location (A9 linkage) provides the axial force restraint.  Primary vertical load paths are through the A8 and A9 linkage to a structural box beam (located inside the centerbody wedge on the centerline) attached to the airframe structure.

The nozzle cooling system design for afterburner operation is comprised of two elements:

1)  All surfaces of the exhaust system upstream of the nozzle exit plane are cooled by fan discharge air;
2)  all the nozzle surfaces downstream of the exit plane are cooled by fan air (subsonically) or by ram air (supersonically).

Further, the cooling distribution system is designed to permit shutting off all cooling flow downstream of the throat plane (duct, sidewalls and centerbody wedge) during all non-augmented thrust modes.  This approach reduces the 2-D nozzle cooling flows to levels less than that required for typical axisymmetric augmentor ducts and C-D nozzles.

Thrust reversing and thrust vectoring capability can be easily incorporated into the centerbody wedge design.  In anticipation of future requirements, thrust reversing and vectoring capability has been included in propulsion system weight estimates.  A detail discussion of the 2-D Airframe Integrated Nozzle design features is presented in References 6, 7, 8 and 9.

Engine Installation and Removal--Installation of the gas generator is accomplished using a standard air-log trailer.  Adequate clearance below the body longeron allows direct placement of the engine below the engine mount lugs.  With the airplane stabilized with jacks or landing gear link locks, the engine is lifted vertically to the mount position.  Visual inspection of the process is provided through the upper access doors over the accessory bay and above the rear engine mount link.  Centering the engine on the two thrust mounts is done with lateral motion of the

60

## 3.3 PROPULSION SYSTEM INSTALLATION (Continued)

trailer. Attaching the rear engine mount to the rear mount frame will permit removal of the ground handling trailer. The inlet stub duct, which is telescoped forward during engine installation, is slid aft and clamped to the compressor face through the engine bay cowl panel. The exhaust nozzle flexible seal is clamped to the gas generator. Connecting fuel, electrical, hydraulic pneumatic, controls and power takeoff shaft to the airplane systems completes the gas generator installation. With inspection completed the non-structural access doors, top and bottom can be reinstalled.

### INSTALLED ENGINE PERFORMANCE

The J101/J/ Study A9 derivative engine provides increased takeoff thrust, increases in altitude combat thrust and improved dry thrust at supersonic cruise over the J101-GE-100. A comparison of the J101/J7 Study A9 and the J101-GE-100 uninstalled thrust levels at key LES flight conditions is presented in Figure 27.

The goal of the LES study is to achieve efficient supersonic cruise at Mach numbers from 1.6 to 2.0. This makes it desirable to operate the engine at intermediate power setting rather than a partial augmented power setting to achieve lower specific fuel consumption: (i.e, at Mach number 1.8 uninstalled specific fuel consumption at intermediate power is 15.5% less). As shown in Figure 28, the intermediate thrust lapse of the derivative engine cycle above Mach number 1.6 makes it difficult to achieve this goal.

Uninstalled engine data were corrected for installation effects using the methods described in "Propulsion System Installation Corrections", AFFDL-TR-72-147 Volumes I-IV. One exception is the bookkeeping of the total inlet spillage drag (reference spillage drag plus the power lever sensitive spillage drag), where the reference spillage drag is included

**61**
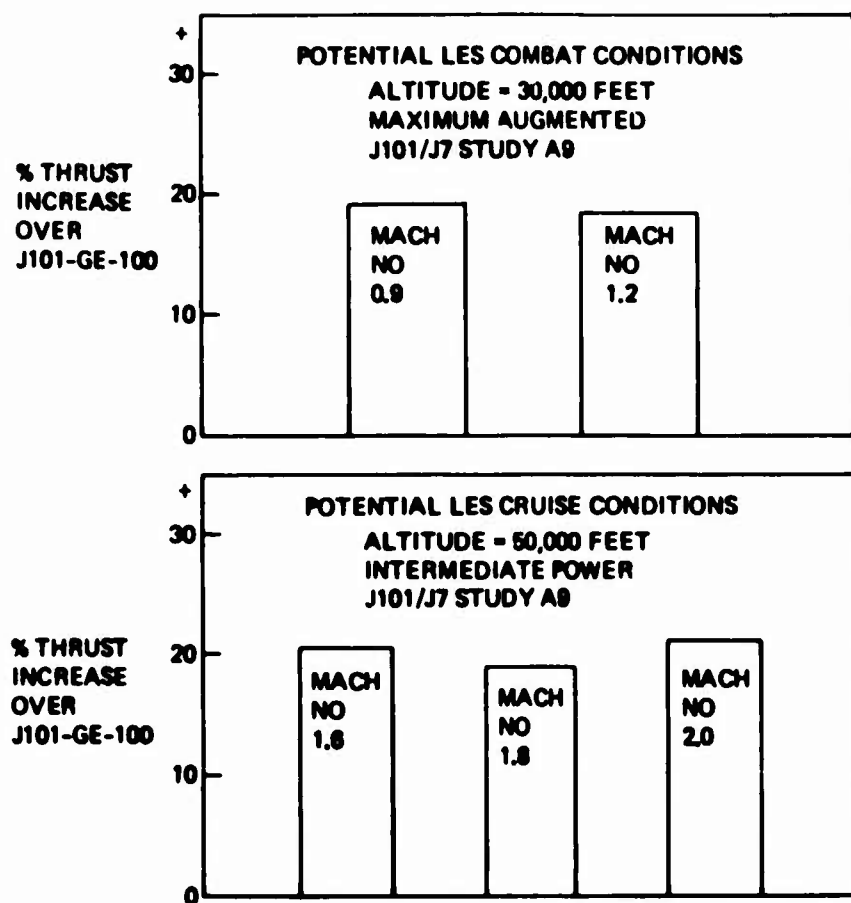
Figure 27. Uninstalled Thrust Comparison — J101/J7 Study A9 Versus J101-GE-100
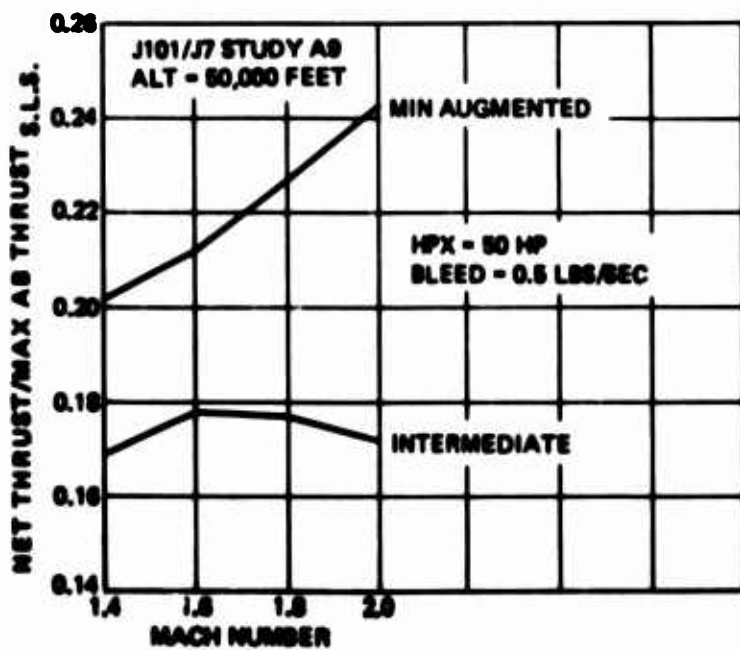


Figure 28. LES Baseline Uninstalled Engine Performance

3.3 PROPULSION SYSTEM INSTALLATION (Continued)

in the installed propulsion system performance. Appendix B further
expands the aero-propulsion bookkeeping methods relied upon in this
study.

Axisymmetric nozzle performance data were used in the exhaust system
installation because 2-D nozzle wind tunnel data was not available in
suitable TEM 333 format for installed engine performance calculations.
A wave drag increment for the 2-D wedge was estimated and included in
the airplane drag polar. Power sensitive afterbody drag estimates
(Figure 29) are based on the Boeing Light-Weight Fighter F-100 nozzle
installation. Subsequent to this LES airplane study, the 2-D AIN wind
tunnel test results were used in an axisymmetric C-D nozzle versus 2-D
nozzle/afterbody evaluation study. This study indicates the above
assumptions are representative of 2-D nozzle/afterbody performance
levels.

Installation penalties as a percentage of uninstalled thrust at the LES
cruise condition are shown in Figure 30. The penalties include the
effects of 50 horsepower extraction and 0.5 lbs. per second high pres-
sure bleed. Note, the installation losses cause a more severe inter-
mediate thrust lapse at Mach numbers above Mach number 1.6 as illus-
trated in Figure 31.
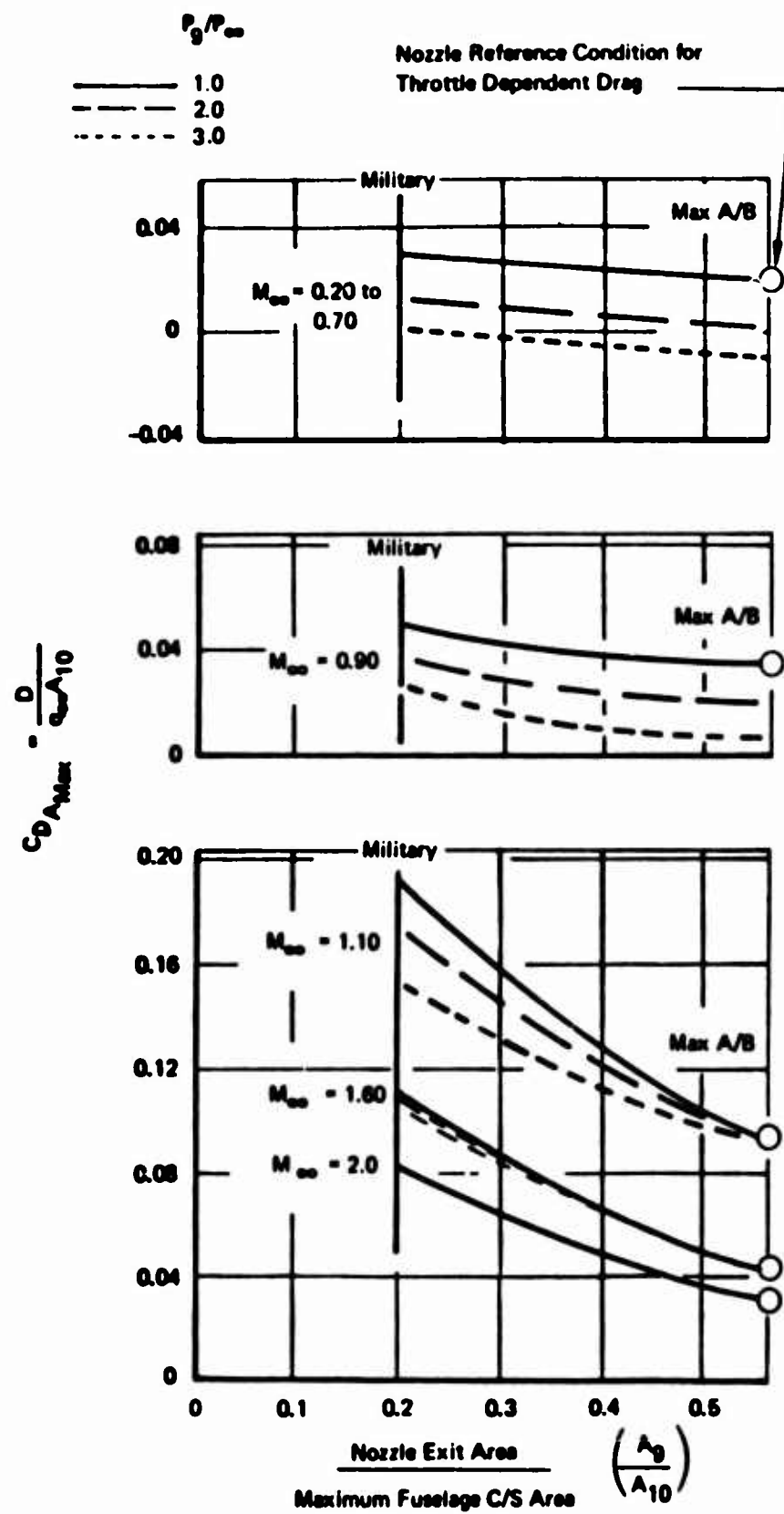
Figure 29. Power Sensitive Aftbody Drag Estimates

**Figure 30.    Installation Penalties at LES Cruise Conditions**
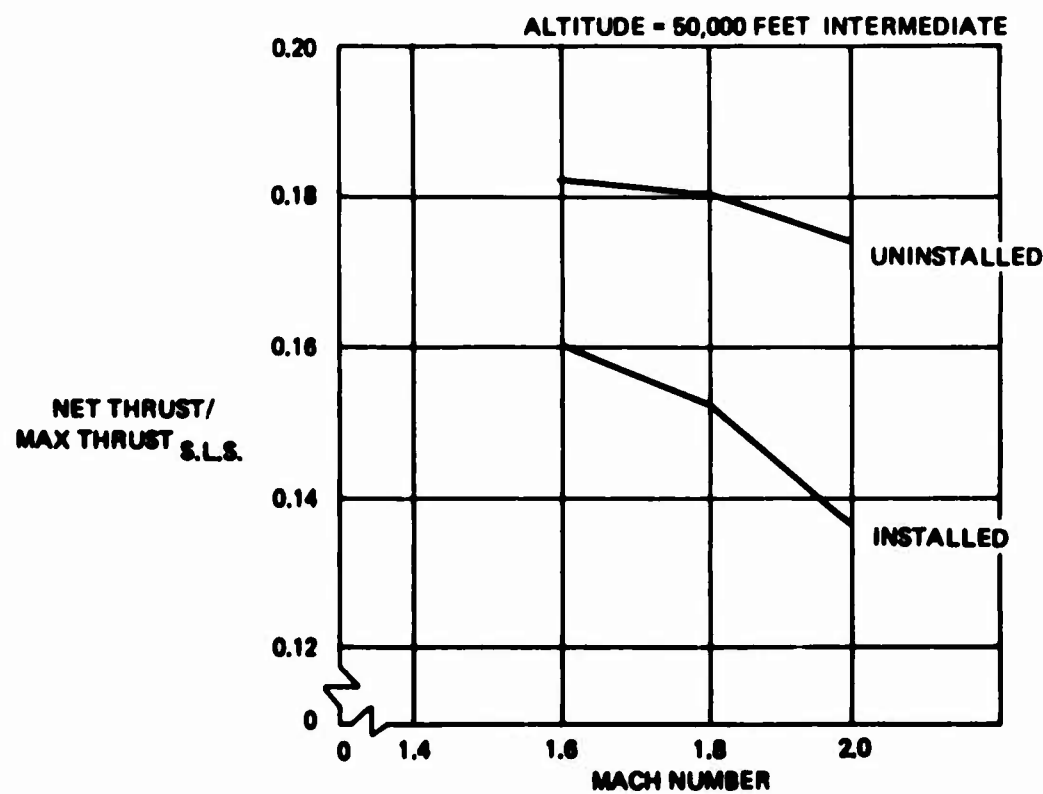


**Figure 31.    LES Baseline Engine Installed Thrust**

3.3  PROPULSION SYSTEM INSTALLATION (Continued)

INLET SELECTION AND DESIGN

An inlet trade study was completed to define the type of inlet which
best matched the LES airplane and the J101/J7 Study A9 engine.  Inlet
geometries reviewed were as follows:

1.  Two-dimensional, three ramp, two ramps variable (Baseline inlet
    for the airplane trade studies).
2.  Two-dimensional, two ramp, one ramp variable.
3.  Two-dimensional, two ramps fixed.
4.  Axisymmetrical half round, three shock, variable body.
5.  Axisymmetrical half round, two shock, fixed centerbody.

All the above inlets were designed for Mach number 2.0 plus operation
in fighter applications.  Each inlet was matched to the J101/J7 Study
A9 engine requirements.  Capture areas for the fixed geometry inlets
were sized in the transonic region and for the variable geometry inlets
at Mach number 1.6.  The effects of ram recovery, bleed drag, spillage
drag, and reference drag were included in the inlet performance.  In
all cases spillage drag increased rapidly above Mach number 1.6 due to
the steep lapse in engine airflow required relative to inlet airflow
supply.

An incremental structure plus cruise fuel weight comparison was completed
for each inlet concept.  A cruise point at Mach number 1.8, altitude
50,000 feet for the -202 configuration was selected for this comparison.
Intermediate thrust was assumed for the entire cruise leg by the mission
(200 n.mi. radius).

Figure 32 presents the increased fuel required to complete the cruise
leg of the mission for each inlet concept relative to the two-dimensional,
three ramp, two ramps variable inlet.  (Baseline inlet for the Parametric
Airplane Study).

3.3 PROPULSION SYSTEM INSTALLATION (Continued)

Class 1 (preliminary) weight estimates were made for each inlet concept based on a constant overall inlet length, Figure 33. The weights were referenced to the two-dimensional, three ramp, two variable ramp inlet (baseline for the Parametric Airplane Study).

The summary results presented in Figure 34 show the two-dimensional, 2 ramp, 1 variable ramp inlet minimizes the incremental structure plus cruise fuel weight. However, all inlets except the half round fixed are very near the minimum incremental structure plus cruise fuel weight.

An incremental number of supersonic turns comparisons was also made for each inlet concept. A constant takeoff gross weight was assumed for the -202 airplane configuration. Operating empty weight was adjusted by the incremental inlet weight. Cruise fuel weight was adjusted for inlet cruise performance ( M - 1.8, Alt. = 50,000 ft.). The remaining fuel was used for turns at Mach 1.8, altitude 50,000 feet and $P_S$ = 0. Figure 35 presents the results of the incremental number of turns comparison relative to the two-dimensional, three ramp, two ramps variable inlet. These results again show all inlet concepts except the half round fixed geometry inlet similar performance.

Based on the above comparisons a two dimensional, two ramp, one ramp variable inlet was selected for the final performance estimates. The configuration for this inlet is shown in Figure 36. The ramp geometry was designed for maximum recovery with shocks on the lip at Mach number 2.2 in anticipation of receiving engine data to Mach number 2.2 (present engine data is limited to Mach 2.0). With the selected fixed ramp angle the second ramp is positioned to achieve near optimum recovery at each Mach number.

Figures 37 through 43 present the inlet performance curves used in generating the installed engine performance data. The inlet recovery

67

## 3.3 PROPULSION SYSTEM INSTALLATION (Continued)

(Figure 37) was computed from supersonic shock losses and subsonic diffuser losses using diffuser loss coefficient, $\Delta P_T/q = 0.12$. The recovery and mass flow ratio for engine match airflow (Figures 38 and 39) were calculated from Figure 37 and the J101/J7 Study A9 engine maximum corrected airflow. The buzz and distortion limits for the inlet are shown in Figure 40.

Boundary layer bleed mass flow rates are plotted against mass flow ratio and Mach number in Figure 41. With this bleed the inlet should be stable over the range of engine corrected flow variation due to altitude changes.

Reference mass flow ratio and reference spillage drag are presented in Figure 42. Bleed drag and spillage drag coefficients are presented in Figure 43 and for the LES study the reference spillage drag was included in the total spillage drag coefficient shown in Figure 43. Normally, the reference spillage drag increment (shown in Figure 38) would be included in the aerodynamic drag, in accordance with the aero-propulsion force accounting procedure documented in Reference (10).

Developing an efficient inlet for flight at Mach numbers up to 2.0 requires detailed analytical studies and wind tunnel testing to investigate inlet recovery, drag, engine/inlet compatibility, and inlet/airframe integration. Unfortunately, it is not usually possible to make all these important investigations in detail during preliminary studies of candidate configurations. For preliminary studies at Boeing, the TEM 333 computer program (PITAP procedure + modifications) is used to calculate installed engine performance. This program uses the set of inlet maps shown in Figures 37 through 43. For purposes of preliminary estimates of inlet/engine compatibility, buzz and distortion limits are included in input data to help avoid regions of possible problems that may require studies in greater detail.
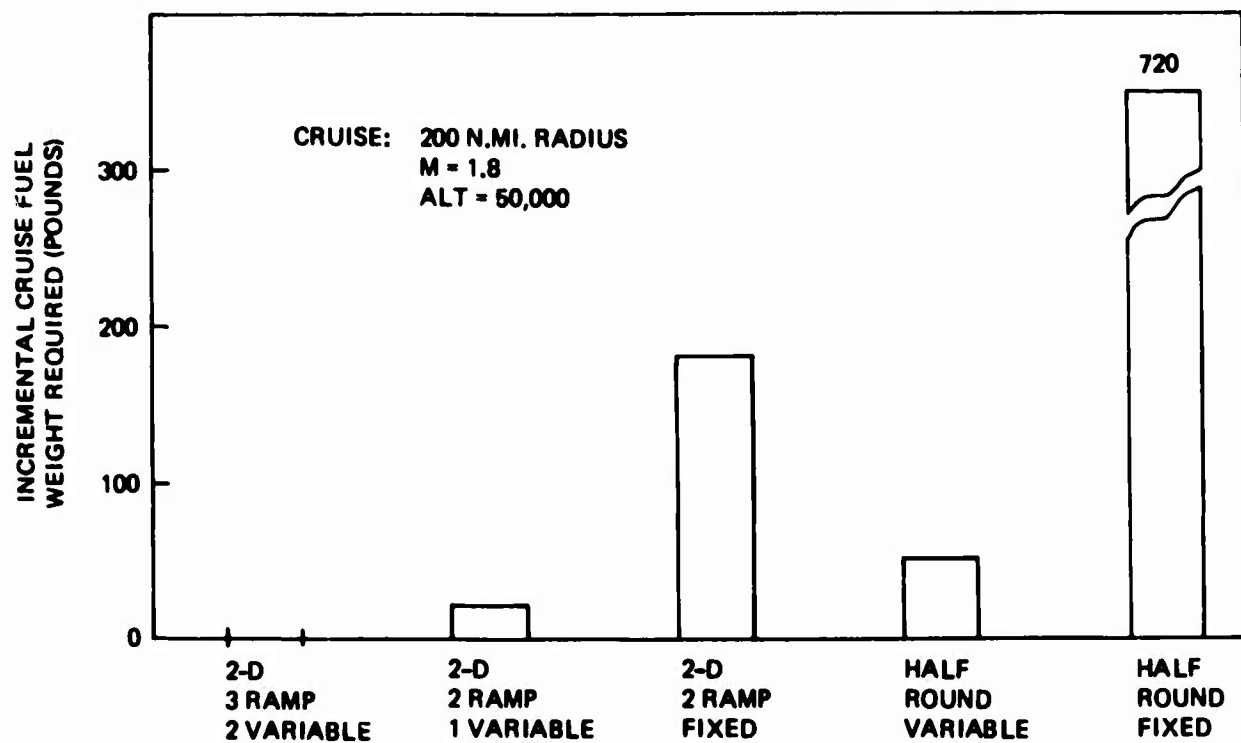
Figure 32.   Inlet Trades — Incremental Cruise Fuel Weight Required
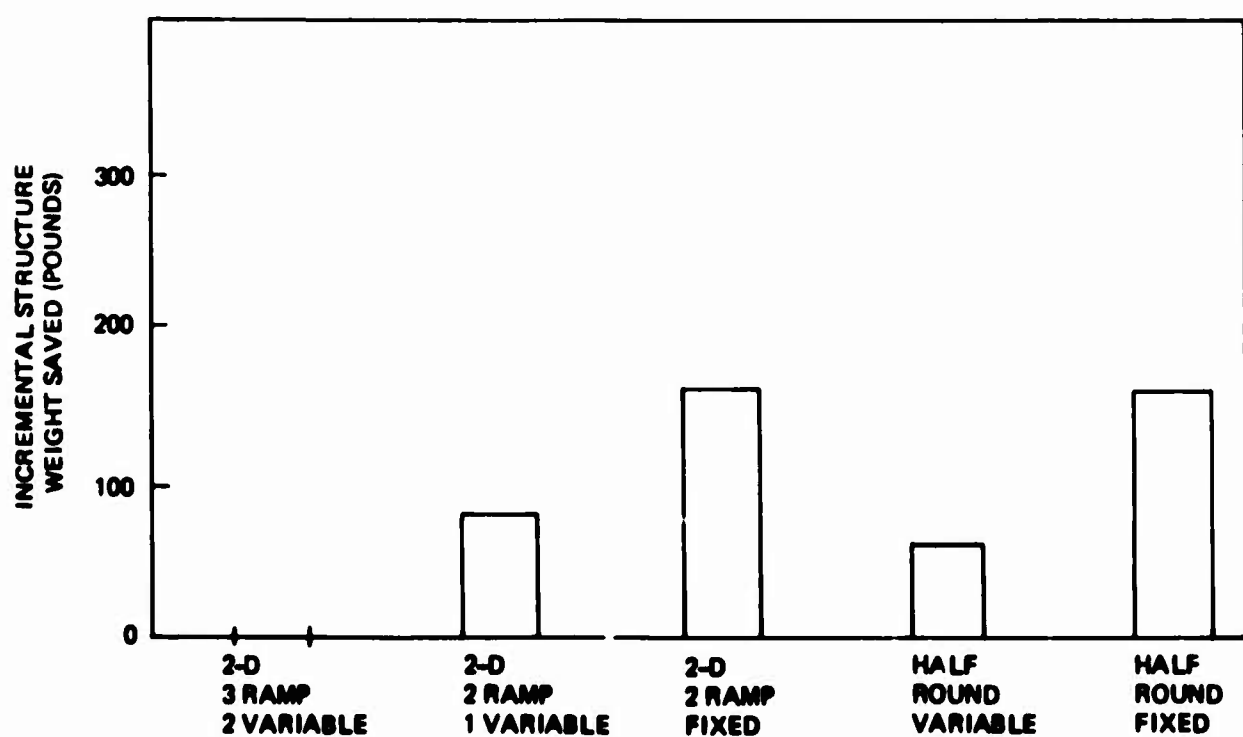


Figure 33.   Inlet Trades — Incremental Structural Weight Saved

69
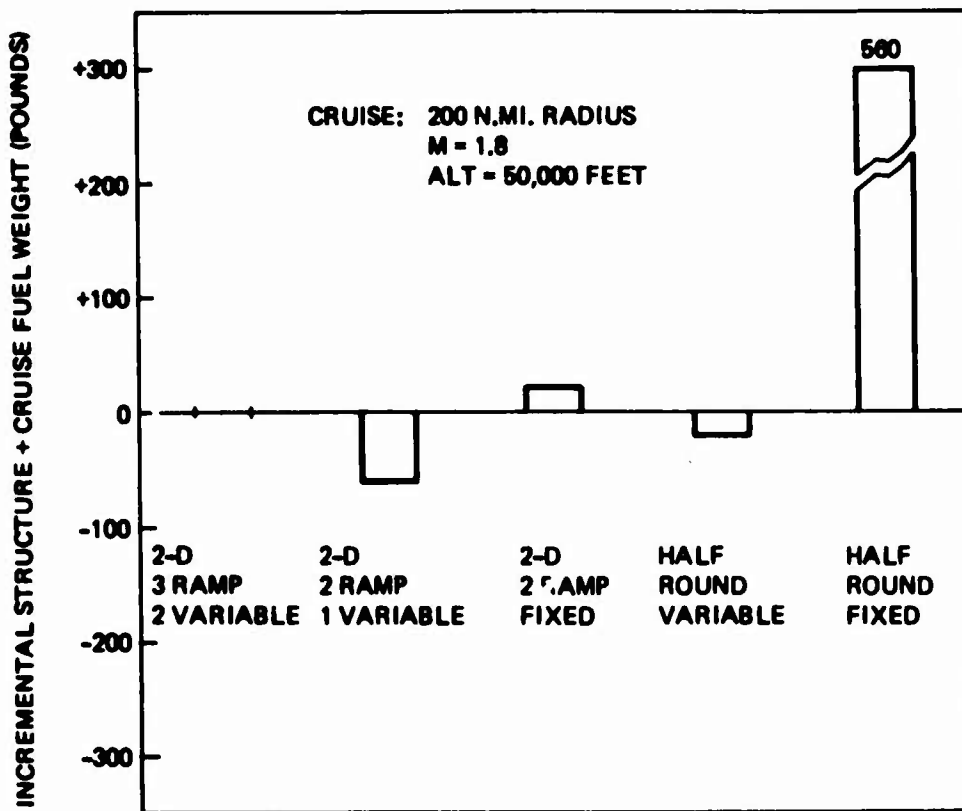
Figure 34. Inlet Trades — Incremental Structural Plus Cruise Fuel Weight

| CRUISE: 200 N.MI. RADIUS, M = 1.8, ALT = 50,000 FEET<br>TURNS: M = 1.8, ALT = 50,000 FEET, $P_S$ = 0 | |
|---|---|
| | Incremental number of turns |
| 2–D, 3 ramps, 2 variable | 0.0 |
| 2–D, 2 ramps, 1 variable | +0.15 |
| 2–D, 2 ramps, fixed | –0.30 |
| 1/2 Round, variable | –0.05 |
| 1/2 Round, fixed | –1.94 |

Figure 35. Inlet Trades — Incremental Number of Turns

70
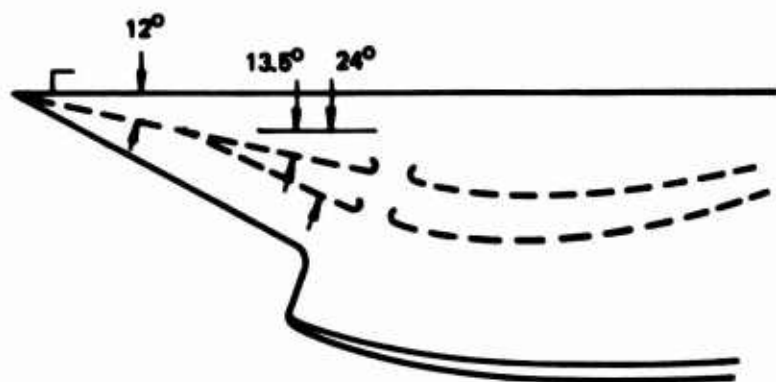
A CAPTURE = 4.07 FEET$^2$ @ M = 1.6 ENGINE DEMAND

Figure 36.    M = 2.20 Inlet Configuration
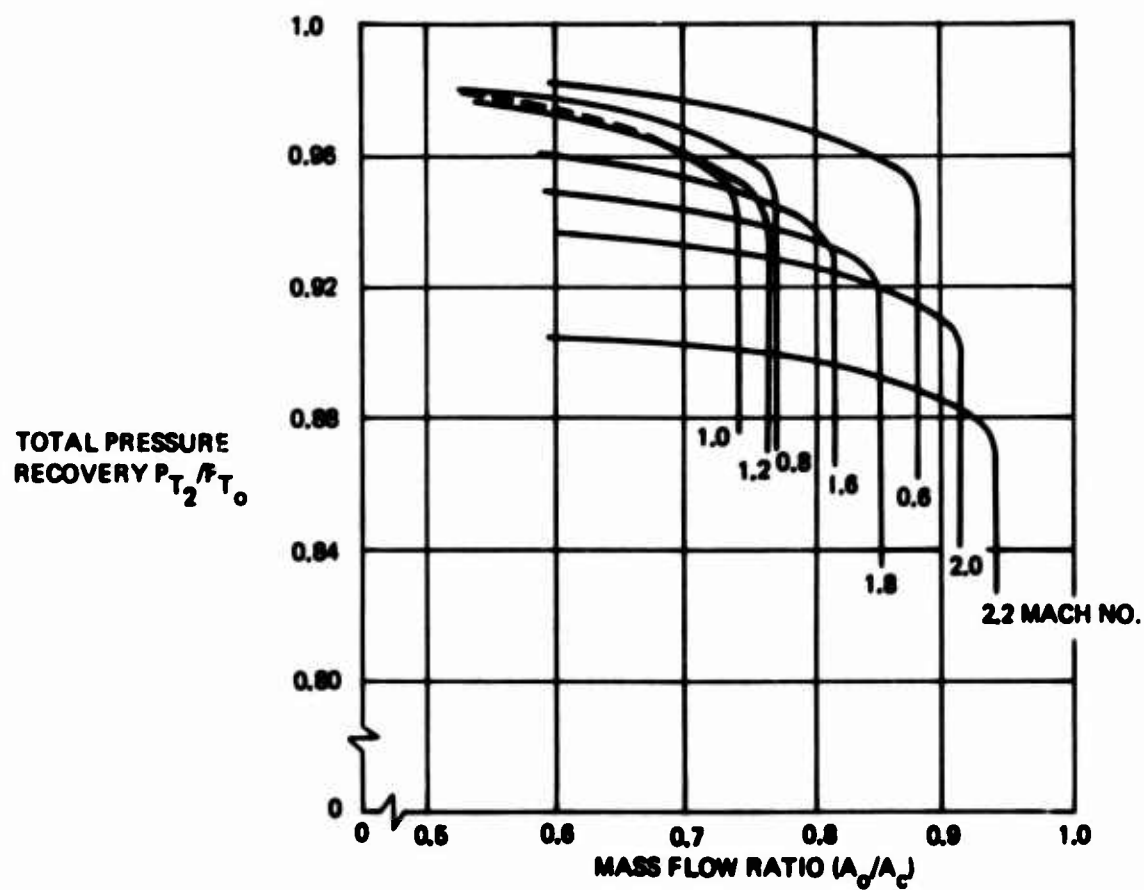


Figure 37.    Inlet Recovery Versus Mass Flow Ratio
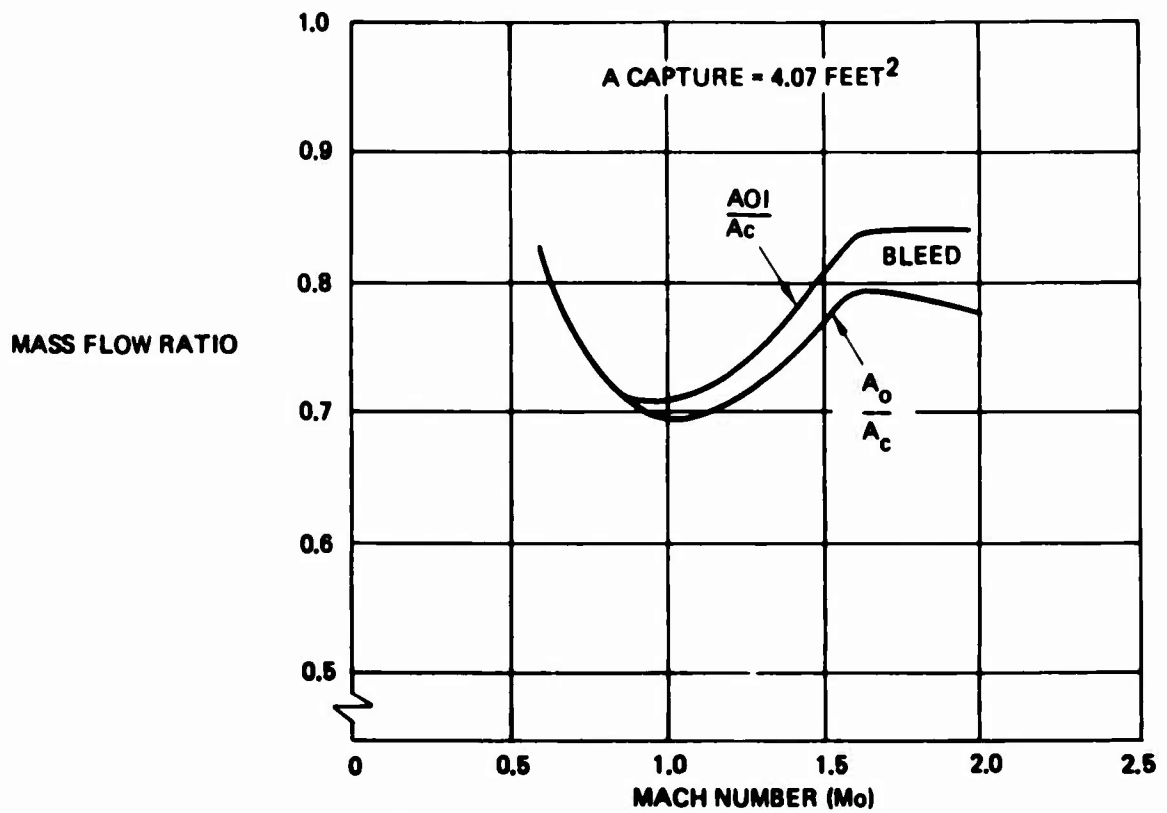
Figure 38. Mass Flow Ratio for Engine Match Airflow
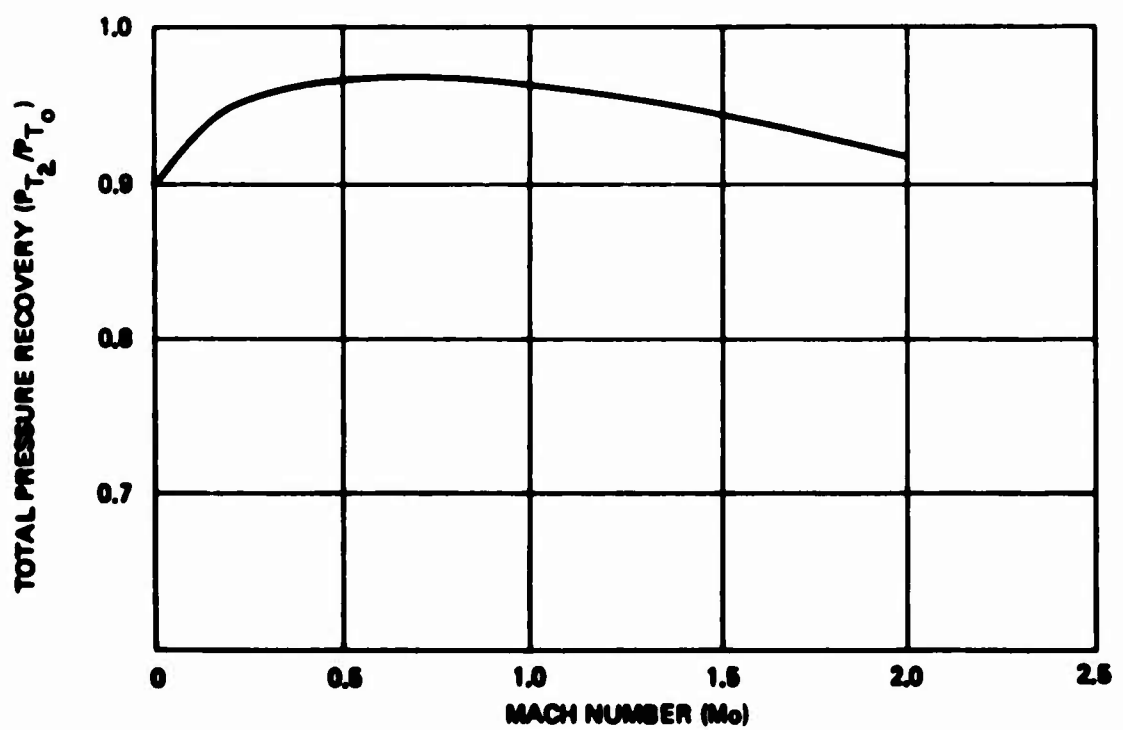


Figure 39. Inlet Recovery for Engine Match Mass Flow

72
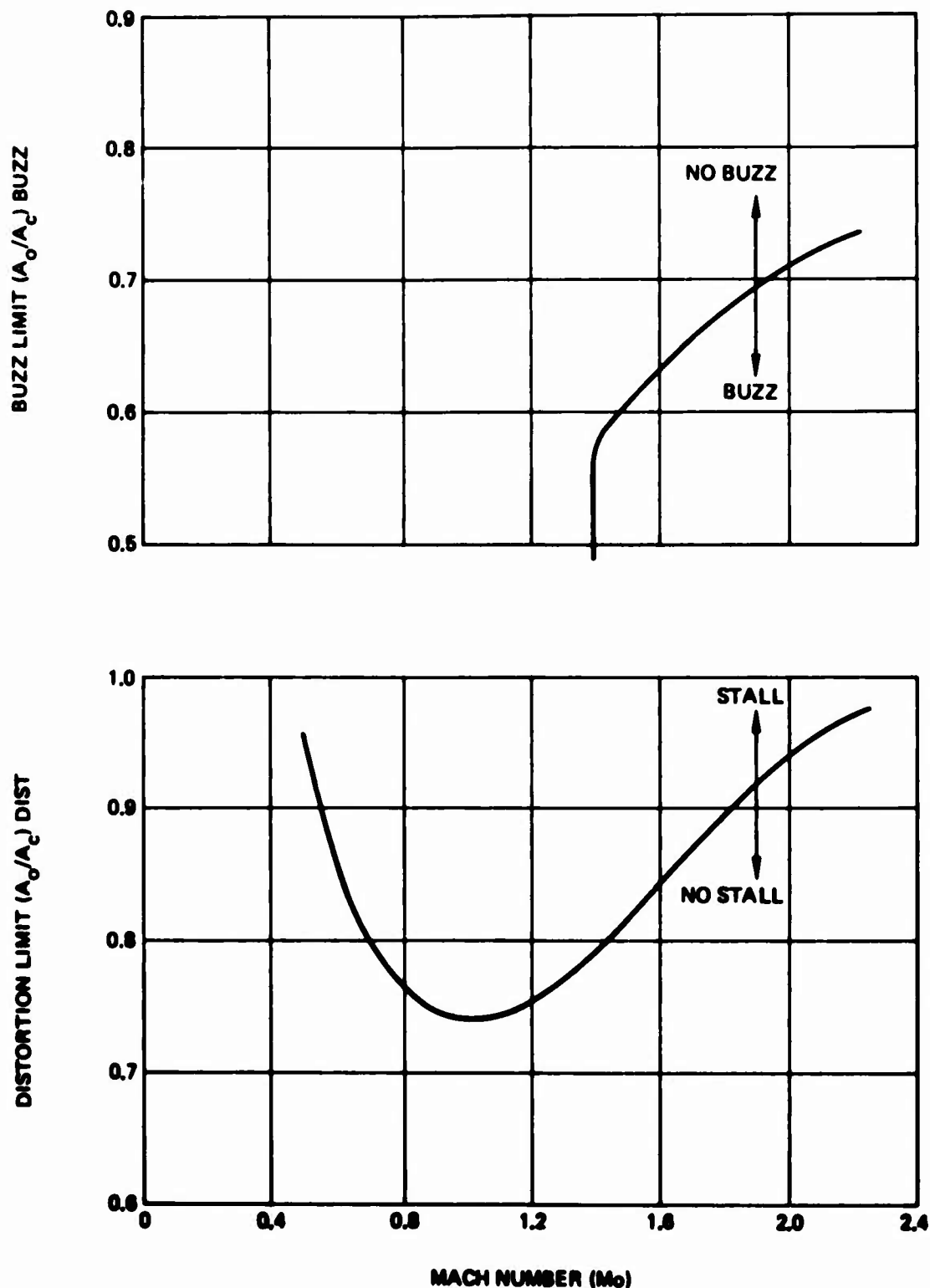
Figure 40. Buzz and Distortion Limits
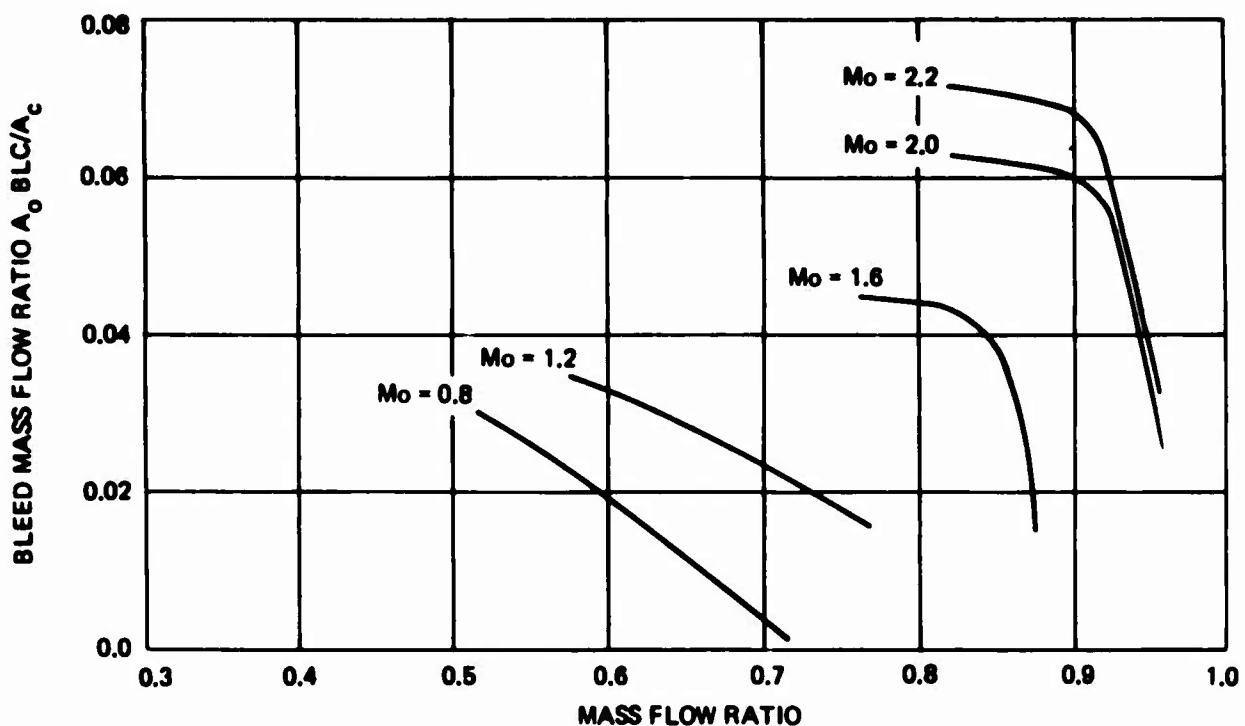
Figure 41. Bleed Mass Flow
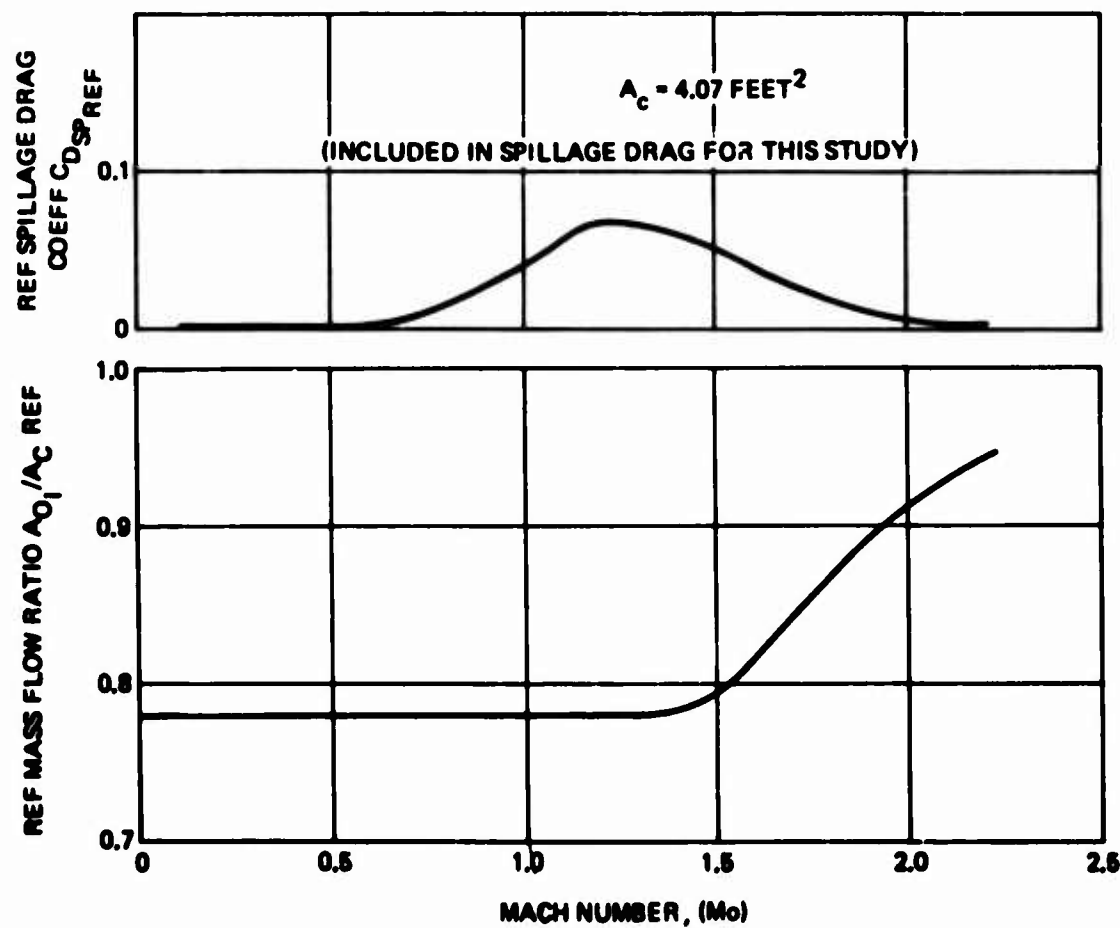


Figure 42. Reference Mass Flow Ratio and Spillage Drag Coefficient
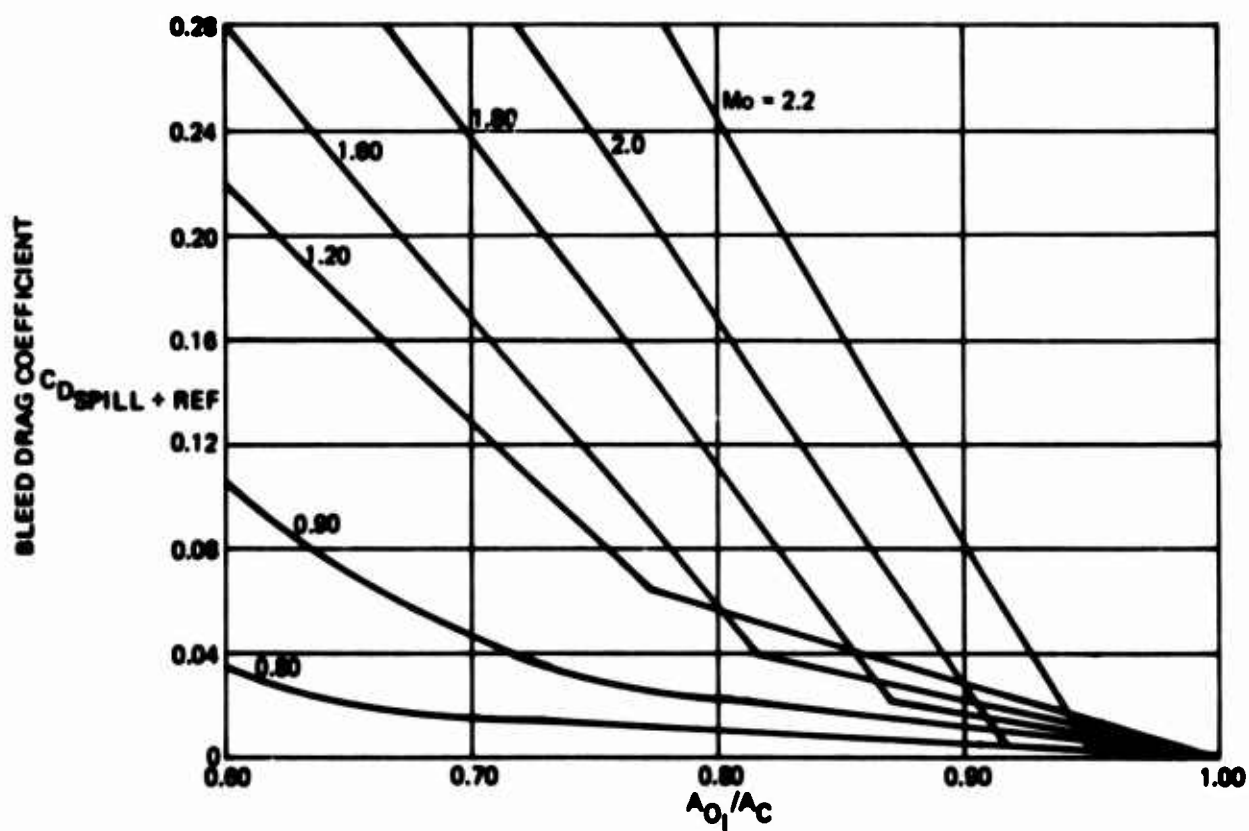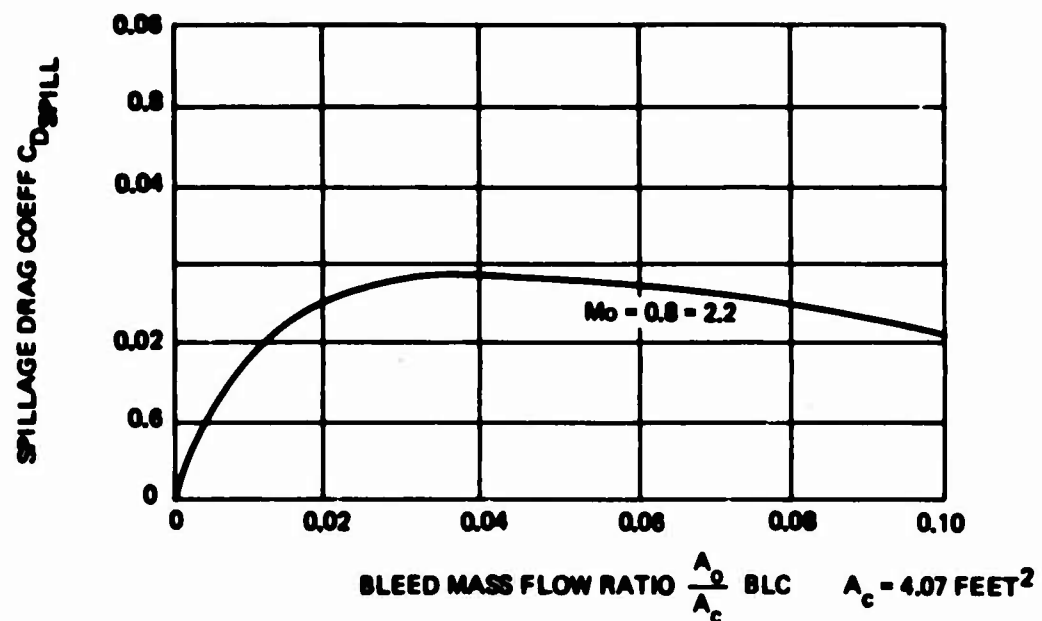
Figure 43. Bleed and Spillage Drag

## 3.3 PROPULSION SYSTEM INSTALLATION (Continued)

Flight test experience with the General Dynamics F-16 has demonstrated
that the under-fuselage inlet location is favorable from the standpoint
of inlet total pressure recovery and inlet/engine compatibility through-
out the flight and maneuver envelope of the airplane (Reference 11).
Boeing wind tunnel tests (Reference 12) for the proposed Boeing LWF
design also demonstrated the under-fuselage inlet location provides
satisfactory total pressure recovery and inlet/engine compatibility
over a wide range of angles of attack, yaw, and Mach number.

### FUEL SYSTEM

Internal fuel is contained in integral fuselage and wing tanks with a
capacity of 3630 pounds (560 gallons) of JP-4 fuel. Provision is made
for carrying 300 gallons of extra fuel in two body conformal drop tanks.
Two main tank compartments are located within, and on each side of the
aircraft fuselage with a single collector tank containing the booster
pumps. This compartmented main tank contains 2430 pounds of fuel. The
wing structure itself is used to form two integral tanks, bounded by
the front and rear spars and between side of body and 100% semi-span
the total wing capacity is 1200 pounds. Wing tip fins house surge tanks
and overboard vents. The tanks are connected to form two groups, each
half of the system can maintain full demand of the engine, thus pro-
viding 50% compartmentization. All tanks incorporate water sump drains.

Fuel pressure at the engine fuel pump inlet shall be maintained at not
less than 5 psi above the true vapor pressure of the fuel and not greater
than 50 psig with a vapor liquid ratio of zero. For design considera-
tions, the aircraft fuel system will be capable of providing fuel flows
as high as 40,000 pph to the engine fuel inlet. The engine has been
designed for operation with fuel that meets the requirements of MIL-T-
5624 grade JP-4 and JP-5, ASTM Types A and B, and NATO Fuel No. F-40
and F-44.

## 3.3  PROPULSION SYSTEM INSTALLATION (Continued)

Engine Feed--Two electrical boost pumps are mounted within a negative "g" housing, located in the bottom of the main tank to maintain a positive pressure at the inlet of the engine driven fuel pump. (Multiple pumps are installed for redundancy and flight reliability). Fuel is allowed to bypass the pump for suction feed or suction defueling. In the event of multiple pump failure, tank pressure and fuel head will help maintain adequate fuel supply. The negative G sump is kept full via normal transfer through balanced spring loaded check valves and during maneuvers or aircraft rapid descent at high negative angles of attack by jet pumps located in the bottom of the main tank operated by fuel supplied from the boost pumps.

Transfer and Vent--Air pressure is supplied to the external drop tank via twin body connections. If these tanks are not used, the air is passed directly to the wing tanks. Fuel is transferred from the lowest point in the wing tank to the highest point in the main tank. Fuel transfer for c.g. control is available over the limits shown in Figure 44. Vapor release valves are located in the top of the main tank float operated to release to the vent system any air or fuel vapors evolved from the fuel or transferred during maneuvers in order to maintain a full main tank.

Pressurization--To allow aircraft operation at high altitude with volatile fuels, it is necessary to pressurize the tanks to suppress fuel boiling. As a positive 5 psig pressure is required for all design missions, it has been found to be practical and economical to pressurize the tanks all the time and utilize this pressure energy for fuel transfer. Pressure is supplied from the engine compressor through a filter and dehumidifier to a control valve. Duplicate reducing valves reduce this high pressure to 10 psig. The pressure control valves relieve excess pressure above 12 psig to the vent system. This valve is overridden (if failed) to allow air to enter the tanks. During ground refueling, pressure is sensed within the refueling line that relieves the tank pressure and allows a greater refueling rate to be obtained.
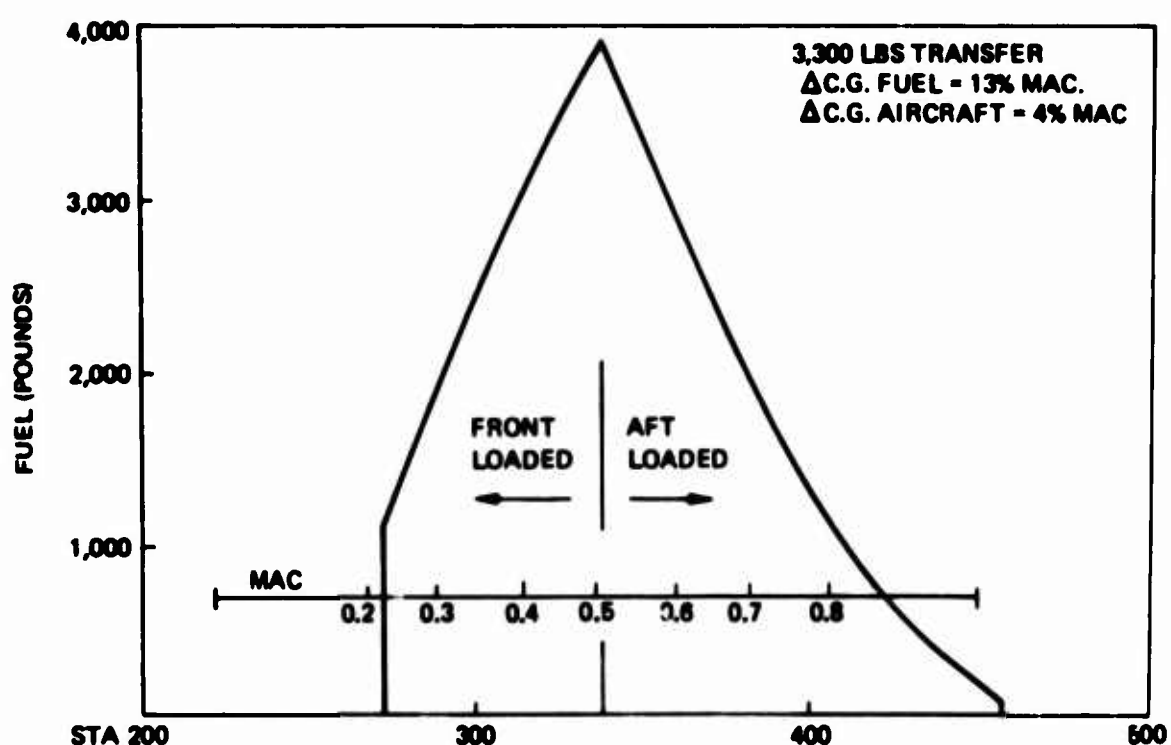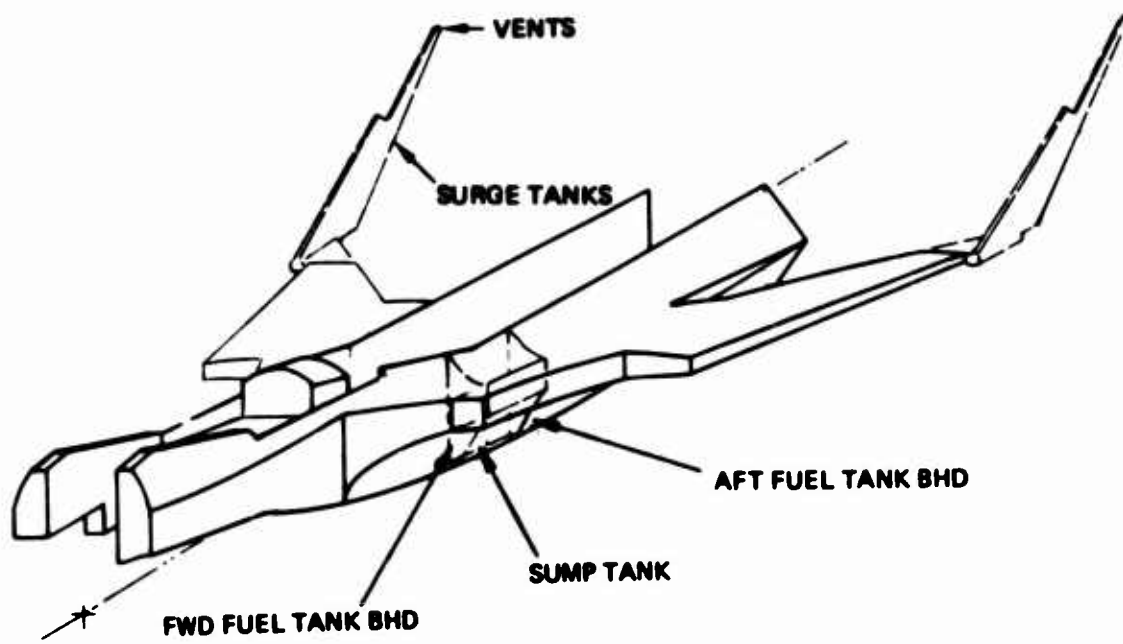
Figure 44. Fuel Transfer Envelope

## 3.4 AERODYNAMICS

This section describes the aerodynamic characteristics of Model 985-213. Complete drag polars, non-lifting elements, camber effects and trim penalties are included along with lift and pitching moment characteristics. The principle methods for aerodynamic estimating are found in Appendix C and the NASA/Boeing Program for supersonic Computer Aided Design (Reference 13). Flexible leading edge variable camber devices were employed to further augment the low wing loading and high thrust to weight ratio effects on transonic maneuver. The impact of these devices and of the basic wing characteristics at subsonic speeds was estimated based on methods derived from previous test data. (Reference 14).

Since the goal of LES is dry thrust cruise at M = 1.8 it is imperative that all drag items be minimized at this condition. Table 3 summarizes the zero lift drag buildup and indicates that wave drag contributes 29% to the total. This study then emphasized the importance of "other" drag items such as excrescence, and miscellaneous items.

These estimates were made from the 985-212 general arrangement drawing. Configuration differences between the -212 and -213 are minor. The associated cross-sectional area distribution shown in Figure 45 was used for wave drag estimates. Notice that the distribution closes to the fully expanded jet area. Therefore, the wave drag increment for the wedge is included in the airplane drag polar. Other elements of non-lifting drag are tabulated in Table 4 and added to the camber and trim drag to produce the total drag at zero lift $(C_{D_0})$ for all cruise speed regimes. Table 4 also identifies individual elements of the miscellaneous drag terms.

Missile drag has been minimized by the semi-submerged installation. No further improvement is expected for an external installation. Internal carriage and tube launch should be investigated.

Table 3. LES-213 Non-Lift Dependent Drag at Mach 1.8, 50,000 Feet

| Drag Component | $C_D$ |
|---|---|
| Wave drag[*] | 0.00497 |
| Skin friction | 0.00587 |
| Excrescence | 0.00183 |
| Inlet diverter | 0.00090 |
| Misc. items | 0.00333 |
| Total | 0.01690 |
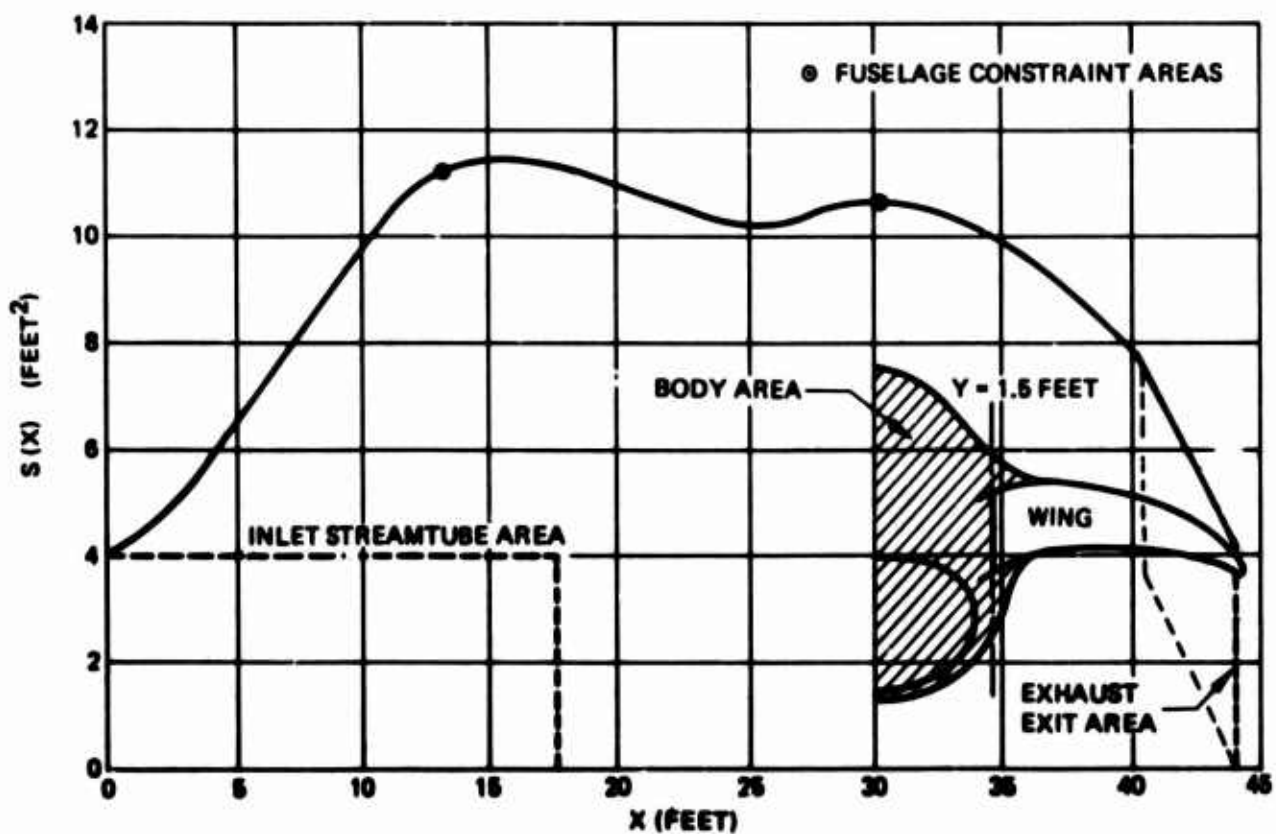


Figure 45. LES-213 Body Area Distribution

## 3.4 AERODYNAMICS (Continued)

Minimum supersonic trim drag has been pursued through wing and body cambering for a design point of Mach 1.8 at 50,000 feet. The basic wing only design characteristics shown in Figure 46 result in the wing twist shown in Figure 47. Airfoil thickness distribution based on the Boeing MAR 55 Section was used (see Section 5.5). Elevon lift and pitching moment drag-due-to-lift characteristics shown in Figure 48. Result in the trim drag characteristics shown in Figure 49. Flying the c.g. locations aft of 0.5 MAC could produce a negative trim drag at higher load factors. The validity of this estimate remains to be verified with wind tunnel data.

The sum result of the preceding estimates are shown in drag polar form in Figures 50 and 51 (c.g. at 55% MAC) for the subsonic Mach = 0.9 condition and for supersonic conditions of Mach = 1.2, and Mach = 1.8, respectively. Subsonic maneuver characteristics are shown with estimated improvements for the flexible skin, variable camber leading and trailing edge devices with trim maintained at 0.55 MAC. Although the maximum benefit curve was used as the performance basis, significant development work would be required to achieve this level with a tailless airplane since trimming must consider the use of wing tip deflections, thrust vectoring, or span-wise warping of the V.C. leading edge. The lower "conservative" estimate represents a level obtainable through L.E. devices alone leaving the trailing edge unburdened for trim. At Mach 1.2 the influence of leading edge flaps is not expected to provide a large improvement so until the effects can be verified, it has been omitted.

Drag for intermediate Mach numbers between 1.2 and 1.5 was interpolated between the two curves in Figure 51. A more refined analysis was not warranted within the scope of this study.

*Table 4. Summary of Zero Lift Drag Estimates*

| Components | M = 0.9 30,000 Feet | M = 1.2 30,000 Feet | M = 1.8 50,000 Feet |
|---|---|---|---|
| Wing $(A_{wet} = 383\ FT^2)$ | 0.00354 | • | 0.00518 |
| Skin friction | 0.00349 | 0.00319 | 0.00305 |
| Form | 0.00005 | —— | —— |
| Wave | —— | • | 0.00213 |
| Body $(A_{wet} = 324\ FT^2)$ | 0.00340 | • | 0.00367 |
| Skin friction | 0.00247 | 0.00226 | 0.00214 |
| Form | 0.00009 | —— | —— |
| Wave | —— | • | 0.00182 |
| Interference (wing-body) | 0.00084 | • | -0.00029 |
| Vertical tails $(A_{wet} = 74\ FT^2)$ | 0.00186 | • | 0.00099 |
| Skin friction | 0.00077 | 0.00071 | 0.00068 |
| Form | 0.00001 | —— | —— |
| Wave | —— | • | 0.00035 |
| Interference (vertical- wing) | 0.00108 | • | -0.00004 |
| Excrescence | 0.00150 | 0.00220 | 0.00183 |
| Inlet diverter • • | 0.00070 | 0.00110 | 0.00090 |
| Misc items | 0.00133 | 0.00333 | 0.00333 |
| Canopy | 0.00025 | | |
| Gun fairing | 0.00010 | 2.5 Factor | 2.5 Factor |
| UHF/IFF antennas (2) | 0.00005 | applied to | applied to |
| Fuel tank vents (4) | 0.00001 | M = 0.9 | M - 0.9 |
| Nav Beacon | 0.00001 | estimate | estimate |
| Air data probe | 0.00011 | | |
| Missiles (2 semi-submerged) | 0.00080 | | |
| Total non-lifting drag | 0.01333 | 0.01875 | 0.01690 |
| Camber and trim drag at $C_L = 0$ | 0 | 0.00770 | 0.00780 |
| Total drag at $C_L = 0$, $C_{D_0}$ | 0.01333 | 0.02645 | 0.02470 |

$S_{ref} = 250\ feet^2$

• Not itemitized; total $C_{D_W}$ @ M = 1.2 = 0.00412

• • Inlet/nozzle reference drag included in engine data

82
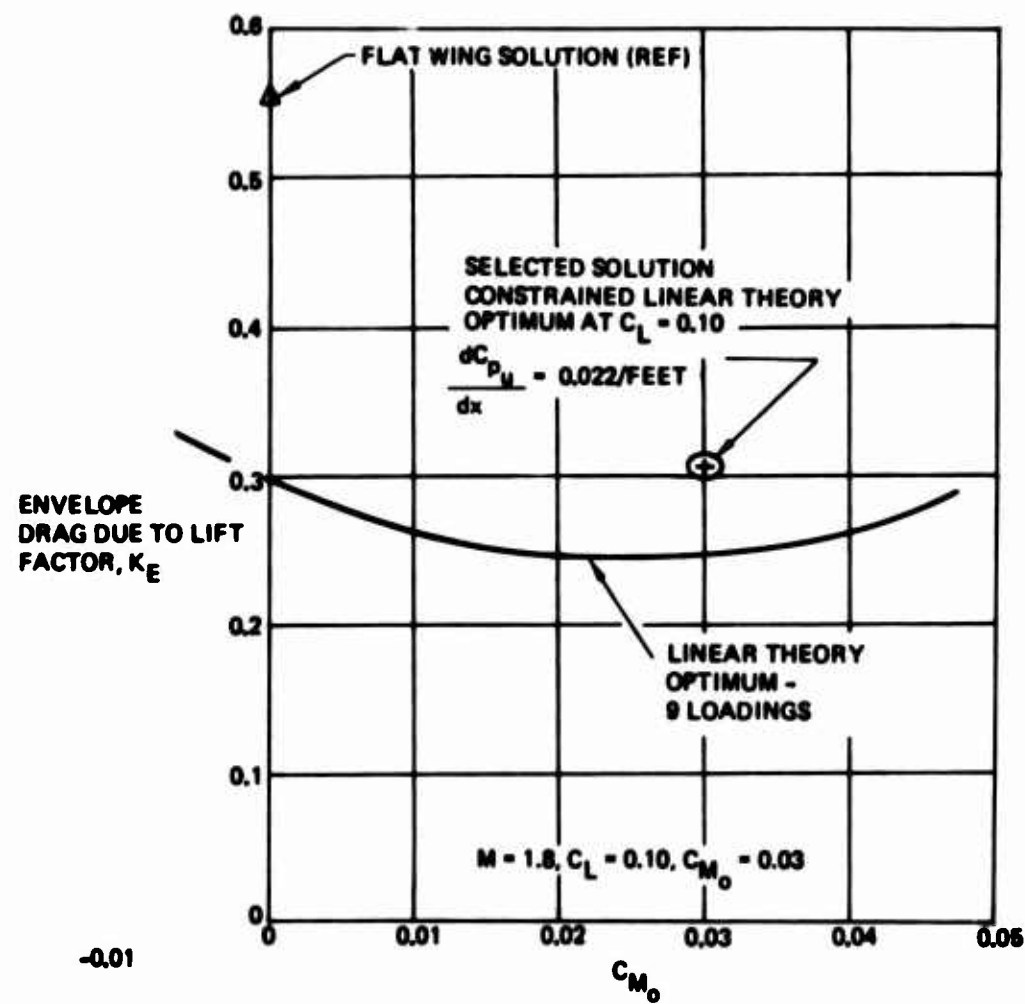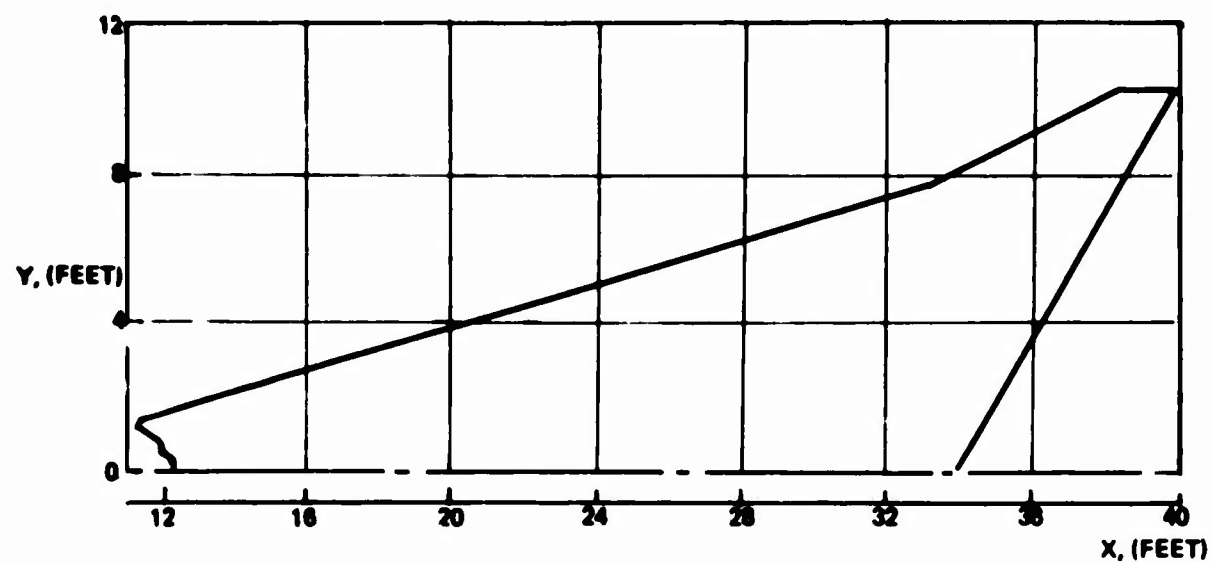
Figure 46. Wing Design Solution
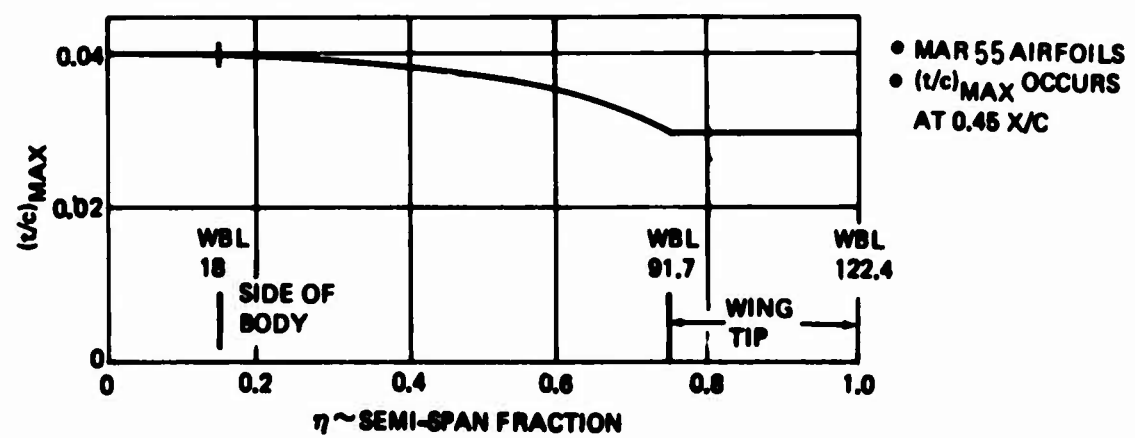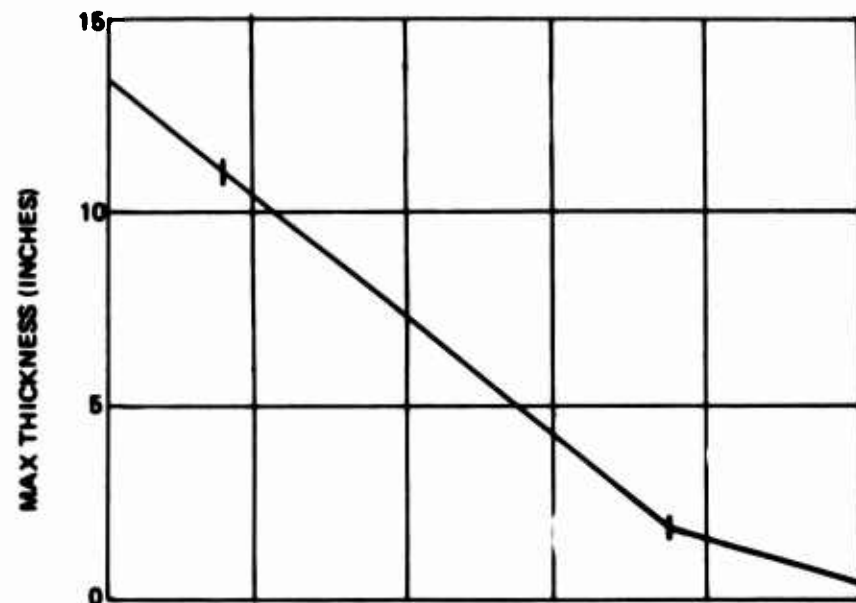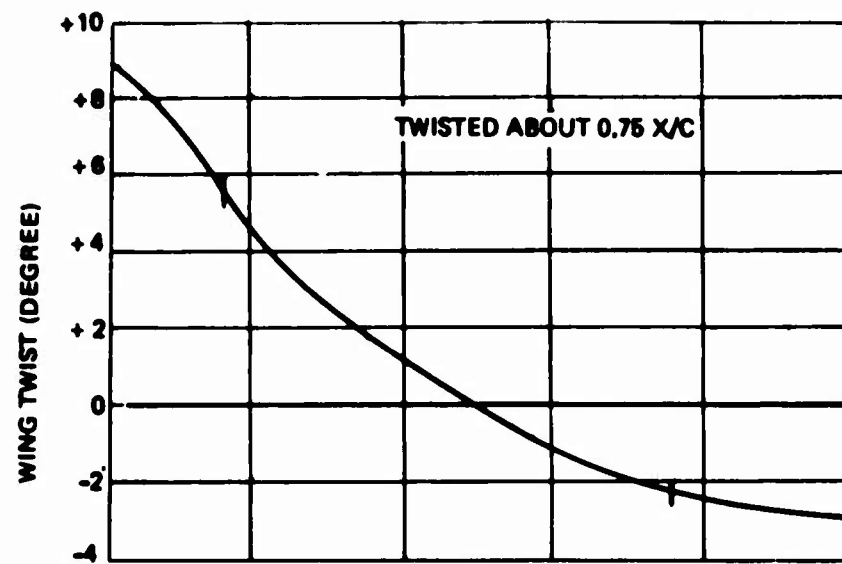
Figure 47. Wing Thickness and Twist Distributions
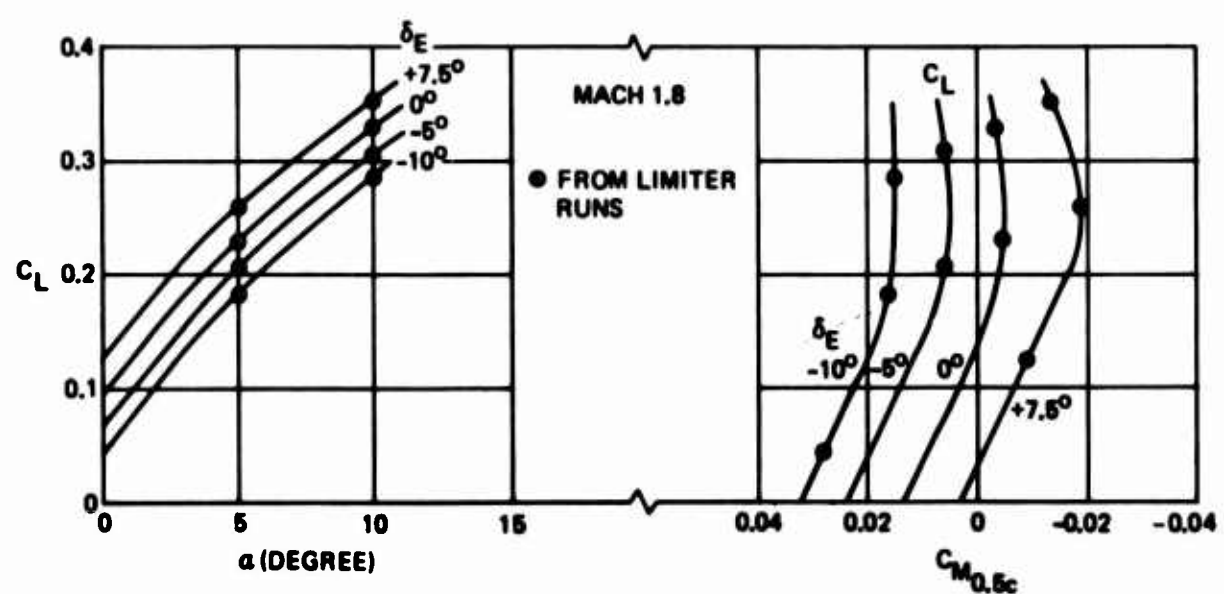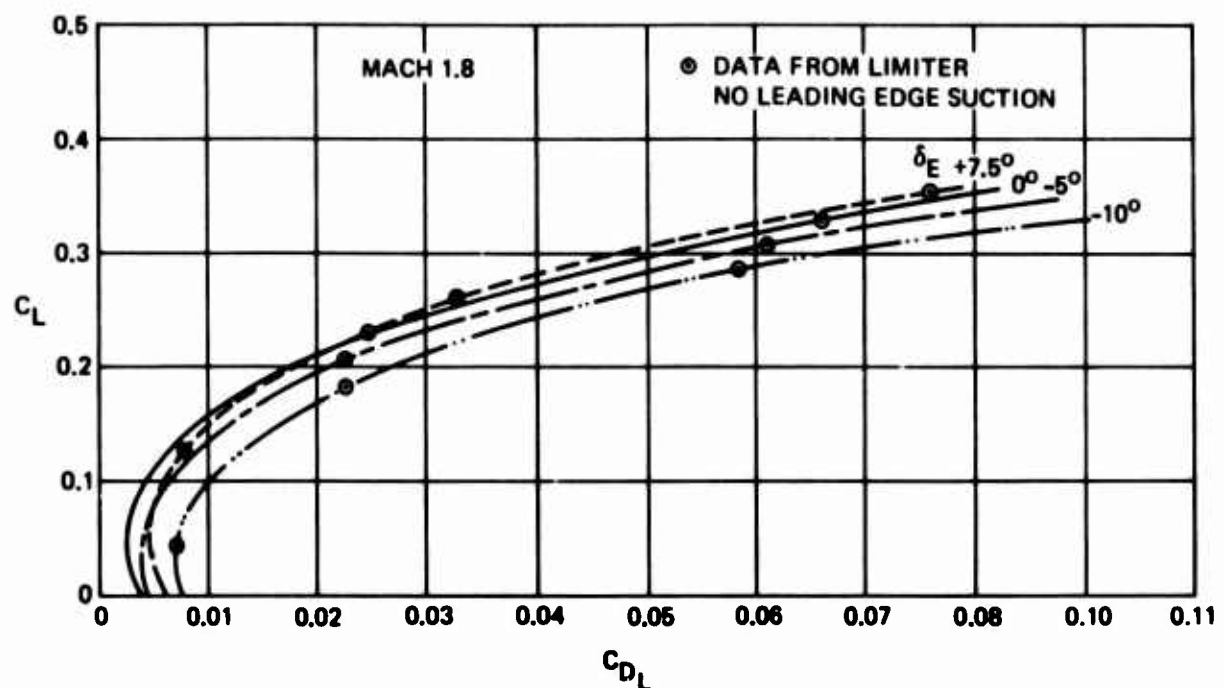
Figure 48. Elevon Characteristics (M = 1.8)

**MACH 1.8**

NOTES: WING TIPS OUT
TRIMMED WITH ELEVONS
Δ'S RELATIVE TO 0°
DEFLECTION
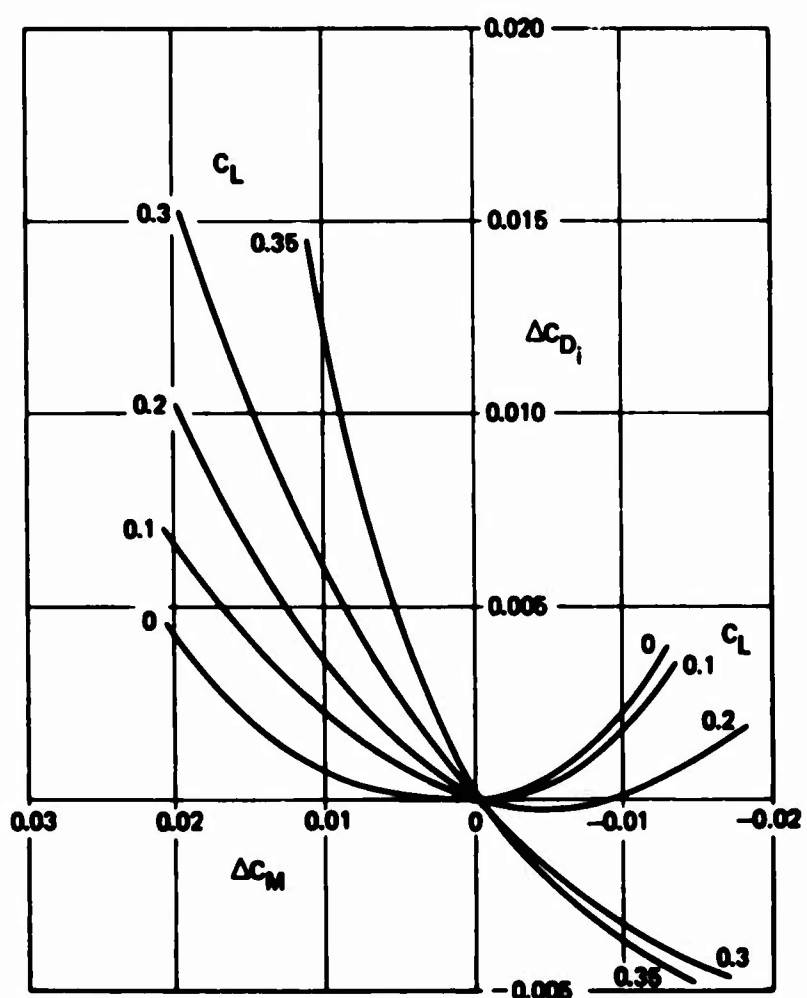
Figure 49. LES-213 Trim Drag Increments
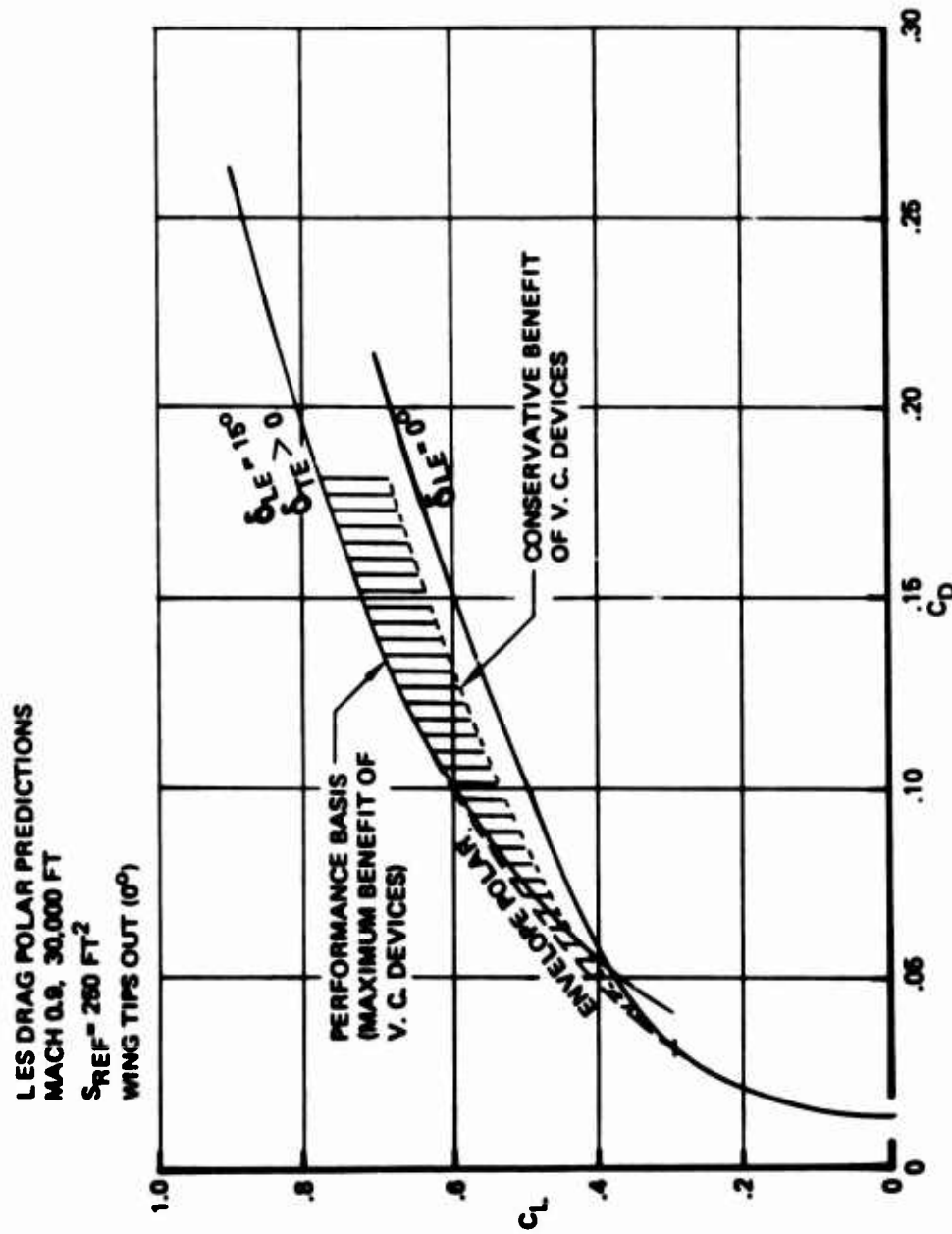
Figure 50. LES-213 Subsonic Trimmed Drag Polar

87

MAC IS DEFINED W/O WING TIPS

$S_{REF}$ = 250 FEET$^2$

WING TIPS OUT (0°)
C.G. AT 55% MAC

MACH 1.2
30,000 FEET

MACH 1.8
50,000 FEET

$C_L$

$C_D$
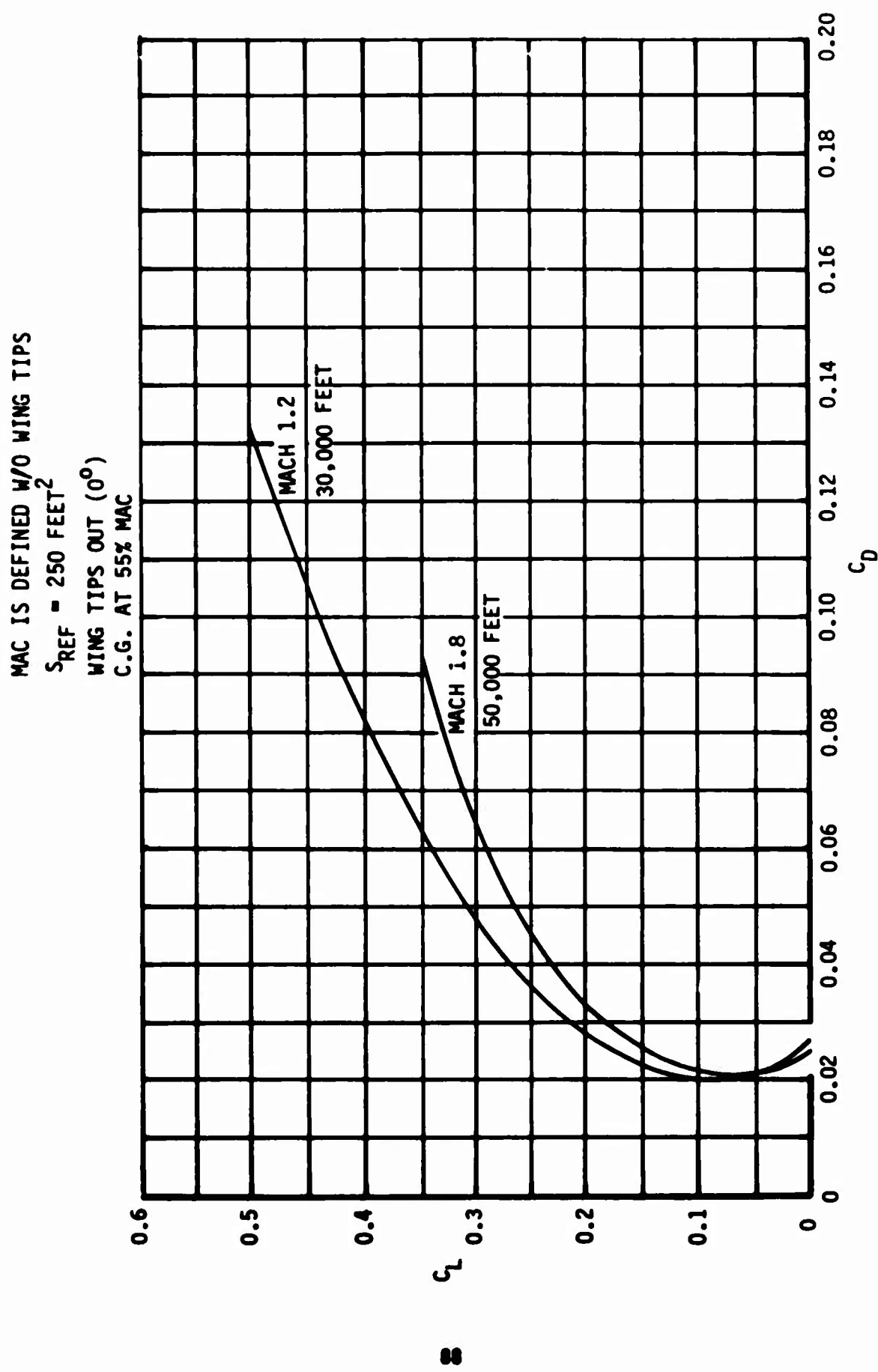
Figure 51. LES-213 Supersonic Trimmed Drag Polars

88

## 3.5 FLIGHT CONTROLS

### STABILITY AND CONTROL

The stability and control analysis is based on the following geometry
(outboard wing panels horizontal): Wing Reference Area, $S_W$ = 267 ft$^2$;
Mean Aerodynamic Chord, MAC = 18.89 ft; Distance from airplane nose to
leading edge of MAC = 16.89 ft; and Aspect Ratio = 1.55.

Small variations in geometry that exist with the evolved airplane at the
end of the preliminary design cycle are considered to have negligible
effect on the results of this study.

Aerodynamic data was computed using the above geometry and the Digital
DATCOM method described in reference (15). The findings were compared
to wind tunnel results of similar configurations (NASA SCAT-15 planform)
presented in references (16), (17), (18), and (19). No attempt was made
to compute aeroelastic effects.

Longitudinal Stability--Estimated aerodynamic center location is presented
in Figure 52. Subsonic a.c. is approximately .50 MAC and supersonic a.c.
at .60 MAC. Airplane c.g. is estimated to be at .54 MAC. In a completely
cycled design, the c.g. should be roughly at .52 - .55 MAC, to allow for
flexibility effects and to minimize demands upon the automatic flight
control system at subsonic speeds, where the airplane will be statically
unstable. Model 985-213, thus is not quite properly balanced, but it is
close enough that moderate changes in the wing-body relationship, or in
internal arrangement will accomplish satisfactory balance.

Longitudinal Control--The incremental lift coefficient that can be
generated with the trailing edge surface acting as elevators $C_{L_{\delta_e}}$ is
shown in Figure 53 as it varies with Mach number.

The control power required for take-off rotation was estimated for a wing
loading of W/S = 62.8 lb/ft$^2$, an elevator deflection of -30 degrees and
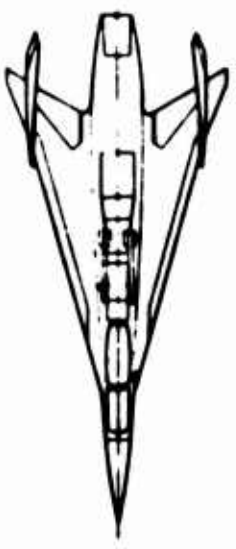
$\bar{C} = 18.89$ FT.
$S_{REF} = 267$ FT$^2$
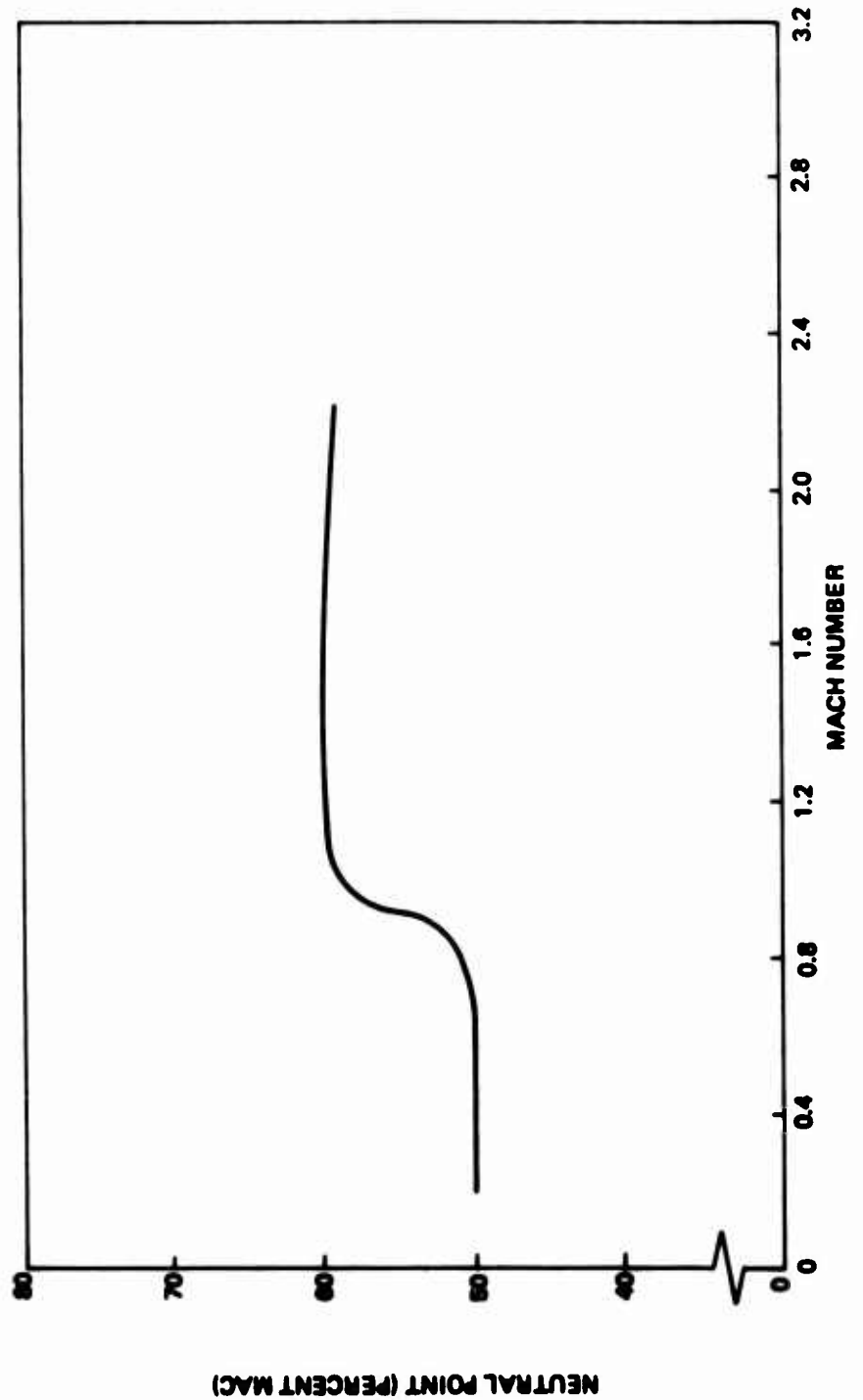


Figure 52   LES Estimated Neutral Point

NEUTRAL POINT (PERCENT MAC)

MACH NUMBER
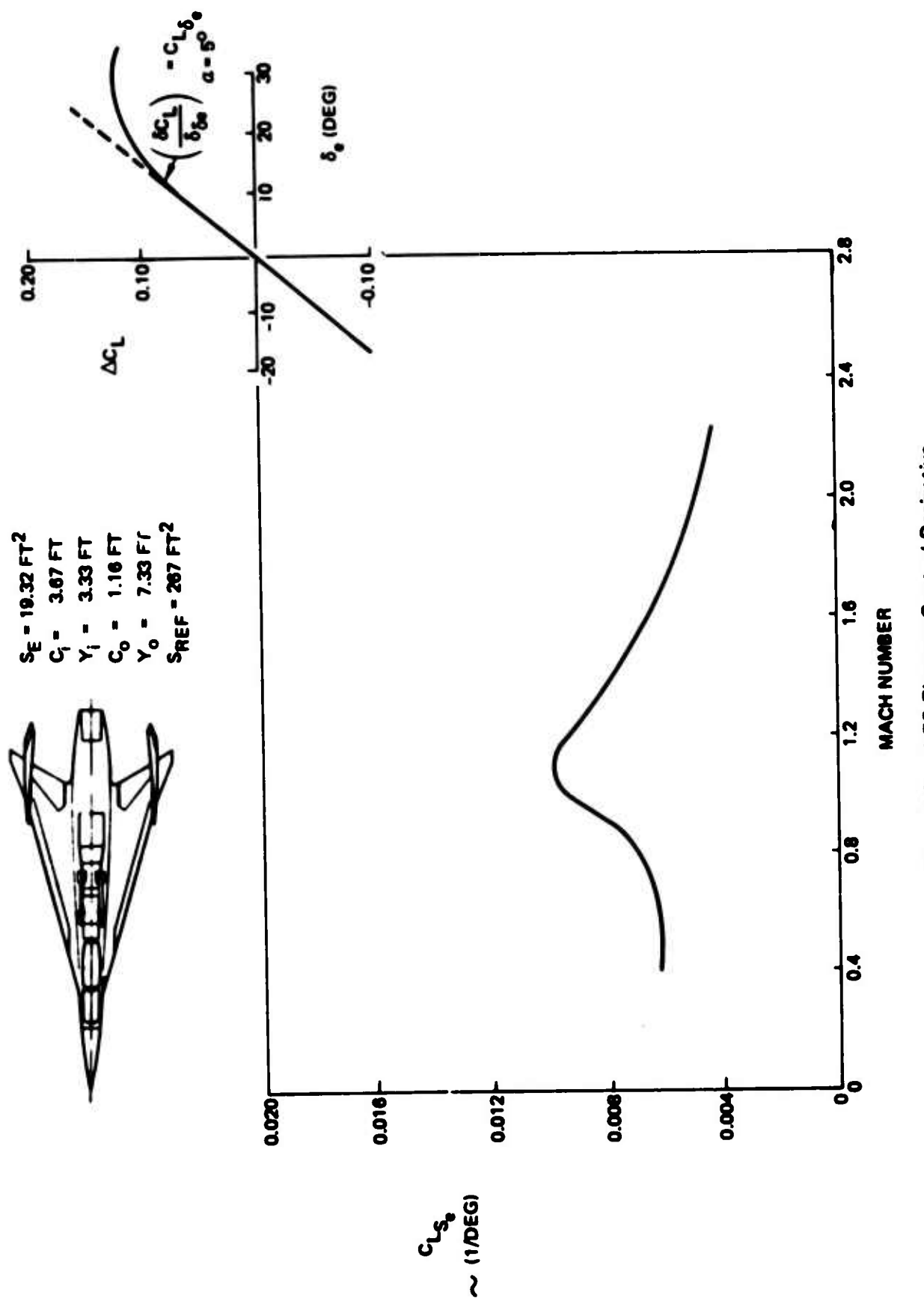
Figure 53    LES Elevator Control Derivative

## 3.5 FLIGHT CONTROLS (Continued)

using the total movable trailing edge surface area ($S_e$ = 19.32 $ft^2$). The elevator moment arm for nose wheel lift-off is .33 MAC with the main gear located at .61 MAC. Sufficient control power is available for rotation with a forward c.g. of .46 MAC and a rotation speed that was 90% of the lift-off speed, thus meeting the requirements of MIL-F-8785B. Based on $C_L$ = 0.50 the lift-off speed is 192 KEAS.

Immediately following lift-off there must be sufficient control power to provide an incremental nose-down pitching-moment to produce a pitch acceleration $\ddot{\theta}$ = -.1 rad/sec$^2$ at the trim $C_L$. For example, at an aft c.g. of .53 $\bar{c}$, a moment arm of .413 $\bar{c}$ and a load factor of 1.5 g's a $\Delta Cm$ = .036 ($\ddot{\theta}$ = .1 rad/sec$^2$) can be generated with 15 degrees of elevator deflection. Figure 54 shows the amount of elevator area that is required to achieve the incremental pitching moment coefficient using $\delta_e$ = 30 degrees. It can be seen that the take-off rotation is the critical requirement using the available trailing edge area between the vertical fins.

At high supersonic speed (Mach = 1.8) and altitude (alt = 60,000 ft) sufficient control power exists for a 7.3 g maneuver.

Directional Stability--The twin vertical fins do not provide sufficient inherent static directional stability at low speed (Mach = .30). The static directional stability was estimated using the methods of DATCOM and for a c.g. at .50 $\bar{c}$, $Cn_B$ = (.00125) + (-.00166) = -.0004/deg, the sum of vertical fin and fuselage + wing contributions. The desired minimum level of $C_{nB}$ is +.0004/deg using the requirements of MIL-F-8785B where the minimum low speed Dutch Roll frequency is $\omega_{nd}$ = 1 rad/sec. Augmentation is required for all flight regimes.

958-213
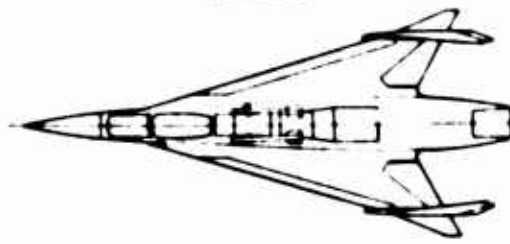
ELEVATOR SIZE STUDY

$S_{REF}$ = 267 ft$^2$

$\bar{C}_W$ = 18.9 ft

XCG = .50$C_W$

$S_{ELEVATOR}$ = 30°
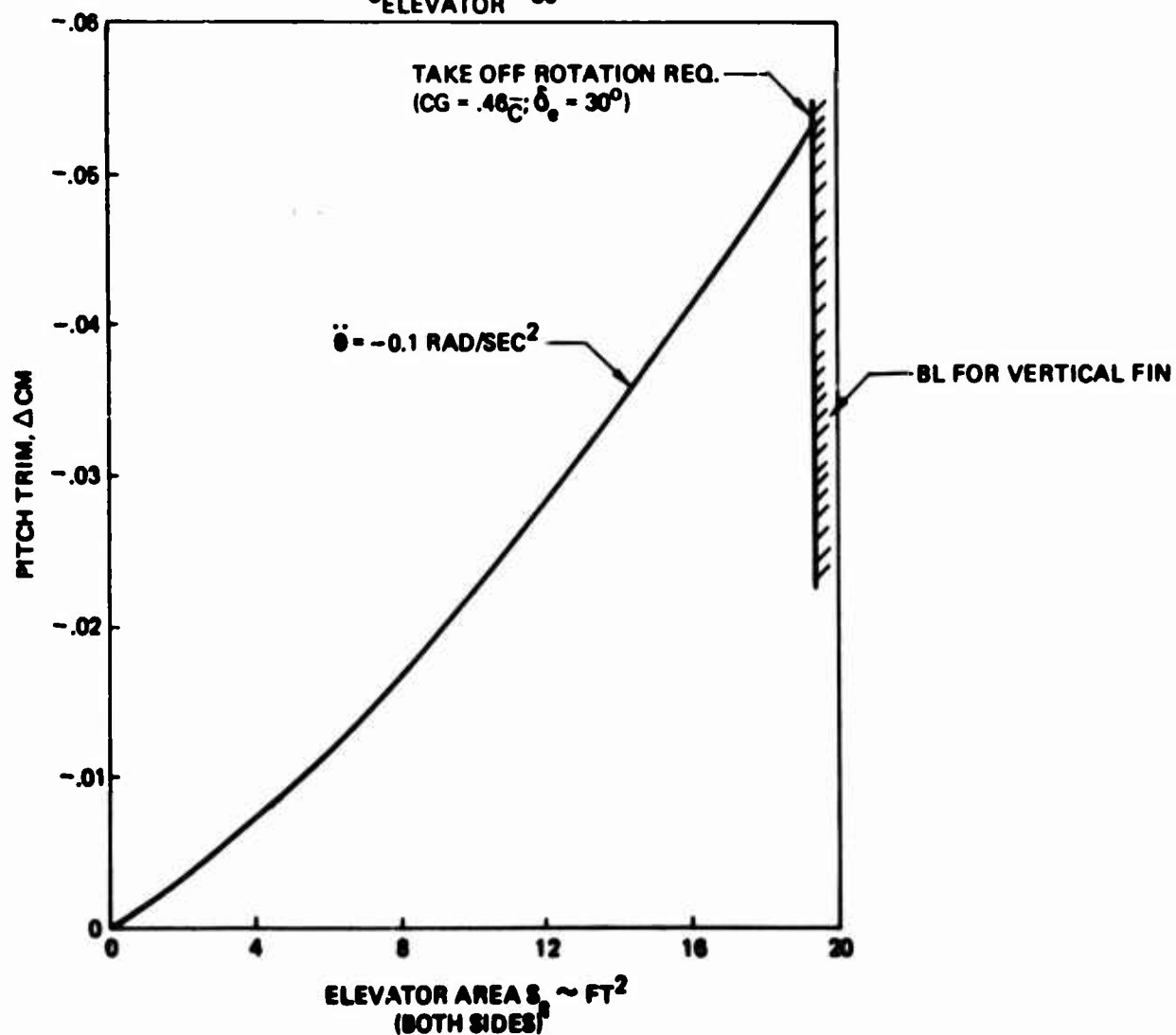


Figure 54. LES Elevator Size Study

3.5 FLIGHT CONTROLS (Continued)

Directional Control--The rudder required to land in a 30 knot crosswind was based on $C_{n_{\delta_R}}$ = -(K) $(C_{n_{\beta_{vt}}})$ = -.000625/deg, (K = .50 per DATCOM). At a speed of 157 knots it takes 7.4 degrees of rudder to cancel an 11 degrees of sideslip assuming the minimum $C_{n_\beta}$ = .004/deg. There is sufficient rudder power to control a 30 knot crosswind at landing level leaving ample rudder authority to overcome adverse yaw and to provide stability augmentation.

Lateral Control--The roll control requirements were evaluated in terms of bank angle reached $\phi$ = 30$^0$ in 1.0 second for takeoff and landing task ($C_\ell$ = .0031); and $\phi$ = 90$^0$ in 1.0 second for the air-to-air combat task ($C_\ell$ = .0095). These requirements are based on MIL-F-8785B requirements for highly maneuverable airplanes (Class IV). The aerial combat requirement ($C_\ell$ = .0095 @ V = 260 KEAS) was the most demanding, based on results (Figure 55) of a one degree of freedom calculation. The inputs to that calculation were $I_x$ = 2,600 slug - ft$^2$, a step aileron with a 0.2 second rise time, a damping derivative in roll adjusted to provide a roll mode time constant commensurate with good flying qualities ($\tau_R$ $\leq$ 1.4 seconds). It is noted that a roll augmentation loop is required to achieve the selected roll mode time constant in all flight regimes.

The lateral control required (Figure 56) to provide sufficient roll power to meet the above roll requirements amounts to the total trailing edge surface (19.32 ft$^2$) deflected 20 degrees. Thus, full roll control limits the available pitch control power.

FLIGHT CONTROLS SYSTEM DESCRIPTION

Referring to Figure 57, the Vehicle Flight Management concept consists of a federated/integrated digital computer complex and data bus architecture, utilizing the merits of each, where applicable. The
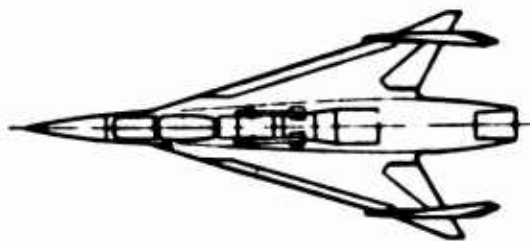
CLASS IV · $\phi_n$ = 30° IN 1.0 SEC (TAKE-OFF & LANDING)

$I_x$ = 2,600 5-FT$^2$
$C_{l_p}$ = .160 °/RAD
$T_R \leqslant$1.00 SEC
RISE TIME: 0.2 SEC



LOW SPEED REQUIREMENT V$_{(KEAS)}$
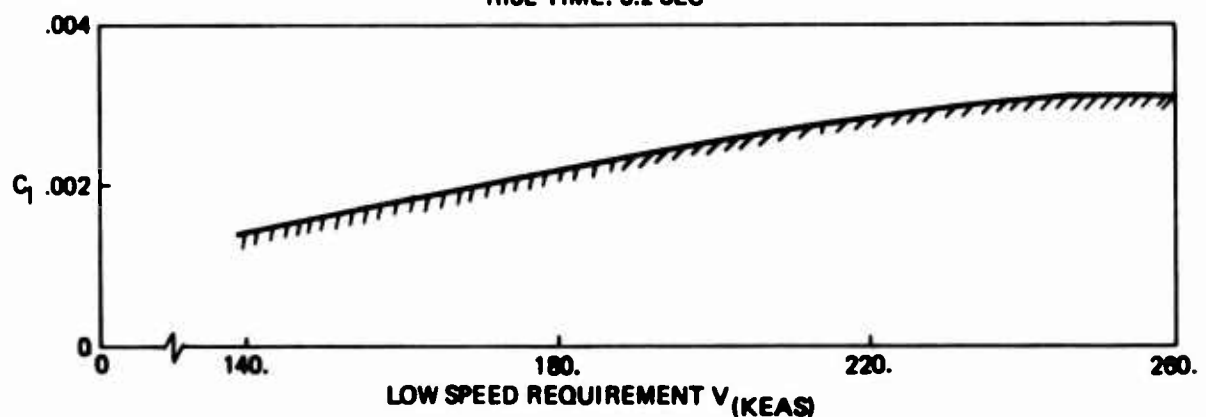
CLASS IV · $\phi_t$ = 90° in 1.0 SEC (AIR-TO-AIR COMBAT)



COMBAT REQUIREMENTS V$_{(KEAS)}$
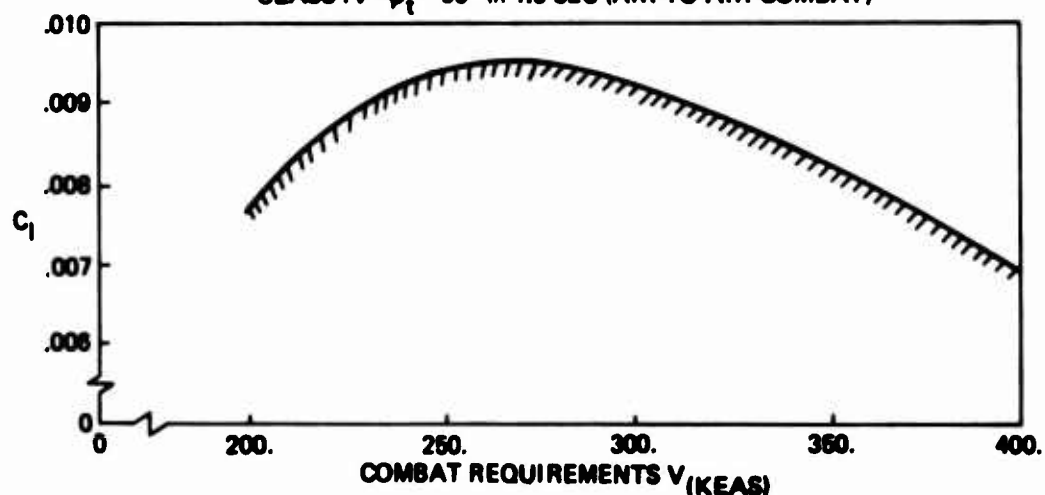
*Figure 55.   LES Roll Power Required*
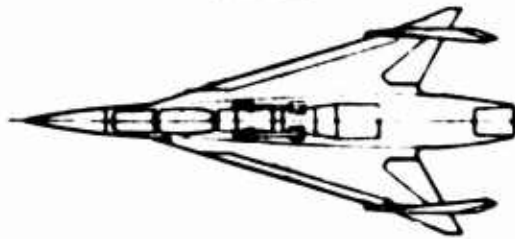
**AILERON SIZING STUDY**

$S_{ref} = 287 \text{ ft}^2$
$b_{ref} = 20.4 \text{ ft}$
$XCG = .50 \, C_W$
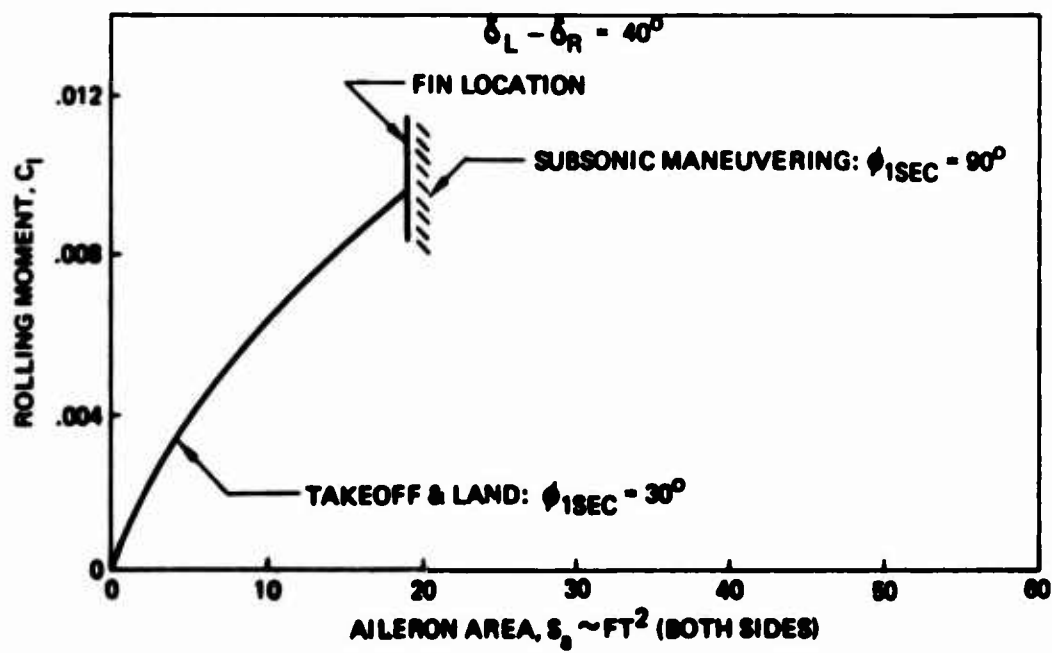


Figure 56. LES Aileron Size Study

## 3.5 FLIGHT CONTROLS (Continued)

federated/integrated system architecture results from a consideration of the criticality of the various required functions.  That is, computation functions that are critical from a flight safety standpoint are integrated into one set of triply redundant computers.  The remaining non-flight-critical computations are performed in a single thread central or mission computer.

Communication between the flight critical computers and the mission computer is accomplished with optical data buses.  This provides electrical isolation and minimizes EMI and EMP problems.

Redundant inertial sensors (gyros and accelerometers) are interfaced directly with the flight critical computers where the strapdown computations are performed.  The processed strapdown data are then optically transmitted to the central computer where guidance and navigation computations are performed.

Modular strapdown sensors are employed; i.e., unique sensor compensation characteristics are defined by PROM's physically located in the sensor LRV's.  Consequently, sensors may be replaced on a modular basis without software changes in the flight critical computers.

A similar approach is used for the air data sensors; all air data computations are performed in the flight critical computers.

Read only memory is used in the triply redundant flight critical computers.

The central computer, data bus, and most of the controls and displays are single-thread; that is non-redundant.  The data bus is used to transfer all non-safety-critical status information to the pilot and between equipments, and most commands to Mission Systems equipment
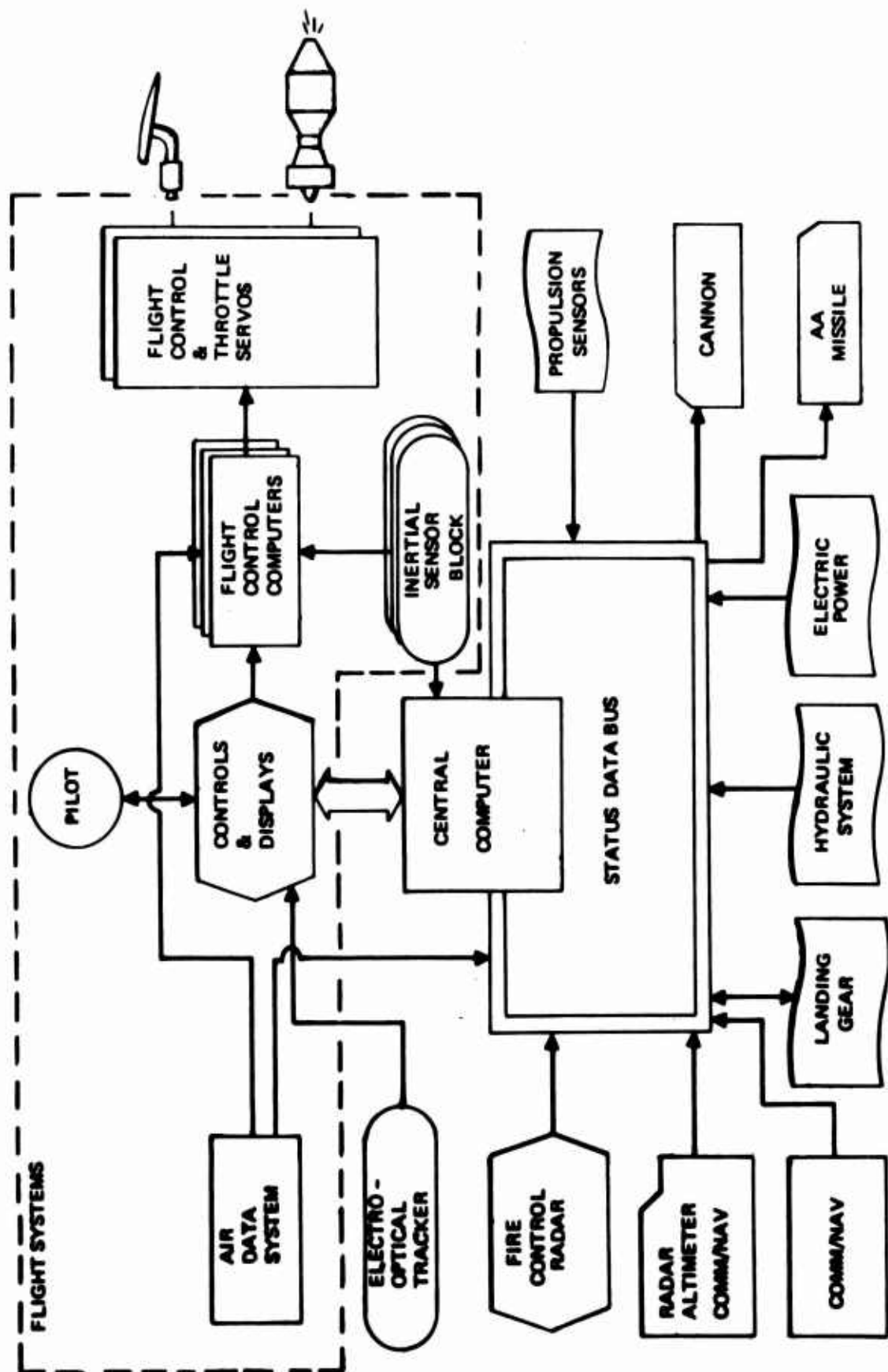
Figure 57. LES – Avionics/Flight Control System Schematic

98

## 3.5  FLIGHT CONTROLS (Continued)

(see Section 3.7).  All functions that have both an automatic and manual mode, such as fore-aft fuel transfer pumps and flap controls, will be commanded through a "MANUAL-AUTOMATIC" model switch, available to the pilot.

Redundancy Management Concept--Functional redundancy is achieved by a combination of triplex hardware redundancy for flight critical equipment and by a reconfigurable computer architecture for the flight critical computers.  That is, the system will be able to operate at the redundancy levels and to effect (automatically) the redundancy level transitions shown as follows:

$$\text{TRIPLEX} \longrightarrow \text{DUPLEX} \longrightarrow \text{SIMPLEX}$$

In effect FAIL-OP$^2$ capability is obtained using triple hardware redundancy.  This is made possible by a combination of in-line computer tests, the use of sensor valids and in-line sensor reasonableness/state estimation computations.  Skewed axis strapdown sensors are used to achieve the required sensor redundancy with minimum hardware.

Dual actuation (FAIL-OP) of control surfaces was chosen as a balance between cost, weight and flight safety.

Outer-loop control of the propulsion unit is basically single-thread.

Control Laws--A normal acceleration command type system is the basic up-and-away control law in the pitch axis.  At low speeds a gradual transition to a pitch-rate command control law is affected.  Automatic trimming and envelope limiting features are also implemented.

The lateral-directional control laws are designed to minimize sideslip due to rolling maneuvers and to provide high roll rate bandwidth. Protection against roll divergence is also provided by the control laws.

## 3.5 FLIGHT CONTROLS (Continued)

Simple pilot relief modes such as attitude hold, Mach hold and attitude hold are also provided. While these are not flight critical, the computations are performed in the flight critical computers since the basic data required already reside in the flight critical computers and since computationally these represent minor additional computations to the basic command augmentation computation risk.

Control laws are scheduled as a function of dynamic pressure and Mach number.

The central computer, keyboard controls, and CRT displays will not be included in the early phases of the LES Prototype program; however, flight deck layout and avionics bays will be configured to avail a smooth transition to a demonstrable weapon system capability, in later phases of the LES prototype.

Integrated Flight Control--Figure 58 depicts the Integrated Flight Control including relevant propulsion controls. Fly-By-Wire (FBW) control, without mechanical backup, is used throughout.
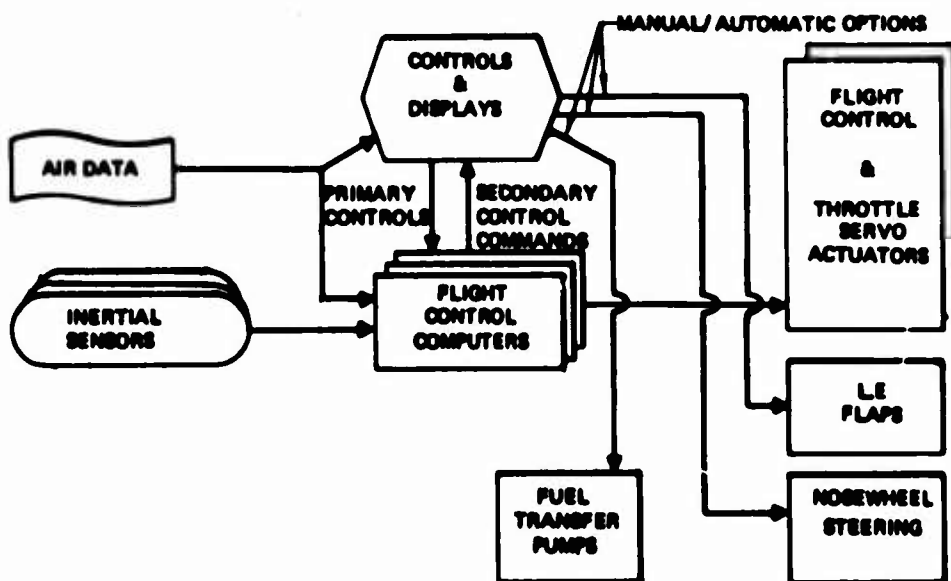


**Figure 58.** *Integrated Flight Control Schematic*

## 3.6  SECONDARY POWER SYSTEM

The configuration of the LES secondary power sytems was developed with particular attention given to considerations of engine restart capability, failure modes of the normal systems and to limitations on aircraft weight and internal space.

Arrangements of electrical, hydraulic, and emergency power generating equipment, weight comparisons and typical failure modes were evaluated. The secondary power subsystem developed from the results of this evaluation are described in this section and is shown in Figure 59.

### HYDRAULIC SYSTEM

Two independent hydraulic systems, each powered by a 3,000 psi variable displacement pump, mounted on the remote engine driven secondary power gear box, supply hydrulic power for flight controls, electrical power generation, for landing gear retraction, nose wheel steering, engine inlet ramp, ram air turbine retraction, and missile launcher trapeze. Wheel brakes are powered by a separate self-contained hydraulic system.

Reduced vulnerability to gunfire is obtained by the maximum practicable separation between the distribution lines of the two separate hydraulic systems.

The engine power take-off shaft may be decoupled to permit engine removal or maintenance without disturbing the secondary power gearbox or the hydraulic pump and engine starter installations.

Emergency hydraulic power, in the event of engine power failure, is provided by engine windmilling power and by an independent power source such as ram air turbine or stored energy system.
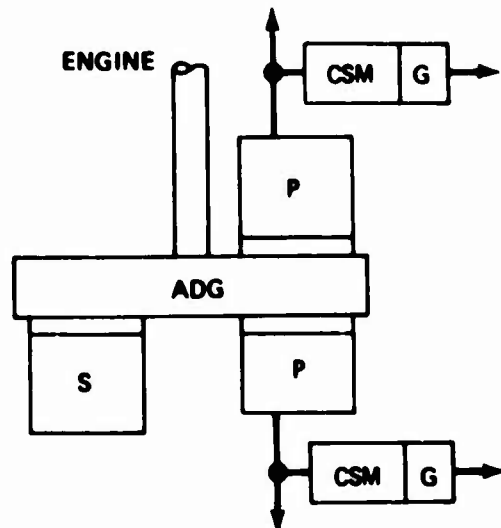
*Figure 59. LES — Secondary Power System Schematic*

| Surface | $M_H$ - Feet-pound per surface | Required rate degrees/seconds | Hydraulic flow total A/P GPM | Extracted H.P./airplane |
|---|---|---|---|---|
| Elevons | 6,750 | 100 | 26.60 | 61.70 |
| Rudders | 2,480 | 30 | 9.36 | 20.10 |
| L.E. flap | 6,670 | 30 | 9.47 | 20.40 |
| * Maximum theoretical instantaneous rate | | Totals | *47.43 | *102.20 |

*Hydraulic Power Requirements, Flight Controls*

| Flight condition | Surface | Rate % | H.P. extracted | SAS H.P. |
|---|---|---|---|---|
| Hi-Q combat | Elevons | 100 | 61.70 | |
| | Rudder | 25 | 5.02 | |
| | | Total | 66.72 | |
| Lo-Q, Hi- ß combat | Elevons | 100 | 61.70 | 20.41 |
| | L.E. flap | 100 | 20.40 | |
| | Rudder | 25 | 5.05 | |
| | | Total | 87.15 | |
| Landing or T/O | Elevons | 100 | 61.70 | |
| | Rudder | 50 | 10.10 | |
| | | Total | 71.80 | |

*Hydraulic Power Extraction For Maneuver*

*Figure 60. LES — Hydraulic Power Requirements*

102

## 3.6  SECONDARY POWER SYSTEM (Continued)

Figure 60 indicates the maximum flow requirements and horsepower extraction at the maximum theoretical rates, and illustrates the horsepower extraction occurring during some maneuver cases.

Electrical generation by constant speed hydraulic motor normally demands 8 gpm or less per generator, with momentary transients possible up to 17 gpm per unit.  See Figure 61 for total hydraulic power extraction including power due to electrical power generation over a typical LES mission.

ELECTRICAL SYSTEM

Two separate electrical sytems incorporating constant speed hydraulic motor driven ac - dc generators powered by separate hydraulic systems, backed up by a battery for certain essential services, provide normal electrical power.

Power sytem survivability and reliability levels to support flight critical functions are achieved through physical separation of the dual redundant systems and their associated wiring.

A master power switch is provided to arm the battery circuit and initiate all automatic functions of the airplane systems.  The electrical system operation is completely automatic with provision for manual deactivation of the individual generators.

Management of the power supply to the triple channel flight control computers will minimize power transients which might occur during engine failure and consequent emergency generator operation.  Figure 62 shows a breakdown of the LES electrical power requirements.

Emergency electrical power, in the event of engine power failure, is provided by engine windmilling power, or by the ram air turbine.
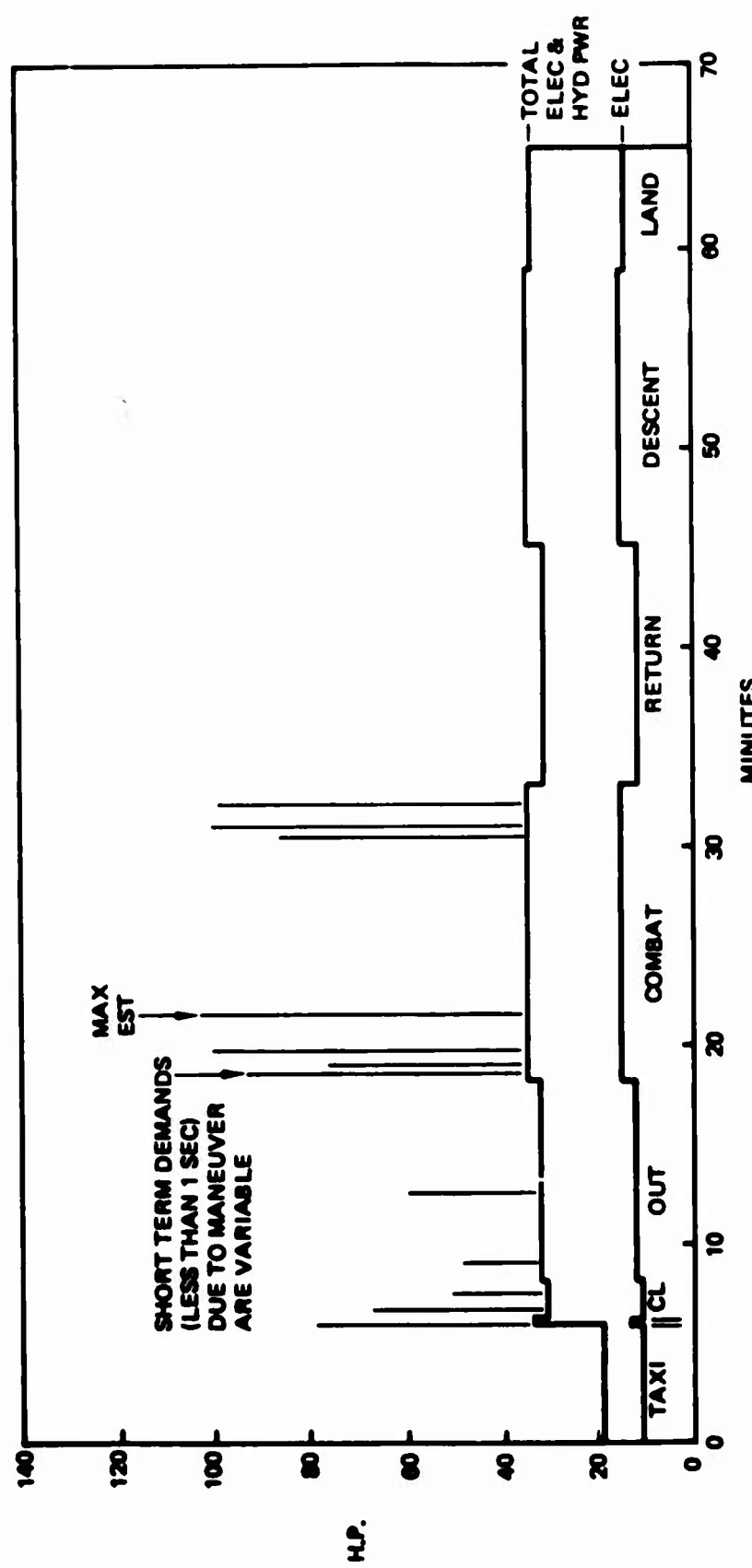
Figure 61. LES Mission – Hydraulic and Electrical Power Requirements

104

| Load item | Normal operation | | | | | Emergency | | |
| | Sys number 1 Gen CSM 5 KVA 50 AMP | | System number 2 Gen CSM 5 KVA 50 AMP | | Batt no 1 11 A-HR | Ram air turbine | | Batt no 1 11 A-HR |
| | AC-VA | DC-W | AC-VA | DC-W | DC-W | AC-VA | DC-W | DC-W |
|---|---|---|---|---|---|---|---|---|
| Fuel boost pump | 2,500 | | | | | 2,500 | | |
| Windshield ht | | | 2,000 | | | | | |
| Env/fuel sys cont | | | 400 | | | | | |
| Batt chg | | | 940 | | | | 280 | |
| Engine instrument | 250 | | 250 | | | 500 | | |
| Avionics | 1,530 | 1,346 | | | | 402 | 1,240 | |
| Panel/cab lts | | | | 224 | | | 224 | |
| Exterior lts | | | 510 | | | | | |
| Hyd press ind | | | | 112 | | | 112 | |
| FBW F/C elec | | | | 265 | 100 | | 165 | 200 |
| Hyd pump EDV | | | | | | | 50 | |
| Totals | 4,280 | 1,346 48 A | 4,100 | 601 21.5A | 100 | 3,402 | 2,071 74A | 200 |

Figure 62.   LES – Electrical Power Requirements

## 3.6 SECONDARY POWER SYSTEM (Continued)

EMERGENCY POWER AND AIR START

The following two important tasks have been defined as objectives in the design of the LES Model 985-213 emergency power subsystem.
o  Assist rapid engine restart in critical flight regimes.
o  Provide hydraulic and electric flight control power for safe flight until either engine power is restored, safe landing is assured, or the pilot ejects from the airplane.

These tasks are in addition to the basic design objectives of achieving integration into the normal secondary power system with a minimum effect on the airplane weight and space allocations and considerations of flight condition, control requirements, pilot reaction time and subsystem response time.

The combination of a ram air turbine and a jet fuel starter (JFS) has been selected as prime candidate to satisfy the objectives for the LES Model 985-213 emergency power subsystem. These units are current state-of-the-art equipment but provide limited performance over several sections of the flight envelope. The engine windmill characteristics are used where possible and normal system power is reduced to low levels during engine shutdown. Figure 63 illustrates the estimated windmill restart envelope for the F404 engine.

To provide an all altitude restart and flight control capability, alternate emergency power systems such as the liquid oxygen (LOX) and jet fuel configuration defined in the Air Force report, AFAPL-TR-75-9, Emergency Power Supply, dated April 1975, show promise of also satisfying LES objectives.

It is therefore recommended that the following subjects be considered for further detailed study:
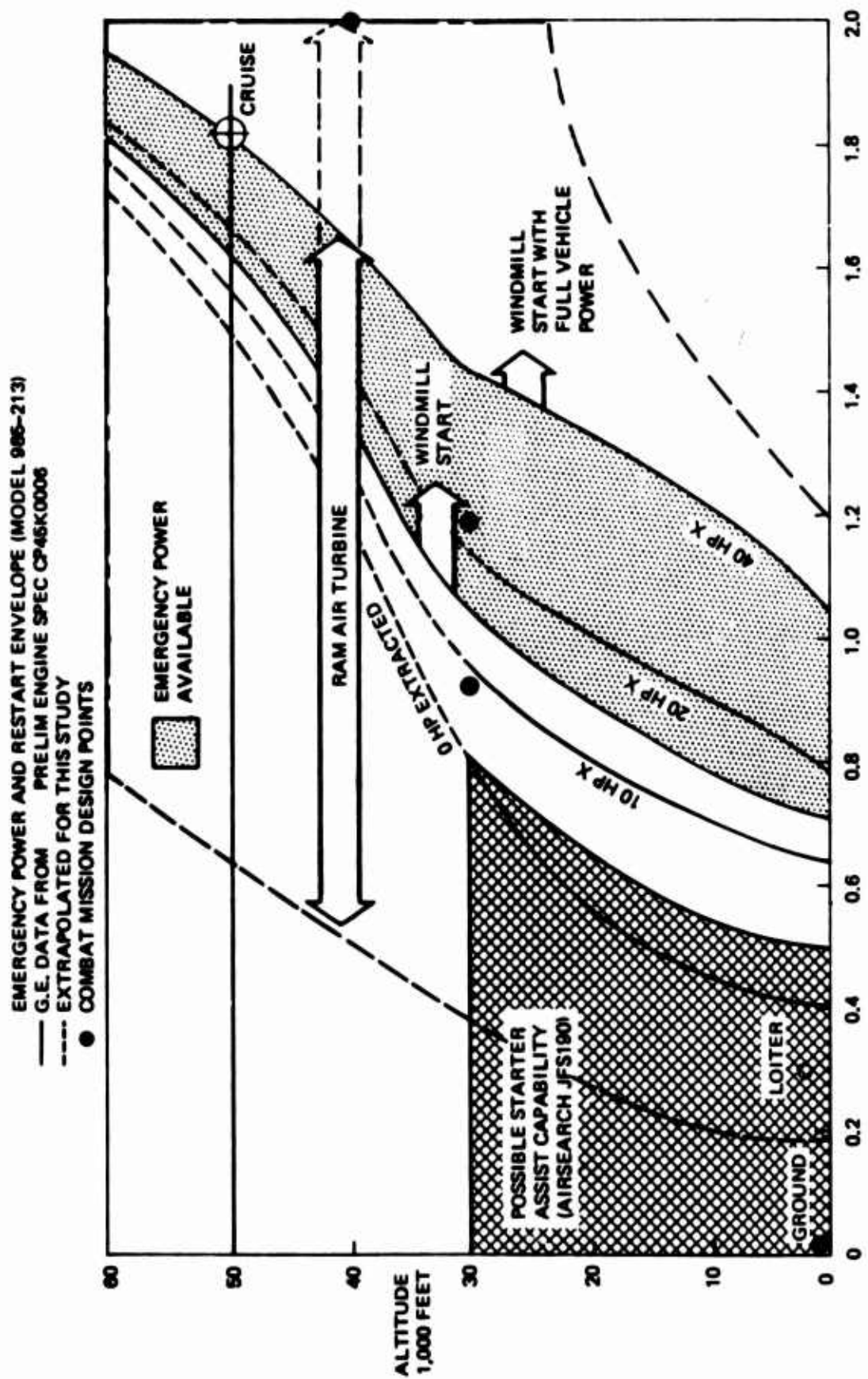
Figure 63. Estimated Windmill Restart Envelope

107

## 3.6  SECONDARY POWER SYSTEM (Continued)

o  Best methods for rapid and reliable detection of interruption of
   normal engine power.

o  Automatic system monitoring and control to reduce hydraulic and
   electrical loads to flight essential services during engine restart
   requirements.

o  Optimization of engine restart performance throughout the flight
   envelope - possible use of techniques such as overhead engine bleed.

o  Obtaining of additional data points to facilitate further study, such
   as engine starting time at various altitudes and temperatures versus
   applied and/or horsepower extraction.

o  Alternate systems such as LOX and jet fuel to supply emergency power
   demands.


ENVIRONMENTAL CONTROL SYSTEM (ECS)

The prototype ECS will be configured utilizing as much off-the-shelf
equipment as is possible to provide the system performance and system
response in accordance with requirements of the LES mission.  The system
schematic is shown in Figure 64.

Bleed Air Subsystem--High stage bleed air is used for pressurizing the
cockpit and to provide the conditioned air source for the cockpit, avionics
cooling, and accessories.  The air from the engine bleed source shall be
pressure, flow, and temperature limited.  A buffer fuel-air heat exchanger
mounted in the engine area precools the bleed air before being ducted to
the cooling package.  Downstream of the engine compartment and where
necessary, ducts shall be insulated to limit duct surface temperatures
to $450^{\circ}F$.

Air Conditioning Subsystem--A simple cycle cooling package is used and
consists of an expansion turbine, fan, heat exchanger, water separator,
and controls.  This unit,manufactured by Hamilton Standard, is the unit
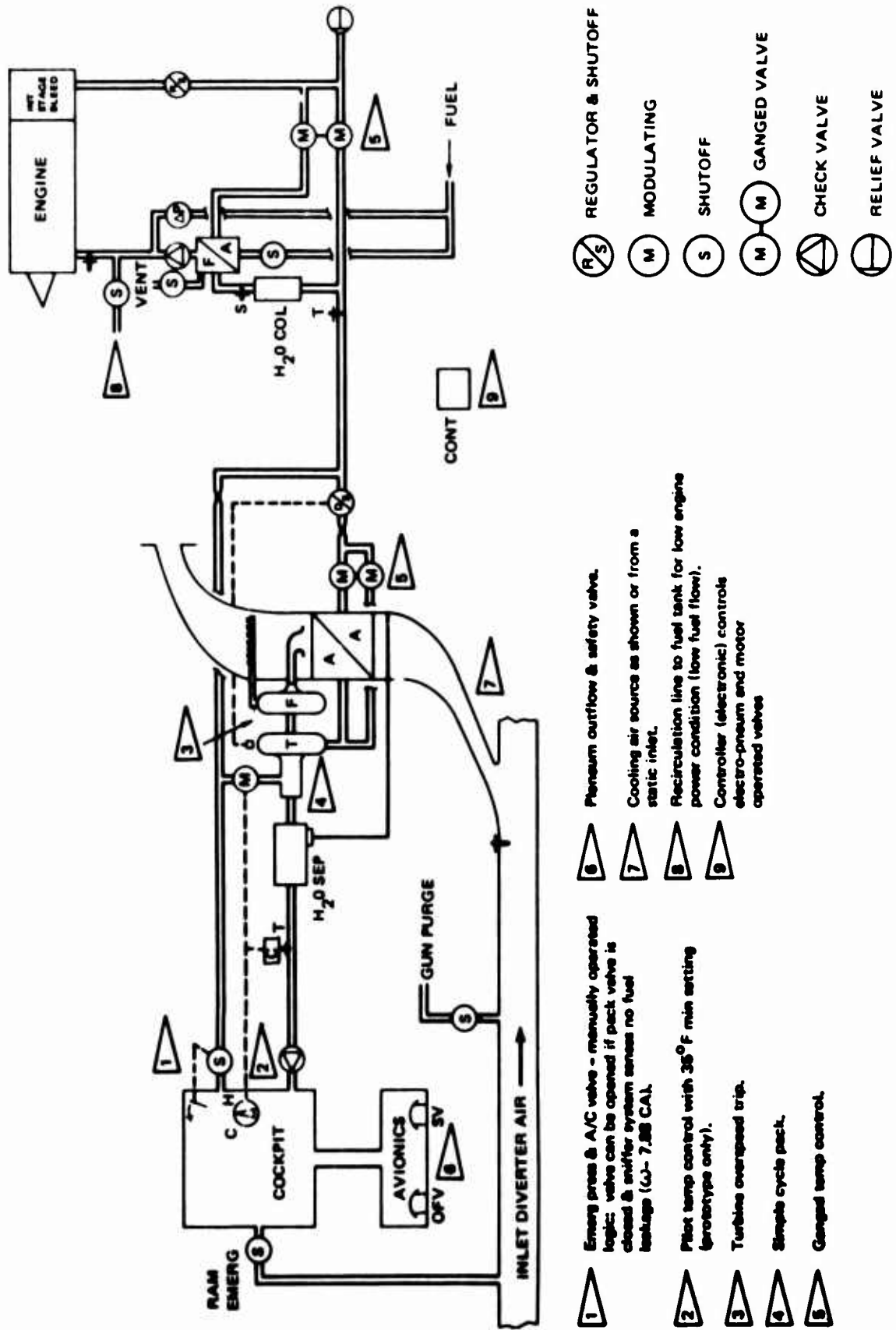
Figure 64. LES Environmental Control System

109

3.6 SECONDARY POWER SYSTEM (Continued)

currently used in the F-5 aircraft. The cooling package will provide
the following performance:

o A maximum cockpit temperature of 80°F for a MIL-STD-210A hot day
  for the flight or ground case.
o A minimum cockpit temperature of 80°F for a MIL-STD-210A cold day
  for the flight or ground case.

Emergency ram air shall be provided for the cockpit and avionics cooling
in the event of failure of the bleed system or cooling package. Avionics
compartment (located in the nose) shall be maintained at the same
compartment pressure as the cockpit. The cooling package shall provide,
as required, the air source for: Fuel tank pressurization, canopy seals;
survival gear, and gun gas purging. Cooling shall also be provided for
secondary power sytems, e.g., hydraulic system, electrical system.

Cockpit Pressurization--The pressurization system shall provide for an
unpressurized cockpit to 8,000' airplane altitude and a 8,000' isobaric
cabin altitude to an airplane altitude of 23,100 feet, and 5.0 psi
differential above 23,100 feet.

Environmental Protection Subsystems--Only Boeing type IV rain repellant
shall be provided for the experimental airplane. Windshield shall be
electrically heated to provide anti-icing and defogging capability. A
standby system that is part of the pilot's foot warmer air system shall
be provided in the event the electrical window heat system malfunctions.
Canopy defog system shall be provided as part of the cockpit air distri-
bution system. No wing or empennage thermal anti-icing is provided.
Engine inlet anti-icing is provided.

Breathing Oxygen Subsystem--A standard 5 liter LOX system shall be used
on the prototype. This system is low cost and easily supportable for
experimental research or production programs.

## 3.7 MISSION SYSTEMS

Mission systems equipment for LES include all avionics except flight control avionics, flight instruments, armament group controls electrical and the armament consisting of cannon and air-to-air missiles. A three barrel 20 mm Gatling gun (G.E. XM-197) was selected to provide an effective cannon at light weight. Low cost dog fight missiles were assumed for LES to be the CLAW concept which provides AIM-9 type performance over shorter ranges at reduced missile weight.

Mission Avionics--The Avionics Suit in Table 5 provides day/night visual capability with fire control for guns and IR missiles for air-to-air missions. For LES the emerging (1978) technology set was selected.

The range only radar has two modes in terms of radar performance. These are the Gun Mode and the Missile Mode, which are under pilot control. In the Gun Mode, the radar searches in range with a fixed angle of 22° in azimuth and in elevation at ranges from 500 ft. to one nautical mile. In the Missile Mode, the radar searches in range of a fixed angle of 6° in azimuth and 4° in elevation at ranges from 500 ft. to 10 nautical miles. In each mode, range lock-on is automatic when a target is encountered; and range search is restarted automatically after a range search in which no target is detected. In addition, the radar provides azimuth angle, elevation angle and radar video. The search rate is 44,000 ft/sec and the range tracking accuracy is ± 50 feet. The target azimuth angle elevation angle and radar video will be displayed on the HUD. The HUD will also display a snapshot presentation in the Gun Mode. Because the radar senses angular position within the beam, it can be used to aim the missile seeker for acquisition by the missile seeker.

The Visual Target Acquisition System (VTAS) mounted on the pilot's helmet will permit SEAM (Sidewinder Expanded Acquisition Mode) capability for the IR missiles. SEAM increases the missiles angular acquisition coverage and permits missile lock-on and track before launch utilizing the VTAS. Missile launch with radar is still possible with SEAM turned off. The VTAS

Table 5. LES Avionics

| Equipment | Emerging (1978) | | |
|---|---|---|---|
| | Weight (lbs) | Volume (feet$^3$) | Power |
| UHF radio no. 1 | 9.25 | 0.12 | 85 Wdc |
| UHF radio no. 2 | 9.25 | 0.12 | 85 Wdc |
| IFF transponder w/crypto | 8.5 | 0.13 | 30 Wdc |
| Control | 2.7 | 0.06 | 5 Wdc |
| KIT-1A/T -sec | 11 | 0.15 | 37 Wac |
| Mounts | 3 | | |
| Secure voice | 26.5 | 0.19 | 5 Wac |
| Data link | 24 | 0.33 | 147 Wac 4 Wdc |
| Intercom | 2.5 | 0.03 | 12 Wdc |
| TACAN | 28.7 | 0.4 | 125 Wac |
| ILS | 11 | 0.14 | 20 Wdc |
| HARS | 31.5 | 0.43 | 300 VA dc |
| Air data computer (ADC) | 15 | 0.17 | 85 Wac |
| Probe | 5 | | 800 Wdc |
| Total air temp. sensor | 1 | | 500 Wdc |
| RHAWS | 36.2 | 0.43 | 321 Wac |
| HUD | 23 | 0.6 | 300VA ac 90 Wdc ▷ |
| Range only radar | 53 | 1.2 | 230 VA |
| VTAS & controls | 9.5 | 0.04 | ▷ |
| | 308.6 | 4.54 | 1,431 Wdc 1,530 VA 115 V, 400 Hz |

▷ Power for VTAS included in HUD.

3.7  MISSION SYSTEMS (Continued)

in effect increases the missile launch envelope by permitting target
acquisition and lock-on of a visual target without radar acqusition.
In the Gun  Mode, the radar provides outputs (range and range rate) to
solve the ballistics computation.  The radar system has no Sparrow
capability.

Armament Installation--The LES has been designed to accommodate a three
barrel gatling gun (BE XM-197) with 250 rounds of 20mm ammunition plus
two light weight and low cost dogfight missiles (CLAW).

The Lightweight M-197 is a derivative of the standard (production) M-197
incorporating the following features:
1. Component material and design changes to reduce gun weight (from 141
   to 126 lbs.)
2. Increase in firing rate (from 1,500 to 3,000 rpm) thru use of self-
   contained rotary gas drive.
3. Incorporation of a new ammo  transfer unit compatible with the
   higher firing rate.
4. Incorporation of breech clearing mechanism and circuitry.

Incorporation of these features permit a total gun system installation
weight (less ammo.) of approximately 260 lbs.  General Electrical Armament
Systems Dept., has estimated the development time for these low risk
features to be well within the LES development time frame.

The LWM-197 best met the following highly desirable characteristics for
a lightly structured, highly maneuverable fighter:
o  lightweight            o  small size
o  low recoil force       o  high fire rate
o  quick fire rate buildup

113

3.7 MISSION SYSTEMS (Continued)

Additionally, the LWM-197 was selected as the best compromise when the important requirements of cost, safety, lethality (e.g. muzzle velocity and output horsepower) and GSE compatibility were considered.

The gun and missile installation is shown in Figure 65 for LES-213.

A comparison of gun installation elements and weights are included on Figure 66 to indicate the reductions possible with this system.

Missiles--The CLAW missile concept is employed for LES. The two weapons are carried in semi-submerged wells in the upper body. Launch is accomplished with a hydraulic powered trapeze to raise the missiles from their carriage wells clear of the airplane to a firing position. Rail launch is assumed.

The CLAW can be easily loaded by two men. The wide field of view and upper hemisphere look angles produce a favorable installation for air-to-air combat.

Semi-submerged carriage on the body was selected over wing tip mounting for low supersonic drag. The selected wing tip geometry does not lend itself to mounting of weapons the size of CLAW or larger. If future wind tunnel testing shows tip geometries that could accommodate low drag carriage and launch this location should be reconsidered.

As drawn, the CLAW installation does interfere with direct access to the aircraft accessory bay. The present location does shield the sensor head from direct airstream erosion and does eliminate extensions of the airplane wing extremities which cause ground damage, but does subject the weapon to damage from maintenance crews working from the upper wing surface. A more desirable weapon installation, and one that would eliminate the above problems, is a tube launched missile buried in the wing structure. Future low cost dog fight missile development should consider this approach.

114
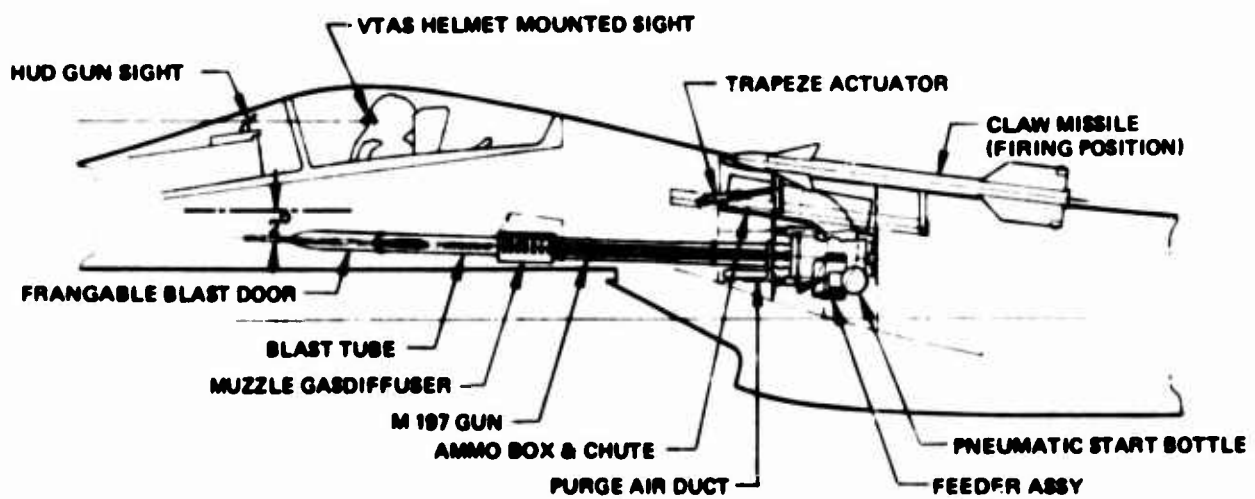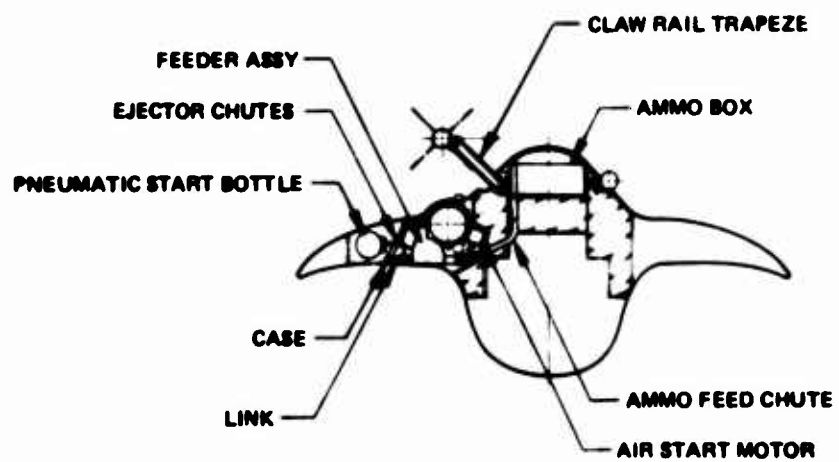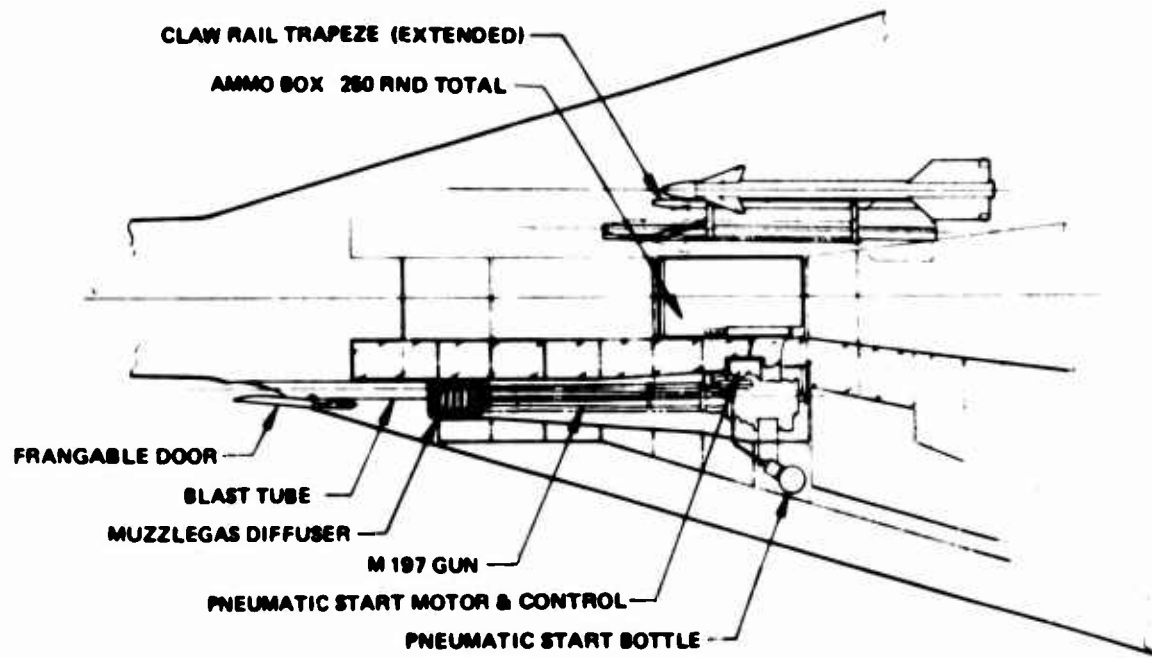
Figure 65. Armament Installation – Model 985-213

115

| | Gun Characteristics (Apprx.) | | | |
|---|---|---|---|---|
| **G.E. LIGHTWEIGHT M-197 (20mm)** | 126 (145 W/ DRIVE) | 3000 | 3400 | 3960 |
| **M-39 (20mm)** | 179 | 1800 | 3300 | 2000 |
| **DEFA/ADEN (30mm)** | 176 | 1250 | 2875 | 2220 |
| **HUGHES CASELESS (25mm)** | 230 (W/FEEDER & EXT. DRIVE) | 2000 | 4000 | 6500 |
| **G.E. LIQUID PROPELLANT GUN (20mm) 6 BARREL** | 400 (W/FEEDER & EXT. DRIVE) | 6000 | 4000 (BASELINE CONFIG.) | 14,750 |
| 100  90  80  70  60  50  40  30  20  10  0  INCHES | WEIGHT (LBS) | RATE OF FIRE (SPM) | MUZZLE VELOCITY (FPS) | MUZZLE OUTPUT HP |

Figure 66.   Gun Comparison

116

3.7  MISSION SYSTEMS (Continued)

Supersonic Weapon Carriage--The design arrangement for LES structure
allows low-drag conformal weapon carriage on the lower body.  The engine
airframe arrangement locates the lower body longeron above the drop out
engine access panel.  This panel can be replaced by a conformal pallet
with capacity for 2 x 2,000 lbs. stores.  The concept is shown in
Figure 67.  To preserve low drag at supersonic cruise speeds, bomb
warheads have been incorporated into a more triangular shape for low
drag and low radar cross section.  The shapes are tangent mounted to the
conformal pallet.  Weapon support structure and ejectors are contained
within the pallet fairing.  Other pallet designs could be employed for
other mission equipment.

With carriage arrangements such as that shown, the Light Experimental
Supercruiser can demonstrate supersonic weapon carriage and release.
Actual target acquisition and kill capability would require further
development of sensors and avionics.

The LES supersonic mission radius for this air-ground configuration is
approximately 250 n. mi.  In this configuration, best supersonic radius
is obtained at cruise Mach = 1.6 with partial afterburning power settings.

3.8  CREW STATION

DESIGN APPROACH

The low profile cockpit is vital to the LES concept to achieve low
supersonic airplane drag.  Volume for the low profile LES cockpit is
essentially equal to that of the Douglas A-4 although the LES volume is
distributed over more body length, reducing the body critical cross
section.  Impact on body cross sectional area distribution could have
been reduced by moving the cockpit aft.  However, this would have
further impaired pilot vision over the nose and side and also resulted

117
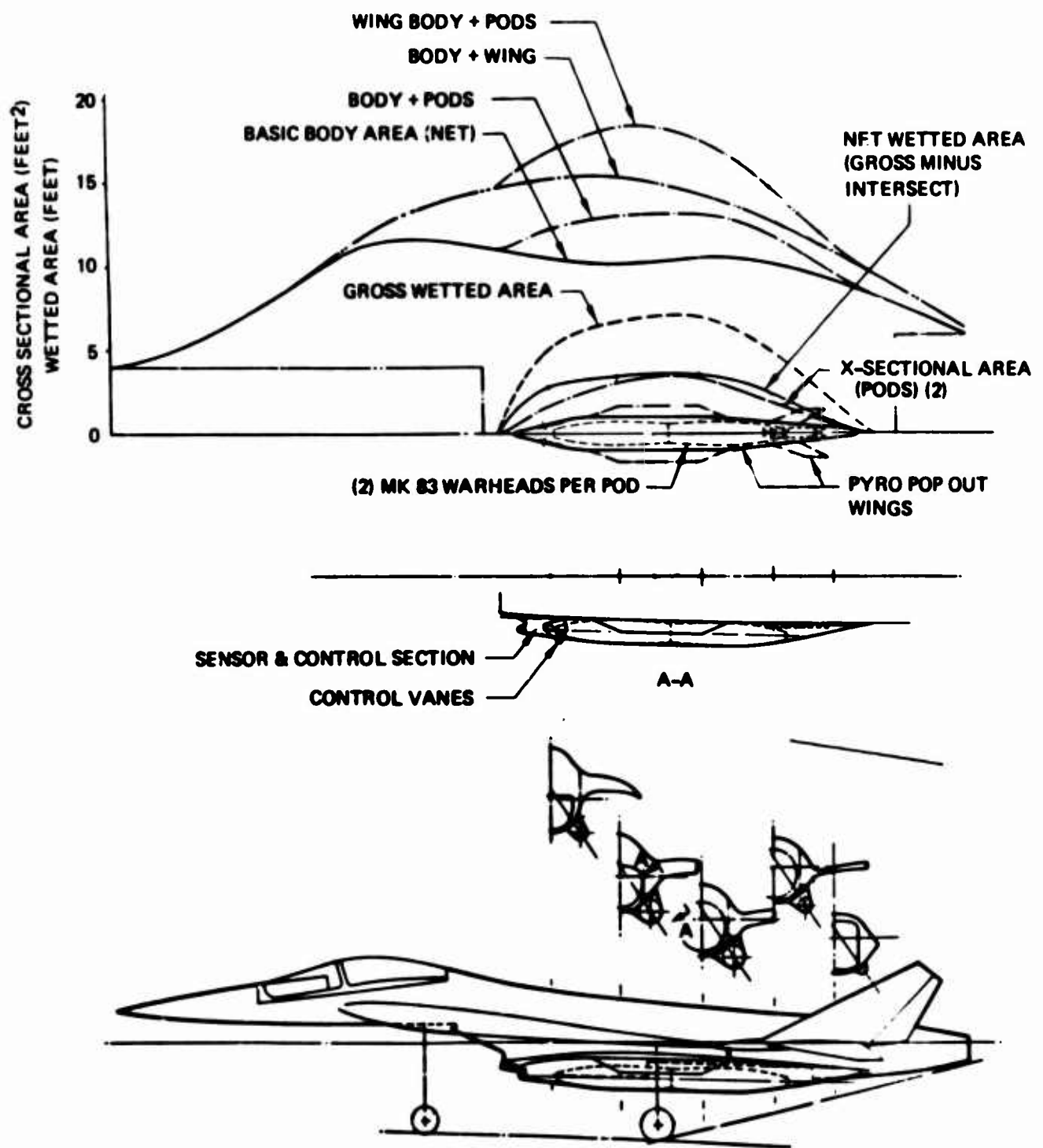
Figure 67. Supersonic Weapon Carriage

3.8  CREW STATION (Continued)

in a reduced body fuel volume.  The $7^O$ "over the nose" pilot vision
envelope is shown in Figure 68, and indicates the pilot's forward vision
is deficient when compared with the standard vision requirements ($11^O$
"over the nose") of MIL-STD-850.  However, if the eyepoint is displaced
4.0 inches from the ariplane centerline, the spec requirements may be
met for an arc of $\pm 5^O$ azimuth where it is deficient by about $4^O$ down
vision.

The cockpit was arranged to encompass controls and displays for the day
visual air-air role, with off-the-shelf hardware.

An integral panel and canopy hatch was used to allow better eye and
reach distances from a supine position.

The instrument panel is fixed to, and moves with the hatch (windshield)
to allow adequate clearance for pilot normal ingress, egress and ejection.

COCKPIT DESCRIPTION

Panel and Seat Arrangement--Arrangement of the instrument panel and
controls shown in Figure 69 is based on a seat at a $50^O$ seat back angle,
a 28 inch distance between eye point and instrument panel, and side
consoles for flight controller, power controller, electrical-electronics
and hydraulics control. A LED (light emitting diode) HUD is located on
the airplane centerline atop the instrument panel.

The cockpit seat relationship has been examined with the aid of mockups.
Results indicate that pilot comfort, internal vision and reach envelopes
are good.  A major limitation is found in aft vision.  The headrest and
parachute package prevent a full view at $180^O$ azimuth.  To aid aft vision,
the canopy was designed with a 26 inch diameter.  This allows pilot head
motion of 4 inches to either side for an aft vision of $180^O$.
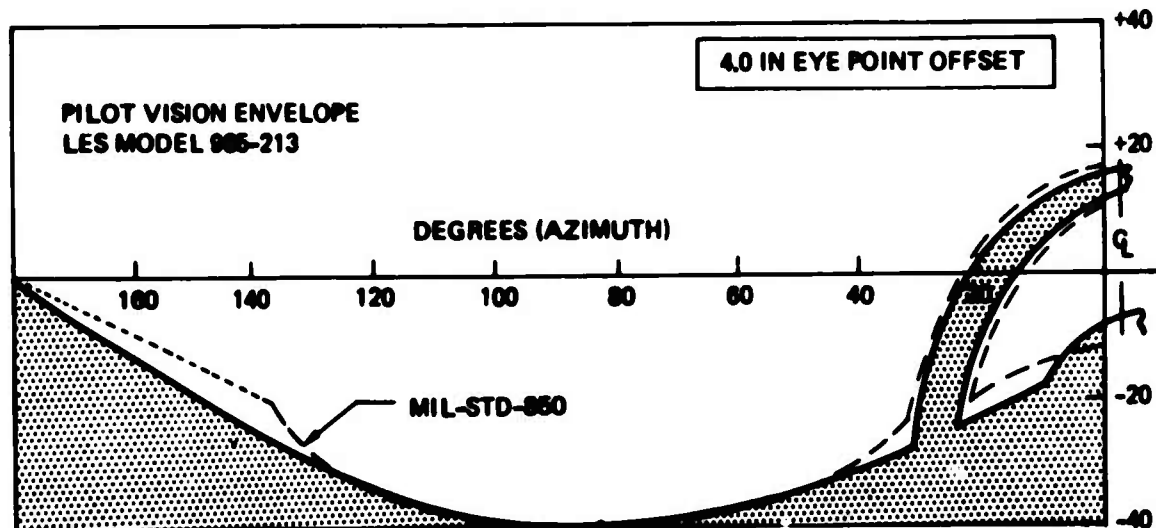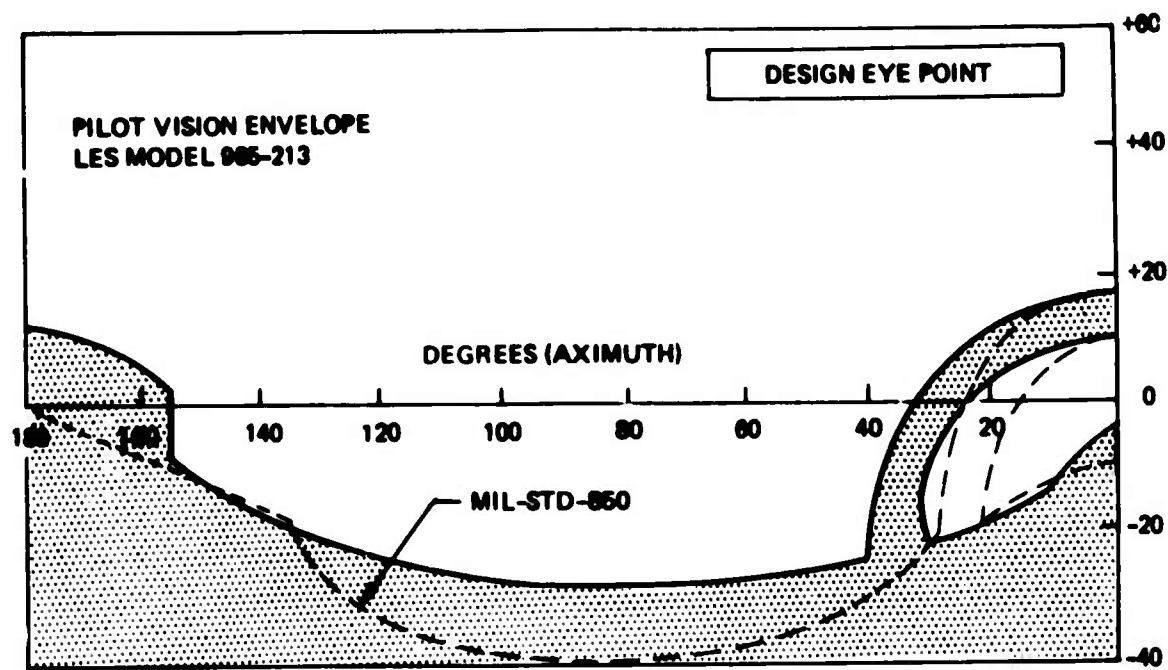
Figure 68.   Pilot Vision Envelopes (985-213)

120

BL

BACK-UP
ALTIMETER
(POP-UP)

BACK-UP
COMPASS
(POP-UP)

BACK-UP
ARTIFICIAL
HORIZON
(POP-UP)

SECTION A-A

BL

LIGHT SWITCH BAR

SECTION B-B
(STA 184)

BL 0.0

LINE OF VISION

PLAN

STA
113.5

BACK-UP
INSTRUMENTS
(POP-UP)

7°

10°

7°

LINE OF VISION

CANOPY BREAK - SEAL PLANE

A

A

WL 100

AUX. VIEW
LIGHT SWITCH BAR

PLAN VIEW

L.H. SIDE VIEW

EJECTION ENVELOPE

EJECTION ENVELOPE

HINGE LINE

STA 184.0

STA 215.0
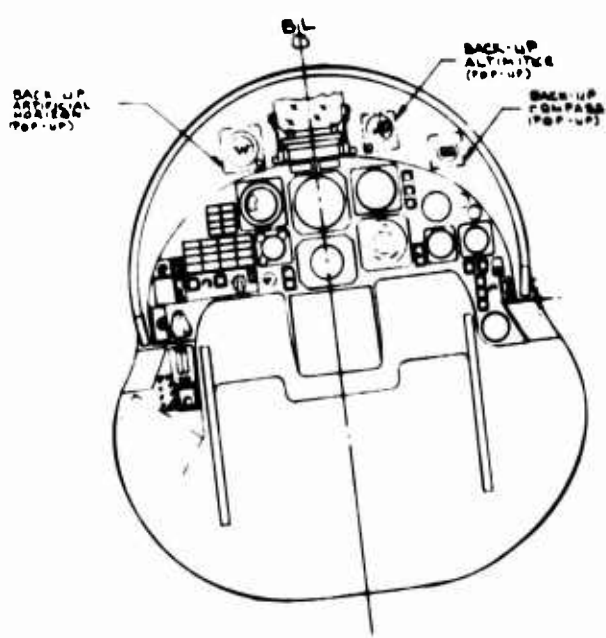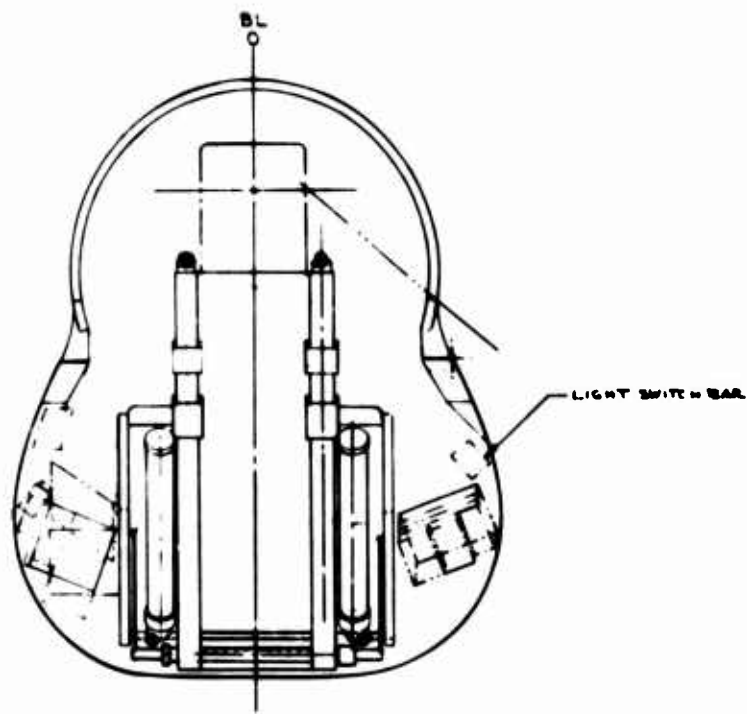
SECTION C-C
(STA 215.0)
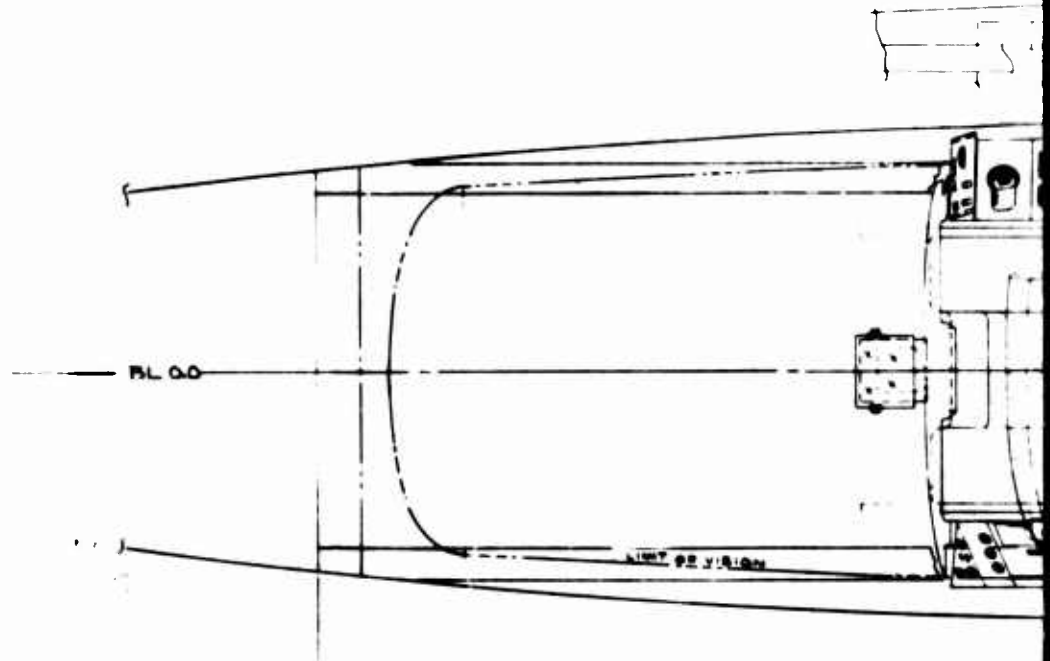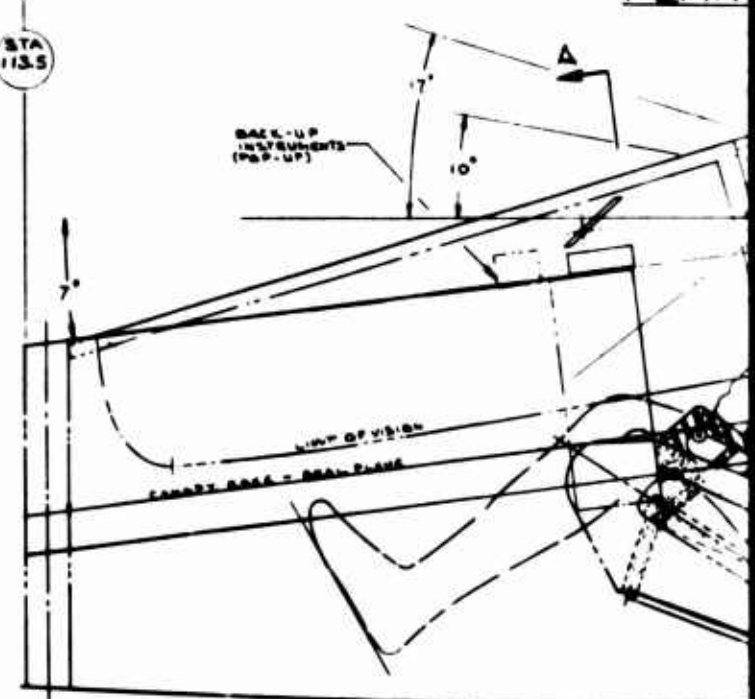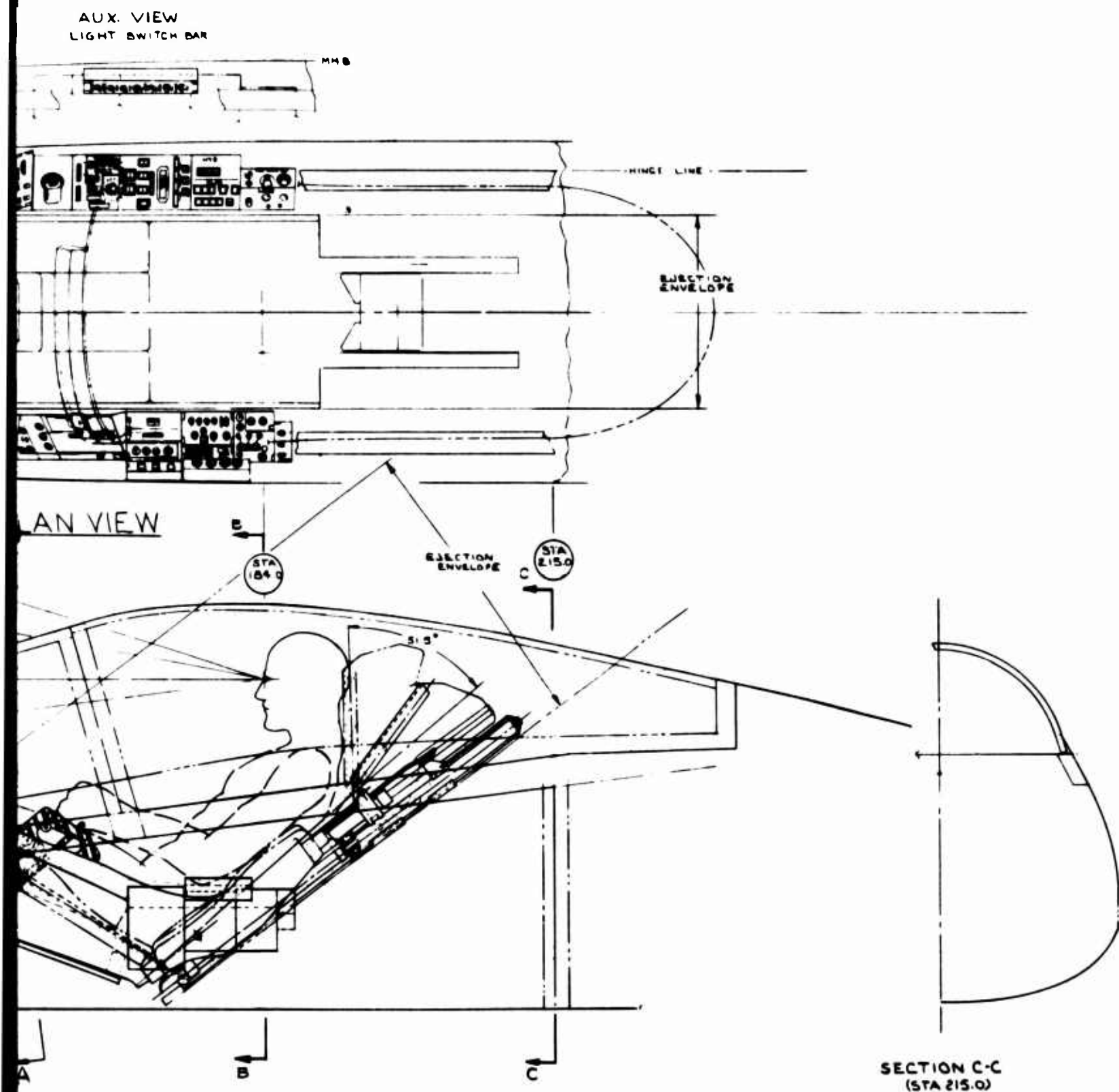
Figure 62. Cockpit Details – LES Model 985-21

121 & 122

## 3.8 CREW STATION (Continued)

The instrument panel and side console layout is based on the "emerging" LES avionics. The left hand console was arranged to bring readouts of radio frequency and channels to direct line of sight from a centerline eye point. The landing gear handle and position indicators were placed in the lower left hand corner of the instrument panel (a portion of the panel fixed to the airframe). Console elements were installed at about $45^o$. This allowed more arm clearance between the seat side and the instrument face, and brought the instrument face more nearly perpendicular to the line of sight. The side arm controller was centered at a natural rest angle. The canted consoles and seat side should give the pilot's arms restraint during high g maneuvers.

The instrument panel, above the level of the canopy hinge and seal, is attached to the canopy hatch assembly. Electrical-electronic umbilical connectors are on the right hand side of the aircraft adjacent to the canopy/hatch hinge line. This will allow free rotation of the hatch during normal operation and a clean release of the umbilical on canopy ejection, or maintenance.

The construction of the canopy/hatch consists of the frame which will include the seal, hinge fittings, ejection fitting and the canopy locking devices. The windshield portion is a cylindrical, polycarbonate transparency attached to the frame and the intermediate arch through a phenolic-glass fabric edging. The aft canopy section is a monolithic polycarbonate shell attached to the frame with a phenolic-glass fabric edging.

Ejection Seat--A fixed existing seat design was sought that would show good ejection performance up to the 600 KT requirement. The ejection seat chosen is the Stencil Aero Engineering Corporation type SIII-S escape system which has been qualified for the AV-8A Harrier and Northrup YF-17 fighter.

123

## 3.8 CREW STATION (Continued)

The seat is a self-contained escape system mounted on a structural bulk-head on the airframe. The seat back tangent line is location at $50^o$ to the vertical, the seat rails and ejection are at $54^o$ from the vertical. The pilot's head rest must be reconfigured to an angle of $51.5^o$ to correctly position the pilot's eye point. The angle between the seat bottom and the seat back tangent line has been modified to $97^o$. This should reduce the possibility of "submarining" through his restraint harness.

### CANOPY JETTISON OPTIONS

Side Opening Operation--The present configuration of cockpit/canopy is designed for a side opening canopy/hatch, Figure 70. During ejection, forward and aft actuators would rotate the assembly clockwise to an ejection position prior to initiation of seat ejection. As all instru-mentation and equipment above the seal plane are attached to the canopy/hatch, pilot egress during ejection would be unimpeded. Latching of the canopy would be accomplished only on the left hand sill beam with the hinges reacting the right hand canopy loads.

Split Canopy Concept--The alternate canopy/hatch arrangement is also shown on Figure 80. The forward windshield is hinged to swing upward and forward to gain access to the attached instrument panel.

The aft canopy is hinged at its aft end allowing it to swing upward and aft for pilot normal access and egress.

During the ejection, the forward canopy section is actuated upward approxi-mately $30^o$. This will allow a complete egress envelope for the pilot's legs and feet and also provide a wind screen during the seat ejection. The aft canopy section would be ejected upward and aft by an actuation system during the seat ejection. This configuration will require two latching systems (forward and aft canopy section) with latches on both left and right hand sill beams and an additional seal at the canopy half interface.

124
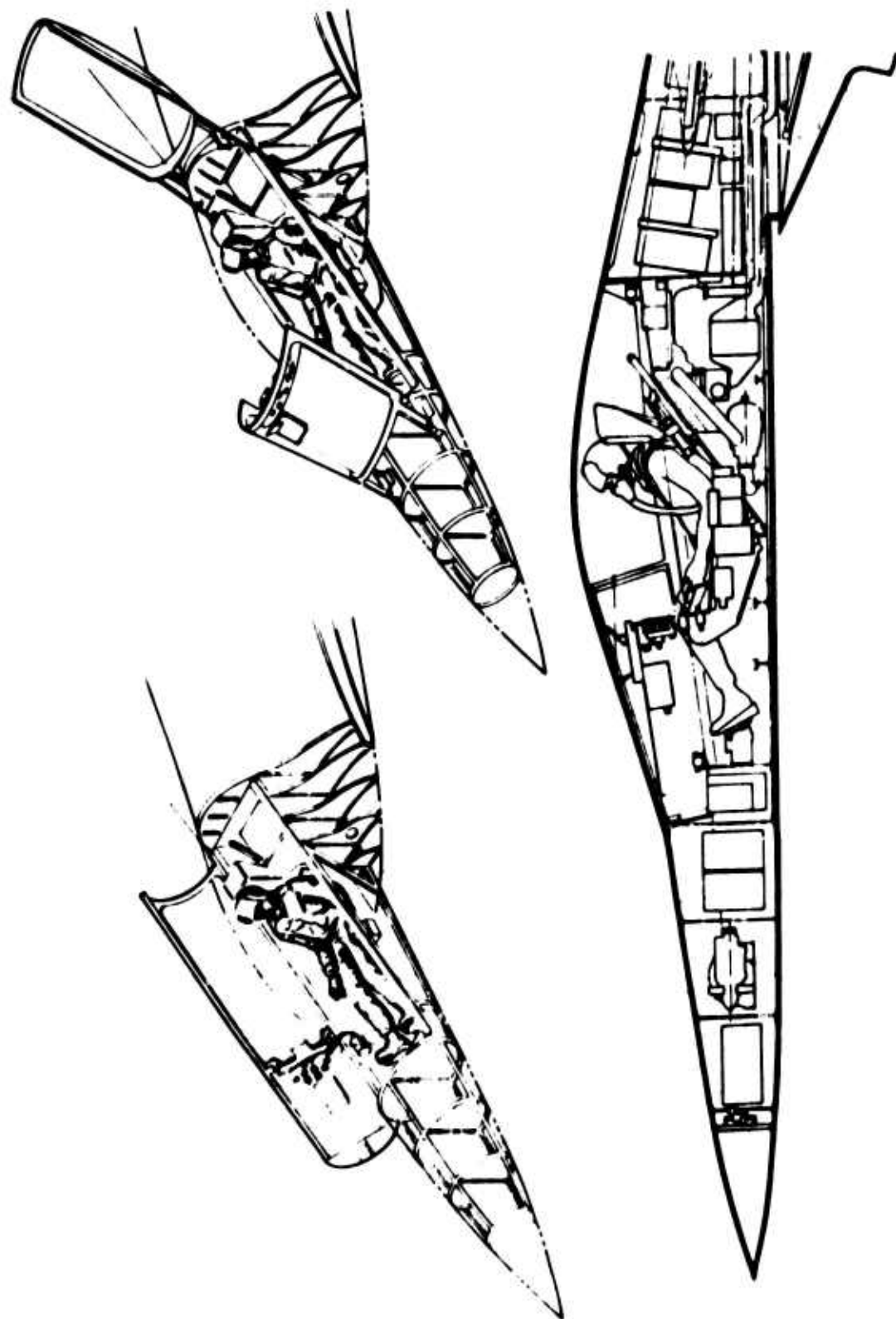
Figure 70.   Low Profile Cockpit Design – Canopy Jettison Options

125

3.9 MASS PROPERTIES

WEIGHT ANALYSIS

The weights for LES Model 985-213 are computed utilizing the methods described in Reference (20) along with the application of appropriate factors to reflect emerging and future technology levels.

The following features were incorporated to minimize weight and cost and to improve performance:

o The majority of aircraft structure is advanced composites (graphite-epoxy).
o Airframe Integrated Nozzle
o Fly-by-wire surface controls.
o Avionics equipment in compliance with statement-of-work requirements.
o Semi-submerged claw missiles (2).
o Final aircraft geometry is the result of aerodynamic and weight parametric trade studies and represents the best compromise for overall performance.
o Lightweight M-197 20mm gattling gun with gas drive.
o Judicious location of gun, ammunition, missiles and fuel such as to minimize CG travel as these items are expended.
o Fuel pumping for trim control.

Structural Weight - The structural weight was calculated utilizing the methods of Reference (20) and adjusted to reflect the extensive use of advanced composites. The adjustment factors for advanced composites were developed during the HIPAAS studies and further substantiated by two current Boeing studies. These studies are the YC-14 elevator (an in-house design study) and the Battle Damage Tolerant Wing Structural Development Program (Reference 5).

126

3.9 MASS PROPERTIES (Continued)

The structural analysis of a 60 sq. ft. portion of the main wing box as discussed in Section 3.2 for the Model 985-211 wing as shown by Figure 22 provides a case for the feasibility of the LES structural design concept. The results of this analysis indicate an idealized structure unit weight of 3.27 lbs/sq. ft. for the 60 sq. ft. of primary wing structure. Idealized primary structure is the upper and lower surface cover material, the main and auxiliary spar chord plus the spar shear webs. Spar web stiffeners, joints, splices, fasteners, bonding, miscellaneous bracketry and supports, access doors, and panels, lightning strike protection, electrical continuity, integral fuel tank treatment as well as exterior finish weights must be added to the idealized structure weight in order to represent a real life structural box weight.

Total wing weight consists of the structural box plus the secondary structure which consists of leading and trailing edge control surfaces, fixed leading and trailings, wing tips, control surface brackets and supports as well as carriages and tracks, hinges and pins.

The combination of real life structural box plus secondary structure is estimated to raise the unit weight for the total wing group to approximately 6.11 lbs/sq. ft. for the 193 sq. ft. of exposed wing area.

Based on the results of the structural analysis and accompanying rationale it was assumed that the unit weights quoted for the advanced composite structures of the LES Model 985-213 are achievable. Additional detail design and analysis should be pursued in order to further verify structural weight advantages .due to the use of advanced composite structural materials.

System and Equipment Weight - System and equipment weight methods are from Reference (20) incorporating the specific requirements of the Light Experimental Supercruiser and cross checked with data generated from the Boeing Lightweight Fighter Proposal.

## 3.9  MASS PROPERTIES (Continued)

Specific requirements and definitions for starting system, hydraulic and electrical system power, avionics equipment, pilot seat, cockpit equipment and gun and provisions lend high confidence to weights reported for these groups.

### AIRCRAFT INERTIAS

Moments and products of inertias were calculated for Model 985-213 using the preliminary design method described in Appendix C of Reference (20), where radii of gyration (K) are expressed as fixed percentages of aerodynamic span and/or overall airplane length and inertia $(I) = m (K)^2$ Slug - $ft^2$.  Radii of gyration are as follows:

$$K_{roll} = 0.127 \ (b) - Ft.$$

$$K_{pitch} = 0.179 \ (L) - Ft.$$

$$K_{yaw} = 0.224 \ \frac{(b+L)}{2} - Ft.$$

Table 6 summarizes moments of inertias calculated for various gross weight conditions.

*Table 6.  Model 985-213 Inertia Data*

| ITEM | | BASIC MISS. FLT. DESIGN WEIGHT | BASIC MISS. TAKEOFF WEIGHT | MAXIMUM TAKEOFF WEIGHT |
|---|---|---|---|---|
| GROSS WEIGHT   - LBS. | | 10,400 | 12,500 | 16,780 |
| $I_{ROLL}$ | SLUG - FT.$^2$ | 2,190 | 2,620 | 3,530 |
| $I_{PITCH}$ | SLUG - FT.$^2$ | 20,030 | 24,020 | 32,390 |
| $I_{YAW}$ | SLUG - FT.$^2$ | 16,860 | 20,210 | 27,260 |

## 3.9  MASS PROPERTIES (Continued)

### WEIGHT AND BALANCE

Aircraft weight and balance is reported in Table 7 to the group weight
statement level of detail.  The weights were calculated per the pre-
ceding discussion and the balance was determined by applying body sta-
tion locations as determined from the general arrangement, Figure 19,
to each of the group weights summing up the moments and dividing by the
appropriate weight.  A center of gravity envelope is shown in Figure 71.
This diagram was constructed to show the worst possible center of
gravity conditions with unrestricted management of disposable useful
load (fuel and weapons) for the design mission.  The subsonic and
supersonic aerodynamic centers and main landing gear location are also
noted on the chart.  The results of this plot indicate that the con-
figuration, as designed, provides satisfactory stability and control
conditions and minimum trim drag for a very simple fuel management
program.

Table 8 contains weight and balance buildups for several design gross
weight conditions.  MIL-STD-1374 Part 1 group weight statement for
Model 985-213 has been completed and is presented in Table 9.

129

Table 7. Group Weight and Balance Statement — LES Model 985-213

| | LES Model 985-213 | | |
|---|---|---|---|
| | WEIGHT LBS. | HORIZONTAL BALANCE | |
| | | BODY STA. | % MAC |
| WING | 1180 | 376 | |
| HORIZONTAL TAIL | - | - | |
| VERTICAL TAIL | 100 | 490 | |
| BODY | 1520 | 316 | |
| MAIN GEAR | 380 | 361 | |
| NOSE GEAR | 110 | 221 | |
| LAUNCH AND RECOVERY GEAR | - | 436 | |
| ENG. SECTION OR NACELLE | 360 | 316 | |
| STRUCTURE | (3650) | (342) | |
| ENGINE & EXHAUST | 2200 | 432 | |
| THRUST REVERSER | | | |
| ENGINE ACCESSORIES | 50 | 400 | |
| ENGINE CONTROLS | 80 | 291 | |
| STARTING SYSTEM | 100 | 373 | |
| FUEL SYSTEM | 340 | 347 | |
| PROPULSION | (2770) | (415) | |
| FLIGHT CONTROLS | 260 | 394 | |
| AUXILIARY POWER PLANT | - | - | |
| INSTRUMENTS | 70 | 178 | |
| HYDRAULIC & PNEUMATIC | 120 | 380 | |
| ELECTRICAL | 270 | 318 | |
| AVIONICS | 390 | 171 | |
| ARMAMENT | 40 | 205 | |
| FURNISHINGS & EQUIPMENT | 180 | 173 | |
| AIR CONDITIONING | 120 | 175 | |
| ANTI-ICING | 10 | 238 | |
| LOAD & HANDLING | 30 | 510 | |
| FIXED EQUIPMENT | (1490) | (262) | |
| WEIGHT EMPTY | 7910 | 352 | 57.1 |
| CREW | 200 | 173 | |
| UNUSABLE FUEL | 30 | 350 | |
| OIL & TRAPPED OIL | 60 | 395 | |
| EXTERNAL TANKS | - | - | |
| GUN INSTALLATIONS | 260 | 275 | |
| WEAPON INSTALLATIONS | 60 | 265 | |
| CREW EQUIPMENT | 10 | 173 | |
| NON-EXP.USEFUL LOAD | (620) | (255) | |
| OPERATING WEIGHT | 8,530 | 345 | 54 |
| FUEL - INTERNAL | 3,630 | 348 | |
| FUEL - EXTERNAL | | | |
| AMMUNITION-250 RNDS 20MM | 180 | 280 | |
| (2) CLAW MISSILES | 160 | 265 | |
| GROSS WEIGHT (MISSION T.O.) | 12,500 | 343.9 | 53.5 |
| BASIC MISS.FLT.DES.WT. | 10,400 | Nose at body sta. 26 | |
| FULL INTERNAL FUEL | 3,630 | LEMAC at body sta. 222.5 | |
| BMFDW | 6,5 | Length of MAC = 226.8 | |

130
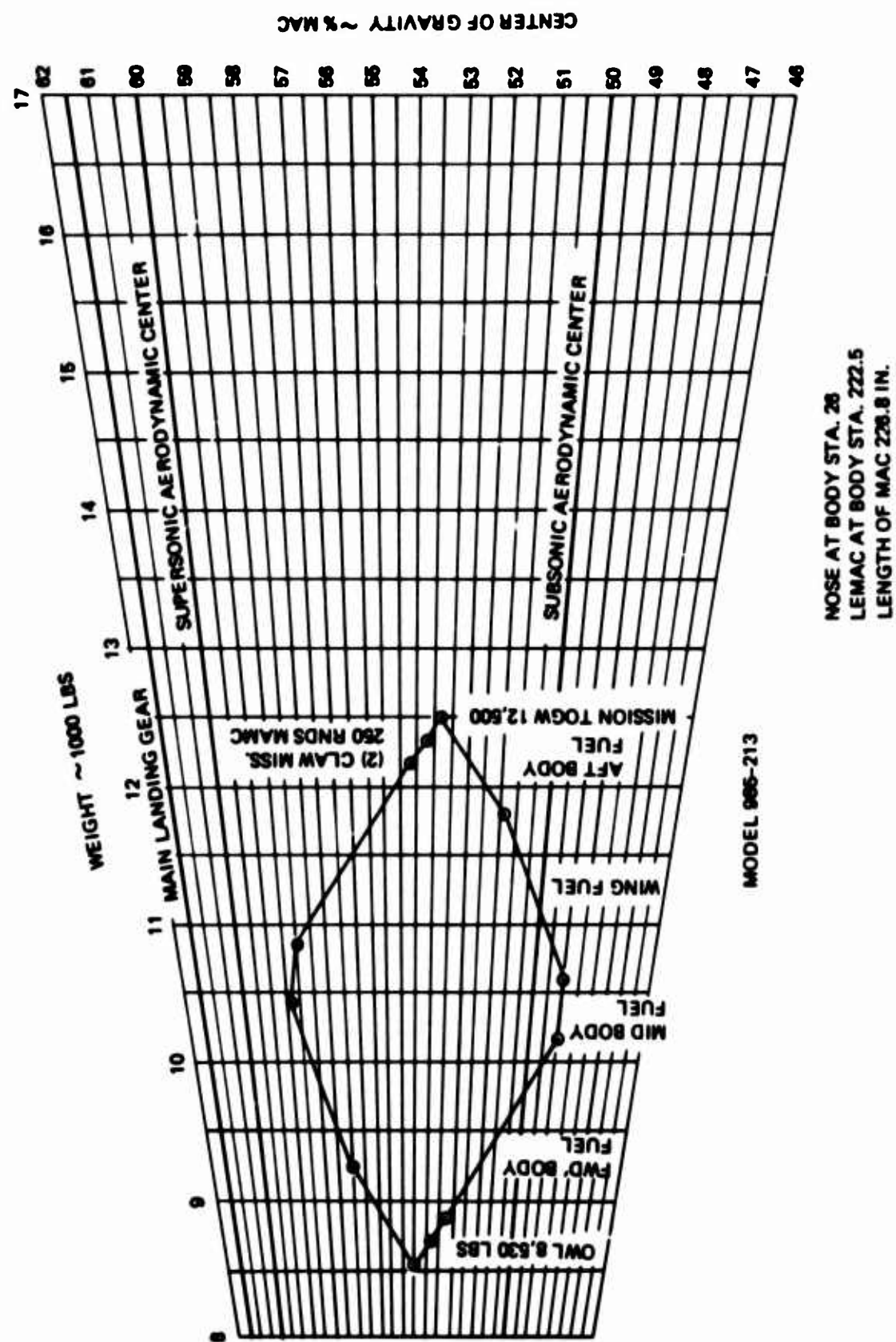
Figure 71. LES Center of Gravity Envelope

MODEL 985-213

NOSE AT BODY STA. 28
LEMAC AT BODY STA. 222.5
LENGTH OF MAC 229.8 IN.

131

## Table 8.   Design Weight Buildups — LES Model 985-213

| ITEM | WEIGHT (LBS.) | HORIZ. C.G. (IN.) |
|------|---------------|-------------------|
| OPERATING WEIGHT | 8,530 | 345 |
| 2 CLAW MISSILES | 160 | 265 |
| 250 ROUNDS AMMUNITION | 180 | 280 |
| BASIC MISSION FLIGHT DESIGN FUEL | 1,530 | 328 |
| BASIC MISSION FLIGHT DESIGN WT. | (10,400) | (340) |
| REMAINDER BASIC MISSION FUEL | 2,100 | 371 |
| BASIC MISSION TAKEOFF WEIGHT | (12,170) | (344.6) |
| | | |
| OPERATING WEIGHT | 8,530 | 345 |
| 2 CLAW MISSILES | 160 | 265 |
| 250 ROUNDS AMMUNITION | 180 | 280 |
| FULL INTERNAL FUEL | 3,600 | 348 |
| FULL INTERNAL FUEL TAKEOFF WT. | (12,470) | (343.9) |
| | | |
| OPERATING WEIGHT | 8,530 | 345 |
| 2 CLAW MISSILES | 160 | 265 |
| 250 ROUNDS AMMUNITION | 180 | 280 |
| FULL INTERNAL FUEL | 3,600 | 348 |
| EXTERNAL FUEL AND PROVISIONS | 4,310 | 380 |
| MAXIMUM TAKEOFF GROSS WT. | (16,780) | (353.2) |

# TABLE 9

# PART I

# GROUP WEIGHT STATEMENT

## MIL-STD-1374

### AIRCRAFT

(INCLUDING ROTORCRAFT)

ESTIMATED

(Cross Out Those Not Applicable)

CONTRACT NO. _____

AIRCRAFT, GOVERNMENT NO. _____

AIRCRAFT, CONTRACTOR NO. _____

MANUFACTURED BY _____

| | | MAIN | AUX |
|---|---|---|---|
| ENGINE | MANUFACTURED BY | GE | |
| | MODEL | A9 STUDY | |
| | NO. | I | |
| | TYPE | | |

| PAGES REMOVED | PAGE NO. |
|---|---|
| | |
| | |
| | |
| | |
| | |

133

## Table 9. Group Weight Statement (Continued)

| # | | Running Gear* | Arrest Gear* | Structure | Controls | | |
|---|---|---|---|---|---|---|---|
| 1 | WING GROUP | | | | | | 1180 |
| 2 | BASIC STRUCTURE · CENTER SECTION | | | | | | |
| 3 | · INTERMEDIATE PANEL | | | | | | |
| 4 | · OUTER PANEL | | | | | 830 | |
| 5 | · GLOVE | | | | | | |
| 6 | SECONDARY STRUCTURE (incl. Wing Fold Weight     Lbs.) | | | | | 90 | |
| 7 | AILERONS (incl. balance weight)   ELEVONS   (Lbs.) | | | | | 120 | |
| 8 | FLAPS · TRAILING EDGE | | | | | | |
| 9 | · LEADING EDGE | | | | | 140 | |
| 10 | SLATS | | | | | | |
| 11 | SPOILERS | | | | | | |
| 12 | | | | | | | |
| 13 | | | | | | | |
| 14 | ROTOR GROUP | | | | | | |
| 15 | BLADE ASSEMBLY | | | | | | |
| 16 | HUB & HINGE (incl. Blade Fold Weight       Lbs.) | | | | | | |
| 17 | | | | | | | |
| 18 | | | | | | | |
| 19 | TAIL GROUP | | | | | | 100 |
| 20 | BASIC & SECONDARY STRUCT. · STABILIZER | | | | | | |
| 21 | · FIN (incl. Dorsal) | | | | | | |
| 22 | VENTRAL | | | | | | |
| 23 | ELEVATOR (incl. Balance Weight       Lbs.) | | | | | | |
| 24 | RUDDERS (incl. Balance Weight       Lbs.) | | | | | | |
| 25 | TAIL ROTOR · BLADES | | | | | | |
| 26 | · HUB & HINGE | | | | | | |
| 27 | | | | | | | |
| 28 | BODY GROUP | | | | | | 1520 |
| 29 | BASIC STRUCTURE · FUSELAGE or HULL | | | | | | |
| 30 | · BOOMS | | | | | | |
| 31 | SECONDARY STRUCTURE · FUSELAGE or HULL | | | | | | |
| 32 | · BOOMS | | | | | | |
| 33 | · SPEEDBRAKES | | | | | | |
| 34 | · DOORS, RAMPS, PANELS, & MISC. | | | | | | |
| 35 | | | | | | | |
| 36 | | | | | | | |
| 37 | ALIGHTING GEAR GROUP (Type: | | | | | | 490 |
| 38 | LOCATION | Running Gear* | Arrest Gear* | Structure | Controls | | |
| 39 | MAIN | 120 | | 200 | 60 | 380 | |
| 40 | NOSE | 10 | | 70 | 30 | 110 | |
| 41 | | | | | | | |
| 42 | | | | | | | |
| 43 | | | | | | | |
| 44 | | | | | | | |
| 45 | ENGINE SECTION or NACELLE GROUP | | | | | | 360 |
| 46 | BODY · INTERNAL | | | | | 70 | |
| 47 | · EXTERNAL | | | | | | |
| 48 | WING · INBOARD | | | | | | |
| 49 | · OUTBOARD | | | | | | |
| 50 | | | | | | | |
| 51 | | | | | | | |
| 52 | AIR INDUCTION SYSTEM | | | | | 290 | |
| 53 | DOORS, PANELS, & MISC. | | | | | | |
| 54 | | | | | | | |
| 55 | | | | | | | |
| 56 | | | | | | | |
| 57 | TOTAL STRUCTURE (To be brought Forward) | | | | | | 3650 |

*Change to Floats & Struts for Water Type Gear.

## Table 9. Group Weight Statement (Continued)

MIL-STD-1374 PART I

Name _____

Date _____

Page _____

Model 985-213

Report _____

| # | | Auxiliary | Main | |
|---|---|---|---|---|
| 1 | PROPULSION GROUP | | | 2770 |
| 2 | ENGINE INSTALLATION + 2D NOZZLE | | 2200 | |
| 3 | | | | |
| 4 | ACCESSORY GEAR BOXES & DRIVE | | 50 | |
| 5 | | | | |
| 6 | EXHAUST SYSTEM | | | |
| 7 | ENGINE COOLING | | | |
| 8 | WATER INJECTION | | | |
| 9 | ENGINE CONTROL | | | |
| 10 | STARTING SYSTEM | | 80 | |
| 11 | PROPELLER INSTALLATION | | 100 | |
| 12 | SMOKE ABATEMENT | | | |
| 13 | LUBRICATING SYSTEM | | | |
| 14 | FUEL SYSTEM | | 340 | |
| 15 | TANKS - PROTECTED | | | |
| 16 | - UNPROTECTED | 40 | | |
| 17 | PLUMBING, etc. | 300 | | |
| 18 | DRIVE SYSTEM | | | |
| 19 | GEAR BOXES, LUB SY & ROTOR BRK | | | |
| 20 | TRANSMISSION DRIVE | | | |
| 21 | ROTOR SHAFTS | | | |
| 22 | JET DRIVE | | | |
| 23 | | | | |
| 24 | FLIGHT CONTROLS GROUP | | | 260 |
| 25 | COCKPIT CONTROLS (Autopilot 90 Lbs.) | | 120 | |
| 26 | SYSTEMS CONTROLS | | 140 | |
| 27 | | | | |
| 28 | | | | |
| 29 | AUXILIARY POWER PLANT GROUP | | | |
| 30 | INSTRUMENTS GROUP | | | 70 |
| 31 | HYDRAULIC & PNEUMATIC GROUP | | | 120 |
| 32 | | | | |
| 33 | ELECTRICAL GROUP | | | 270 |
| 34 | | | | |
| 35 | AVIONICS GROUP | | | 390 |
| 36 | EQUIPMENT | | 310 | |
| 37 | INSTALLATION | | 80 | |
| 38 | | | | |
| 39 | ARMAMENT GROUP (incl. Passive Prot. Lbs.) | | | 40 |
| 40 | FURNISHINGS & EQUIPMENT GROUP | | | 180 |
| 41 | ACCOMMODATION FOR PERSONNEL | | | |
| 42 | MISCELLANEOUS EQUIPMENT | | | |
| 43 | FURNISHINGS | | | |
| 44 | EMERGENCY EQUIPMENT | | | |
| 45 | | | | |
| 46 | AIR CONDITIONING GROUP | | | 120 |
| 47 | ANTI - ICING GROUP | | | 10 |
| 48 | GUN INSTALLATION & PROVISIONS | | | |
| 49 | PHOTOGRAPHIC GROUP | | | |
| 50 | | | | |
| 51 | LOAD & HANDLING GROUP | | | 30 |
| 52 | AIRCRAFT HANDLING | | 30 | |
| 53 | LOAD HANDLING | | | |
| 54 | | | | |
| 55 | MANUFACTURING VARIATION | | | |
| 56 | TOTAL FROM PAGE 2 | | | 3650 |
| 57 | WEIGHT EMPTY | | | 7910 |

BEST AVAILABLE COPY

## Table 9. Group Weight Statement (Continued)

MIL-STD-1374 PART 1

Name _____

Date _____

Page _____

Model __985-213__

Report _____

| # | LOAD CONDITION | | | | | BASIC | | | |
|---|---|---|---|---|---|---|---|---|---|
| 1 | LOAD CONDITION | | | | | BASIC | | | |
| 2 | | | | | | MISSION | | | |
| 3 | CREW (No. 1 ) | | | | | 200 | | | |
| 4 | PASSENGERS (No. 1 ) | | | | | | | | |
| 5 | FUEL | Location | Type | Gals. | | | | | |
| 6 | UNUSABLE | | | 4.6 | | 30 | | | |
| 7 | INTERNAL | WING | | 184.6 | | 1200 | | | |
| 8 | | BODY | | 373.8 | | 2430 | | | |
| 9 | | | | | | | | | |
| 10 | | | | | | | | | |
| 11 | EXTERNAL | | | | | | | | |
| 12 | | | | | | | | | |
| 13 | | | | | | | | | |
| 14 | OIL | | | | | | | | |
| 15 | TRAPPED | | | | | 20 | | | |
| 16 | ENGINE | | | | | 40 | | | |
| 17 | | | | | | | | | |
| 18 | FUEL TANKS (Location ) | | | | | | | | |
| 19 | WATER INJECTION FLUID ( Gal.) | | | | | | | | |
| 20 | CREW PROVISIONS | | | | | 10 | | | |
| 21 | BAGGAGE | | | | | | | | |
| 22 | CARGO | | | | | | | | |
| 23 | | | | | | | | | |
| 24 | GUN INSTALLATIONS | | | | | 260 | | | |
| 25 | GUNS | Location | Fin. or Flex | Quantity | Caliber | | | | |
| 26 | | | | | | | | | |
| 27 | | | | | | | | | |
| 28 | AMMO. | | | 250 | 20MM | 180 | | | |
| 29 | | | | | | | | | |
| 30 | | | | | | | | | |
| 31 | SUPPTS | | | | | | | | |
| 32 | WEAPONS INSTALL. (incl. Submarine Detection Expendables) | | | | | | | | |
| 33 | CLAW MISSLES (2) | | | | | 160 | | | |
| 34 | EJECTORS | | | | | 60 | | | |
| 35 | | | | | | | | | |
| 36 | | | | | | | | | |
| 37 | | | | | | | | | |
| 38 | | | | | | | | | |
| 39 | | | | | | | | | |
| 40 | | | | | | | | | |
| 41 | | | | | | | | | |
| 42 | | | | | | | | | |
| 43 | | | | | | | | | |
| 44 | | | | | | | | | |
| 45 | | | | | | | | | |
| 46 | EQUIPMENT | | | | | | | | |
| 47 | | | | | | | | | |
| 48 | SURVIVAL KITS & LIFE RAFTS | | | | | | | | |
| 49 | | | | | | | | | |
| 50 | OXYGEN | | | | | | | | |
| 51 | | | | | | | | | |
| 52 | | | | | | | | | |
| 53 | | | | | | | | | |
| 54 | | | | | | | | | |
| 55 | TOTAL USEFUL LOAD | | | | | 4590 | | | |
| 56 | WEIGHT EMPTY | | | | | 7910 | | | |
| 57 | GROSS WEIGHT | | | | | 12500 | | | |

*If Removable and Specified as Useful Load

**List Stores, Missiles, Sonobuoys, etc. Followed by Racks, Launchers, Chutes, etc. Not Part of Weight Empty.
List Identification, Location, and Quantity for All Items Above Including Installation.

136

## Table 9. Group Weight Statement (Continued)

MIL-STD-1374 PART I

Name _____

Date _____

Page _____

Model __985-213__

Report _____

| # | WING, ROTOR & TAIL GROUPS | | | | | | |
|---|---|---|---|---|---|---|---|
| 1 | WING, ROTOR & TAIL GROUPS | | | | | | |
| 2 | WING | 15.28 | 44.83 | 330 | 13.2 | 62.7 | 1.88 B.L. 91.7 |
| 3 | | | | | | | |
| 4 | MAIN ROTOR (Blades/Rotor ) | | | | | | |
| 5 | TAIL ROTOR (Blades/Rotor ) | | | | | | |
| 6 | HORIZ TAIL | | | | | | |
| 7 | VERT TAIL | | | | | | |
| 8 | | | | | | | |
| 9 | AREAS - (Sq. Ft.) | Wing | | | Horiz. Tail | Vert. Tail | Dorsal |
| 10 | (Theo. for Wing & Rotor, All Others Exposed) | 266 | | | | 38 | |
| 11 | | Speed Brks. | Flaps (L.E.) | Flaps (T.E.) | Slots | Spoilers | Ailerons |
| 12 | AREAS - (Sq. Ft.) | | | 22 | | | 19 |
| 13 | BODY & NACELLE GROUPS | Length (Ft.) | Depth (Ft.) | Width (Ft.) | WETTED AREA SQ FT | Vol. (Cu. Ft.) | VOL PRESS CU FT |
| 14 | FUSELAGE or HULL | 44 | 4.08 | 4.5 | 417 | | |
| 15 | BOOMS | | | | | | |
| 16 | NACELLES | | | | | | |
| 17 | | | | | | | |
| 18 | | | | | | | |
| 19 | ALIGHTING GEAR GROUP | Length - Oleo Ext. | | Oleo Travel | | Length - Arrest Hook | |
| 20 | | Axle to ℄ Trunnion | | Ext. to Collapsed | | Hook Trunnion to Pt. | |
| 21 | LOCATION | NOSE | MAIN | NOSE | MAIN | | |
| 22 | DIMENSIONS (Inches) | 72 | 61 | 10 | 8 | | |
| 23 | | | | | | | |
| 24 | PROPULSION GROUP | | | | | | |
| 25 | ENGINES | S.L.S. THRUST IN LBS/ENG WITH AFTERBURNER | | S.L.S. THRUST IN LBS/ENG WITHOUT AFTERBURNER | | MAX S.L.S. SHAFT HP | SHAFT RPM AT MAX HP |
| 26 | MAIN | 16500 | | | | | |
| 27 | AUXILIARY | | | | | | |
| 28 | ROTOR DRIVE SYSTEM | Design H.P. | Input R.P.M. | OUTPUT RPM AT GROSS | RATED ROTOR RPM | NUMBER GEAR BOXES | |
| 29 | | | | | | | |
| 30 | | Protected | | Unprotected | | Integral | |
| 31 | FUEL - INTERNAL *** LOCATION | No. Tanks | Gallons | No. Tanks | Gallons | No. Tanks | Gallons |
| 32 | WING | | | | | | 184.6 |
| 33 | FUSELAGE | | | | | | 373.8 |
| 34 | EXTERNAL *** | | | | 610 | | |
| 35 | | | | | | | |
| 36 | OIL | | | | | | |
| 37 | ELECTRICAL & LOAD & HANDLING GROUPS | | QTY AC | QTY AC | | CARGO FLOOR AREA | |
| 38 | | 2 | 50A | 5KVA | | | |
| 39 | | | | | | | |
| 40 | STRUCTURAL DATA - CONDITION | | | FUEL IN WINGS LBS | | GROSS WEIGHT | Ult. L.F. |
| 41 | FLIGHT - MANEUVER | | | | | 10400 | 9.75 |
| 42 | - GUST | | | | | | |
| 43 | LANDING | | | | | | |
| 44 | | | | | | | |
| 45 | MAX. GROSS WITH ZERO WING FUEL | ✕ | ✕ | ✕ | | 15580 | 6.50 |
| 46 | CATAPULTING | ✕ | | | | | |
| 47 | LIMIT LANDING SINK SPEED (Ft./Sec.) | ✕ | | | | ✕ | |
| 48 | WT ASSUMED FOR LANDING WEIGHT CONDITION Ft. W | ✕ | | | | ✕ | |
| 49 | STALL SPD - LDG. CONFIG. - POWER OFF | ✕ | | ✕ | | ✕ | |
| 50 | RESULTING CABIN ALT DIFFER WITH DIFFERENTIAL PRESS P.M. | ✕ | | ✕ | | ✕ | |
| 51 | ROTOR TIP SPD AT DESIGN LIMIT | R.P.M. | Power | Ft./Sec. | COMPRESSIBILITY MACH FACTOR | | |
| 52 | | | | | | | |
| 53 | % DESIGN LOAD | Wing | | Rotor | | Rotor | |
| 54 | DESIGN SPEED AT S.L. (Knots) | Level | 790 | Dive | | | |
| 55 | DESIGN SPD AT OTHER ALTITUDES | 1188 | Alt. 50000 | | Alt. | | |
| 56 | | | | | | | |
| 57 | DCPR WEIGHT (Airframe) | | | | | | |

*Nose to aft tip of fuselage including equipment protuberances
**Parallel to ℄ or ℄ Aircraft for Wing & Tail. Insert inches from ℄ Rotor for Rotors.
***Total Usable Capacity
****Insert inches from ℄ Rotor to Blade Attachment for Rotors.

BEST AVAILABLE COPY

## 3.10 PERFORMANCE

Mission performance, takeoff and landing, and energy maneuver charac-
teristics of the Model 985-213 airplane are presented in this section.

### MISSION PERFORMANCE

Flight profiles described in Section 2.2 were calculated based on the
drag assessment from Section 3.4. Although it is anticipated that
significant improvements in performance will result with continued con-
figuration development, the airplane as currently defined is unable to
comply with the DESIGN/MISSION objective. Mission trades depicted on
Figure 72 indicate that at a cruise altitude of 50,000 feet and a radius
of 200 nautical miles, 26 percent of the desirable combat fuel is
available. Because of the initial wing geometry selection, considerable
advantage is gained through cruising at 60,000 feet. As discussed in
Section 2.3.2, detailed cockpit design work would be required to allow
operation at this higher altitude without encountering serious drag
penalties associated with pressure suit requirements. General perform-
ance level degradations were suffered as a result of the intermediate
thrust characteristics of the J101/J7 study A9 engine. A reduction in
thrust with speed above Mach 1.6 required the use of partial augmenta-
tion at the design cruise condition of Mach 1.8. The interpolation
procedure between intermediate thrust and minimum augmentation as
shown in Figure 73 was used for this study. Further development in
cockpit design, wing geometry, miscellaneous drag assessment and
engine ratings can result in attainment of the specified mission
objectives.

It should be noted that the maximum estimated potential for variable
camber devices from Section 3.4, was assumed for these calculations.
If the conservative estimate were used, a reduction in maneuver load
factor of 0.5g and an increase in combat fuel of 6 percent would
result. This emphasizes the importance of the development work
required in this area.
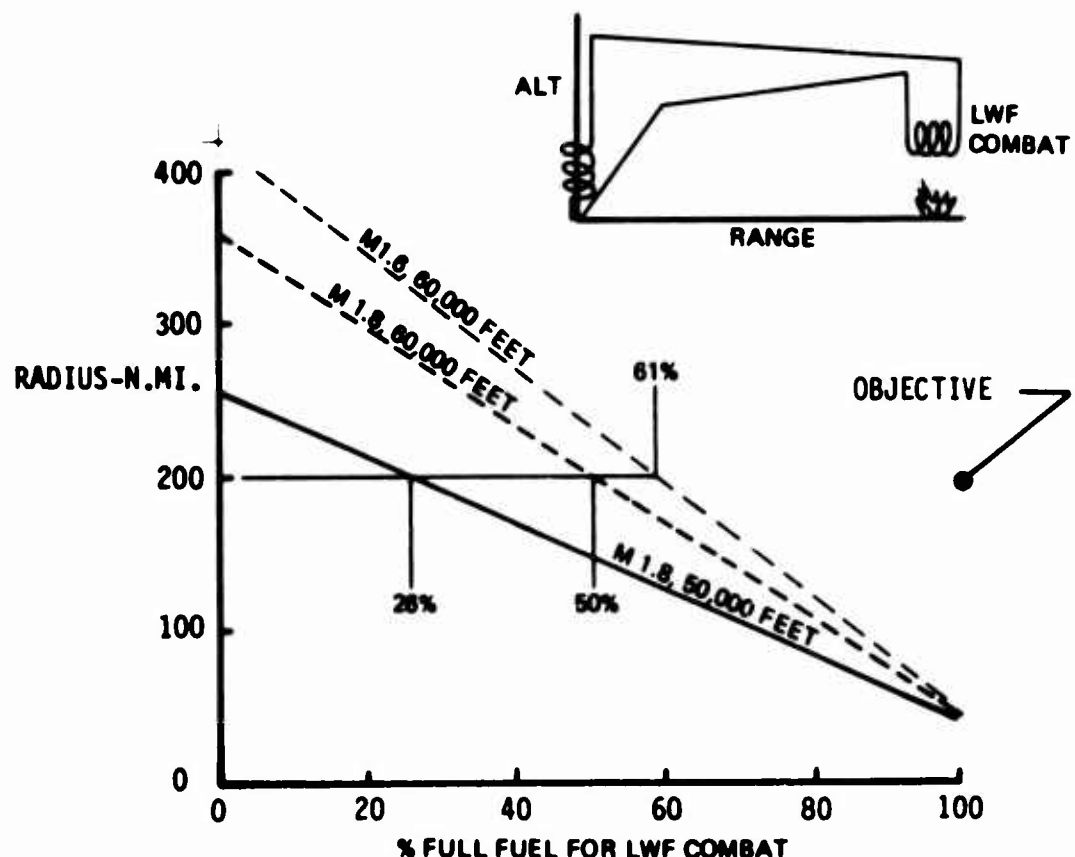
Figure 72. Design Mission Performance
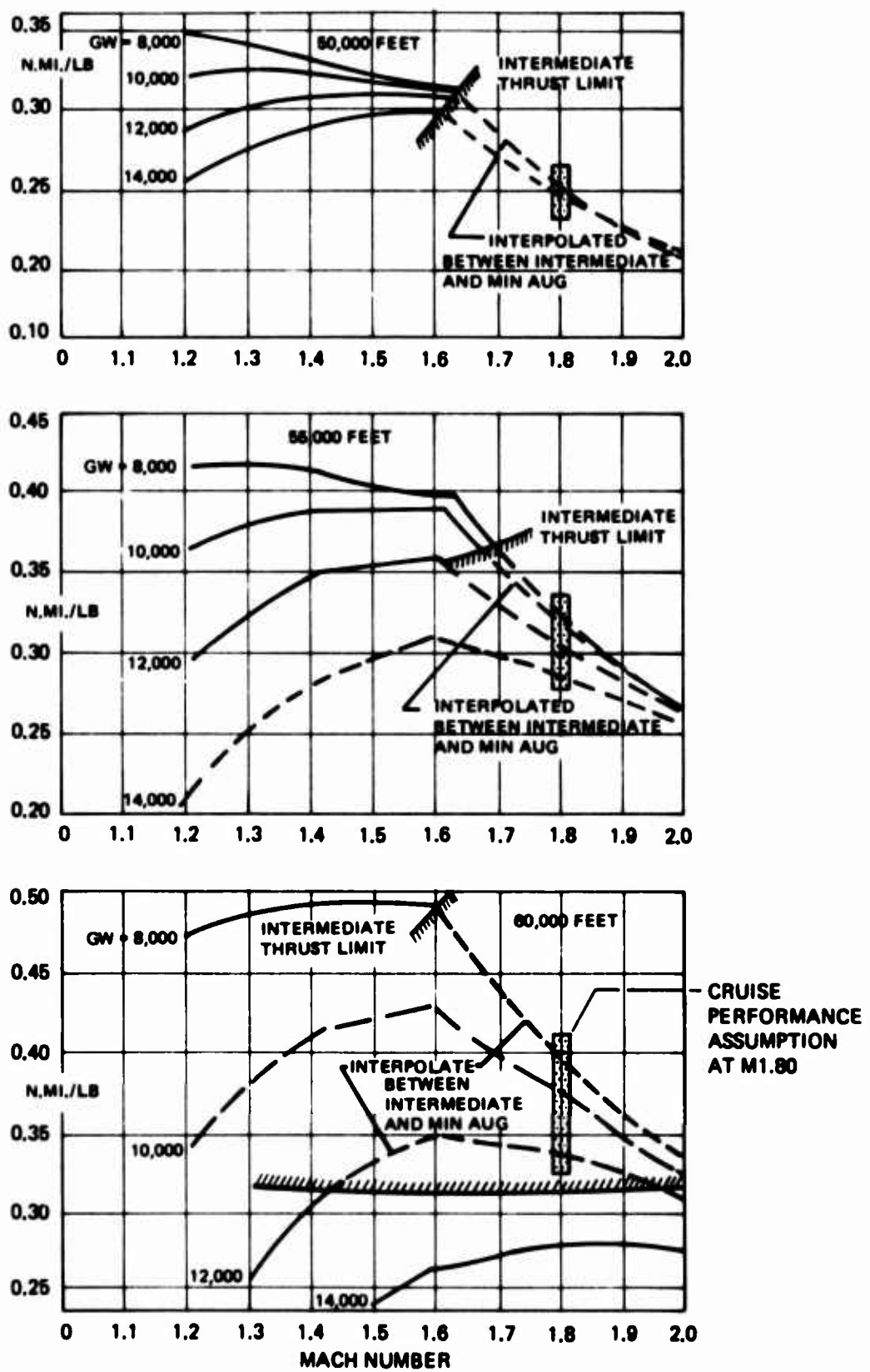
Figure 73. Supersonic Specific Range

3.10 PERFORMANCE (Continued)

A time, fuel, and distance tabulation for the DESIGN/MISSION calcula-
tion at 50,000 feet cruise and 200 nautical mile radius is presented
in Table 10.

Cruise speed and altitude trades for the MAXIMUM SUPERSONIC RADIUS
mission are shown in Figure 74. Here again, the relative advantages of
the higher cruise level is evident. Use of the partial augmentation
thrust results in a very significant effect of cruise Mach number.
Persistence options with radius are shown in Figure 75. Cruising
at the penalizing altitude of 50,000 feet, the following equivalent
combat allowances are possible at a 200 nautical mile radius:

| MACH NUMBER | ALTITUDE FT. | NUMBER OF TURNS |
|-------------|--------------|-----------------|
| 0.9 | 30,000 | 2.7 |
| 1.2 | 30,000 | 1.7 |
| 2.0 | 40,000 | 1.0 |

Takeoff and Landing performance at presented in Figures 76 and 77,
respectively. Because of the low wing loading and high thrust to
weight ratio, the airplane has outstanding takeoff potential. At a
reduced thrust level of 57 percent of dry rating, a respectable
ground roll distance of 2,500 feet is still realized relative to
1,350 feet using full thrust.

Approach speed varies from 150 knots at 12,000 pounds to 130 knots
at 9,000 pounds of gross weight. Because of these relatively high
speeds, landing distances are significantly longer than those required
for takeoff. If 30 percent thrust reversing is assumed, however, a
reasonable match with takeoff is realized.

3.10 PERFORMANCE (Continued)

Energy maneuver has been estimated using the USAF Energy Maneuver
program, (Reference 21), to show global persistence, specific excess
power, and maximum maneuver capability. Persistence capability is
presented in Figure 78. These data indicate the number of sustained
$360^{o}$ turns possible using maximum thrust and a mission radius of
200 nautical miles.

Specific excess power, $P_s$ is presented for load factors of 1g, 4g, and
7g in Figures 79, 80, and 81, respectively. These parameters can be
related to dimensional aerodynamic parameters as follows:

$$P_s = \frac{(T-D)V}{W} = \left[ \frac{T}{W} - \frac{C_D}{q(W/S)} \right] V$$

$$N = q \left[ \frac{C_L}{W/S} \right]$$

For convenience, normalized drag polars are provided in Figure 82 for
Mach numbers of 0.9, 1.2, and 1.8.

*Table 10.  Design Mission Summary*

| | RADIUS = 200 N MI | | |
|---|---|---|---|
| | INITIAL WEIGHT -Lb. | DISTANCE - N MI | FUEL - lb |
| TAXI | 12,500 | 0 | 160 |
| TAKEOFF | 12,340 | ·0 | 50 |
| ACCELERATE | 12,290 | 2 | 60 |
| CLIMB | 12,230 | 31 | 660 |
| CRUISE | 11,570 | 167 | 690 |
| COMBAT | 10,880 | 0 | 470 |
| EXPEND PAYLOAD | 10,410 | 0 | --- |
| TURN AROUND | 10,070 | 5 | 220 |
| CRUISE | 9,850 | 195 | 810 |
| LOITER | 9,040 | 0 | 510 |
| OW | 8,530 | | (3630) |
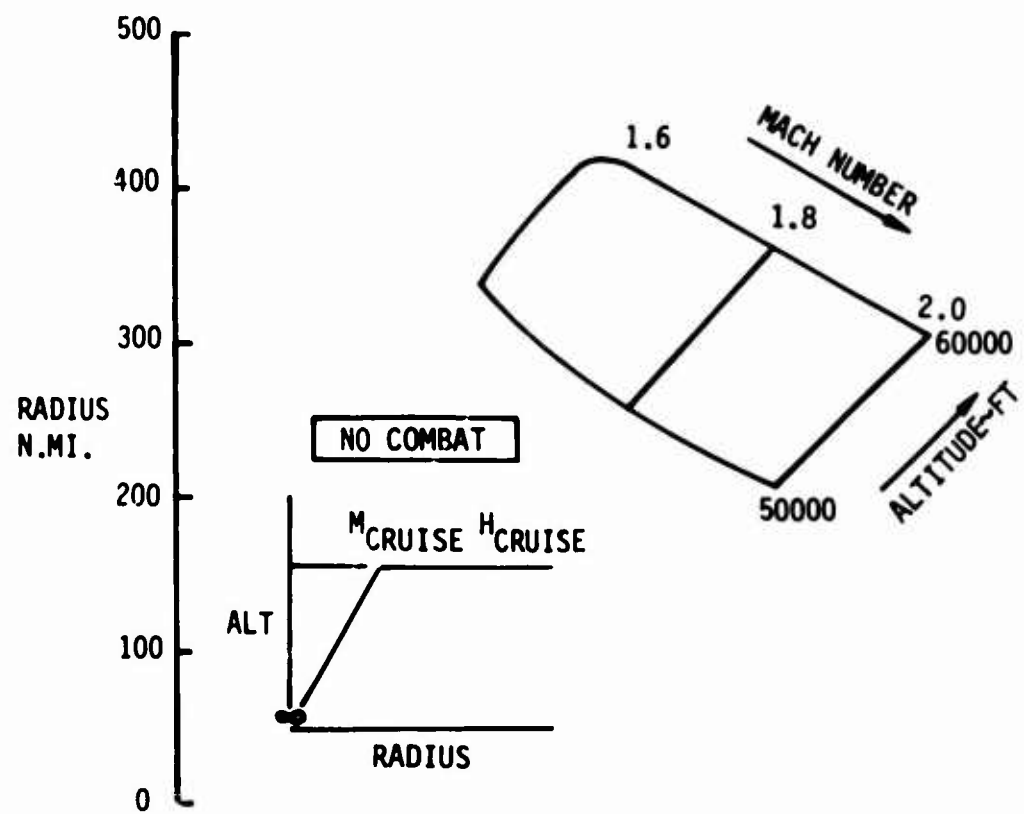
**Figure 74. Mission RAdius Versus Cruise Mach Number and Altitude**
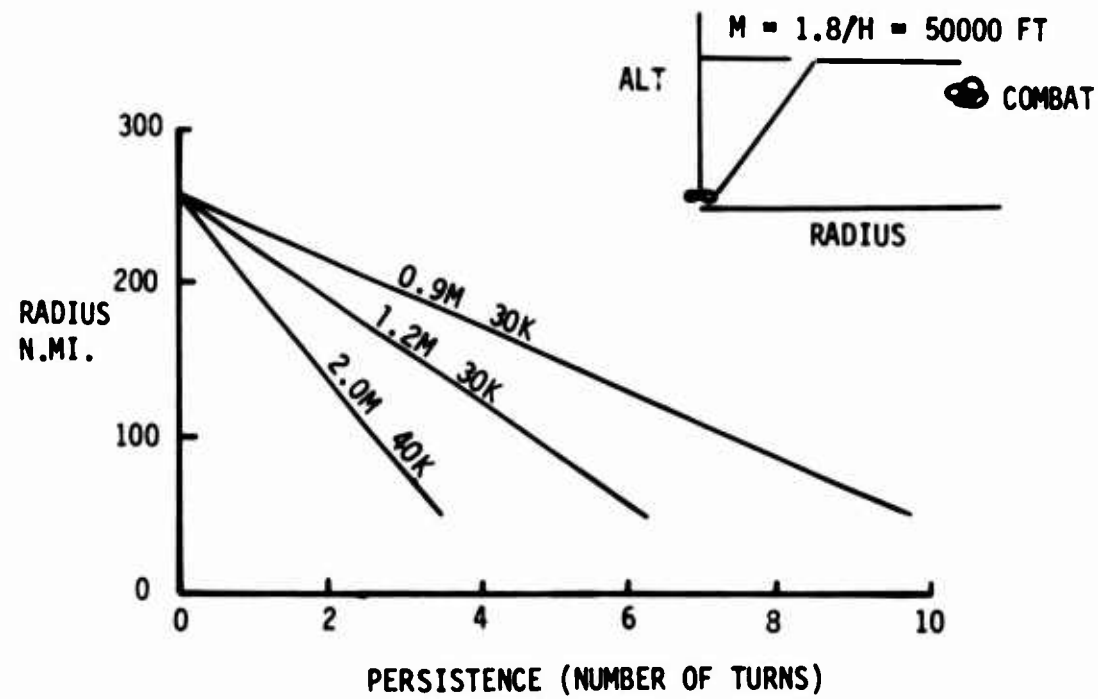


**Figure 75. Persistence Variation With Supersonic Radius**

143
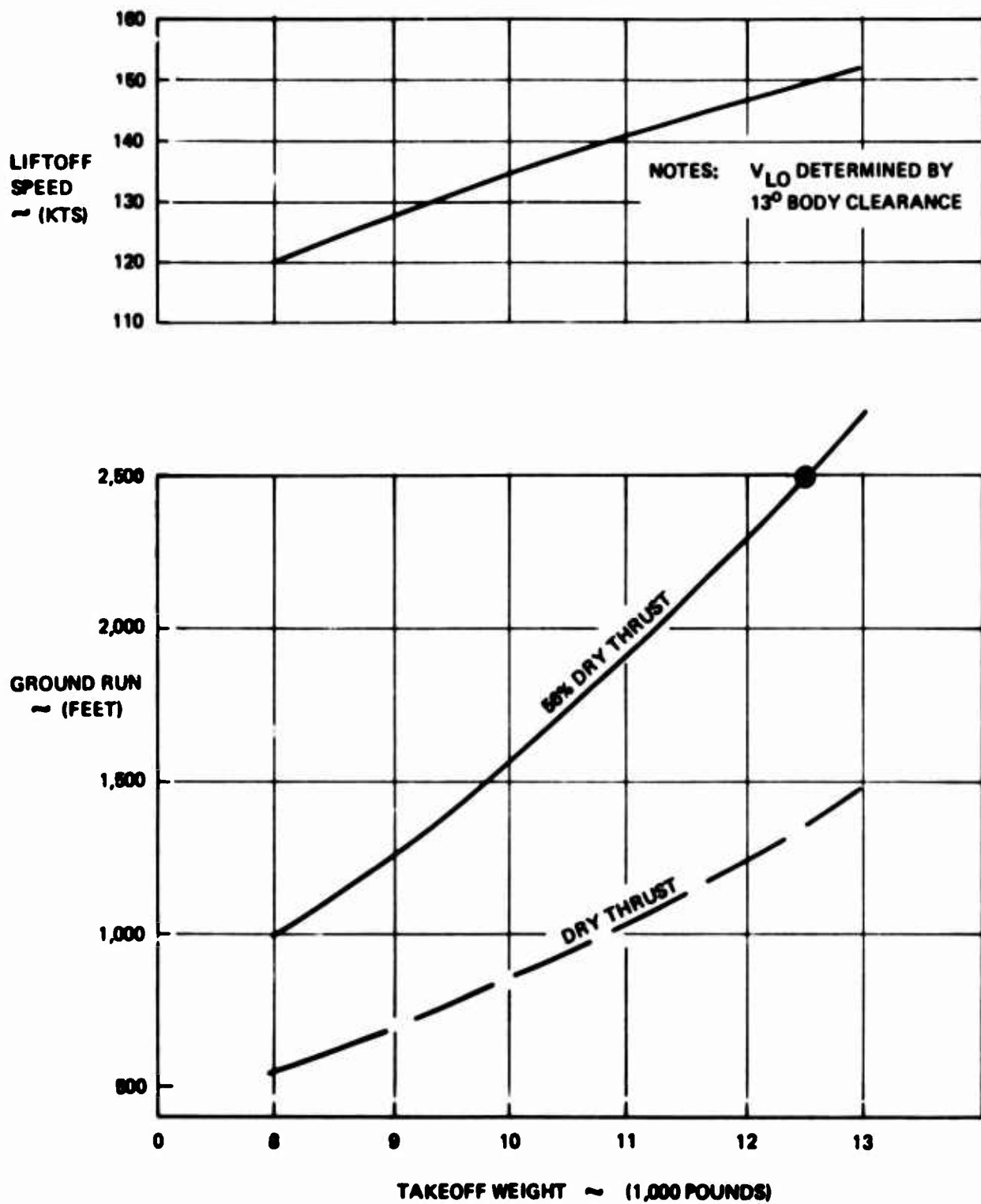
Figure 76. Takeoff Performance (985-213)

144
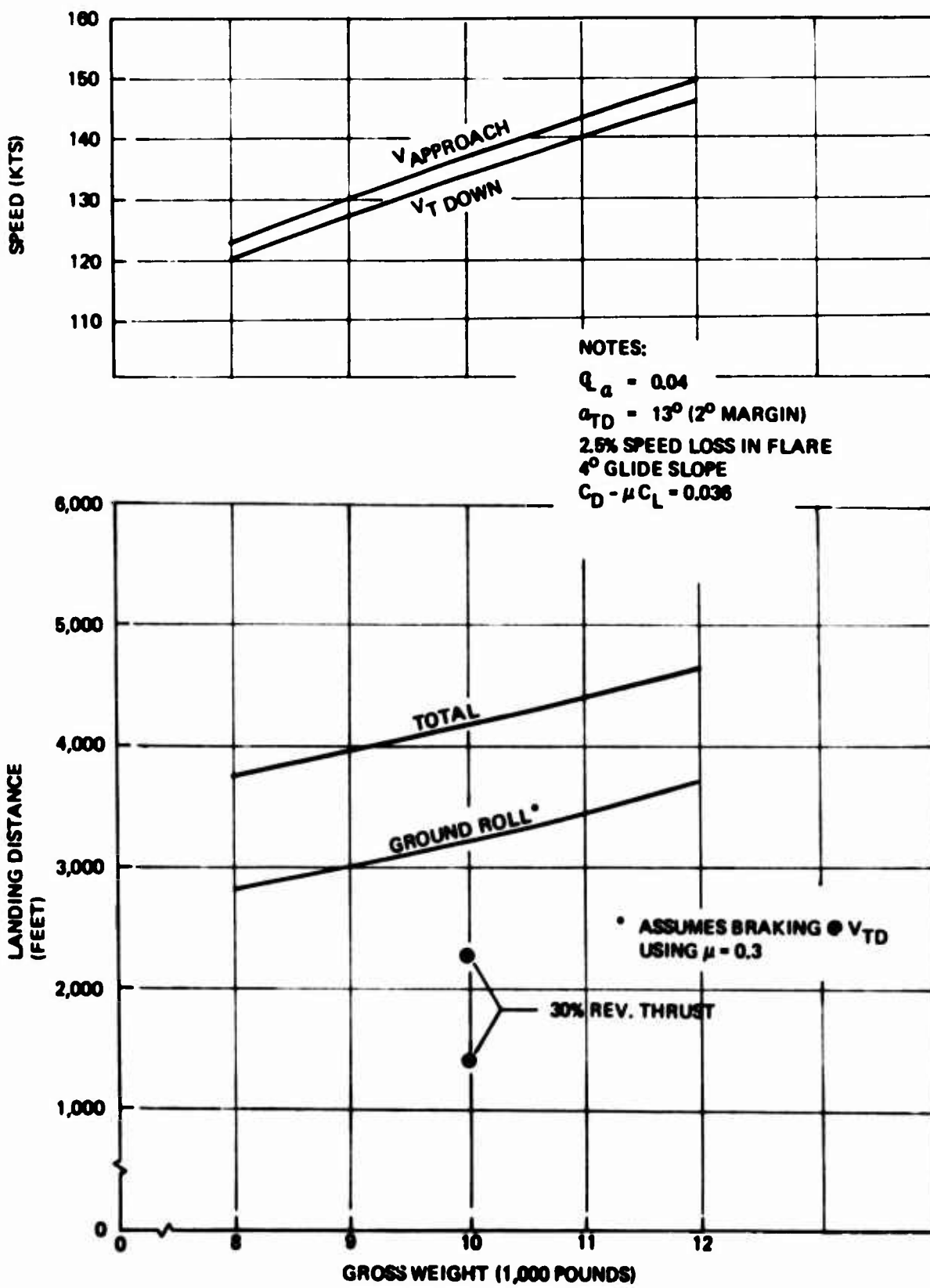
Figure 77. Landing Performance
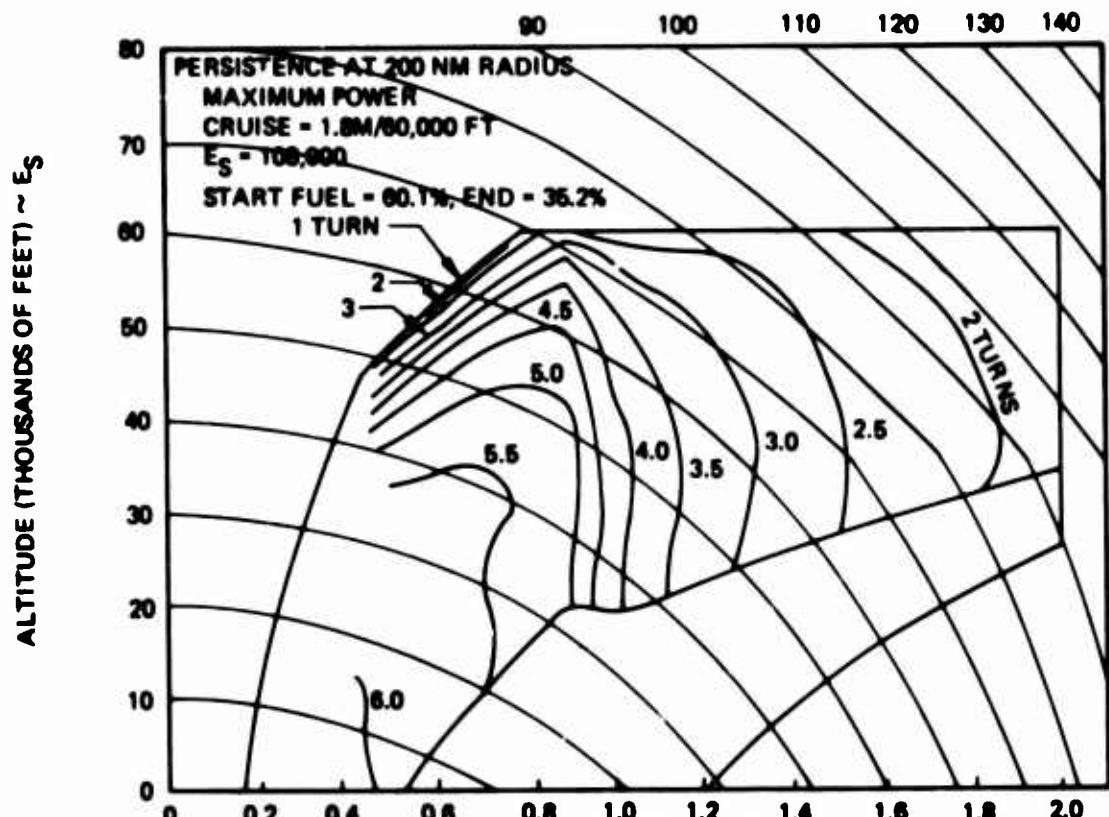
Figure 78. Global Persistence (985-213)
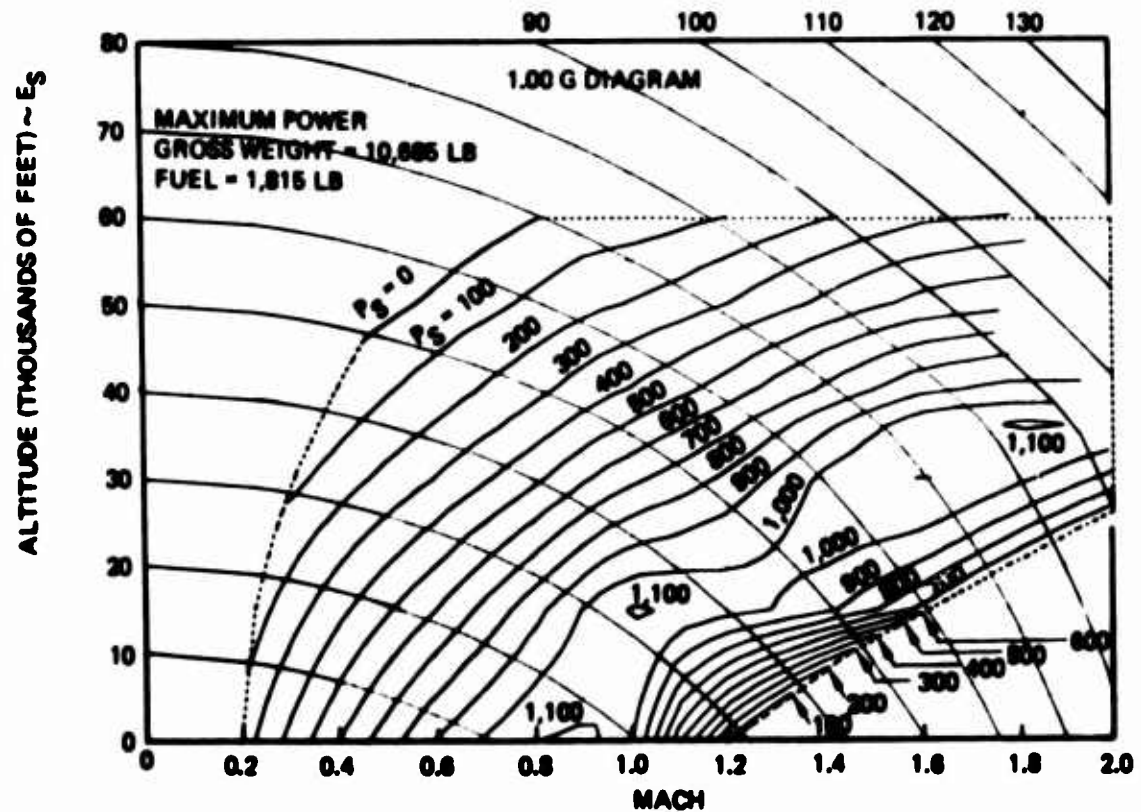


Figure 79. Specific Excess Power – 1g (985-213)

146

Figure 80.    Specific Excess Power – 4g (985-213)



Figure 81.    Specific Excess Power – 7g (985-213)

147
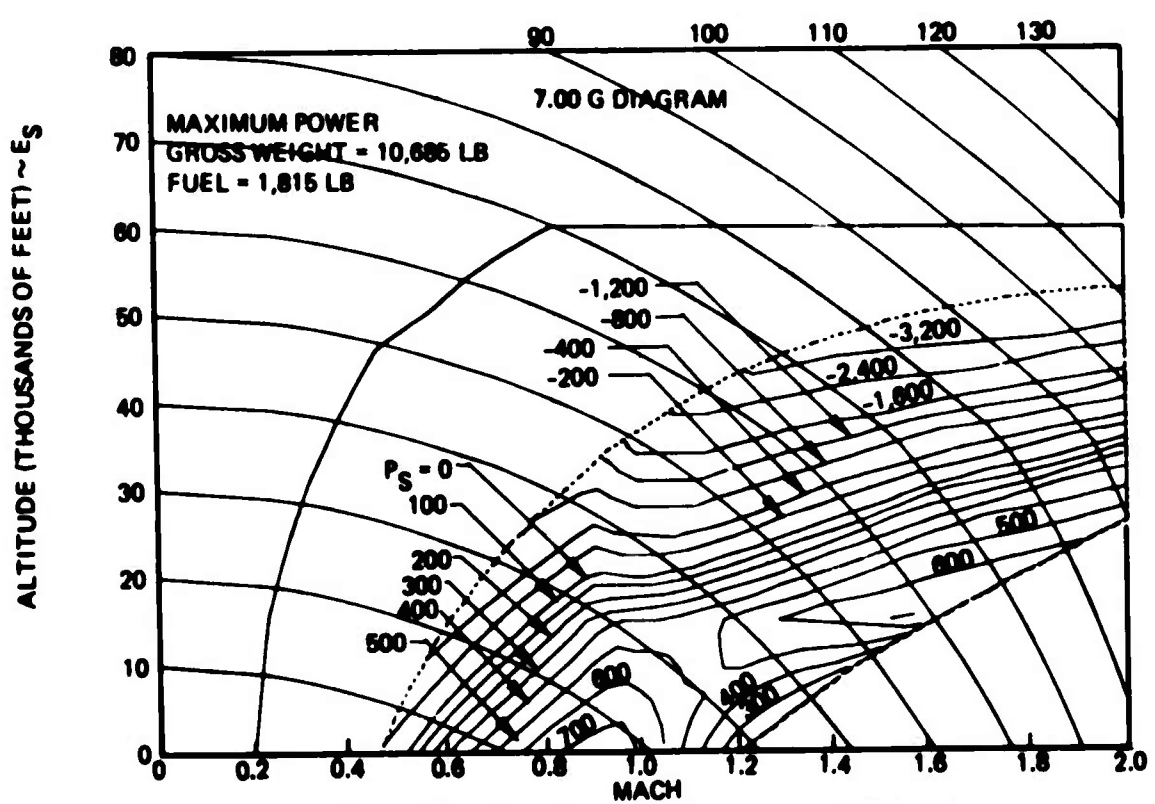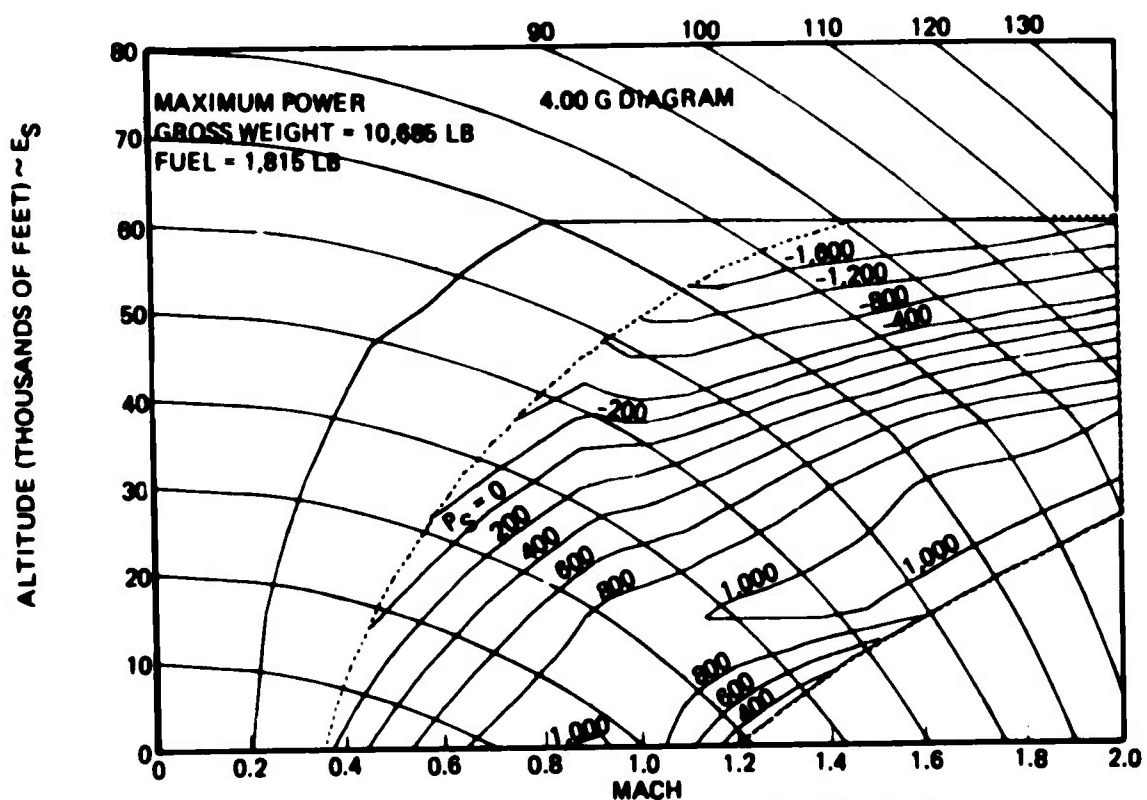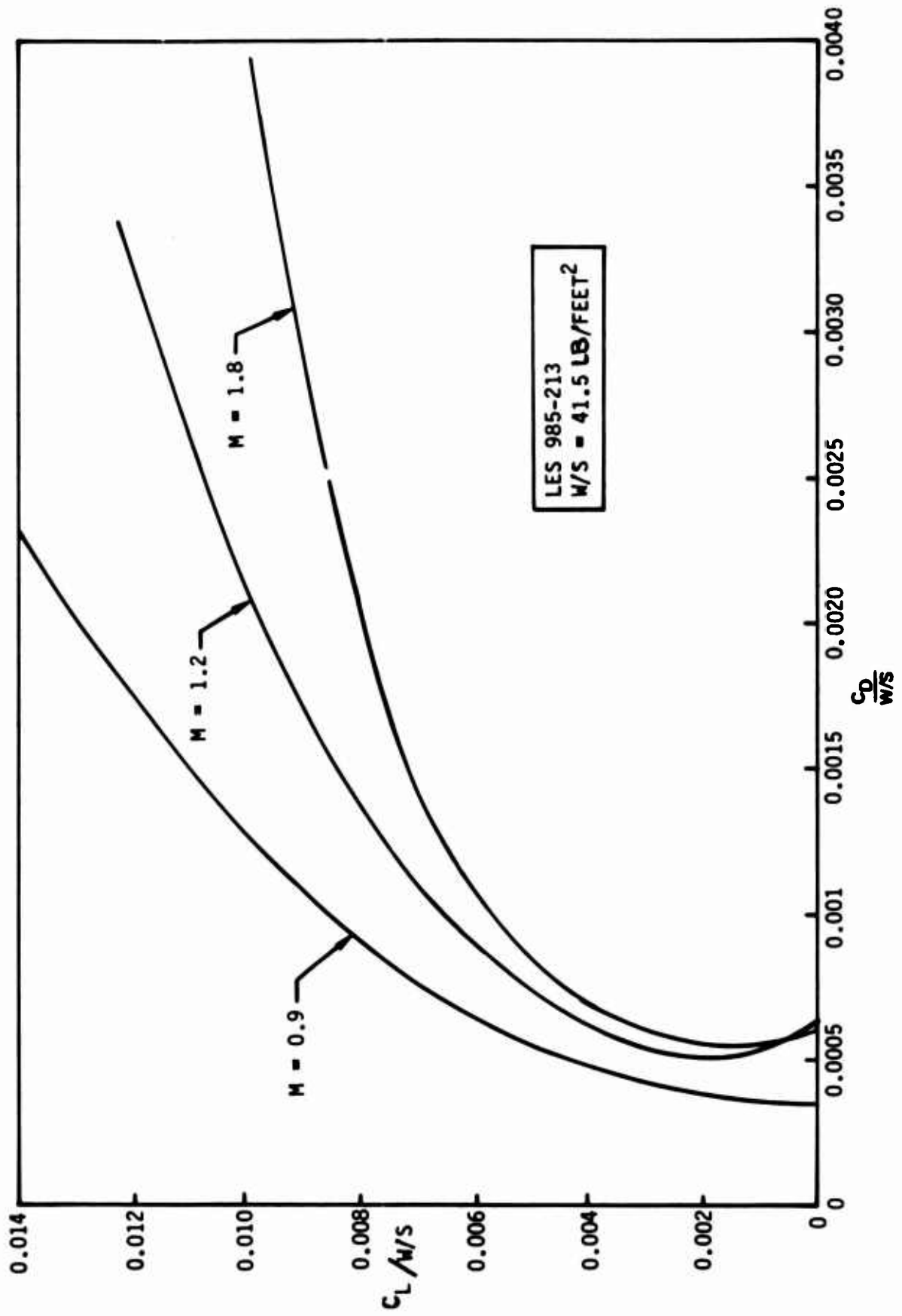
Figure 82    Normalized Drag Polers

## 3.11    PROTOTYPE COSTS

The prototype cost estimate for the LES was developed based on the following ground rules and assumptions:

    a.   2 Experimental Research Vehicles would be built

    b.   New Cockpit

    c.   New Airframe Development (Composite, MODEL 985-213)

    d.   Flight Control System Development

    e.   LWF Type Avionics and Subsystems

    f.   Prototype Cost in Constant 1976 Dollars

    g.   Excludes Armament

    h.   J101/J7 Study A9 Engine

The stated AMPR weight as furnished by Engineering for the LES Prototype was 5,390 lbs.  Based on Boeing and Industry data, this weight was adjusted by 125% to arrive at an estimated weight of an aluminum airplane.  The aluminum airplane was then priced by element of cost (Table 11) using Boeing Prototype History with adjustment for Speed using Rand Corporation data.  These data were compared to reported industry data for reasonableness, and resulted in the estimated cost as shown.

The estimated cost of the Composite Airplane as shown on Table 11 was arrived at by adjustments to each element of cost, as a result of weight, estimated part card count, and comparison to Boeing and Industry Composite data.

Several elements of cost as shown on Table 11 needing explanation are:

    &deg;   TOOL AND PRODUCTION PLANNING (T/PP)

    &deg;   Purchased Equipment

    &deg;   Outside Production

    &deg;   Distributable Labor

## 3.11   PROTOTYPE COSTS (Continued)

Table 11. Cost Summary — 1976 Dollars

| BASE A/P LESS DIGITAL FLIGHT CONTROL & EXHAUST NOZZLE DEV. | | | | |
|---|---|---|---|---|
| | ALUM | | BASED ON INDUSTRY DATA   COMPOSITE | |
| AMPR WEIGHT | 6,738# | | 5,390# | |
| PART CARD EST. | 100% | | 67% | |
| COST & HRS. IN 000's | HOURS | $ | HOURS | $ |
| ENGINEERING | 560 | 16,722 | 410 | 12,243 |
| DEVELOPMENTAL | 134 | 3,166 | 205 | 4,844 |
| TOOLING | 110 | 2,599 | 76 | 1,796 |
| PRODUCTION | 403 | 9,641 | 332 | 7,845 |
| T. & P.P. | 62.5 | 1,477 | 44.5 | 1,052 |
| Q.C. | 54.5 | 1,438 | 76 | 2,005 |
| DISTRIBUTABLE | 222 | 5,246 | 220 | 5,199 |
| MFG. RESEARCH | 12 | 300 | 22 | 550 |
| DEV. MAT'L. | $1.56/hr. | 209 | | 400 |
| TOOL MAT'L. | $1.62/hr. | 178 | | 123 |
| PROD. MAT'L. | $ .89/hr | 363 | $60/Lb. | 650 |
| P.E./O.P. | | 945 | | 945 |
| FLIGHT TEST | | 5,000 | | 5,000 |
| SUBTOTAL | | 47,284 | | 42,652 |
| FEE | | 3,783 | | 3,412 |
| SUBTOTAL AIRFRAME | | 51,067 | | 46,064 |
| AVIONICS | | 5,100 | | 5,100 |
| ENGINES | | 2,000 | | 2,000 |
| TOTAL AIRBORNE 1976 $ | | 58,167 | | 53,164 |

3.11 PROTOTYPE COSTS (Continued)

TOOL AND PRODUCTION PLANNING (T/PP)

Tool and Production labor translates the engineering designs and speci-
fication into work plans and task descriptions which provide direction
to shop personnel for fabrication and assembly of end items of hardware.
Tool and Production Planning (T/PP) is also responsible for the  task of
hardware management from a technical as well as schedule standpoint.

T/PP analyses make or buy requirements, prepares the manufacturing plans
and production processes and sequences the flow of work.  It identifies
the special tool and test equipment requirements, the unique processes,
equipment, space and special skills required resulting from the produc-
tion plans.

PURCHASES EQUIPMENT AND OUTSIDE PRODUCTION (PE/OP)

Purchased Equipment --This element of cost is for equipment  items that
are operable or functional components of systems normally outside the
company's product line and manufacturing objectives.  These items are
governed by Boeing specifications and drawings which may require that
suppliers comply with existing Boeing Quality Control requirements.

Outside Production--Outside production is parts and assemblies manu-
factured to Boeing's drawings which are within the scope of the com-
pany's product line and manufacturing objectives, however, is procured
on contract from suppliers because of shop loading, etc.

Distributable Labor--Within the context of the job order cost system
employed by Boeing certain functions which are of a direct nature, but,
due to their benefit relationship to more than one job order within a
homogenous cost objective can be accounted for more economically through
the employment of a redistribution technique.  All Distributed Direct
Support function factors are presented and negotiated with the local AFPRO
and must be used by all BAC projects and programs.

## 3.11 PROTOTYPE COSTS (Continued)

Cost Data--This estimate is based on the airplane cost as shown on Table 12 with modifications to arrive at the "Total Cost" as shown. Estimating data for the requalification of Ejector Seat; Digital Flight Control; Exhaust Nozzle Development are based on preliminary pricing data obtained from suppliers and inhouse estimate.

*Table 12.   Preliminary Cost  —  1976 Dollars*

| LES - MODEL 985-213 | |
|---|---|
| | BASIC |
| BASE AP'S | $53M |
| ADD | |
| REQUALIFICATION OF EJECTOR SEAT | 1M |
| DIGITAL FLIGHT CONTROL | 5M |
| ANALOG FLIGHT CONTROL | |
| EXHAUST NOZZLE - FULL DEVELOPMENT | 10M |
| SUBTOTAL | $69M |
| CONTINGENCY (20%) | 14M |
| TOTAL | $83M |

## 4.0 PARAMETRIC TRADE STUDIES

Conceptual parametric design studies have been conducted with a growth derivative of the J101 engine on two airframe concepts:

1) Close Coupled Canard
2) SCAT-15 Arrow Wing

The primary goal is to achieve efficient supersonic cruise to cruise speeds double those of current fighters, and at the same time, have outstanding combat performance.

The parametric results indicate that a maximum supersonic radius (no combat allowance) on the order of 800 n. mi. can be achieved. The resultant combat capability as measured in sustained g's is on the order of 3 to 4 at Mach = 0.9 and 30,000 feet. The basic levels of performance are the same for both concepts with a slight edge to the arrow wing concept in terms of supersonic radius.

Designs selected for maximum sustained load factor are in direct conflict with those selected for maximum radius in terms of takeoff gross weight and wing loading. Load factor is increased by about 2 g's at Mach = 0.9 and 30,000 feet, however, radius falls off by a factor of 4 to about 200 n. mi. Again the levels of performance for the two concepts are similar.

Four point design airplanes were selected for more detailed performance evaluation. The general characteristics of these designs are summarized in Table 13.

*Table 13. Point Design Characteristics*

| CONCEPT | DESIGNATION | W/S | $\Lambda_{LE}$ | AR | SUPERSONIC RADIUS - NO COMBAT |
|---------|-------------|-----|------|-----|------------------------------|
| CANARD | I | 120 | 65 | 3.0 | 550 |
| CANARD | II | 66 | 45 | 3.0 | 390 |
| ARROW | III | 80 | 74 | .94 | 550 |
| ARROW | IV | 40 | 74 | .94 | 390 |

4.0    PARAMETRIC TRADE STUDIES (Continued)

All four designs have a takeoff gross weight of 12,000 lbs.  Designs I
and III have been selected on the basis of supersonic cruise radius where-
as designs II and IV were selected by emphasizing sustained maneuver load
factor.  Additional information on these points designs is presented in
Appendix E.

Point design IV, the low wing loading arrow wing concept, was selected for
further refinement in this study.

4.1    BASELINE CONFIGURATION AND SELECTION CRITERIA

This study has originated from three independent efforts:
1)  USAF/AFFDL unpublished design studies.
2)  A supercruiser design from the Boeing Commercial Airplane Company.
3)  An Advanced Technology Light Fighter design from the Boeing
    Aerospace Company.

These activities have promoted the present study to define the character-
istics of a Light Experimental Supercruiser.  The Boeing concepts are
shown in Figure 83 and serve as baselines for this conceptual parametric
study.  The concepts are intended to represent two extreme approaches in
the search for a fighter with efficient cruise capability at supersonic
speeds.

The objectives and methods used in conducting the LES parametric study are
outlined in Figure 84.

The two basic airframe concepts considered in the parametric study are
shown in Figure 85 along with the corresponding design variables, and
their upper and lower limits.  Note that two wing planform variables,
sweep and aspect ratio, were eliminated for the 985-210 (arrow) study.
It was assumed that the wing leading edge was always a constant increment

154

## 4.1 BASELINE CONFIGURATION AND SELECTION CRITERIA (Continued)

behind the Mach cone. This related wing sweep directly to cruise Mach number. Also, the relationship between wing leading and trailing edge sweep and wing area determines aspect ratio.



**ARROW WING CONCEPT (SCAT 15)**
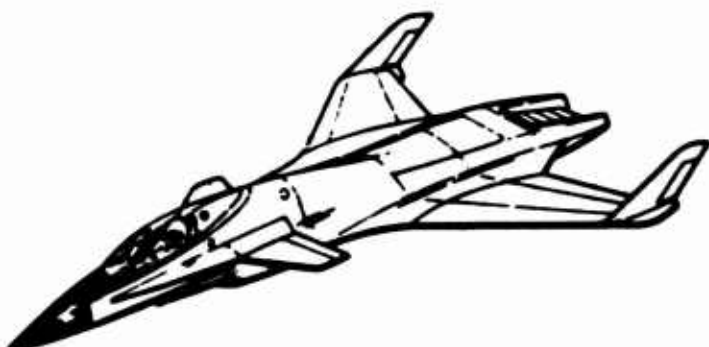


**ADVANCED TECHNOLOGY
LIGHT FIGHTER CONCEPT (ATLF)**

*Figure 83. Parametric Baselines*

**Objectives**

> Provide Information and Trade

> Data for the Selection of the

> Task II Configuration

**Methods**

> Sensitivity Analysis

> ARES Methodology – Optimization

> Carpets

*Figure 84.   LES Parametric – Task 1*

Model 985-202
_____

$60 \leqslant W/S \leqslant 160$

$2 \leqslant AR \leqslant 5$

$0.02 \leqslant t/c \leqslant 0.06$

$45 \leqslant LE \leqslant 65$

$10,000 \leqslant TOGW \leqslant 16,000$

$1.4 \leqslant M_{cr} \leqslant 2.0$

Model 985-210
_____

$40 \leqslant W/S \leqslant 100$

$0.02 \leqslant t/c \leqslant 0.06$

$10,000 \leqslant TOGW \leqslant 16,000$

$1.4 \leqslant M_{cr} \leqslant 2.0$

*Figure 85.   LES Parametric – Study Variables*

## 4.2 PARAMETRIC STUDY METHODS

The basis for the data presented in Section 4.0 is a parametric airplane sizing and performance program. The program is shown schematically in Figure 86. The major elements of the program as shown are:

- o Geometry calculation
- o Weight estimation
- o Drag buildup
- o Performance evaluation

The geometry module calculates the lengths, wetted areas, and the volumes required for the weight and the drag modules. A key loop in the sizing program is the adjustment of fuselage length to satisfy fuel volume requirements.

A Class I weight estimating procedure is then used to calculate operating weight and fuel available. The basic Class I methods are described in Reference 20. The basic methods were modified so as to better predict the mass properties of the LES configurations.

The parametric drag buildup procedures account for variations in airplane wetted areas and cross sectional area, wing planform variations, and airplane operating condition.

The final block in the sizing and performance program is the performance evaluation itself. Both mission performance and energy-maneuver data are calculated. The missions and the energy-maneuver points are shown in Figure 87. The basic mission is all supersonic with a 200 n. mi. radius. Combat persistence and maximum sustained load factor are calculated for the eight Mach number, altitude points shown. Alternate missions are the maximum supersonic radius with no combat, and a four thousand pound overload mission.

Four other computer programs were used in addition to the basic airplane sizing and performance program. These programs are shown in Figure 88.

157
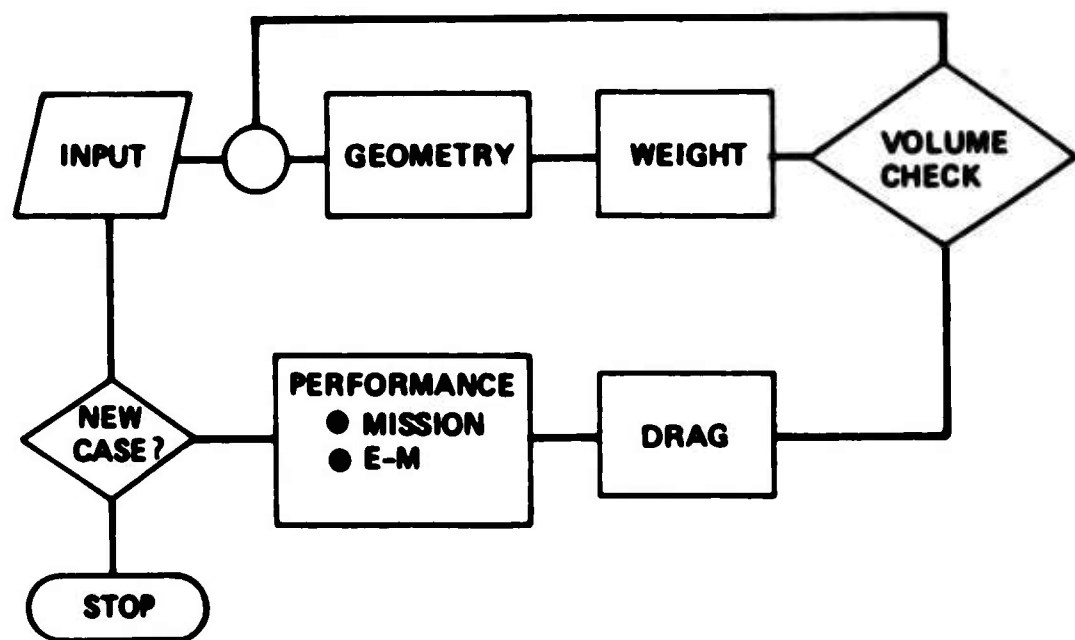
Figure 86. LES Parametric Sizing and Performance Program
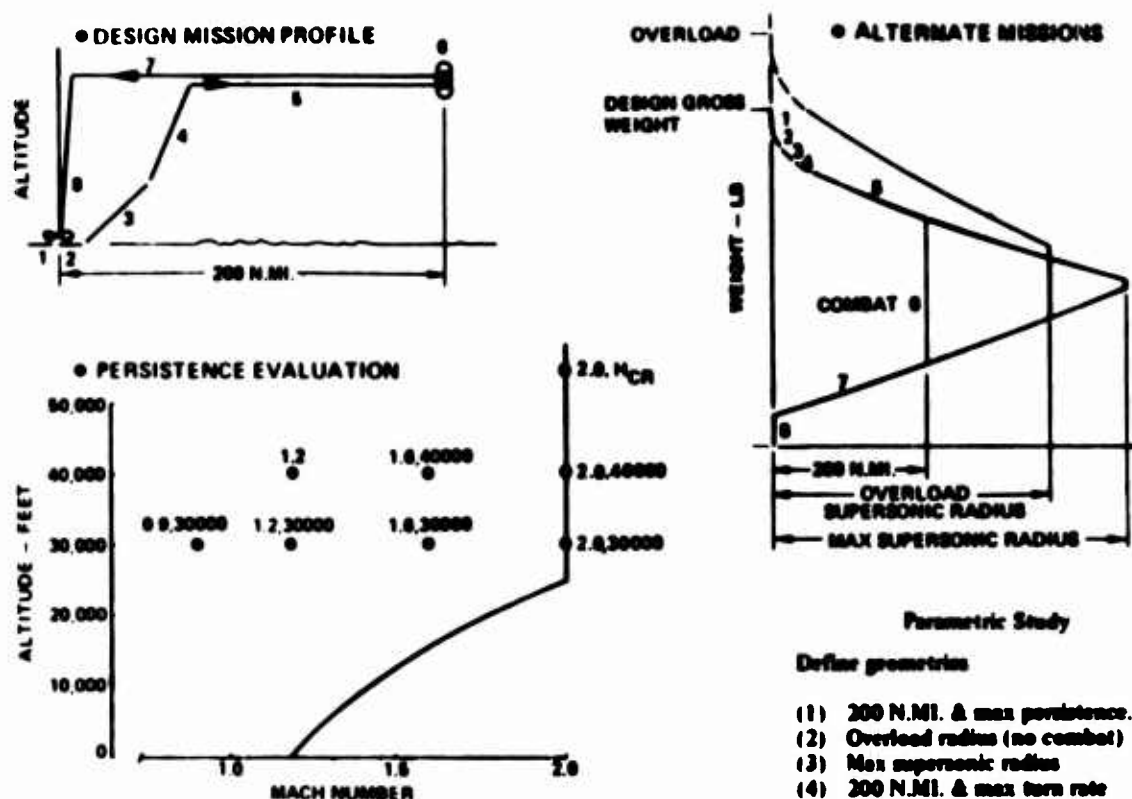
Figure 87. Parametric Performance Evaluation
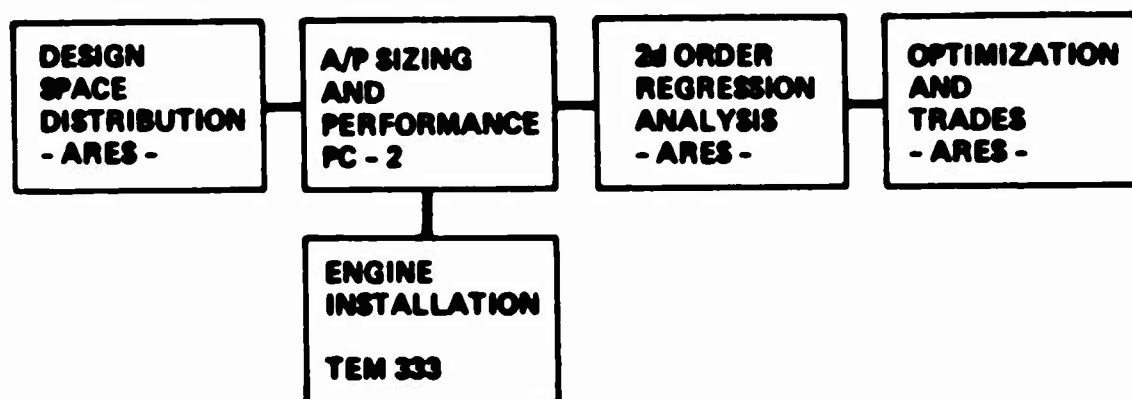


Figure 88. LES Parametric Computer Programs

159

## 4.2 PARAMETRIC STUDY METHODS (Continued)

Three of these programs are related to the Airplane Responsive Engine Selection (ARES) regression and optimization methodology, Reference 22. This method is briefly described in the following paragraphs.

For a given set of design variables and a region of interest, points are determined by the design space distribution program for evaluation in the airplane sizing and performance program. The performance results are then input to a regression analysis program which determines the coefficients for a second order surface fit. The simple second order equations are then used in place of the airplane sizing and performance program to do optimization and trade studies. Appendix D summarizes the regression analysis.

Examples of the regression equations and design carpets which can be derived from these regression equations are shown in Figure 89.

## 4.3 VEHICLE PARAMETRIC TRADES

Phase I parametric trades are presented for both the canard configuration concept and the arrow wing concept in the following sections:

CANARD CONCEPT

The baseline design for the canard concept parametric study is shown in Figure 90. This concept has evolved from recent Micro-Fighter/Advanced Light Fighter studies. Once again the study variables for this concept are:

o Takeoff gross weight - TOGW
o Cruise Mach number - $M_{cr}$
o Wing leading edge sweep angle - $\Lambda_{LE}$
o Wing average thickness ratio - t/c
o Wing aspect ratio - AR
o Wing loading - W/S

REGRESSION EQUATION:

$$R = -4352 + 6.817 \times W/S + .2384 \times TOGW + 3065 \times M_{cr} + 15.03 \times T/C \times W/S$$
$$+ .0002744 \times W/S \times TOGW - .0669 \times W/S^2 - .000007067 \times TOGW^2 - 930.5 \times M_{cr}^2$$

- T/C = .06
- $M_{cr}$ = 1.65
- 4000 LB OVERLOAD

RADIUS ~ NMI

1000
800
600
400
200
0

TOGW
16000
14000
12000
10000

W/S
100 80 60 40
OPT

REGRESSION EQUATION:

$$N = 14.09 + 2.108 \times T/C - .1316 \times W/S - .1316 \times W/S - 3.356 \times M_{cr} + .000001096$$
$$\times W/S \times TOGW + .01927 \times W/S \times M_{cr} + .0003526 \times W/S^2 - .0000000039$$
$$\times TOGW^2$$

T/C = .06
—— $M_{cr}$ = 1.4
‑ ‑ ‑ $M_{cr}$ = 1.8

- M = .9
- H = 30000

LOAD FACTOR

6
5
4
3
2
1
0

TOGW
10000 12000 14000 16000
40
60
80
100
W/S

Figure 89.  Example Regression Equations and Carpets
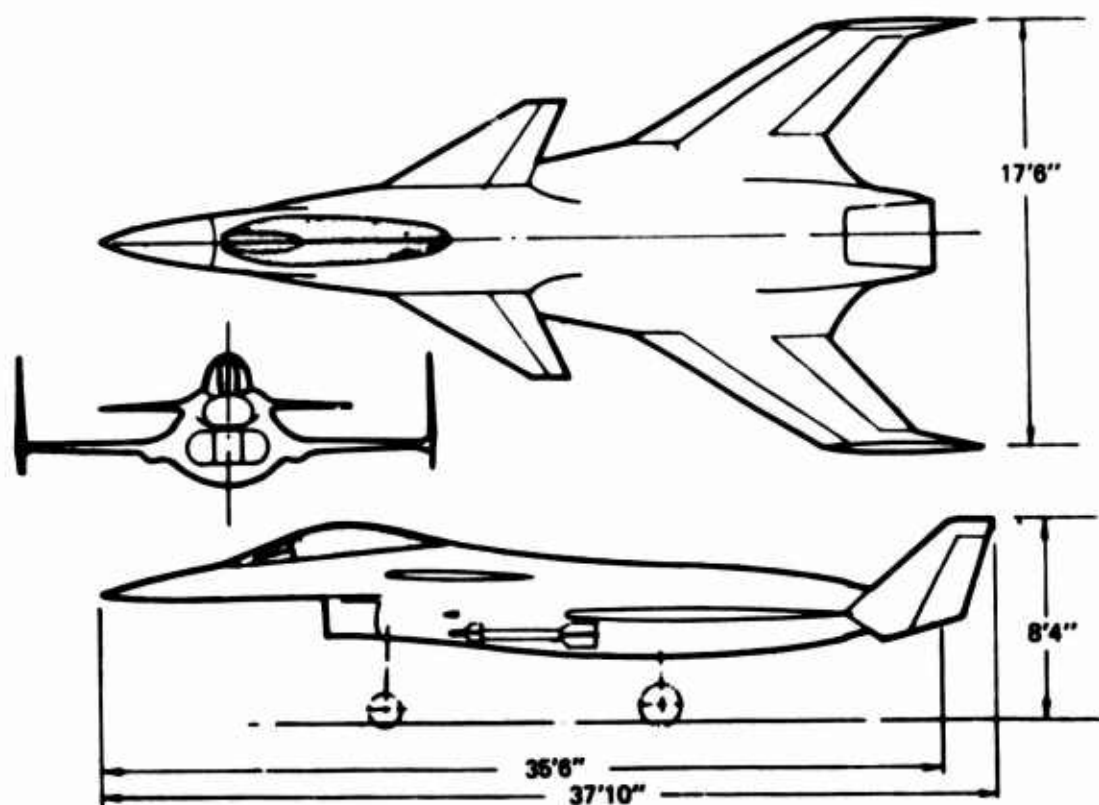
*Figure 90.  LES — Canard Concept Baseline*

TAKEOFF GROSS WEIGHT = 10,000 LB
W/S = 100 —·—
70 ——
40 -----
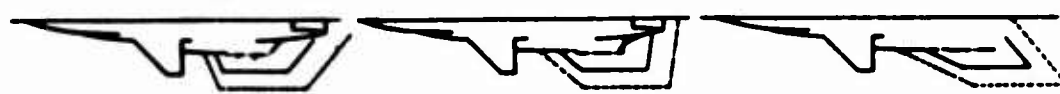


ASPECT RATIO = 1

ASPECT RATIO = 3.2

ASPECT RATIO = 5

SWEEP = 25°     SWEEP = 50°     SWEEP = 60°

*Figure 91.  LES — Wing Planform Variations — Canard*

162

4.3   VEHICLE PARAMETRIC TRADES (Continued)

The wide range of wing planforms which were included in the study are
shown in Figure 91.  Figure 92 lists the designs which were evaluated
in the airplane sizing and performance program to form the regression
analysis data base.

The following sections discuss the impact of varying the above design
variables on supersonic radius, combat persistence, and combat sustained
load factor.  Sensititivity analysis, regression analysis, and traditional
carpet plots are used to present results.  Designs are selected which
optimize each of the key performance items.

Supersonic Radius--One of the key figures of merit is supersonic radius.
The impact of varying each of the design variables individually on
supersonic radius is shown in Figure 93.  The variables in the order of
decreasing importance are:

o  TOGW
o  W/S
o  $M_{cr}$
o  t/c
o  $\Lambda_{LE}$
o  AR

The first two variables, takeoff gross weight and wing loading load have
by far the largest impact on supersonic radius.

These sensitivity results were confirmed by the regression analysis
when only TOGW and W/S terms were included in the equation for supersonic
radius.  All other terms had zero or negligible coefficients.

$$R = -1652 + 8.824 \times W/S + 1803 \times GW - .12/2 \times W/S^2 + .0003955 \times W/S$$
$$\times GW - .00001097/2. \times GW^2.$$

A carpet based on this equation is shown in Figure 94.

| CASE | SUP MACH | TOGW | SWEEP | W/S | T/C | AR |
|---|---|---|---|---|---|---|
| 1 | 1.400 | 10000 | 45.0 | 60.0 | .020 | 2.0 |
| 2 | 1.500 | 11000 | 48.3 | 76.7 | .027 | 2.5 |
| 3 | 1.600 | 12000 | 51.7 | 93.3 | .033 | 3.0 |
| 4 | 1.700 | 13000 | 55.0 | 110.0 | .040 | 3.5 |
| 5 | 1.800 | 14000 | 58.3 | 126.7 | .047 | 4.0 |
| 6 | 1.900 | 15000 | 61.7 | 143.3 | .053 | 4.5 |
| 7 | 2.000 | 16000 | 65.0 | 160.0 | .060 | 5.0 |
| 8 | 1.500 | 12000 | 55.0 | 126.7 | .053 | 5.0 |
| 9 | 1.600 | 13000 | 58.3 | 143.3 | .060 | 2.0 |
| 10 | 1.700 | 14000 | 61.7 | 160.0 | .020 | 2.5 |
| 11 | 1.800 | 15000 | 65.0 | 60.0 | .027 | 3.0 |
| 12 | 1.900 | 16000 | 45.0 | 76.7 | .033 | 3.5 |
| 13 | 2.000 | 10000 | 48.3 | 93.3 | .040 | 4.0 |
| 14 | 1.400 | 11000 | 51.7 | 110.0 | .047 | 4.5 |
| 15 | 1.600 | 14000 | 65.0 | 76.7 | .040 | 4.5 |
| 16 | 1.700 | 15000 | 45.0 | 93.3 | .047 | 5.0 |
| 17 | 1.800 | 16000 | 48.3 | 110.0 | .053 | 2.0 |
| 18 | 1.900 | 10000 | 51.7 | 126.7 | .060 | 2.5 |
| 19 | 2.000 | 11000 | 55.0 | 143.3 | .020 | 3.0 |
| 20 | 1.400 | 12000 | 58.3 | 160.0 | .027 | 3.5 |
| 21 | 1.500 | 13000 | 61.7 | 60.0 | .033 | 4.0 |
| 22 | 1.700 | 16000 | 51.7 | 143.3 | .027 | 4.0 |
| 23 | 1.800 | 10000 | 55.0 | 160.0 | .033 | 4.5 |
| 24 | 1.900 | 11000 | 58.3 | 60.0 | .040 | 5.0 |
| 25 | 2.000 | 12000 | 61.7 | 76.7 | .047 | 2.0 |
| 26 | 1.400 | 13000 | 65.0 | 93.3 | .053 | 2.5 |
| 27 | 1.500 | 14000 | 45.0 | 110.0 | .060 | 3.0 |
| 28 | 1.600 | 15000 | 48.3 | 126.7 | .020 | 3.5 |
| 29 | 1.800 | 11000 | 61.7 | 93.3 | .060 | 3.5 |
| 30 | 1.900 | 12000 | 65.0 | 110.0 | .020 | 4.0 |
| 31 | 2.000 | 13000 | 45.0 | 126.7 | .027 | 4.5 |
| 32 | 1.400 | 14000 | 48.3 | 143.3 | .033 | 5.0 |
| 33 | 1.500 | 15000 | 51.7 | 160.0 | .040 | 2.0 |
| 34 | 1.600 | 16000 | 55.0 | 60.0 | .047 | 2.5 |
| 35 | 1.700 | 10000 | 58.3 | 76.7 | .053 | 3.0 |
| 36 | 1.900 | 13000 | 48.3 | 160.0 | .047 | 3.0 |
| 37 | 2.000 | 14000 | 51.7 | 60.0 | .053 | 3.5 |
| 38 | 1.400 | 15000 | 55.0 | 76.7 | .060 | 4.0 |
| 39 | 1.500 | 16000 | 58.3 | 93.3 | .020 | 4.5 |
| 40 | 1.600 | 10000 | 61.7 | 110.0 | .027 | 5.0 |
| 41 | 1.700 | 11000 | 65.0 | 126.7 | .033 | 2.0 |
| 42 | 1.800 | 12000 | 45.0 | 143.3 | .040 | 2.5 |
| 43 | 2.000 | 15000 | 58.3 | 110.0 | .033 | 2.5 |
| 44 | 1.400 | 16000 | 61.7 | 126.7 | .040 | 3.0 |
| 45 | 1.500 | 10000 | 65.0 | 143.3 | .047 | 3.5 |
| 46 | 1.600 | 11000 | 45.0 | 160.0 | .053 | 4.0 |
| 47 | 1.700 | 12000 | 48.3 | 60.0 | .060 | 4.5 |
| 48 | 1.800 | 13000 | 51.7 | 76.7 | .020 | 5.0 |
| 49 | 1.900 | 14000 | 55.0 | 93.3 | .027 | 2.0 |
| 50 | 2.000 | 11000 | 51.7 | 110.0 | .047 | 4.5 |
| 51 | 1.400 | 12000 | 55.0 | 126.7 | .053 | 5.0 |
| 52 | 1.500 | 13000 | 58.3 | 143.3 | .060 | 2.0 |
| 53 | 1.600 | 14000 | 61.7 | 160.0 | .020 | 2.5 |
| 54 | 1.700 | 15000 | 65.0 | 60.0 | .027 | 3.0 |
| 55 | 1.800 | 16000 | 45.0 | 76.7 | .033 | 3.5 |
| 56 | 1.900 | 10000 | 48.3 | 93.3 | .040 | 4.0 |
| 57 | 1.900 | 12000 | 58.3 | 160.0 | .027 | 3.5 |
| 58 | 2.000 | 13000 | 61.7 | 60.0 | .033 | 4.0 |
| 59 | 1.400 | 14000 | 65.0 | 76.7 | .040 | 4.5 |
| 60 | 1.500 | 15000 | 45.0 | 93.3 | .047 | 5.0 |
| 61 | 1.600 | 16000 | 48.3 | 110.0 | .053 | 2.0 |
| 62 | 1.700 | 10000 | 51.7 | 126.7 | .060 | 2.5 |
| 63 | 1.800 | 11000 | 55.0 | 143.3 | .020 | 3.0 |
| 64 | 1.800 | 13000 | 65.0 | 93.3 | .053 | 2.5 |
| 65 | 1.900 | 14000 | 45.0 | 110.0 | .060 | 3.0 |
| 66 | 2.000 | 15000 | 48.3 | 126.7 | .020 | 3.5 |
| 67 | 1.400 | 16000 | 51.7 | 143.3 | .027 | 4.0 |
| 68 | 1.500 | 10000 | 55.0 | 160.0 | .033 | 4.5 |
| 69 | 1.600 | 11000 | 58.3 | 60.0 | .040 | 5.0 |
| 70 | 1.700 | 12000 | 61.7 | 76.7 | .047 | 2.0 |
| 71 | 1.700 | 14000 | 48.3 | 143.3 | .033 | 5.0 |
| 72 | 1.800 | 15000 | 51.7 | 160.0 | .040 | 2.0 |
| 73 | 1.900 | 16000 | 55.0 | 60.0 | .047 | 2.5 |
| 74 | 2.000 | 10000 | 58.3 | 76.7 | .053 | 3.0 |
| 75 | 1.400 | 11000 | 61.7 | 93.3 | .060 | 3.5 |
| 76 | 1.500 | 12000 | 65.0 | 110.0 | .020 | 4.0 |
| 77 | 1.600 | 13000 | 45.0 | 126.7 | .027 | 4.5 |
| 78 | 1.600 | 15000 | 55.0 | 76.7 | .060 | 4.0 |
| 79 | 1.700 | 16000 | 58.3 | 93.3 | .020 | 4.5 |
| 80 | 1.800 | 10000 | 61.7 | 110.0 | .027 | 5.0 |
| 81 | 1.900 | 11000 | 65.0 | 126.7 | .033 | 2.0 |
| 82 | 2.000 | 12000 | 45.0 | 143.3 | .040 | 2.5 |
| 83 | 1.400 | 13000 | 48.3 | 160.0 | .047 | 3.0 |
| 84 | 1.500 | 14000 | 51.7 | 60.0 | .053 | 3.5 |
| 85 | 1.500 | 16000 | 61.7 | 126.7 | .040 | 3.0 |
| 86 | 1.600 | 10000 | 65.0 | 143.3 | .047 | 3.5 |
| 87 | 1.700 | 11000 | 45.0 | 160.0 | .053 | 4.0 |
| 88 | 1.800 | 12000 | 48.3 | 60.0 | .060 | 4.5 |
| 89 | 1.900 | 13000 | 51.7 | 76.7 | .020 | 5.0 |
| 90 | 2.000 | 14000 | 55.0 | 93.3 | .027 | 2.0 |
| 91 | 1.400 | 15000 | 58.3 | 110.0 | .033 | 2.5 |

*Figure 92. Canard Configuration Latin Square Design Selection*
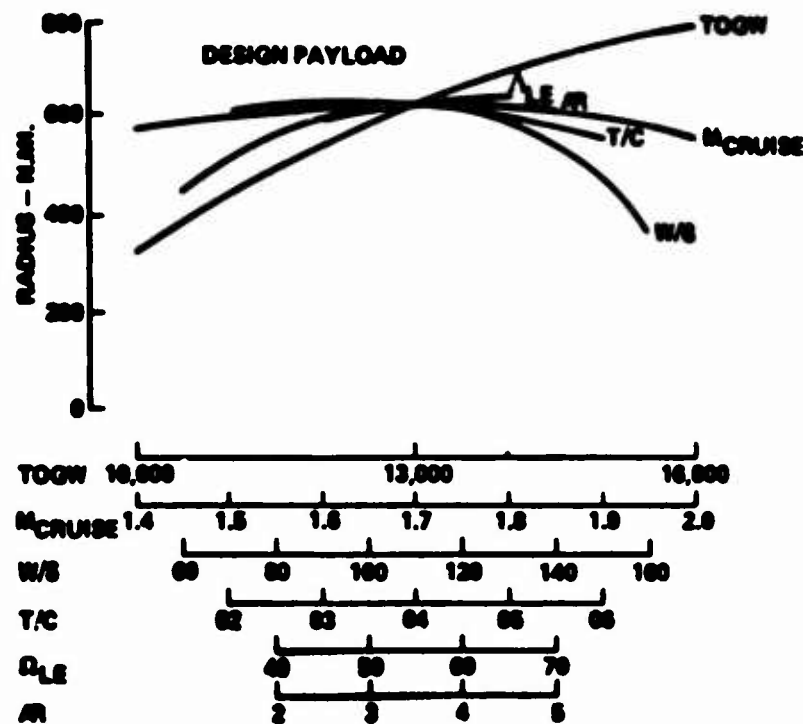
Figure 93. Canard Supersonic Radius Sensitivity Analysis
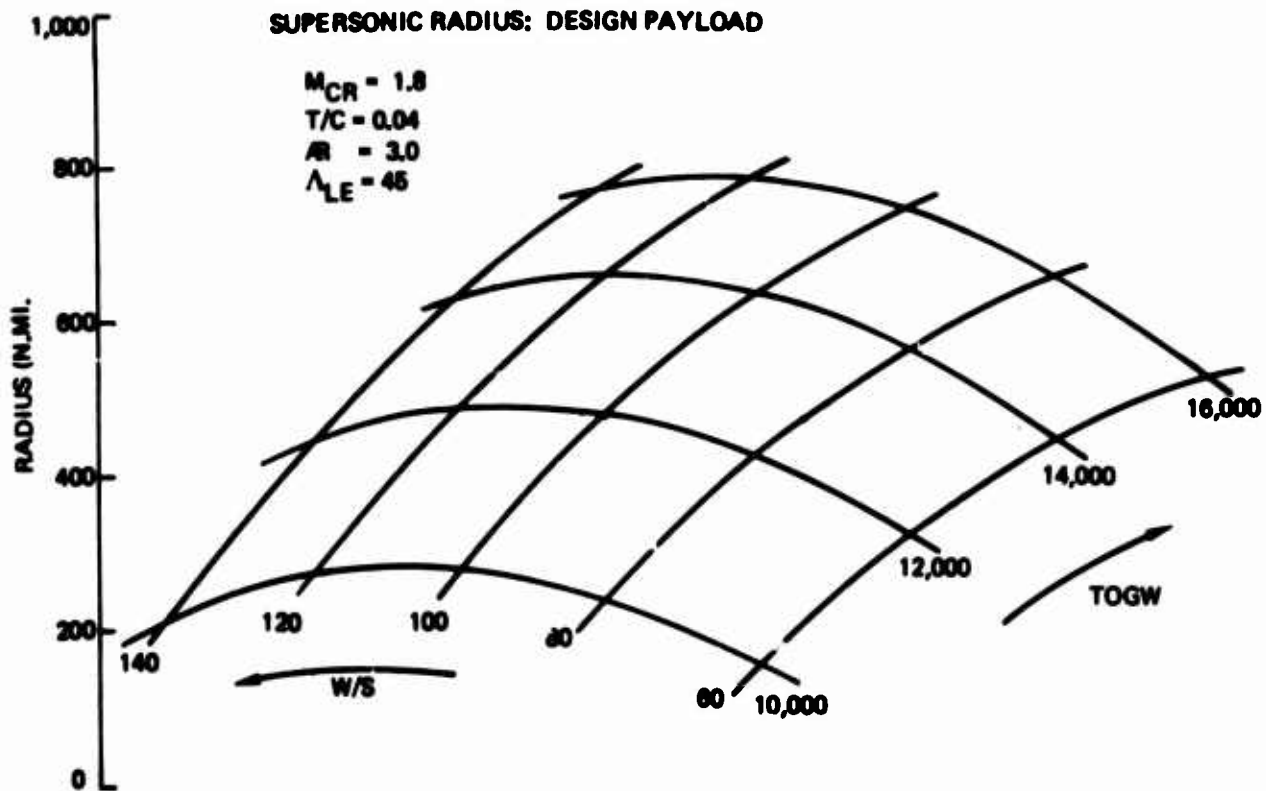


Figure 94. Canard Supersonic Radius Versus TOGW and W/S

## 4.3 VEHICLE PARAMETRIC TRADES (Continued)

Additional information can be gained from the equation by looking at the partial derivatives.

$$\frac{dR}{dW/S} = 8.824 - .12 \times W/S + .0003955 \times GW$$

$$\frac{dR}{dGW} = .1803 + .0003955 \times W/S - .00001097 \times GW$$

Setting both partial derivatives to zero:

$$W/S_{opt} = 73.53 + .0033 \times GW$$

$$GW_{opt} = 16440 + 36.05 \times W/S.$$

These two equations show that wing loading for maximum radius is a linearly increasing function of gross weight, and similarly that gross weight for maximum range is a linearly decreasing function of wing loading.

Finally solving for the optimum wing loading, gross weight, and the corresponding maximum radius:

$$W/S_{opt} = 145 \text{ lb/ft}^2$$

$$GW_{opt} = 21,670 \text{ lb.}$$

$$R_{Max.} = 940 \text{ n. mi.}$$

These results must be viewed with some caution because the gross weight is extrapolated well past the upper limit of the original data. However, when reexamining the sensitivity plot in Figure 93 and looking ahead to the carpet in Figure 95, it does appear that radius peaks out somewhere in gross weight range of 18,000 to 22,000 lbs.

Figure 95 shows the relatively small effect of wing leading edge sweep angle on supersonic radius. The points I and II spotted on the carpets are the two canard concept point designs selected for mid-term evaluation. For additional information on these two designs, see Appendix E.

SUPERSONIC RADIUS
DESIGN PAYLOAD
$M_{CR} = 1.8$
$AR = 3$
$T/C = 0.04$
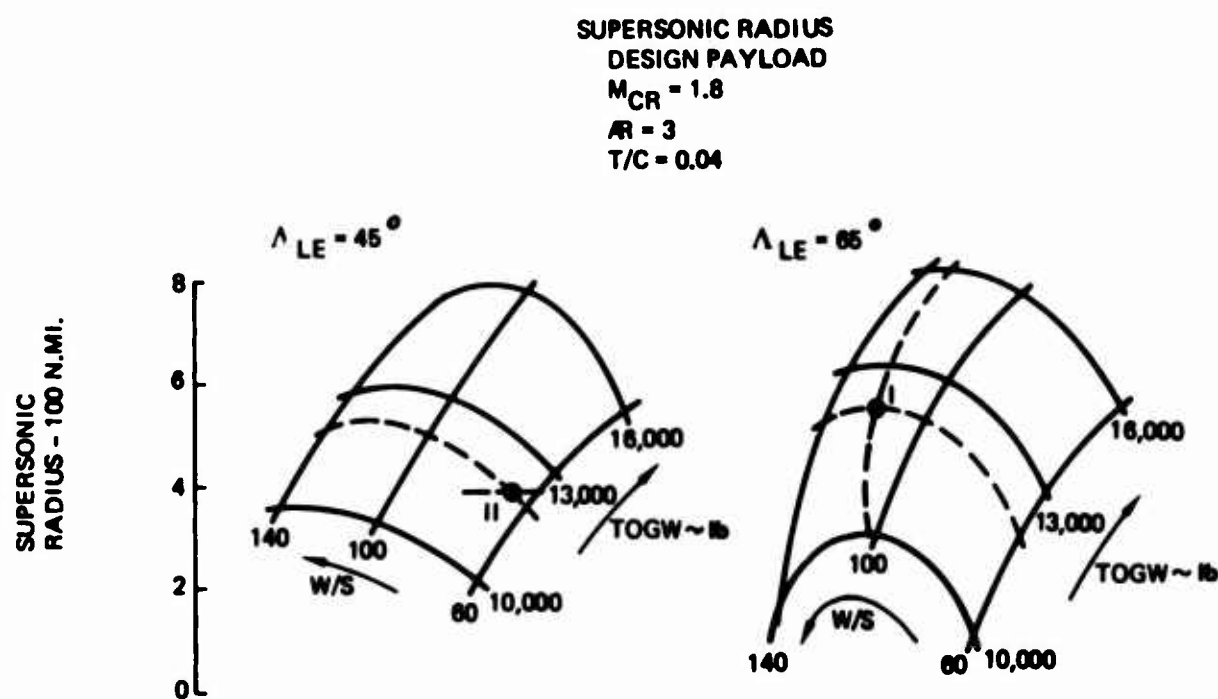
Figure 95.    Canard Point Design Supersonic Radius Carpet



Regression Analysis

$M_{CR} = 1.8$
$T/C = 0.04$
$AR = 3.0$
$\Lambda_{LE} = 45°$
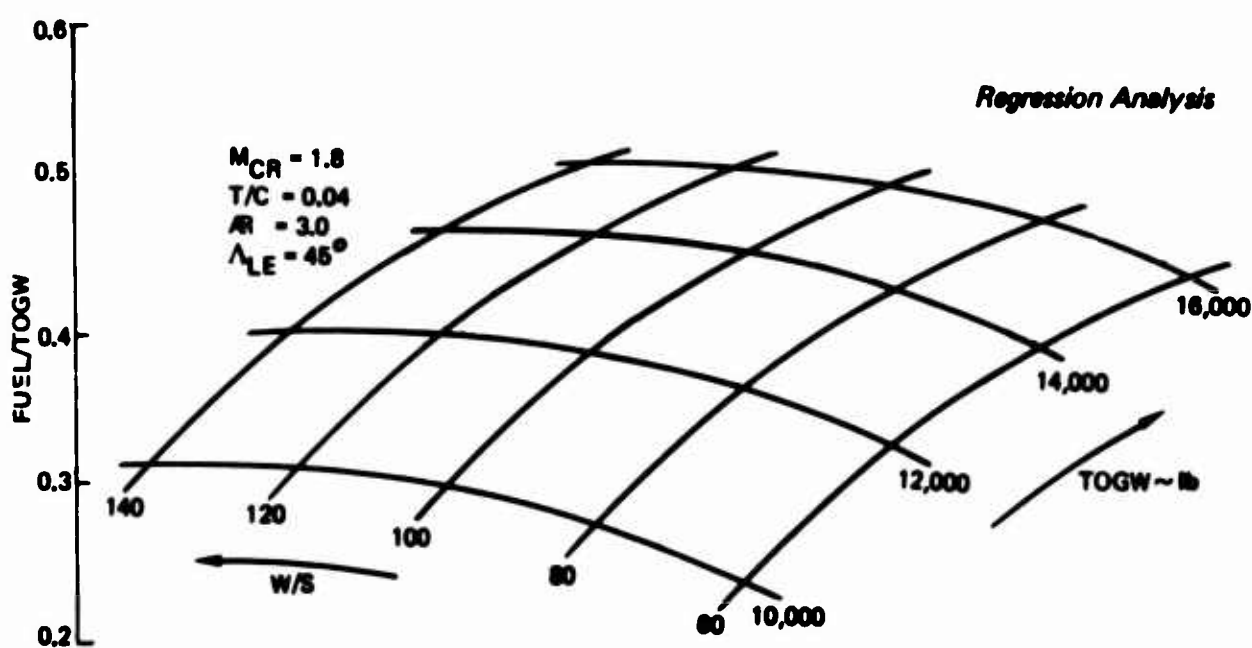
Figure 96.    Canard Fuel Fraction Versus TOGW and W/S

167

## 4.3 VEHICLE PARAMETRIC TRADES (Continued)

In order to better understand the variation of supersonic cruise radius with the design variables, the next few paragraphs will look at fuel frction (Fuel/TOGW) and cruise efficiency (M x L/D/SFC).

The variation of fuel fraction with W/S and TOGW is shown in Figure 96. Note the dominant influence of TOGW, and also that fuel fraction is starting to level off with increasing TOGW. Also, at a constant gross weight, fuel fraction approaches a constant as the wing approaches zero area.

For the case shown in Figure 96, there was little variation in cruise efficiency M(L/D) SFC = 5.4. Thus, the change in radius with W/S and TOGW is mainly due to the change in fuel fraction.

The impact of two primary wing variables, leading edge sweep and aspect ratio, on fuel fraction and cruise efficiency are shown in Figures 97 and 98. The variations in fuel fraction and cruise efficiency tend to cancel each other. That is, increased sweep increases cruise efficiency but decreases fuel fraction. Similarly, increased aspect ratio increases cruise efficiency but reduces fuel fraction.

It would appear from Figures 97 and 98 that apsect ratio has the greater impact on fuel fraction and in order to maximize radius, aspect ratio should be as low as possible. Although the trade between sweep appears to be a toss-up, increased sweep probably will increase radius.

If supersonic radius were the only criteria for design selection, the optimum airplane based on the data presented would have the following characteristics:

o  TOGW    -  16,000 lb
o  W/S     -  120 lb/ft$^2$
o  AR      -  1
o  $\Lambda_{LE}$    65 deg
o  Radius  -  800 N.MI.
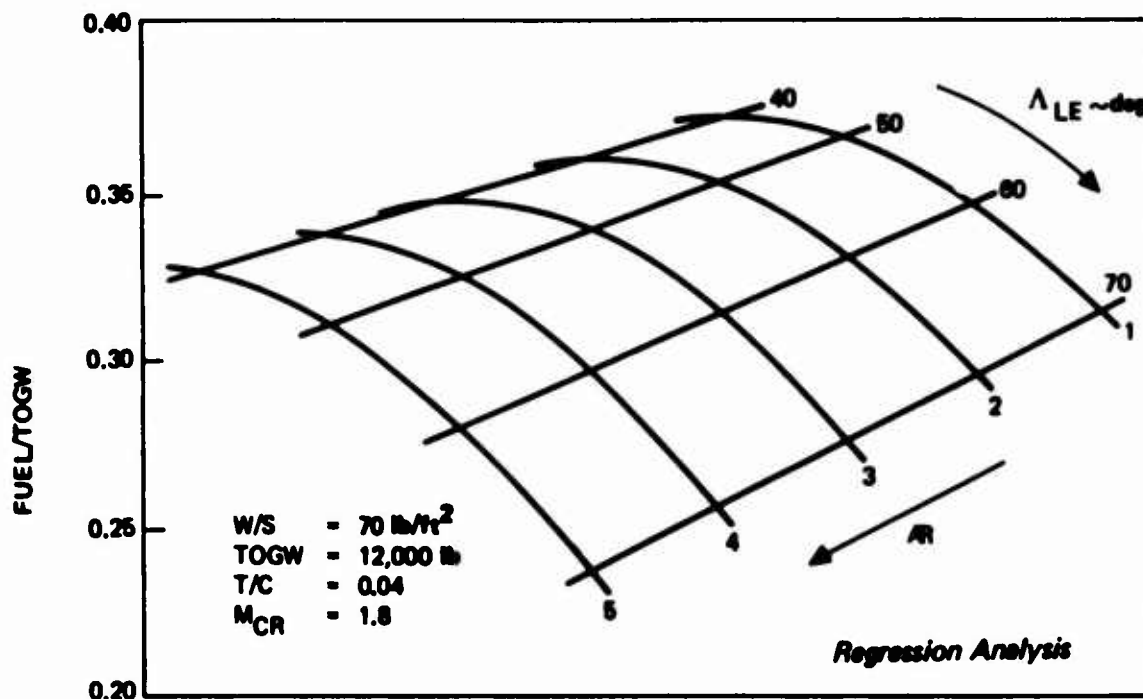
Figure 97. Canard Fuel Fraction Versus AR and $\Lambda_{LE}$
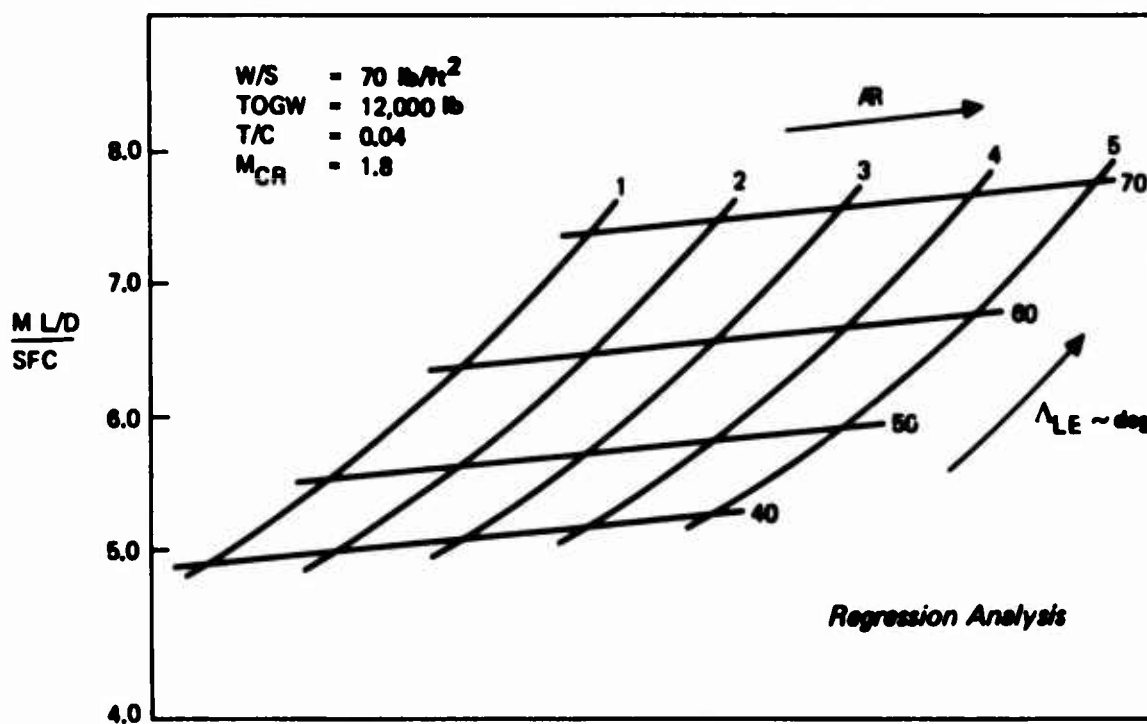


Figure 98. Canard Cruise Efficiency Versus AR and $\Lambda_{LE}$

169

4.3    VEHICLE PARAMETRIC TRADES (Continued)

Combat Persistence--The next figure of merit to consider is combat
persistence.  Persistence is defined as the number of turns which can
be made using the fuel variable at a radius of 200 n. mi.  Load factor,
turn rate, and fuel flow for the turn calculations are based on maximum
afterburning thrust.

The results of the sensitivity analysis, where each variable is perturbed
individually, are shown in Figure 99 for subsonic and supersonic
persistence.

Takeoff gross weight (TOGW) is the dominant variable followed by wing
loading (W/S) and in the case of subsonic persistence, by leading edge
sweep angle.  Wing aspect ratio and thickness ratio have a negligible
impact on persistence.

Figure 100 illustrates the sensitivity of persistence to variations in
W/S and TOGW.  The carpets shown are based on the regression equations.

Figure 101 presents persistence as a function of aspect ratio and wing
leading edge sweep angle.  Note that persistence at each of the flight
envelope points shown increases with decreasing sweep and increasing
aspect ratio.

The persistence carpets for the two canard point designs are shown in
Figure 102 (points I and II).  The results in general are the same as
those obtained from the previous persistence figures.  TOGW is again the
primary variable followed by W/S and  $\Lambda_{LE}$.

Using the data presented in this section, an airplane optimized for combat
persistence would have the following characteristics:

o   TOGW  =   16,000 lb
o   W/S   =   100 lb/ft$^2$
o   AR    =   1.0
o   $\Lambda_{LE}$   =   45 deg
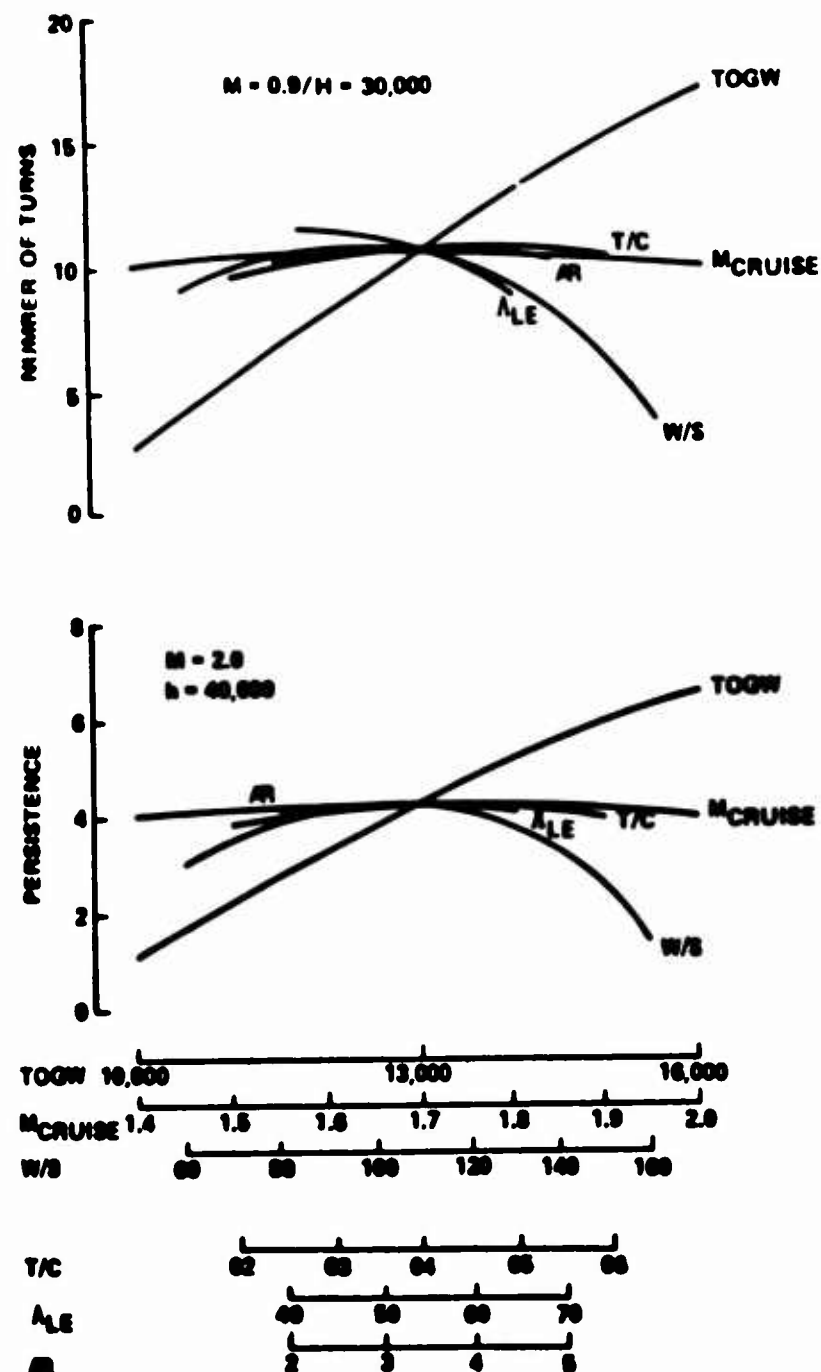
Figure 99.   Canard Persistence Sensitivity Analysis

171
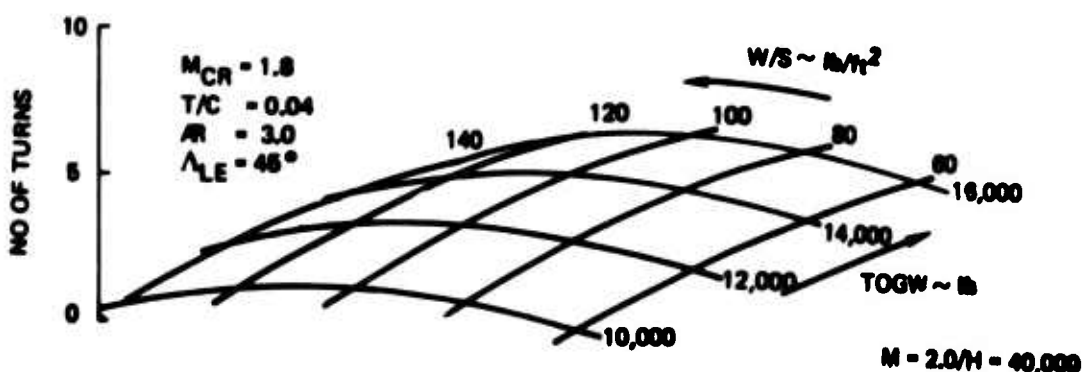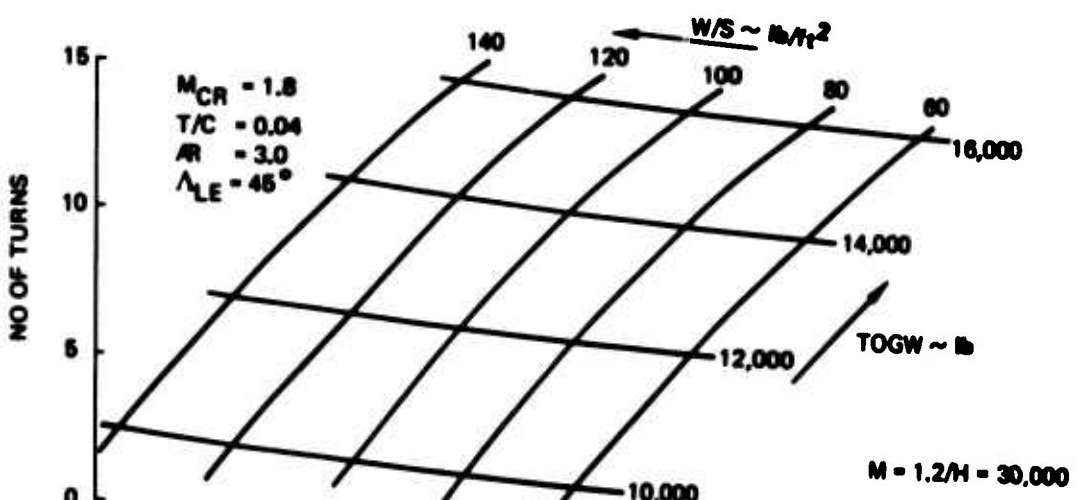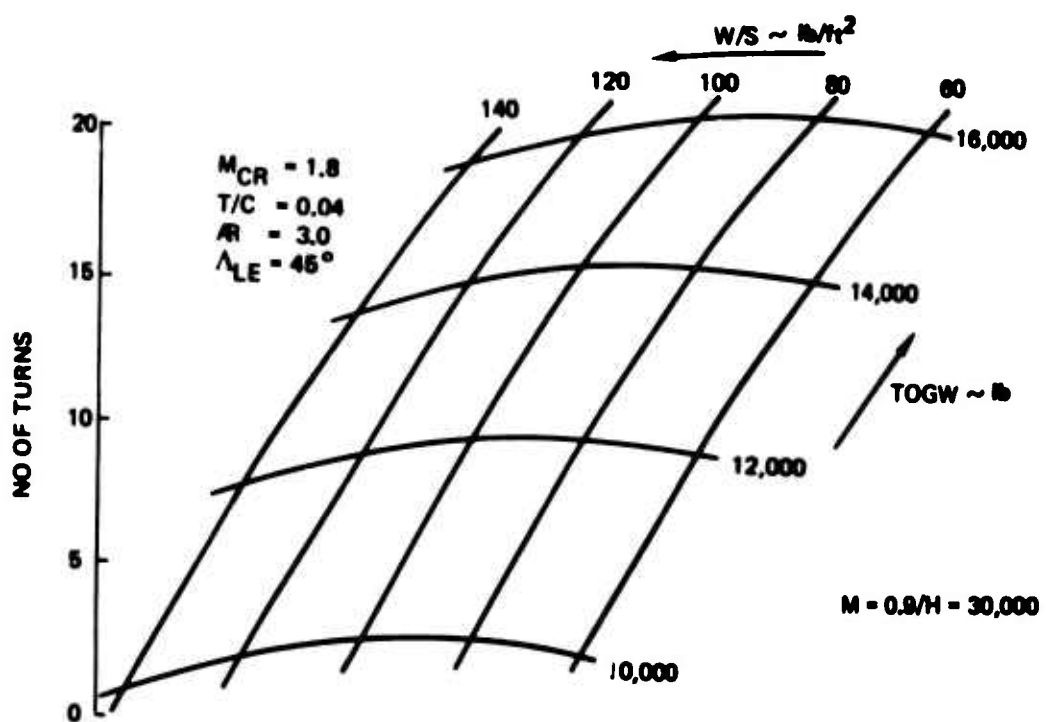
Figure 100. Canard Persistence Versus TOGW and W/S
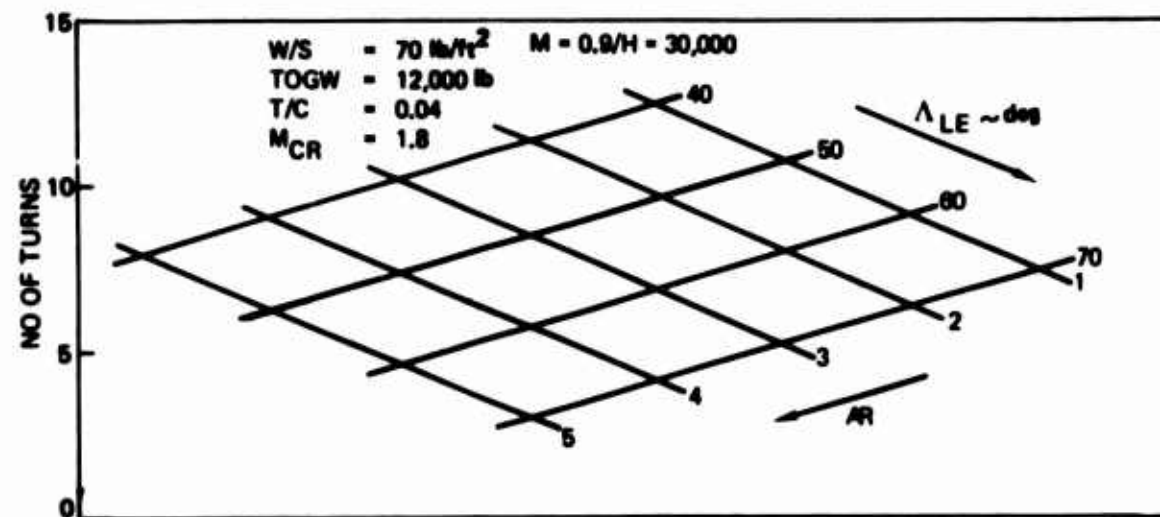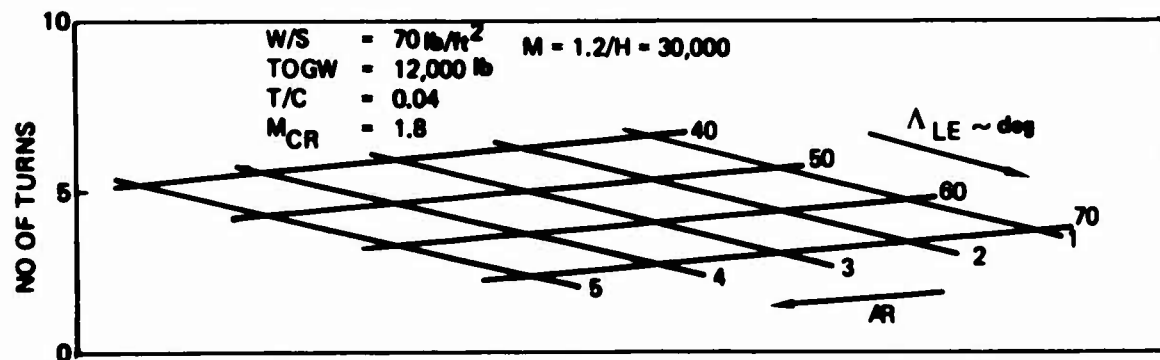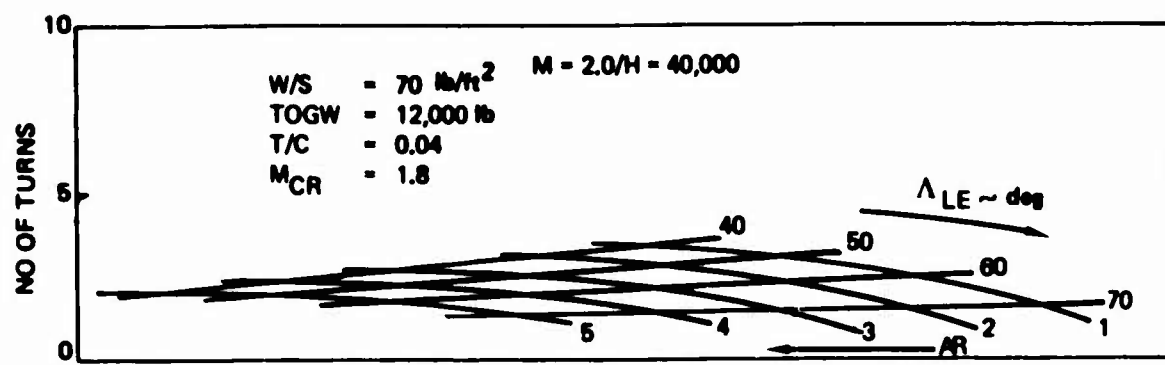
Figure 101. Canard Persistence Versus $\Lambda_{LE}$ and AR
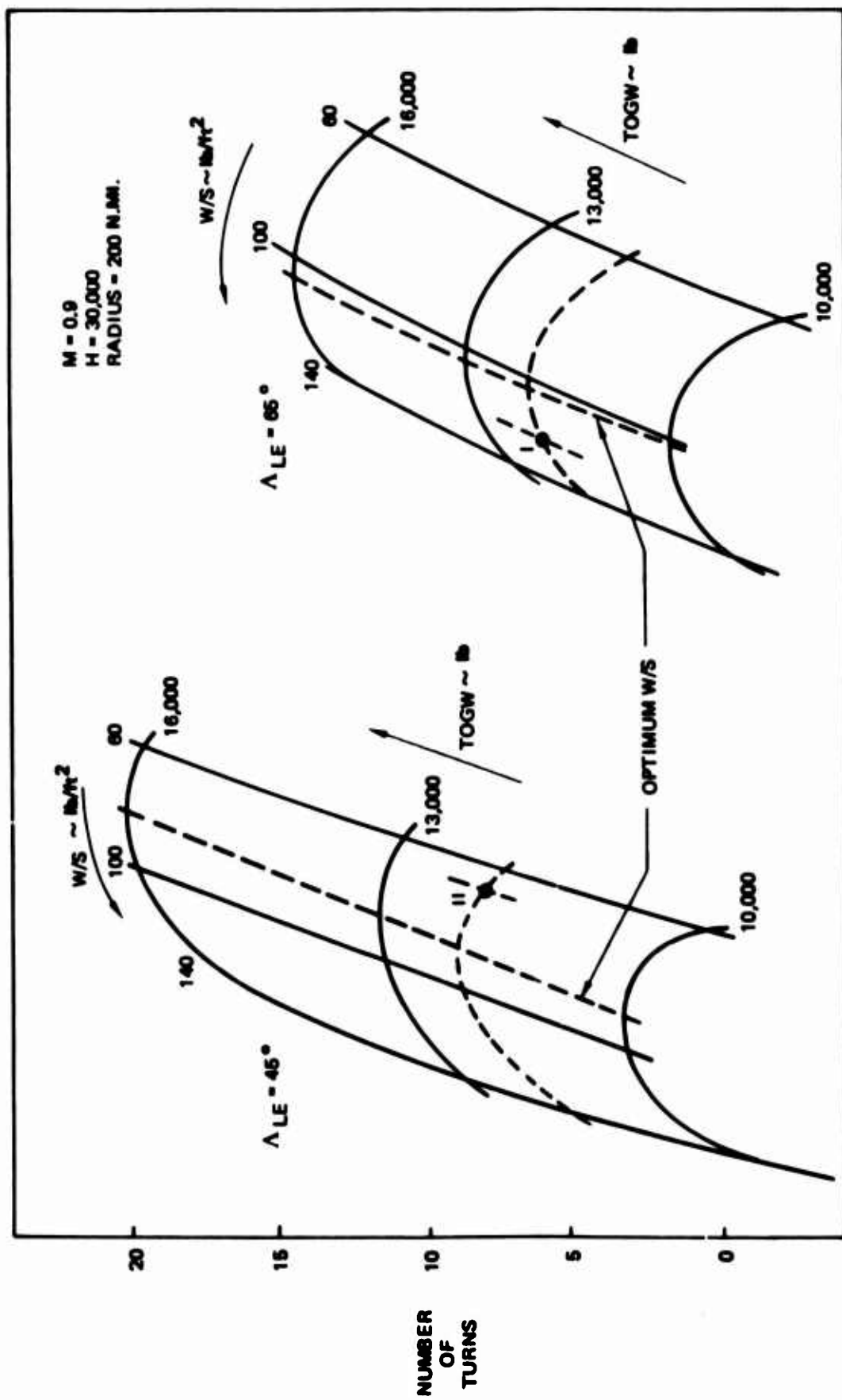
173

Figure 102. Canard Point Design Persistence Carpet

174

## 4.3 VEHICLE PARAMETRIC TRADES (Continued)

Note that the TOGW and AR are the same as the supersonic cruise optimized design. W/S is down 20 $lb/ft^2$ from 120 $lb/ft^2$. The big change is in $\Lambda_{LE}$ which has shifted from the upper design limit to the lower design limit.

Sustained Load Factor--The third and final figure of merit to be considered for the canard concepts is sustained load factor. Sustained load factor is calculated for an average combat weight at a radius of 200 n. mi. using maximum afterburning thrust. Results are presented for both subsonic and supersonic conditions in the following paragraphs.

The results of the sensitivity analysis on load factor are shown in Figure 103. The variable with the biggest impact on load factor is wing loading. Both subsonic and supersonic load factor obtain their maximum values with wing loading set to its lower limit of 60 $lb/ft^2$. The second most important variable is leading edge sweep angle, $\Lambda_{LE}$. Note, however, that while higher leading edge sweep angle increases supersonic load factor, it decreases subsonic load factor. Aspect ratio (AR) is the third most important variable. Increasing AR improves both the subsonic and the supersonic load factors. The fourth most important variable is takeoff gross weight. As to be expected, increasing TOGW decreases sustained load factor.

Sustained load factor carpets based on the regression analysis equations are shown in Figures 104 and 105. Figure 106 illustrates the impact of TOGW and W/S. For all three flight envelope points shown, load factor is maximized by minimizing W/S and TOGW. This result is consistent with the sensitivity analysis and is in direct conflict with the W/S and TOGW for maximum radius.

The effect of aspect ratio, AR, and wing leading edge sweep angle, $\Lambda_{LE}$, on load factor shown in Figure 101. Note that increasing AR improves load factor in all three cases. On the other hand, increasing $\Lambda_{LE}$ only improves load factor at M - 2.0/H - 40,000.
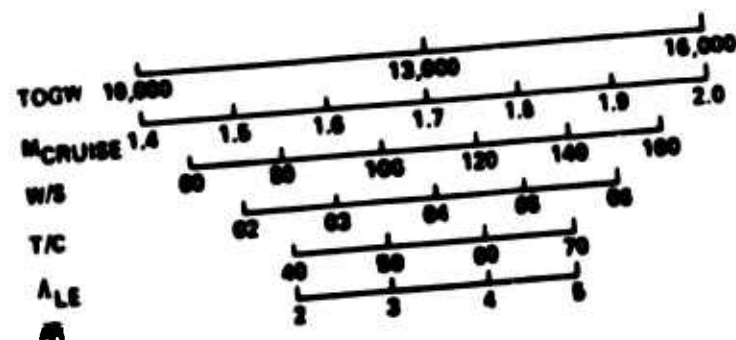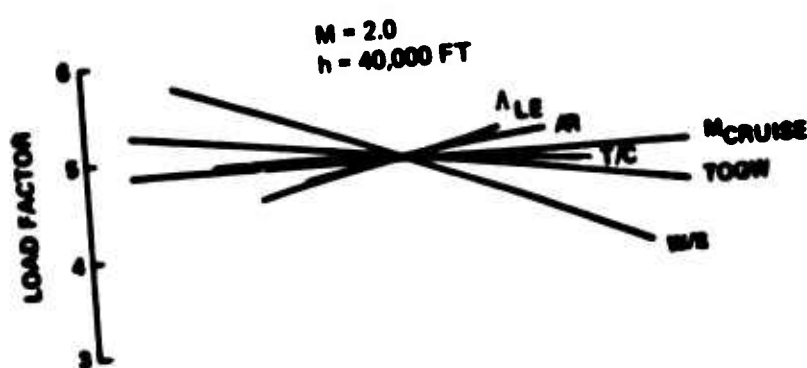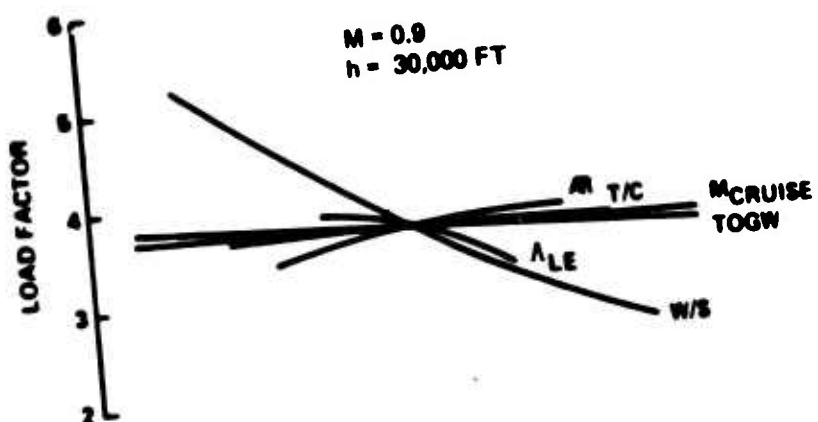
Figure 103. Canard Sustained Load Factor Sensitivity Analysis
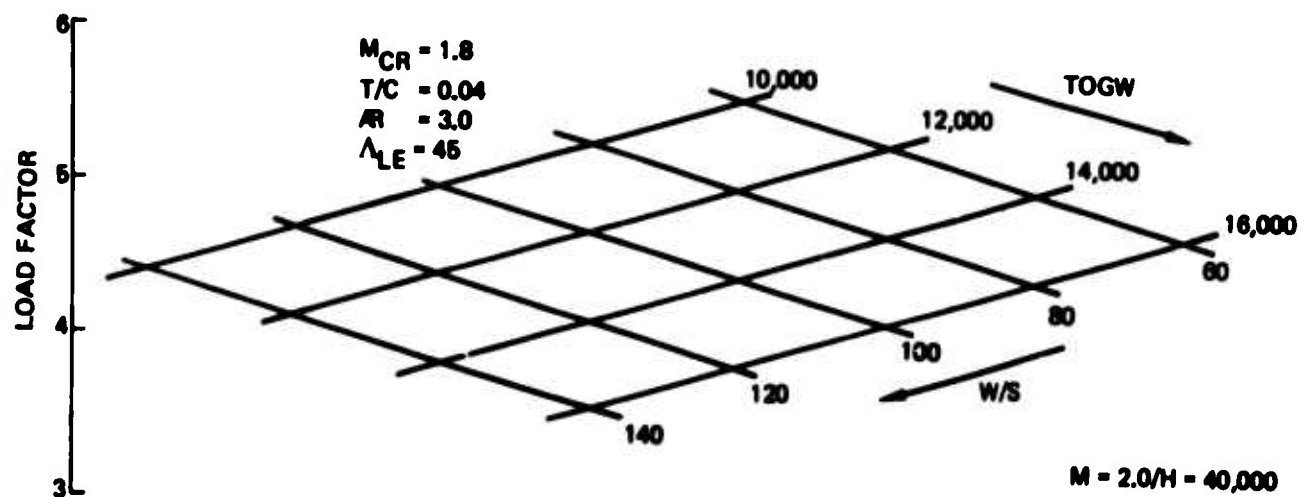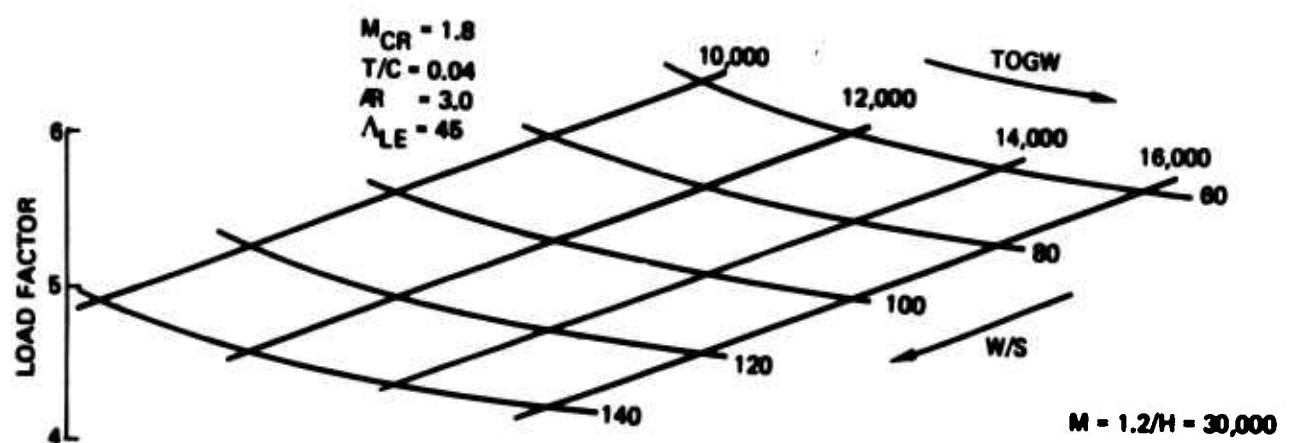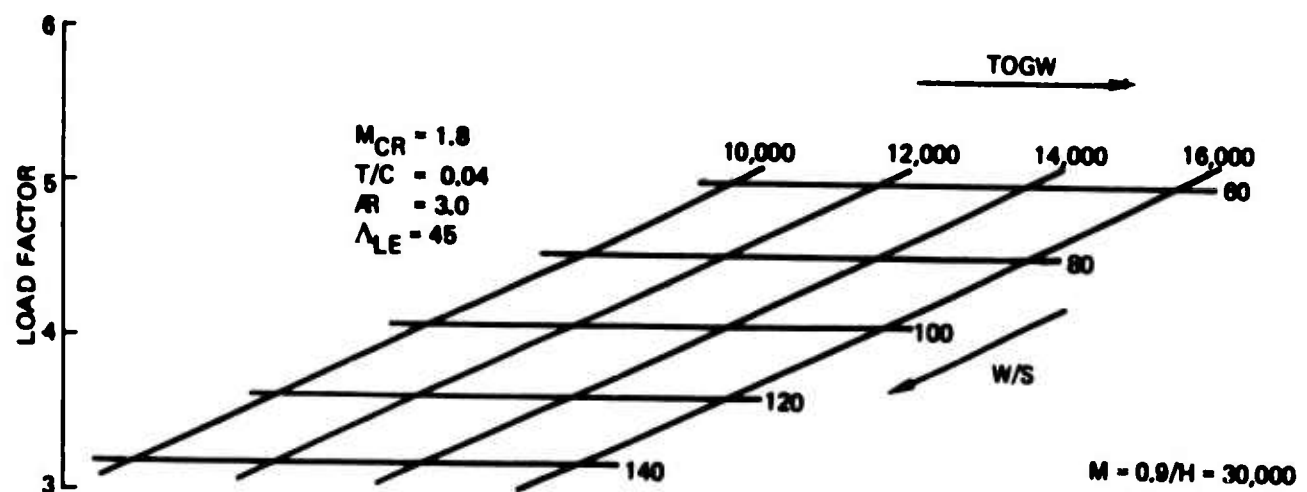
Figure 104.    Canard Sustained Load Factor Versus TOGW and W/S

**M = 0.9/H = 30,000**

W/S = 70    T/C = 0.04
TOGW = 12,000    $M_{CR}$ = 1.8

**M = 1.2/H = 30,000**

W/S = 70    T/C = 0.04
TOGW = 12,000    $M_{CR}$ = 1.8

**M = 2.0/H = 40,000**

W/S = 70    T/C = 0.04
TOGW = 12,000    $M_{CR}$ = 1.8
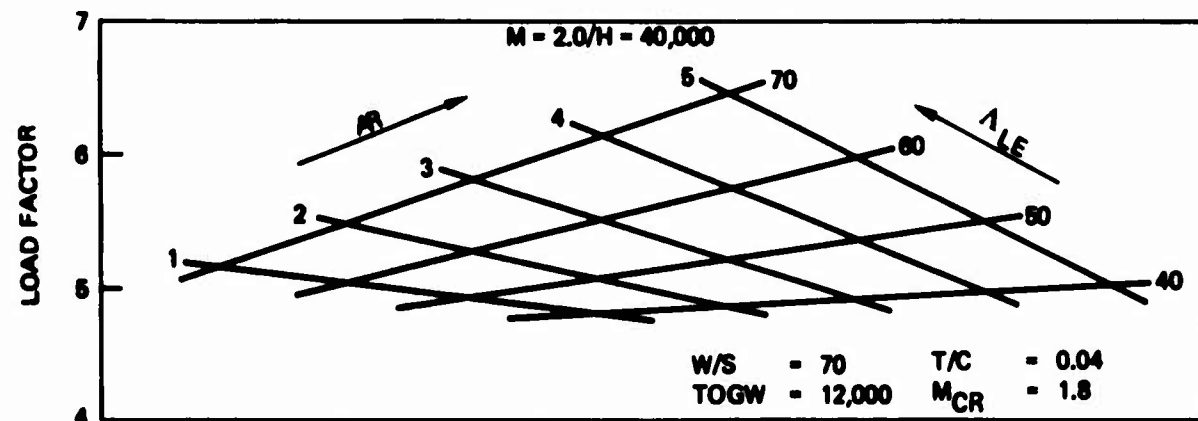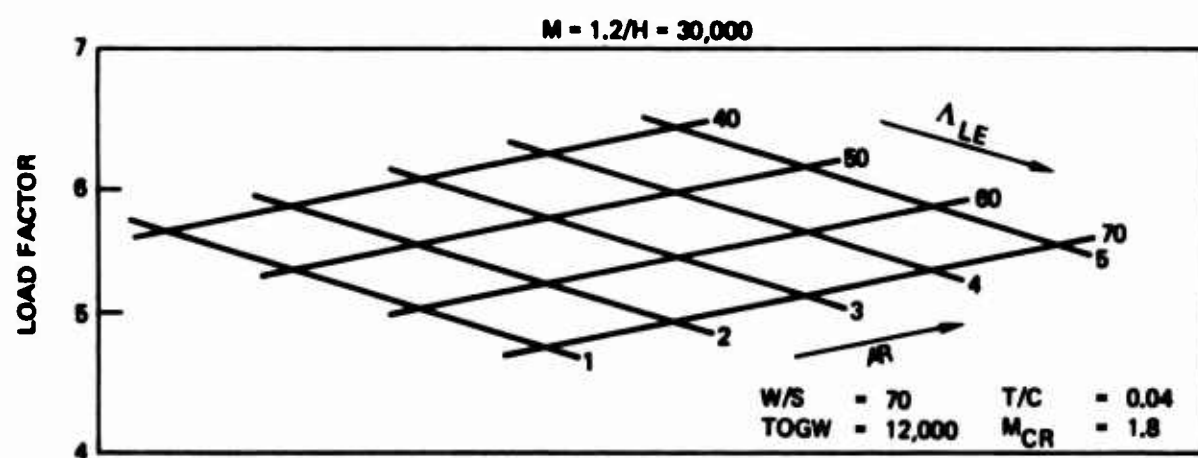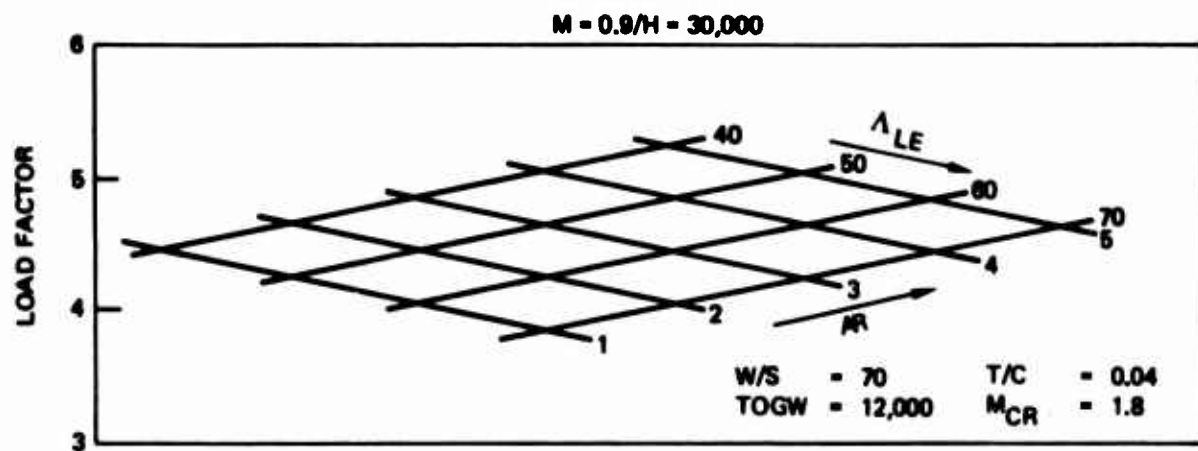
*Figure 105.    Canard Sustained Load Factor Versus $\Lambda_{LE}$ and AR*
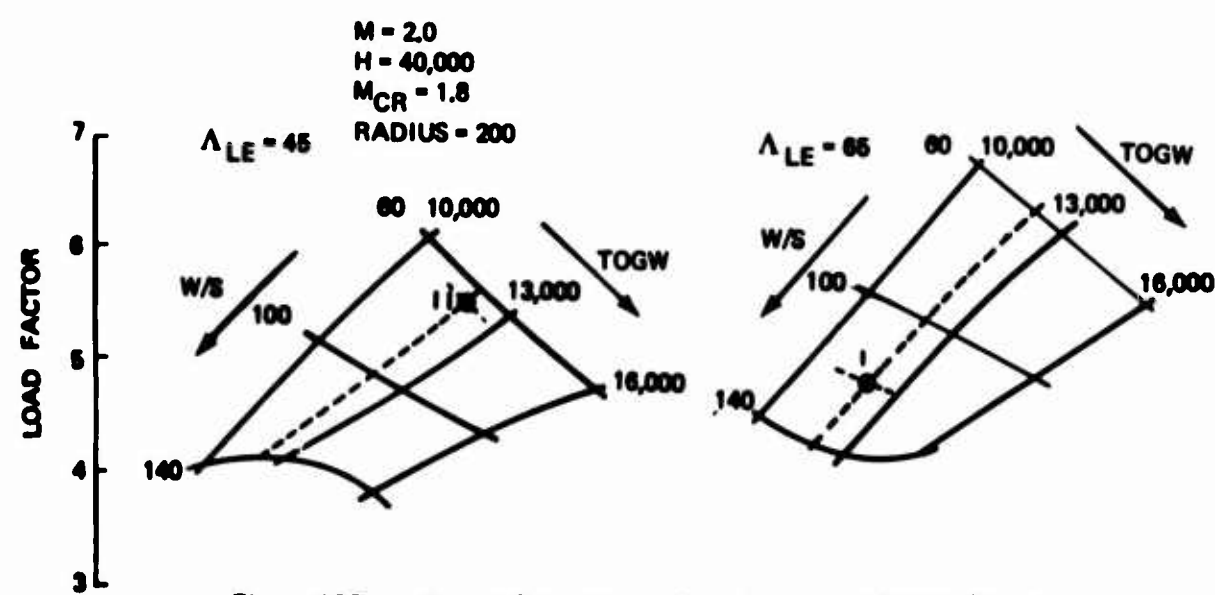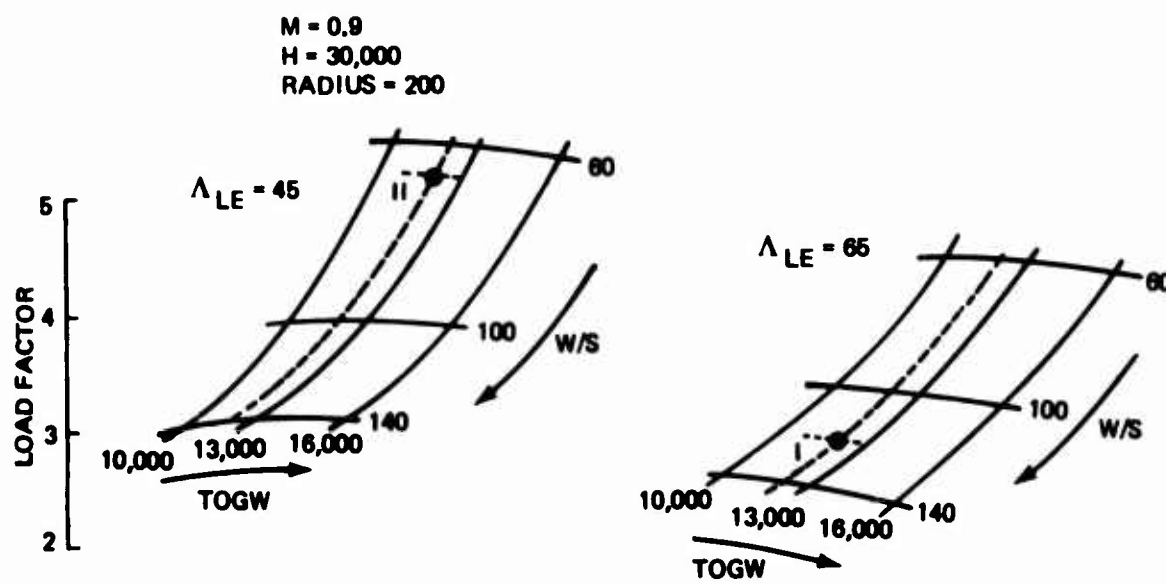
Figure 106. Conrad Point Design Sustained Load Factor Carpet

179

## 4.3 VEHICLE PARAMETRIC TRADES (Continued)

Similar results are presented in Figure 102 for the point design carpets.

ARROW CONCEPT

Following the canard concept parametric study, a similar evaluation was made of the arrow concept shown in Figure 107. The major difference in the two parametric evaluations was the elimination of wing leading edge sweep and aspect ratio from the arrow concept study. For the arrow design, the wing leading edge was set a constant increment behind the Mach one. Therefore, there was a direct relationship between cruise Mach number and wing leading edge sweep eliminating one of the previous design variables. The variation of wing planform geometry with cruise Mach number is shown in Figure 108. The relationship between the wing leading and trailing edge sweep angles along with wing area lead to a unique expression for wing aspect ratio thus eliminating the second design variable.

In review, the design variables for the arrow parametric are:
o  Takeoff gross weight
o  Wing loading
o  Cruise Mach number
o  Wing thickness ratio

The effects of these parameters on supersonic cruise performance, combat persistence, and combat load factors are discussed in the following sections. Sensitivity plots, regression equations and carpet plots are used to present the data. Figure 109 shows the fourty-five designs which were evaluated in the sizing and performance program to establish the data base for the regression equations.
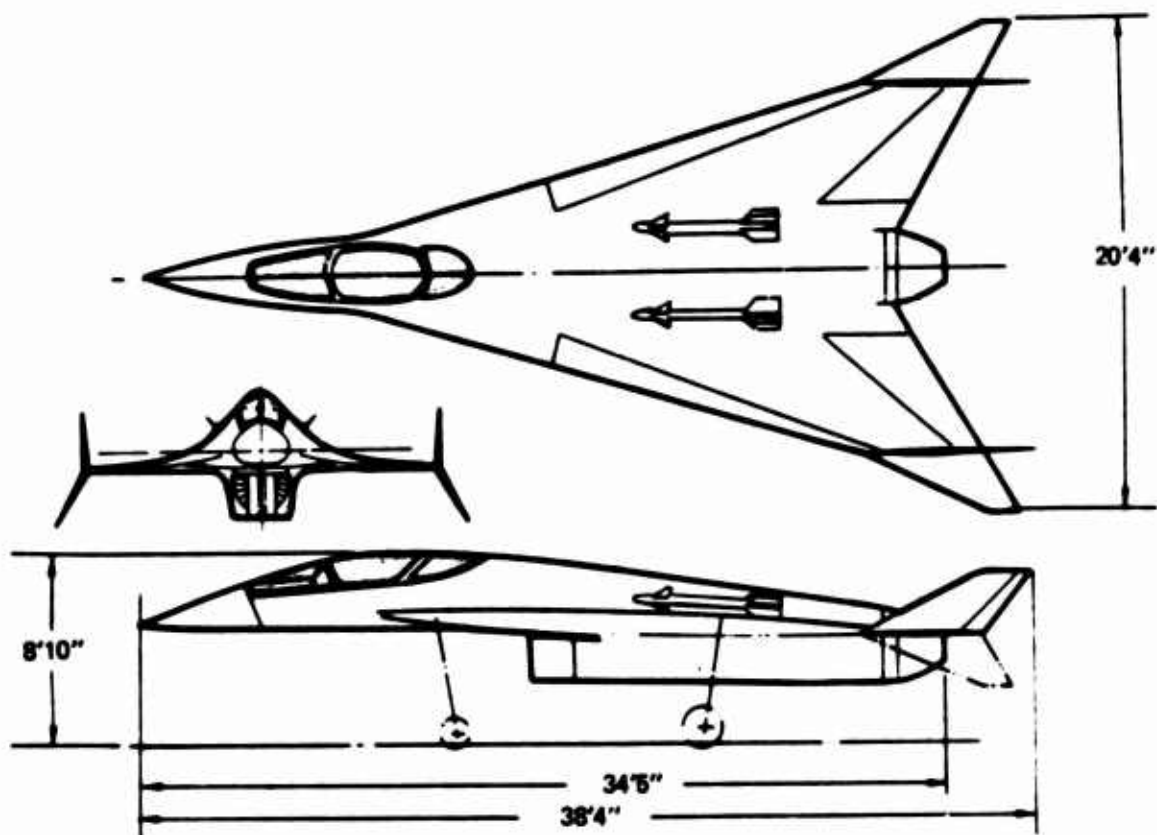
Figure 107.    LES – Arrow Concept Baseline.
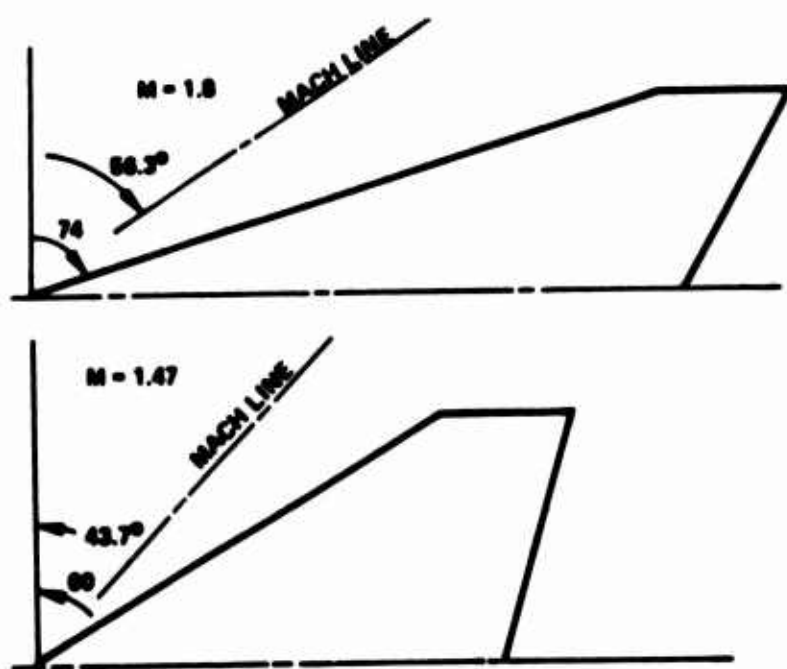


Figure 108.    Arrow Concept Wing Planform Geometry

| CASE | SUPMACH | TOGW | W/S | T/C |
|------|---------|-------|-------|------|
| 1 | 1.400 | 10000 | 40.0 | .020 |
| 2 | 1.550 | 11500 | 55.0 | .030 |
| 3 | 1.700 | 13000 | 70.0 | .040 |
| 4 | 1.850 | 14500 | 85.0 | .050 |
| 5 | 2.000 | 16000 | 100.0 | .060 |
| 6 | 1.550 | 13000 | 85.0 | .060 |
| 7 | 1.700 | 14500 | 100.0 | .020 |
| 8 | 1.850 | 16000 | 40.0 | .030 |
| 9 | 2.000 | 10000 | 55.0 | .040 |
| 10 | 1.400 | 11500 | 70.0 | .050 |
| 11 | 1.700 | 16000 | 55.0 | .050 |
| 12 | 1.850 | 10000 | 70.0 | .060 |
| 13 | 2.000 | 11500 | 85.0 | .020 |
| 14 | 1.400 | 13000 | 100.0 | .030 |
| 15 | 1.550 | 14500 | 40.0 | .040 |
| 16 | 1.850 | 11500 | 100.0 | .040 |
| 17 | 2.000 | 13000 | 40.0 | .050 |
| 18 | 1.400 | 14500 | 55.0 | .060 |
| 19 | 1.550 | 16000 | 70.0 | .020 |
| 20 | 1.700 | 10000 | 85.0 | .030 |
| 21 | 2.000 | 14500 | 70.0 | .030 |
| 22 | 1.400 | 16000 | 85.0 | .040 |
| 23 | 1.550 | 10000 | 100.0 | .050 |
| 24 | 1.700 | 11500 | 40.0 | .060 |
| 25 | 1.850 | 13000 | 55.0 | .020 |
| 26 | 2.000 | 11500 | 70.0 | .050 |
| 27 | 1.400 | 13000 | 85.0 | .060 |
| 28 | 1.550 | 14500 | 100.0 | .020 |
| 29 | 1.700 | 16000 | 40.0 | .030 |
| 30 | 1.850 | 10000 | 55.0 | .040 |
| 31 | 1.850 | 13000 | 100.0 | .030 |
| 32 | 2.000 | 14500 | 40.0 | .040 |
| 33 | 1.400 | 16000 | 55.0 | .050 |
| 34 | 1.550 | 10000 | 70.0 | .060 |
| 35 | 1.700 | 11500 | 85.0 | .020 |
| 36 | 1.700 | 14500 | 55.0 | .060 |
| 37 | 1.850 | 16000 | 70.0 | .020 |
| 38 | 2.000 | 10000 | 85.0 | .030 |
| 39 | 1.400 | 11500 | 100.0 | .040 |
| 40 | 1.550 | 13000 | 40.0 | .050 |
| 41 | 1.550 | 16000 | 85.0 | .040 |
| 42 | 1.700 | 10000 | 100.0 | .050 |
| 43 | 1.850 | 11500 | 40.0 | .060 |
| 44 | 2.000 | 13000 | 55.0 | .020 |
| 45 | 1.400 | 14500 | 70.0 | .030 |

*Figure 109. Arrow Concept Latin Square Design Selection*

182

## 4.3  VEHICLE PARAMETRIC TRADES (Continued)

Supersonic Radius--The results of the sensitivity analysis on supersonic radius are shown in Figure 110. Takeoff gross weight has by far the largest impact on radius followed by wing loading, cruise Mach number and wing thickness ratio. Note that supersonic radius peaks at a cruise Mach number of about 1.65 and a wing loading of about 84. Also, note that although wing thickness has the smallest impact, radius increases with increasing wing t/c over the range of thickness ratios considered.

The regression equation for supersonic radius and the first partial derivatives are:

$$R = 4867 + 6.6487 \times W/S + .2859 \times TOGW + 3,414 \times M_{cr}$$
$$+ 18.433 \times t/c \times W/S - .07074 \times W/S^2 + .000317 \times W/S \times TOGW$$
$$- .00000883 \times TOGW^2 - 1032 \times M_{cr}^2.$$

$$\frac{\delta R}{\delta TOGW} = 6.6487 + 18.433 \times t/c - .14148 \times W/S + .000317 \times TOGW$$

$$\frac{\delta R}{\delta M_{CR}} = .2859 + .000317 \times W/S - .0001766 \times TOGW$$

$$\frac{\delta R}{\delta M_{CR}} = 3414 - 2064 \times M_{CR}$$

$$\frac{\delta R}{\delta t/c} = 18.433 \times W/S$$

By inspection of these equations, it can be seen that radius will be a maximum when:

o  t/c = 0.6 (the upper limit)

o  $M_{CR}$ = 1.65

Setting wing thickness ratio and cruise Mach number to these optimal values, the variation of radius with the two remaining desgin variables is shown in Figure 111.
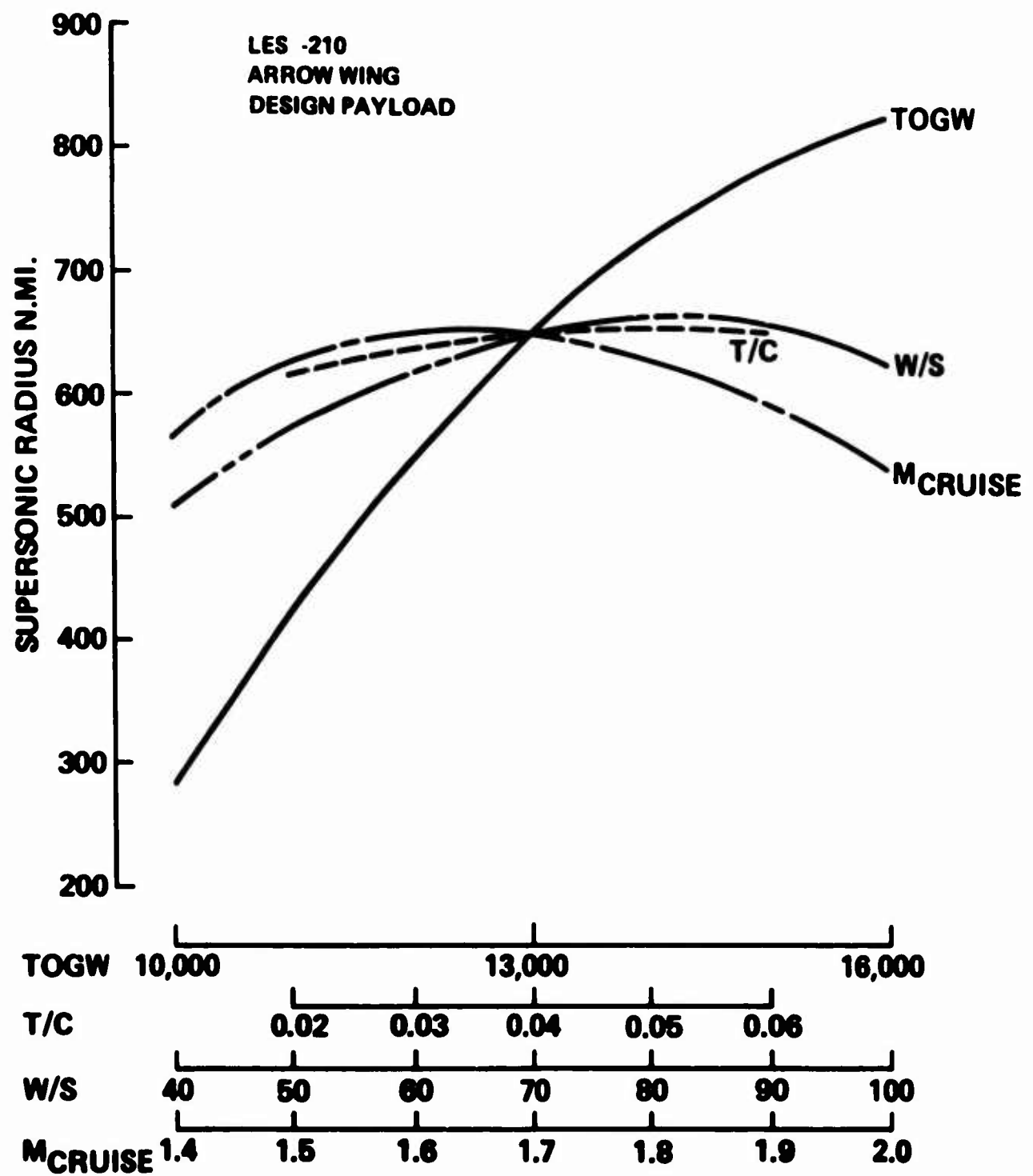
Figure 110. Arrow Supersonic Radius Sensitivity Analysis
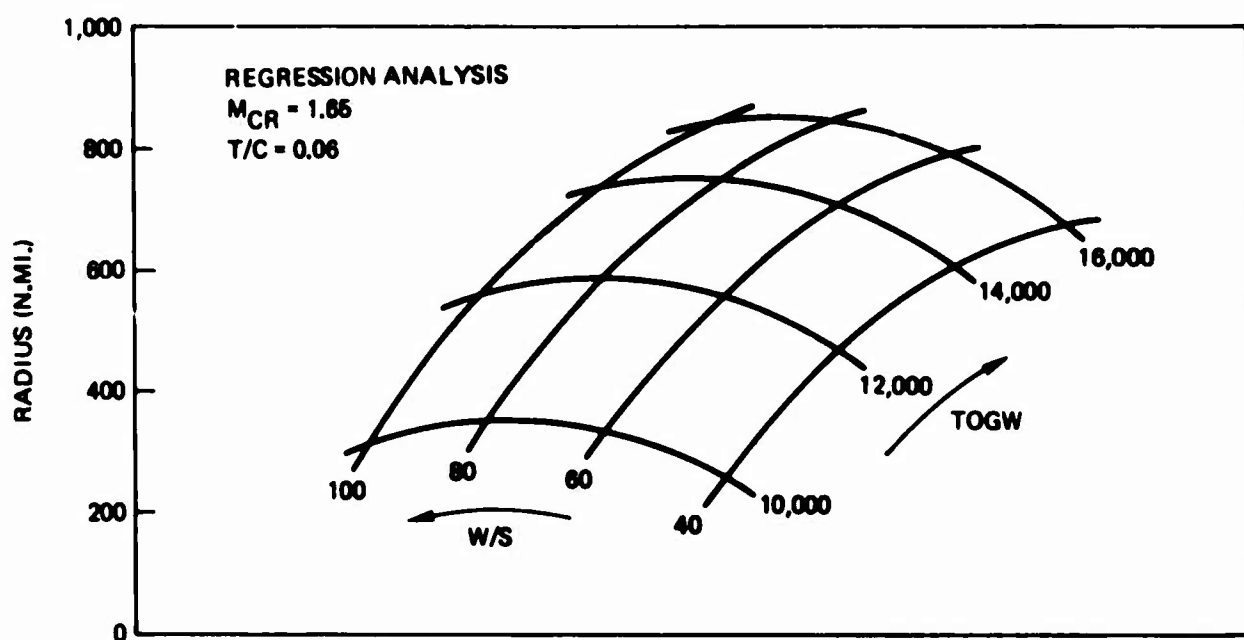
Figure 111.    Arrow Supersonic Radius Versus TOGW and W/S
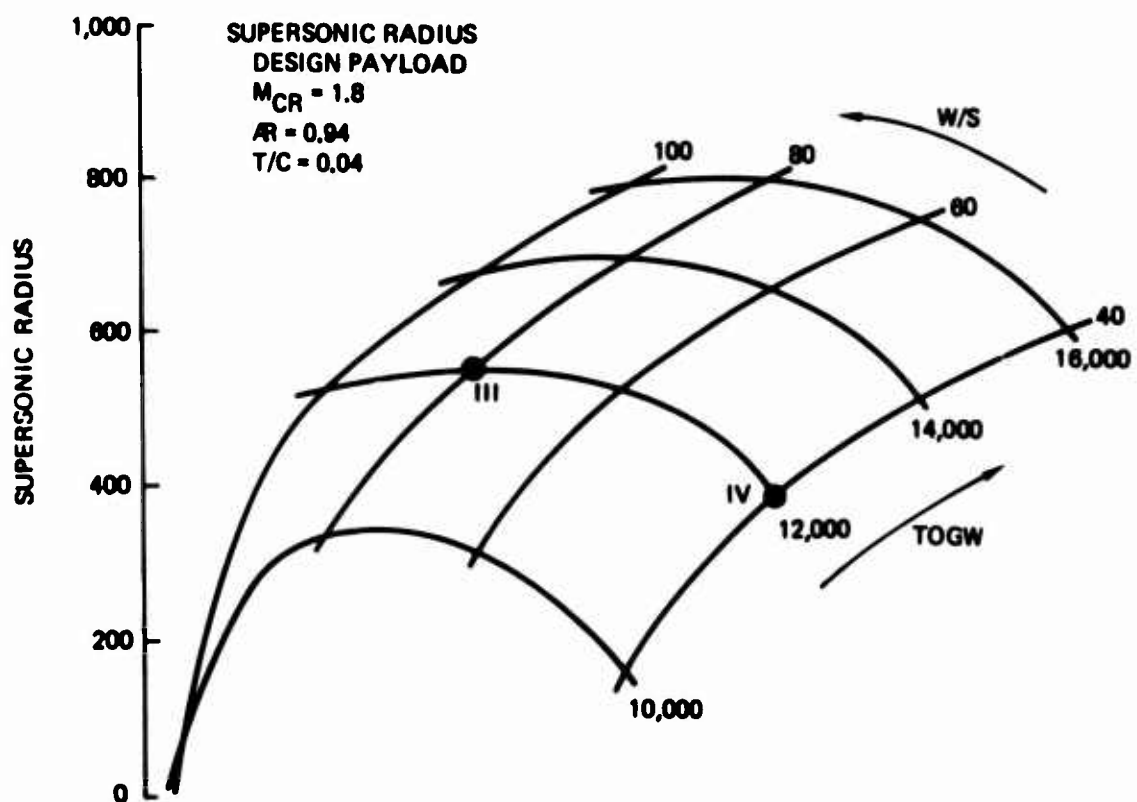


Figure 112.    Arrow Point Design Supersonic Radius Carpet

## 4.3 VEHICLE PARAMETRIC TRADES (Continued)

The results are similar to the sensitivity analysis. TOGW again has the greatest impact on supersonic radius followed by W/S. The wing loading for maximum radius is a function of takeoff gross weight and varies from about 70 at the low takeoff gross weight of 10,000 to about 90 at the high gross weight of 16,000.

The two arrow concept point designs selected for the mid-term review are shown on the W/S - TOGW carpet in Figure 112 (Point III and IV. Point III represents the best supersonic cruise airplane with a takeoff gross weight less than or equal to 12,000 lbs. Point IV is the best maneuver airplane (in terms of sustained load factor) at the 12,000 lb. TOGW. The points used to construct the carpet in Figure 112 were obtained from the sizing and performance program. In general, there is good agreement with the regression equation results presented in Figure 112.

The large influence of TOGW and W/S on supersonic radius is better understood by looking at their respective influence on cruise efficiency and fuel fraction. In Figure 113, it is seen that M x L/D/SFC increases with gross weight and decreases with wing loading. In Figure 114, fuel fraction increases with both gross weight and wing load. Thus, increasing gross weight increases both of the terms in the radius equation explaining the large impact of gross weight on radius. On the other hand, increasing wing loading only pays off up to about 80 lbs/ft$^2$ where gains in fuel fraction begin to level off and are more than offset by the corresponding losses in cruise efficiency.

Based on data examined thus far, an arrow wing design optimized for supersonic cruise radius would have the following characteristics:

o  TOGW  -  16,000 lbs.

o  W/S  -  90 lb/ft$^2$

o  $M_{cr}$  -  1.65

o  t/c  -  .06
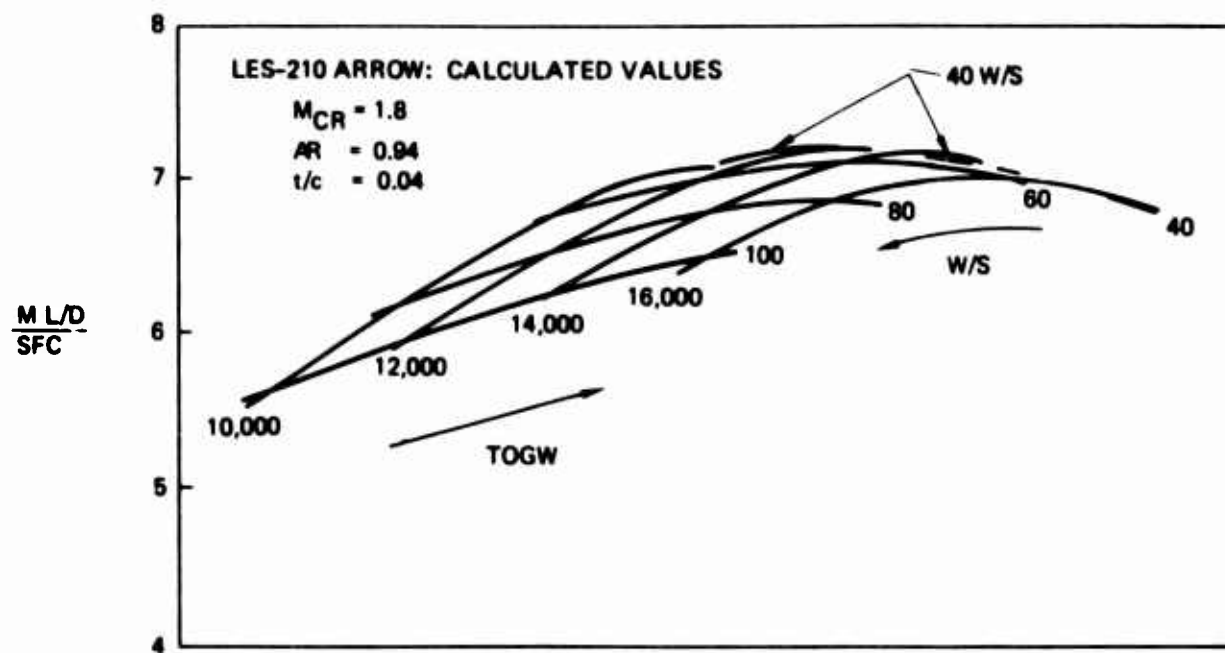
Figure 113.    Arrow Cruise Efficiency Versus TOGW and W/S
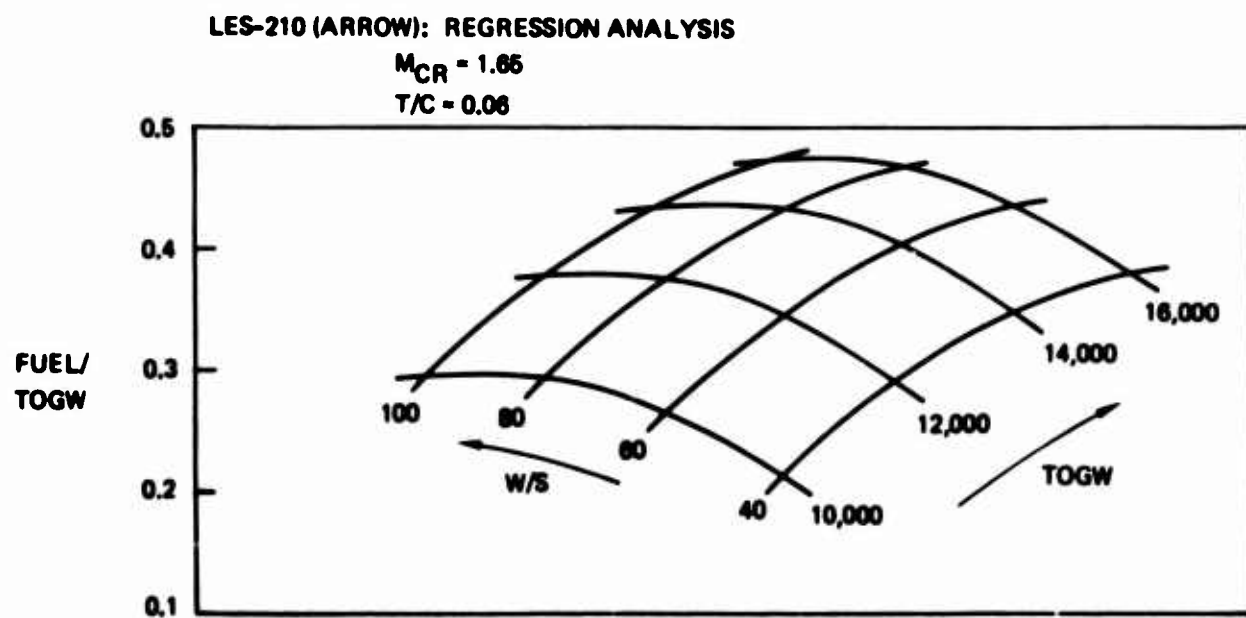


Figure 114.    Arrow Fuel Fraction Versus TOGW and W/S

## 4.3    VEHICLE PARAMETRIC TRADES (Continued)

Combat Persistence--The next figure of merit to be looked at is combat
persistence.  Persistence is the number of turns that can be made with
the fuel available at a 200 n. mi. radius.  The turns are calculated at
maximum afterburning thrust.

The sensitivity analysis results are shown in Figure 115 for subsonic
(Mach 0.9, 30,000 ft.) and supersonic (Mach 2.0, 40,000 ft.) combat
persistence.  The most apparent result is again the large impact of
takeoff gross weight on persistence.  This result is related to the
fact that the large airplanes have large fuel fractions (see Figure 114)
and at a constant radius, have more fuel to burn during the combat.

Figure 115 indicates that persistence reaches a peak at a wing loading
of about 70 lb/ft$^2$.  As to be expected, this is a lower wing loading
than the value for maximum radius.  The variation in persistence with
wing thickness ratio is the same as the variation of radius with t/c.
That is, persistence increases with increasing t/c.  Different trends
are indicated for the variation of subsonic and supersonic persistence
with cruise Mach number.  Subsonic persistence obtains its maximum
value at a cruise Mach number of 1.4 while supersonic persistence peaks
out at about 1.7.

The regression analysis results showing the interaction between gross
weight and wing loading on combat persistence are shown in Figure 116.
These data also include persistence at Mach 1.2, 30,000 feet.  For
subsonic persistence, the optimum wing loading varies from about 70 lb/ft$^2$
at low gross weight of 10,000 lbs to about 50 lb/ft$^2$ at high
gross weight of 16,000 lbs.  At low supersonic Mach numbers (M = 1.2)
wing loading appears to have little or no effect on persistence.  At
the highest supersonic Mach number shown, persistence increases with
wing loading up to the upper bound of 100 lb/ft$^2$, although the increase
is small.
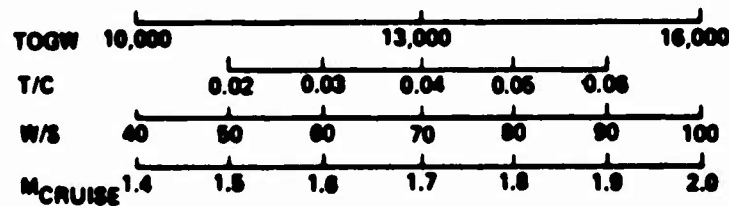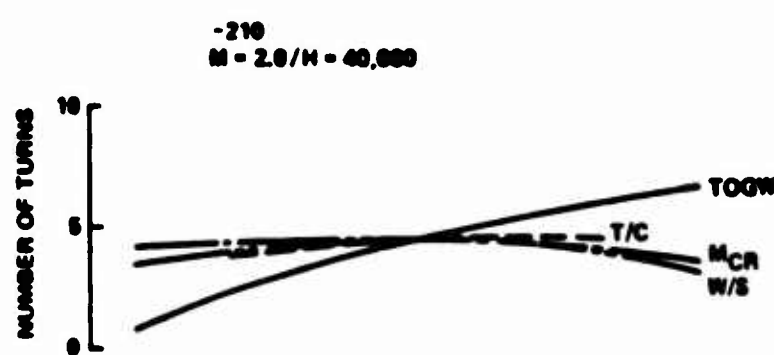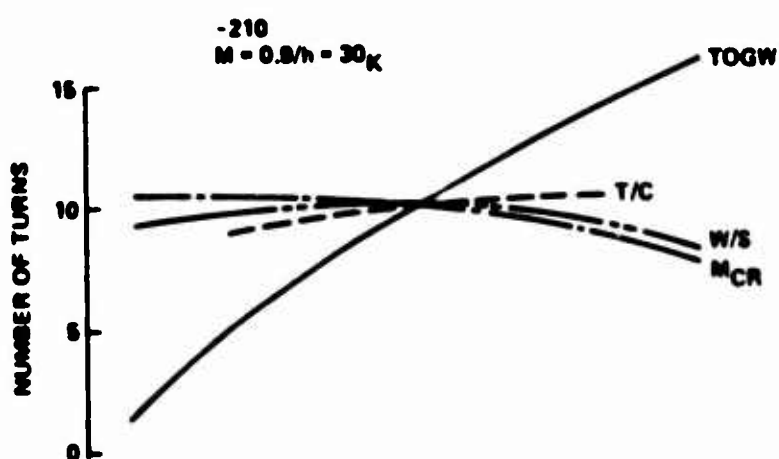
Figure 115.    Arrow Persistence Sensitivity Analysis
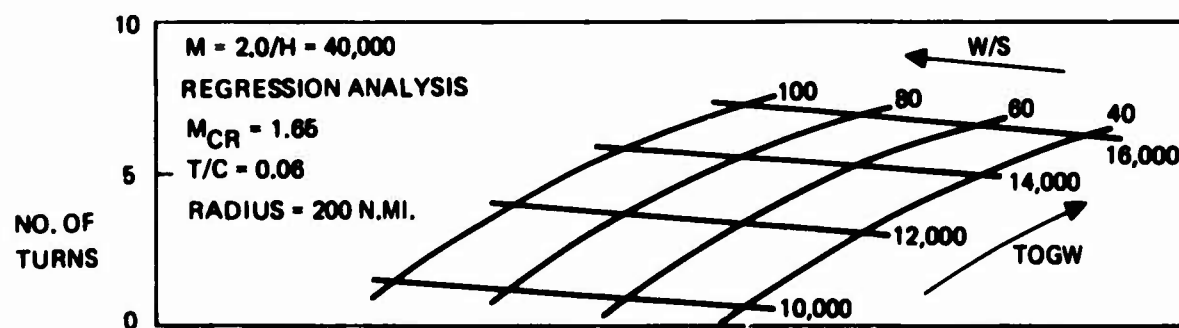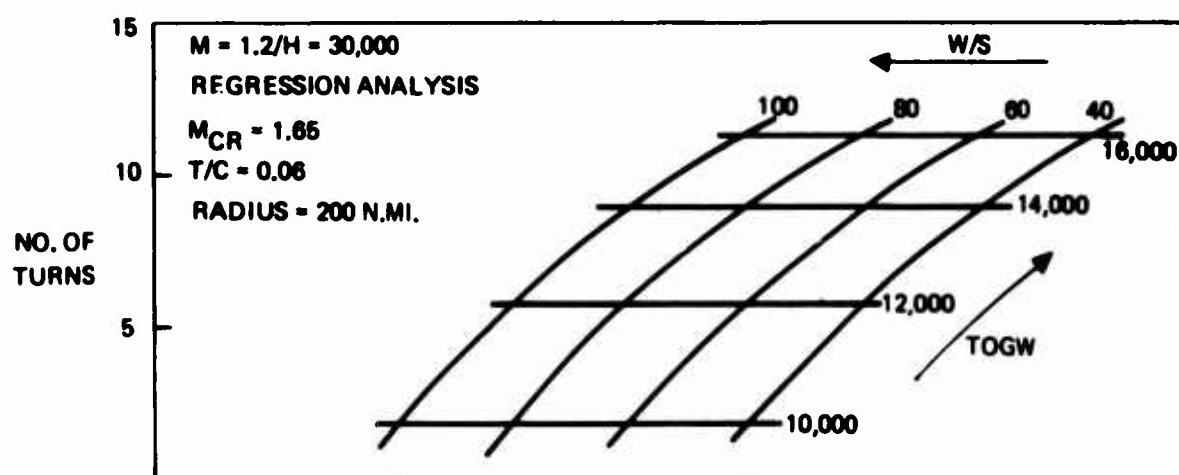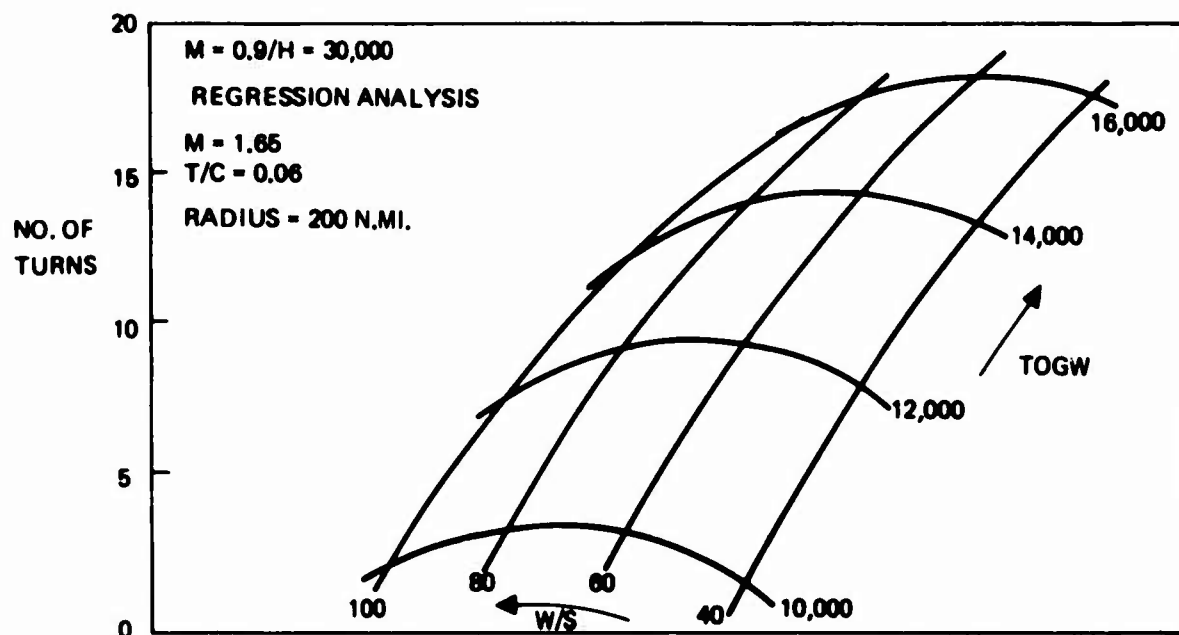
Figure 116. Arrow Persistence Versus TOGW and W/S

4.3    VEHICLE PARAMETRIC TRADES (Continued)

Figure 117 shows the interaction between the two remaining design
varaibles, cruise Mach number and wing thickness ratio, on combat
persistence.  The carpets which are derived from the regression
equations are for a takeoff gross weight of 12,000 lbs. and a wing
loading of 40 lb/ft$^2$.  Persistence falls off at cruise Mach number above
1.6.  There appears to be an increase in optimum cruise Mach number with
increasing combat Mach number.  Persistence increases monotonically with
wing thickness ratio at the three combat Mach numbers shown.  Note
however, that the rate of increase decreases with increasing combat Mach
number.

The persistence carpets for the two mid-term point designs are shown in
Figure 118 (Point III & IV).  The subsonic persistence carpet is similar
to the corresponding regression analysis carpet.  However, the variation
of supersonic persistence with wing loading shows an optimum at about
60 lb/ft$^2$ whereas the regression results indicate that persistence
continues to increase with an increasing wing loading.

If combat persistence were the sole design criteria, an optimum arrow
concept would be characterized by:

o   TOGW       - 16,000 lbs.
o   W/S        - 80 lb/ft$^2$
o   $M_{cr}$       -  1.6
o   t/c        - .06

This design is essentially the same as the design for maximum radius.
Thus, there is no conflict between the radius and persistence
requirements.
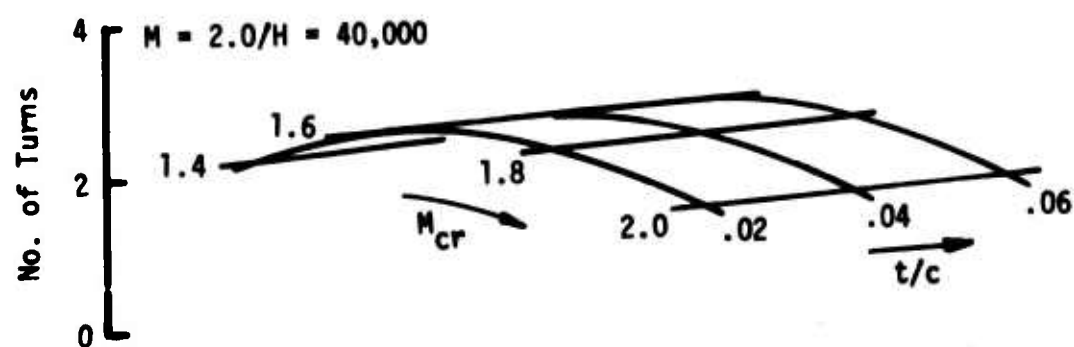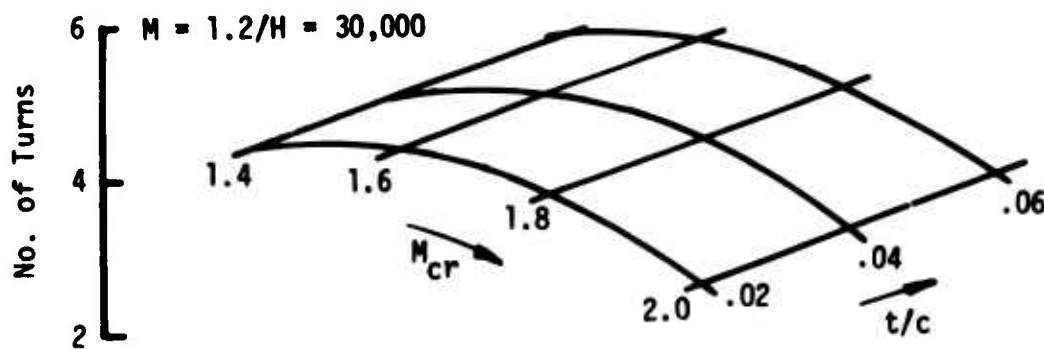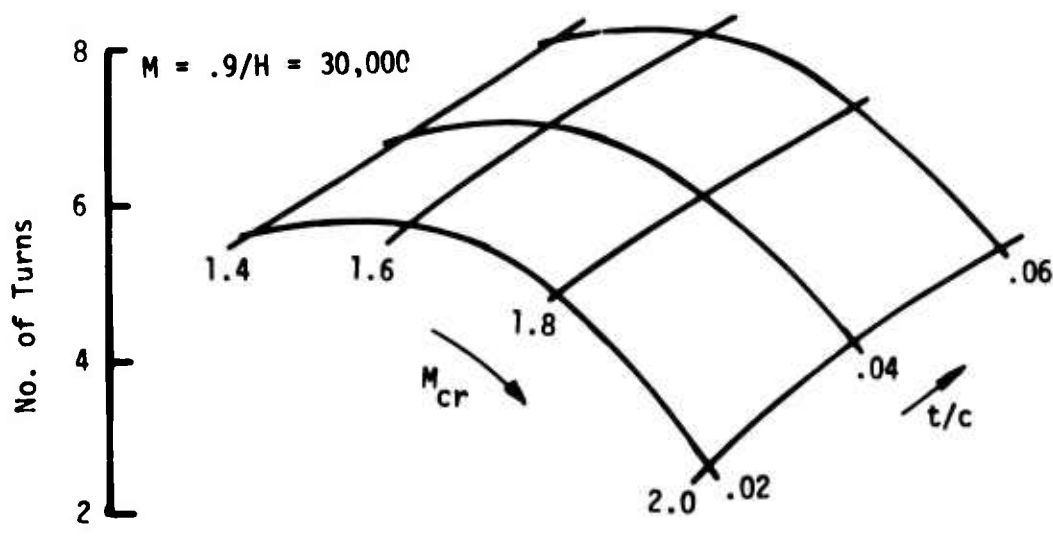
Figure 117. Arrow Persistence Versus $M_{CR}$ and t/c
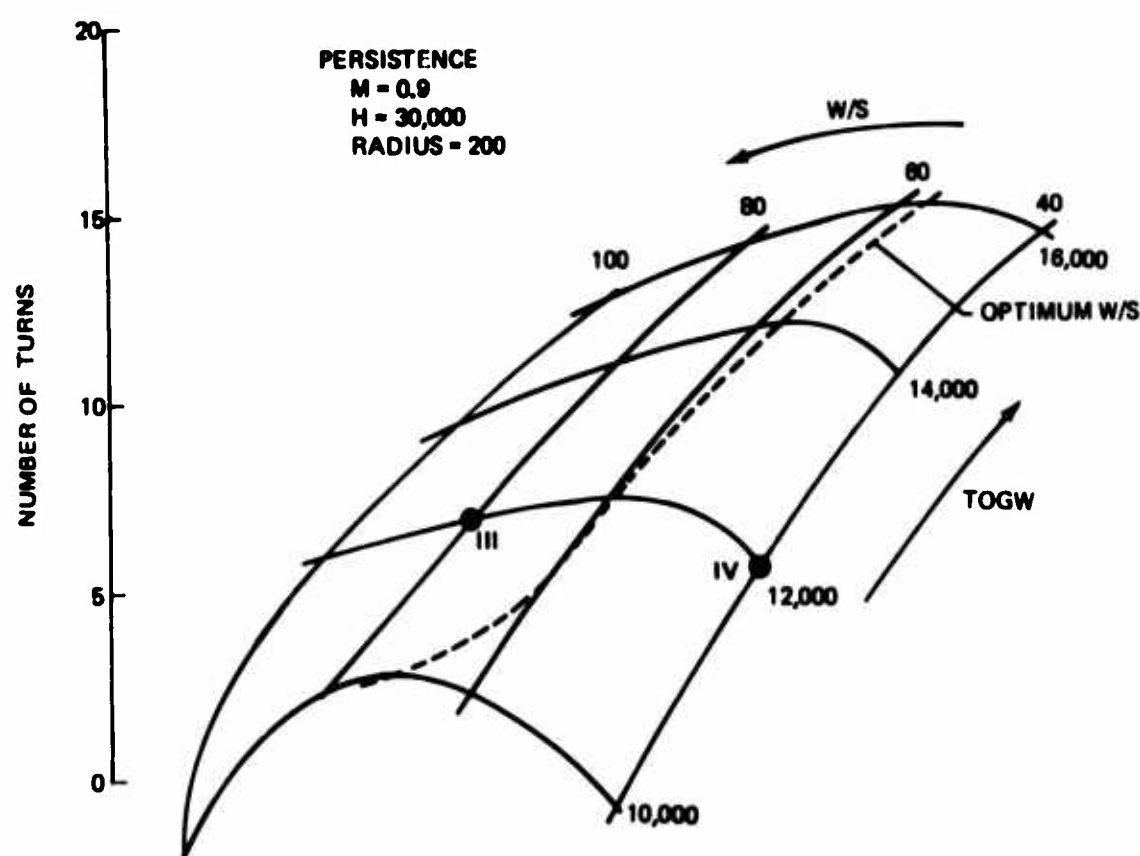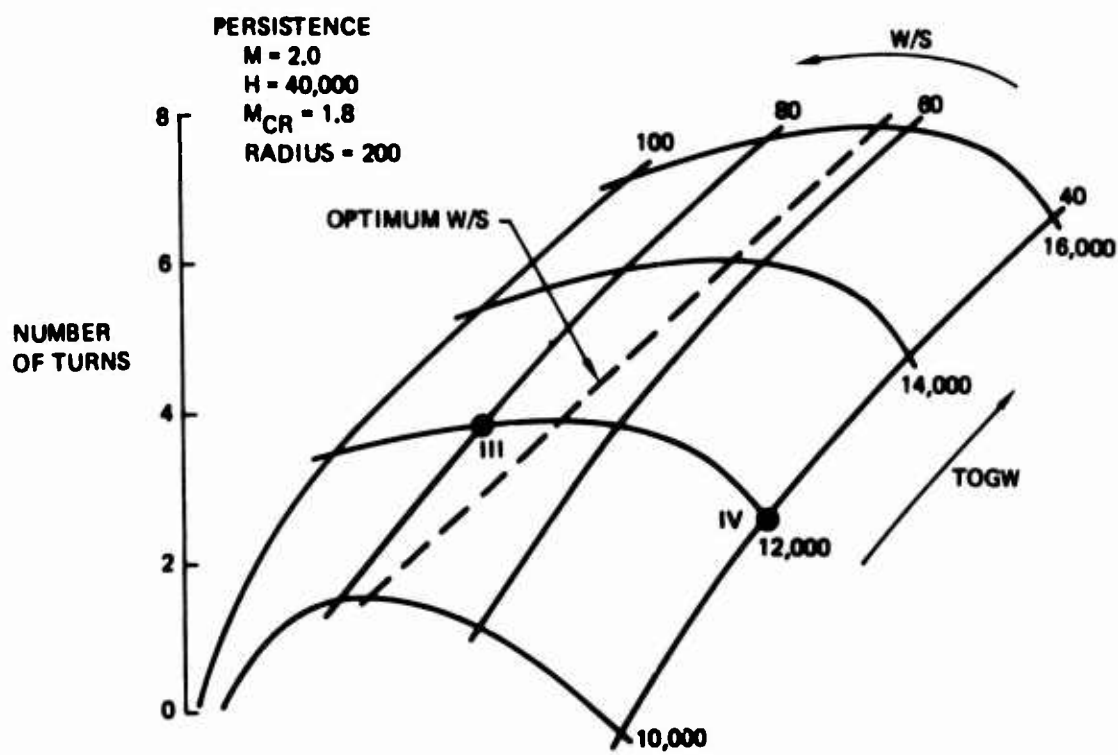
Figure 118.    Arrow Point Design Persistence Carpet

4.3    VEHICLE PARAMETRIC TRADES (Continued)

Sustained Load Factor--The third figure of merit to be examined is
sustained load factor.  The sustained load factor is calculated at an
a·erage combat weight at a 200 n. mi. radius with maximum afterburning
thrust.

The sensitivity results are shown in Figure 119 for subsonic and super-
sonic sustained load factor.  The variable with the biggest impact in
both the subsonic and supersonic cases is wing loading.  Load factor
obtains its maximum value at the lower limit of wing loading (W/S =
40 lb/ft$^2$).  Although the sensitivity is not as great, sustained load
factor is also a maximum at the lower limits of takeoff gross weight
and cruise Mach number.  Wing thickness ratio has little impact on
sustained load factor.

The results of the regression analysis are presented in Figures 120 and
121.  Figure 120 shows the effect of wing loading and takeoff gross
weight on sustained load factor for cruise Mach number equal to 1.65
and wing thickness ratio equal to .06.  These results, in general, are
the same as the sensitivity analysis results.  For the three combat
conditions shown, sustained load factor is a maximum at the lower limits
of wing loading and takeoff gross weight, (W/S = 40 and TOGW = 10,000 lbs).
Note that the impact of TOGW becomes more pronounced at the higher combat
Mach numbers.

Figure 121 presents the influence of cruise Mach number and wing thickness
ratio on sustained load factor for a takeoff gross weight of 12,000 lbs.
and a wing loading of 40 lb/ft$^2$.  Cruise Mach number is the dominant
variable with the maximum load factor at the minimum value of cruise Mach
number.

Wing thickness ratio has a slight impact on subsonic load factor, but
none at all on supersonic load factor.

194

## 4.3   VEHICLE PARAMETRIC TRADES (Continued)

The point design wing loading, thrust to weight carpets of sustained
load factor are shown in Figure 122.  Once again, the carpets from the
sizing and performance program give results similar to those from the
regression equations.

If sustained load factor were the single figure of merit, the resulting
design is substantially different from a radius or persistence optimized
and it has the following characteristics:

o   TOGW    -10,000 lbs.

o   W/S     - 40 lb/ft$^2$

o   $M_{cr}$   - 1.4

o   t/c     - .06

TOGW, W/S and $M_{cr}$ are all at their lower limits whereas t/c is at its
upper limit.  Since the lower limit of TOGW which maximizes load factor
minimizes radius and combat persistence, a trade between these performance
parameters will have to be made in the selection of the final TOGW.
A similar choice will also have to be made for W/S.
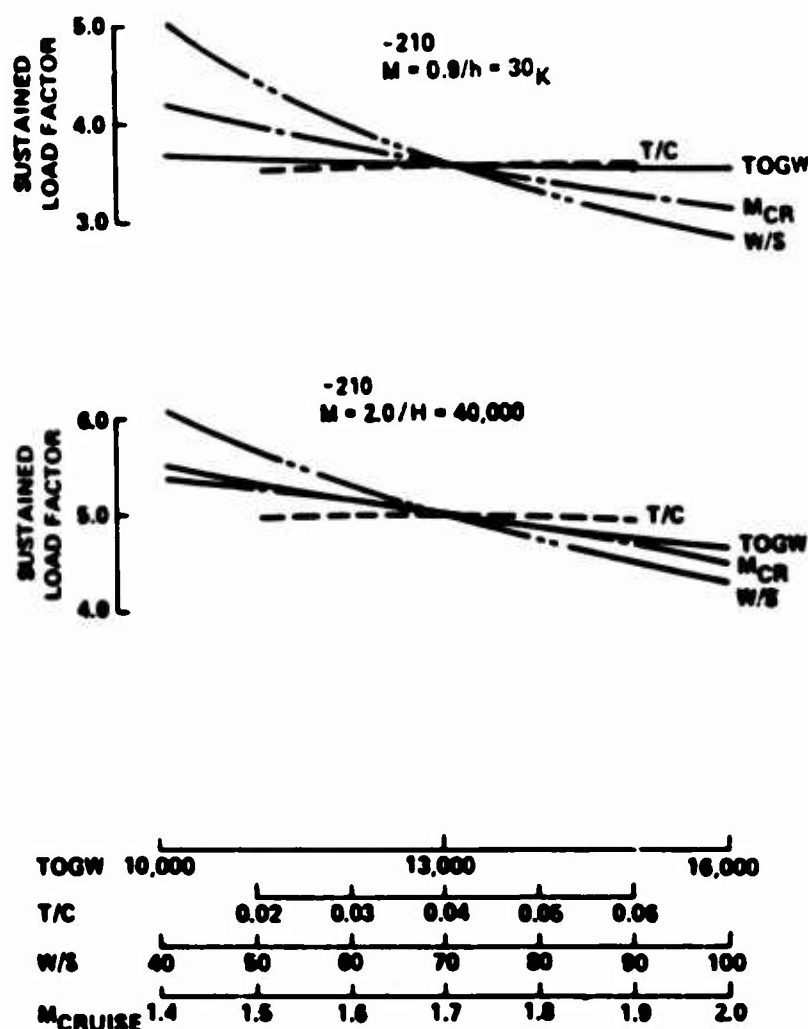
Figure 119. Arrow Sustained Load Factor Sensitivity Analysis
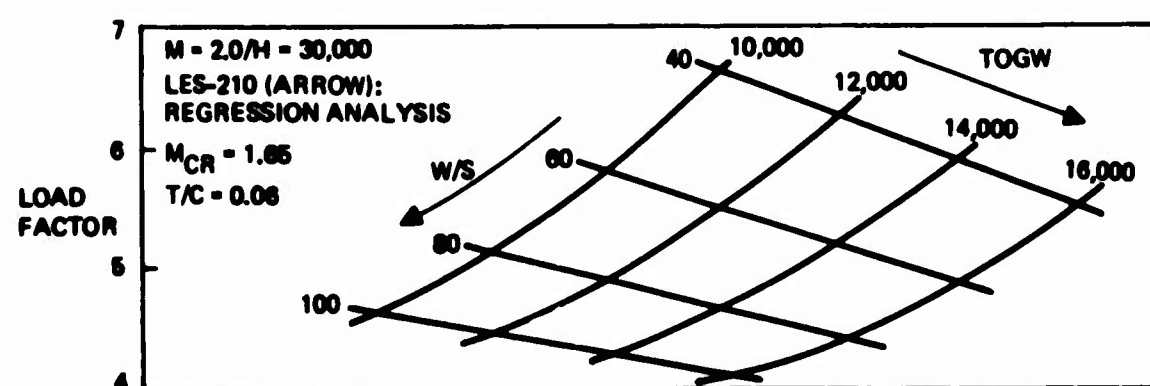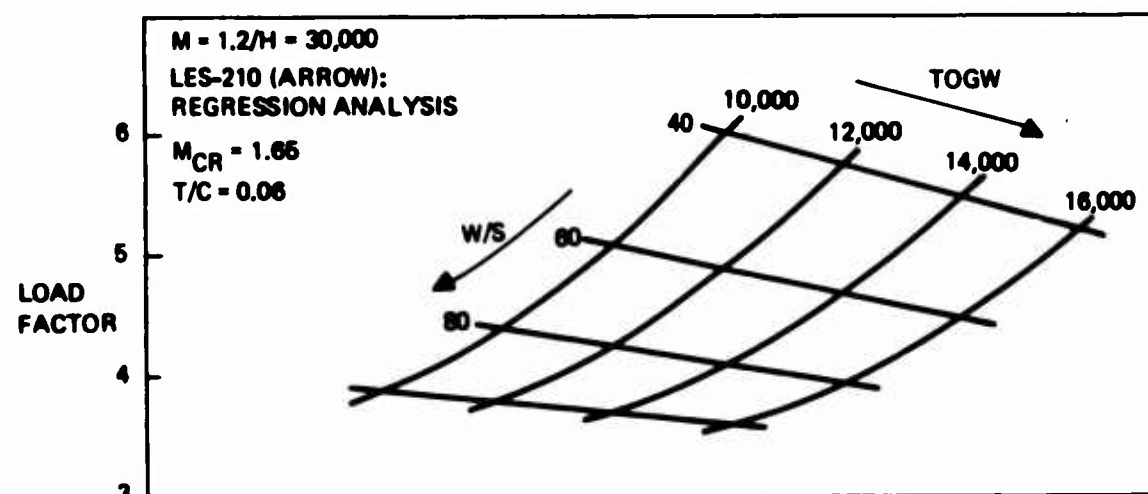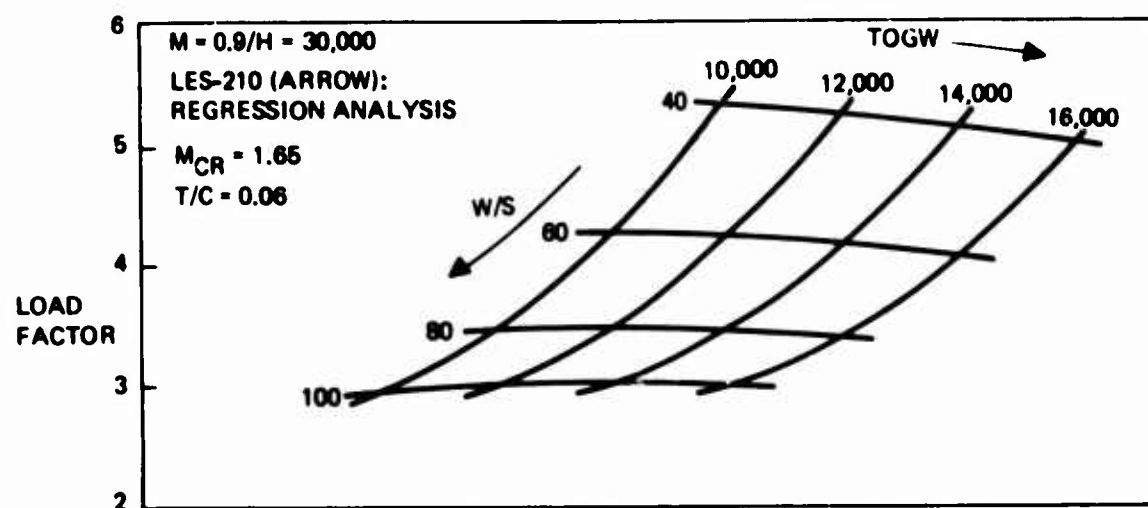
*Figure 120. Arrow Sustained Load Factor Versus TOGW and W/S*
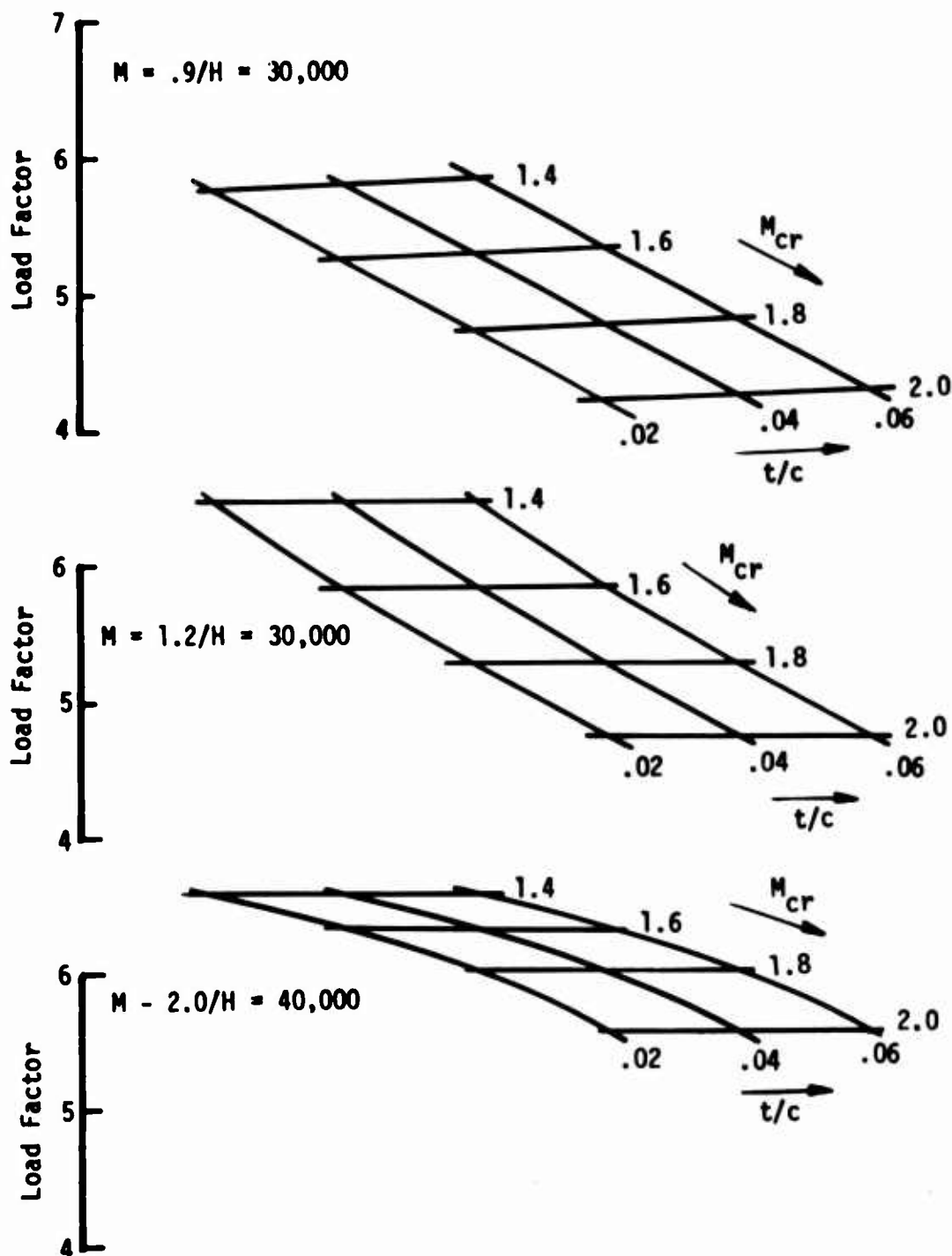
Figure 121. Arrow Sustained Load Factor Versus $M_{CR}$ and t/c
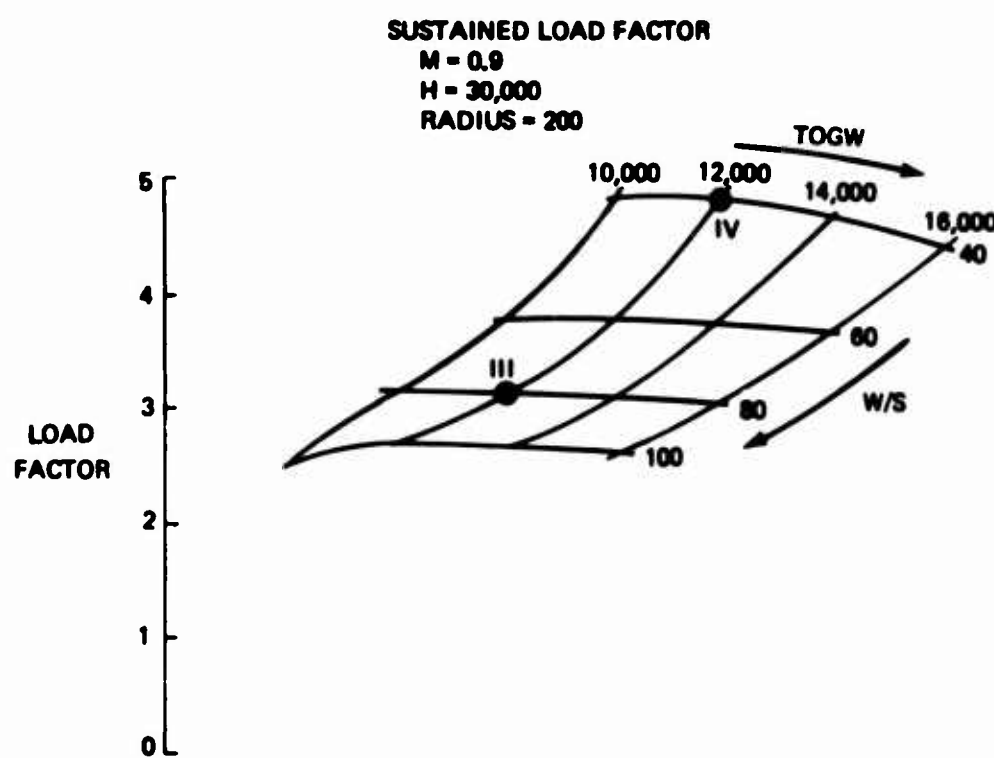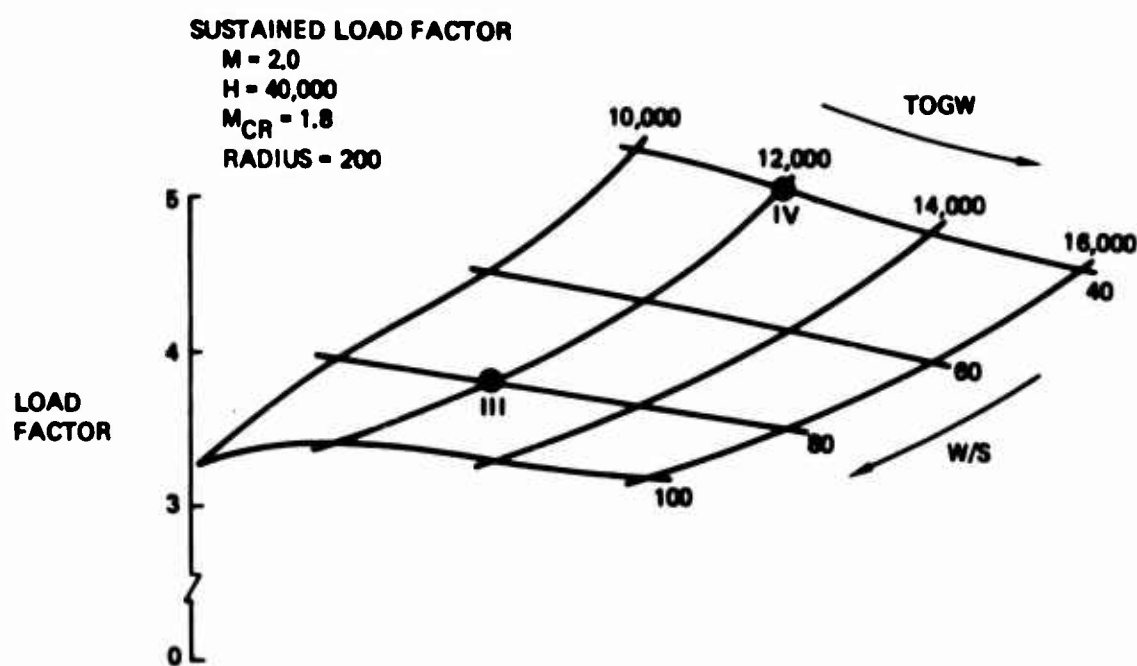
Figure 122.    Arrow Point Design Sustained Load Factor Carpets

## 5.0 AERODYNAMIC CONFIGURATION STUDIES

Development of the current LES arrow wing configuration started with an analysis of two separate concepts, the -202 canard configuration and the -210 arrow wing configuration. The -202 canard configuration shown in Figure 123 was oriented toward combat maneuverability with supersonic cruise capability. The -210 arrow wing configuration shown in Figure 124 was oriented toward supersonic cruise efficiency without emphasizing combat capability.

Preliminary design work, operational considerations and performance analysis based on parametric design studies with these baseline configurations led to the selection of the arrow wing concept for detailed study and analysis.

The following is a brief description of the two original concepts, the -202 canard configuration and the -210 arrow wing configuration.

### 5.1 CANARD CONFIGURATION

The first iteration analysis of the canard configuration (-202) was conducted to compare with the arrow wing concept and to identify potential areas of improvement. Initial analysis indicated a longer body would provide a major improvement by reducing the aft closure slopes. Further analysis on wing design, canard location, incidence and size could lead to improved drag-due-to-lift and trim characteristics.

### CONFIGURATION REPRESENTATION - BODY OPTIMIZATION

The far-field wave drag computer representation of the canard configuration is shown in Figure 125. The planform goemetry used is shown in Figure 126. The airfoil section thickness distribution used for the wing, canard and fin is based on the MAR 56 Airfoil section, see Figure 127. The body representation for the supersonic design program was obtained by measuring the cross-sectional areas from the configuration
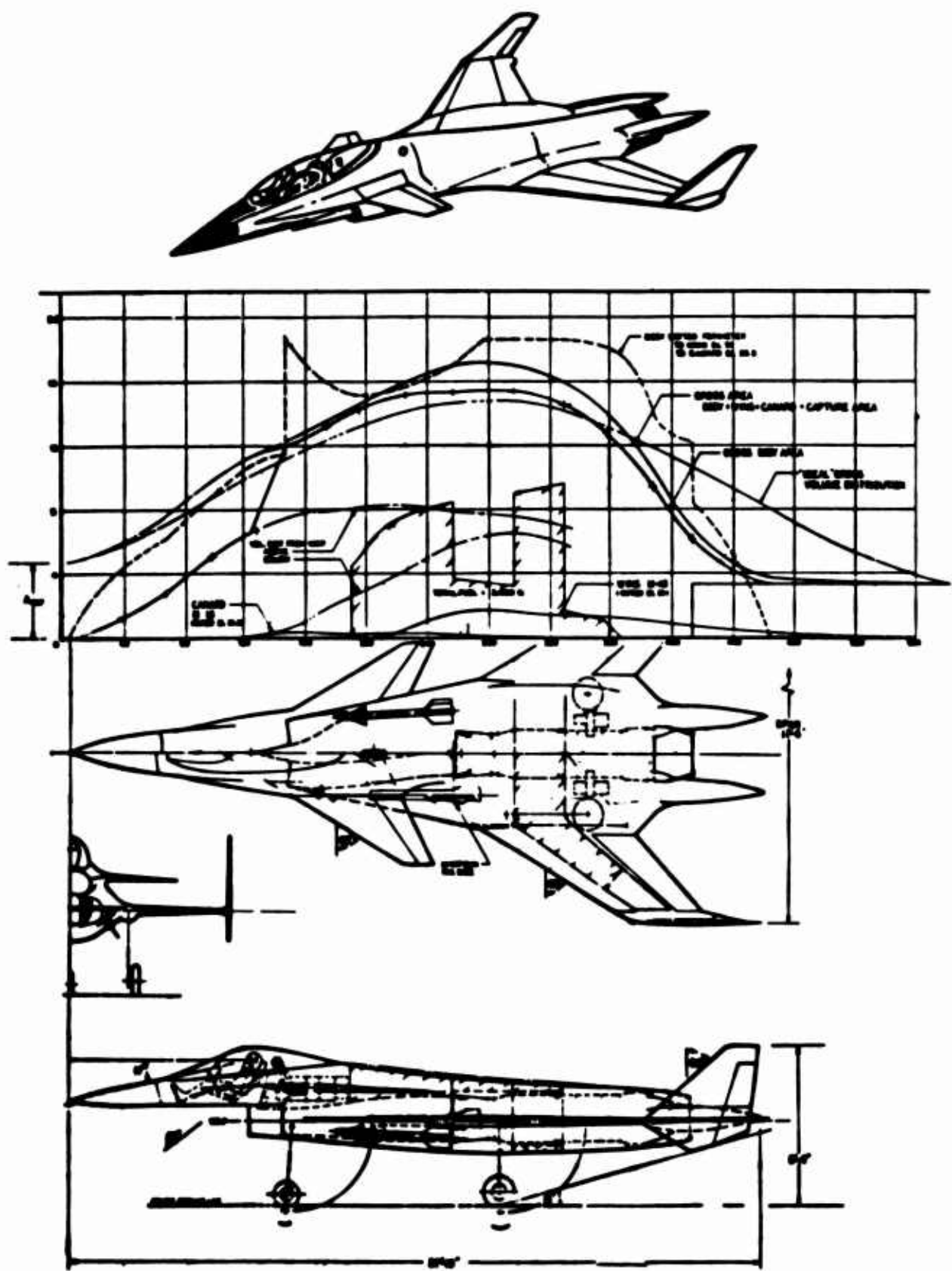
Figure 123. Canard Configuration – Model 985-202

202
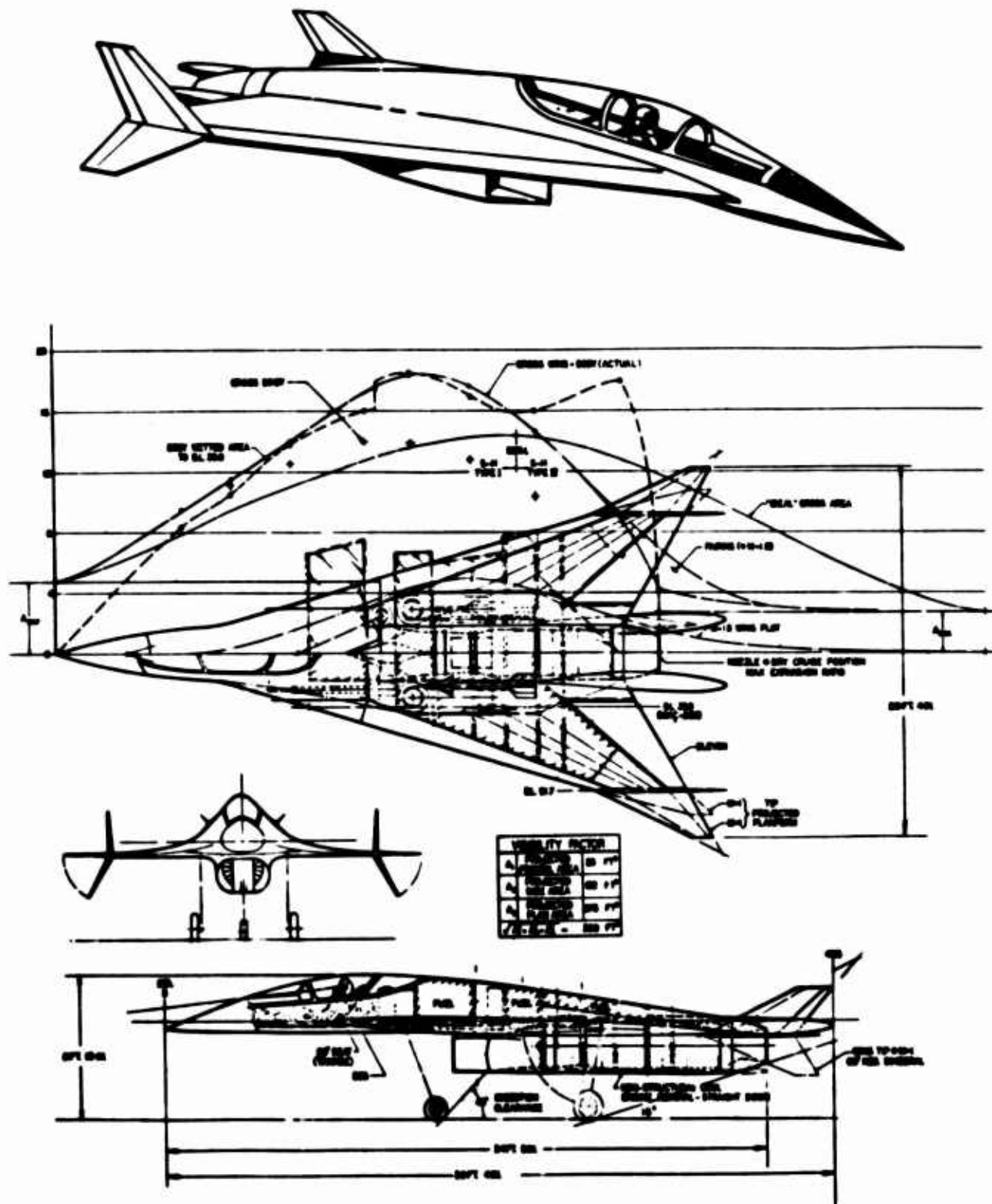
**Figure 124.    Arrow Wing Configuration — Model 985-210**

**FRONT VIEW**
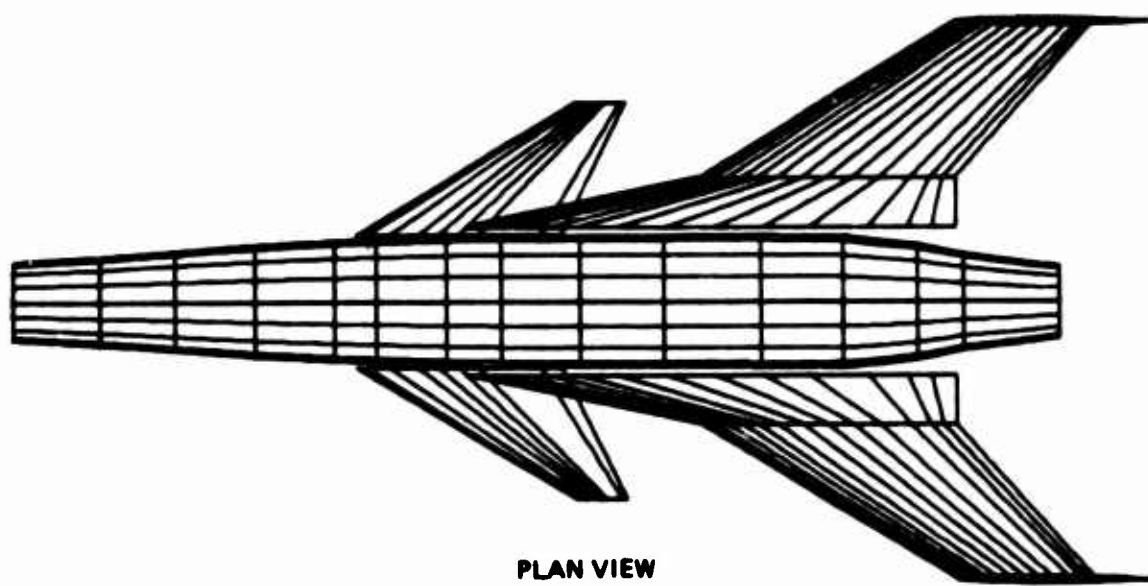
**PLAN VIEW**
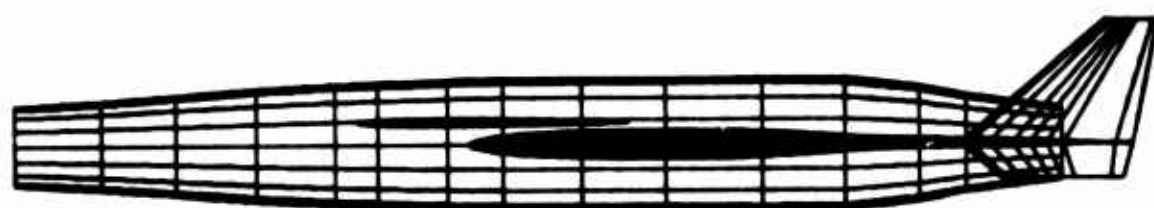
**SIDE VIEW**

*Figure 125.     Far Field Wave Drag Computer Representation of – 202 Configuration*
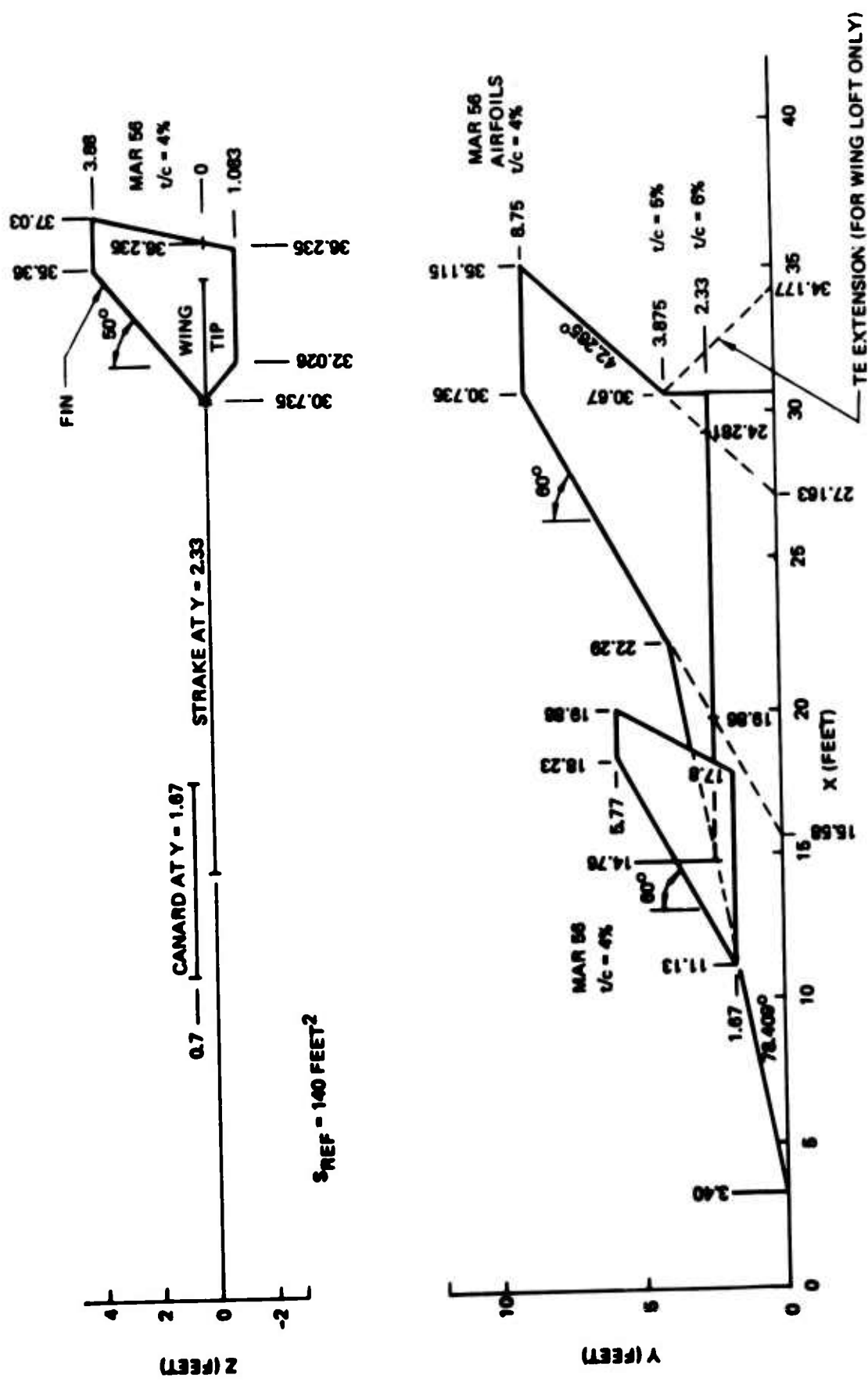
Figure 126. Canard Configuration — Reference Planform Geometry

205

5.1 CANARD CONFIGURATION (Continued)

drawing. The resulting body area plot was input as circular sections.
Preliminary work had indicated that including the inlet streamtube area
would best represent the configuration for calculation of the far-
field wave drag. The body was optimized at Mach 1.8, in the presence
of the wing, canard and fins. Two constraint points, one at the cock-
pit and one at the aft spar, resulted in the optimum area distribution
shown in Figure 128. The rapid area reduction required between the
aftbody constraint point and the nozzle exit contributes approximately
75 percent of the body wave drag as shown in Figure 129. To get a
reasonable rate of area closure, a combination of things could be done;
increase the nozzle fineness ratio, increase the afterbody length and
if possible, reduce the aftbody constraint area.

WING DESIGN

A preliminary wing design was performed using the defined wing and
canard planforms. The wing camber and twist were designed for a $C_L$ =
0.20 at Mach 1.8. The pressure limiting feature was employed,
$(C_{P_{Limit}} = 0.7C_{P_{Vac}})$. The influence of the canard on the wing was taken
into account by running the body and canard at $\alpha$ = 1° with the wing
camber slopes set equal to zero. This generates the body and canard
influences in the plane of the wing for the wing design module. The
resulting curve of optimum drag-due-to-lift factor ($K_E = C_{Di}/C_L^2$) versus
zero lift pitching moment ($C_{Mo}$) for a 6 term loading case is shown in
Figure 130. No positive $C_{Mo}$ constraint was imposed because the minimum
drag-due-to-lift occurred at a relatively high positive $C_{Mo}$ value of
0.113. A first estimate for the drag polar shape used the camber lines
directly as generated by the wing design module. Normally the camber
lines from the wing design module are plotted and smoothed before the
actual geometric wing lofting is done. The wing twist was revised to
smooth out variations caused by the wing strake, canard influence, and
body upwash. Twist inboard of the side of body is not used. Figure 131

207
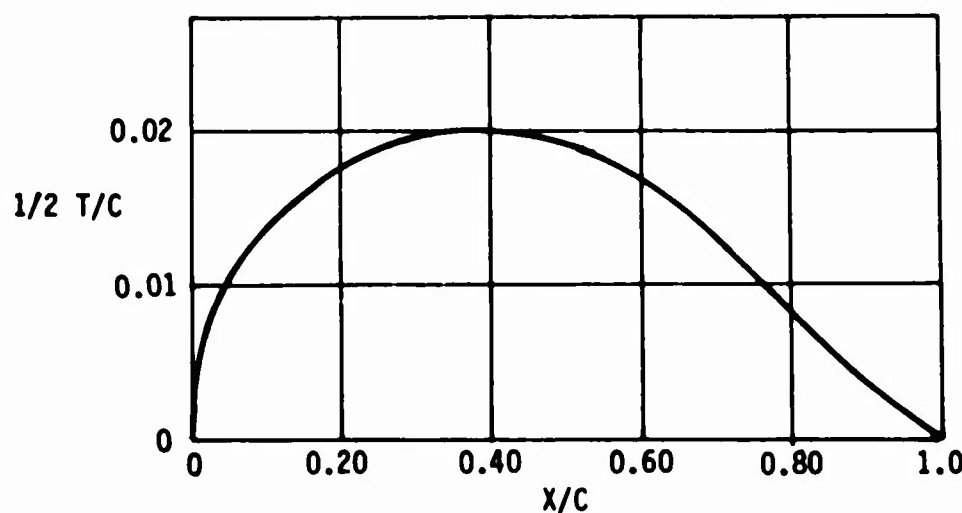
Figure 127. Airfoil Thickness Distribution
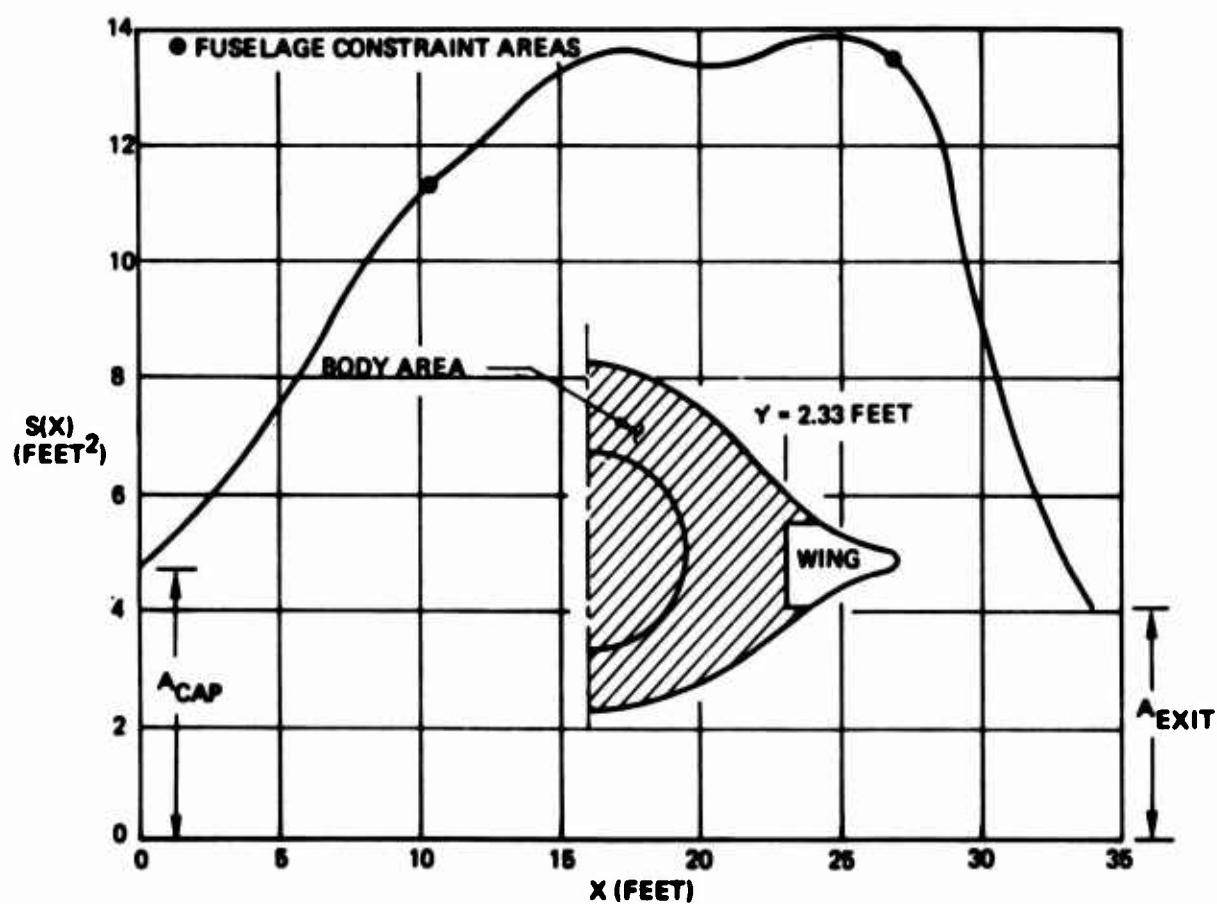


Figure 128. Canard Configuration — Body Area Distribution

206
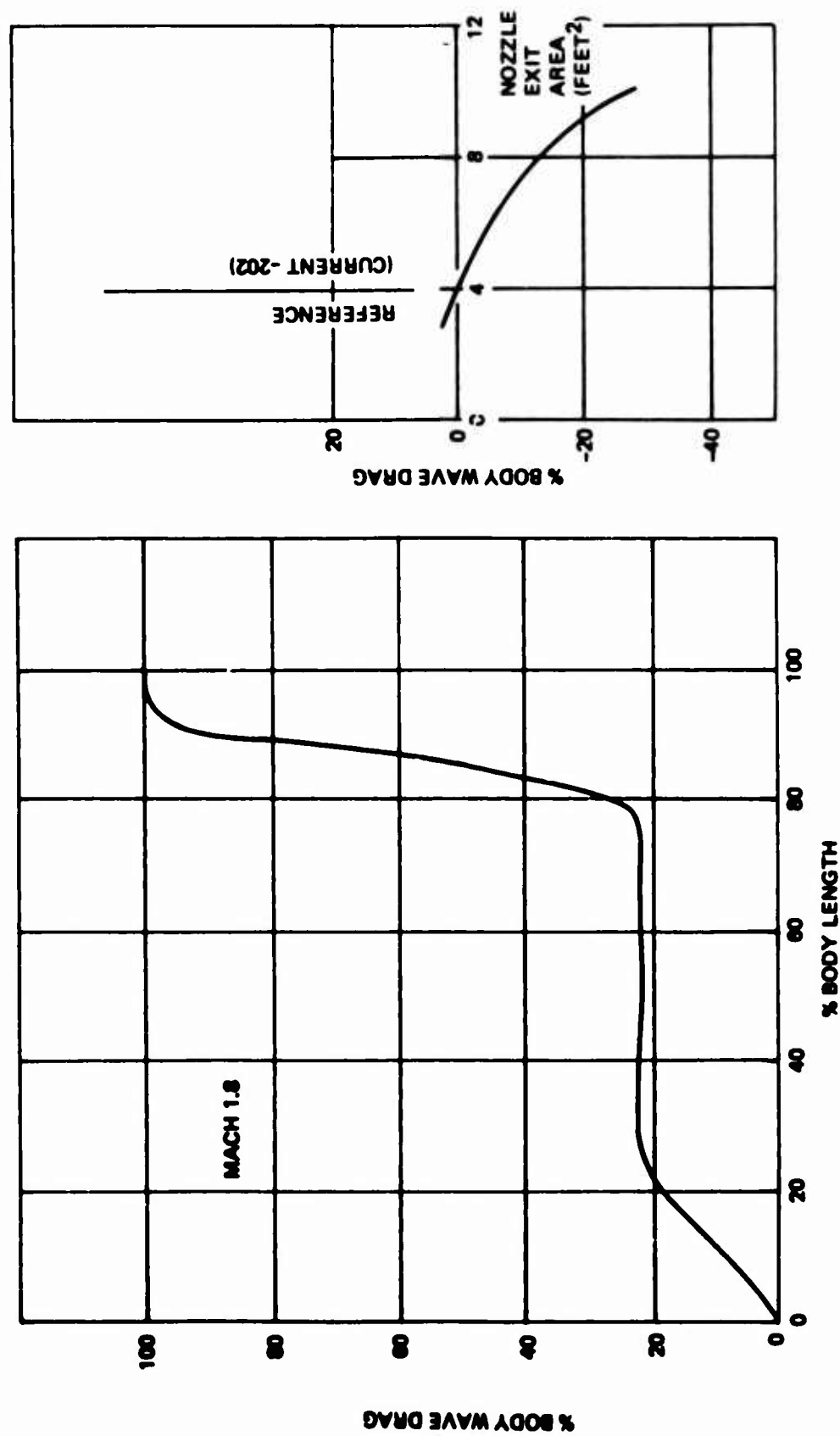
Figure 129. Canard Configuration – Body Wave Drag Distribution
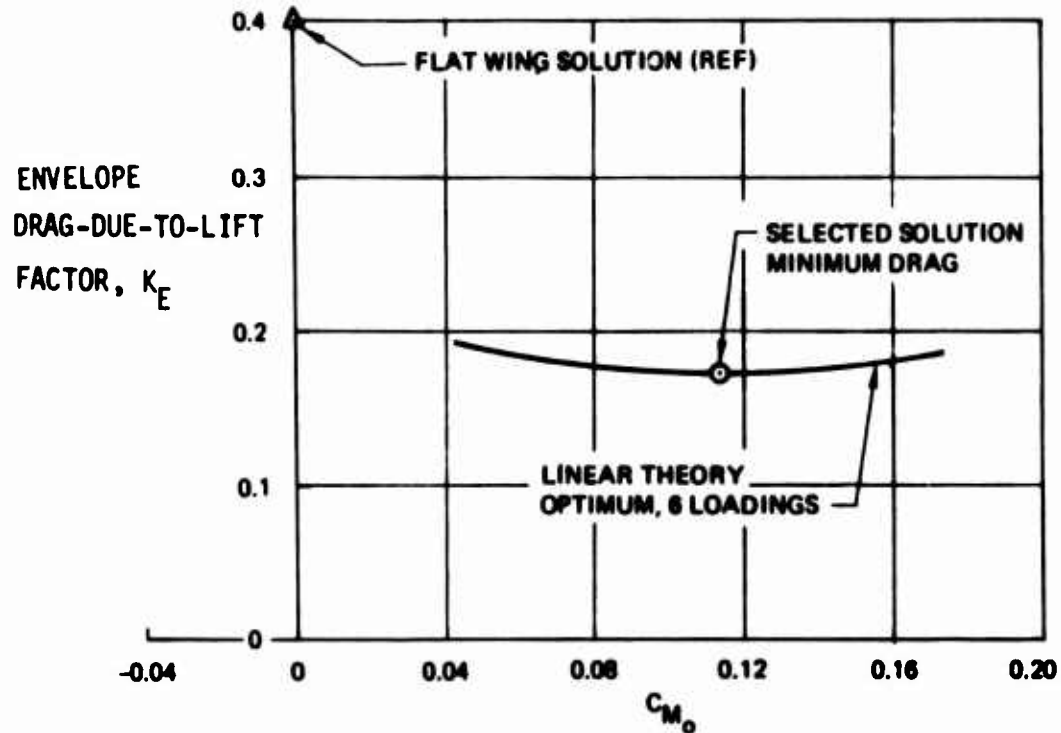
Figure 130.    Canard Configuration — Wing Design Solution

```
GEOM NEW
-202  NO BODY CAMBER  OPTIMIZED BODY INCLUDING STREAMTUBE AREA
  1 -1 -1  0   1  1  0  9 17  1  9 15                                    2 10  1 19CODE
                                                                              REF
140.     8.523  24.08                                                         X1C
0.       .2     .6     2.     5.     10.    16.    22.    30.    40.           X1C
50.      60.    70.    82.    90.    95.    100.                              X1C
14.760  2.33   0.    19.91                                                    W1
22.292  5.875  0.     8.378                                                   W2
50.735  8.75   0.     4.38                                                    W3
0.       .290   .516   .968  1.530  2.073  2.454  2.703  2.911  3.0           W1 T/C
2.888   2.544  1.969  1.094   .540   .253   .041                             W1 T/C
0.       .241   .630   .806  1.275  1.727  2.045  2.252  2.425  2.5           W2 T/C
2.406   2.120  1.660   .911   .450   .211   .034                             W2 T/C
0.       .193   .344   .665  1.020  1.382  1.636  1.802  1.941  2.0           W3 T/C
1.925   1.696  1.313   .729   .360   .169   .027                             W3 T/C
0.      2.75   5.17   7.75  10.38  11.8   14.08  15.88  18.38  21.08          FUS X
24.25   27.0   29.41  30.92  34.0                                             FUS X
                                                                              FUS Z
                                                                              FUS Z
4.75    6.05   7.65   9.70  11.30  11.85  12.87  13.47  13.55  13.38          OPT BODY
13.85   13.50  10.25   7.25   4.0                                             OPT BODY
50.735  8.75   0.     5.5   35.36  8.75   3.88   1.67                         FIN 1
 .       .6    5.    16.    30.    40.    50.    60.    90.    100.           FIN X/C
0.       .344  1.020  1.636  1.941  2.00   1.925  1.696   .360   .027         FIN T/C
50.735  8.75   0.     5.5   32.026  8.75  -1.083 3.917                        FIN 2
0.       .6    5.    16.    30.    40.    50.    60.    90.    100.           FIN X/C
0.       .344  1.020  1.636  1.941  2.00   1.925  1.696   .360   .027         FIN T/C
11.13   2.10    .70   6.67  18.23   6.20   0.7    1.63                        CAN LOG
0.       .6    5.    16.    30.    40.    50.    60.    90.    100.           CAN X/C
0.       .344  1.020  1.636  1.941  2.00   1.925  1.696   .360   .027         CAN T/C
FFWD
-202 CONFIGURATION
1.      1.     0.     1.     1.
003     1.8    50.    36.
FND
NFWD
-202 WING THICKNESS PRESSURES FOR WING DESIGN PROGRAM
0.      0.
0.      1.8    0.     2.                                                      INPUTS
7.10   -1.    -1.

END
ANLZ
-202 CONFIGURATION
1.      0.     1.     0.
12.     12.    1.     0.
0.      12.    3.    -1.     0.    -1.
7.10    0.     0.     0.     0.
1.8            1.
   .000  9.000 10.000 20.000 30.000 40.000 50.000 60.000 70.000 80.000       X/C
 90.000100.000                                                               X/C
   .000 10.000 15.000 20.000 30.000 40.000 50.000 60.000 70.000 80.000       2V/A
 90.000100.000                                                               2V/B
   .000  -.024 -2.128 -5.533 -9.537-13.837-18.179-22.430-26.309-29.704       0.
 -32.560-34.784
   .000   .063  -.416 -2.623 -5.397 -8.290-11.093-13.530-15.443-16.767       .10
 -17.339-17.078
   .000   .843  1.107  -.223 -2.381 -4.952 -7.480 -9.819-11.789-13.291       .15
 -14.240-14.540
   .000  1.387  2.367  2.494  1.139  -.748 -2.070 -4.975 -7.001 -8.873       .20
 -10.505-11.831
   .000  1.221  2.334  3.207  3.182  2.602  1.722   .611  -.582 -1.801       .30
  -3.012 -4.189
   .000  1.298  2.347  3.806  4.199  4.288  4.180  3.933  3.576  3.131       .40
  2.611  2.013
   .000   .557  1.039  1.849  2.358  2.699  2.938  3.067  3.127  3.111       .50
  3.028  2.912
   .000   .114   .449   .975  1.247  1.387  1.455  1.433  1.404  1.329       .60
  1.234  1.112
   .000  -.032   .415   .876  1.197  1.464  1.672  1.832  1.952  2.047       .70
  2.116  2.173
   .000   .203   .372   .622   .630   .522   .341   .107  -.148  -.451       .80
  -.746 -1.074
   .000  -.041  -.019   .420   .475   .427   .351   .156  -.083  -.400       .90
  -.806 -1.299
   .000  -.269  -.210   .499  1.299  2.121  2.956  3.783  4.594  5.382       1.0
  6.151  6.877
   .000 10.000 15.000 20.000 30.000 40.000 50.000 60.000 70.000 80.000       2V/A
 90.000100.000                                                               2V/B
-7.48   0.     0.     0.     0.     .203   0.    -.923   .495   -.365         DEL TWIST
0.      4.784                                                                 DEL TWIST
-2.     0.     2.                                                             CA ALPHA
 .20
FND
```

**Figure 131.    Wing Thickness and Twist Distributions — Canard Configuration**

210

## 5.1 CANARD CONFIGURATION (Continued)

gives the computer listing used to estimate the -202 wave drag and drag-due-to-lift. For the drag-due-to-lift analysis, the body included the streamtube area, a side of body definition of Y = 2.1 ft. and the canard was at 0° relative to the freestream. Note that the wing twist table in the computer listing is only the difference required to smooth out the basic twist as defined via the camber lines. Preliminary twist and maximum thickness distributions suitable for a preliminary wing lift are shown in Figure 132. The lift, drag and moment characteristics at Mach 1.8 are shown in Figure 133. Also included is the effect of $\pm2°$ canard incidence. No trim drag, i.e., flap deflection data, or high angle of attack data with the pressure limiting feature were run.

## DRAG CHARACTERISTICS

Detailed drag characteristics for the -202 configuration were not made. The non-lifting drag estimates shown in Figure 134 are only preliminary in nature and only suitable for parametric type comparisons. The estimates for the -210 arrow wing configuration were made on the same basis. The preliminary Mach 1.8 drag polar for the -202 canard configuration is shown in Figure 135. The drag-due-to-lift estimate is taken from Figure 133 with the canard incidence at zero. Drag estimates above $C_L = 0.2$, are not shown because high angle of attack data with the pressure limiting feature were not run during the preliminary evaluations. Trim drag increments are not included. Canard incidence, size, camber and twist were not considered in this comparison and are potential items to be investigated for improvement of the drag-due-to-lift characteristics.

## 5.2 ARROW WING CONFIGURATION

A first iteration analysis of the arrow wing configuration (-210) was conducted to compare with the canard configuration and to identify
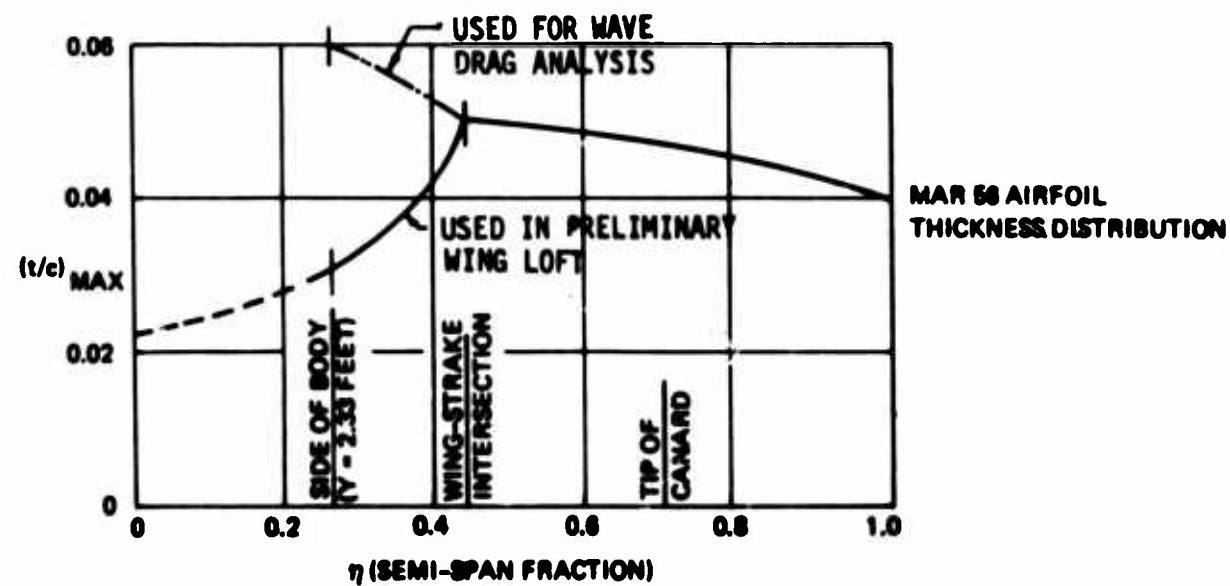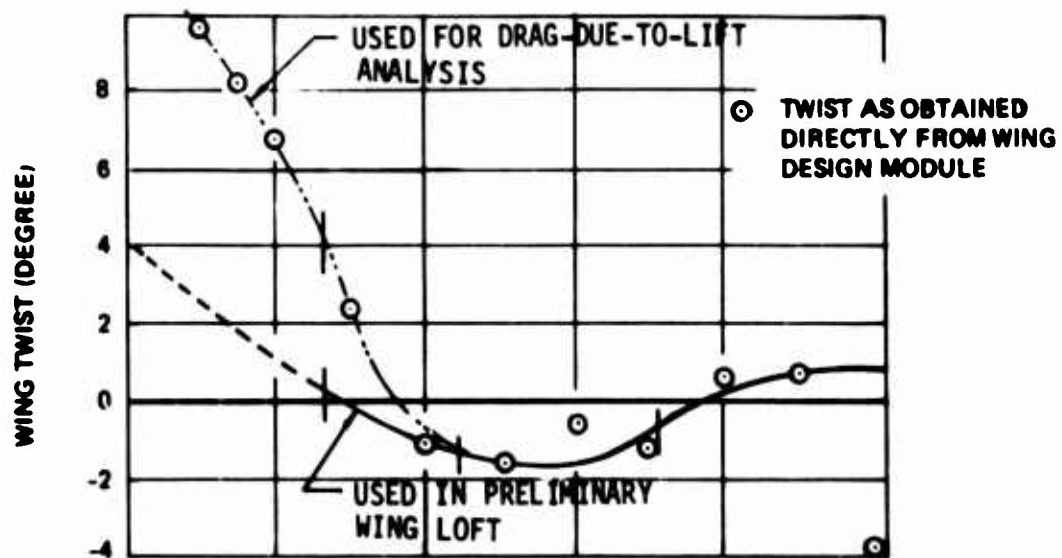
Figure 132. Wing Thickness and Twist Distributions — Canard Configuration
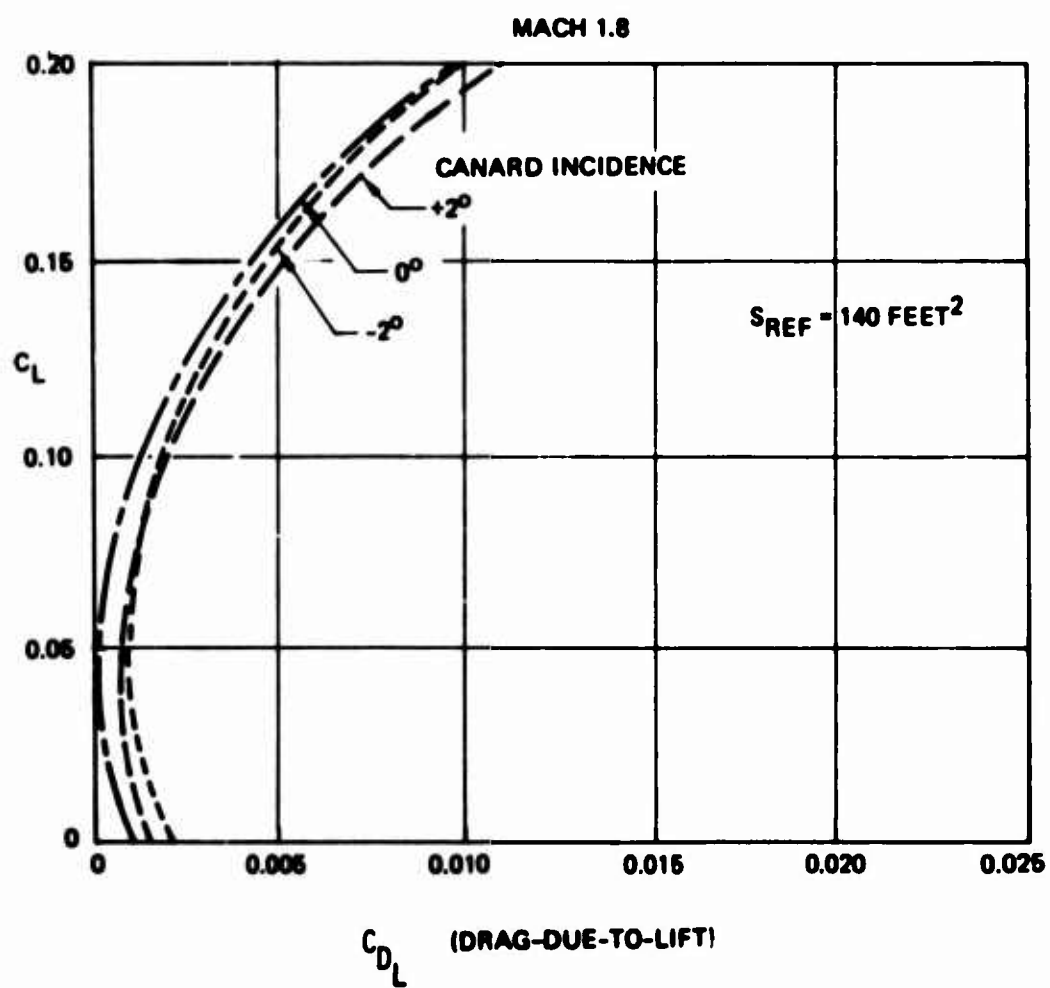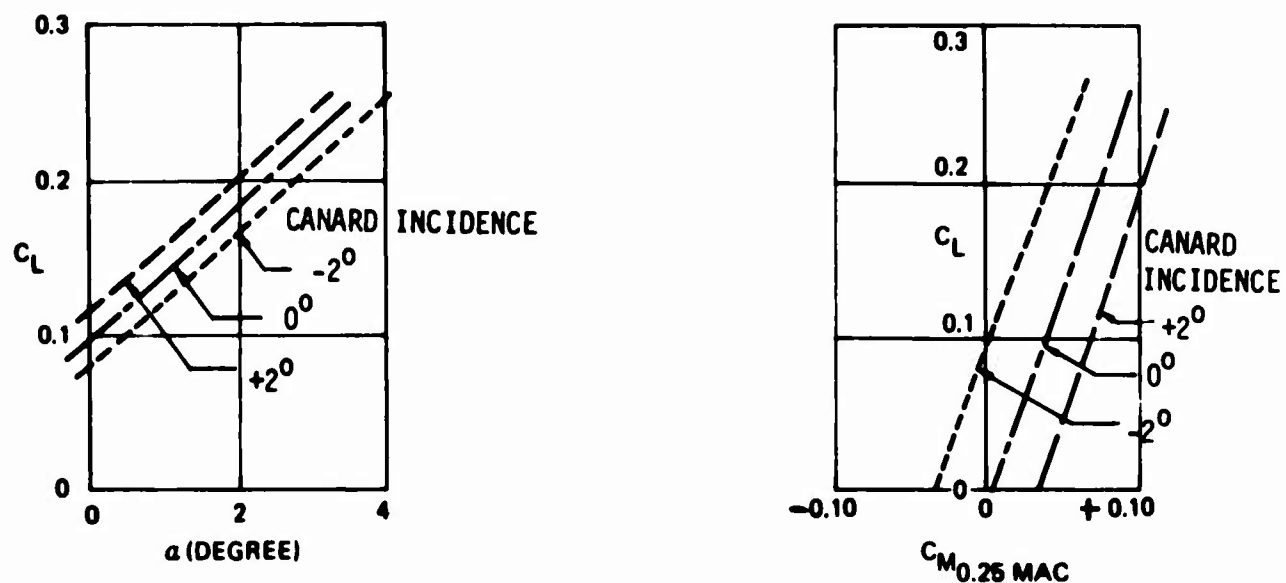
Figure 133.    Canard Configuration — Lift, Drag and Moment Characteristics, M = 1.8

Mach 1.8, 50,000 feet

| Drag component | Canard -202 D/q (Feet$^2$) |
|---|---|
| Wave drag | 2.814 |
| Skin friction | 1.532 |
| Excrescence | 0.224 |
| Inlet diverter | — |
| Misc. items | 0.098 |
| Total D/q | 4.668 |

Figure 134.    Canard Configuration – Non-Lifting Drag Comparison
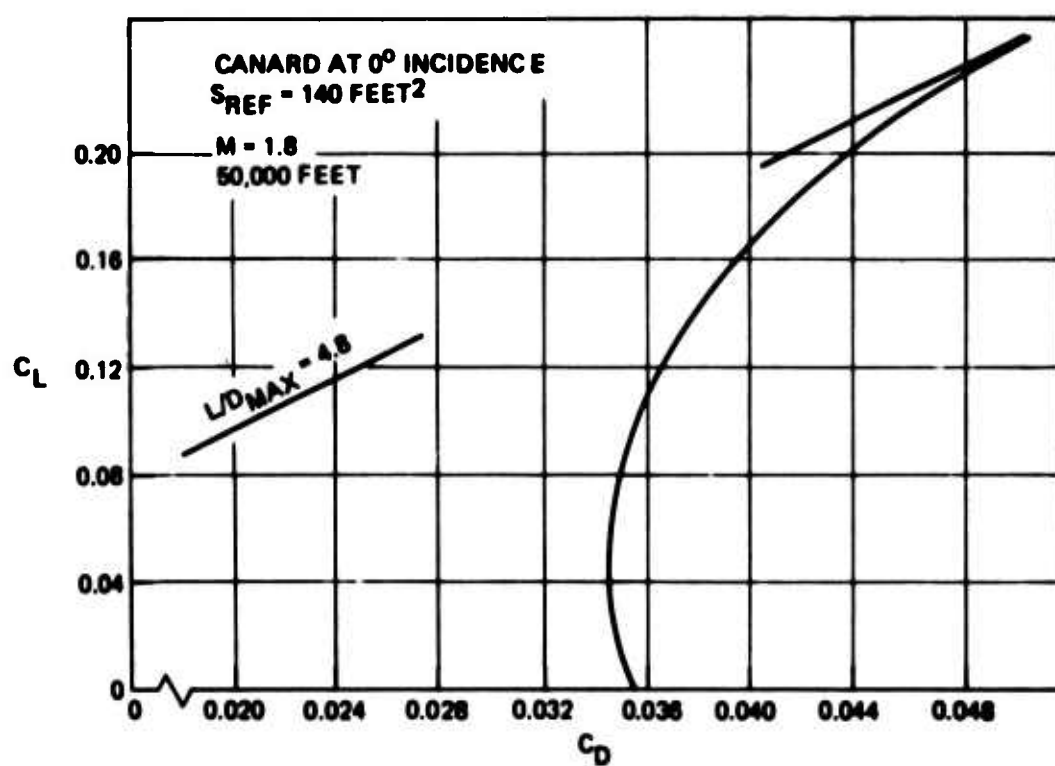


Figure 135.    Canard Configuration – Drag Characteristics M = 1.8, 50,000 Feet

5.2  ARROW WING CONFIGURATION (Continued)

potential areas of improvement.  Subsequent analysis was conducted on
a refined design (-212) which served as a basis for the final perform-
ance representing the LES -213 concept capability.  This section pre-
sents -210 estimates.

CONFIGURATION REPRESENTATION - BODY OPTIMIZATION

The far-field wave drag computer representation on the arrow wing con-
figuration was similar to that shown for the canard configuration.  The
planform goemetry used for the -210 analysis is shown in Figure 136.
The MAR 56 airfoil section thickness distribution used for the wing is
the same one used on the canard configuration (Figure 127).  The body
representation for the supersonic design program was obtained by measur-
ing the cross-sectional areas from the configuration drawing.  The
resulting body area plot was input as circular sections.  Preliminary
work had indicated that including the inlet streamtube area would best
represent the configuration for calculation of the far-field wave drag.
The body was optimized at Mach 1.8, in the presence of the wing and fins.
Two constraint points, one at the cockpit and one at the aft spar engine
area resulted in the optimum area distribution shown in Figure 137.  The
rapid area reduction required between the aft body constraint point and
the nozzle exit, contributes approximately 65 percent of the body wave
drag as shown in Figure 138 as compared to approximately 75 percent on
the canard configuration.  As with the canard concept, to get a reason-
able rate of aft body closure, a combination of things could be done;
increase the nozzle fineness ratio, increase the afterbody length and if
possible, reduce the aft body constraint area.

WING DESIGN

The wing planform shown in Figure 136 is based on the SCAT 15.  The wing
design solution was done on a planform that did not include the wing

215
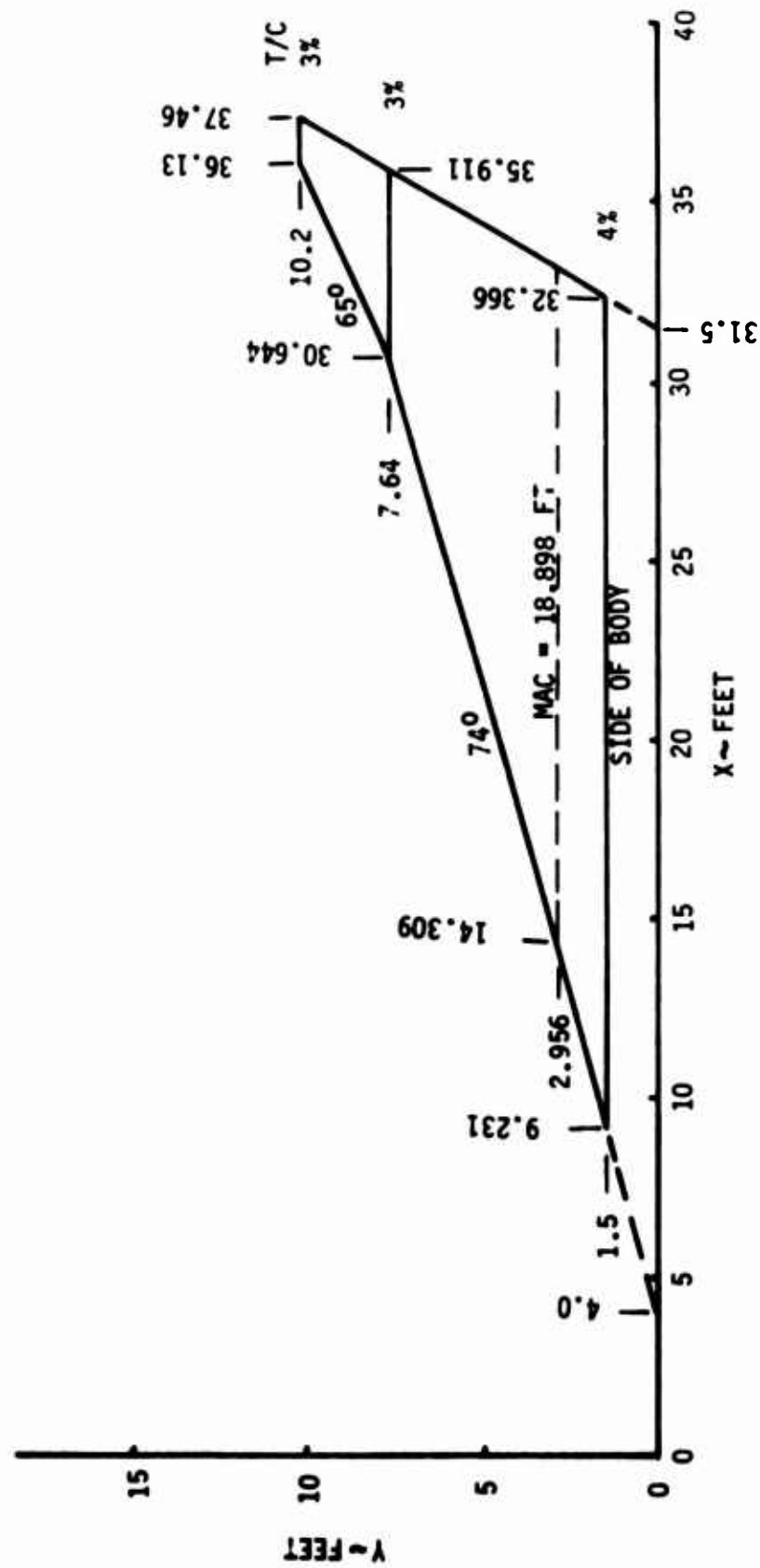
Figure 136. Arrow Configuration — Reference Planform Geometry

216
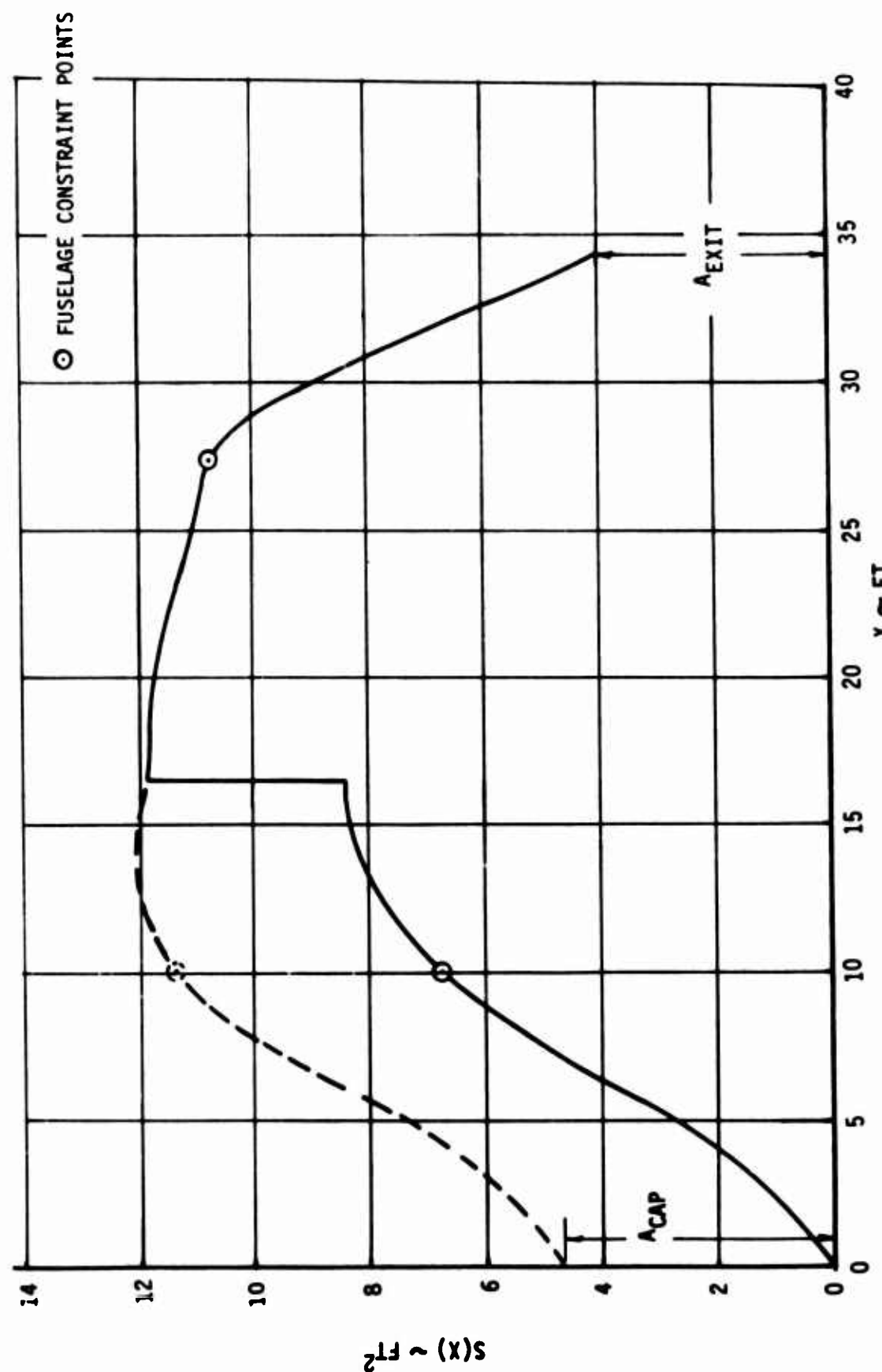
Figure 137. Arrow Configuration — Body Area Distribution
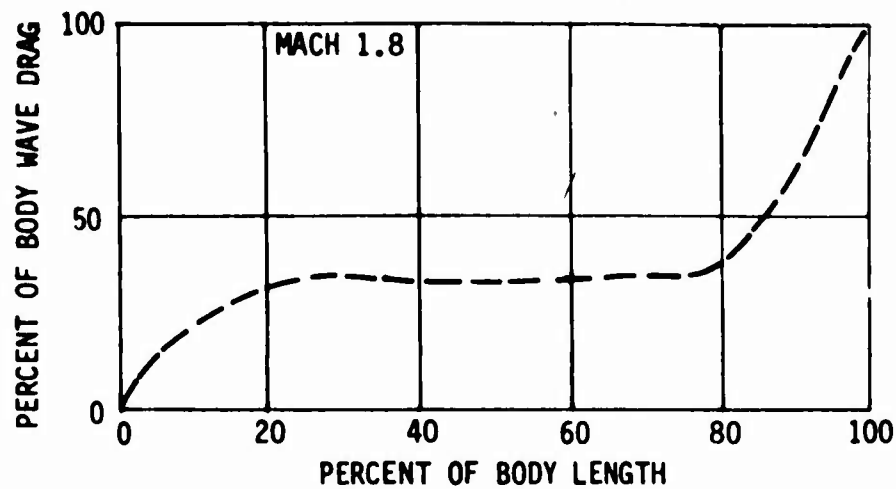
Figure 138. Arrow Configuration – Body Wave Drag Distribution

WING ONLY DESIGN SOLUTION
MACH 1.8, $C_L$ = 0.10, $C_{M_o}$ = 0.02

$S_{REF}$ = 250 $FT^2$

C = MAC = 18.9 FT

MOMENT REFERENCE = .5 MAC = 23.76 FT
WING TIPS DEFLECTED DOWN (90°)
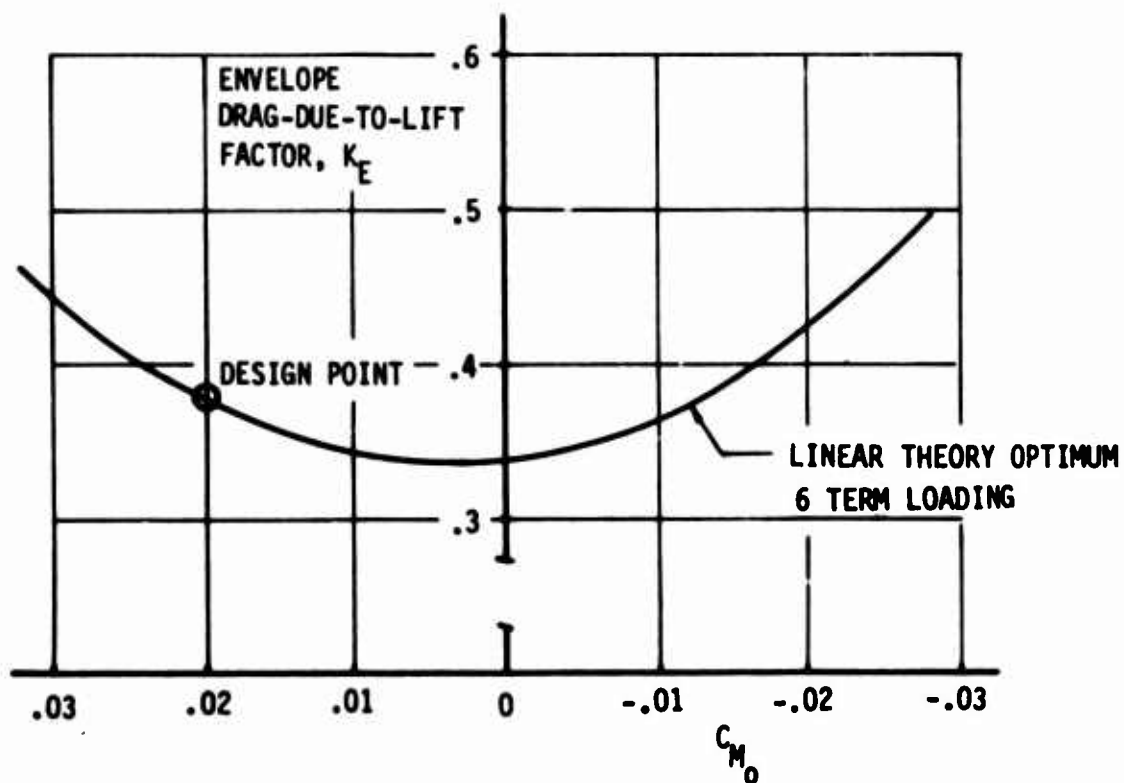


Figure 139. Arrow Configuration – Wing Design Solution

218

## 5.2 ARROW WING CONFIGURATION (Continued)

tips. On a wing alone basis, the wing camber and twist were designed
at Mach 1.8 for a $C_L$ = 0.10 and a positive $C_{Mo}$ constraint of 0.02. The
resulting curve of the optimum drag-due-to-lift factor ($K_E = C_{Di}/C_L^2$)
versus zero lift pitching moment ($C_{Mo}$) for a 6 term loading case is
shown in Figure 139. The airplane was designed to be in trim at
Mach 1.8, $C_L$ = 0.10 with an assumed c.g. position at 50% of the wing
MAC.

### DRAG CHARACTERISTICS

As with the -202 configuration, detailed drag characteristics for the
-210 configuration were not made. The non-lifting drag estimates were
only preliminary in nature and only suitable for parametric type com-
parisons. The estimates were made on the same basis as for the -202
and are compared in Figure 140. The preliminary Mach 1.8 drag polar
for the -210 arrow wing and canard configuration are compared in
Figure 141. Drag estimates at high lift values are not shown because
high angle of attack data with the pressure limiting feature were not
run during the preliminary evaluations.

| Mach 1.8,  50,000 feet | | |
|---|---|---|
| Drag Component | Canard<br>-202<br>D/q (Feet$^2$) | Arrow<br>-210<br>D/q (Feet$^2$) |
| Wave Drag | 2.814 | 1.815 |
| Skin Friction | 1.532 | 1.280 |
| Excrescence | 0.224 | 0.175 |
| Inlet Diverter | --- | --- |
| Misc. Items | 0.098 | 0.100 |
| TOTAL D/q | 4.668 | 3.350 |

*Figure 140.    Canard and Arrow Configurations — Non-Lifting Drag Comparison*
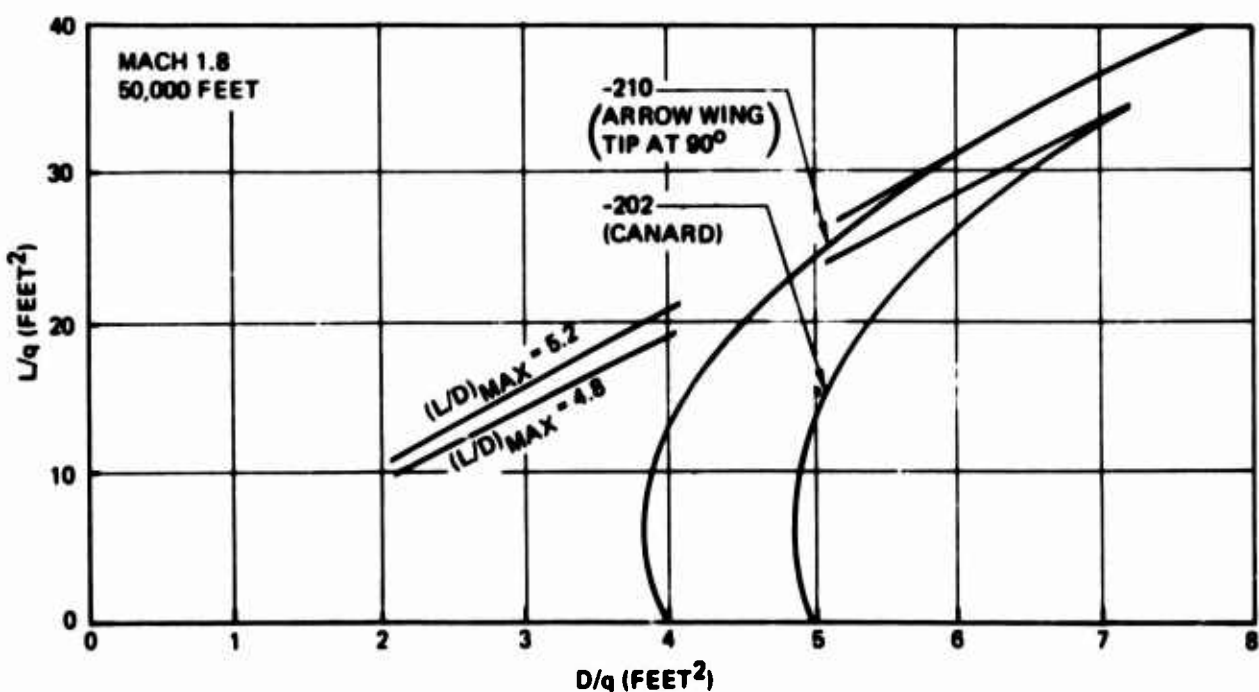


*Figure 141.    Canard and Arrow Configurations — Comparison of Drag Characteristics*

## 5.3 FOREBODY AND COCKPIT DRAG STUDY

A body variation was studied to investigate the effect of increasing the cockpit area to accommodate a standard pressure suit. Pressure suit requirements increase the cockpit constraint area by 35 percent relative to that assumed for the -213 airplane. The Mach 1.8 wave drag penalty for the increased cockpit cross section is $C_{D_W} = 0.0017$ assuming the optimized body area distribution shown in Figure 142. Additional skin friction and canopy drag increments would be on the order of $C_{D_{Fric.}} \approx 0.0002$ to $0.0004$ for a total drag penalty on the order of $C_{D_{Cockpit}} \approx 0.0020$.
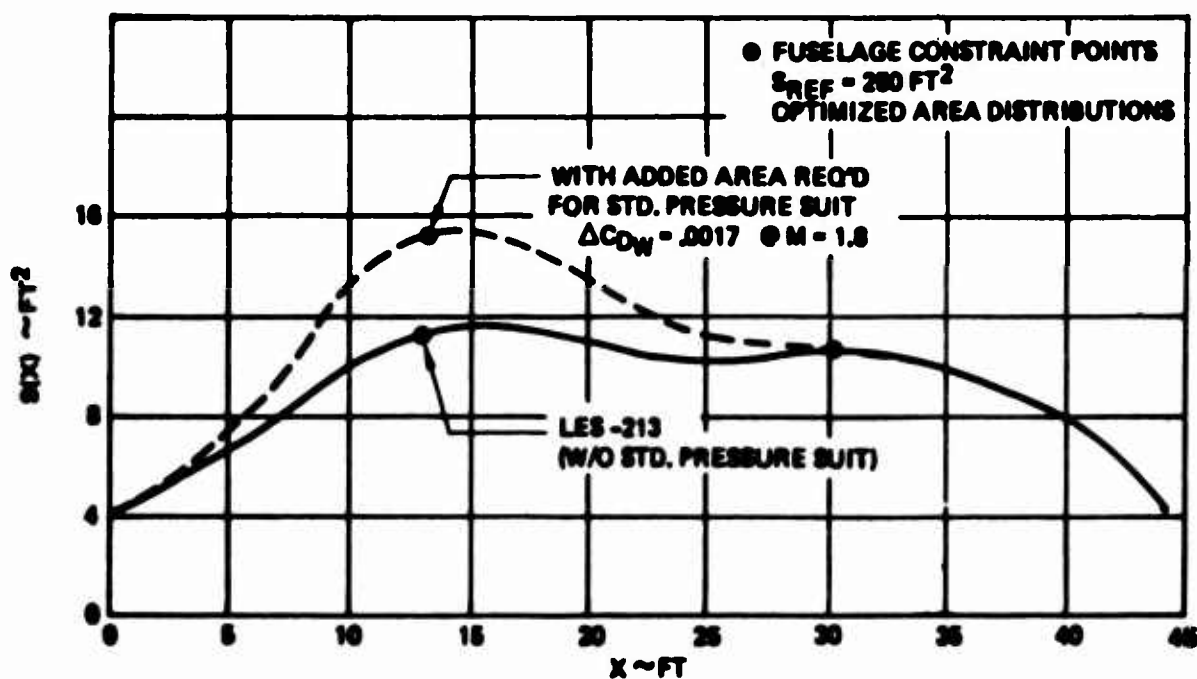


Figure 142. Fuselage Area Change Due to Cockpit Area Change

## 5.4 AFTBODY/NOZZLE TRADE STUDY

The LES airplane design has been configured with a two-dimensional wedge aftbody/exhaust system. However airplane performance was estimated for this study using a J101 derivative engine (J101/J7 Study A9) and axisymmetric C-D nozzle thrust performance, with power sensitive nozzle drag increments based on Boeing LWF proposal data for the F100 PW100 axisymmetric nozzle installation. Only the estimates for friction drag, wave drag at zero lift (based on -213 area plot) and weight r.-flect the 2-D Airframe Integrated Nozzle installation (2-D AIN) as shown on the LES configuration. To approximate the 2-D AIN performance, a wave drag increment for the 2-D wedge was estimated, Figure 143, and included in the -213 airplane drag polar. This approach was taken because the 2-D AIN wind tunnel test data (references 7, 8 and unpublished Mach 2.0 NASA test data) was not available in a suitable TEM 333 format to perform installed engine performance calculations.

This nozzle study was initiated to compare the performance of different axisymmetric aftbody geometries to the 2-D AIN installation and to compare the document performance levels estimated under the assumptions stated above. The results of this study shows the -213 airplane performance at Mach 1.8, dry thrust (based on the previously noted propulsion performance assumptions) to be 2.4% optimistic in equivalent drag compared to the same airplane geometry evaluated with 2-D nozzle thrust performance estimates. However a refined 2-D AIN aftbody closure shows a slight improvement in equivalent drag performance compared to the -213 estimate.

### AFTBODY/NOZZLE GEOMETRY COMPARISON

In this initial investigation, the basic LES-213 max body cross-sectional area and the engine location were held common to all aftbody geometry variations. The 2-D AIN geometry, as drawn on the -213 was evaluated using the 2-D wind tunnel test data and compared to a short axisymmetric C-D nozzle, a refined 2-D AIN, a long axisymmetric
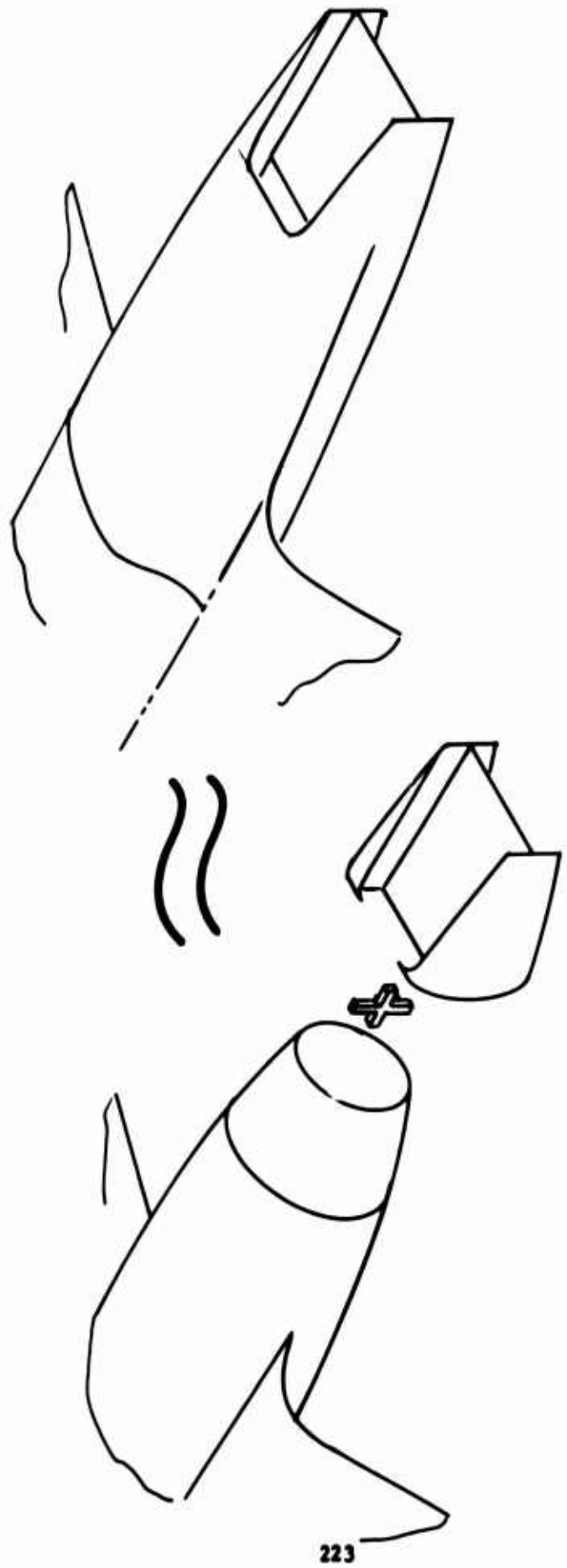
Figure 143 LES Installed 2-D Nozzle Performance Assumption

## 5.4 AFTBODY/NOZZLE TRADE STUDY (Continued)

C-D nozzle and a short axisymmetric C-D nozzle with speed booms astride
the nozzle. The five aftbody/nozzle arrangements studied are schemat-
ically shown in Figure 144. No attempt was made to optimize each aft-
body shape to include the correct fuel volume and maintain the document
airplane operating weight, however, the effects of the resulting aft-
body designs on operating weight (OW) internal fuel, OW balance require-
ments, drag and nozzle performance were examined. Wave drag was esti-
mated using an equivalent axisymmetric representation for all aftbody
shapes using the Integral Mean Slope (IMS) drag prediction technique
(Reference 30). Table 14 presents the friction drag, net thrust,
pressure drag, and weight estimates of this study. Table 15 summarizes
the aftbody structural weight and fuel differences plus the required
ballast to maintain the operating weight c.g. of the LES document air-
plane. The sum of these terms represent the change in gross weight of
the airplane aftbody modifications as drawn, without regard to main-
taining the same mission capability as the basic -213 airplane.

As a figure of merit the force increments of friction drag and thrust
minus pressure drag estimates at Mach 1.8 were compared to the -213
performance estimates and the excess forces were combined and treated
as equivalent drag changes (summarized in Table 14). As shown in Table
15, these data normalized around the Mach 1.8 reference drag of the
-213 LES study configuration, shows the refined 2-D AIN (Configuration
5) to have the lowest equivalent drag. The refined 2-D AIN aftbody
installation shows good agreement with the performance assumptions made
for this LES study. Figure 145 shows all other geometries studied to
have higher drag (hence less max speed capability) than the -213
reference airplane.

**224**

LES-213 2D-AFTBODY
• AXI SYM THRUST
• WEDGE WAVE DRAG

LES-213 2D AFTBODY
• 2D NOZZLE THRUST

SHORT AFTBODY
• AXI-SYM C-D NOZZLE

REFINED 2-D AIN AFTBODY
• 2-D NOZZLE THRUST

LONG AFTBODY
• AXI- SYM C-D NOZZLE

SHORT AFTBODY
• AXI-SYM C-D NOZZLE
  WITH SPEED BUMPS
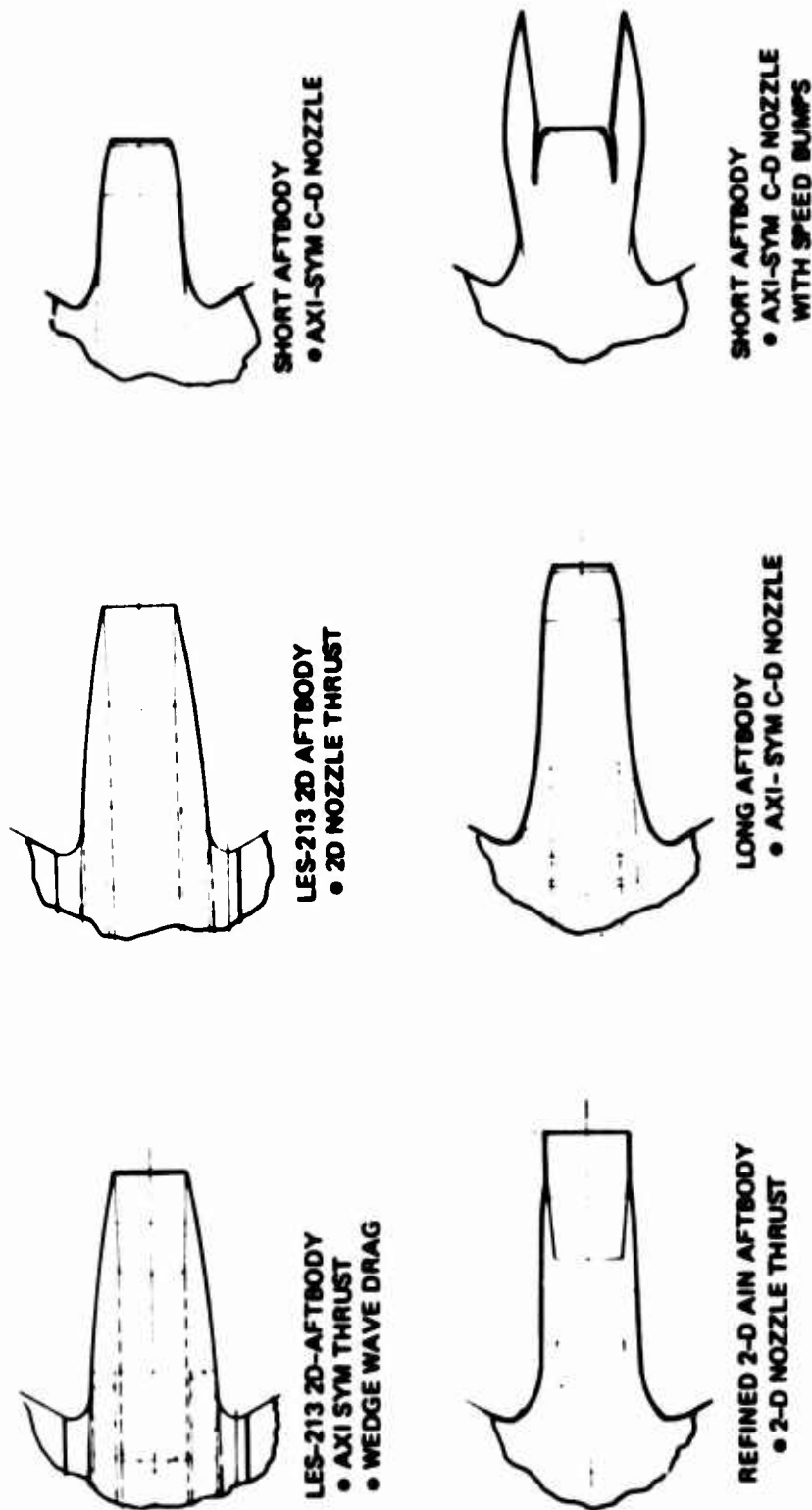
Figure 14i.    Trade Study – Aftbody/Nozzle Geometry Concepts

225

## 5.4  AFTBODY/NOZZLE TRADE STUDY (Continued)

### 2-D AIN DESIGN REFINEMENT

Two geometry revisions to the 2-D AIN design for the as drawn -213
were incorporated in this LES aftbody study.  These revisions better
match the exhaust expansion area requirements at Mach 1.8 by reducing
the projected area of the 2-D nozzle exit plane and using a smaller
centerbody with shallow wedge closure angles to improve the aftbody
area distribution and thus reduce wave drag.  The refined sidewall
geometry also reflects the design study conclusions (reference 6)
that minimize external surface cooling requirements during the after-
burner operation.

*Table 14.  Equivalent Drag Comparison at Mach 1.8*

| AFTBODY SHAPE | FRICTION | | | NET THRUST MINUS PRESSURE DRAG | | | | TOTAL $\Delta$'s $\Delta$ FORCE IN TERMS OF DRAG | EQUIVALENT DRAG COUNTS |
|---|---|---|---|---|---|---|---|---|---|
| | $C_{D_F}$ COUNTS | DRAG LBS | $\Delta$ DRAG LBS | $\dfrac{F_N - D_P}{F_N}$ | $F_N$·LBS | $F_N - D_P$ | $\Delta$ $(F_N - D_P)$ | | |
| LES-213 2D AFTBODY AXI-SYM NOZZLE THRUST WEDGE WAVE DRAG | 9.7 | 134 | REF | .920 | 2860 | 2631 | REF | REF | REF |
| LES-213 2D AFTBODY 2D NOZZLE THRUST | 9.7 | 134 | 0 | .931 | 2751 | 2561 | -70 | +70 | +5.1 |
| SHORT AFTBODY AXI-SYM NOZZLE THRUST | 8.4 | 116 | -18 | .893 | 2860 | 2554 | -77 | +59 | +4.3 |
| REFINED 2D AFTBODY 2D NOZZLE THRUST | 9.5 | 131 | -3 | .960 | 2751 | 2641 | +10 | -13 | -0.9 |
| LONG AFTBODY AXI-SYM NOZZLE THRUST | 10.9 | 151 | +17 | .899 | 2860 | 2571 | -60 | +77 | +5.6 |
| SHORT AFTBODY AXI-SYM NOZZLE THRUST PLUS SPEED BUMPS | 10.4 | 144 | +10 | .822 | 2860 | 2351 | -280 | +290 | +21.0 |

▶

q $S_{ref}$ · 138126 LBS @ M1.8

50K

$S_W$· 250 F $\bar{\imath}^2$

▶ THIS COLUMN USED IN %$\Delta$FORCE CALC ON TABLE 16.

Table 15. As Drawn Aftbody Weight and Normalized Drag Comparison

| AFTBODY SHAPE | Δ OW, LBS (8530 REF) | Δ FUEL, LBS (3830 REF) | BALLAST TO BALANCE OW @54% MAC | Δ GW, LBS (12,500 REF) | % Δ FORCE MACH 1.8 (2900 LBS REF) | NORMALIZED DRAG @ M1.6 |
|---|---|---|---|---|---|---|
| LES-213 2D AFTBODY • AXI-SYM NOZZLE THRUST • WEDGE WAVE DRAG | REF | REF | REF | REF | REF | 1.10 REF △ |
| LES-213 2D AFTBODY • 2D NOZZLE THRUST | 0 | 0 | 0 | 0 | +2.41% | 1.1285 |
| SHORT AFTBODY • AXI-SYM NOZZLE THRUST | -220 | -250 | +490 | +20 | +2.03% | 1.1223 |
| REFINED 2D AFTBODY • 2D NOZZLE THRUST | 0 | -100 | 0 | -100 | -0.45% | 1.0951 |
| LONG AFTBODY • AXI-SYM NOZZLE THRUST | +240 | -50 | +300 | +460 | +2.66% | 1.1293 |
| SHORT AFTBODY • AXI-SYM NOZZLE THRUST • PLUS SPEED BUMPS | -110 | -250 | +260 | -100 | +10.0% | 1.210 |

△ SEE TABLE 14

△ SEE FIGURE 148 FOR NORMALIZED -213 REFERENCE DRAG AT MACH 1.8, $DRAG_{M1.8} = 1.10\ F_{N_{M1.6}}$

227
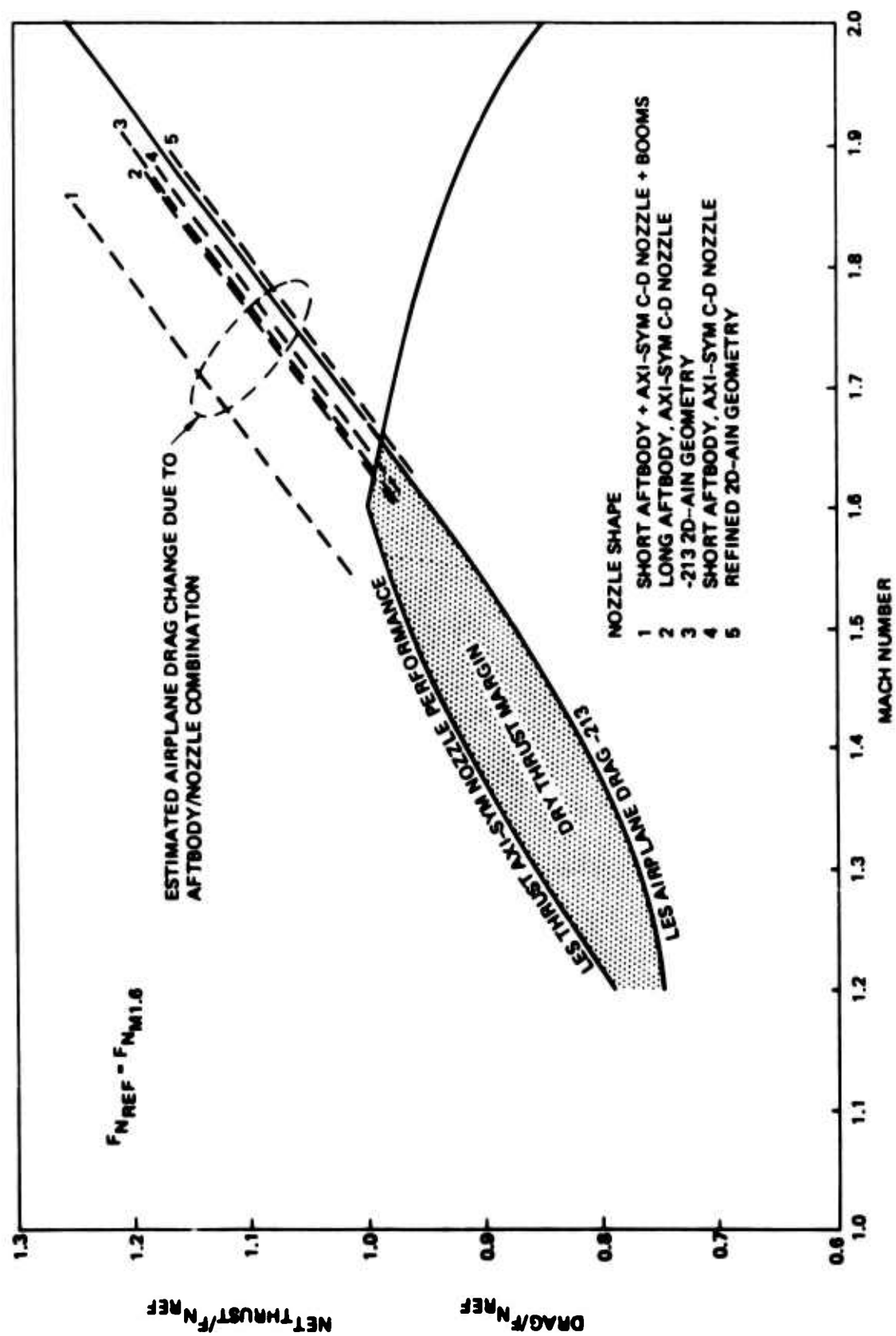
Figure 145. LES Maximum Speed Trades for Various Aftbody Designs

228

## 5.5 MISCELLANEOUS AERODYNAMIC TRADE STUDIES

Airfoil Section Thickness - The effect of airfoil thickness distribu-
tion on wave drag at Mach 1.8 was investigated.  Airfoil sections
based on two advanced technology airfoil thickness distributions were
applied to the basic wing planform,  Figure 146.  The MAR 55 airfoil
thickness had a larger leading edge radius than the MAR 56 airfoil and
had more volume (depth) in the region of the rear spar ($X/C$ = .75 to
.80).  Though the wave drag increment was approximately    $\Delta C_{D_W}$ = .0005,
the MAR 55 airfoil was selected due to better leading edge    suction
characteristics and more depth for actuators and spars in the aft part
of the airfoil section.



* NEAR-FIELD WAVE DRAG, M = 1.8
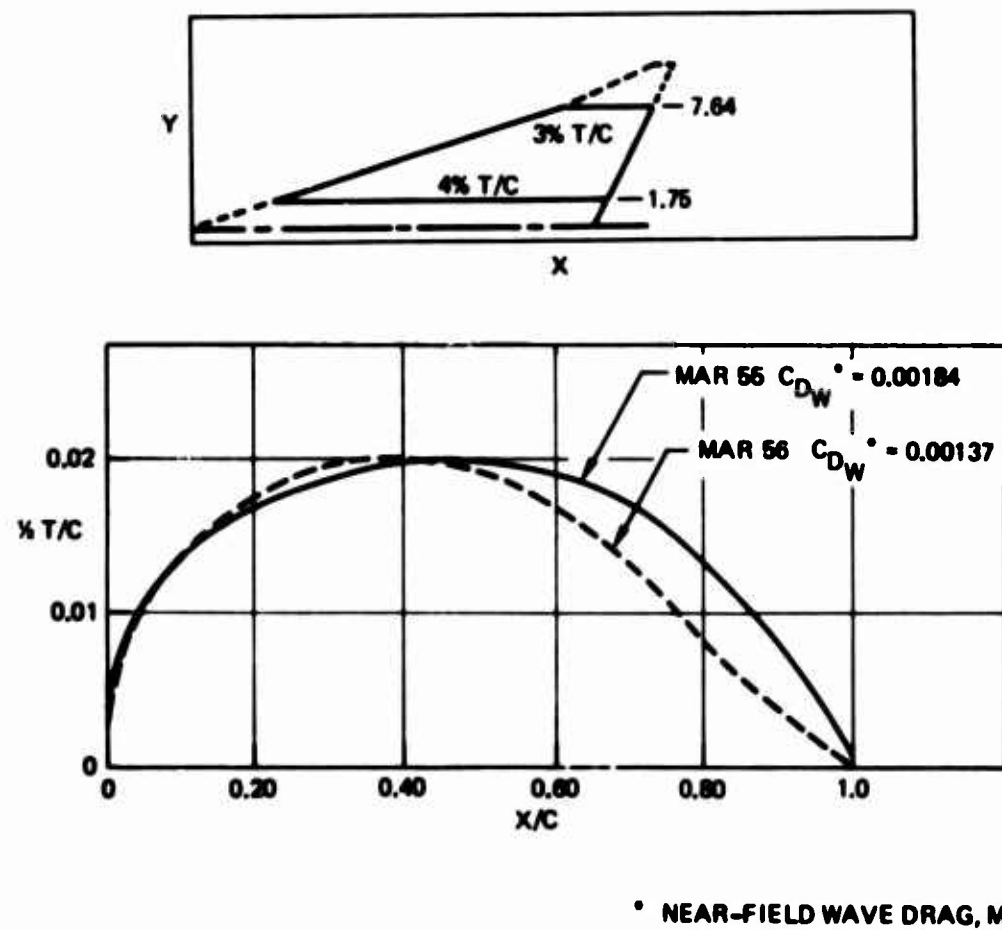
*Figure 146.    Airfoil Thickness Comparison*

229

## 5.5 MISCELLANEOUS AERODYNAMIC TRADE STUDIES (Continued)

Wing Sweep Variations - The effect of reduced wing sweep at cruise
condition (Mach 1.8, 50,000 feet, $C_L$ = 0.10) was investigated using
a configuration similar to the -213 as a reference. As shown in
Figure 147, wing area was held constant, the 50 percent MAC station
(MAC is defined without the wing tips) was fixed to a given body
station, the absolute wing thickness at the side of the body was held
constant, and the chord length where the verticals were attached to
the wing remain fixed. Component drag increments and total drag
variation as a function of wing sweep indicated that no significant
cruise drag penalty would be incurred until the wing leading edge
reduction approached 65 degrees. The reduced sweep would improve the
maneuver characteristics but would decrease the potential for higher
Mach number capability without a significant drag penalty.

Wing Tip Deflection - For the different wing tip deflections, the
expected variation in drag-due-to-lift and the A.C. position is shown
in Figure 148. The subsonic, 0° tip variation is based on SCAT 15
wind tunnel test data. Further improvements in drag-due-to-lift could
be investigated using the wing tips to control the A.C. position and
redesigning the wing for different $C_{Mo}$ constraints. Trades between
trim and drag-due-to-lift resulting from deflecting the wing tip for
various c.g. positions could provide optimum maneuvering character-
istics for a given wing sweep.
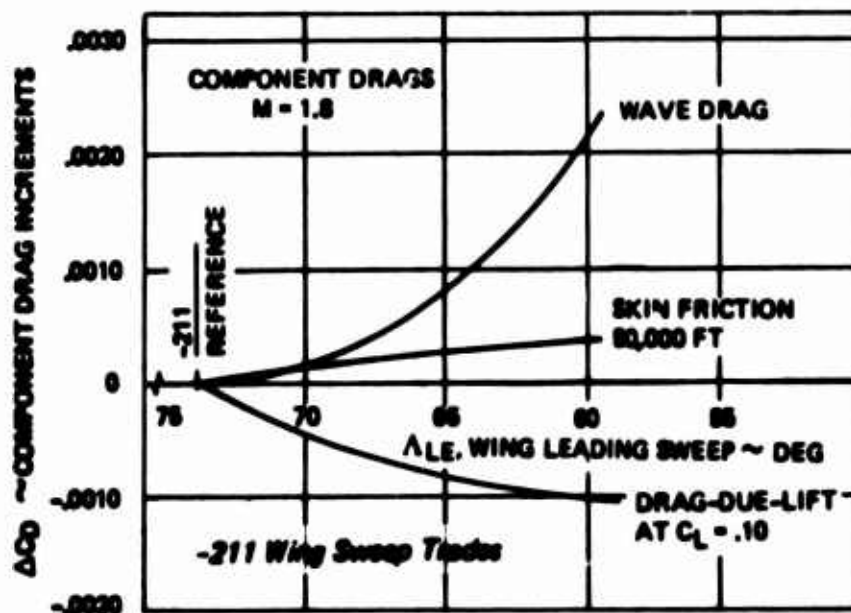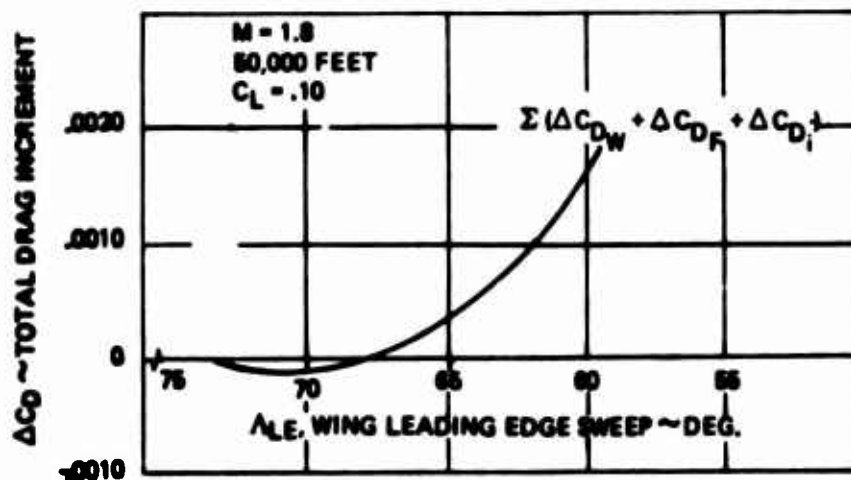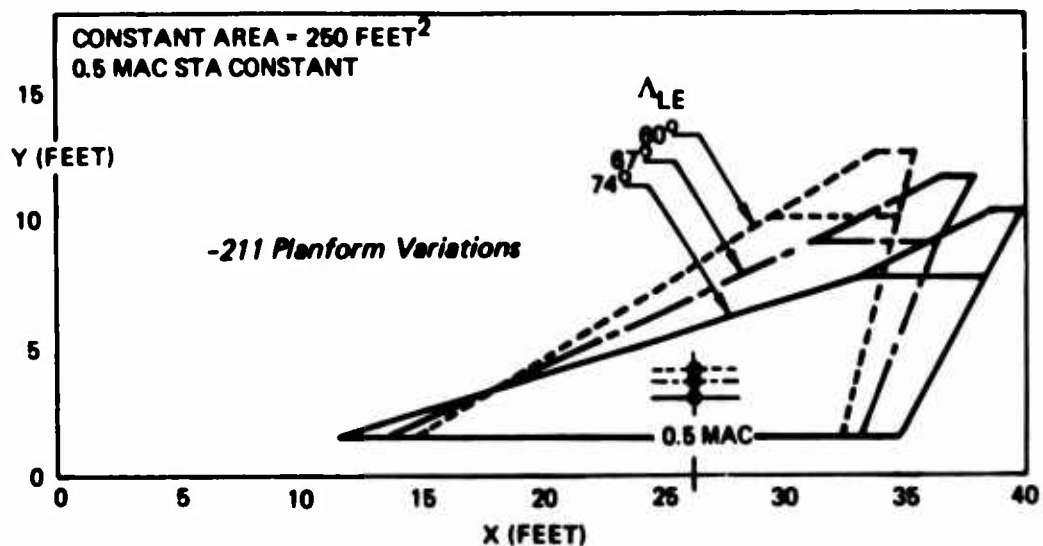
Figure 147. Wing Sweep Variations

Figure 148. Effect of Wing Tip Deflection

232
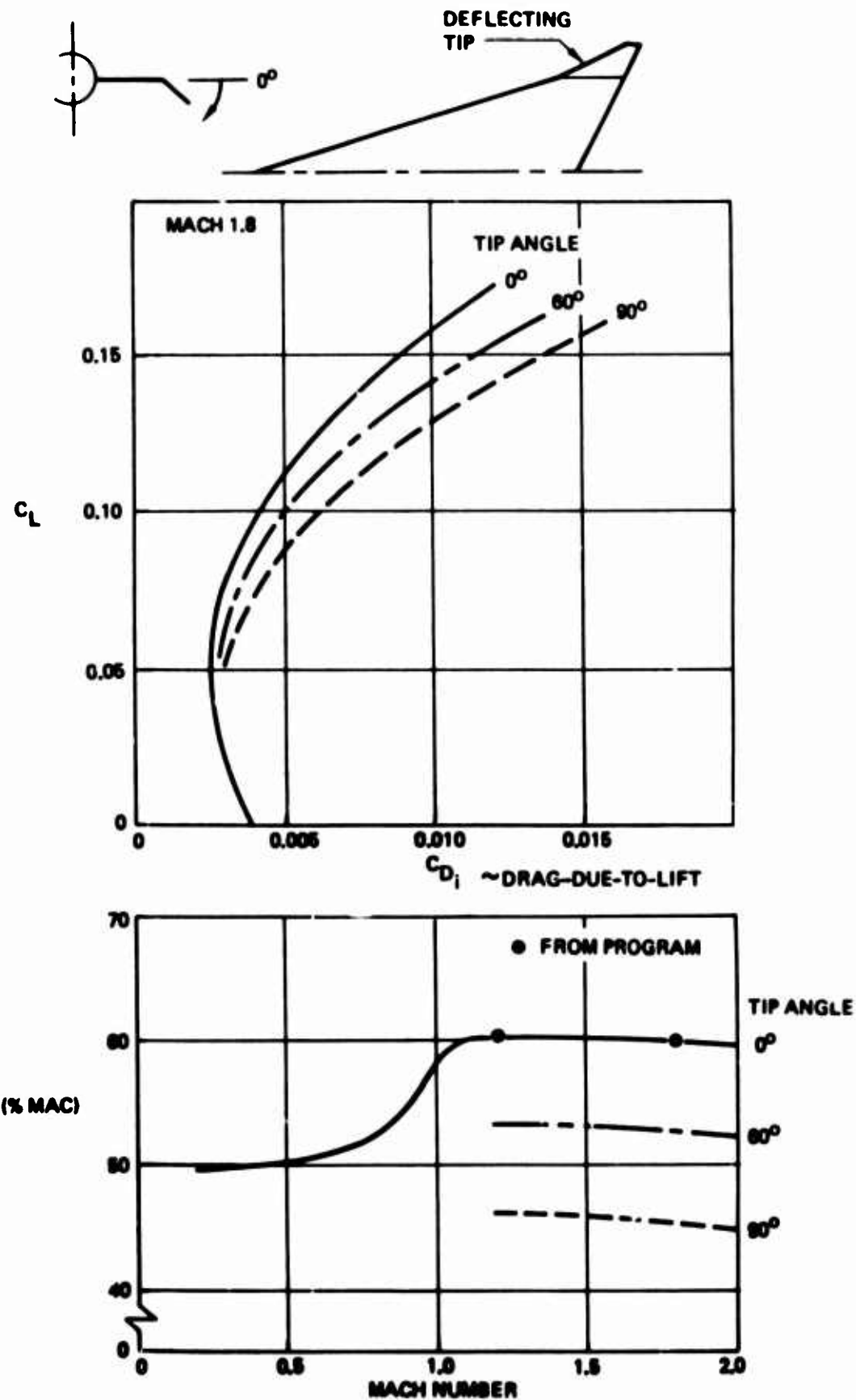
## 5.6 WIND TUNNEL TEST REQUIREMENTS

Wind tunnel model test data will provide the reference aerodynamic parameters necessary to confirm the vehicle performance and establish stability and control characteristics. The type of configuration, desired aerodynamic parameters, model test facilities and the method used to correct the model test data to full scale airplane estimates all have an impact on the model design and test planning.

Before any wind tunnel model testing is contemplated, a method for correcting the wind tunnel model data to full scale airplane estimates is required. This method must consider the thrust minus drag bookkeeping system. Such a system is outlined in Appendix D.

The airplane configuration, test facility and type of data will be the major factors in determining the model mounting system, the number of parts required and the model size. For a performance test, a six component internal strain gauge balance on an aft sting mount protruding from the nozzle exit is preferred. This allows a flow through nacelle and minimizes mounting interference effects on the model. Removable model parts are required to determine the effects of major configuration components and component variations. As most thrust minus drag type bookkeeping systems us a reference mass flow to determine the thrust/drag split, mass flow ratio variations through the flow through nacelle system should encompass or allow extrapolation to zero inlet spillage. Blockage, buoyance, shock reflections and shock induced starting loads must be considered in determing the model size and test limits.

A test designed to establish and/or confirm basic vehicle performance parameters should include testing at the design and important off-design Mach numbers, sufficient variations in major configuration variables to determine their impact on the configuration, mass flow variations required for extrapolation to zero spillage to allow correlation with analytical estimates, and control deflections necessary

233

## 5.6 WIND TUNNEL TEST REQUIREMENTS (Continued)

to determine trim drag penalties. Flow visualization runs; i.e. oil
flows, schlieren, etc., are required to assist with the data analysis
and to determine where configuration design changes could reduce the
drag by improving the local flow conditions.

Performance confirmation of the LES arrow wing configuration should be
conducted over a Mach and angle of attack range that encompasses both
supersonic and subsonic cruise and maneuver conditions. The aft body
should be represented by a simple shape which assures a surface flow
condition amenable to analysis using existing theoretical methods.
The major configuration variables to be tested should include the
effect of the leading and trailing edge variable camber devices,
verticals and wing tip deflections. Model parts required would include
the basic wing-body, a set of vertical tails, wing tips that can be
deflected down (30°, 60°, 90°) and exit nozzles (3) for varying the
mass flow. Instrumentation would include a six component internal
strain gauge balance mounted on an aft sting through the exit nozzle.
Internal drag measurements and mass flow variations require pressure
rakes mounted at the plane of the nozzle exit (in the annulus between
the sting and nozzle) to measure the momentum loss (internal drag).
Static pressures are required along the length of the internal duct
and at the exit to determine the mass flow through the internal duct
and the velocity distribution within the duct. Base pressures are
required on any blunt base areas not representative of the airplane
and in the region of the metric break with the sting.

For the LES configuration, the wing definition was created using a
geometry lofting system which combined the camber, twist and thickness
distributions from the computer inputs. Sections from the numerical
wing definition created for the current LES wing design are shown in
Figure 149. The wing definition is also suitable for using numerical
control machining techniques to build the wind tunnel model wing.

234
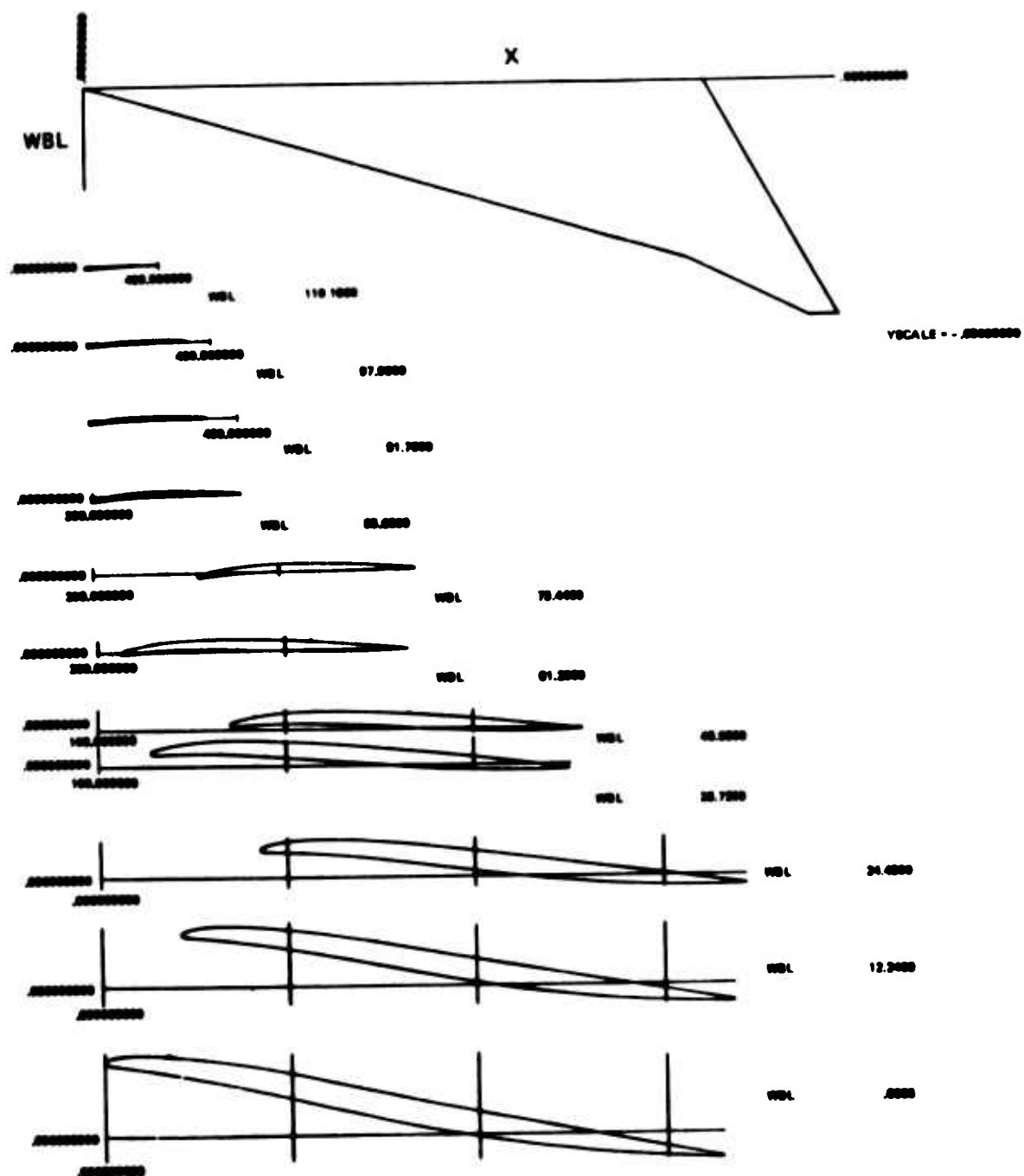
Figure 149. LES Lofted Wing

## 5.6 WIND TUNNEL TEST REQUIREMENTS (Continued)

The control surfaces (sizes and location) are taken from the general arrangement drawing or as defined by analysis work. Brackets are required to hold the vertical tails and the wing tip at its various deflection angles. The variable camber leading edge deflections would require the deflected shape to be defined and the wing relofted with the deflected leading edge.

A LES body definition with the 2-D nozzle and aft body has been defined using the same lofting program that created the wing definition. Body station cuts and top, side, and bottom views of this definition are shown in Figures 150 and 151. Due to the highly blended wing-body intersection, the body definition was carried out to WBL 28. Inlet details were not included as it is best to make the inlet separately.

Inlet details have to be worked out so as to minimize deviations from the external contours due to the model mounting sytstem. With the sting, sufficient flow area must be provided in the annulus to pass the maximum amount of air flow captured by the inlet. Lesser airflows for mass flow variations are controlled by reducing the nozzle exit diameter. To prevent flow instabilities in the internal duct, the flow area between the inlet throat and the nozzle exit should be large enough to assure subsonic flow throughout ($M \leq .6$) and then close down so the flow becomes choked at the nozzle exit. For the LES configuration, a unique problem exists at the inlet/diverter location. Further redesign of the inlet/boundary layer diverter region is required to accommodate a conventional boundary layer diverter installation.

The plan of test outlined in Figure 152 would provide the wind tunnel data necessary for confirming the full scale airplane estimates of the LES configuration and provide sufficient information for evaluating the potential use of wing tip deflections for controlling trim drag and directional stability. The first runs of the test should be to

236
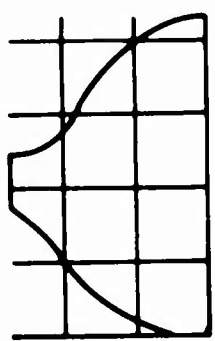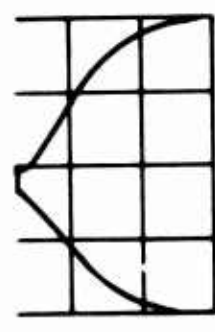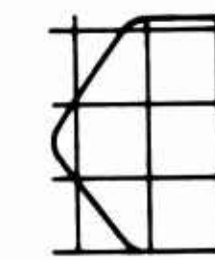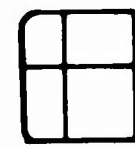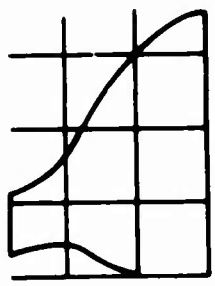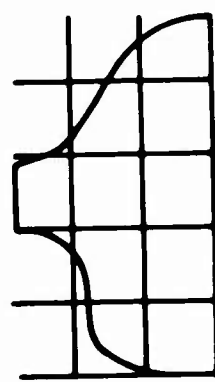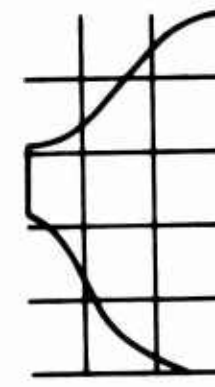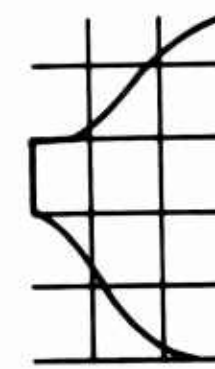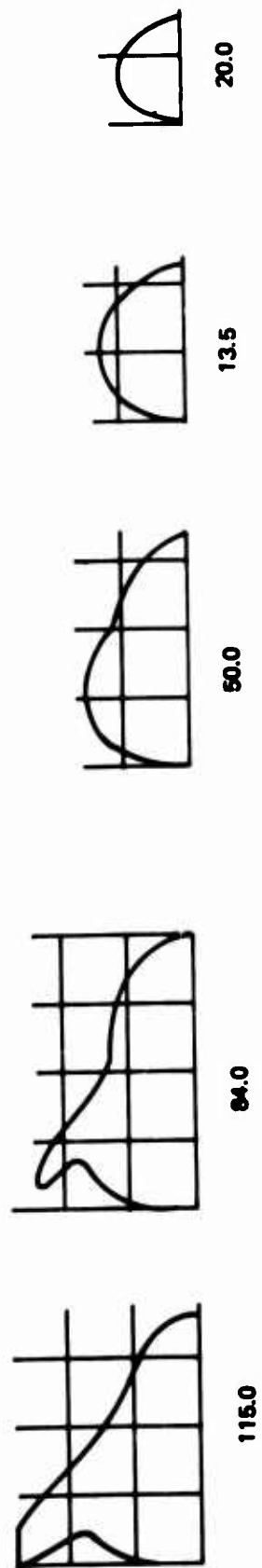
Figure 150. LES Lofted Body Station Cuts

TOP VIEW

SIDE VIEW
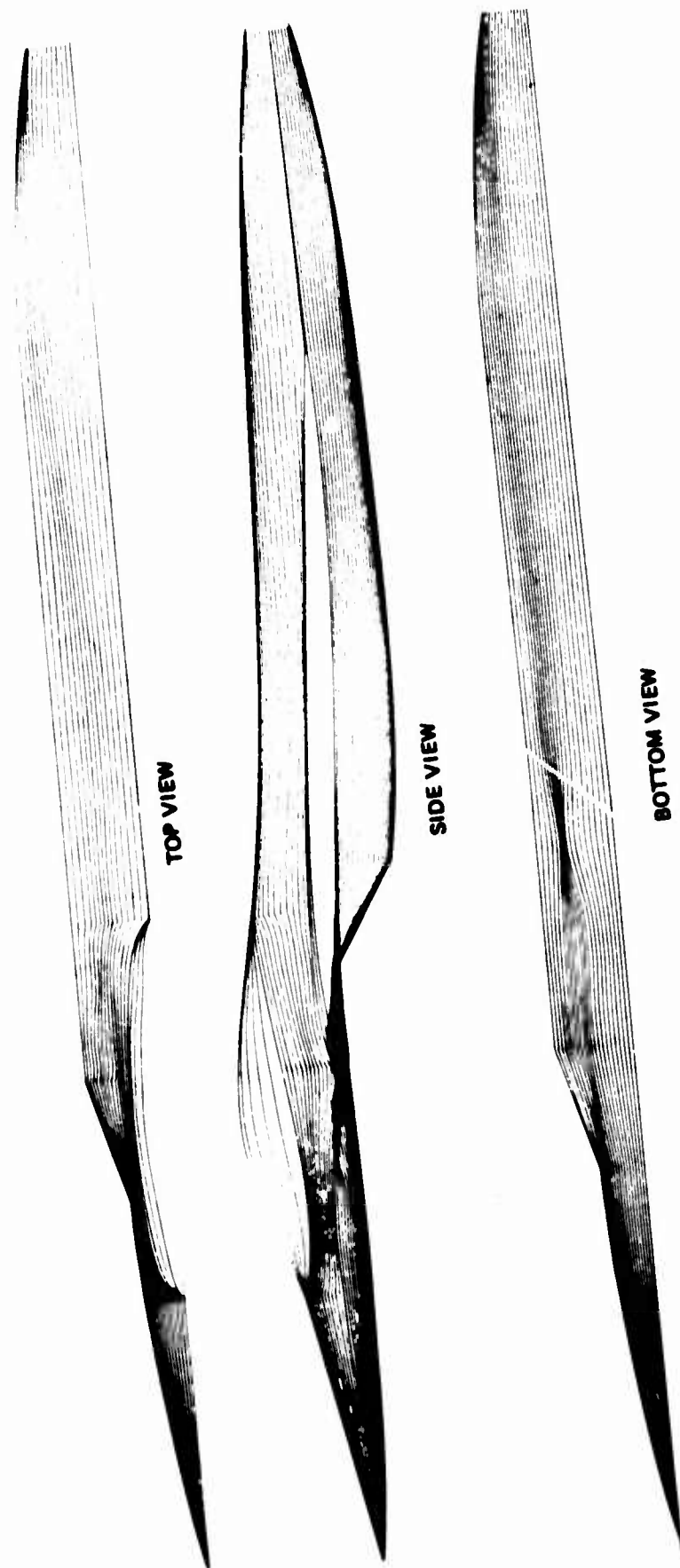
BOTTOM VIEW

Figure 151.    LES Lofted Body-Top, Side and Bottom Views

238

Figure 152. LES Preliminary Plan of Test

| Purpose | Configuration | Type of data | δ_LE | δ_TC | δ_TIP | 0.50 | 0.70 | 0.80 | 0.80 | 0.90 | 0.925 | 0.950 | 0.975 | 1.05 | 1.2 | 1.6 | 1.8 | 2.0 | 2.2 |
|---|---|---|---|---|---|---|---|---|---|---|---|---|---|---|---|---|---|---|---|
| Mass flow variations (internal drag) Pressure data | Wing + body + nozzles → | Pressure | 0° → | 0° → | Off → | X | X | X |  | X |  |  |  | X | X | X | X | X | X |
| Mass flow variations force data |  |  |  |  |  | X | X | X |  | X |  |  |  | X | X | X | X | X | X |
| Effect of wing tip and basic configuration Drag rise characteristics | Wing + body + tip | Force (pitch) | 0° → | 0° → | 0° → | X | X | X | X | X | X | X | X | X | X | X | X | X | X |
| Effect of verticals | Wing + body + tip + verticals |  | +2.5° +7.5° +15° |  |  | X | X | X | X | X | X | X | X | X | X | X | X |  | X |
| Effect of L.E. deflections |  |  | +7.5° → |  |  | X X X |  | X X X |  |  |  |  |  | X X X | X X X X X |  | X X X X X |  | X X X X X |
| Trim drag with L.E. deflections |  |  | 0° → | +15° +7.5° -7.5° |  | X X X X X |  | X X X X X |  |  |  |  |  | X X X | X X X X X |  | X X X X X |  | X X X X X |
| Trim drag w/o L.E. deflection |  |  |  | -7.5° -15° +7.5° +15° 0° |  | X X X |  | X X X |  |  |  |  |  |  | X X X | X X X | X X X | X X X | X X X |
| Effect of wing tip deflections on A.C. position and drag-due-to-lift |  |  |  | 0° → | 30° 60° 90° → | X X X X |  | X X X X |  |  |  |  |  |  | X X X X | X | X X X X |  | X X X X |
| Trim drag with wing tip down |  |  |  | 0° +7.5° +15° -7.5° | 90° → | X X X X |  | X X X X |  |  |  |  |  |  | X X X X |  | X X X X |  | X X X X |
| Wing tip effectiveness on directional stability |  | Force (yaw) → | 0° → | 0° → | 90° 60° 30° 0° → | X |  | X |  |  |  |  |  |  | X |  | X |  | X |
| Vertical tail effectiveness | Wing + body + tip → |  |  |  | 0° → |  |  |  |  |  |  |  |  |  |  |  |  |  |  |
| Flow visualization and configuration improvement | As required |  |  |  |  | As required → |  |  |  |  |  |  |  |  |  |  |  |  |  |

Mach numbers

## 5.6 WIND TUNNEL TEST REQUIREMENTS (Continued)

determine the internal drag with the different nozzles used to control
the mass flow variation. The pressure instrumentation is then removed
and the force data obtained using a single nozzle or the nozzles most
appropriate for the Mach range being tested. Data up to Mach 2.2
(or higher) is suggested to provide further understanding of the con-
figuration and a data basis for higher Mach number requirements in the
future. A complete Mach range is run to determine the basic wing-body
characteristics. Additional Mach numbers including 0.85, 1.10 and 1.4
may be desired to better define the transonic variation of drag with
speed. This is useful for data continuity, test-theory comparisons and
providing a data basis for other studies which are LES configuration
oriented. Wing tip effectiveness is also obtained.

The remainder of the data is run only at selected Mach numbers. Lead-
ing edge effectiveness for maneuver and low speed are run next. Trim
drag data at one leading edge deflection are run to compare the total
increments relative to zero degree leading edge deflection. The effect
of deflecting the wing tip down will provide data to influence the
wing design with regard to trim drag ($C_{M_0}$), A.C. shift, and drag-due -
to lift during maneuver and cruise. The directional stability (yaw
data) characteristics with the wing tips down will influence the size
of vertical tail required. The last part of the test should include
time for trying configuration improvements, running of additional data
if required and for flow visualization. Unless the test objective is
strictly limited to a data gathering role, a thorough flow visualiza-
tion is imperitive. Flow visualization data in the form of oil flow,
schlierens and possibly vapor screens on key configurations and at
critical flight conditions are necessary in both analyzing the data
and identifying adverse interaction problems. In the absence of signi-
ficant external pressure instrumentation, flow visualization is the only
source of information defining shock locations and regions of separated
flow including vortex formation on the wing.

## APPENDIX A   INTEGRATED STRUCTURAL ANALYSIS SYSTEM (ISAS)

The ISAS Program is used for in-depth analysis during preliminary design.   The full ISAS module flow chart is shown in Figure A1 with the procedures used in the present study marked in bold outline.   Specifically, solution activity begins with the use of Procedures 1 and 2 to describe the structural model in terms of nodes, spars, ribs, webs and cover plates.   Thicknesses are obtained by interrogating the geometric description tape (Procedure 9) which is also used to loft wind tunnel models.   Initial structural properties and geometries are selected and the data is assorted and ordered by Procedure 4.   Net rigid external loads on the elevator balanced airplane are received from Procedure 19 and distributed to the structural model nodes by Procedure 11.   Implementation of the main redundant structural analysis program in Procedure 22 provides a complete description of internal loads in the given structure.   The structure is then optimized for minimum weight by the Procedure 13 resize module that considers materials, allowables, minimum gage and load distribution instructions in defining and weighing each structural element.   This new model is analyzed to obtain a flexibility matrix for Procedure 18 to use preparatory to calculating new airloads in the flexible airplane in Procedure 19.   A single iteration that extended through the Procedure 13 resize module completed the aeroelastic cycle in the present study.

Descriptions of the chief ISAS modules are given below:

PROCEDURE 1 - NODE

The NODE program is used for the generation of modal data for ISAS. NODE can generate nodal data independently, or with the Geometry Control System (GCS).   NODE can modify or add to nodal data generated by any of the other nodal data generation programs in ISAS (such as the ASTRA SAIL Procedure 3, or the Master Dimensions Node extraction Procedures 32 through 36).

241
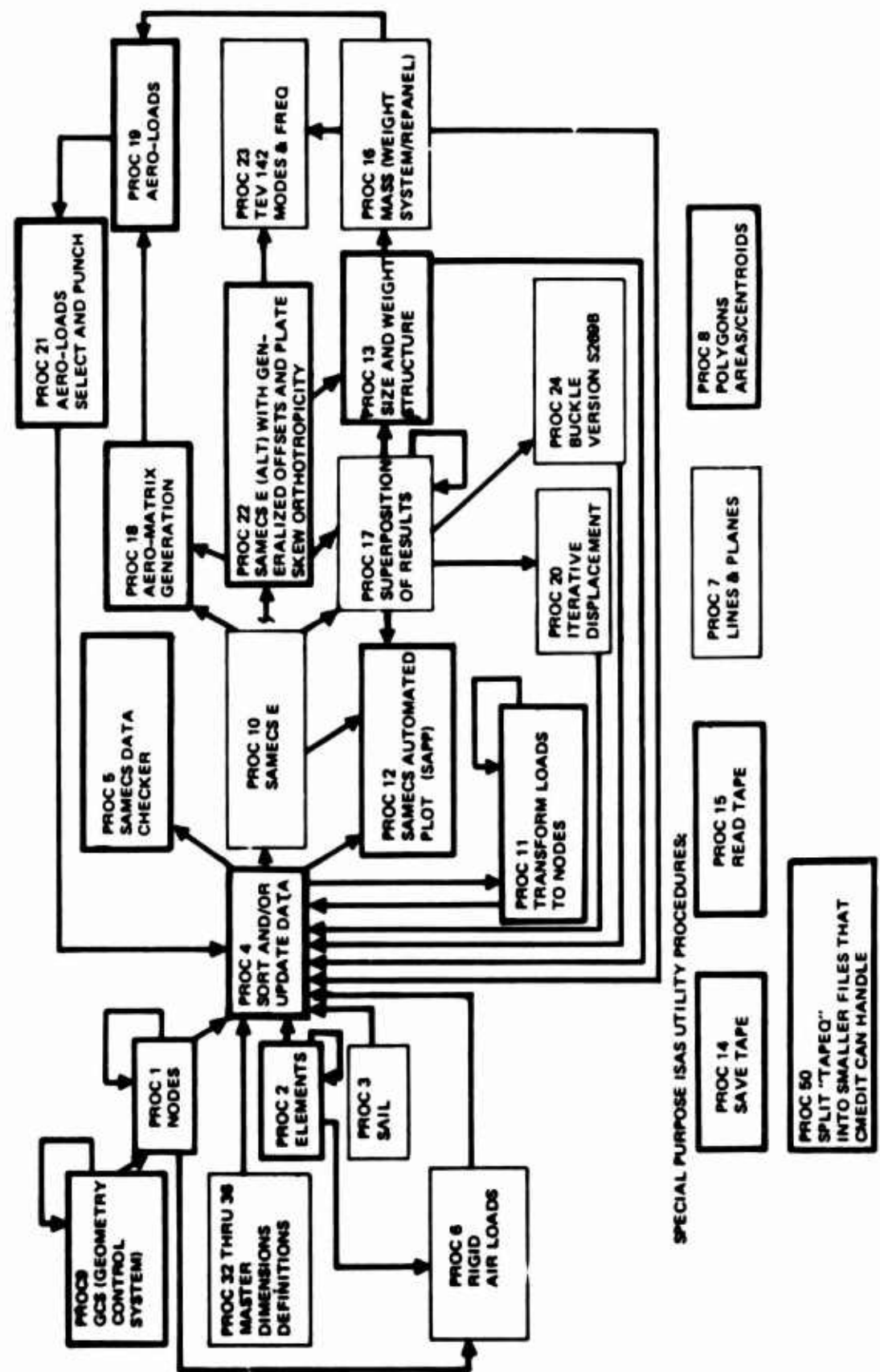
Figure A1. ISAS Procedures Flowchart

APPENDIX A    INTEGRATED STRUCTURAL ANALYSIS SYSTEM (Continued)

PROCEDURE 2 - ELEMENT

The ELEMENT program is used for the generation of finite element data
for ISAS.  ELEMENT generates two kinds of elements:  structural finite
elements of plate and beam types, and loaded (or weighted) finite ele-
ments of point, line, triangular area, and quadrilateral area types.

PROCEDURE 5 - SAMECS DATA CHECKER

The SAMECS DATA CHECKER is used to check SAMECS E input data for confor-
mance with the SAMECS E input format specifications prior to SAMECS exe-
cution.  It's primary advantage is that in checking the data set before
it is submitted to SAMECS E it saves computer budget.

PROCEDURE 9 - GEOMETRY CONTROL SYSTEM (GCS)

The Geometry Control System (GCS) is a powerful engineering tool which
can rapidly construct three-dimensional shapes of wing-like and body-
like structures using user supplied defining sections.  The system fits
curves (straight lines, circles, and/or cubics) between the defining
sections per instructions from the user.

PROCEDURE 11 - TRANSFORMATION OF EXTERNAL LOADS TO NODE LOAD S

The loads transformation program is used to produce node loads on struc-
tural nodes for internal loads analyses.  The comprehensive equili-
brium checks built into the program and the manner in which data pro-
cessing is arranged guarantee the quality of the node loads produced by
the procedure.  It is not necessary to use node loads from any other
source to complete any structural internal loads analysis node loads.

APPENDIX A - INTEGRATED STRUCTURAL ANALYSIS SYSTEM (Continued)

PROCEDURE 12 - SAMECS AUTOMATED PILOT PROGRAM (SAPP)

The SAMECS automated pilot program is used to plot input and output data
for SAMECS.  The plots are produced on a cal-comp plotter.  Plan, side,
front, and 45 degree views are available as well as 3-D views with axes
oriented in any direction from 0 through 360 degrees, as selected by
the user.

The "RESIZE" program is an interactive computer program that will auto-
matically resize a SAMECS data set for strength, with stiffness, buck-
ling, and minimum gage constraints imposed.  The resize program is cap-
able of treating composite as well as metallic structure.

PROCEDURE 18 - AEROELASTIC MATRIX (A/M) AND MATRIX RE-ORDERING PROGRAM

The AEROELASTIC MATRIX program was originally written to produce air-
load panel flexibility and slope-flexibility matrices for aeroelastic
loads analyses.  It has since been used to reduce the size and/or re-
order flexibility matrices, and to reorder stiffness matrices.

PROCEDURE 19 - AEROELASTIC LOADS

The AEROELASTIC LOADS PROGRAM TEA196 is used to:  1) claculate the down-
wash and aerodynamic matrix, 2) correct the aerodynamic matrix by any
correction factors available from wind tunnel data, 3) solve the aero-
elastic problem to obtain unit or balanced solutions for air loads in-
cluding VMD (shear, moment torsion integrated loads) data, and 4) to
calculate the effects of aeroelasticity on stability and control para-
meters.

APPENDIX A - INTEGRATED STRUCTURAL ANALYSIS SYSTEM (Continued)

PROCEDURE 22 - STRUCTURAL ANALYSIS METHOD FOR EVALUATION OF
COMPLEX STRUCTURES VERSION E (SAMECS E)

SAMECS is used to analyze structures idealized as plate and beam elements (connected at nodes) to obtain deflections, rotations, internal loads, stresses, reactions, and reduced stiffness, flexibility, deflection, and load matrices. (Other types of elements may be included as required via the pre-merge feature available in SAMECS). Input data to SAMECS consists of nodes, plates, beams, node loads, externally generated stiffness and loads matrices, and problem option selection.

APPENDIX B - PROPULSION INSTALLATION BOOKKEEPING METHODS

INTRODUCTION

The need for a performance integration system in an airplane development
program arises largely from the inability to determine the performance
of the complete airplane system, with simulataneous real inlet and ex-
haust system operation, in one test or one calculation.  Furthermore, it
is usually desirable to optimize the inlet and exhaust system in sepa-
rate tests which are independent of the general aerodynamic drag test-
ing of the basic airplane configuration.  Thus, a well-defined performance
mance integration system is required to insure that the performance es-
timated for the various elements (i.e., inlet, exhaust system, airframe,
turbomachinery) of the airplane system are properly integrated to yield
an accurate prediction of averall system performance.

The approaches taken by the major airframe contractors (References B1
through B9, in treating this problem are all similar in concept.  The
aerodynamic drag testing of the basic airplane configuration is done
with some reference inlet and exhaust system condition.  Most commonly
this testing is done with the propulsion system represented by a flow
nacelle (i.e., flow-through duct).  Thus, the reference inlet and ex-
haust system simulation on the airplane drag model is that which is
achievable under flow-through conditions.  To extrapolate from this con-
dition to the full scale airplane condition in flight, separate inlet
and exhaust system tests are conducted with a portion of the airplane
geometry and flow properties duplicated in the region of the inlet or
exhaust system being studied.  These separate tests include full engine
simulation so as to allow measurement of drag increments of the opera-
ting condition relative to that which is produced on the airplane re-
ference flow nacelle.  For the nozzle this requires blowing high pres-
sure air through the exhaust system to produce the pressure ratios and
external nozzle geometry consistent with the installed engine in flight.
For the inlet this requires varying the mass flow and inlet geometry on
the flow-through nacelle.  The inlet and exhaust system drag increments

thus obtained are then combined with the internal propulsion system thrust and airplane drag to obtain a prediction of overall thrust-minus-drag performance of the airplane system as depicted in Figure B1.

Fundamental to this performance integration is the definition adopted for the thrust and drag forces. Herein lies the controversy or book-keeping differences that currently afflict the industry. From a performance calculation standpoint it is immaterial how the split is made between thrust and drag provided that all forces exerted on the airplane system are accounted for once and only once as either a drag force or a thrust force. The split defined however has implications in accuracy, test technique employed, accountability and comparison of component performance between airplanes. These implications can be made evident by considering a specific example. Assume that the split or bookkeeping definition is established by the condition of the flow nacelle on the airplane drag model. Further, assume the reference flow-nacelle condition is one which passes airflow equal to the inlet capture area through the duct for all Mach numbers (i.e., MFR = 1.0).

Both the inlet and nozzle geometry are significantly altered relative to the operating condition of the propulsion system to achieve this condition. Thus, as shown in Figures B2 and B3, the propulsion force increment measured relative to this reference will contain a significant drag increment that is associated with the flow-through simulation of the propulsion system geometry on the reference flow nacelle. These "configuration change" drag increments will ultimately have to be assigned to airplane drag (i.e., scaled from model test data) when comparison is made with flight test data; when evaluating performance of competing airplane configurations or when attempting to develop a technology base for prediction drag of the real airplane in flight. This is completely correct and consistent bookkeeping. However, consider that with this kind of reference significant configuration dependent drag increments for the airplane system are measured on inlet and nozzle component

247
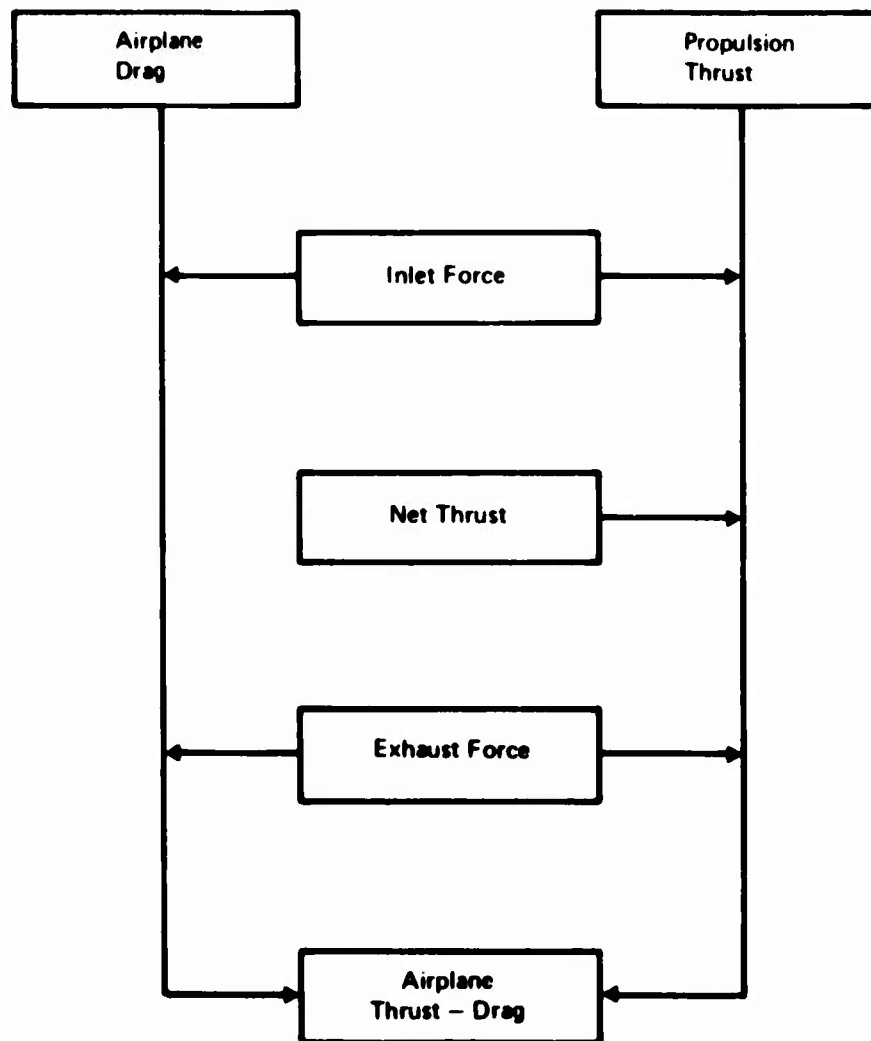
Figure B1.   Airplane Thrust/Drag Bookkeeping

248
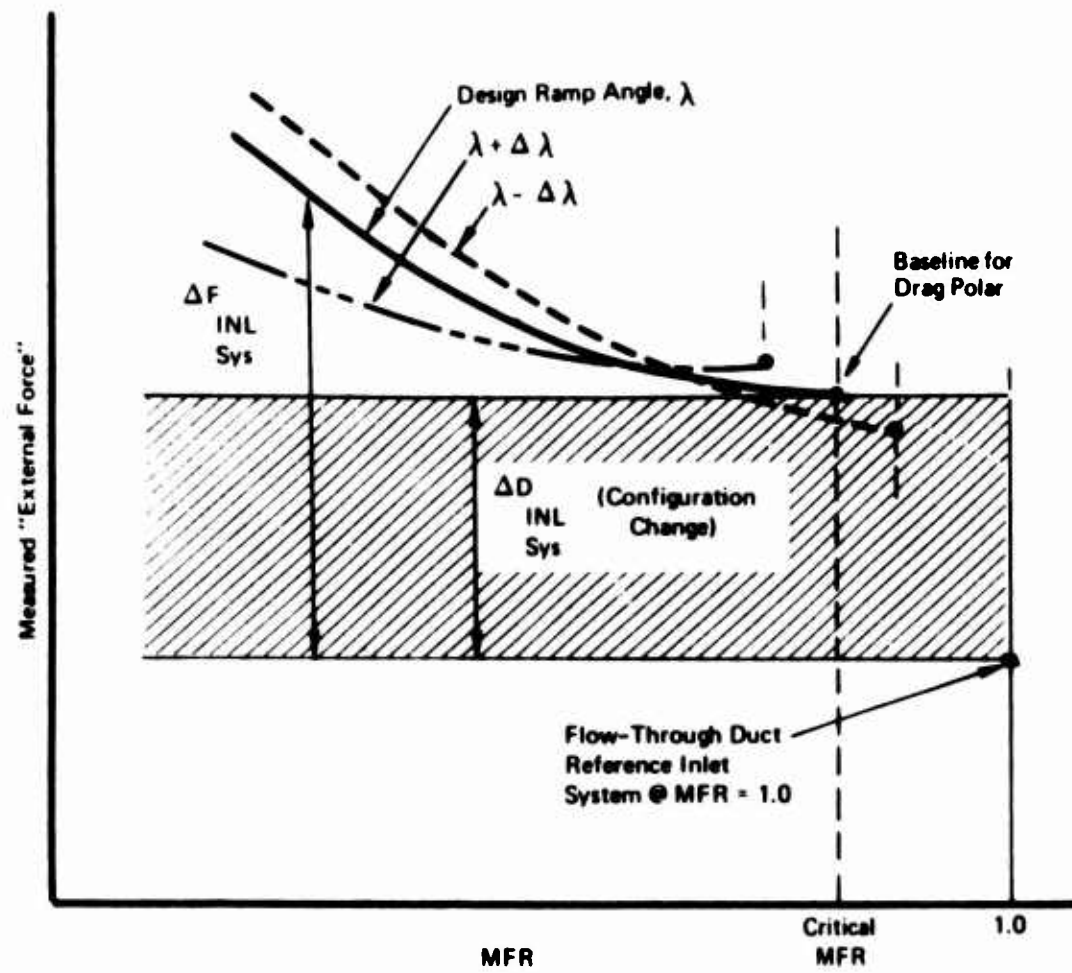
Figure B2. Inlet System Drag Relative to Flow Nacelle Reference

249
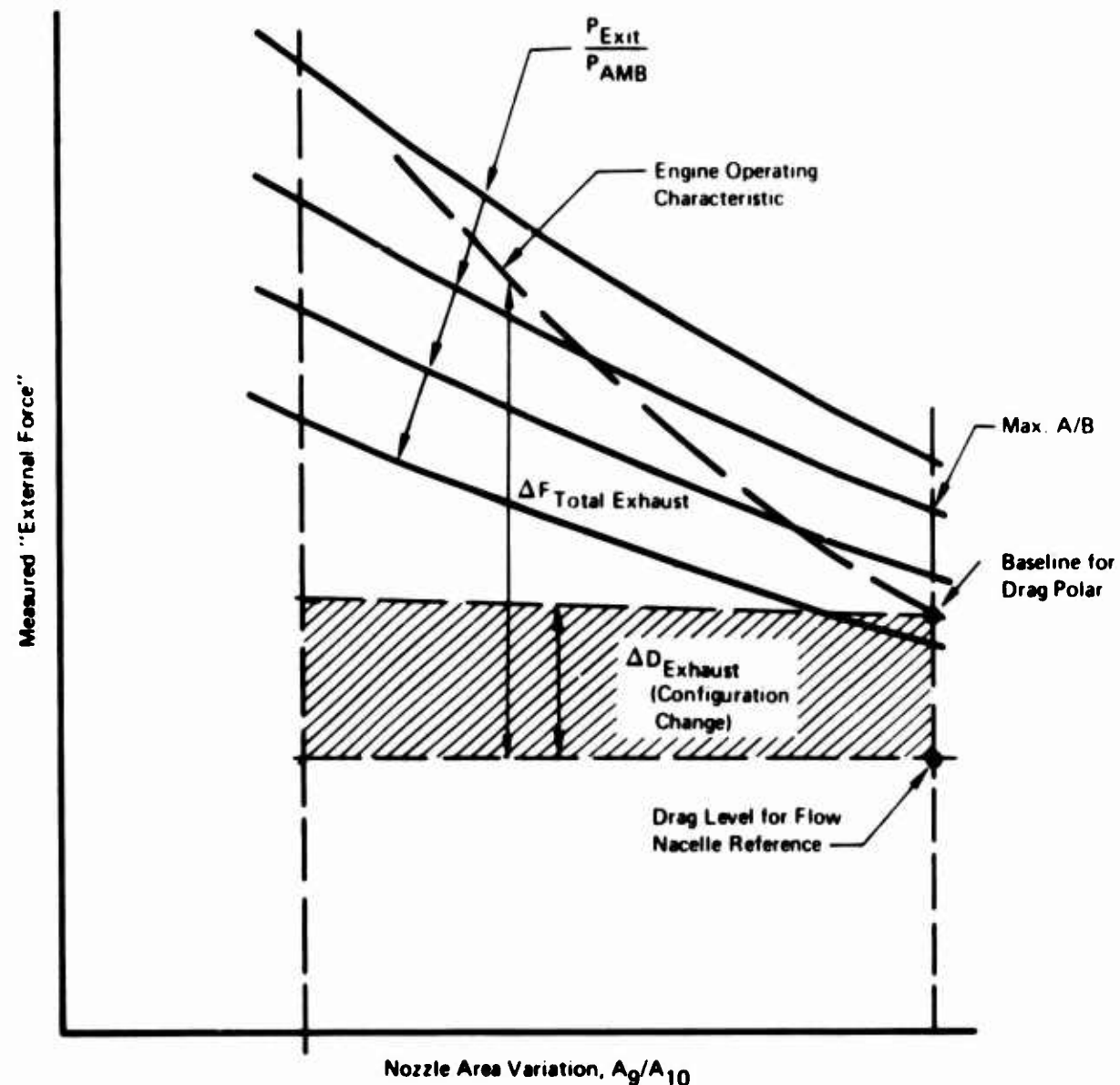
Figure B3. Exhaust System Drag Data Relative to Flow Nacelle Reference

250

APPENDIX B - PROPULSION INSTALLATION BOOKKEEPING METHODS (Continued)

models which are designed to accurately measure external force changes
associated with engine flow and pressure/ratio change rather than on the
airplane drag model which is used to develop the airplane configuration.
Referring to Figure B2, by simply changing the flow nacelle condition
then the configuration change drag increment becomes a part of the total
measured for the airplane, the airplane drag contains the interference
associated with it. Note some small correction to the drag polar may
still be required due to differences in the inlet ramp angle. This in-
crement, however, as indicated in the figure will usually be quite small
and on a scaled basis will not significantly affect the airplane drag
buildup accuracy.

From this brief example it is apparent arbitrary selection of the book-
keeping is not desirable if one strives to meet overall objectives for
airplane system performance prediction accuracy. Rather, selection
should be based on satisfying criteria derived from the overall objec-
tive.

First of all, accuracy of simulation and measurement in the wind tunnel
is required, not only for the propulsion system components, but also for
the airplane system. Thus, all aspects of the propulsion system such
as external geometry and inlet flow that can be obtained with the flow
nacelle simulation shold be attempted on the airplane drag model pro-
vided the reference condition so obtained can be accurately reproduced
on the propulsion model. Secondly, the performance integration defini-
tion and integration procedure must afford as much visibility as possi-
ble of the behavior of the components involved (inlet, nozzle, airframe,
engine) consistent with the accuracy requirement, in order to provide a
basis for comparison, evaluation and development of component technol-
ogy. This is best obtained by selecting references for the inlet, nozzle
and airplane which not only provide a near operating condition but at the
same time are sufficiently general to be adopted for a variety of air-
plane systems and types.

251

APPENDIX B - PROPULSION INSTALLATION BOOKKEEPING METHODS (Continued)

Finally, it is desirable that a single performance integration system can be found that would be applicable throughout the entire airplane development cycle (e.g., from the initial theoretical design through flight test). This will make it possible to trace the evolution and adequacy of the performance prediction of the airplance system relative to component or subsystems performance over the total life of the program.

With these criteria, and review of bookkeeping (References B1 - B9) a performance integration method described below was evolved.

SYSTEM DEFINITIONS

The basis for a complete accounting of forces acting on the airplane system in flight is to a large extent derived from the test techniques used to simulate the propulsion and airframe subsystems. Hence, the performance integration system definitions are derived from a wind tunnel reference based on the following:

1) Engine thrust is established from a static full scale thrust measurement with inlet internal pressure and exhaust system altitude condition reproduced in the test cell.

2) Airplane drag is derived from a reference full airplane force and moment model having a flow nacelle simulator of the propulsion system at a specified mass flow condition.

3) Inlet drag is derived either from the full airplane model or a partial airplane model using a flow nacelle simulation and the same reference condition as 2).

4) Exhaust system drag is derived from a full or partial airplane model having faired over inlets and blown nacelle simulation for jet effects and the same reference condition as 2).

252

APPENDIX B - PROPULSION INSTALLATION BOOKKEEPING METHODS (Continued)

The reference condition is established with the airplane model. It is
a measurable repeatable condition which is accurately duplicated on
the inlet and exhaust nozzle models and serves as the connector for the
experimental buildup of the drag polar for the "baseline" airplane.

The "baseline" for the full scale airplane drag is a specified inlet and
exhaust system geometry and flow condition, wherein the propulsion sys-
tem throttle dependent drag is defined to be zero. All engine throttle
conditions different from the baseline conditions produce a throttle
dependent drag which is charged to the engine net thrust. Thus the
"baseline" definition constitues the bookkeeping definition for splitting
thrust and drag on the full scale airplane.

With these definitions the total force for the airplane in the flight
direction is given by

$$F_{TOTAL} = \overbrace{\sum_{i=1}^{n} F_{N_{R_i}} + \Delta F_{N_{EXH}} + \Delta F_{N_{INL}}}^{F_{N_A}} - \overbrace{D_{REF} - \Delta D_{EXH_{A/P}} - \Delta D_{INL_{A/P}}}^{D_{A/P}} \quad (1)$$

The first three terms on the right side of equation (1) combine to form,
by definition, the propulsion system net thrust, $F_{N_A}$. (There n is the
number of engines on the airplane). The three terms subtracted at the
end combine to form the airframe system drag, which is independent of
engine throttle setting, $D_{A/P}$. All drag variations associated with
changes in throttle setting are included in the inlet and exhaust sys-
tem force increments, $\Delta F_{N_{INL}}$ and $\Delta F_{N_{EXH}}$, respectively.

All of the terms on the right side of equation (1) are defined below.

253

APPENDIX B - PROPULSION INSTALLATION BOOKKEEPING METHODS (Continued)

ENGINE NET THRUST, $F_{N_R}$

The engine net thrust $F_{N_R}$ is defined to be the difference betwee n the gross thrust of the exhaust system in quiescent air, at a specified pressure ratio, and the ram drag on the engine streamtube at the specified flight conditions.  The engine streamtube includes by definition all of the airflow demand at the engine face as well as any secondary airflow captured by the engine inlet and ducted around the engine to the exhaust system.  Any additional airflow captured by the inlet and ducted overboard through bleed or bypass systems, or simply lost by leakage, is not part of the engine streamtube.

The effects of inlet internal performance, i.e., inlet total pressure recovery and steady-state and dynamic distortion, are accounted for in the engine net thrust.  Thus, identical engines in a multi-engine airplane might produce different engine net thrusts because of different inlet installations.

The effects of engine bleed, engine power extraction, and exhaust system internal performance are also accounted for in the engine net thrust.

The term "gross thrust" used in this definition of engine net thrust is the force that would be measured on the balance in a blowing test, in quiescent air, if the inlet air were introduced in a direction normal to the thrust direction.  For most exhaust systems the gross thrust equals the integral of total momentum (axial momentum flux plus pressure increment above ambient) across the nozzle exit plane.  For a plug nozzle it also includes the force (in quiescent air) on the part of the plug extending beyond the exit plane.

The "ram drag" used in this definition is the product of the mass flow in the engine streamtube and the flight velocity.

254

APPENDIX B - PROPULSION INSTALLATION BOOKKEEPING METHODS (Continued)

Thus, the engine net thrust $F_{NR}$ can be determined in an altitude chamber with an available engine using conventional techniques. The effects of inlet internal performance would be simulated, and the measured thrust would be corrected to the proper ram drag for the flight conditions being simulated.

INLET THRUST INCREMENT, $\Delta F_{N_{INL}}$

The inlet thrust increment (inlet throttle dependent drag) is the drag increment between the inlet at its baseline condition and its operating condition. It is derived from:

$$\Delta F_{N_{INL}} = \Delta F_{TOTAL\ INL} - \Delta D_{INL-A/P}$$

where

$\Delta F_{TOTAL\ INL}$ is the total inlet drag measured relative to the reference flow nacelle condition.

$\Delta D_{INL-A/P}$ is the drag increment between the reference flow nacelle and baseline inlet.

The relationship between the various increments thus defined a re shown geometrically in Figure B4. Note that the reference and baseline condition for the inlet is intended to be the same and usually differ only because of difficulty in achieving the full scale baseline condition on the small scale reference airplane model. Thus $\Delta D_{INL-A/P}$ is usually quite small and is used to correct the reference airplane drag to the baseline airplane drag. The inlet baseline condition is defined at each Mach number as shown in Figure B5. These conditions were chosen because:

a)    it corresponds to an accurate reference and measurable condition for the real inlet,

255
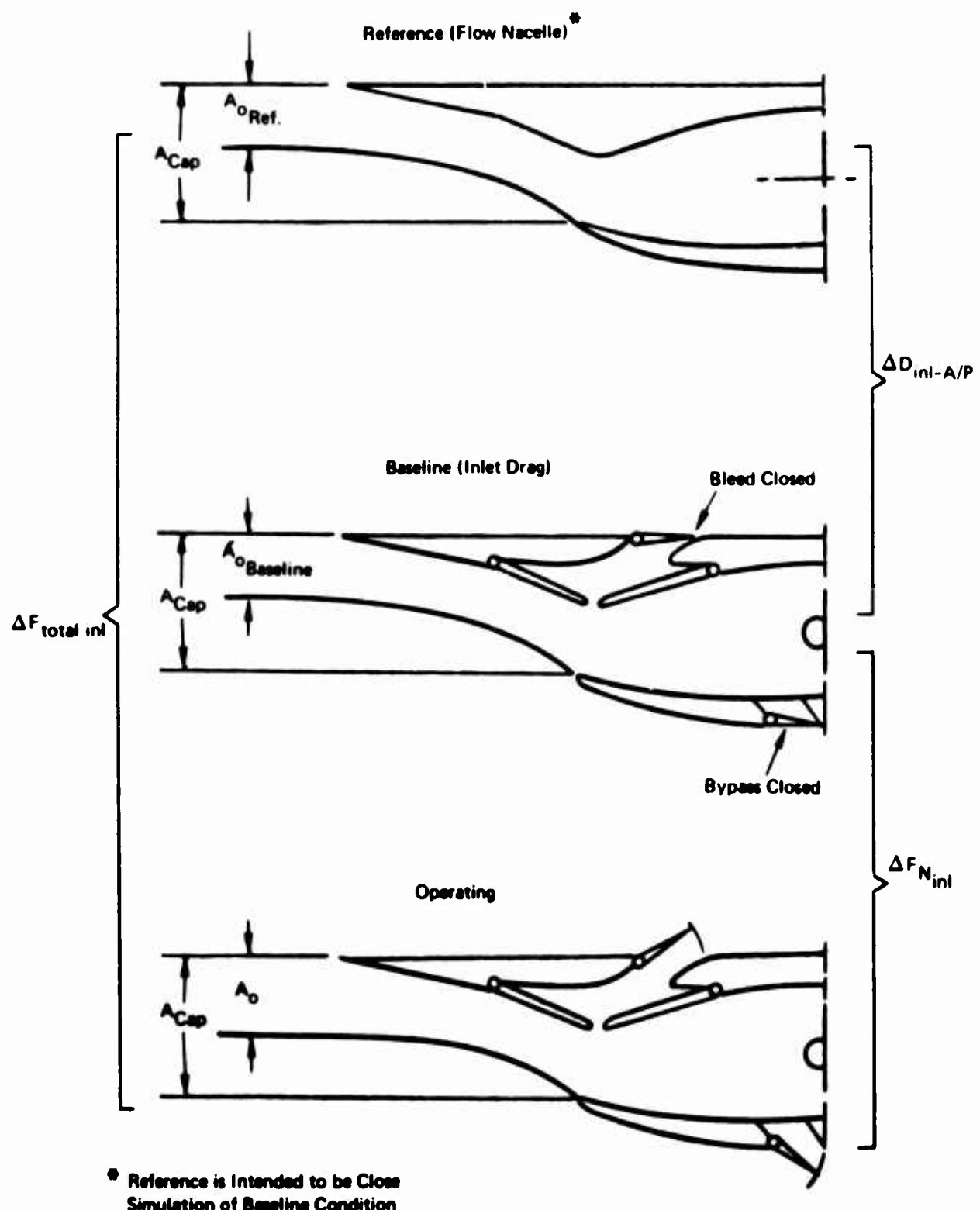
Figure B4. Inlet Drag Definition
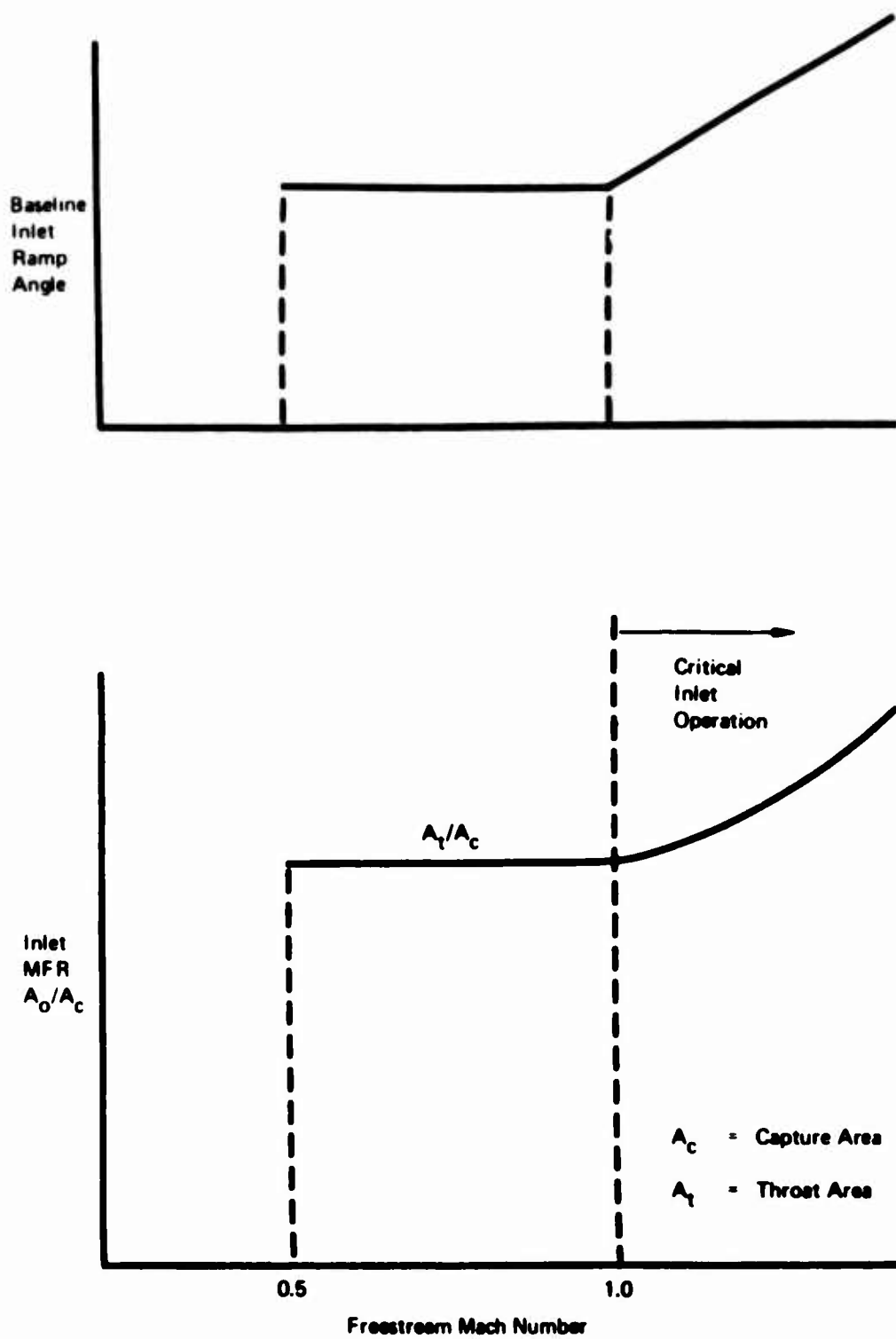
Figure B5.  Baseline Inlet Condition Versus Mach Number

257

b)   it corresponds to a condition when inlet spillage drag is minimum
(i.e., minimum lip separation and therefore less error in scaling),

c)   it is near the operating condition of the inlet (airplane reference
model therefore contains major inlet interference effects).

Figure B6 compares the theoretical buildup of the total inlet d rag with
the experimental definition established above.  The experimental build-
up of the inlet forces from balance and flow nacelle measurements is
defined in Figure B7.  Figures B8 and B9 show the experimental results
schematically for the subsonic and supersonic conditions respectively.

Typical data thus obtained from a full airplane model is shown in Figure
B10.  The corresponding total inlet drag derived from the data is shown
in Figure B11.

EXHAUST SYSTEM THRUST INCREMENT, $\Delta F_{N_{EXH}}$

As for the inlet, the exhaust system thrust increment is the throttle
dependent drag increment between the baseline exhaust system condition
and its operating condition.  It is derived from:

$$\Delta F_{N_{EXH}} = \Delta F_{TOTAL\ EXH} - \Delta D_{EXH\ SYS}$$

where

   $\Delta F_{TOTAL\ EXH}$ is the total exhaust system drag measured relative
   to the reference flow nacelle nozzle condition,

   $\Delta D_{EXH-A/P}$ is the drag increment between the reference and base-
   line nozzle conditions.

The relationship between the various increments thus defined are shown
geometrically in Figure B12.  The difference between the reference and
baseline condition will be greater for the exhaust system because of

$$\Delta F^{*}_{tot\,inl} = \left[ \overbrace{D_{Add} + D_{Press + S.F.}}^{D_{Spill}} + D_{Bleed} + D_{Bypass} \right]_{\substack{Real\ MFR \\ Real\ Geom}} - \left[ \overbrace{D_{Add} + D_{Press + S.F.}}^{D_{Spill}} \right]_{\substack{Ref.\ MFR \\ Ref.\ Geom}} \longleftarrow Theoretical$$

$$\Delta F_{tot\,inl} = \underbrace{\left( \overline{\begin{array}{c} External\ Force \\ For\ Real \\ Inlet\ Condition \end{array}} \right)}_{F_{ext}} - \underbrace{\left( \overline{\begin{array}{c} External\ Force \\ For\ Reference \\ Inlet\ Operation \end{array}} \right)}_{F_{ext_{ref}}} \longleftarrow Experimental$$

Where:

$D_{Bleed}$ and $D_{Bypass}$     =   Drag associated with momentum loss and exit doors of respective systems.

$D_{Add}$     =   Integrated pressure along inlet captured stream tube

$D_{Press + S.F.}$     =   Integrated pressure and skin friction over all surfaces affected by spillage.

\*   If secondary air is removed from inlet or leakage differences occur between model and full scale then these drag losses must be included as well.

*Figure B6.   Total Inlet Drag Buildup*

259

$$F_{Ext} \equiv F_{Bal\ Corr} - D_{Int}$$

$F_{Bal\ Corr}$    $\equiv$ Balance measurement corrected for tare, mounting effects and base pressure on flow nacelle model.

$D_{int}$    $\equiv$ Internal drag of flow nacelle which is difference in momentum and pressure force in flow nacelle exit jet relative to free stream condition of captured stream tube.

*Figure B7.  External Force Determination From Flow Nacelle/Force Balance*
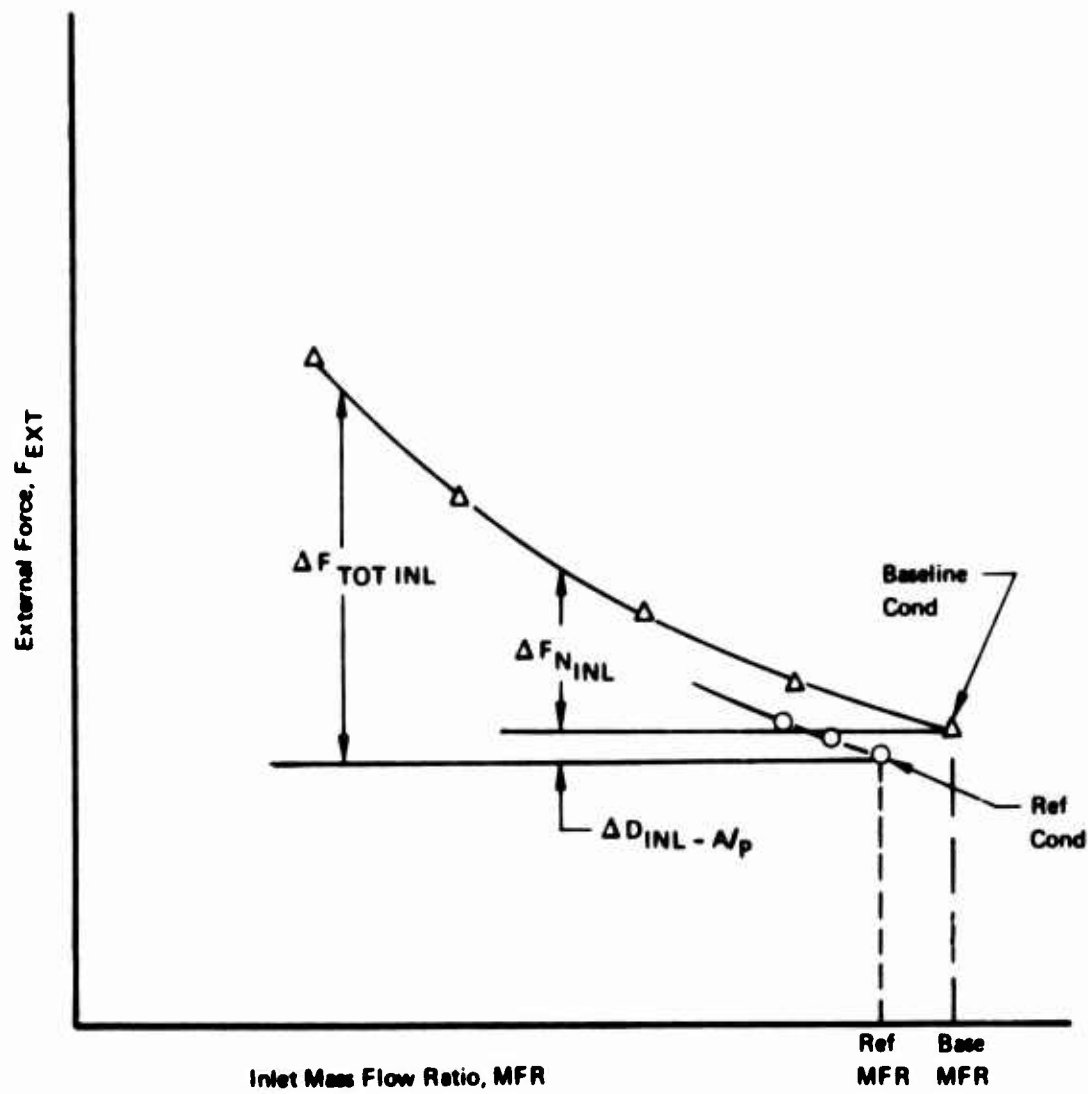
Figure B8. Subsonic Inlet Drag
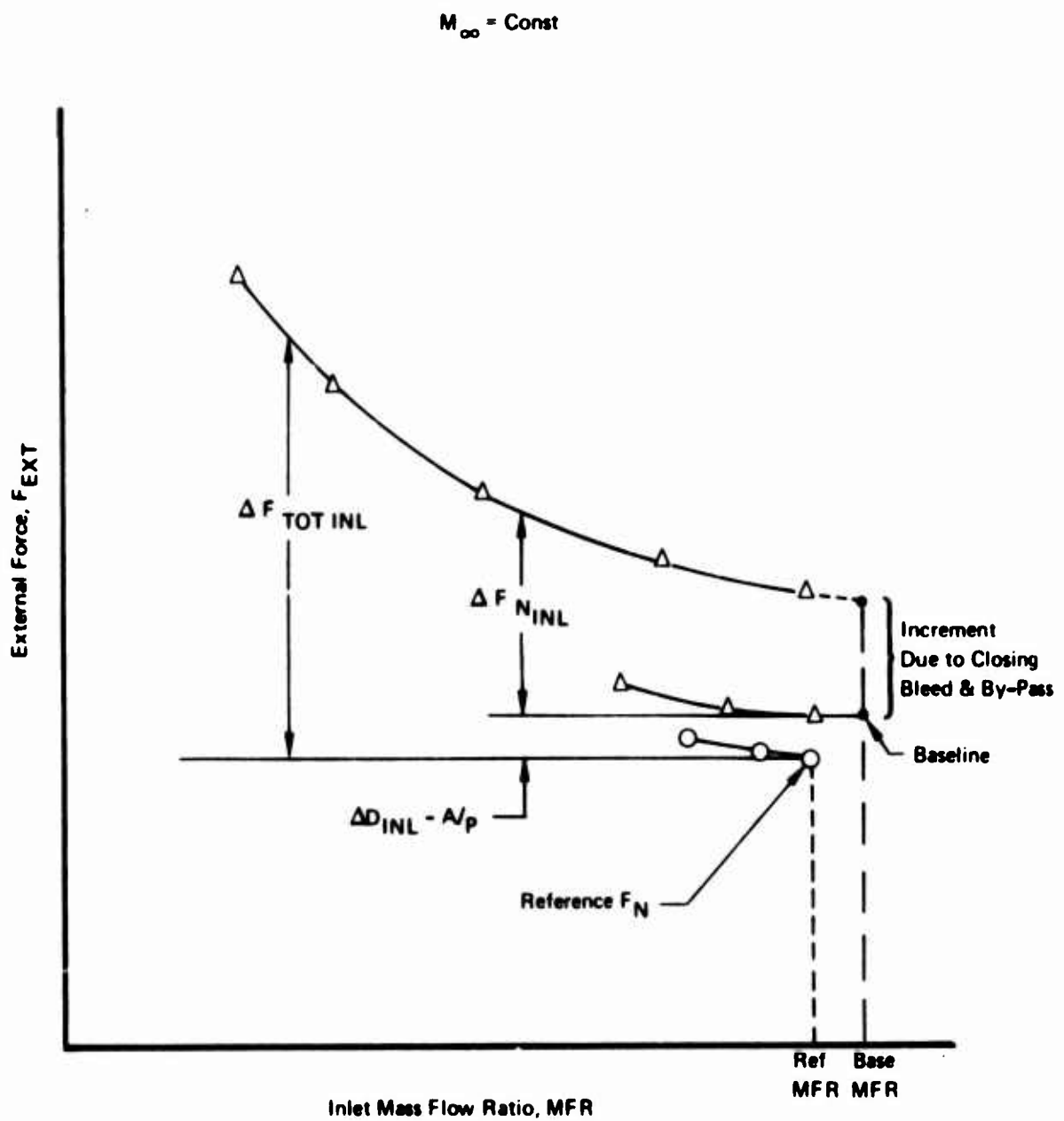
Figure 29. Supersonic Inlet Drag
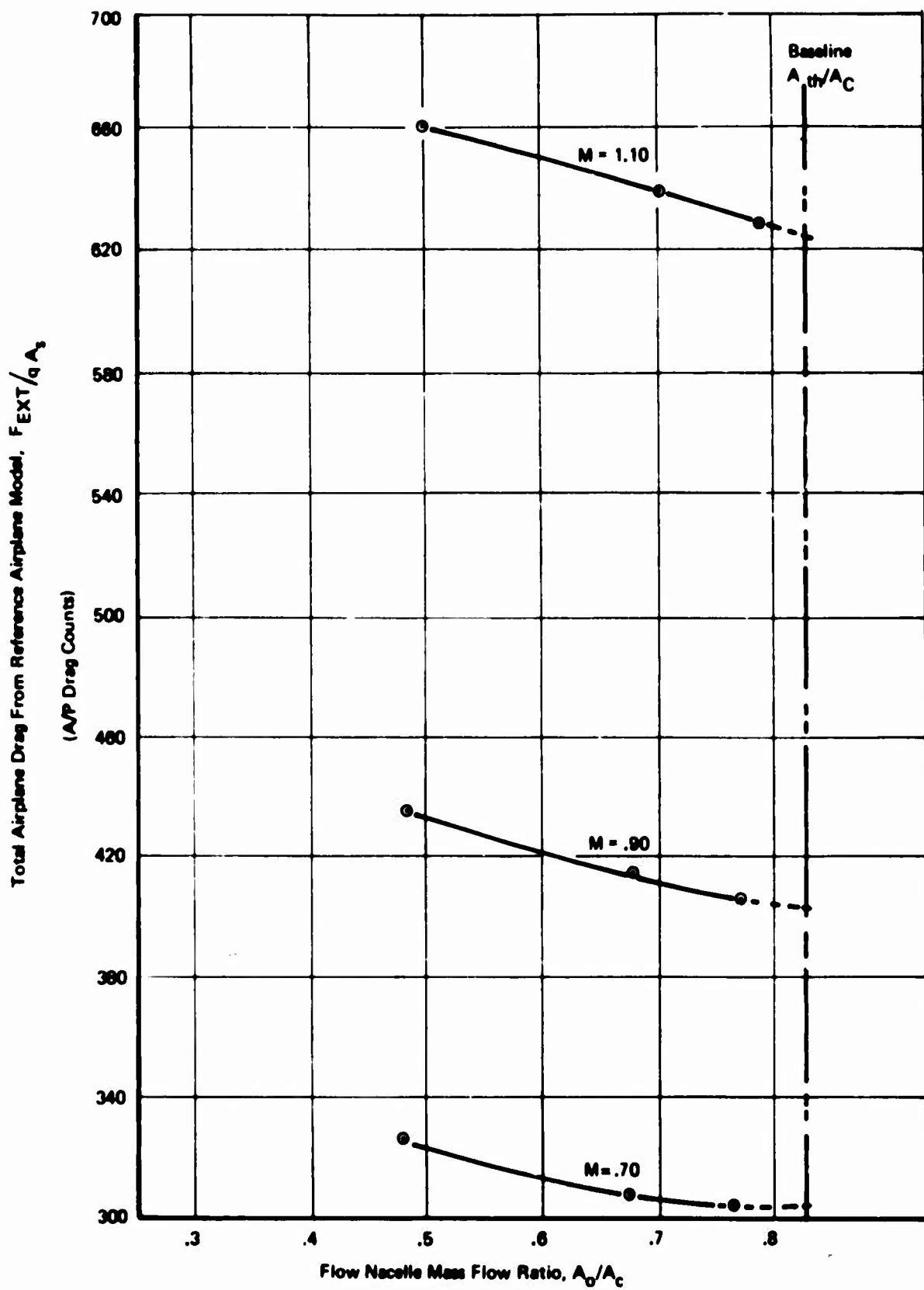
Figure B10. External Force Measurement; Airplane Versus
Mass Flow For Full A/P Model

263

$$\frac{A_{th}}{A_c} = .85$$
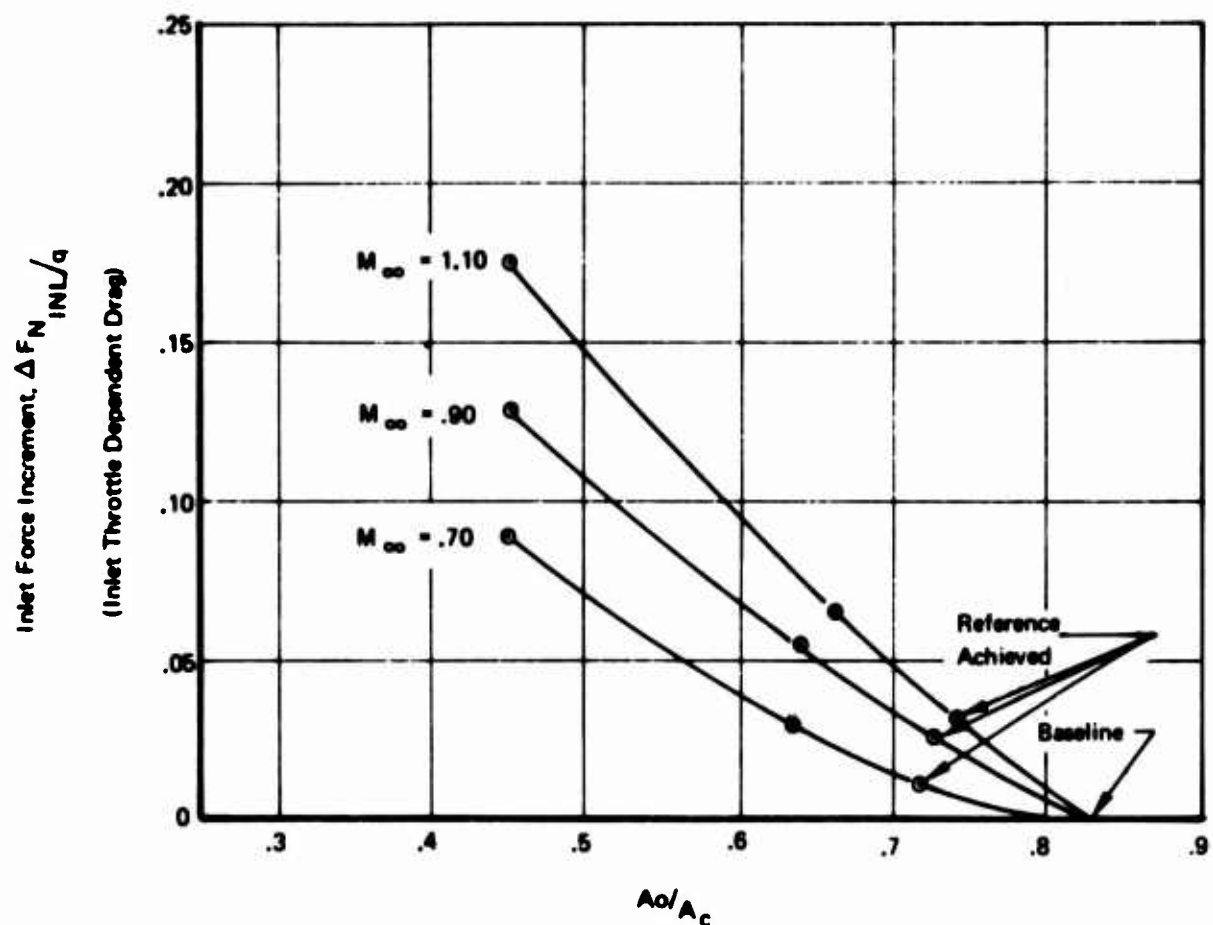


Figure B11. Inlet Data Derived from Full Model Measurements

264

Reference

$D_{Ref}$
Corresponds
to this
Condition

Ram Pressure *
Ratio

$\Delta D_{Exh}$
Sys

Baseline

Real
(Baseline)
* Pressure Ratio

Exhaust
System
Total

Airplane
Drag Polar
Corresponds
to this
Condition

$\Delta F_{tot\ exh}$
Measured

Operation
(Throttle-Dependent)

$\Delta F_{N_{Exh}}$
Sys

Real
* Pressure Ratio
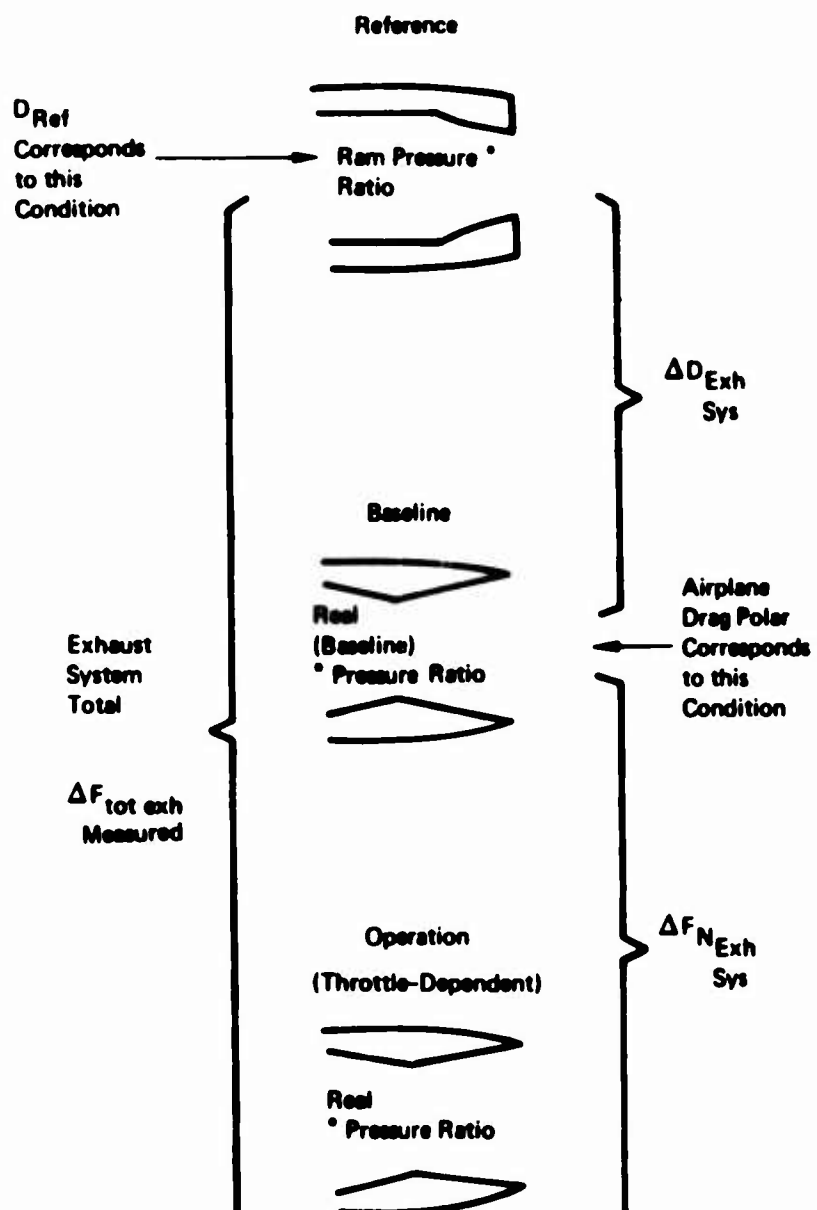
* Pressure Ratio = Jet Exit Static to Free Stream Pressure Ratio

*Figure B12. Exhaust System Drag Definition*

265

inability to simulate both inlet and exhaust system baseline condition simultaneously with a flow nacelle. Thus, $\Delta D_{EXH-A/P}$ is the airplane drag correction bridging the gap between the flow nacelle nozzle and real baseline nozzle. The baseline condition selected for the nozzle was maximum afterburning external geometry and a jet exit static pressure ratio of 1.0. This allowed duplication of real external nozzle geometry while at the same time providing sufficient base area for maximum inlet mass flow requirements.

The theoretical buildup of the exhaust system drag is shown in Figure B13 compared to the experimental definition. A schematic of the blown nacelle installation used in the experimental buildup is shown in Figure B14. The blown nacelle is alternately operated with tunnel off (wind-off static thrust) and with wind tunnel on at desired Mach number condition. The measurements thus obtained are combined as shown in Figure B15 to establish the total exhaust system drag. Figure B16 graphically portrays the results. Typical data is shown in Figure B17.

AIRPLANE SYSTEM DRAG, $D_{A/P}$

The airplane drag, $D_{A/P}$, is established for the defined inlet and nozzle baseline condition. It is derived by scaling the model data to full scale. It is made up of these terms, namely:

$$D_{A/P} = D_{REF} + \Delta D_{INL-A/P} + \Delta D_{EXH-A/P}$$

where the inlet and nozzle increments are derived from the propulsion wind tunnel models or theoretical buildup and $D_{REF}$ is derived by scaling the external force measurements of the reference airplane wind tunnel model. Figures B18 and B19 illustrate the buildup to the full scale baseline airplane drag polar from model scale data for both the subsonic and supersonic case, respectively.

APPENDIX B - PROPULSION INSTALLATION BOOKKEEPING METHODS (Continued)

Note that the flow nacelle reference inlet spillage is reflected in the shape of the measured drag polar which is unchaged in the scaling to full scale. This is a prime reason for attempting to reduce the increment $\Delta C_{D_{INL-A/P}}$ that is added to correct the drag polar from the reference to baseline condition.
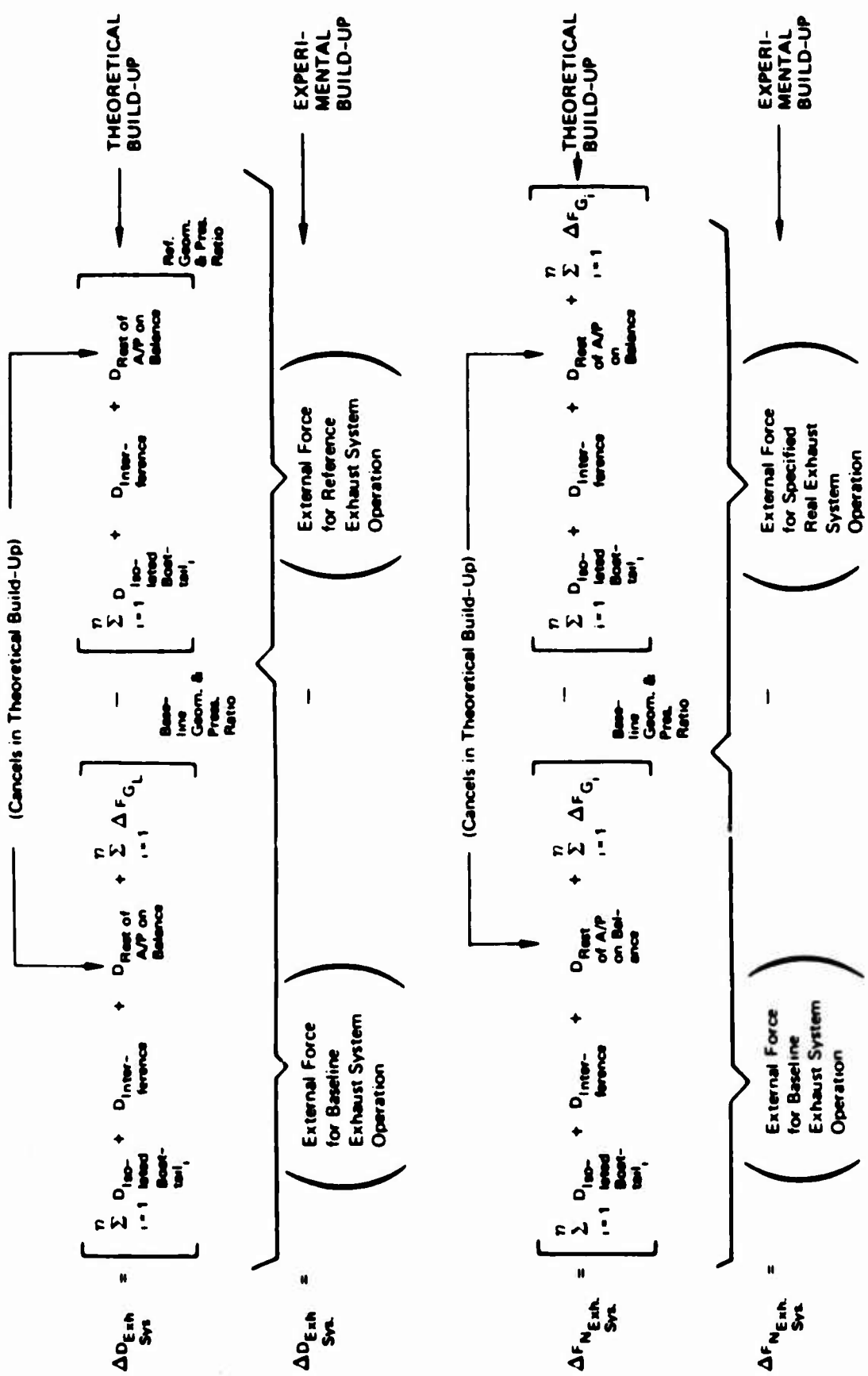
Figure B13. Exhaust System Drag Buildup

268

Reference
Nozzle

Total Pressure
Rake

Choke Plates

Inlet
Fairing

Air
Plenum

Floor Strut

Test
Nozzle

Tunnel Floor

High Pressure
Air Supply

ASME Flow Nozzle

Tunnel Balance
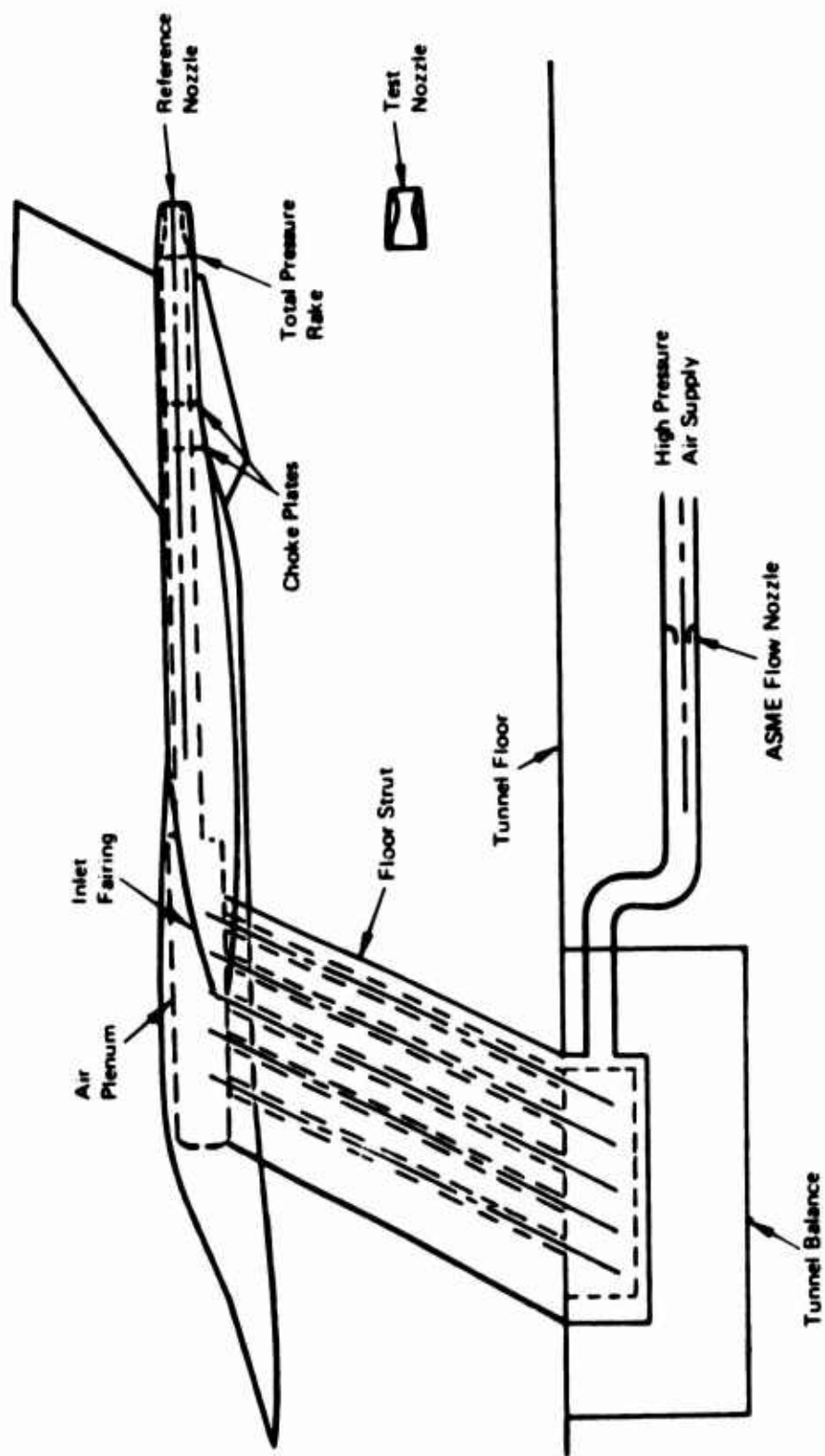
*Figure B14.  Schematic of Blown Nacelle Model Using Single Balance*

- Flow Nacelle Reference Nozzle Installed and Operated

$$F_{Ext\ Ref.} = \left[ \frac{\dot{M}_{W.O.}}{\dot{M}_{Static}} \quad \bar{F}_{\substack{Bal \\ Cor}}\ (\text{Wind-Off}) - F_{\substack{Bal \\ Cor}}\ (\text{Wind-On}) \right]_{\substack{Ref. \\ Noz.}}$$

- Replace Flow Nacelle Nozzle with Real Nozzle

$$F_{Ext\ Test} = \left[ \frac{\dot{M}_{W.O.}}{\dot{M}_{Static}} \quad \bar{F}_{\substack{Bal \\ Cor}}\ (\text{Wind-Off}) - F_{\substack{Bal \\ Cor}}\ (\text{Wind-On}) \right]_{\substack{Test \\ Noz.}}$$

- Total External Force Increment

$$\Delta F_{Tot\ Exh} = F_{Ext\ Test} - F_{Ext\ Ref.}$$

Note: $\quad C_{V_{Static}} = \bar{F}_{\substack{Bal \\ Cor}}\ (\text{Wind-Off}) / \dot{M}_{Static} \times V_{Ideal}$

*Figure B15.  Experimental Buildup From a Single Balance Measurement
(Blown Nacelle/Force Balance)*
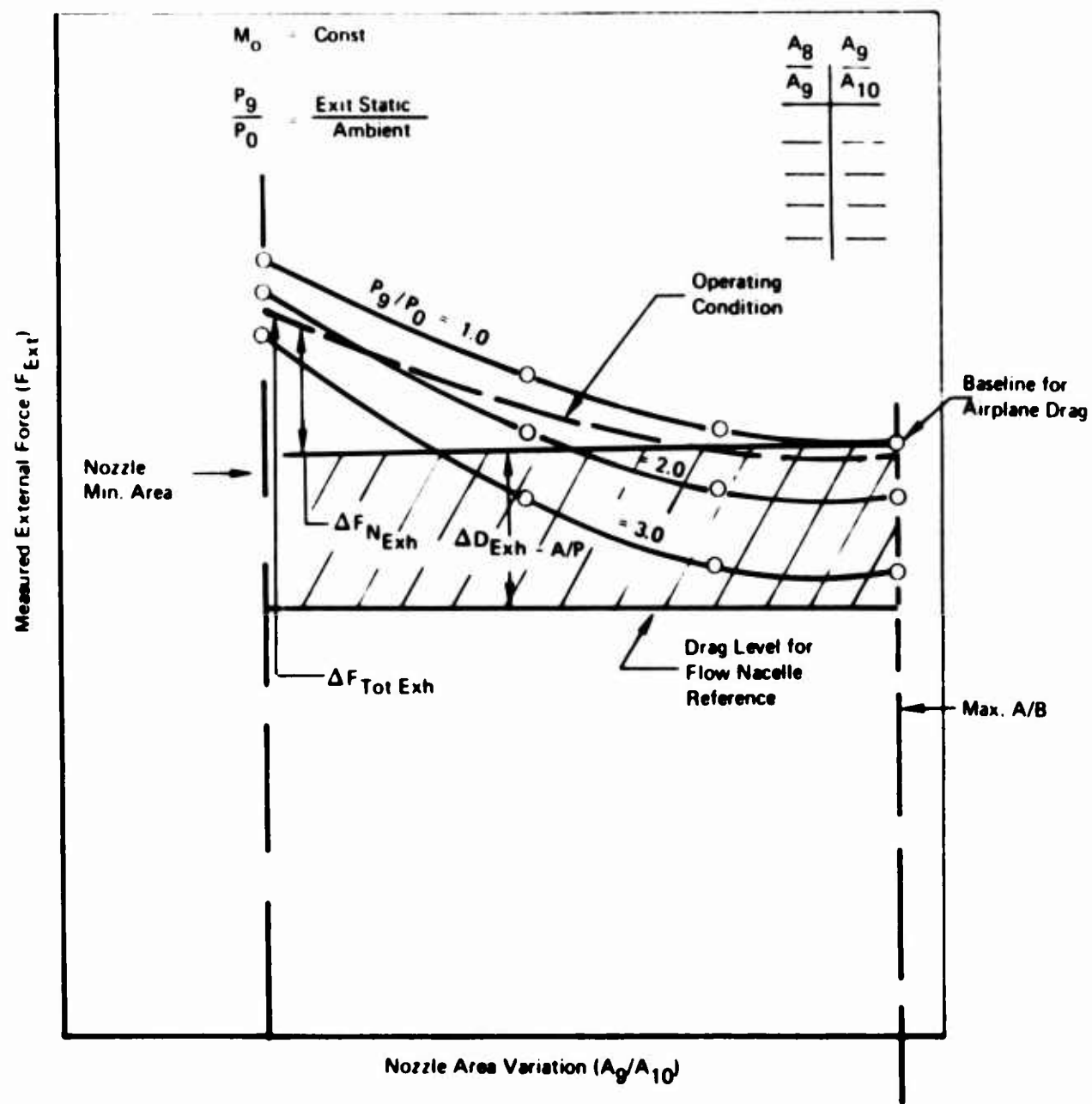
*Figure B16.  Exhaust System Drag Schematic*

271
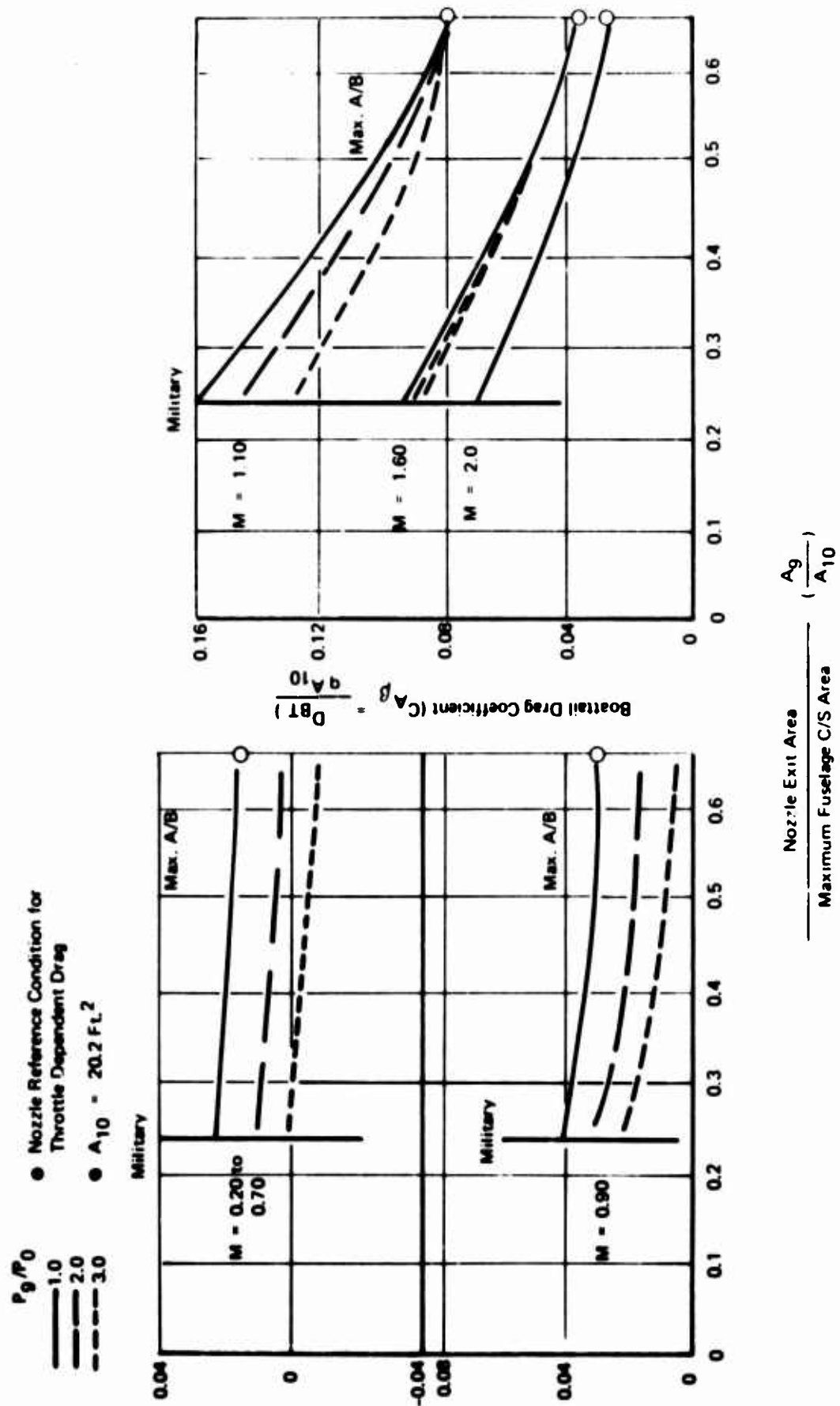
Figure B17. Exhaust System Drag Data

# SUBSONIC AERODYNAMIC DATA
## WIND TUNNEL DATA
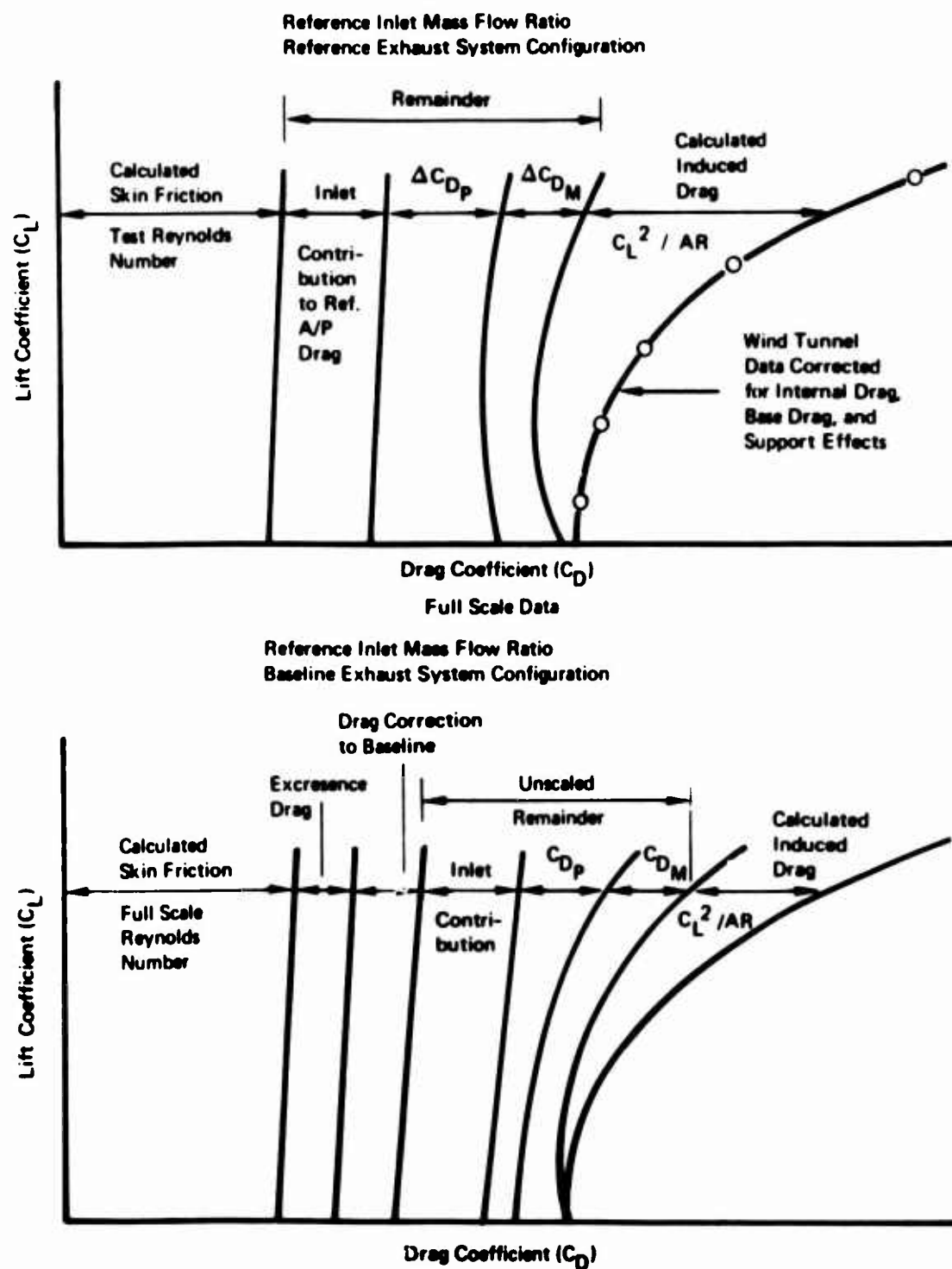


Figure B18. Subsonic Drag Polar Buildup for Baseline Airplane
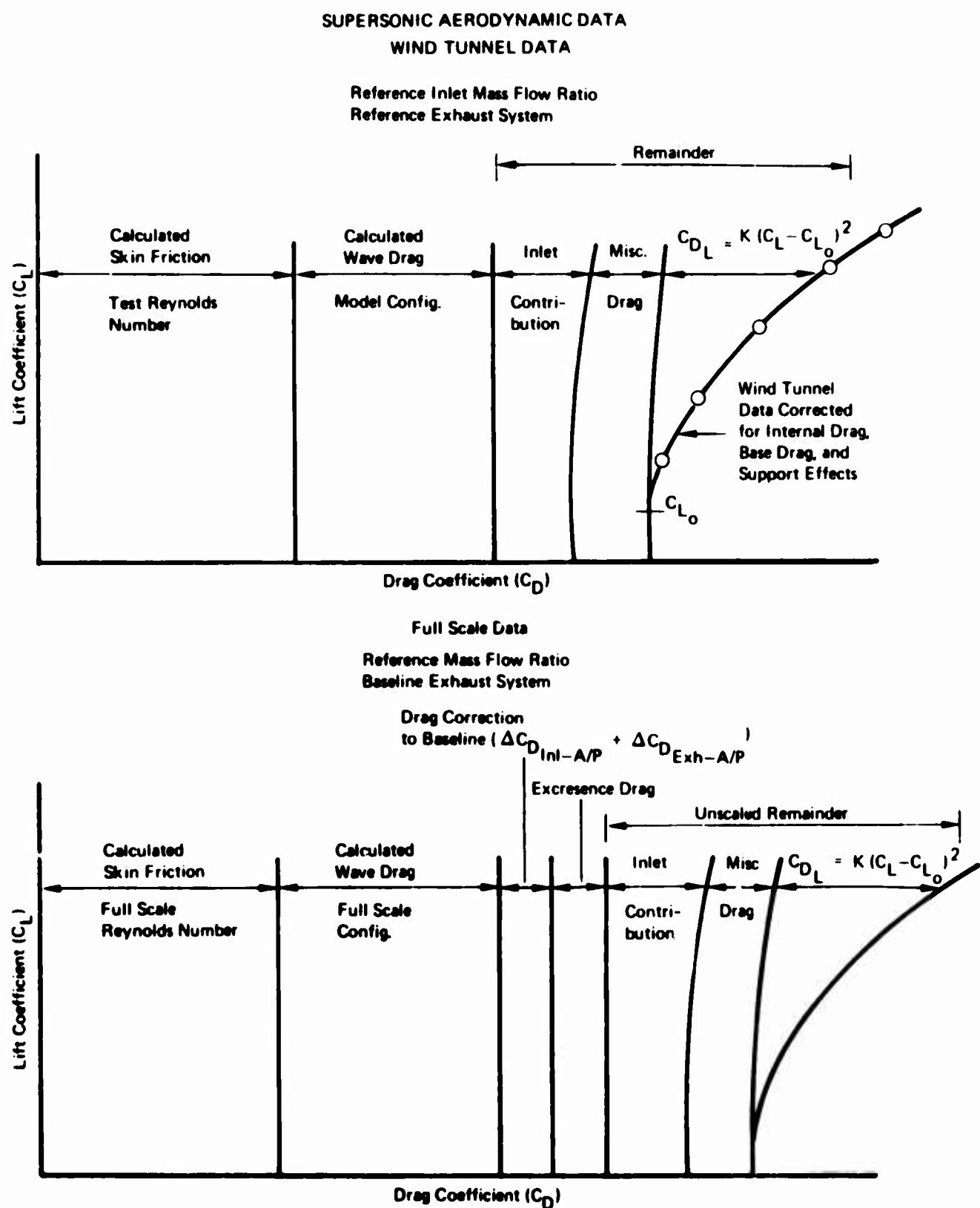
Figure B19. Supersonic Drag Polar Buildup for Baseline Airplane

# APPENDIX B REFERENCES

(B1.)  Johnson, R. H., et al., "Propulsion System Integration and Test Program (Steady State) Summary:  Part I, Integration Technique and Test Activities", AFAPL-TR-69-36, Part I, Air Force Aero Propulsion Laboratory, June 1969.

(B2.)  Schreiber, L. H., "A Plan for Bookkeeping of the Propulsion and Aerodynamic Elements of Airplane Performance", presented at the Airframe Propulsion Compatibility Symposium at Miami Beach, June 24-26, 1969.

(B3.)  Anderson, R. D., Lee, C. C., and Martens, R. E., "A Thrust/Drag Accounting Procedure Applicable to Engine Cycle Selection Studies", MDC A1197, McDonnell Douglas Corporation, June 1971.

(B4.)  Harner, P., (Naval Air Systems Command), Presentation at AIAA Sixth Propulsion Joint Specialist Conference, San Diego, June 15-19, 1970.

(B5.)  Harner, P., Private Communication, August 20, 1970.

(B6.)  Armstrong, R. S., and Miller, S. R., "Subsonic Aerodynamic Performance of Nozzle Installations in Supersonic Airplanes", presented at the AIAA Third Propulsion Joint Specialist Conference, Washington D.C., July 1967.

(B7.)  Migdal, D., Miller, E. H. and Schnell, W. C., "An Experimental Evaluation of Exhaust Nozzle/Airframe Interference", AIAA Paper No. 69-430, presented at the Fifth Propulsion Joint Specialist Conference, Colorado, June 9-13, 1969.

(B8.)  Chamberlain, D., "Measurement of Drag from Interaction of Jet Exhaust and Airframe," Journal of Aircraft, Volume 6 No. 2, March-April, 1969.

(B9.)  Migdal, D. and Greathouse, W. K., "Optimizing Exhaust-Nozzle/ Airframe Thrust Minus Drag", SAE Paper No. 680294, presented at Air Transportation Meeting, New York, April 29 - May 2, 1968.

## APPENDIX C - AERODYNAMIC ANALYSIS TECHNIQUES

Configuration aerodynamic design and analysis is carried out using the "Aerodynamic Design and Analysis System for Supersonic Aircraft," by W. D. Middleton, et al., and documented in a NASA-contractor report, NASA CR 2520, dated 1975. This is an integrated system of computer programs that has been developed for the design and analysis of supersonic configurations. The system consists of a main program and seven modules as shown in Figure C1. All the aerodynamic programs use common geometry inputs as defined via the geometry module. Skin friction is computed assuming flat plate turbulent flow. Wave drag can be calculated using a near-field theory (integrates surface pressures) or the far-field theory (supersonic area rule concepts). The near-field theory is used for obtaining surface pressures due to thickness effects. The far-field method is used for wave drag coefficient estimates and wing-body optimization using area rule concepts. The drag-due-to-lift (analysis) and the wing design modules use "Mach-box" rectilinear elements in a linear theory solution. Both drag-due-to-lift modules have a pressure limiting feature which, when combined with the thickness pressures from the near-field wave module, can limit wing surface pressures as the angle of attack increases or not allow the angle of attack to increase if a specified value of pressure coefficient is encountered.

Drag polars are estimated using superposition, i.e. all drag components are additive. In the absence of wind tunnel data, the drag polars are estimated using the following components.

$$C_{D_{Total}} = C_{D_{Wave}} + C_{D_{Friction}} + C_{D_{Form}} + C_{D_{Interference}} + C_{D_{Mach}}$$
$$+ C_{D_{Excrescence}} + C_{D_{Inlet/Nozzle}} + C_{D_{Misc.}} + C_{D_{Lift}} + C_{D_{Trim}}$$

where

$C_{D_{Wave}}$ = Total configuration wave drag from the far-field wave drag module.

276

## APPENDIX C - AERODYNAMIC ANALYSIS TECHNIQUES

$C_{D_{Friction}}$    = Skin friction using the skin friction module.

$C_{D_{Form}}$    = Drag associated with thickness effects, empirical estimates. (subsonic only)

$C_{D_{Interference}}$    = Interference drag between components, empirical estimates. (subsonic only)
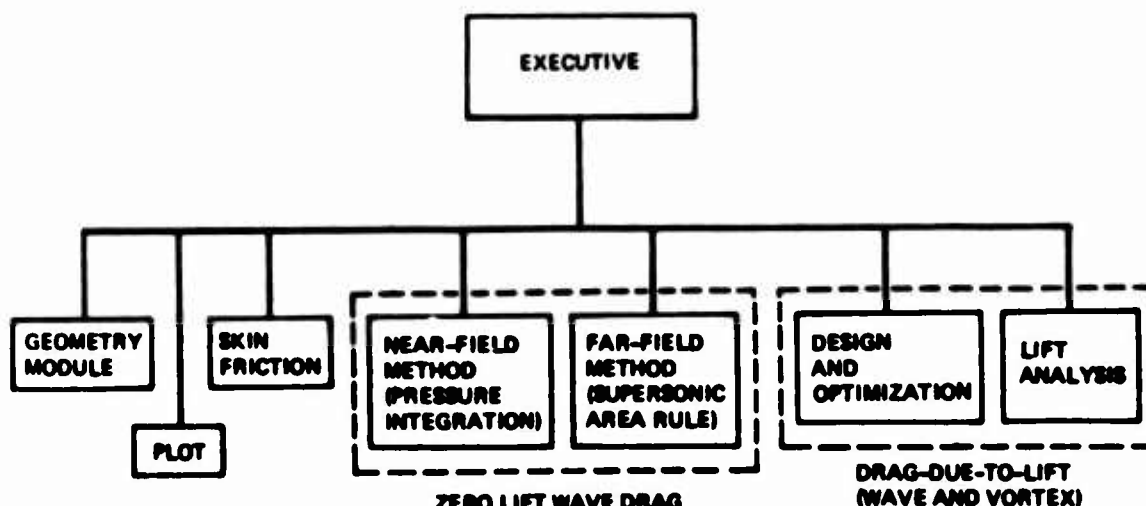


Figure C1. *Integrated Supersonic Design and Analysis System*

$C_{D_{Mach}}$    = Drag increase due to Mach number effects at high subsonic Mach numbers. (subsonic only)

$C_{D_{Excrescence}}$    = Drag, in addition to skin friction, which accounts for surface irregularities, small protuberances, gaps, mismatches, leakage, etc. Based on total wetted area and Mach number.

$C_{D_{Inlet/Nozzle}}$    = Drag associated with the inlet and nozzle details (diverter and aft-body closure effects), empirical estimates.

APPENDIX C - AERODYNAMIC ANALYSIS TECHNIQUES

$C_{D_{Misc.}}$     = Drag associated with small but discrete items
                      such as antennas, beacons, fuel vents, weapons,
                      etc.; based on empirical data.

$C_{D_{Lift}}$      = Drag-due-to-lift (including parasite drag sub-
                      sonically) includes leading edge suction when
                      applicable. Supersonically, from the lift ana-
                      lysis module, subsonically, emperical methods,
                      based on wind tunnel and flight test data.

$C_{D_{Trim}}$      = Drag-due-to-lift associated with trimming the
                      airplane to a given c.g. position.

Power sensitive drag items are included in the engine data. For this
study only, the inlet/nozzle reference drags were allowed to remain in
the engine data.

The LES configuration representation in the supersonic design and ana-
lysis program is shown in Figure C2. The open nose results from in-
cluding the inlet streamtube in the body area distribution. The wing
definition shown in Figure C3 begins at Y = 1.5 ft. and includes the
wing tip. Cross-sectional area inside of Y = 1.5 and area due to the
wing-body fairing extending outboard of Y = 1.5 ft. is included in the
fuselage area distribution. Body area distribution shown in Figure C4
are input as circular sections including the inlet streamtube area.
This representation of the configuration was used for the wave drag cal-
culations (far-field method). For the drag-due-to-lift module, body
camber and wing camber were added and the inlet streamtube area was re-
moved to better approximate the fuselage upwash field. Supersonic trim
drag data were generated using the trailing edge flap option in the
drag-due-to-lift (analysis) module. Configuration geometry inputs to
the supersonic design and analysis program are shown in Figures C5 and
C6.

278
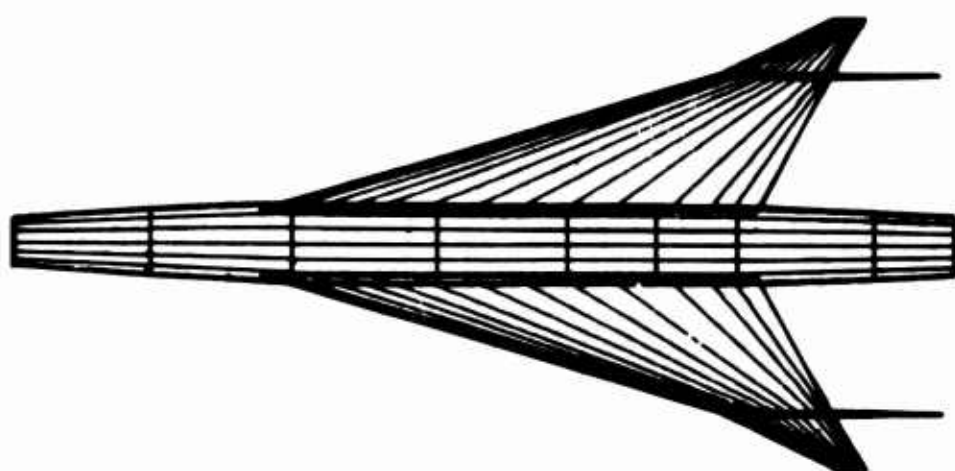
Figure C2. LES Far-Field Wave Drag Computer Representation

279
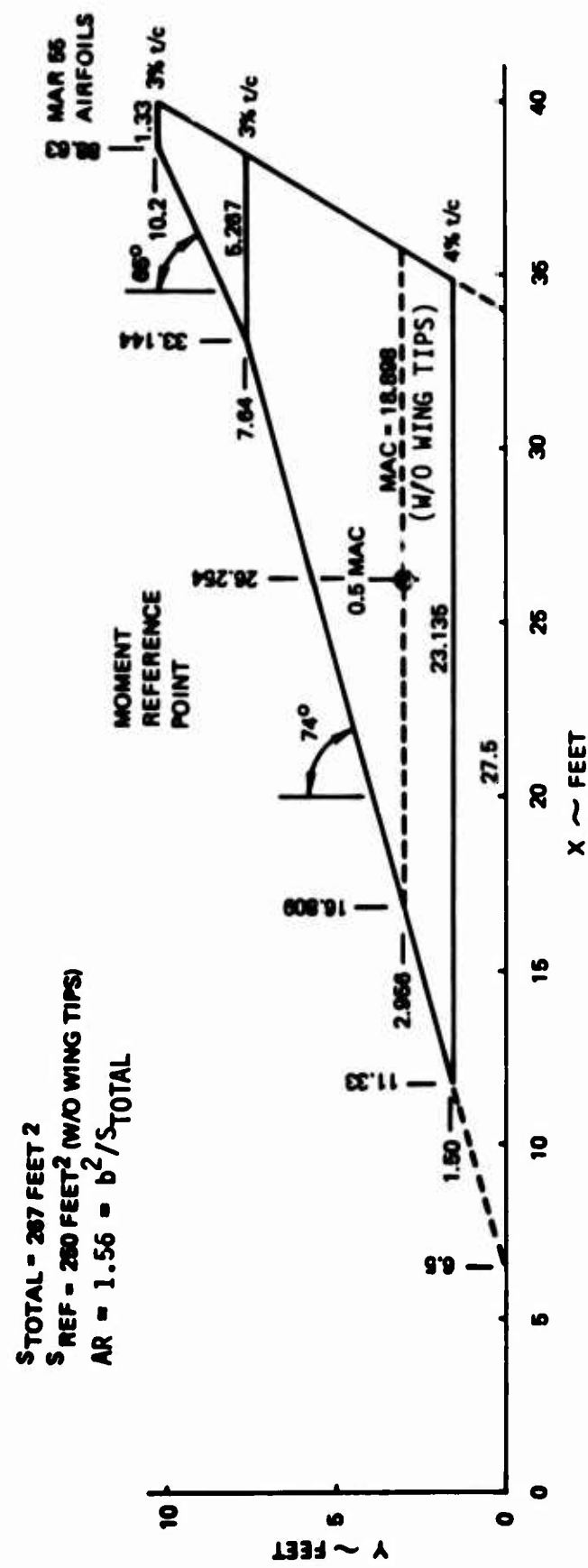
Figure C3. -212 (-213) Reference Plan Form Geometry

280
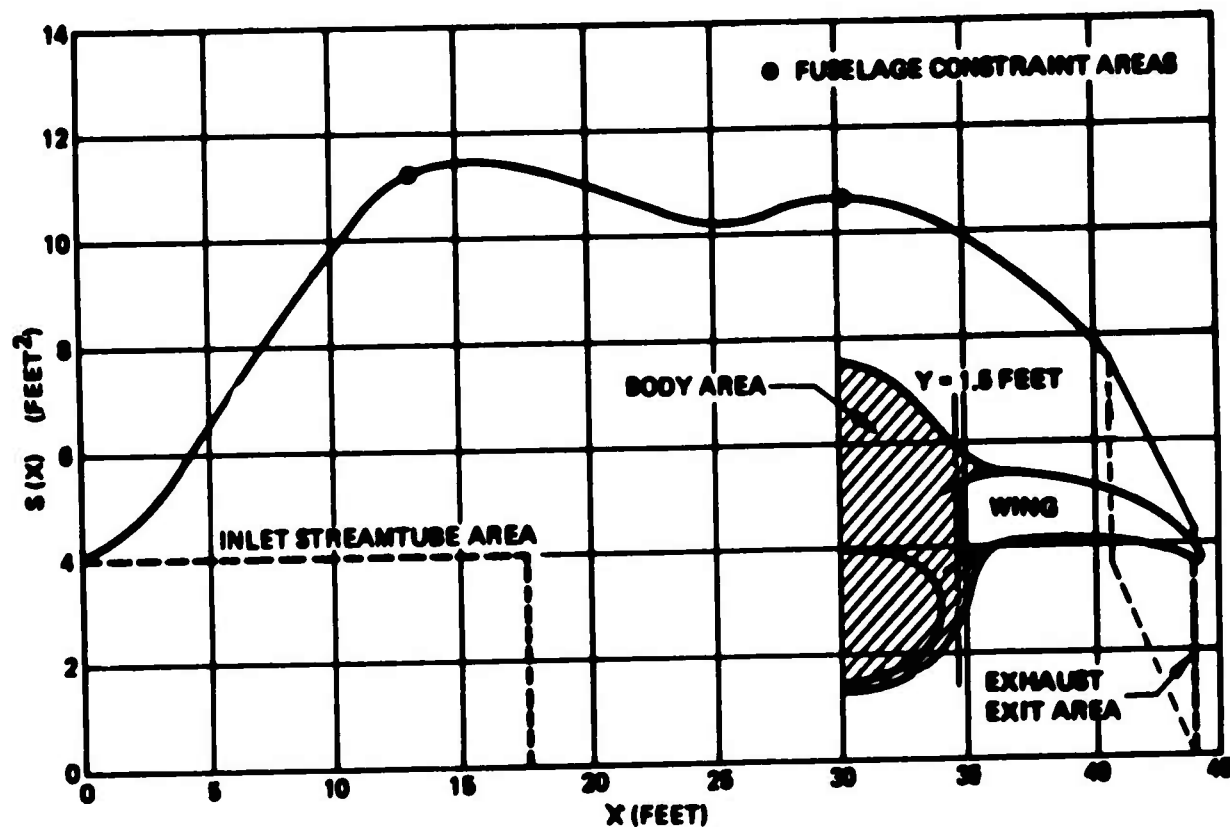
Figure C4. Body Area Distribution

281

```
GEOM NEW
-212 CONFIGURATION REPRESENTATION  WING-BODY-FIN  NO CAMBER  BODY INCLUDES ACAP
   1 -1 -1     1         3 17  1  9  9                              1  4
250.    18.9   26.26                                               REF GEOM
0.      .2     .6      2.     5.    10.    16.    22.    30.    40.  X/C
50.     60.    70.     82.    90.   95.    100.                      X/C
11.73   1.5    0.      23.135                                        W1
33.144  7.64   0.      5.267                                         W2
38.63   10.2   0.      1.33                                          WING TIP
0.      .255   .449    .761   1.048 1.347  1.578  1.734  1.880  1.984 T/C-55-4
2.      1.908  1.713   1.274  .823  .472   .073                      T/C-55-4
0.      .191   .337    .571   .786  1.010  1.184  1.300  1.410  1.488 T/C-55-3
1.5     1.431  1.285   .956   .617  .354   .073                      T/C-55-3
0.      .191   .337    .571   .786  1.010  1.184  1.300  1.410  1.488 T/C-55-3
1.5     1.431  1.285   .956   .617  .354   .073                      T/C-55-3
0.      6.5    13.2    19.8   26.0  30.2   34.0   40.3   44.0        FUSE X
                                                                    FUS Z
4.0     7.45   11.19   10.94  10.15 10.60  10.15  7.75   4.1        212 OPTA
33.144  7.64   0.      7.83   40.77 7.64   3.58   2.5               FIN
0.      32.5   67.5    100.                                          FIN X/C
0.      1.5    1.5     0.                                            FIN T/C
FFWD
-212 WING- BODY-FIN   MACH 1.8
1.      1.     0.      1.     0.
   1    1.8    50.     36.    0.                                    4
END
NFWD
-212 CONFIGURATION  NEAR FIELD THICKNESS PRESSURES
0.                                                                  3
-1.     1.8                   20.    11.                            4
1.5            -1.                                                  5
0.      2.     4.      6.     8.    10.    12.    14.    16.    18.  7
20.                                                                 7
FND
PLOT
-212 CONFIGURATION
1.      1.     0.      1.
X Z                                              5.0  ORT
Y Z                                              5.0  ORT
X Y                                              5.0  ORT
END
```

Figure C5.  Computer Inputs for -212 (-213) Far-Field Wave Drag

```
GEOM NFW
-212 DEFINITION FOR DRAG-DUE-TO-LIFT DATA  RODY CAMBERED  POINTED NOSE
  1 -1 -1                   3 14  1  9 17                        CODE
250.    10.9   26.26                                            REF DATA
0.      5.     10.    16.    22.    30.    40.    50.    60.    70.    X/C
82.     90.    95.    100.                                      X/C
11.73   1.5    1.729  23.139                                   W1
33.144  7.64   -.16   5.267                                    W2
38.63   10.2   0.     1.35                                     W3
0.      1.040  1.347  1.570  1.734  1.88   1.984  2.    1.908  1.713  T/C-1
1.274   .029   .472   0.                                       T/C-1
0.      .786   1.010  1.184  1.300  1.410  1.488  1.500  1.431  1.285  T/C-2
.956    .617   .354   0.                                       T/C-2
0.      .786   1.010  1.184  1.300  1.410  1.488  1.500  1.431  1.285  T/C-3
.956    .617   .354   0.                                       T/C-3
0.      4.     7.3    10.    11.5   13.2   16.0   18.7   22.5   24.3   FUS X
26.0    30.2   32.    34.    37.    40.3   44.                  FUS X
1.6     1.75   1.9    2.1    2.18   2.25   2.2    1.45   .5     .3     FUS Z
.15     0.     -.05   -.13   -.25   -.35   -.35                 FUS Z
0.      1.85   3.8    5.75   6.4    6.85   7.1    6.85   6.1    5.92   FUS A
5.9     6.3    6.25   5.85   4.87   3.5    .1                   FUS A
NFWD
M81.8 THICKNESS PRESSURES    -212 CONFIGURATION
0.                                                             3
-1.     1.8                  20.    11.                        4
1.5            -1.                                             5
0.      2.     4.     6.     8.     10.    12.    14.    16.    18.    7
20.                                                            7
END
ANL2
M81.8 POLARS   PRESSURE LIMITED  FLAP DEFLECTED  67.9 DEGREES
1.                                                             3
12.     12.    1.                   20.    5.                  4
1.      12.                                                    5
1.5                   1.                                       6
1.8     1.                                                     8
0.      5.     10.    20.    30.    40.    50.    60.    70.    80.    X/C
90.     100.                                                   X/C
0.      15.    20.    30.    40.    50.    60.    70.    74.9   80.    2Y/B
90.     100.                                                   2Y/B
0.      .84    1.24   1.41   1.29   .74    .37    -.10   -.52   -.37   211RL.15
-.27    0.                                                     211RL.15
0.      .84    1.24   1.41   1.29   .74    .37    -.10   -.52   -.37   211RL.15
-.27    0.                                                     211RL.15
0.      .847   1.316  1.596  1.419  1.039  .608   .224   -.051  -.182  .20 -211
-.160   0.                                                     .20 -211
0.      .862   1.460  1.938  1.937  1.699  1.343  .951   .586   .292   .30 -211
.095    0.                                                     .30 -211
0.      .872   1.525  2.096  2.206  2.048  1.721  1.337  .930   .550   .40 -211
.236    0.                                                     .40 -211
0.      .781   1.494  2.138  2.351  2.244  1.981  1.592  1.177  .737   .50 -211
.341    0.                                                     .50 -211
0.      .694   1.344  2.130  2.398  2.400  2.173  1.827  1.407  .919   .60 -211
.446    0.                                                     .60 -211
0.      .647   1.204  2.074  2.472  2.478  2.287  1.933  1.512  1.035  .70 -211
.526    0.                                                     .70 -211
0.      .565   1.03   1.75   2.13   2.17   2.00   1.70   1.33   .90    .749-211
.465    0.                                                     .749-211
0.      .320   .610   1.102  1.383  1.440  1.396  1.259  1.021  .728   .80 -211
.385    0.                                                     .80 -211
0.      .184   .350   .627   .851   .976   .979   .882   .736   .535   .90 -211
.285    0.                                                     .90 -211
0.      .075   .14    .27    .375   .45    .49    .49    .42    .31    1.0 -211
.165    0.                                                     1.0 -211
0.      15.    20.    30.    40.    50.    60.    70.    74.9   80.    2Y/B
90.     100.                                                   2Y/B
5.65    5.65   4.25   2.38   1.08   -.05   -1.12  -1.98  -2.29  -2.46  ATWIST
-2.70   -2.97                                                  ATWIST
31.6    2.7    37.0   7.3    7.5                               FLAP DEF
.7                                                             20  VAC
0.      5.     10.                                             ALPHAS
END
```

CAMBER LINES

Figure C6.   Computer Inputs for -212 (-213) Drag-Due-To-Lift Analysis

APPENDIX C (Continued)

DRAG ESTIMATES

The subsonic drag and miscellaneous drag estimates are calculated using the following methods:

Form Drag -- The form (or profile) drag is calculated using factors in emperical relationships. The wing and vertical tail form drag is calculated using the following:

$$C_{D_{Form}} = (K_t + K_c) K_A K_L \; C_{D_{Friction}}$$

$K_t$ and $K_c$ are airfoil dependent (thickness and camber) and have been developed for advanced technology airfoils using boundary layer theory, simple sweep theory and two-dimensional experimental data. $K_A$ is a function of wing sweep and $K_L$ is determined by the amount of laminar flow expected. A value for $K_L = 1.0$ was assumed for the LES evaluation. These factors then adjust the flat-plate skin friction for that particular component. The body form drag is computed as follows:

$$C_{D_{Form}} = K_F \; C_{D_{Friction}}$$

Where $K_F$ adjusts the flat plate evaluation for all three-dimensional effects and is a function of the body fineness ratio and Reynolds number. Extreme afterbody upsweep or closure would be accounted for separately.

Interference Drag -- Interference drag calculations account for body-wing and vertical-wing interference effects. The general form of the equation is:

$$C_{D_{Interference}} = (K_i \; C_{D_{Friction}}) N_i$$

284

APPENDIX C (Continued)

For the wing and vertical tails, the interference drag factor, $K_i$, is a function of sweep, taper ratio and aspect ratio. $N_i$ accounts for the number of surfaces intersecting the body or wing.

Excrescence Drag -- The form drag and skin friction drag calculations assume the aircrafts exterior (wetted) surface is smooth. In actuality, the external surface is not smooth but has gaps, mismatches, surface waviness, small protuberances, leakage through control surfaces, etc. Although it is anticipated that a composite structure will reflect considerable advantages in this respect, relative to a built-up aluminum design, drag assessment methodology reflecting the latter was applied for this initial study phase. To account for these surface irregularities, an excrescence drag is calculated based on the surface (wetted) area, the total vehicle's skin friction, form and interference drags.

$$C_{D_{Excrescence}} = K_E K_M (C_{D_{Friction}} + C_{D_{Form}} + C_{D_{Interference}})$$

$K_E$ is a function of the total airplane wetted area and $K_M$ is a function of Mach number. For the supersonic estimates the form of the equation is:

$$C_{D_{Excrescence}} + K_E K_M C_{D_{Friction}}$$

Miscellaneous Drag -- The drag of discrete items such as antennas, refueling probes, gun fairings, external stores, blunt bases or steps, canopy, external gear bumps, flap track fairings, etc. is calculated separately. Generally the parasite drag of these items is calculated using the following equation:

$$C_{D_{Misc}} = C_{D_\pi} \frac{A_\pi}{S_{Ref}}$$

285

APPENDIX C (Continued)

where $C_{D_\pi}$ is the drag coefficient of the particular item based on its projected frontal area, $A_\pi$ . The values of $C_{D_\pi}$ as a function of Mach number for different items are generally available from publications, flight test data or wind tunnel test data.

Nozzle/Inlet Reference Drag -- Nozzle and inlet reference drags are a function of the component designs, size and engine erference mass flow. In the case of this current LES study, a reference mass flow schedule was not available in time to make a definite thrust/drag Consequently, propulsion system reference drags were included in the engine data.

Inlet Diverter Drag -- The inlet diverter drag evolved from an earlier configuration which assumed an airscoop arrangement because of the inlet, wing, body proximity of that region. For the scoop, air from one half of the inlet width was taken on board -- the remaining was diverted away to the sides in a more conventional fashion. The drag calculation assumed a 50 percent momentum loss from free-stream of the air passing into the scoop while the diverter portion was assessed using Boeing B-1 Wind Tunnel data. Subsequently the design was changed to that shown for the -213 where a minimal scoop was used. In lieu of a detailed analysis, the diverter assessment was reduced by $\Delta C_D$ = 0.0010 or about half of the original penalty. The remaining compares quite favorably with that used for earlier studies such as for the LWF. For this LES design scoping phase, it was felt that a more detailed study was not warranted.

Drag-Due-To-Mach-Number -- The drag calculations for the major airplane components discussed above do not take into account compressibility effects with increased Mach number. Because of the high body fineness ratio and the thin, highly swept wing, the LES configuration does not display a significant drag rise effect at 0.9 Mach.

APPENDIX C (Continued)

Drag-Due-To-Lift - At Mach 0.9 the equation used to calculate the drag-due-to-lift of the wing-body combination is given below.

$$c_{D_{L_{WING}}} = \left\{ (c_L - c_{L_{DES}})^2 \left[ \frac{1}{c_{L\alpha}} + (\frac{s}{s_{MAX}}) s_{MAX} (\frac{1+\delta}{\pi AR} - \frac{1}{c_{L\alpha}}) \right] + \frac{c_{L_{DES}}}{\pi AR} (2c_L - c_{L_{DES}}) \Delta c_D \right\} \left\{ 1 + (\frac{d}{b})^2 \right\}$$

The method includes standard aerodynamic parameters such as lift curve slope, aspect ratio and a planform correction factor, $1 + \delta$ . In addition, leading edge suction is accounted for in the parameter $s_{max}$ (maximum leading edge suction) which is a function of leading edge Reynolds number and in the parameter $s/s_{max}$, which accounts for the variation of leading edge suction with $C_L$ and is a function of leading edge radius. For airfoils which incorporate leading and/or trailing edge devices, the term $\Delta C_{D_f}$ accounts for an increment in camber drag over and above that accounted for in the parasite drag calculations. This term is a function of the increase in airfoil camber over and above that of the basic airfoil. A body carryover correction factor, $1 + (d/b)^2$ accounts for the effect of the fuselage on the wing spanwise lift distribution. The value of $C_{L_{des}}$ is a function of the average geometric wing camber which is adjusted for wing sweep effects. When $C_L$ is equal to the wing design $C_L$, $C_{L_{DES}}$ , the drag due-to-lift is then just equal to the recognized drag-due-to-lift form of $C_L^2 / \pi AR$ with the addition of $\Delta C_{D_f}$ and the body correction factor. Note that this method includes the variation of parasite drag-due-to-lift which is often referred to as $\Delta C_{D_p}$ . The parameters used in the equation for $C_{D_L}$ are from sources such as the RAS data sheets (for $C_{L_\alpha}$ and $1 + \delta$ ) or have been derived from wind tunnel test data ($s_{max}$ and $s/s_{max}$).

287

## APPENDIX D    REGRESSION ANALYSIS SUMMARY

The prime measure of goodness of the surface fit equations, the multiple correlation coefficient squared, is presented in Table D1   for both configuration concepts.   The closer the coefficient is to 1.0 the better the surface fit.

In general the surface fit results are quite good.   Only three out of the twenty-two parameters shown have surface fits which might be considered unacceptable.   These are supersonic cruise altitude for both the -202 and the -210 and supersonic cruise efficiency for the -210.   The reason for the poor fit of these three parameters is not understood at this time.

The regression equations are presented in tabular form in Table D2 and D3 for the -202 canard concept and the -210 arrow concept respectively. The dependent variable name are listed across the top of the table.   The terms that go into a second order polynomial equation are listed on the left hand side.   The body of the table lists the coefficients of each of the terms.   The terms with zero coefficients do not appear in the equation.

For example looking at Table D2, the equation for cruise radius in more familiar terms is:

$$SUPR2 = -1652 + 8.824 \times W/S + .1803 \times TOGW + .0600 \times W/S^2$$
$$+ .0003955 \times W/S \times TOGW - .000005 \times TOGW^2$$

## Table D1. Regression Parameters and Statistics

| Variable | Description | Multiple Correlation Coefficient Squared | |
|----------|-------------|:-----:|:-----:|
| | | (-202) | (-210) |
| SUPALT | Supersonic Cruise Altitude | .6789 | .6408 |
| SUPR1 | Supersonic radius, design payload | .929 | .9530 |
| SUPR3 | Supersonic radius, overload payload | .8576 | .9643 |
| FUELF | Fuel fraction: Fuel/TOGW | .9940 | .9970 |
| SUPMLS | Supersonic cruise efficiency, ML/D/SFC | .8543 | .5841 |
| TURN1 | Persistence, $M = .9/h = 30,000$ | .9594 | .9226 |
| TURN2 | Persistence, $M = 1.2/h = 30,000$ | .9374 | .9597 |
| TURN7 | Persistence, $M = 2.0/h = 40,000$ | .9887 | .9555 |
| XLS1 | Sustained load factor, $M = .9/h = 30,000$ | .9420 | .9942 |
| XLS2 | Sustained load factor, $M = 1.2/h = 30,000$ | .9630 | .9956 |
| XLS7 | Sustained load factor, $M = 2.0/h = 40,000$ | .9511 | .9863 |

289

Table D2. Canard Concept Regression Equations

| | SUPALT | SUPRL | SUPR3 | FUELF | SUPMLS |
|---|---|---|---|---|---|
| CONSTANT | 46790 | −1652 | −1477 | −.6169 | −18.88 |
| $A\!R$ | 0 | 0 | 0 | 0 | 0 |
| $t/c$ | 0 | 0 | 0 | 0 | 0 |
| $W/S$ | 0 | 8.824 | 4.478 | .002429 | 0 |
| $\Omega_{LE}$ | 0 | 0 | 0 | 0 | 0 |
| TOGW | 0 | .1803 | .1732 | .0001019 | 0 |
| $M_{CR}$ | 0 | 0 | 0 | 0 | 29.67 |
| $A\!R^2$ | 0 | 0 | 0 | 0 | 0 |
| $A\!R \times t/c$ | 0 | 0 | 0 | 0 | 0 |
| $A\!R \times W/S$ | 0 | 0 | 0 | 0 | 0 |
| $A\!R \times \Omega_{LE}$ | 0 | 0 | 0 | .0002767 | 0 |
| $A\!R \times$ TOGW | 0 | 0 | 0 | 0 | .00004417 |
| $A\!R \times M_{cr}$ | 680.8 | 0 | 0 | 0 | −.2369 |
| $t/c^2$ | 0 | 0 | 116900. | 0 | 0 |
| $t/c \times W/S$ | 0 | 0 | −79.29 | −.01546 | 0 |
| $t/c \times \Omega_{LE}$ | 0 | 0 | 0 | .0507 | 0 |
| $t/c \times$ TOGW | 0 | 0 | 0 | 0 | −.003670 |
| $t/c \times M_{cr}$ | 0 | 0 | 0 | 0 | 0 |
| $W/S^2$ | 0 | .0600 | 0 | −.00001499 | 0 |
| $W/S \times \Omega_{LD}$ | 0 | 0 | 0 | .00004490 | 0 |
| $W/S \times$ TOGW | −.005807 | .0003955 | −.0004712 | 0 | 0 |
| $W/S \times M_{cr}$ | 0 | 0 | 3.781 | 0 | 0 |
| $\Omega_{LE}^2$ | 0 | 0 | 0 | −.00006258 | .0007652 |
| $\Omega_{LE} \times$ TOGW | 0 | 0 | 0 | 0 | 0 |
| $\Omega_{LE} \times M_{cr}$ | 0 | 0 | 0 | 0 | 0 |
| $\text{TOGW}^2$ | 0 | $-5.484 \times 10^{-6}$ | 0 | $-2.623 \times 10^{-9}$ | 0 |
| TOGW $\times M_{cr}$ | .2435 | 0 | −.03443 | 0 | 0 |
| $M_{cr}^2$ | 0 | 0 | 0 | 0 | −9.016 |

|  | TURN1 | TURN2 | TURN7 | XLS1 | XLS2 | XLS7 |
|---|---|---|---|---|---|---|
| CONSTANT | -65.99 | -46.15 | -16.10 | 5.309 | 10.29 | 5.847 |
| $R$ | 0 | 0 | -1.968 | 0 | 0 | 0 |
| t/c | 0 | 0 | -32.73 | 0 | 0 | 0 |
| W/S | 0 | 0 | .1090 | 0 | 0 | 0 |
| LE | .2453 | .3356 | 0 | 0 | 0 | 0 |
| TOGW | .008143 | .005447 | .001928 | 0 | -.0004399 | 0 |
| $M_{cr}$ | 6.419 | 0 | 0 | 0 | 0 | 0 |
| $R^2$ | 0 | 0 | 0 | 0 | 0 | 0 |
| $R$ x t/c | 0 | -8.440 | 0 | 4.794 | 0 | 0 |
| $R$ x W/S | .03702 | 0 | .002802 | 0 | 0 | 0 |
| $R$ x LE | 0 | 0 | .01137 | 0 | 0 | .008954 |
| $R$ x TOGW | 0 | 0 | .00007739 | 0 | -.00001663 | -.00002485 |
| $R$ x $M_{cr}$ | -2.056 | 0 | 0 | 0 | 0 | 0 |
| $t/c^2$ | -2193 | 0 | -778.1 | 0 | 0 | -21.54 |
| t/c x W/S | 0 | .5550 | 0 | -.2342 | 0 | 0 |
| t/c x LE | 4.234 | 0 | 1.978 | 0 | 0 | .6170 |
| t/c x TOGW | 0 | 0 | 0 | 0 | 0 | -.001750 |
| t/c x $M_{cr}$ | 0 | 0 | 0 | 6.319 | 0 | 0 |
| $W/S^2$ | -.0006365 | 0 | -.001329 | 0 | 0 | 0 |
| W/S x LE | 0 | 0 | .0005250 | -.0002932 | -.0004096 | -.0003139 |
| W/S x TOGW | 0 | 0 | 0 | 0 | 0 | 0 |
| W/S x $M_{cr}$ | 0 | 0 | 0 | 0 | 0 | 0 |
| $LE^2$ | 0 | 0 | -.001691 | 0 | 0 | 0 |
| LE x TOGW | -.00004830 | -.00003562 | 0 | 0 | 0 | 0 |
| LE x $M_{cr}$ | 0 | 0 | 0 | 0 | 0 | 0 |
| $TOGW^2$ | $-1.150 \times 10^{-7}$ | $-7.115 \times 10^{-8}$ | $-4.944 \times 10^{-8}$ | 0 | $1.09 \times 10^{-8}$ | 0 |
| TOGW x $M_{cr}$ | 0 | 0 | 0 | 0 | 0 | 0 |
| $M_{cr}^2$ | 0 | 0 | 0 | 0 | 0 | 0 |

*Table D3. Arrow Concept Regression Equations*

| CONSTANT | SUPALT | SUPR2 | SUPR3 | FUELF | SUPMLS |
|---|---|---|---|---|---|
| CONSTANT | 54180 | -4867 | -4352 | -.8166 | 7.8684 |
| t/c | 0 | 0 | | 2.767 | 0 |
| W/S | 0 | 6.649 | 6.817 | .006025 | 0 |
| TOGW | 0 | .2859 | .2384 | .0001015 | 0 |
| $M_{cr}$ | 0 | 3414 | 3065 | 0 | 0 |
| t/c x t/c | 0 | 0 | 0 | -16.65 | 0 |
| t/c x W/S | 0 | 18.43 | 15.03 | -.01177 | -.19186 |
| t/c x TOGW | 0 | 0 | 0 | 0 | 0 |
| t/c x $M_{cr}$ | 0 | 0 | 0 | .1856 | 0 |
| W/S x W/S | 0 | -.07074 | -.06690 | -.00006097 | 0 |
| W/S x TOGW | -.005985 | .0003175 | .0002744 | $3.377 \times 10^{8}$ | $1.701 \times 10^{-6}$ |
| W/S x $M_{cr}$ | 0 | 0 | 0 | 0 | -.021583 |
| TOGW x TOGW | 0 | $-8.829 \times 10^{-6}$ | $-7.087 \times 10^{-6}$ | $-2.887 \times 10^{9}$ | 0 |
| TOGW x $M_{cr}$ | 0 | 0 | 0 | 0 | 0 |
| $M_{cr}$ x $M_{cr}$ | 0 | -1032 | -930.5 | 0 | 0 |

Table D3, Continued

|  | TURN1 | TURN2 | TURN7 | XLS2 | XL | XLS3 |
|---|---|---|---|---|---|---|
| CONSTANT | -114.9 | -68.90 | -46.13 | 14.09 | 19.25 | 14.11 |
| $t/c$ | 59.86 | 35.66 | 0 | 2.108 | 0 | 0 |
| $W/S$ | .3298 | 0 | 0 | -.1316 | -.1012 | -.07787 |
| TOGW | .008728 | .005865 | .003372 | 0 | -.0003476 | -.0005140 |
| $M_{cr}$ | 52.51 | 34.51 | 26.88 | -3.356 | -6.358 | 0 |
| $t/c \times t/c$ | 0 | 0 | 0 | 0 | 0 | 0 |
| $t/c \times W/S$ | 0 | 0 | .2596 | 0 | 0 | 0 |
| $t/c \times$ TOGW | 0 | 0 | 0 | 0 | 0 | 0 |
| $t/c \times M_{cr}$ | 0 | 0 | 0 | 0 | 0 | 0 |
| $W/S \times W/S$ | -.0017 | 0 | 0 | .0003526 | .0002461 | .0002001 |
| $W/S \times$ TOGW | -.00000808 | 0 | 0 | $1.096 \times 10^{-6}$ | $1.447 \times 10^{-6}$ | $1.6\ 5 \times 10^{-6}$ |
| $W/S \times M_{cr}$ | 0 | 0 | 0 | -01926 | .01035 | 0 |
| TOGW$^2$ | -.00000014 | $-9.839 \times 10^{-8}$ | $-7.014 \times 10^{-8}$ | $-3.9 \times 10^{-9}$ | 0 | 0 |
| TOGW $\times M_{cr}$ | -.001264 | -.001040 | -.0003722 | 0 | .00009313 | .1593 |
| $M_{cr} \times M_{cr}$ | -12.31 | -7.372 | -7.906 | 0 | .5726 | -1.039 |

## APPENDIX E - MID-TERM POINT DESIGNS

This appendix briefly describes the selection criteria for the mid-term point design airplanes and presents their persistence and specific excess power charts.

Four airplanes (Table E1) were selected for presentation at the mid-term oral, two canard concepts and two arrow concepts. The original selection criteria was to select the best supercruise and the best maneuver design for each concept. By coincidence, the best supercruise airplanes both had a radius of 550 n. mi. at a takeoff gross weight. Next, in selecting the best maneuver (highest sustained load factor) designs, the wing loading on the canard concept was compromised slightly (increased from 60 to 66 lb/ft) to match the radius capability of best maneuver arrow concept.

*Table E1. Point Design Characteristics*

| CONCEPT | W/S | $\Lambda_{LE}$ | R | RADIUS |
|---------|-----|------|-----|--------|
| Canard  | 120 | $65^0$ |     | 550 |
| Canard  | 66  | $45^0$ | 3.0 | 390 |
| Arrow   | 80  |      |     | 550 |
| Arrow   | 40  | $74^0$ | .94 | 390 |

Combat performance, sustained load factor, and persistence, is shown in Figure E 1 for two flight envelope conditions, Mach 0.90/40,000 ft. and Mach 2.0/40,000 ft.

1 and 5g Ps followed by persistence is presented in Figures E 2 through E 7 for the two canard concept airplanes. Corresponding data follows in Figures E 8 through E 13 for the two arrow configurations. All data is calculated at maximum thrust. The 60,000 ft. altitude limit was imposed by the engine.

294
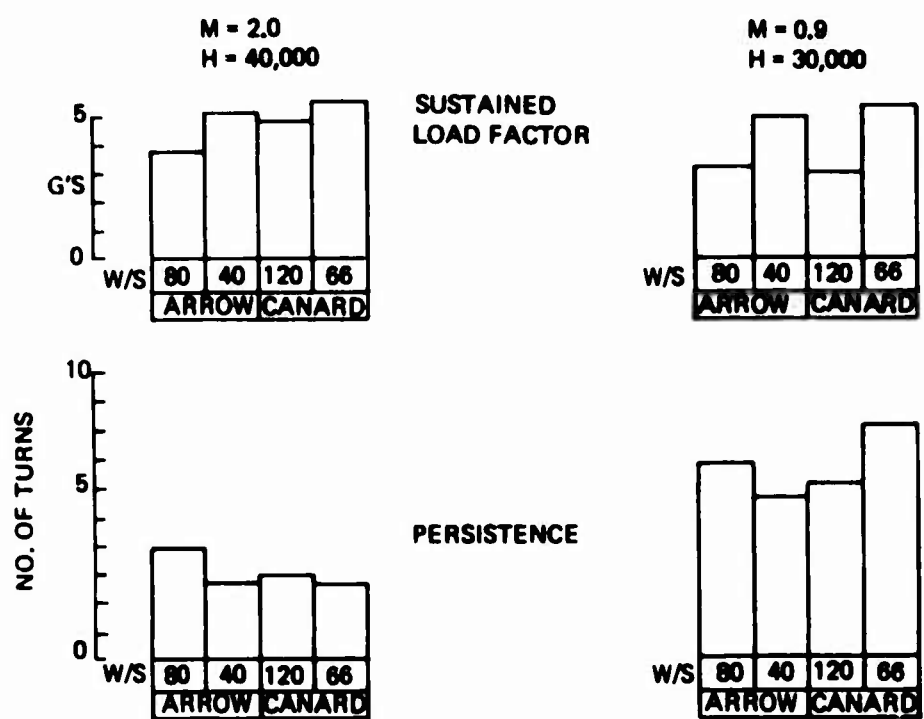
Figure E1. LES Combat Performance Summary
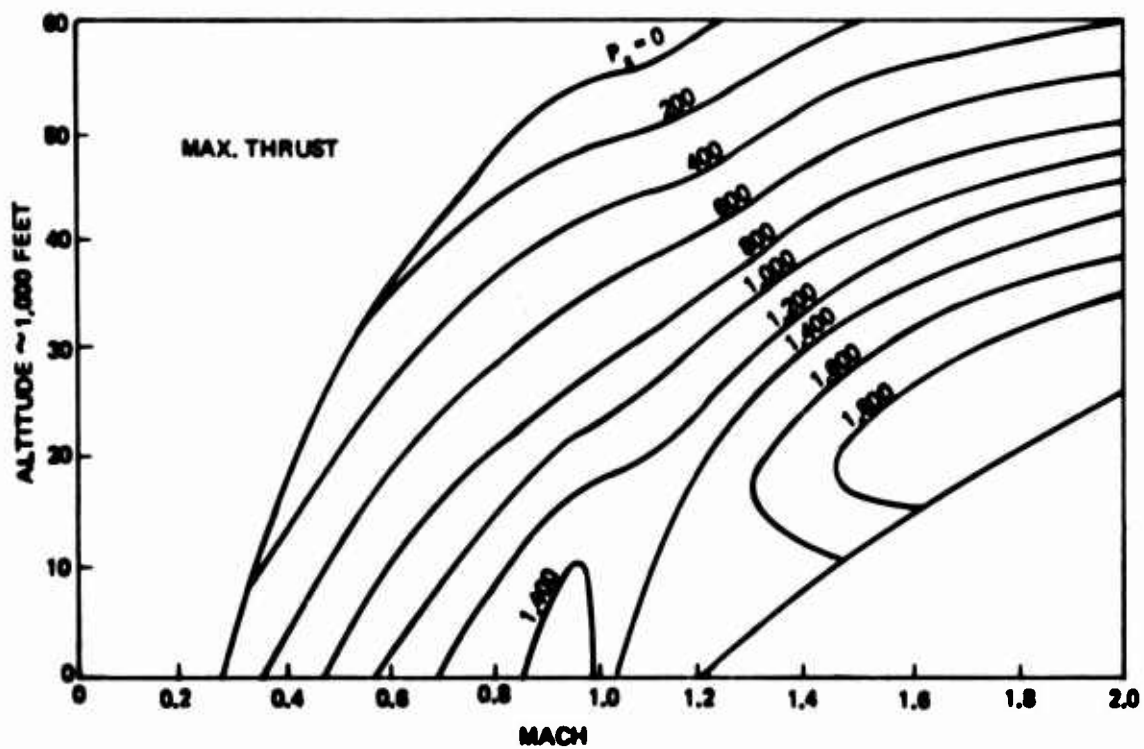
Figure E2.   LES-202 (Canard) 1G - $P_S$ W/S = 120 PSF
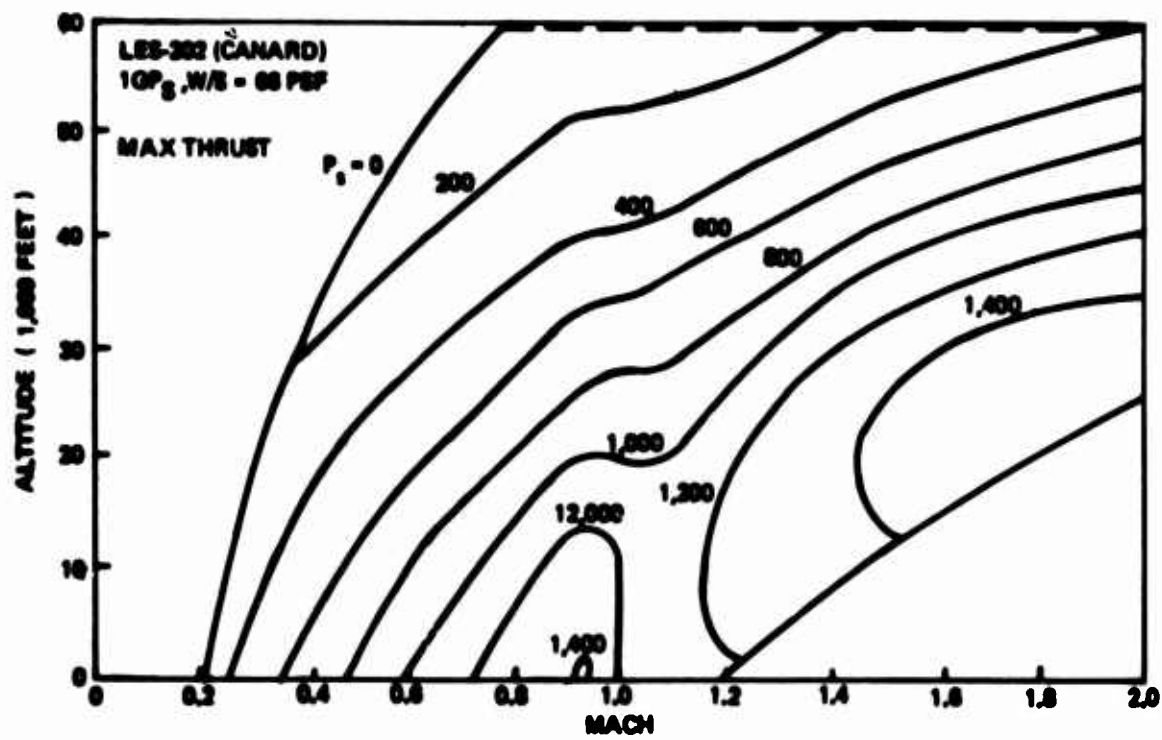


Figure E3.   LES-202 (Canard) 1G- $P_S$ W/S = 66 PSF
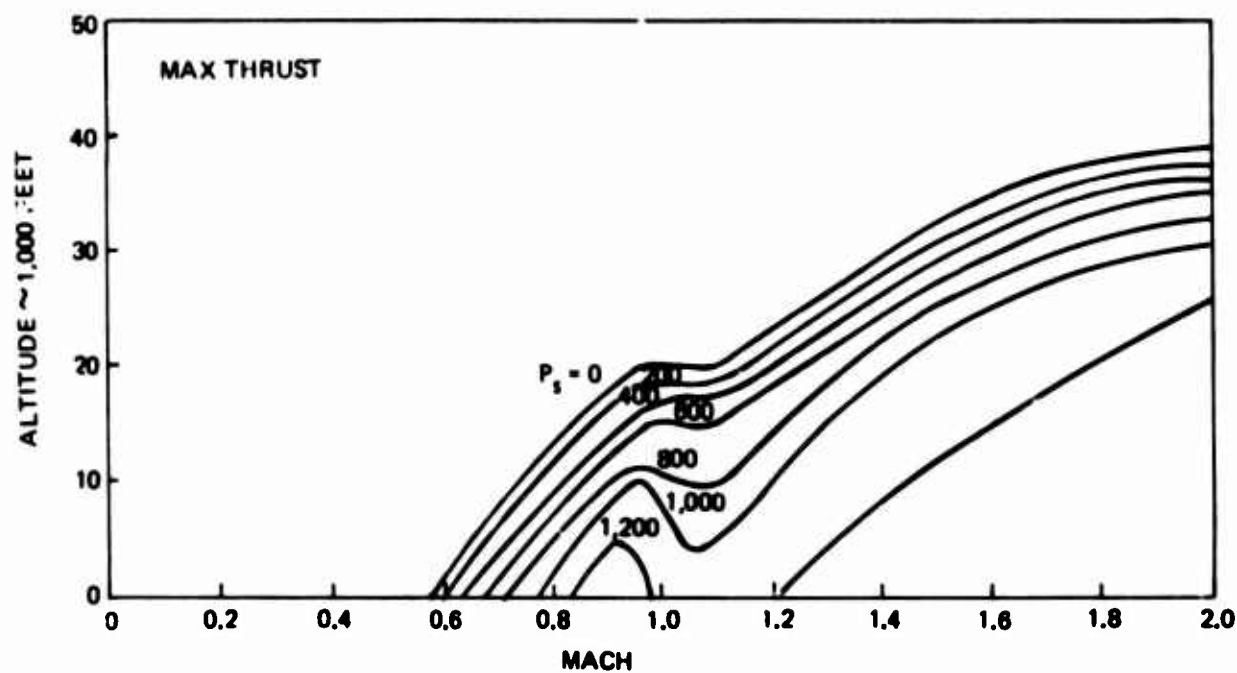
Figure E4.   LES-202 (Canard) 5G = $P_S$ W/S = 120 PSF
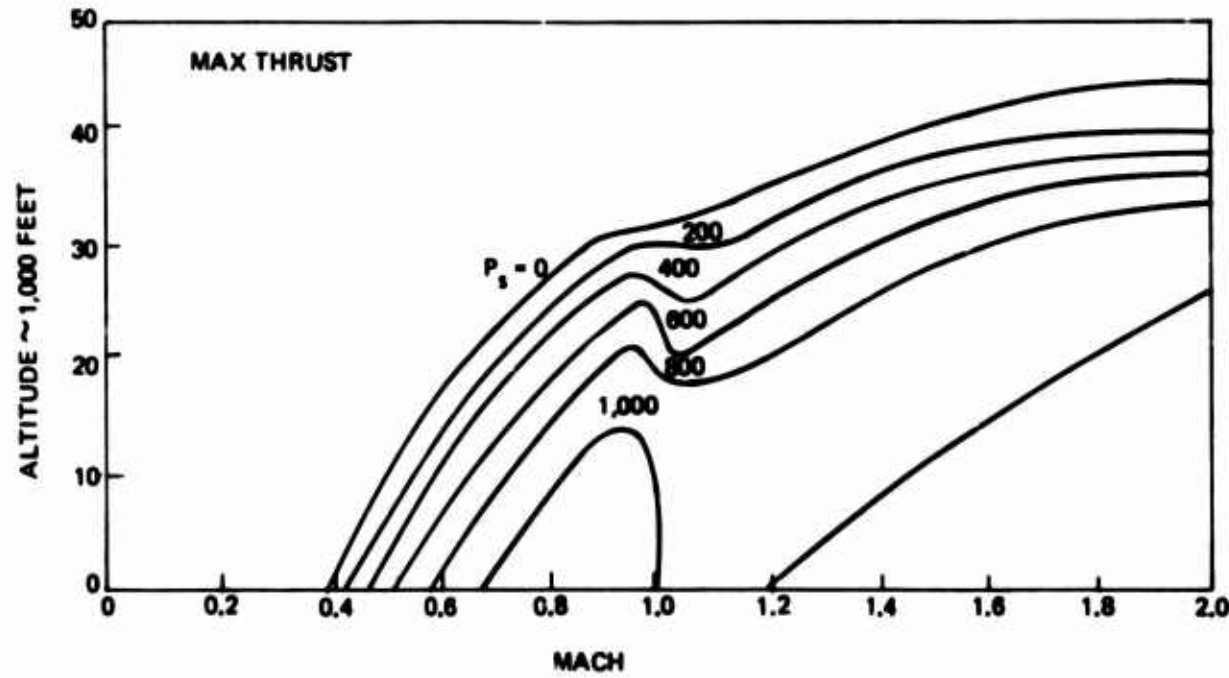


Figure E5.   LES-202 (Canard) 5G = $P_S$ W/S = 66 PSF
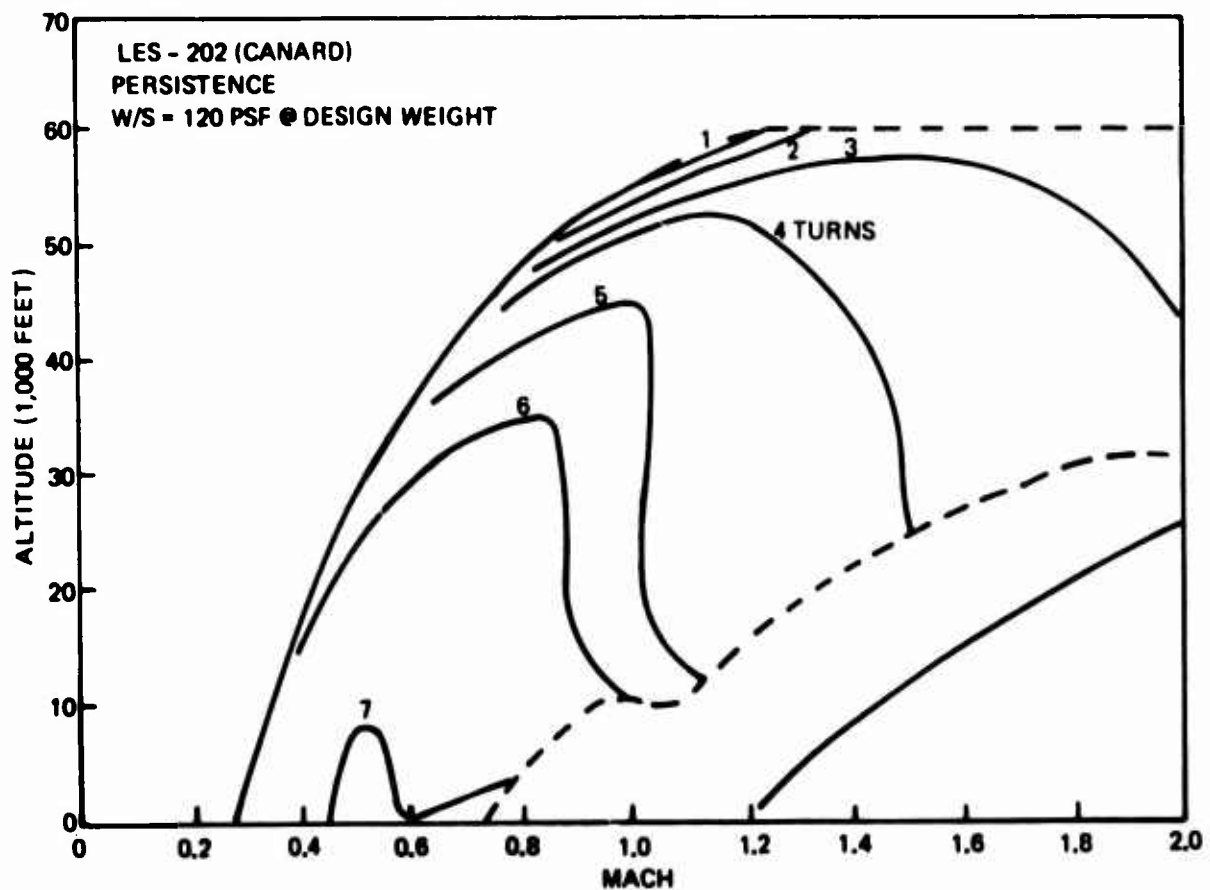
Figure E6.   LES-202 (Canard) Persistence, W/S = 120 PSF
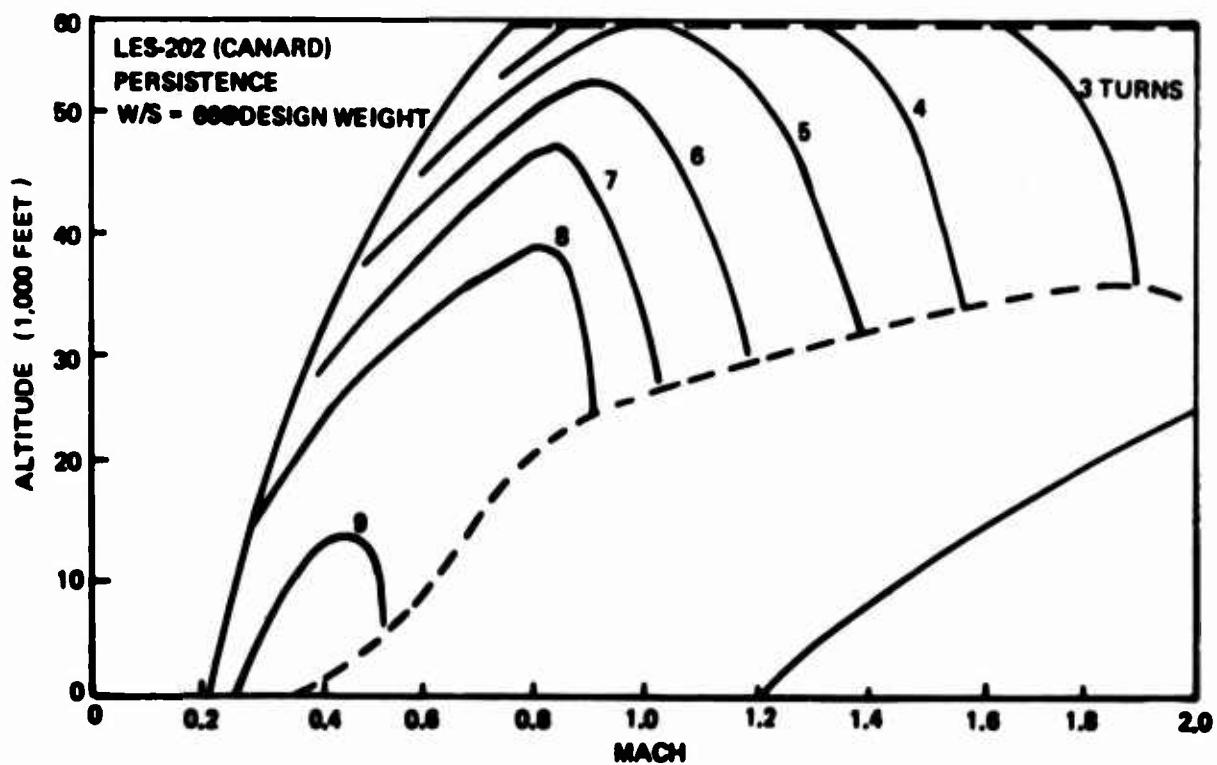


Figure E7.   LES-202 (Canard) Persistence, W/S = 66 PSF
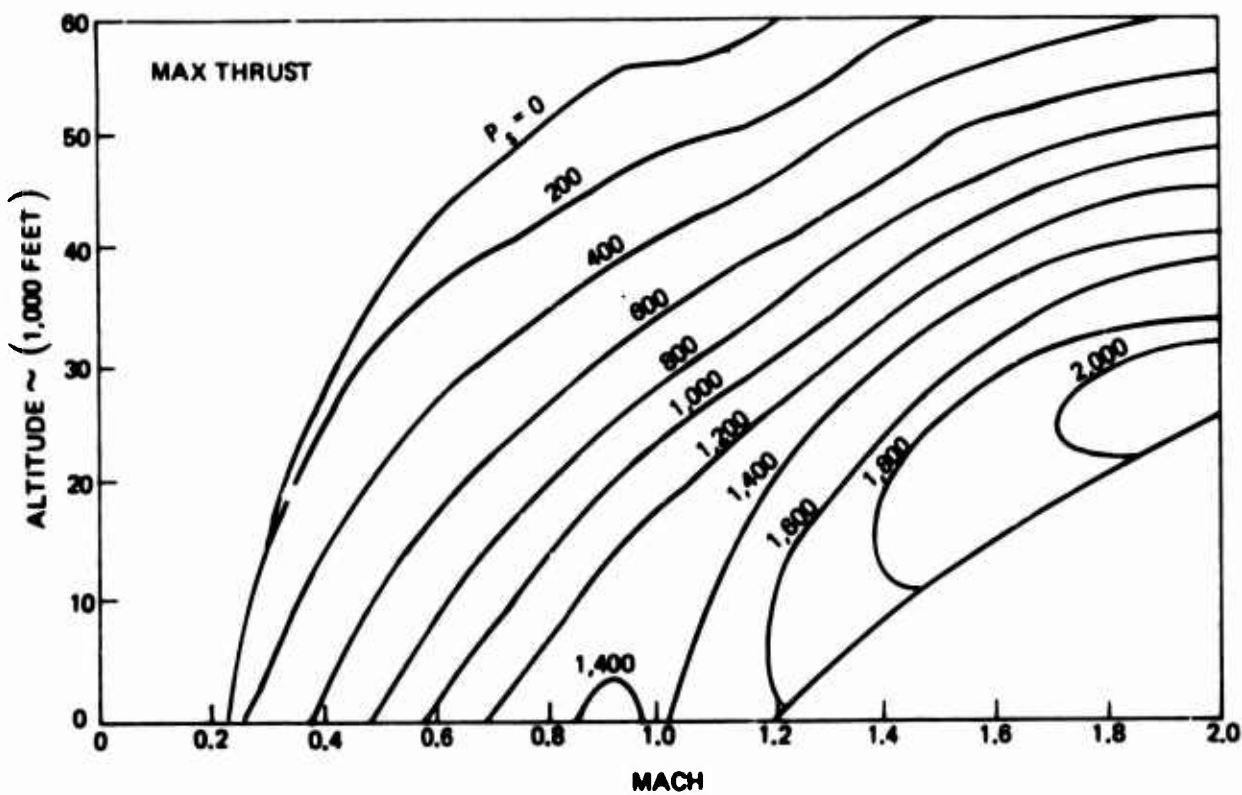
Figure E8. LES-210 (Arrow) 1G = $P_S$ W/S = 80 PSF
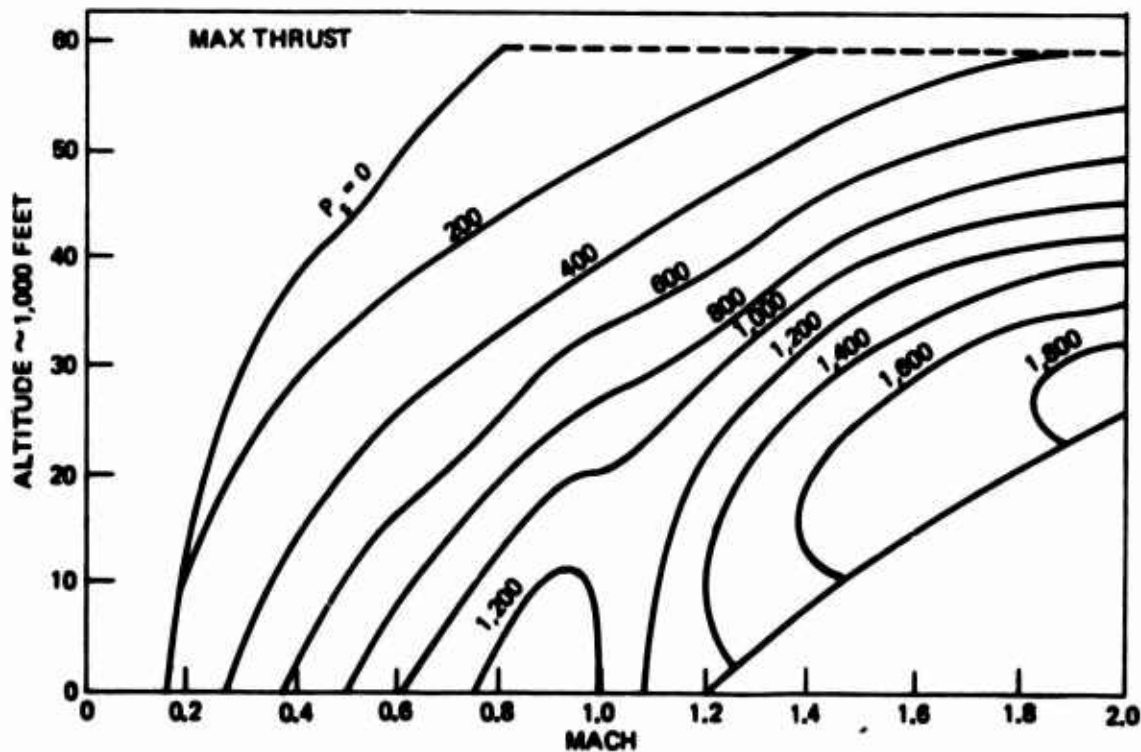


Figure E9. LES-210 (Arrow) 1G - $P_S$ W/S = 40 PSF
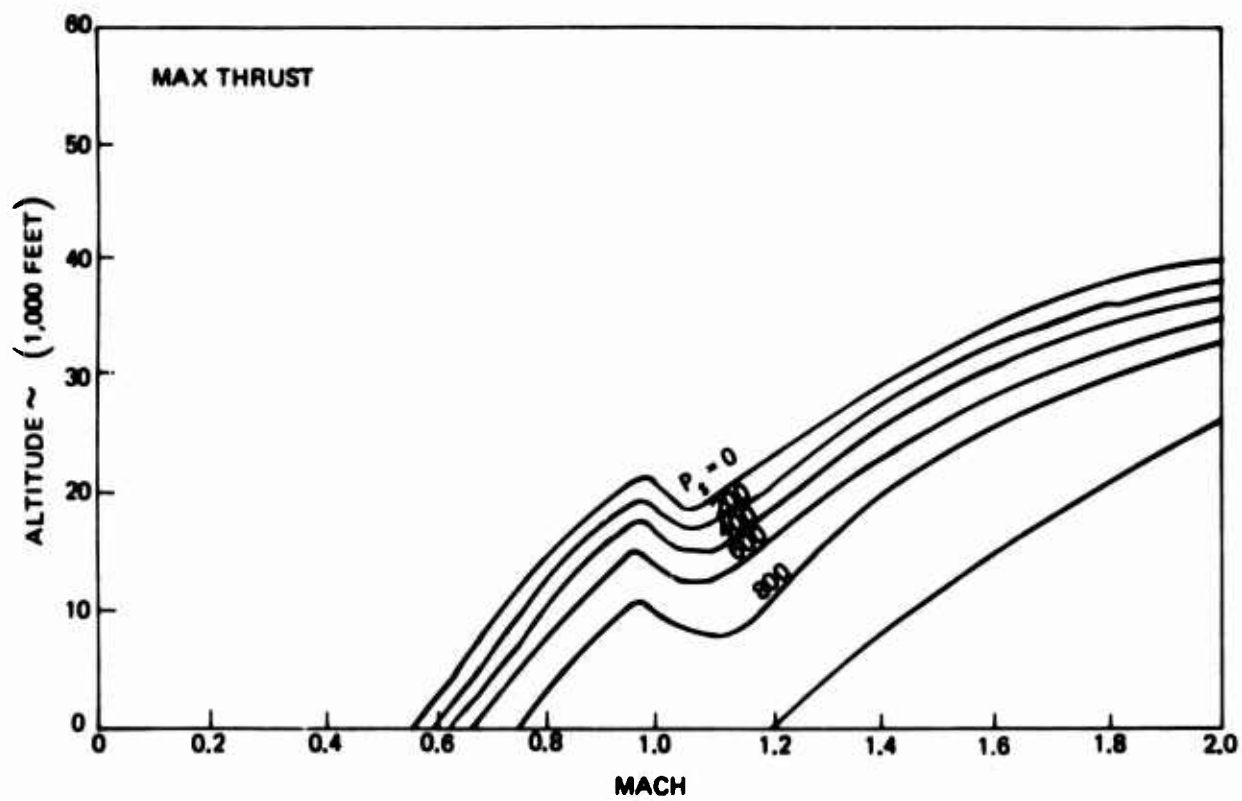
Figure E10. *LES-210 (Arrow) 5G - $P_S$ W/S = 80 PSF*
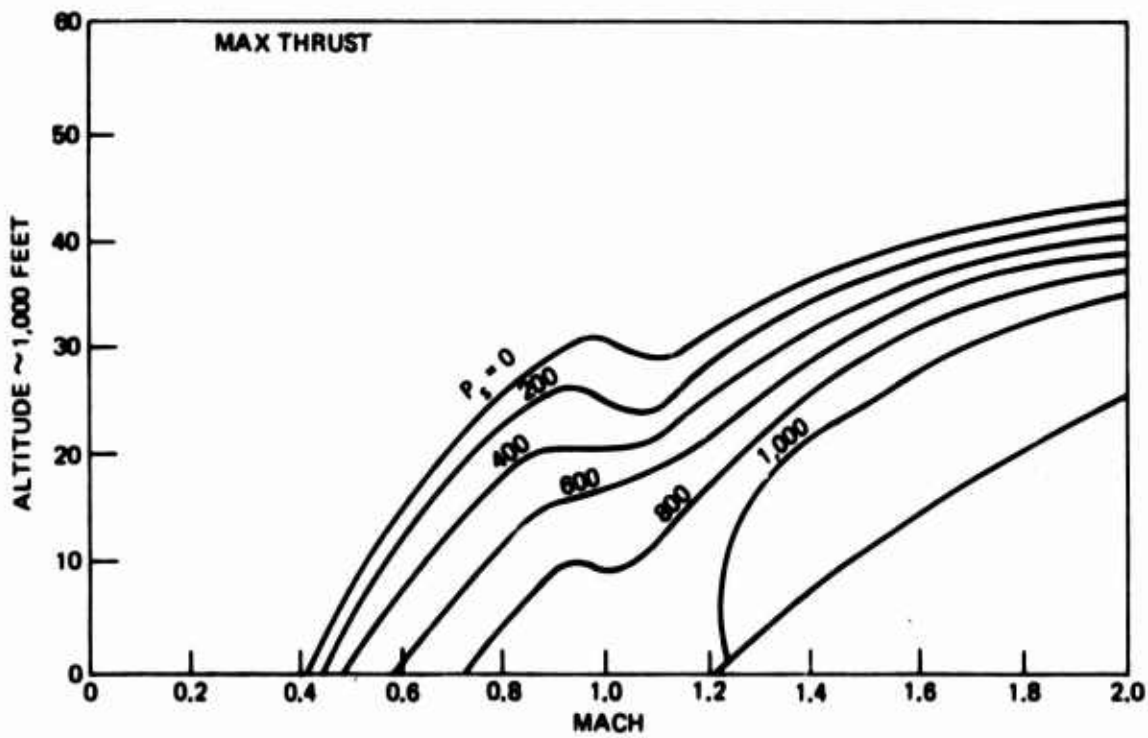


Figure E11. *LES-210 (Arrow) 5G = $P_S$ W/S = 40 PSF*

300
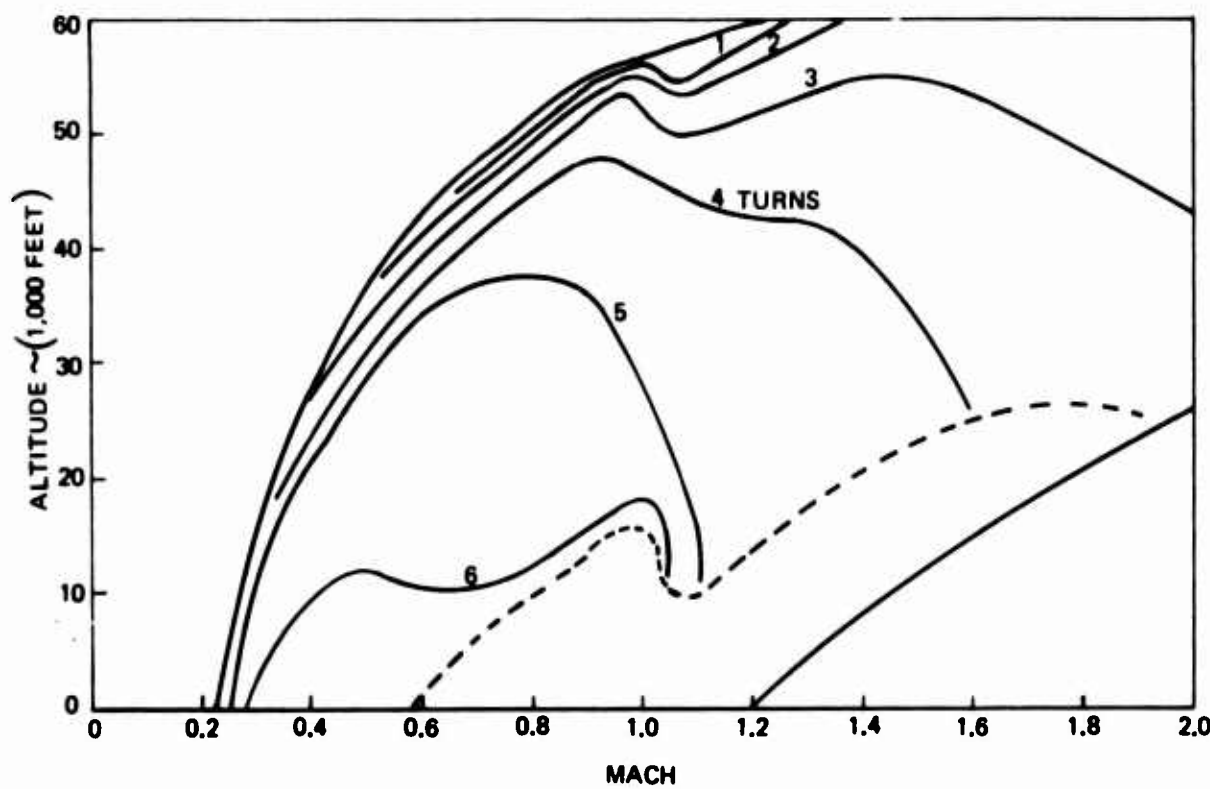
Figure E12.   LES-210 (Arrow) Persistence, W/S = 8C
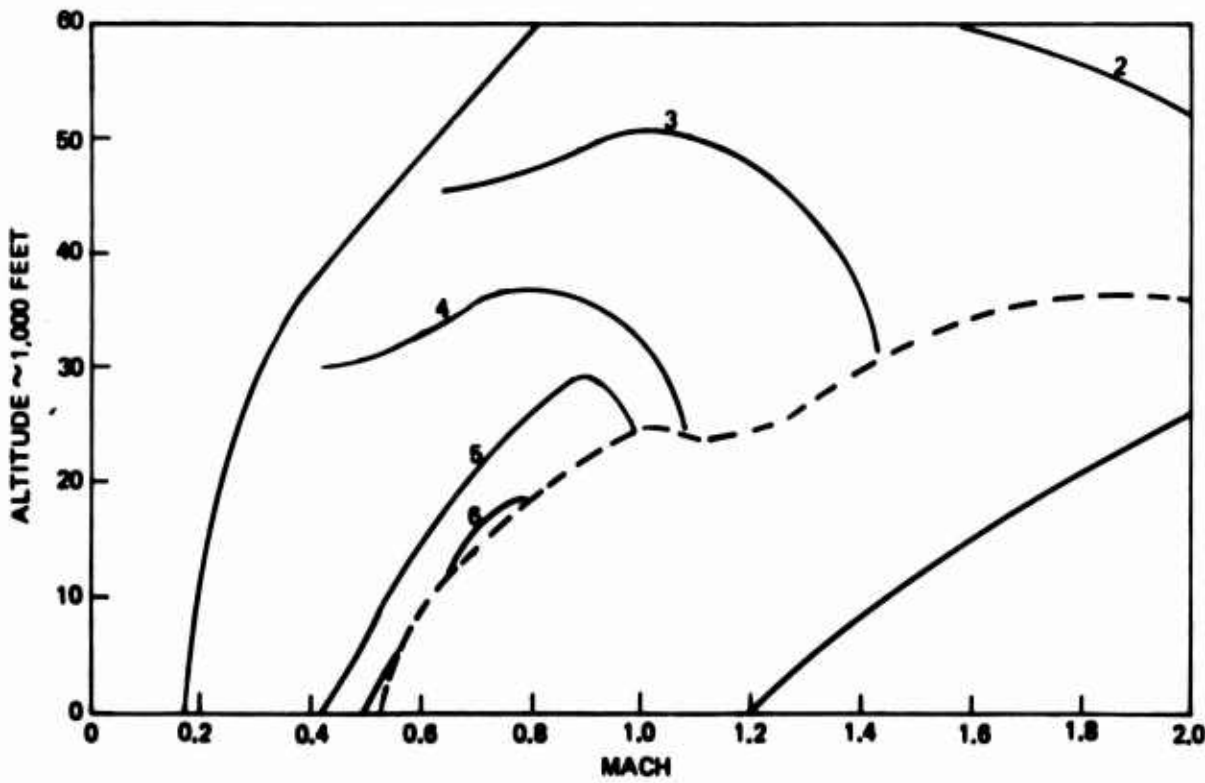


Figure E13.   LES-210 (Arrow) Persistence, W/S = 40

301

## 6.0 REFERENCES

(1)     D.R. Kozlowski, et. al., "Advanced Tactical Fighter Target Acqui-
        sition and Weapon Delivery Study", McDonnell Aircraft Company,
        McDonnell Douglas Corporation, Technical Report ASD/XR-74-21,
        October 1974.

(2)     H.H. Album, Major, USAF, "Technological Feasibilities for an
        Advanced Strike Fighter", Technical Report AFFDL-TR-71-184,
        July 1971.

(3)     D.A. Reddan, "Advanced Tactical Fighter Preliminary Design Study",
        McDonnell Aircraft Company, McDonnell Douglas Corporation, Tech-
        nical Report ASD/XR-72-31, Volume II, "Technology Assessment",
        July 1972.

(4)     S.K. Jackson, Jr., "Parametric and Point Design Studies of an Ad-
        vanced Tactical Fighter", Convair Aerospace Division of General
        Dynamics Corporation, Technical Report ASD/XR-72-32, Volume II,
        "Technology Assessment", July 1972.

(5)     K. deBooy, et. al., "Battle Damage Tolerant Wing Structural De-
        velopment Program", Quarterly Reports to NASC under Navy Con-
        tract N00019-75-C-0178, Boeing Aerospace Company D180-18697-1,
        March 1975, D180-18894-1, July 1975 and D180-19508-1 (to be
        published) May 1976.

(6)     G.F  Goetz, et. al., "Exploratory Development of an Integrated
        Engine Exhaust System - Design Feasibility Study of an Airframe
        Integrated Nozzle Concept", Final Report to NAPTC under Navy Con-
        tract No. N000140-73-C-0027, Boeing Aerospace Company D180-19106-1,
        November 1975.

6.0    REFERENCES (Continued)

(7)    G.F. Goetz and J.E. Petit, "Exploratory Development of an Inte-
       grated Engine Exhaust System.  Integrated Nozzle Wind Tunnel Test
       Results", Final Report to NAPTC under Contract No. N00140-73-C-
       0027, Boeing Aerospace Company, D180-18166-1, July 1974.

(8)    J.E. Petit, "Twin Integrated Nozzle Wind Tunnel Test Results",
       Boeing Aerospace Company, D180-18544-1, November 1975.

(9)    K deBooy, et. al., "Study of an Airframe Integrated Nozzle for In-
       fra Red Suppression to Improve Aircraft Survivability".  Technical
       Proposal to NASC, Boeing Aerospace Company D180-18114-1, May 1974.

(10)   W.H. Ball, "Propulsion System Installation Corrections", Final
       Report to AFFDL under Contract F33615-72-C-1580, AFFDL-TR-72-147,
       Volume IV, December 1972.

(11)   J.E. Hawkins, "YF-16 Inlet Design and Performance", AIAA Paper
       No. 74-1062, AIAA 10th Propulsion Conference, October 21-23, 1974.

(12)   P.A. Ross, "Propulsion System Development for Lightweight Fighter -
       Inlet/Engine Compatibility", Boeing Aerospace Company D180-14475-2
       TN, March 20, 1974.

(13)   W.D. Middleton, et. al., "Aerodynamic Design and Analysis System
       for Supersonic Aircraft", NASA CR-2520, 1975.

(14)   D.K. Gould, "Variable Camber Wing - Phase I", Final Report to ONR
       under Navy Contract N00014-73-C-0244, Boeing Aerospace Company,
       D180-17606-1, October 1973.

(15)   D.E. Hoak, "USAF Stability and Control DATCOM", Revised February
       1972.

6.0    REFERENCES (Continued)

(16)   LWP-573, "Updated Studies of an Intercontinental SST Utilizing the
       SCAT-15F Configuration Concept", by Staff of Langley Research Center
       March 1968.

(17)   S.C. Murrary, et. al., "The USAF Stability and Control Digital
       DATCOM Users Manual", McDonnell Douglas Astronautics Company,
       AFFDL-TR-74-68, February 1974.

(18)   LWP-723, "Aerodynamic Characteristics of a Fixed Wing Supersonic
       Transport Configuration (SCAT-15-F-9898). Stability and Perfor-
       mance Characteristics at Mach Numbers from 0.60 to 1.20",
       February 1969.

(19)   LWP-725, "The Aerodynamic Characteristics of a Fixed Arrow Wing
       SST Configuration (SCAT-15-F-9898). Stability and Performance
       Characteristics at Supersonic Mach Numbers of 2.30, 2.70 and
       2.95", February 1969.

(20)   "Guidelines for Mass Properties Estimating - Level I", The Boeing
       Company, D6-15095-TN, REvision E, June 1974.

(21)   USAF Energy Maneuver Program.

(22)   G.J. Eckard, et. al., "Airplane Responsive Engine Selection,
       (ARES)". Phase I Report to AFFDL under Contract F-33615-73-C-2084,
       Boeing Aerospace Company, D180-18895-1, October 1975.

(23)   W.D. Middleton, J.L. Lundry, R.G. Coleman, "Aeronautical Design
       and Analysis System for Supersonic Aircraft NASA 1-12052,
       November 1974.

6.0    REFERENCES (Continued)

(24)    J.P. Decker, "The Aerodynamic Characteristics of A Fixed Arrow
        Wing Supersonic Transport Configuration (SCAT 15F-9898). Part
        V-Stability and Performance Characteristics at Mach Numbers from
        0.60 to 1.20", NASA LWP-723, October 1969.

(25)    "NASA SCAT 15F Feasibility Study", Boeing Aerospace Company,
        D180-19048-1, September 1975.

(26)    "Mid-Term Report, LWF Supercruiser Study", Boeing Aerospace
        Company, D180-19048-1, September 1975.

(27)    D.K. Gould and D.W. Eastman, "Methods Used to Determine Aero-
        dynamic Drag and Installed Propulsion Thrust for the Boeing
        Lightweight Fighter", Boeing Aerospace Company, D199-10003-1,
        1972.

(28)    L.M. Nicolai, "Fundamentals of Aircraft Design", - University of
        Dayton, 1975.

(29)    J.D. Kelly, et. al., "Design of Naval Fighter Attack Aircraft for
        Low Radar Cross Section", Final Report to ONR under contract
        N00014-71-C-0207, Boeing Aerospace Company, D180-14192-1, (Secret)
        January 1972.

(30)    J.E. Postlewaite, et. al., "Exhaust System Integration Program,
        Exhaust System Handbook - Volume 12". Final Report to ;FFDL under
        contract F33615-70-C-1450, Boeing Aerospace Company, D162-10467-12,
        April 1973.